Development of Heck and Desaturation Reactions Involving Novel Hybrid Palladium-Radical Intermediates

BY

MARVIN PARASRAM
B.S., Stony Brook University, Stony Brook, NY 2010

THESIS

Submitted as partial fulfillment of the requirements
for the degree of Doctor of Philosophy of Chemistry
in the Graduate College of the
University of Illinois at Chicago, 2017

Chicago, Illinois

Defense Committee:

Prof. Vladimir Gevorgyan, Chair and Advisor
Prof. Daesung Lee
Prof. Justin T. Mohr
Prof. Leslie N. Aldrich
Dr. Arthur R. Gomtsyan, AbbVie

This thesis is dedicated to my parents, Tularam and Parbattie Parasram, my brother, Melvin Parasram, my longtime companion, Araceli Leal, my extended family, my friends, and to those who believed in me.

ACKNOWLEDGMENTS

First and foremost, I would like to thank my advisor, Distinguished Professor Vladimir Gevorgyan, for his guidance and unwavering support over the years of my study. Under his advisement, I have become a far greater scientist than I would have ever imagined. Our countless scientific discussions and development of new projects for the laboratory during the 2016 proposal is certainly one my favorite moments of my graduate career. I am very appreciative of the great level of independence and trust he has extended to me during my career, as it allowed me to become an innovator and a leader of his laboratory. I have learned a tremendous amount from him, not only in the art of synthetic research but also on becoming a well-rounded individual. In my view, he is the highest standard of an accomplished professor and I hope to advance his philosophical ideals and enthusiasm for synthetic chemistry in my future endeavors.

I would also like to give thanks to Professors Daesung Lee, Justin T. Mohr, Leslie N. Aldrich, and Doctor Arthur R. Gomtsyan for serving as members of my thesis committee. Professor Daesung Lee has been there for me since the start of my career and his passion and knowledge of organic chemistry continues to inspire me today. In addition, I would like to express my gratitude to Professor Lee for instilling how to critically think of reaction mechanisms and for supporting me during my Ph.D. career. I would like to thank Professor Justin T. Mohr for providing me with valuable advice and support during my postdoctoral job search, which was arguably one of my most challenging moments. I am also thankful to Professor Aldrich and Doctor Gomtsyan for their suggestions, criticism, and support.

I would like to thank all current and former members of Professor Gevorgyan's research group for their fruitful friendship and support. I was very fortunate to work on exciting research projects with many intelligent and enthusiastic young scientists from the

laboratory: Mr. Padon Chuentragool, Mr. Maxim Ratushnyy, and Ms. Daria Kurandina. Engaging in scientific discussions with you all has been truly a heartwarming and joyful experience.

I express thanks to the entire staff of the Department of Chemistry for their help during these years, especially Ms. Rhonda Staudohar, Ms. Silvia Solis, Ms. Pat Ratajczyk, Dr. Randall Puchalski, Dr. Dan McElheny and Mr. Yonilo Lim.

I would like to give my sincerest thanks to my friends from the chemistry department. To the brilliant and incomparable Ms. Jenny S. Martinez, whose unwavering positive attitude and willingness to help anyone is something that I admire, dearly. She has always been a better friend to me than I ever was to her and I am truly blessed to have her in my life. I smile more because of her. To my classmate, Mr. Anthony Savushkin, the ladies man, I thank you for all the great moments we have shared over this long journey. To Dr. Neil Miranda, thank you for providing advice and help throughout my career.

Lastly, and most importantly, I would like to thank my family. To my mother, Ms. Parbattie Parasram, and my father, Mr. Tularam Parasram, I would not have made it this far without their love, hard work, and emotional support over these years. They are the best parents a stubborn child like me could ever ask for. To my twin brother, Dr. Melvin Parasram, I would like to thank him for selflessly supporting and encouraging me over these years. Words cannot express how fortunate I am to have a brother like him. Finally, a very special thank you goes to my longtime companion, Araceli Leal. She has seen the best and worst of me throughout my Ph.D. career. Unfortunately, she has seen more of the latter but because of her endless love, unconditional support, and belief in me; I have made it this far. Because of her, I was able to amaze and astonish. I thank her with all of my heart.

TABLE OF CONTENTS

TABLE OF CONTENTS

TABLE OF CONTENTS

LIST OF SCHEMES

LIST OF TABLES

LIST OF ABBREVIATIONS

Ac	acetyl
Alk	alkyl
aq	aqueous
Ar	aryl
atm	atmosphere
Bn	benzyl
Boc	*tert*-butoxycarbonyl
Bz	benzoyl
n-Bu	butyl
t-Bu	*tert*-butyl
Calcd	calculated
cat.	catalytic amount
COD	1,5-cyclooctadiene
δ	chemical shifts in parts per million downfield from tetramethylsilane (NMR)
2D	two-dimensional (NMR)
d	doublet
dba	dibenzylidene acetone
DCM	dichloromethane
DCE	1,2-dichloroethane
DCE	1,2-dichloroethane
DEPT	distortionless enhancement by polarization transfer

LIST OF ABBREVIATIONS (continued)

DFT	Density Functional Theory
DMA	dimethylacetamide
DMB	2,4-dimethoxybenzyl
DMF	dimethylformamide
DMSO	dimethylsulfoxide
EDG	electron-donating group
EE	ethoxyethyl
EI	electron impact ionization (in mass spectrometry)
Et	ethyl
eq, equiv.	molar equivalent
EWG	electron-withdrawing group
ΔG	group, Gibbs free energy
g	gram
GC	gas chromatography
h, hrs	hour(s)
HAT	hydrogen atom transfer
HMBC	heteronuclear multiple-bond correlation spectroscopy (NMR)
HMQC	heteronuclear multiple-quantum coherence spectroscopy (NMR)
HR	high resolution (mass spectrometry)
Hz	Hertz
IPr	1,3-bis(2,6-diisopropylphenyl) imidazole-2-ylidene
J	spin-spin coupling constant (NMR)

LIST OF ABBREVIATIONS (continued)

L	ligand
LDA	lithiumdiisopropyl amide
m	multiplet (NMR)
mp	melting point
m	micro
[M]	metal
M	molar
MS	mass spectrometry
MS	molecular sieves
Me	methyl
Mes	mesityl
MIDA	*N*-methyliminodiacetic acid
mg	milligram
min	minute
mL, ml	milliliter
mm	millimeter
mmol	millimole
mol	mole
MHz	megahertz
m/z	mass to charge ratio
NHC	*N*-heterocyclic carbene
NMR	nuclear magnetic resonance

LIST OF ABBREVIATIONS (continued)

Ph	phenyl
PIDA	Pinen-derived iminodiacetic acid
Piv	pivaloyl, trimethylacetyl
PMB	*p*-methoxybenzyl
ppm	parts per million
Pr	propyl
i-Pr	isopropyl
n-Pr	propyl
q	quartet (NMR)
quint	quintet (NMR)
rt	room temperature
s	singlet (NMR)
sept	septet (NMR)
t	triplet (NMR)
TBS	*tert*-butyldimethylsilyl
Tf	trifluoromethanesulfonyl
THF	tetrahydrofuran
TLC	thin layer chromatography
TM	transition metal
TMS	trimethylsilyl
Tol, tol	tolyl
Ts	*p*-toluenesulfonyl

SUMMARY

This thesis describes the development of palladium-catalyzed Heck and desaturation reactions of silyl-tethered phenols/alkenols and alcohols, respectively, involving novel Pd-hybrid radical intermediates.

Chapter 1 describes a brief overview of transition metal-catalyzed intramolecular Heck reaction of unactivated alkyl halides. Selected examples are highlighted to demonstrate the reaction scope, limitations, and reaction mechanism of the transformation. Also, Chapter 1 highlights *endo*-selective cyclization trends in the area of radical chemistry involving halomethylsilyl tethers.

Chapter 2 describes the development of the first *endo*-selective Pd-catalyzed silyl methyl Heck reaction of iodomethylsilyl ethers of phenols and aliphatic alkenols. Our methodology enabled the synthesis of 7-, 8-, and 9-membered *endo*-siloxycycles in high yield and regioselectivity. Mechanistic studies involving radical clock and deuterium labeling tests revealed that this silyl methyl Heck reaction operates via a hybrid Pd-radical process and that the silicon atom is crucial for the observed *endo* selectivity and it also enables post-modification of the obtained products. Thus, the obtained siloxycycles can be oxidized to form *Z*-allylic alcohols or can be further functionalized via the intramolecular Hosomi-Sakurai reaction to produce spiro benzofuran skeleton. We envision that this protocol may become a useful tool for a formal *Z*-hydroxymethylation of a broad range of alkenols. The experimental details for the palladium-catalyzed silyl methyl Heck reaction are presented in Chapter 3.

The second part of the thesis begins with Chapter 4. This chapter covers the two state-of-the-art areas for desaturation of aliphatic systems: transition metal-catalyzed and oxidative radical approaches. The next chapter (chapter 5) describes work that pertains to the direct photoinduced formation of an aryl hybrid Pd-radical species capable of hydrogen-atom-transfer (HAT). This transformation enabled the direct α-/β-desaturation of silyl ethers in synthetically valuable silyl enol ethers. Various mechanistic studies were conducted, which supported an aryl hybrid Pd-radical pathway of the transformation and not the conventional concerted-metalation-deprotonation (CMD) pathway for Pd-catalyzed C–H functionalization reactions. Chapter 6 discloses my recent work on the visible-light induced palladium-catalyzed remote desaturation of aliphatic alcohols. This strategy involves the employment of easily installable/removable Si-tethers possessing hydrogen atom abstracting groups, which allowed for site-controlled desaturation at unactivated C(sp^3)–H sites. The mechanism of the transformation operates via a hybrid Pd-radical pathway, where the formed intermediates possess both radical and Pd character that enables a radical-type HAT reaction and a Pd-involved β-hydride elimination endgame event to occur. The latter feature of the mechanism allows for the formation of alkenols with superior degrees of regioselectivity compared to the prior state-of-the-art desaturation methods. The experimental details for both visible light induced Pd-catalyzed α-/β-desaturation of silyl ethers and selective β-/γ-, γ-/δ-, and δ-/ε-desaturation of alcohols, featured in Chapters 5 and 6, are described in Chapter 7.

CONTRIBUTION OF AUTHORS

Several parts of this thesis are reproduced from previously published articles co-authored with collaborators, who contributed significantly to the presented work.

The first part of this thesis is written based on the previously published article ("Endo-Selective Pd-Catalyzed Silyl Methyl Heck Reaction" Parasram, M.; Iaroshenko V. O.; Gevorgyan, V. *J. Am. Chem. Soc*. **2014**, *136*, 17926). Thus, as a major contributor of this work, I designed and performed experiments (Chapter 2), and wrote the manuscript. Dr. Viktor O. Iaroschenko, a postdoctoral researcher of our group at the time, partially contributed to the mechanistic studies of the project (Chapter 2.6.). Distinguished Professor Vladimir Gevorgyan guided the research and contributed to the discussion of the results and manuscript writing.

The second part of the thesis is adapted and reproduced from a previously published research article ("Photoinduced Formation of Hybrid Aryl Pd-Radical Species Capable of 1,5-HAT: Selective Catalytic Oxidation of Silyl Ethers into Silyl Enol Ethers" Parasram, M.; Chuentragool, P.; Sakar, D.; Gevorgyan, V. *J. Am. Chem. Soc.* **2016***, 138*, 6340), in which I conceive the concept of the project, conducted mechanistic experiments, and wrote the manuscript (Chapter 5). Padon Chuentragool, a graduate student of our group and co-first author of the project, and Dhruba Sakar, a graduate student of our group at the time, both developed the scope of project and had significant contributions in executing the project (Chapter 5.2.). Distinguished Professor Vladimir Gevorgyan guided the research and contributed to the discussion of the results and manuscript writing.

PART ONE: ENDO-SELECTIVE PALLADIUM-CATALYZED SILYL METHYL HECK REACTION (Previously Published as Parasram, M.; Iaroshenko, V. O.; Gevorgyan, V. "Endo-Selective Pd-Catalyzed Silyl Methyl Heck Reaction." *J. Am. Chem. Soc.* 2014, *136*, 17926.)

1. Introduction

The Mizoroki-Heck reaction is a fundamental transformation that enables coupling of carbohalides/pseudohalides with olefins to form substituted alkenes.[1] Since its discovery,[2] numerous advances have been made involving C(sp^2)–X, aryl and vinyl halides, in both inter- and intramolecular fashion (Scheme 1). Between the two pathways, the intramolecular mode enables facile construction of carbo- and heterocycles and thus has been extensively featured in various total syntheses toward important natural products and various pharmaceutically relevant compounds.[3] A range of ring sizes can be formed, from small (*n*=3-4), normal (*n*=5-7), medium (*n*=8-14), to large (*n*>14) sized rings, as defined by Oestreich.[1] Depending on the ring size, cyclization can either occur via *exo*- or *endo*-*trig*-cyclization. In most cases, the regiochemical outcome follows Baldwin's rules for radical cyclization.[4] Hence, *exo*-*trig*-cyclization is favored for small to normal sized rings and *endo*-*trig*-cyclization is predominant for medium to large sized rings. Although very rare, intramolecular Heck reaction of C(sp^2)–X producing normal sized rings can occur *endo* selectively based on steric interactions upon cyclization,[5] additives,[6] and electronic bias of the alkene.[7] However, reported *endo* selective Heck reactions can be ambiguous. In 1992, Negishi and co-workers informed the scientific community on apparent 6-*endo* selective outcomes for Heck reactions of vinyl halides.[8] After extensive mechanistic studies, they reported that formation of the

thermodynamically favored *6-endo* adduct occurs via *5-exo-trig/3-exo-trig* cascade reaction, followed by rearrangement of the formed cyclopropane.

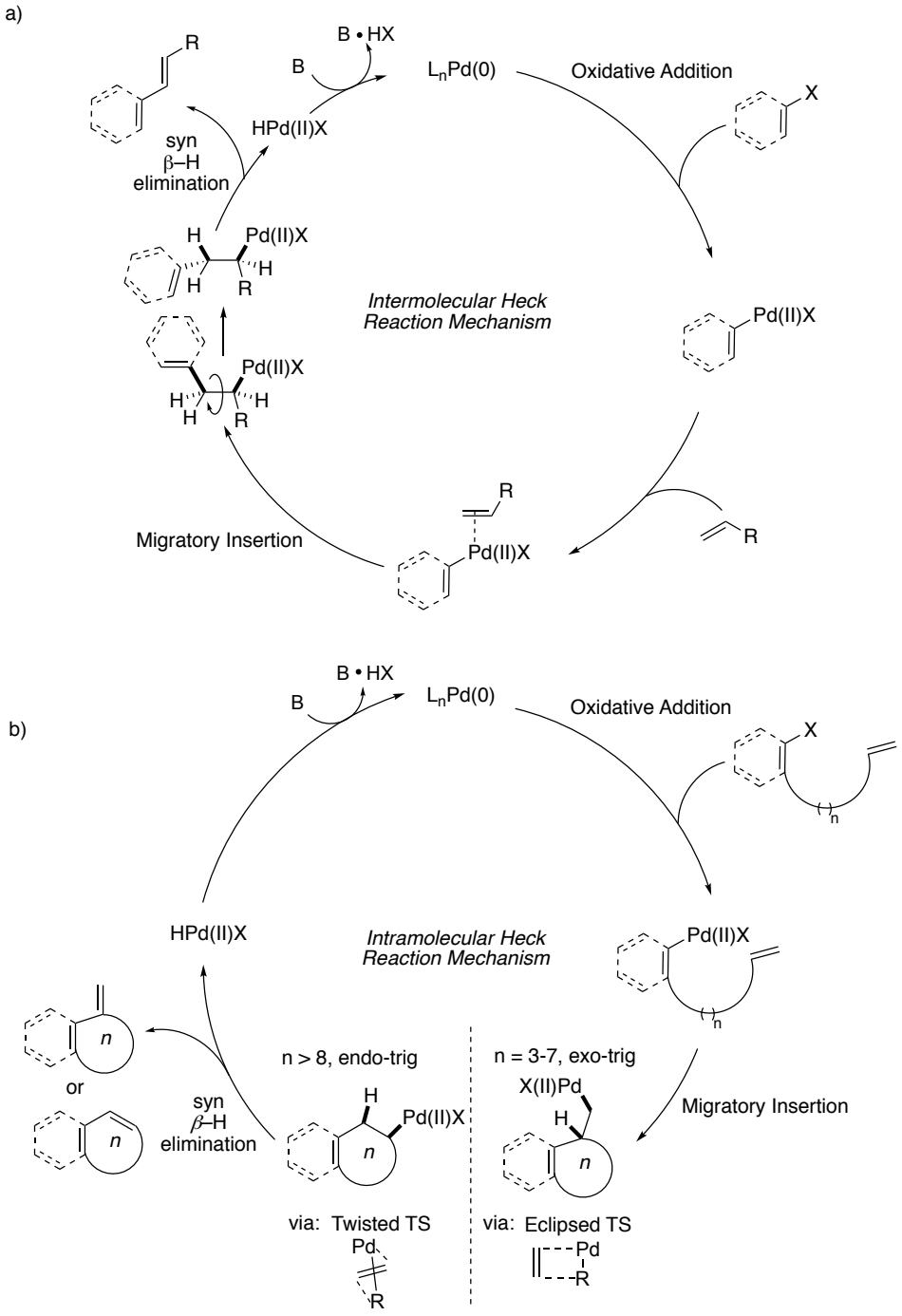

Scheme 1: Mechanism of the (a) intermolecular/(b) intramolecular Heck reaction of aryl/vinyl halides.

Another underdeveloped area of the Heck reaction is the alkyl Heck reaction. Limitations of this reaction are due to a premature β-hydride elimination issue (Scheme 2).[9] Employment of transition metals (TM) other than Pd, such as Ti[10] and Co,[11] has successfully facilitated the intramolecular alkyl Heck reaction. However, these cases require stoichiometric amounts of Grignard reagents to form the active metal species, which limits the scope of the reaction. In his pioneering work, Fu realized the first Pd-catalyzed intramolecular Heck reaction of unactivated bromides and chlorides.[12] The success of the reaction was due to the employment of bulky NHC ligands, which promoted migratory insertion over the competing premature β-hydride elimination pathway. Later, Alexanian[13] and co-workers reported an elegant intramolecular Heck reaction of alkyl iodides occurring via a novel hybrid Pd-radical mechanism.[14] The nature of the mechanism allows for the formation of radical intermediates that are less susceptible to premature β-hydride elimination. Since their report, alkyl Heck-type reactions have flourished. However, intramolecular modes are still limited to *5-exo*-trig/*6-exo*-trig cyclization. Prior to our studies, no *endo*-selective alkyl Heck reactions have been reported. Development of an *endo*-selective Heck transformation will not only be interesting from a conceptual perspective, but also from a synthetic standpoint as it would provide a novel retrosynthetic disconnection toward endocyclic cycloalkenes.

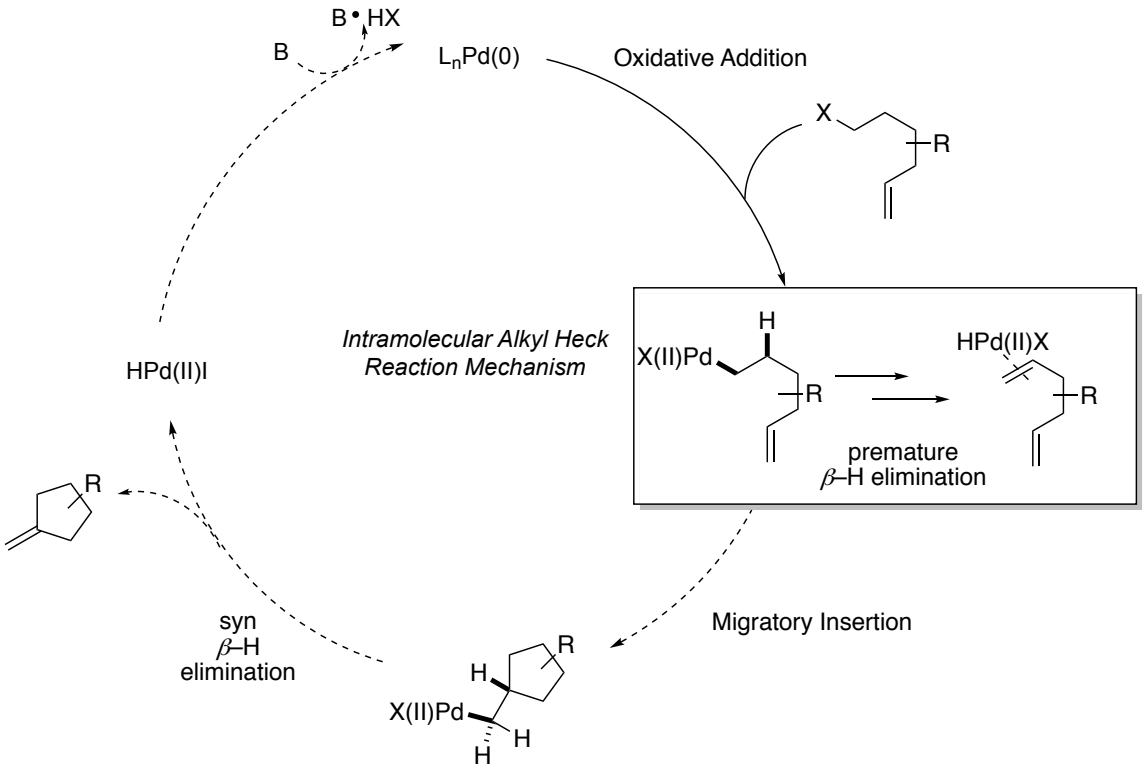

Scheme 2: Mechanism of the intramolecular alkyl-Heck reaction.

Endo-selective trends in Heck-type reactions are rare but are established in reductive radical transformations, specifically for halomethylsilanes tethers. In 1981, Wilt and co-workers studied the kinetics of radical cyclization of halomethylhomoallylsilanes.[15] It was found that *endo-trig* cyclization was favored over *exo-trig* cyclization. Later, Koreeda supported Wilt studies in his work on the *7-endo-trig* cyclization of halomethylsilyl tethered homoallylic alcohols, which served as a general tool for the formation of 1,5 diols.[16] These studies indicate that the inherent features of the halomethylsilane moiety can enable selective *endo-trig* cyclization. Thus, employing this moiety for a Pd-catalyzed Heck-type could potentially generate the first *endo*-selective alkyl Heck reaction.

1.1. Intramolecular Alkyl Heck-Type Reactions

In 2006, Oshima reported the first Co-catalyzed alkyl Heck reaction of unactivated alkyl iodides.[11] However, employment of excess Grignard reagents were required to form the active Co-complex in order to promote the transformation, which resulted in limited substrate scope. Nevertheless, an impressive number of examples were reported (Scheme 3). Intramolecular Heck reaction of alkyl iodides **1** resulted in *5-exo-trig*-cyclization to afford cyclopentene derivatives **2** in good yield. In some cases, however, the products were generated with low diastereoselectivity due to the radical nature of the transformation, a common mechanistic feature when first-row metals are employed.[17]

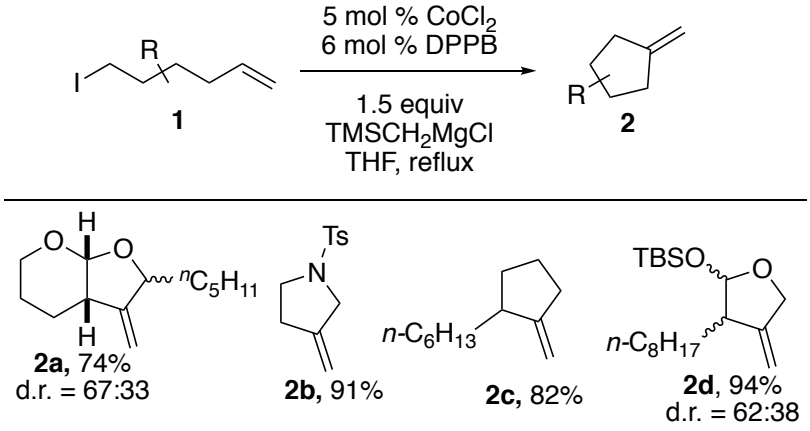

Scheme 3: Oshima's Co-catalyzed alkyl Heck reaction.

An interesting application for a Co-catalyzed alkyl Heck reaction was featured in Carreira's total synthesis of (+)-daphmanidin E.[18] In the presence of cobaloxime catalyst **A** and visible light, cyclization of alkyl iodide **3** resulted in the formation of (+)-daphmanidin E core **4** in excellent yield (Scheme 4). Notably, the reaction followed the

endo mode of cyclization due to the polar effects of the alkene. In his follow-up report using neutral/non-biased alkenes, intramolecular Heck cyclization occurred *exo*-selectively (Scheme 5).[19]

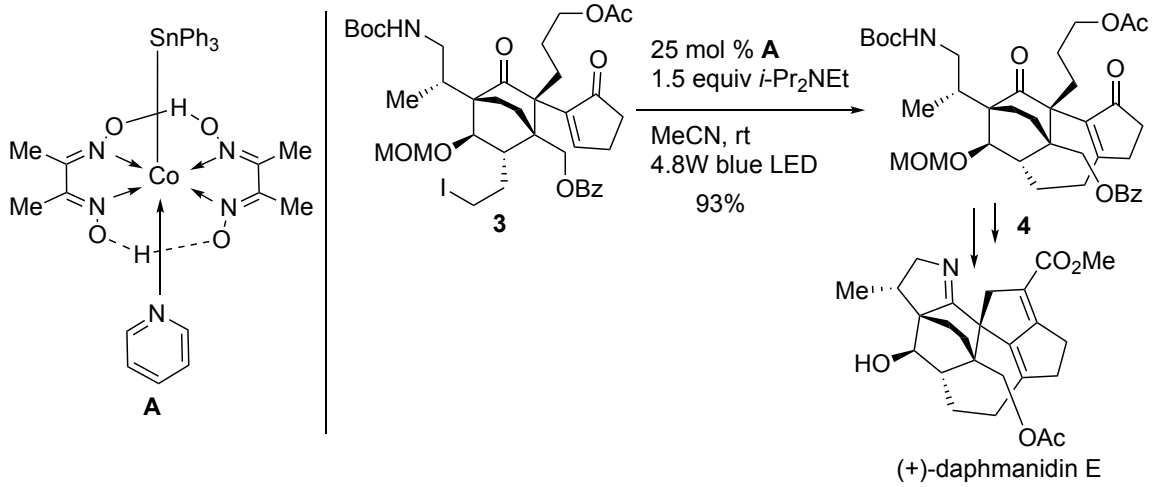

Scheme 4: Carreira's alkyl Heck reaction en route to (+)-daphmanidin E.

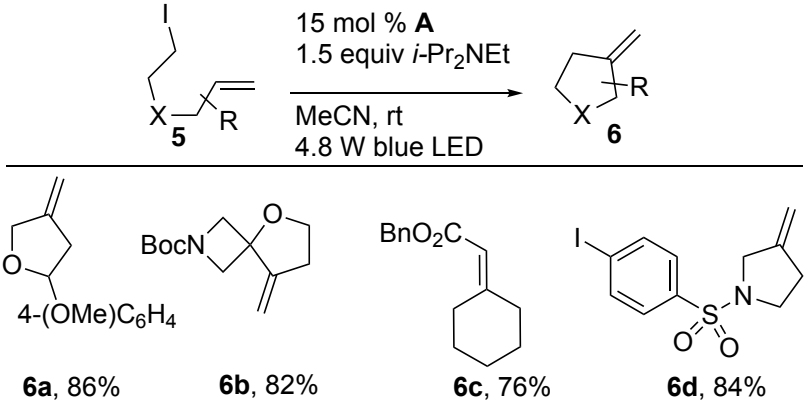

Scheme 5: Scope of Carreira's alkyl Heck reaction.

In 2012, Cuerva reported Ti/Ni multimetallic system for intramolecular Heck cyclization of alkyl iodides.[20] Their protocol operates at room temperature with catalytic amounts of Ni and substoichiometric amounts of Ti. The scope of the transformation was found to be quite broad; *exo-trig* adducts were formed with generally good yields

(Scheme 6). The endgame mode of the transformation, formation of the alkene, was speculated to occur via the Ni-involved *β*-Hydride elimination or via a direct H-abstraction with the Ti- reagent.

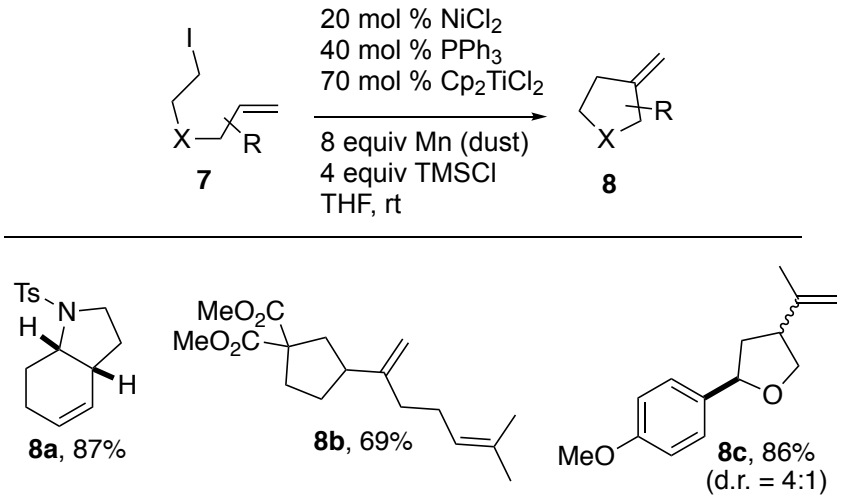

Scheme 6: Cuerva's multimetallic alkyl Heck reaction.

Thus far, alkyl Heck-type reactions with substrates bearing *β*-hydrogens have been successful for first-row TM because of the inherent radical features of the metals employed. Utilization of conventional Heck reaction conditions, involving Pd-catalysis, has been met with challenges due to a premature *β*-hydride elimination process (Scheme 2). In 2007, Fu reported that a Pd-catalyzed Heck reaction of unactivated halides could be achieved (Scheme 7).[12] The scope of the transformation was found to be quite broad, as both alkyl bromides and chlorides bearing terminal alkenes underwent smooth *exo-trig*-cyclization, generating cyclopentene derivatives in good yields. Conversely, substrates possessing secondary alkyl halides and substituted olefins were not tolerated under the reaction conditions. Also, formation of cyclohexene derivatives could not be achieved. The success of the reaction was contingent upon the catalyst and the ligand combination

employed. It was found that the electron-rich substituent on the dba ligand of Pd_2(OMe-dba)$_3$ allows for an increase of reaction rates due to a facile release of the less tightly-bound ligand from Pd(0) (Scheme 8).[21] Moreover, the bulky NHC ligand employed prevents β-agostic interactions of the OA intermediate **15** (Scheme 9),[22] as well as blocks a vacant pre-coordination site, both requisites for β–H elimination, and thus promotes the migratory insertion over competing β–H elimination (**15→18).** In order to distinguish if the operative mechanism occurs via a classical or radical pathway, the authors studied the reaction outcome of deuterium labeled substrate **19** (Scheme 10). Subjecting **19** to the reaction conditions resulted in **20** as a single diastereomer, which is consistent with an S_N2 mechanism for OA and, thus, is distinct from the aforementioned radical type-pathways.

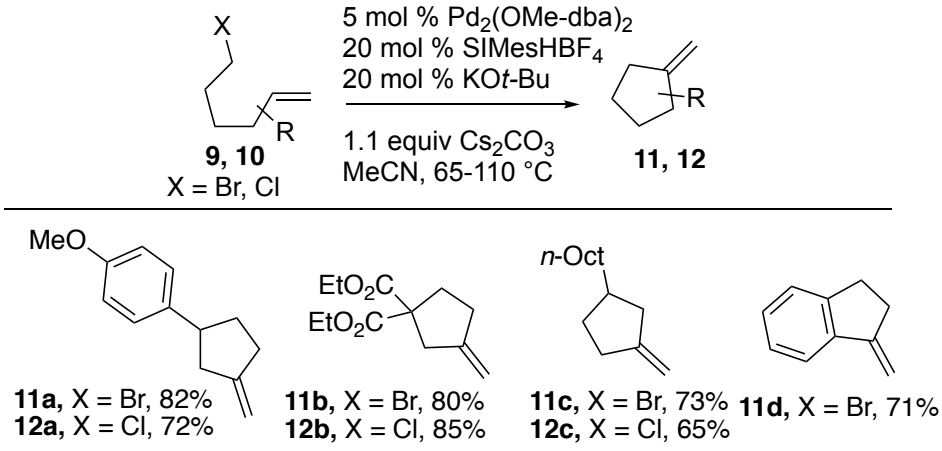

Scheme 7: Scope of Fu's alkyl Heck reaction.

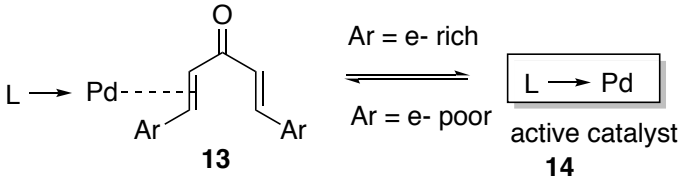

Scheme 8: Rationale for employment of Pd_2(OMe-dba)$_3$.

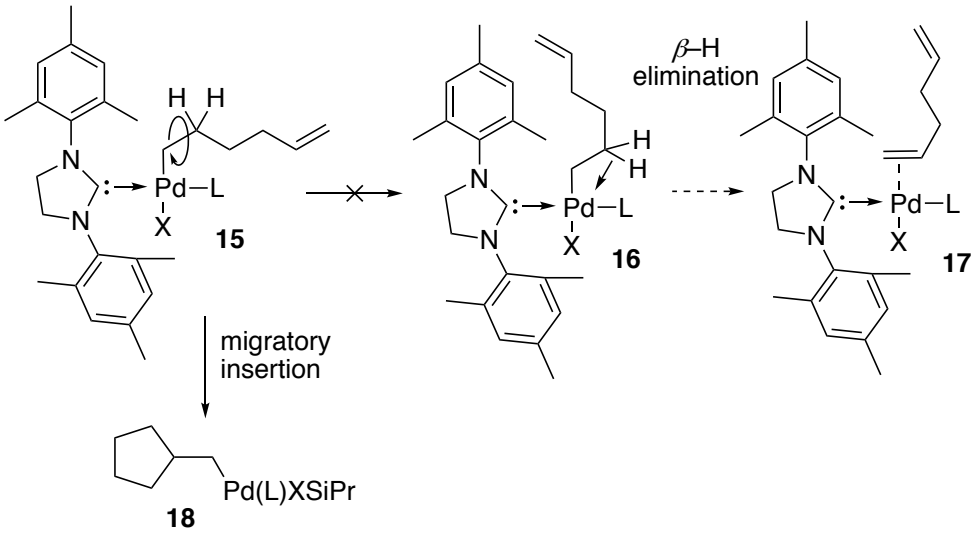

Scheme 9: Effect of SiPr ligand.

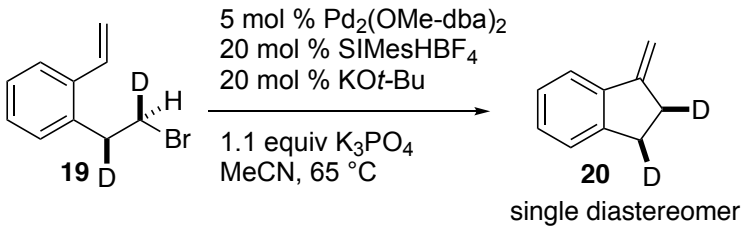

Scheme 10: Fu's deuterium labeled study.

Heck reactions of unactivated alkyl iodides remained elusive until Alexanian's groundbreaking work in 2011.[13] His report featured an efficient intramolecular Heck reaction of alkyl iodides using simple $Pd(PPh_3)_4$ catalyst under positive CO pressure (Scheme 11). Interestingly, no formation of carbonylative Heck products were detected under these reactions conditions, thus it was speculated that CO forms a less electron-rich Pd(0) complex that promotes the transformation. The scope of the reaction was found to complement that of Fu's alkyl Heck reaction as various substituted alkenes and secondary alkyl electrophiles were tolerated. Moreover, *6-exo*-trig cyclization of **21b** into **22b** occurred efficiently. The authors probed the reaction mechanism by addition of TEMPO

to the reaction conditions, which resulted in TEMPO trapped adduct **23** in 24% NMR yield along with unreacted starting material (Scheme 12). This result supported involvement of radical intermediates via a hybrid Pd-radical mechanism (Scheme 13).[14] The authors proposed that the active Pd(0) species undergoes a SET process with alkyl halide **21b** to generate **24** and a putative Pd(I)I species. *Exo-trig*-cyclization of **24** forms secondary radical intermediate **25**. Recombination of **25** with Pd(I)I and a subsequent β-H elimination results in alkyl Heck product **22b**. It should be mentioned that due to the nature of this process, a premature β–H elimination is not competitive since the formed radical species (**24**) are less predisposed toward 1,2-elimination.

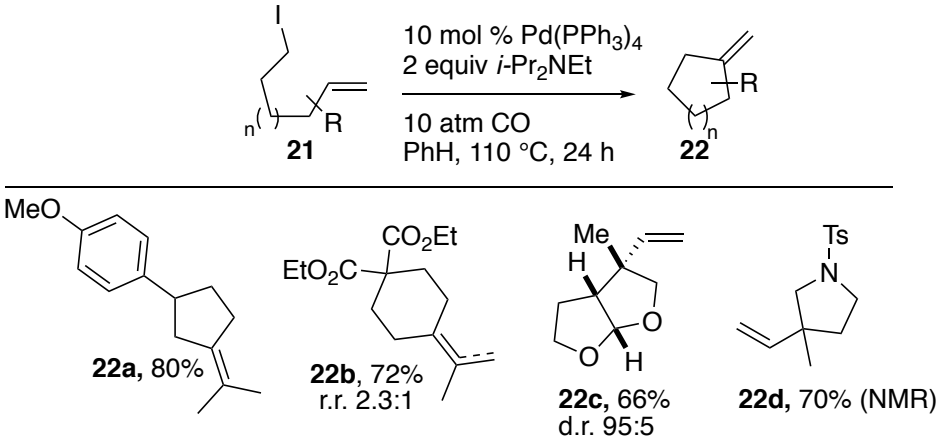

Scheme 11: Alexanian's Heck reaction of unactivated alkyl iodides.

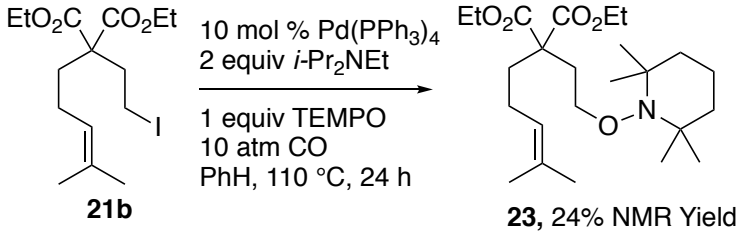

Scheme 12: Alexanian's TEMPO trapping study.

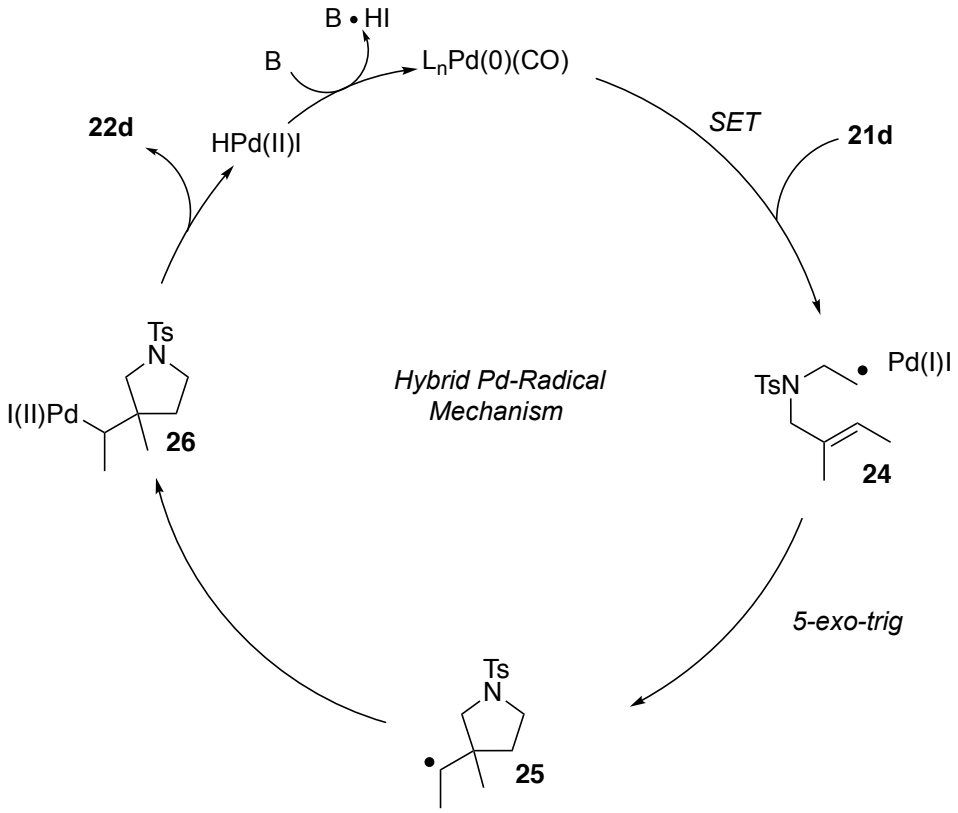

Scheme 13: Hybrid Pd-radical mechanism of Alexanian's alkyl Heck reaction.

Liu and co-workers reported a Pd-catalyzed *6-endo*-selective alkyl Heck reaction (Scheme 14).[23] Their strategy allowed for rapid access to bioactive endocyclic tetrahydropyridine derivatives in good yields with high *endo* selectivity (**27→30**). Similar to Alexanian's report, the authors proposed a hybrid-Pd-radical mechanism.[14] However, the scope of the reaction is limited to use of α-phenyl substituted alkenes, which drives cyclization to occur via *endo-trig* cyclization due to the formation of a more stable tertiary benzyl radical intermediate **29** compared to the less stable primary radical **28,** which would form via *exo-trig* cyclization.

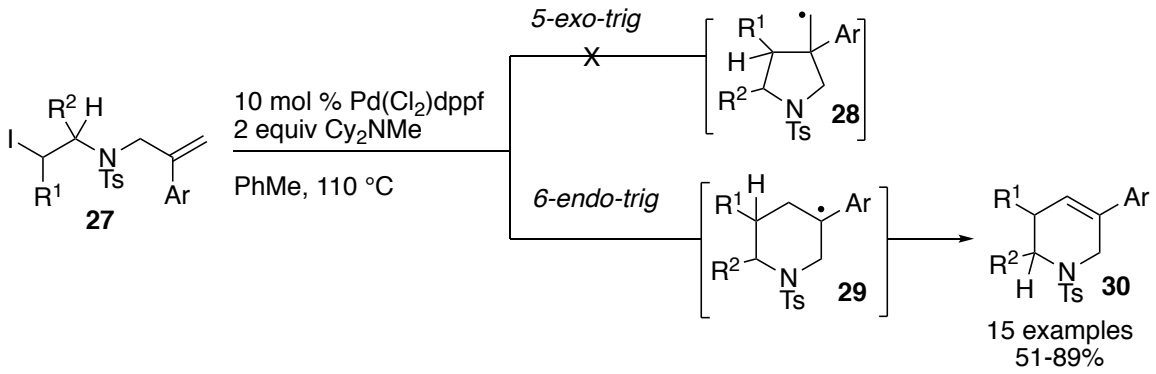

Scheme 14: Liu's *6-endo*-selective alkyl Heck reaction.

Although the works presented above represents a significant advance for the area of intramolecular alkyl Heck reactions, considerable limitations exist. Firstly, the scope of these reactions is limited to the formation of 5/6-memebered cyclopentenes via *5/6-exo*-trig cyclization. Secondly, harsh reaction conditions are typically employed to promote the alkyl Heck transformation. Lastly, no non-biased *endo*-selective alkyl reactions have been reported.

1.2. *Endo*-Selective Radical Cyclizations of Halomethylsilanes

In 1981, Wilt and co-workers studied the rate of radical cyclization of 2-sila-5-hexenyl and its carbon analog (Table 1, entries 1-2).[15] As expected, the latter underwent smooth *5-exo-trig* cyclization, preferably (entry 2). In sharp contrast, radical cyclization of 2-sila-5-hexenyl led to a reversal in regioselectivity; the *endo-trig*-cyclization product was obtained as the major isomer. The profound regioselecivity preference is attributed to several factors: 1) decreased rate of *5-exo*-trig cyclization; 2) longer Si–C bond length that enable efficient cyclization at the terminal end of the alkene; 3) favorable polar effects of the *endo* ring closure transition state (Scheme 15).[24] The *6-endo-TS* bears a partial negative charge α- to the silane moiety, which is favored, and a partial positive

charge developed on the secondary carbon (**32**). The *exo-TS*, however, is disfavored due to the developed partial positive charge on the primary carbon (**31**).

Table 1: Wilt's studies on 5-Hexenyl radical cyclizations.

Entry	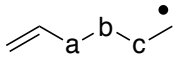	10^{-4} *5-exo* 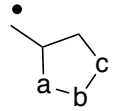	10^{-4} *6-endo* 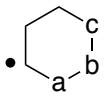
1	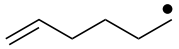	24	0.3
2	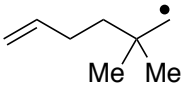	>200	0.2
3	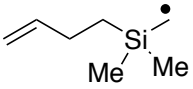	0.7	1.6
4	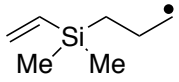	6.3	0.4

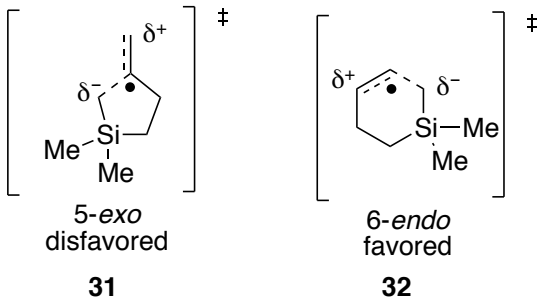

Scheme 15: *Exo-* and *endo*-transition states of radical cyclization of silyl methyl radical.

A few years later, Nishiyama employed bromomethylsilanes as a formal tool for hydro-hydroxymethylation of cinnamyl alcohols (Scheme 16).[25] In all cases, products of *5-exo-trig* cyclization were formed selectively. However, for terminal alkenes, appreciable amounts of the *6-endo*-trig adduct were obtained (Table 2). The formation of

the *6-endo-trig* by-products supported the observation disclosed by Wilt and co-workers. It should be mentioned that after Nishiyama's report, several research groups have employed this concept in many natural product syntheses, specifically, for the formation of *syn*-1,3- diols from allylic alcohols.[24]

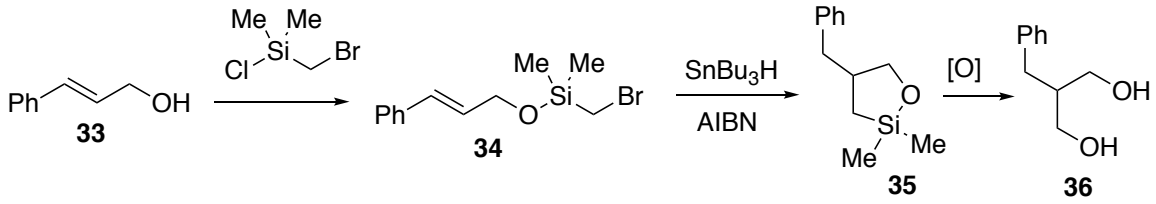

Scheme 16: Nishiyama's hydro-hydroxymethylation of allylic alcohols.

Table 2: Scope of Nishiyama's transformation with terminal alkenes.

Entry	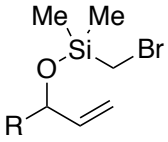	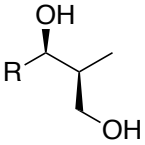 *5-exo-syn*	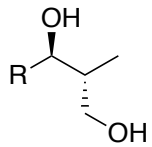 *5-exo-anti*	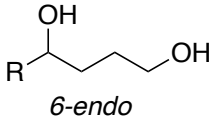 *6-endo*
1	R = Me	66%	14%	15%
2	R = *i*-Pr	74%	-	16%
3	R = *t*-Bu	66%	-	26%
4	R = vinyl	52%	9%	24%
5	R = Ph	48%	4%	36%

In 1986, Koreeda and co-workers reported an interesting *6-endo-trig* cyclization of bromomethylsilane-tethered steroids (Scheme 17).[26] The authors' approach enabled the formation of two new stereogenic centers (C-17 and C-20) upon cyclization.

Moreover, upon facile oxidation of the formed silyloxycycle, 1,4-diols were generated. Although confirmation effects and employment of a geometrically defined substituted alkene increased the inherent propensity for *endo-trig* cyclization, this constituted a significant advance for *endo*-selective reactions of alkyl radicals.

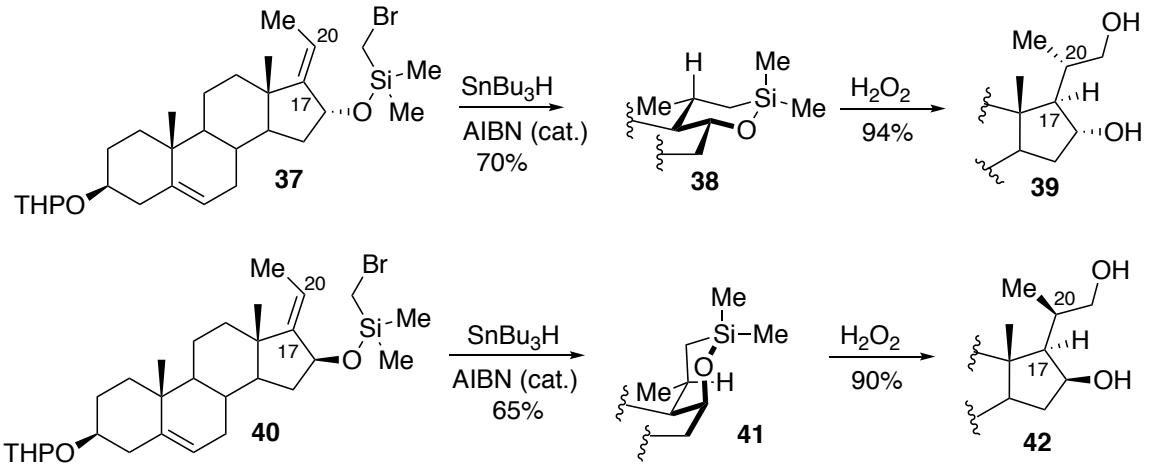

Scheme 17: Koreeda's *6-endo-trig* cyclization of bromomethylsilane-tethered steroids.

The same group reported a novel chirality transfer reaction of homoallylic alcohols via *6-exo-trig* cyclization of bromomethylsilane-tethered alkenols (Scheme 18).[16] Under the reaction conditions, cyclization of bromomethylsilane with substituted alkenes generally produced the *6-exo-trig* products (**44**, **49**) with high yields and regioselectivity. In contrast, when unbiased terminal alkenes were employed, a *7-endo*-trig cyclization occurred, resulting in **46** and **51** as the *sole regioisomers.* This unexpected outcome was rationalized due to the lower energy TS for *endo*-trig-cyclization (**53**) compared to that of *exo*-trig cyclization (**54**) (Scheme 19), which is in agreement with Wilt's observations.[15] Notably, the obtained *6-exo-trig* adducts were formed due to unfavorable steric interactions of the alkyl groups at the β-position of the alkene and the

silyl methyl radical, which redirected the mode of cyclization from *endo* to *exo*. Although Koreeda did not capitalize on this unique *endo*-selective outcome, it showcased the potential for using halomethylsilane tethers as a tool for *endo*-selective cyclization, as well as for hydro-hydromethylation of homoallylic alcohols toward 1,5-diols.

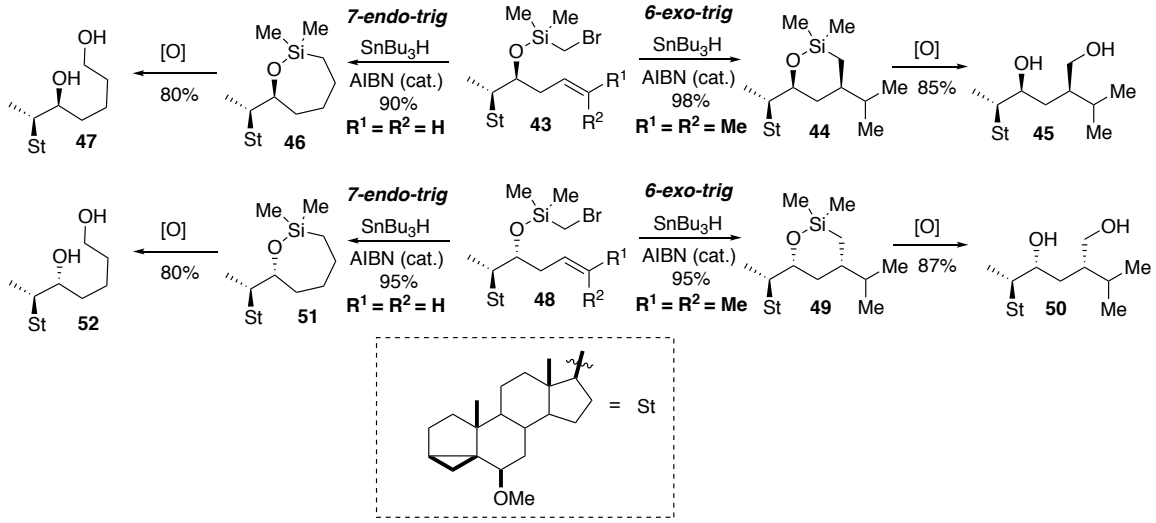

Scheme 18: Koreeda's chirality transfer reaction of homoallylic alcohols via *6-exo-trig* cyclization and *7-endo-trig* cyclization depending on the substitution pattern at the alkene.

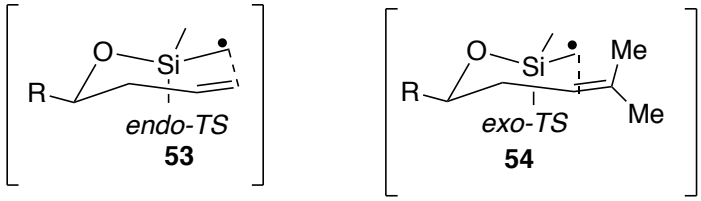

Scheme 19: Transition states for *endo* and *exo* modes of cyclization with differently substituted alkenes.

1.3. Conclusions

Since the discovery of the Heck reaction in the early 1970's, numerous advances and methodological developments have been accomplished. The intramolecular Heck reaction has become a mainstream approach toward formation of carbocycles and heterocycles when sp^2 electrophiles are employed. Much less developed, however, is the alkyl Heck reaction. Although advances have been reported in this area, significant limitations still exist, specifically for the mode of cyclization. All reported intramolecular alkyl Heck reactions occur via either *5/6-exo-trig* cyclization. To date, no precedents for an *endo*-selective Heck reaction have been reported. Undoubtedly, the discovery of the *endo* selective alkyl Heck reactions will be a considerable advance, as it would allow for the facile formation of endocyclic systems, which are prevalent in various natural products and pharmaceutically relevant compounds. Delightfully, reports in the area of reductive radical chemistry has left clues toward achieving an *endo* selective alkyl Heck reaction using halomethylsilanes. Studies indicate that these moieties undergo *endo-trig* cyclization selectively. Thus, if this preferred regiochemical outcome could be translated to a Heck-type reaction, it would allow for the first *endo*-selective alkyl Heck reaction.

2. ENDO-SELECTIVE PALLADIUM-CATALYZED SILYL METHYL HECK REACTION (Previously Published as Parasram, M.; Iaroshenko, V. O.; Gevorgyan, V. "Endo-Selective Pd-Catalyzed Silyl Methyl Heck Reaction." *J. Am. Chem. Soc.* 2014, 136, 17926.)

2.1. Reaction Development

As discussed above, Heck reactions employing alkyl electrophiles are rare, but *endo*-selective alkyl Heck reactions are virtually non-existent. Inspired by Koreeda's report[16] on the selective *endo-trig*-cyclization of halomethylsilyl-tethered homoallylic alcohols under typical radical conditions (Scheme 20, **54→55**), we hypothesized that if this unique selectivity outcome would translate into a Heck-type reaction, it would allow for the first *endo* selective alkyl Heck reaction (Scheme 20, **58→59**). Moreover, it would allow for the selective formation of valuable *Z*-allylic silanes (**59**), which can be further oxidized into important *Z*-1,5-alkenol-diols (**60**). Overall, the proposed method will serve as a formal tool for *Z*-hydroxymethylation of alkenols (**57→60)**.

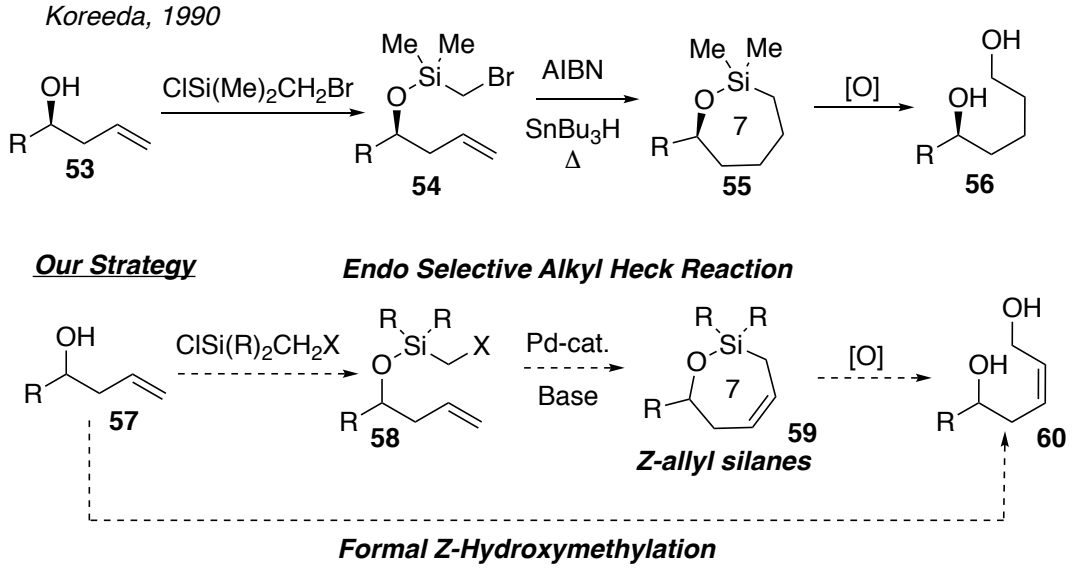

Scheme 20: Proposed *endo*-selective silyl methyl Heck reaction.

2.2. Synthesis of Iodomethyldiisopropylsilane Tether

Based on the mechanism of the Heck reaction,[1] oxidative addition of Pd(0) with iodomethylsilane moiety is required. In 2009, Cloke and co-workers studied the oxidative addition of (iodomethyl)trimethylsilanes **62** with Pd(0) NHC complex **61**. However, the expected oxidative addition adduct **63** was not obtained; instead products of carbon–silicon bond activation were obtained (**64**, **65, 66**, Scheme 21).[27] Based on this observation, we envisioned that employment of a bulkier iodomethylsilyl tether might circumvent this potential pathway and promote oxidative addition. Hence, we focused our efforts toward the synthesis of (iodomethyl)diisopropylsilane **69** (Scheme 22). It was surmised that the *i*-Pr-groups on silicon tether would not only provide the required steric bulk, but also increase stability and possibly increase the rate of cyclization via Thorpe-Ingold effect reactivity.[28] First, alkylation of commercially-available diisopropylchlorosilane **67** followed by a Finkelstein reaction, generated iodomethyl silane product **68**. A subsequent chlorination reaction using trichloroisocyanuric acid (TCCA) resulted in **69** in overall 50% yield (for 3-steps). The iodomethylchlorosilane reagent **69** can be installed onto homoallylic alcohols using established coupling procedures developed in our laboratory.[28]

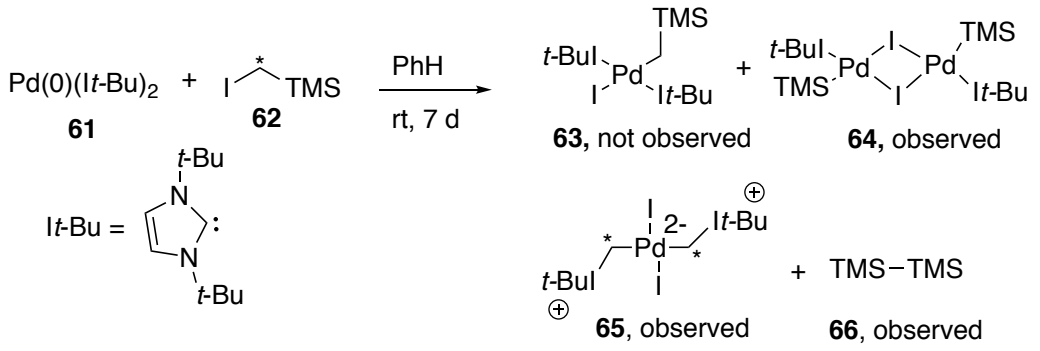

Scheme 21: Cloke's seminal work on OA of halomethylsilanes with Pd(0).

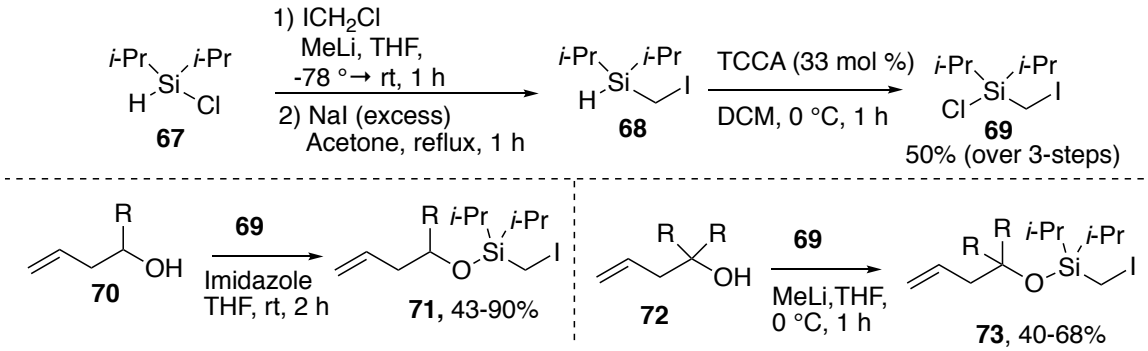

Scheme 22: Synthesis of **69** and its coupling with alcohols.

2.3. Optimization of the Reaction Conditions

Next, optimization of the reaction conditions was conducted. Obviously, by design, a premature *β*-hydride elimination event is not a competitive pathway for the iodomethylsilane tether. Our optimization studies commenced using conformationally biased substrate **74** tested under reported Pd-catalyzed conditions (Fu[12] and Alexanian's[13] conditions) for alkyl Heck reaction (Table 3). However, these reaction conditions were not effective (entries 1-2). In addition, use of monodentate ligands was inefficient (entries 3-5). Excitingly, employment of dppf ligand resulted in selective formation of the *endo* adduct **75a**, albeit in low yield, 24% (entry 6). Interestingly, addition of AgOTf increased the reaction yield to 60% (entry 7). Screening other ligands from the ferrocene family, such as ligand **L**, worked but did not increase the overall yield

(entries 8-10). Lowering the reaction temperature from 120 to 85 °C shut down the reaction (entry 11), however, employment of ligand **L** at this temperature led to a dramatic increase in overall yield 76% (entry 12). Next, it was found that AgOTF did not help the overall reaction efficiency at lower temperatures (entry 13). Lowering the reaction temperature to 75 °C proved to be optimal, as **75a** was generated in high yield (92% GC yield, 79% isolated yield, entry 14). Finally, a control study indicated that the Pd-catalyst is required for this transformation (entry 15).

Table 3: Optimization of the reaction conditions.

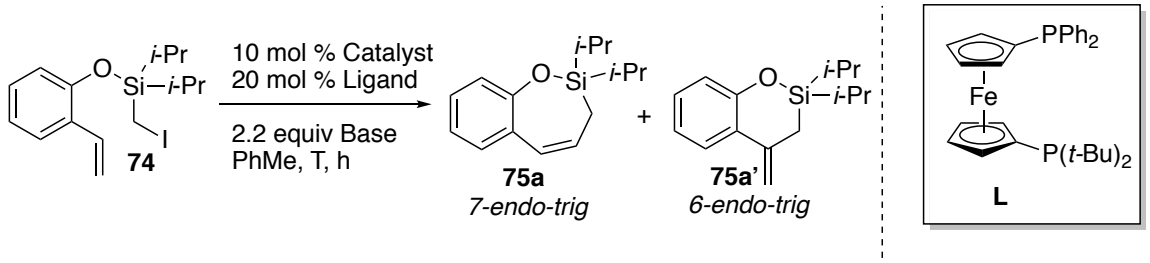

Entry	Catalyst	Ligand	Base	Additive	T (°C)	h	**75a** : **75a'**	GC Yield, %, of **75a**[a,b]
1	$Pd(PPh_3)_4$	-	PMP	-	110	24	-	NR[c]
2	$Pd_2(4OMe\text{-}dba)_3$	$SIMesHBF_4$	Cs_2CO_3	KO*t*Bu	65	24	-	Decomp[d,e]
3	Pd_2dba_3	*t*-$BuPPh_2$	*i*-Pr_2NEt	-	120	24	1 : 1	10[d]
4	$Pd(OAc)_2$	P^tBuHBF_4	*i*-Pr_2NEt	-	120	24	1 :2.3	23
5	$Pd(OAc)_2$	$P(ad)_2n$-Bu	*i*-Pr_2NEt	-	120	24	1 :1	5
6	$Pd(OAc)_2$	dppf	*i*-Pr_2NEt	-	120	24	40 : 1	24
7	$Pd(OAc)_2$	dppf	*i*-Pr_2NEt	AgOTf	120	24	50 : 1	60
8	$Pd(OAc)_2$	diprpf	*i*-Pr_2NEt	AgOTf	120	24	50 : 1	20
9	$Pd(OAc)_2$	dtbupf	*i*-Pr_2NEt	AgOTf	120	24	50 : 1	11
10	$Pd(OAc)_2$	**L**	*i*-Pr_2NEt	AgOTf	120	24	50 : 1	40
11	$Pd(OAc_)_2$	dppf	*i*-Pr_2NEt	AgOTf	85	24	-	NR
12	$Pd(OAc)_2$	**L**	*i*-Pr_2NEt	AgOTf	85	24	50 : 1	76 (68)

13	$Pd(OAc)_2$	**L**	*i*-Pr_2NEt	-	85	3	40 : 1	89 (73)
14	**$Pd(OAc)_2$**	**L**	***i*-Pr_2NEt**	**-**	**75**	**12**	**40 : 1**	**92 (79)**
15	$Pd(OAc)_2$	**L**	*i*-Pr_2NEt	-	65	24	-	50%. conv
16	-	-	*i*-Pr_2NEt		75	12		<2

[a]GC was calibrated using tetradecane as an internal standard. [b]Isolated yields are in parentheses. [c]Reaction was conducted under 10 atm of CO. [d]5 mol % of catalyst was used. [e]MeCN was used as solvent.

2.4. Scope and Limitations

After identifying the optimized conditions, the generality of the transformation was tested on arene-tethered substrates. Pleasantly, the regiochemical outcome was unaffected by the electronic nature of the substituents at the arene moiety (Table 4, entries 2-8). Next, it was found that this method enables a facile synthesis of medium size rings via *8-endo-trig*- and *9-endo-trig* cyclization of **74i** and **74j**, respectively. Importantly, employment of secondary bromomethylsilane **74k** worked well, as the *7-endo*-aryl-substituted allylsilane product **75k** was obtained in 67% yield. Next, we turned our attention to the effect of the substitution pattern at the alkene on the regiochemical outcome of the reaction. It was revealed that cyclization of substrates possessing substituents at the *β*-position proceeded uneventfully; producing the *endo* adducts, **75l** and **75m**, selectively. In contrast, substitution at the *α*-position of alkene led to a regioselectivity reversal; *exo-trig* products **75n** and **75o** were formed exclusively (entries 14, 15). The observed reversal of the regioselectivity trend is in agreement with Koreeda's observation on the impediment of the *endo-trig* cyclization due to steric effects at the terminal end of the alkene (Scheme 19).[16]

Table 4: *Endo* silyl methyl Heck reaction of arene-tethered substrates.

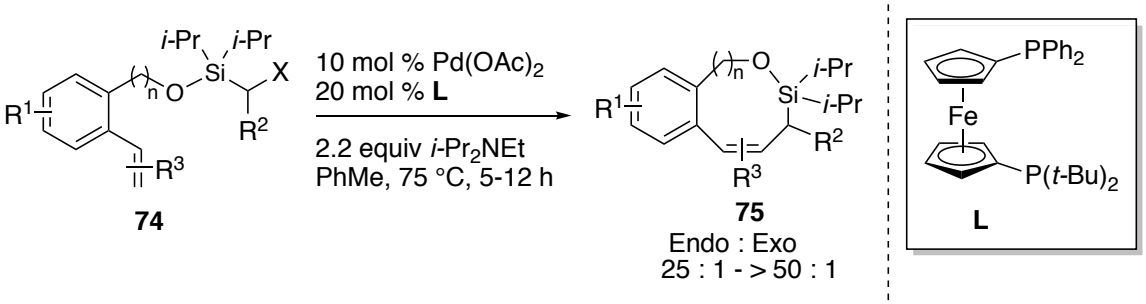

#	74		75		Yield, %[a]	
1		**74a**		**75a**	R=H	79 (73[b])
2		**74b**		**75b**	OMe	87
3		**74c**		**75c**	F	74
4		**74d**		**75d**	Me	76
5		**74e**		**75e**	Cl	71
6		**74f**		**75f**	NO_2	33
7		**74g**		**75g**	OMe	90
8		**74h**		**75h**	F	74
9		**74i**		**75i**		60[c,d]
10		**74j**		**75j**		33[c,e]
11		**74k**		**75k**		67[c,d]

12	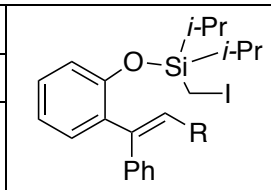	**74l**	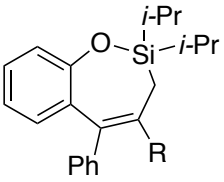	**75l**	H	96
13		**74m**		**75m**	Ph	64[c,g]
14	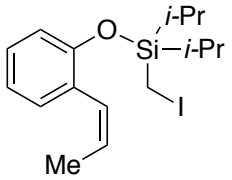	**74n**	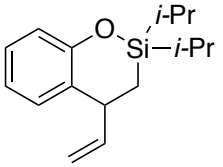	**75n**		78[h]
15	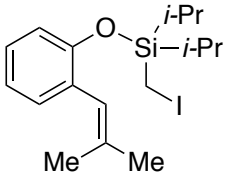	**74o**	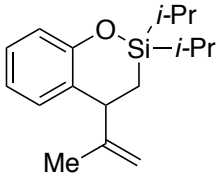	**75o**		76

[a]Isolated yields. [b]Reaction performed at 3.8 mmol scale. [c]Reaction performed at 120 °C. [d]NMR ratio of product to hydro-dehalogenation side product is 12 : 1. [e]NMR ratio of product to hydro-dehalogenation side product is 1.6 : 1. [f]Reaction time = 36h. [g]Ag(OTf) was used as an additive. [h]Mixture of isomers.

Next, we tested this method on challenging homoallylic alcohols. For these cases, the regiochemical outcome of the cyclization seemed uncertain since they are sterically unbiased and hence less predisposed toward *endo*-selective cyclization. Also, due to the availability of alternative sites for β-hydride elimination, other regioisomers, such as *homoallylic* silanes, may form. Indeed, it was found that subjecting **76a-c** to the reaction conditions resulted in formation of homoallylic silanes **77a-c** in good yields with excellent *endo* selectivity (Table 5). Interestingly, it was found that increasing the steric bulk (two geminal substituents) at the α-position of the alcohol (**76d, e**) resulted in the selective formation of allylic silanes via *endo-trig* cyclization (**77d, e**). Apparently, sterics at the α-position of alcohol plays a curial role during the β-H elimination event, where increasing substitution pattern favors allylic silane formation over the homoallylsilane

(*vide infra*). This observed phenomenon is in agreement with Waston's observation on the steric influence on the regiochemistry of *β*-H elimination of the intermolecular silyl Heck reaction.[29] Gratifyingly, *8-endo-trig*- and *9-endo-trig*-cyclization of **76g** and **76h** was achieved, resulting in formation of medium sized rings **77g** and **77h** in 85% and 44% yield, respectively. Finally, applying this method to naturally occurring terpene, isopulegol, resulted in two isomers of *7-endo-trig* cyclization, from which the homoallylsilane **77j** was isolated as the major product.

Table 5: *Endo* silyl methyl Heck reaction of homoallylic alcohols.

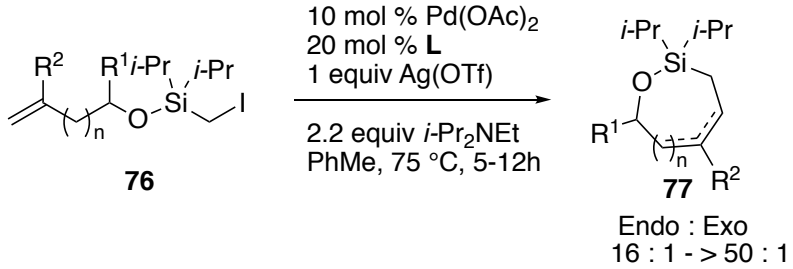

76 **77**

#	**76**		**77**		Yield, %[a]	
1		**76a**		**77a**	R=^{n}Pr	65
2		**76b**		**77b**	^{n}Pent	76
3		**76c**		**77c**	Ph	84
4		**76d**		**77d**		79[b,c]
5		**76e**		**77e**		75[b,c]

6	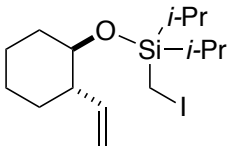	**76f**	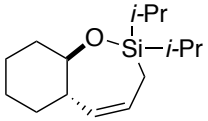	**77f**		71
7	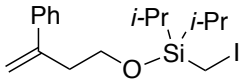	**76g**	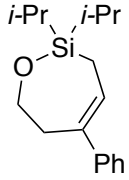	**77g**		80[d]
8	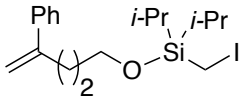	**76h**	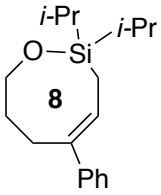	**77h**		85[e]
9	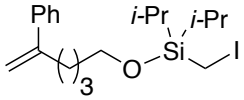	**76i**	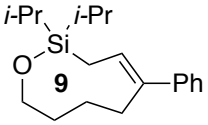	**77i**		44[f,g]
10	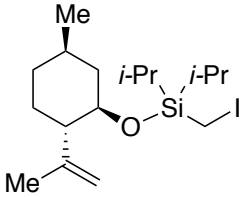	**76j**	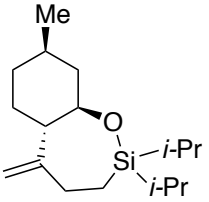	**77j**		45 (90[h])

[a]Isolated yields [b]DABCO was used instead of $^{i}Pr_2NEt$. [c]Ag(OTf) was not used as an additive. [d]Major product shown, ratio of major product to homoallylic side product is 7 : 1. [e]Major product shown, ratio of major product to homoallylic side product is 17 : 1. [f]Reaction performed at 130 °C. [g]Major product shown, ratio of major product to hydrodehalogenation side product is 1 : 1. [h]Major product shown, ratio of major product to allylic side product is 3.5 : 1. Isomers were separated.

2.5. Further Transformations of Obtained Siloxycyclic Products

The formed allylic siloxycycles are valuable entities that are widely used as reactive substrates toward further functionalizations.[30] Thus, the synthetic utility of the reaction products were investigated. First, Tamao oxidation of **75a** resulted in formation

of *Z*-1,5-alkenoldiol **78** in excellent yield (Scheme 23). This transformation highlights our protocol as a formal tool for *Z*-hydroxymethylation of alkenols. Next, Hosomi-Sakurai[30a] reaction of **75a** with ketoacetal 1,1-dimethoxycyclohexane was attempted, however, only traces of the reaction product **80** were observed. It was speculated that steric encumbrance of the *i*-Pr groups at the silane moiety of **75a** prevented the Hosomi-Sakurai reaction to occur. To this end, in order to form a more flexible and, thus, less encumbered allyl silane, a ring opening of **75a** with MeLi was conducted, which resulted in formation of **79** in 70% yield. Exposure of **79** to standard Hosomi-Sakurai reaction conditions in the presence of 1,1-dimethoxycyclohexane resulted in smooth formation of **80** in excellent yield. The latent preference of silyl-tethered alkyl iodide toward *endo*-selective Heck reaction, as well as potential for development of regiodivergent cyclizations, were highlighted in cyclization of dienol **81**. Remarkably, due to the influence of the silane moiety, *6-endo-trig* of **81** occurred first, followed by "normal" *5-exo-trig* cyclization to produce the tricyclic compound **82** as a single product. It should be mentioned that this example constitutes a rare cascade Heck reaction initiated by *endo-trig* cyclization.[31] A subsequent Woerpel oxidation[32] of **82** resulted in 1,4-indenediol **83** in good yield. Lastly, testing complex steroid **84** highlighted the late-stage applicability of the transformation. It was found that *endo*-selective silyl methyl Heck reaction and successive Tamao oxidation[33] of **84** occurred smoothly, furnishing diol **86** in good yield.

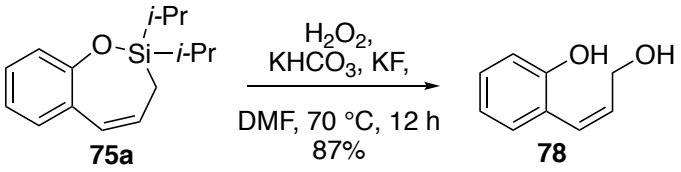

Scheme 23: Tamao oxidation of the *endo*-Heck product **75a**.

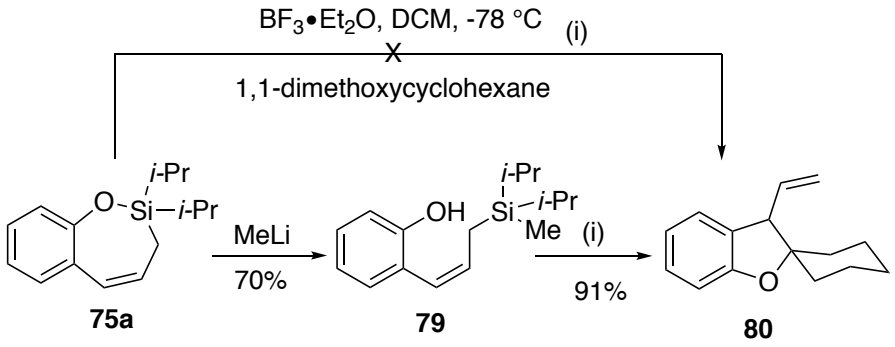

Scheme 24: Hosomi-Sakurai reaction of **75a**.

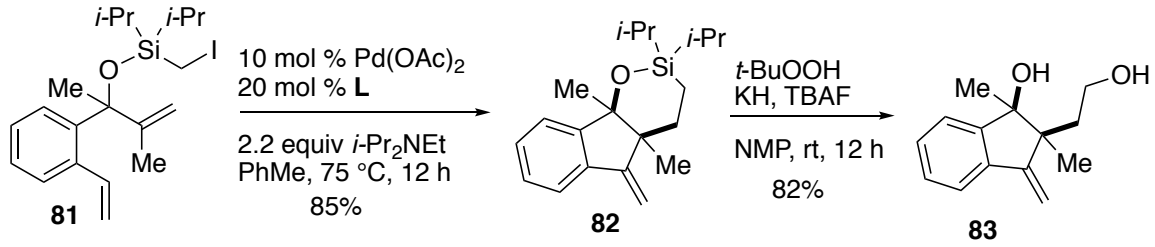

Scheme 25: Novel cascade *6-endo*/*5-exo* Heck reaction of **81** into **82** and its subsequent oxidation.

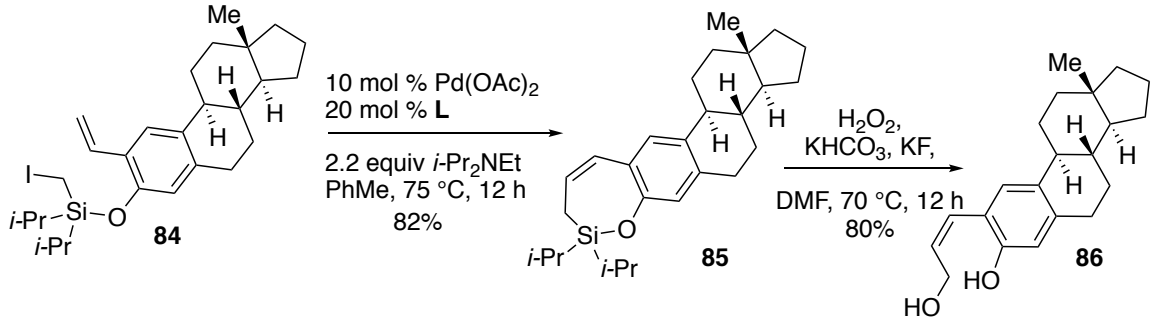

Scheme 26: Complex molecule application.

2.6. Mechanistic Considerations

Naturally, after the scope of the reaction was established, the mechanism of the transformation was investigated. Two mechanistic scenarios were envisioned for the transformation, a classical-Heck-type[1] (Scheme 2) or a hybrid Pd-radical mechanism[14] (Scheme 13). Since the regiochemical outcome of the transformation matched the *endo* trends reported for radical cyclization of halomethylsilanes (Table 1 and Scheme 18), it

was speculated that radical intermediates were involved in our transformation. To confirm this, radical-trapping experiments were conducted (Table 6). Employment of BHT did not affect the reaction outcome, but faster radical traps such as galvinoxyl and TEMPO resulted in lower reaction efficiency or complete shut down the reaction, respectively. For the latter case, however, the TEMPO adduct **87** was not detected. Due to the ambiguity of the aforementioned studies,[34] we decided to employ radical clock studies to probe the nature of the transformation.

Table 6: Radical trap studies for *endo* silyl methyl Heck reaction.

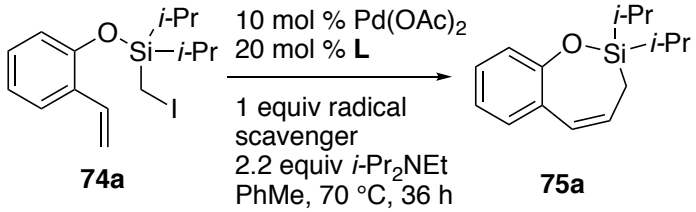

Entry	Radical Scavenger	GC Yield, %, of **75a**[a,b]
1	none	92
2	BHT	92
3	Galvinoxyl	68
4	TEMPO	NR

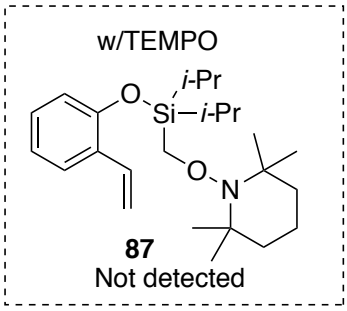

Scheme 27: TEMPO trapped adduct **87**.

Since Newcomb's systematic studies[35] on the rates of radical ring-opening of methylcyclopropanes (Scheme 28), these systems have been implemented for probing the

rates of many radical-type transformations. More recently, they have been employed as useful tools for detection of radical intermediates in transition metal-catalyzed transformations.[36] Hence, the nature of cyclization of compound **94** (Scheme 29), possessing a radical clock, was tested. It was found that **94** underwent cyclization and subsequent ring-opening of the cyclopropane unit, resulting in 1:1 mixture of **96** and **97**. Notably, reaction product with intact cyclopropane unit (**95**) was not detected. However, this probe did not allow for distinguishing between radical opening of the cyclopropylmethyl (Scheme 28) and the *β*-C elimination process of cyclopropylmethyl palladium species (Scheme 30),[37] which has been well documented for methylcyclopropanes. Therefore, our transformation was tested on unambiguous radical clock **104** (Scheme 31). This probe can verify whether the nature of cyclization occurs via involvement radical- or a carbopalladated intermediates based on the regiochemical outcome of ring-opening of the cyclopropane unit. If the Pd-involved cyclization is operative, then, it is anticipated that **104** will produce a mixture of **106** and **107** based on an unselective Pd-involved *β*-C elimination process (**101→102→103**, Scheme 30). Conversely, if radical intermediates are involved, then formation of **106** is expected to be the sole product (**92→93**, Scheme 30). It was found that exposure of **104** to our optimized conditions resulted in sole formation of ring-opening product **106** and thus strongly supports the radical nature of our transformation (Scheme 31).

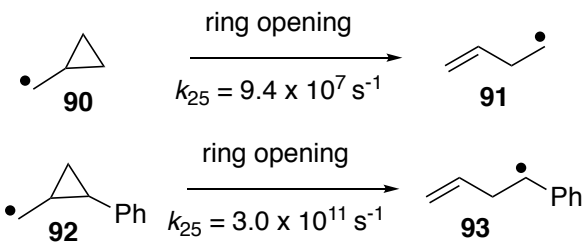

Scheme 28: Newcomb's radical clocks.

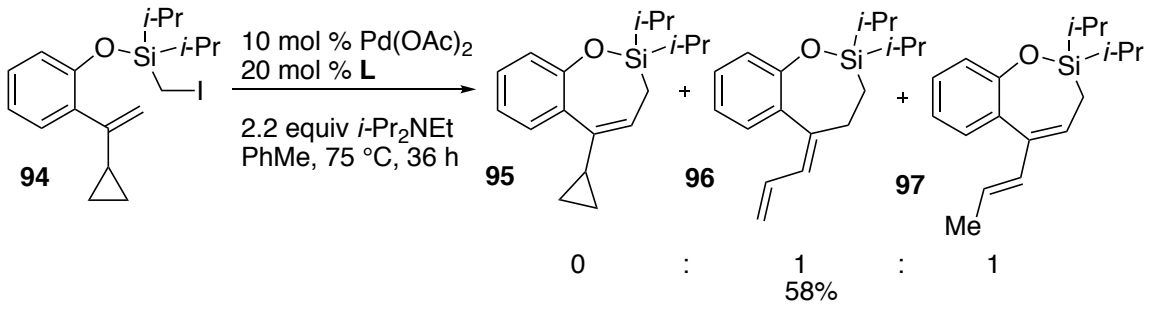

Scheme 29: Radical clock test of **94**.

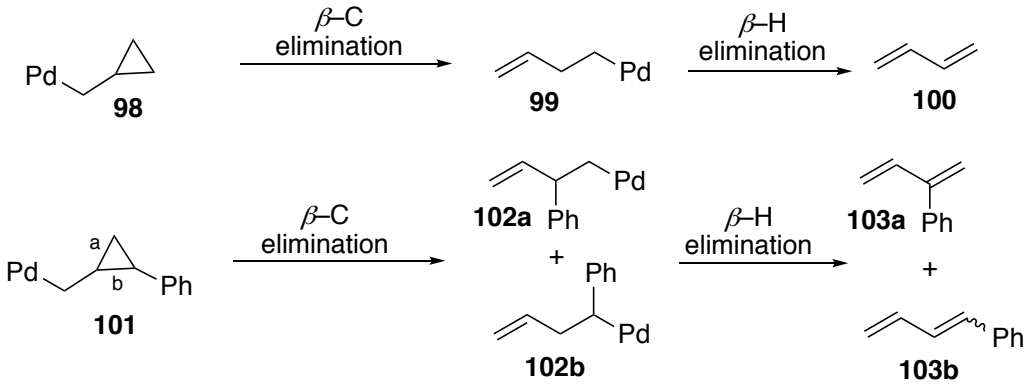

Scheme 30: Pd *β*–C elimination of methylcyclopropanes.

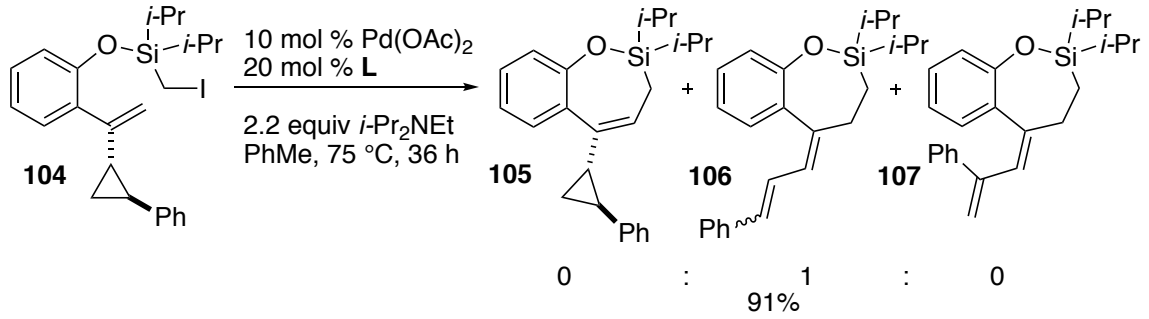

Scheme 31: Radical clock test of **104**.

In order to provide additional evidence on whether the cyclization step follows a classical Heck mechanism, involving carbopalladated intermediates, or a radical pathway, *endo*-Heck reaction of deuterium-labeled substrate **108** was studied (Scheme 32). If a classical Heck pathway were operative, then a stereo-defined alkyl palladium species would be produced upon cyclization (**108→111)**, which will undergo *syn β*-hydride

elimination resulting in complete retention of deuterium (**111→112**). In contrast, upon radical cyclization (**108→114)**, the recombination of an alkyl radical with putative Pd(I) could occur from either face, producing a non-stereodefined alkyl palladium intermediate (**115**). This intermediate, upon *β*-hydride elimination, would result in a product with a loss of nearly half of deuterium label at the alkene moiety (**112b**). Hence, under our optimized conditions, **108**, with 88% deuterium incorporation, underwent *endo*-trig cyclization to generate **112a** with the substantial loss of deuterium (47% deuterium incorporation), which supported a hybrid-Pd radical pathway for this transformation (Scheme 33).

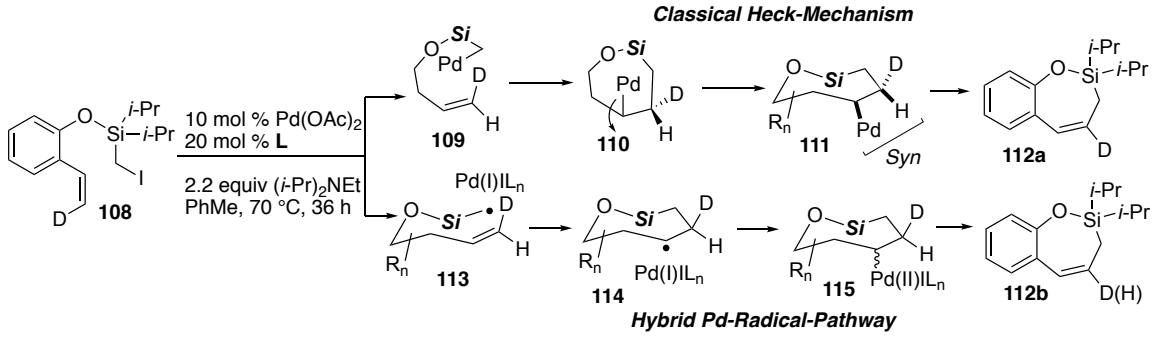

Scheme 32: Rationale for deuterium-labeled study of the *endo*-selective silyl methyl Heck reaction.

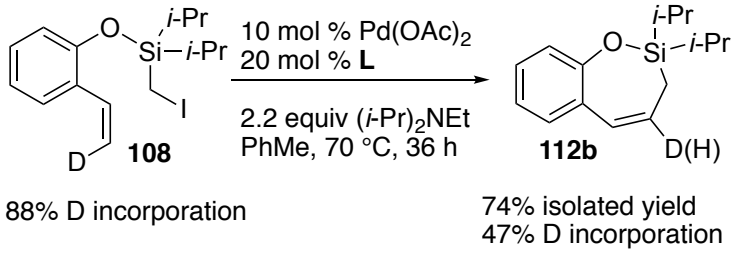

Scheme 33: Results of the deuterium labeled study.

Next, we wanted to verify further that the silicon atom is responsible for the observed *endo*-selective outcome. Hence, a comparison study was implemented. The

regiochemical outcome of substrate **116** was tested against its carbon analog **118** under the same reaction conditions (Scheme 34). As expected, it was found that *only* the silyl methyl substrate **116** underwent selective *endo*-trig cyclization (**116→117a**), whereas the carbon analog **118** generated the *exo-trig* adduct **119b** selectively. Thus, confirming that the silicon atom is crucial for the observed *endo* selectivity for the transformation.

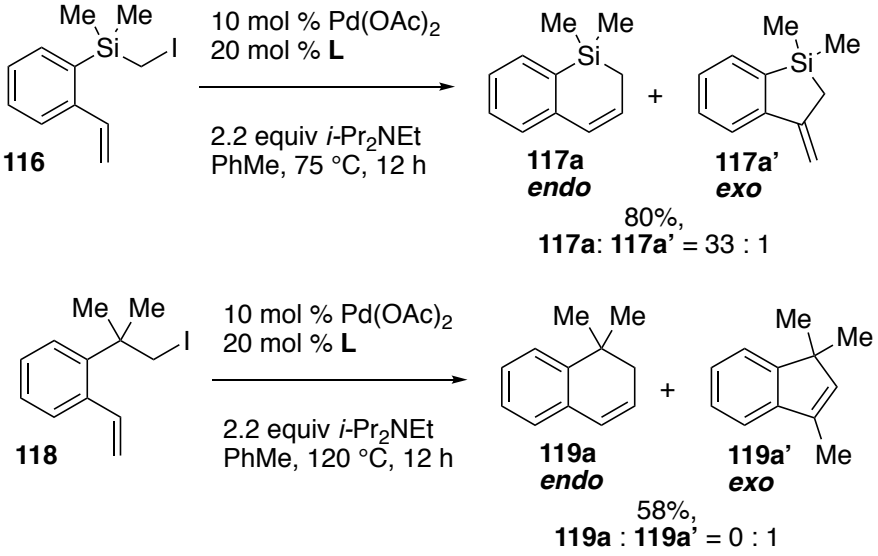

Scheme 34: Comparison study on the regiochemcial outcome of Heck cyclization of iodomethylsilane **116** and carbon analog **118**.

Based on the above mechanistic studies, a hybrid Pd-radical mechanism[14] is proposed for the *endo*-selective silyl methyl Heck reaction (Scheme 35). First, a SET process occurs with the active Pd(0) species and the iodomethylsilane moiety **120**, which produces the putative Pd(I)I species and the silyl methyl radical intermediate **121**. The latter intermediate, possessing radical character, will follow typical cyclization trends reported by Koreeda and Wilt for silyl methyl radicals (*vide supra*). Hence, for substrates

possessing substituent(s) at the β-position of alkene, *endo-trig* cyclization is impeded and *exo*-trig cyclization occurs selectively (**121→122**). However, with substrates possessing terminal double bond, **121** undergoes selective *endo-trig* cyclization to generate radical silyloxycyle **123**. This regiochemical outcome is due to several reasons (1) elongated Si-C bond length that allows for efficient cyclization at the terminal end of the alkene; (2) slower relative rate of competitive *exo* cyclization; (3) and favorable stability of the *endo* transition state proposed for radical cyclizations of halomethylsilanes. Next, recombination of **123** with Pd(I)I results in formation of alkylpalladium intermediate **124**. Evidently, **124** contains two β-hydrogens, $\mathbf{H_h}$ and $\mathbf{H_a}$, for Pd-β-hydride elimination to occur, which can lead to either *homoallylic*- (**125**) or *allylic* silanes (**126**), respectively. Based on the analysis of the substrate scope, it was found that sterics at the α-position of the homoallylic alcohol plays an important role during the β-hydride elimination event, where increasing substitution pattern favors allylic silane formation. After Pd-β-hydride elimination, the *endo* products are formed and the active catalyst is regenerated.

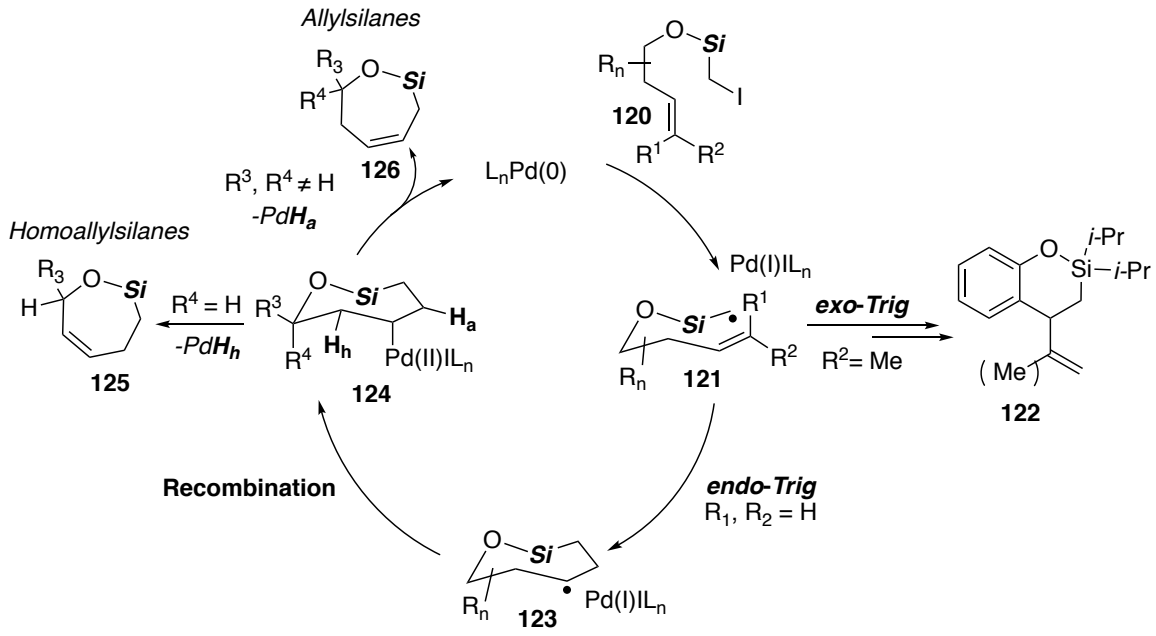

Scheme 35: Hybrid Pd-radical mechanism for the *endo*-selective silyl methyl Heck reaction.

2.7. Summary

In summary, we have shown that iodomethylsilanes are capable tethers for enabling the first *endo-selective alkyl Heck reaction* of 2-vinylphenols and homoallylic alcohols. This protocol allowed for a facile access of synthetically versatile allylic siloxycycle derivatives, which were functionalized via an intramolecular Hosomi-Sakurai reaction to produce a spiro benzofuran skeleton. Moreover, the reaction products were efficiently oxidized into *Z*-alkenol-diols, which highlights our method as a formal tool for *Z*-hydroxymethylation of alkenols. Furthermore, we have shown the broad applicability of this transformation by developing a novel cascade alkyl Heck reaction commenced by *endo-trig*-cyclization. The mechanistic studies involving radical clock and deuterium

labeled experiments supports that a hybrid Pd-radical mechanism is operative. This dual radical and transition metal-type nature of this transformation allows for both an inherent *endo-trig* cyclization of silyl methyl radical intermediate, and a *β*-hydride elimination event, which enabled the formation of the *endo*-selective Heck reaction products.

3. Experimental Section (Previously Published as Parasram, M.; Iaroshenko, V. O.; Gevorgyan, V. "Endo-Selective Pd-Catalyzed Silyl Methyl Heck Reaction." *J. Am. Chem. Soc.* 2014, 136, 17926.)

3.1. General Information

NMR spectra were recorded on BrukerAvance DRX-500 (500 MHz) or DPX-400 (400 MHz) instrument. LRMS and HRMS analyses were performed on Micromass 70 VSE mass spectrometer. GC/MS analysis was performed on a Hewlett Packard Model 6890 GC interfaced to a Hewlett Packard Model 5973 mass selective detector (15 m x 0.25 mm capillary column, HP-5MS). Column chromatography was carried out employing Silicycle Silica flash chromatography (40-63 μm) and/or Florisil® (60-100 mesh). Precoated silica gel plates F-254 were used for thin-layer analytical chromatography. All manipulations with transition metal catalysts were conducted in oven-dried glassware under inert atmosphere using a combination of glovebox and standard Schlenk techniques. Anhydrous solvents purchased from Aldrich were additionally purified on PureSolv PS-400-4 by Innovative Technology, Inc. purification system and/or stored over calcium hydride. All other starting materials were purchased from Strem Chemicals, Aldrich, Gelest Inc., Alfa Aesar, or TCI.

3.2. Endo-Selective Pd-Catalyzed Silyl Methyl Heck Reaction

3.2.1. Preparation of Starting Materials

Synthesis of chloro(iodomethyl)diisopropylsilane tether 69:

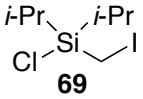

69

To an oven-dried 250 mL Schlenk flask charged with a stir-bar and septum under Ar, a solution of chlorodiisopropylsilane (6.8 mL, 1 equiv, 40 mmol) and chloroiodomethane (4.4 mL, 1.5 equiv, 60 mmol) in THF (50 mL) was added. This mixture was cooled to -78 °C. Then, MeLi-LiBr complex (1.5 M in ether, 40 mL, 60 mmol) was added dropwise. The reaction mixture was stirred at -78 °C for 1 h and then allowed to warm to room temperature before being quenched with saturated ammonium chloride solution (10 mL. The aqueous layer was extracted with hexane (3x50 mL). The combined organic layers was dried over anhydrous magnesium sulfate and concentrated *in vacuo.* The crude product, (chloromethyl)diisopropylsilane, was used for the next step without further purification.

To a solution of NaI (18 g, 3 equiv, 120 mmol) in ACS standard acetone (40 mL), crude (chloromethyl)diisopropylsilane in acetone (5 mL) was added. The resulting reaction mixture was refluxed at 85 °C for 1 h. Then, the reaction was cooled to room temperature before being quenching with saturated solution of $Na_2S_2O_3$ (50 mL). The aqueous layer was extracted with hexane (3x50 mL). The combined organic layer was dried over anhydrous magnesium sulfate and concentrated *in vacuo*. The crude product, 5.1g, (50% yield) (iodomethyl)diisopropylsilane, was used for the next step without further purification.

To a solution of TCCA (1.67 g, 0.36 equiv, 7.2 mmol) in dry DCM (40 mL), (chloromethyl)diisopropylsilane (5.1 g, 1 equiv, 20 mmol) in DCM (5 mL) was added dropwise under argon at 0 °C. The reaction mixture was stirred at 0 °C for 1 h. Then, the mixture was allowed to warm to r.t. Next, the reaction mixture filtered through Celite and concentrated. The residue was then dissolved in hexanes and again re-filtered through Celite. Finally, the solution was concentrated *in vacuo* to yield chloro(iodomethyl)diisopropylsilane (quantitative, 5.8 g) as a pink/purple oil. The crude product, >95% purity, chloro(iodomethyl)diisopropylsilane, was used for the next step without further purification.

Yield = 50% over three steps.

^{1}H NMR (500 MHz, $CDCl_3$): δ ppm 2.22 (s, 2H), 1.41-1.47 (m, 2H), 1.12 -1.14 (dd, 12H). ^{13}C NMR (126 MHz, $CDCl_3$): δ ppm 13.4, 16.9, 17.3. HRMS (EI) calcd. for $C_7H_{16}ISiCl$ [M+H]: 289.9755, found: 289.9759.

Synthesis of secondary chloro(bromo(phenyl)methyl)diisopropylsilane (74k-Tether):

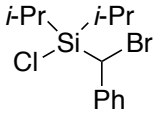

74k-Tether

To an oven-dried 50 mL Schlenk flask charged with a stir-bar and septum under Ar, a solution of diisopropylamine (0.7 mL, 1 equiv, 5 mmol) in THF (10 mL) was added. This mixture was cooled to -78 °C. Then, a solution of *n*-BuLi (2.63 M in hexanes, 1.9 mL, 5 mmol) was added dropwise at -78 °C. The reaction mixture was stirred at 0 °C for 0.5 h and then allowed to warm to room temperature for 0.5 h. The reaction mixture was then cooled down to -100 °C (EtOH and Liquid N_2), followed by addition of BnBr (0.6 mL, 1

equiv, 5 mmol) and chlorodiisopropylsilane (1.02 mL, 1.1 equiv, 6 mmol) in THF:Hex - 1:1 (14 mL). The reaction was stirred overnight at -100 °C to r.t. before being quenched with saturated ammonium chloride solution (20 mL). The aqueous layer was extracted with hexane (3 x 30 mL). The combined organic layer was dried over anhydrous magnesium sulfate and concentrated *in vacuo*. The crude product, (bromo(phenyl)methyl)diisopropylsilane (52% yield, 830 mg), was used for the next step without further purification.

To a solution of TCCA (0.15 g, 0.36 equiv, 0.64 mmol) in dry DCM (10 mL), (chloromethyl)diisopropylsilane (0.513 g, 1 equiv, 1.8 mmol) in DCM (5 mL) was added dropwise under Ar at 0 °C. The reaction mixture was stirred at 0 °C for 1 h. Then, the mixture was allowed to warm to r.t. Next, the reaction mixture filtered through Celite and concentrated. The residue was then dissolved in hexanes and again re-filtered through Celite. Finally, the solution was concentrated *in vacuo* to yield chloro(bromo(phenyl)methyl)diisopropylsilane (quantitative) as a white solid. The crude product, chloro(bromo(phenyl)methyl)diisopropylsilane (>95% purity, quantitative), was used for the next step without further purification (*vide infra*).

Synthesis of silyl-tethered phenols 74a-o and alcohols 76a-3j:

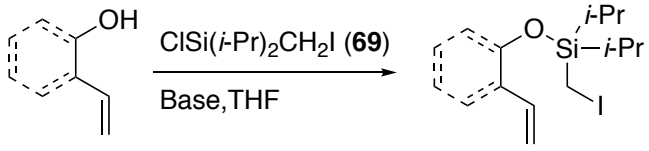

Method A: To a stirred mixture of imidazole (450 mg, 6.6 mmol, 2.2 equiv) and THF (20 mL), chloro(iodomethyl)diisopropylsilane (**69**) (872 mg, 3 mmol, 1 equiv) was added at r.t. under argon atmosphere. To this mixture, phenol/alcohol (3.3 mmol, 1.1 equiv) in 5 mL of THF was added. The mixture was stirred until completion of the reaction (3 h) as

judged by GC/MS. To this mixture, hexane (20 mL) was added and filtered. The filtrate was then concentrated under reduced pressure. The residue was purified by column chromatography in hexanes.

Method B: To a stirred mixture of DMAP (18.3 mg, 0.15 mmol, 5 mol %), chloro(iodomethyl)diisopropylsilane (**69**) (872 mg, 3 mmol, 1 equiv), triethylamine (0.3 mL, 3 mmol, 1 equiv) DCM (10 mL), phenol/alcohol (3.3 mmol, 1.1 equiv) in 5 mL of DCM was added at 0 °C under argon atmosphere. The mixture was stirred until completion of the reaction (1 h) as judged by GC/MS. After completion the mixture was quenched with saturated ammonium chloride solution and extracted with DCM (3 x 50 mL). The combined organic layer was washed with brine. The organic layer was dried with Na_2SO_4, filtered, and then evaporated by rotary evaporator under reduced pressure. The residue was purified by column chromatography in hexanes.

Method C: To a stirred mixture of phenol/alcohol (3.3 mmol, 1.1 equiv) and THF (10 mL), MeLi (2.06 mL, 1.5 M, 3.3 mmol, 1.1 equiv) was added dropwise at 0 °C under argon atmosphere. To this mixture, chloro(iodomethyl)diisopropylsilane (**69**) (872 mg, 3 mmol, 1 equiv) in 5 mL of THF was added at 0 °C. The mixture was stirred until completion of the reaction (1 h) as judged by GC/MS. After completion the mixture was quenched with saturated ammonium chloride solution and extracted with DCM (3 x 50 mL). The combined organic layer was washed with brine. The organic layer was dried with Na_2SO_4, filtered, and then evaporated by rotary evaporator under reduced pressure. The residue was purified by column chromatography in hexanes.

Method D: To a stirred mixture of phenol/alcohol (3.3 mmol, 1.1 equiv) and THF (10 mL), MeLi (2.06 mL, 1.5 M, 3.3 mmol, 1.1 equiv) was added dropwise at 0 °C under

argon atmosphere. To this mixture, HMPA (0.57 mL, 3.3 mmol, 1.1 equiv) was added, followed by, chloro(iodomethyl)diisopropylsilane (**69**) (872 mg, 3 mmol, 1 equiv) in 5 mL of THF was added at 0 °C. The mixture was stirred until completion of the reaction by (1 h) GC/MS. After completion the mixture was quenched with saturated ammonium chloride solution and extracted with DCM (3 x 50 mL). The combined organic layer was washed with brine. The organic layer was dried with Na_2SO_4, filtered, and then evaporated by rotary evaporator under reduced pressure. The residue was purified by column chromatography in hexanes.

Benzene tethered substrates, 74a-74o:

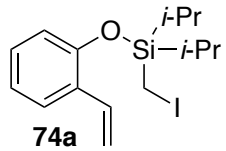

74a

Coupling of 2-vinyl-phenol[38] with **69** using Method A.

Isolated yield = 84%, 943 mg.

^{1}H NMR (500 MHz, $CDCl_3$): δ ppm 7.52 (dd, *J*=7.70, 1.83 Hz, 1 H), 7.07 - 7.18 (m, 2 H), 6.95-7.01 (m, 1 H), 6.85 (dd, *J*=8.07, 1.10 Hz, 1 H), 5.71 (dd, *J*=17.97, 1.47 Hz, 1 H), 5.28 (dd, *J*=11.00, 1.47 Hz, 1 H), 2.26 (s, 2 H) 1.40-1.50 (m, 2 H) 1.12-1.21 (m, 12 H). ^{13}C NMR (126 MHz, $CDCl_3$): δ ppm 12.7, 17.4, 17.7, 114.1, 119.3, 121.8, 126.2, 128.7, 128.9, 131.8, 152.3. HRMS (ESI) calcd. for $C_{15}H_{23}IOSi$ [M+H]: 375.0641, found: 375.0647

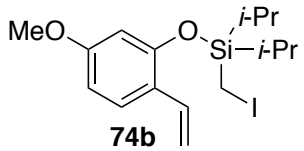

74b

Coupling of 5-methoxy-2-vinylphenol[39]with **69** using Method A.

Isolated yield = 62%, 752 mg.

^{1}H NMR (500 MHz, $CDCl_3$): δ ppm 7.43 (d, *J*=8.77 Hz, 1 H), 7.00 (dd, *J*=17.54, 11.11 Hz, 1 H), 6.54 (dd, J=8.77, 2.34 Hz, 1 H), 5.57 (dd, *J*=17.83, 1.46 Hz, 1 H), 5.14 (dd, *J*=11.11, 1.17 Hz, 1 H), 3.79 (s, 3 H) 2.25 (s, 2 H) 1.35-1.54 (m, 2 H) 1.09-1.19 (m, 12 H). ^{13}C NMR (126 MHz, $CDCl_3$): δ ppm 12.7, 17.4, 17.7, 55.4, 105.5, 107.3, 111.8, 121.9, 126.8, 131.3, 151.2, 160.1. HRMS (ESI) calcd. for $C_{16}H_{25}IO_2Si$ [M+H]: 405.0747, found: 405.0751.

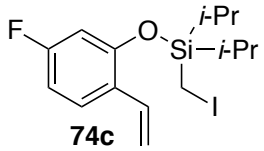

74c

Coupling of 5-fluoro-2-vinylphenol[38] with **69** using Method A.

Isolated yield = 69%, 812 mg.

^{1}H NMR (500 MHz, $CDCl_3$): δ ppm 7.40-7.50 (m, 1 H), 6.99 (dd, *J*=17.69, 10.96 Hz, 1 H), 6.65-6.74 (m, 1 H), 6.51 - 6.62 (m, 1 H), 5.61 (d, *J*=17.83 Hz, 1 H), 5.23 (d, *J*=11.11 Hz, 1 H), 2.21-2.28 (m, 2 H), 1.35-1.50 (m, 2 H), 1.08-1.18 (m, 12 H). ^{13}C NMR (126 MHz, $CDCl_3$): δ ppm 12.7, 17.3, 17.6, 106.7, 106.9, 108.8, 108.9, 113.7, 125.3, 125.4 127.1, 127.2, 130.9, 153.1, 161.7, 163.6. HRMS (ESI) calcd. for $C_{15}H_{22}FIOSi$ [M+H]: 393.0547, found: 393.0551.

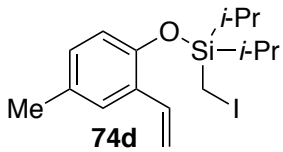

74d

Coupling of 4-methyl-2-vinylphenol[39] with **69** using Method A.

Isolated yield = 68%, 792 mg.

^{1}H NMR (500 MHz, $CDCl_3$): δ ppm 7.17 (dd, *J*=9.65, 2.92 Hz, 1 H), 7.02 (ddd, *J*=17.76, 11.03, 1.61 Hz, 1 H), 6.74 - 6.88 (m, 2 H), 5.67 (dd, *J*=17.83, 0.88 Hz, 1 H), 5.26 - 5.36 (m, 1 H), 2.29 (s, 3H), 2.23 (s, 3H), 1.37-1.45 (m, 2H), 1.05 -1.18 (m, 12H). ^{13}C NMR (126 MHz, $CDCl_3$): δ ppm 12.7, 17.4, 17.7, 20.7, 113.7, 119.1, 126.6, 128.4, 129.3, 130.9, 131.9, 150.1. HRMS (EI) calcd. for $C_{16}H_{25}IOSi$ [M]: 388.0719, found: 388.0716.

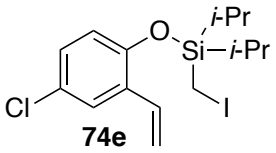

74e

Coupling of 4-chloro-2-vinylphenol[40]with **69** using Method A.

Isolated yield = 84%, 1.03 g.

^{1}H NMR (500 MHz, $CDCl_3$): δ ppm 7.46 (d, *J*=2.93 Hz, 1 H), 7.09 (dd, *J*=8.44, 2.57 Hz, 1 H), 7.01 (dd, *J*=17.79, 11.19 Hz, 1 H), 6.75 - 6.81 (m, 1 H), 5.70 (d, =17.97 Hz, 1 H), 5.31 (d, *J* =11.00 Hz, 1 H), 2.24 (s, 2H), 1.39-1.46 (m, 2H), 1.11 -1.15 (m, 12H). ^{13}C NMR (126 MHz, $CDCl_3$): δ ppm 12.7, 17.4, 17.7, 115.4, 120.5, 126.1, 126.8, 128.4, 130.5, 130.8, 150.6. HRMS (EI) calcd. for $C_{15}H_{22}IClOSi$ [M+H]: 408.0173, found: 408.0172

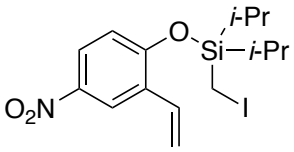

Coupling of 4-nitro-2-vinylphenol[38] with **69** using Method A.

Isolated yield = 48%, 603 mg.

^{1}H NMR (500 MHz, $CDCl_3$): δ ppm 8.40 (d, *J*=2.93 Hz, 1 H), 7.99 - 8.12 (m, 1 H), 7.03 (dd, J=17.61, 11.00 Hz, 1 H), 6.86 - 6.96 (m, 1 H), 5.79 - 5.93 (m, 1 H), 5.37 - 5.48 (m, 1 H), 2.26 (s, 2H), 1.41-1.49 (m, 2H), 1.13 -1.17 (m, 12H). ^{13}C NMR (126 MHz, $CDCl_3$): δ

ppm 12.7, 17.3, 17.5, 117.2, 119.3, 122.2, 124.2, 129.9, 130.0, 142.4, 157.6. HRMS (ESI) calcd. for $C_{15}H_{22}INO_3Si$ [M+H]: 420.0492, found: 420.0489.

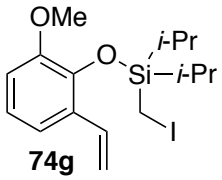

74g

Coupling of 2-methoxy-6-vinylphenol[41] with **69** using Method A.

Isolated yield = 43%, 521 mg.

^{1}H NMR (500 MHz, $CDCl_3$): δ ppm 7.08 - 7.19 (m, 7H), 6.85-6.92 (m, 1H), 6.76 (dd, *J*=8.0, 1.6 Hz, 1H), 5.67 (dd, *J*=17.7, 1.3 Hz, 1H), 5.26 (dd, *J*=11.1, 1.5 Hz, 1H), 3.80 (s, 3H), 2.26 (s, 2H), 1.36-1.44 (m, 2H), 1.08 -1.13 (m, 12H). ^{13}C NMR (125 MHz, $CDCl_3$): δ ppm 13.3, 17.6, 17.8, 55.1, 110.5, 114.2, 117.8, 121.2, 129.6, 131.9, 142.0, 150.0. HRMS (EI) calcd. for $C_{16}H_{25}IO_2Si$ [M]: 404.0669, found: 404.0671.

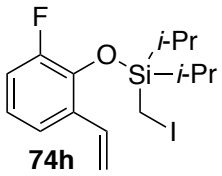

74h

Coupling of 2-fluoro-6-vinylphenol[42]with **69** using Method A.

Isolated yield = 61%, 717 mg.

^{1}H NMR (500 MHz, $CDCl_3$): δ ppm 7.23 - 7.30 (m, 1 H), 7.03 - 7.13 (m, 1 H), 6.93 - 7.01 (m, 1 H), 6.83 - 6.93 (m, 1 H), 5.67 - 5.76 (m, 1 H), 5.32 (d, *J*=11.11 Hz, 1 H), 2.27 (s, 2H), 1.41-1.49 (m, 2H), 1.11 -1.17 (m, 12H). ^{13}C NMR (126 MHz, $CDCl_3$): δ ppm 12.9, 17.3, 17.6, 106.7, 106.9, 108.8, 108.9, 113.7, 125.4, 127.0, 127.1, 130.1, 153.1, 161.67, 163.6. HRMS (EI) calcd. for $C_{15}H_{22}FIOSi$ [M+H]: 392.0469, found: 392.0467.

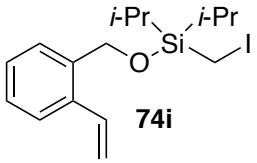

74i

Coupling of 2-vinylbenzylol[40] with **69** using Method B.

Isolated yield = 70%, 815 mg.

^{1}H NMR (500 MHz, $CDCl_3$): δ ppm 7.48 (s, 2 H), 7.22-7.36 (m, 3 H), 6.96 (ddd, *J*=17.24, 11.00, 3.30 Hz, 1 H), 5.66 (dt, J=17.24, 1.65 Hz, 1 H), 5.32 (dt, J=10.73, 1.79 Hz, 1 H), 4.95 (s, 2H), 2.13 (s, 2H), 1.24-1.34 (m, 2H), 1.11-1.12 (m, 12H). ^{13}C NMR (126 MHz, $CDCl_3$): δ ppm 12.4, 17.5, 17.7, 63.7, 116.0, 125.6, 126.9, 127.4, 127.7, 133.9, 135.8, 137.6. HRMS (EI) calcd. for $C_{16}H_{25}IOSi$ [M]: 388.0719, found: 388.0720.

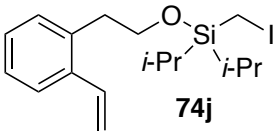

74j

Coupling of 2-vinylphenethanol[38] with **69** using Method B.

Isolated yield = 70%, 845 mg.

^{1}H NMR (500 MHz, $CDCl_3$): δ ppm 7.45 - 7.55 (m, 3 H), 7.15 - 7.25 (m, 11 H), 7.05 (dd, *J*=17.24, 11.00 Hz, 1 H), 5.65 (d, *J*=17.24 Hz, 1 H), 5.31 (d, *J*=11.00 Hz, 1 H), 3.89 (t, *J*=7.15 Hz, 2 H), 2.98 (t, *J*=7.15 Hz, 2 H), 2.00 (s, 2H), 1.17-1.21 (m, 2H), 1.03-1.05 (m, 12H). ^{13}C NMR (126 MHz, $CDCl_3$): δ ppm 12.2, 17.4, 17.6, 36.7, 64.3, 115.7, 125.7, 126.7, 127.7, 130.5, 134.7, 136.0, 137.0. HRMS (ESI) calcd. for $C_{17}H_{27}IOSi$ [M+H]: 403.0954, found: 403.0958.

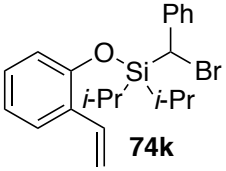

74k

Coupling of 2-vinylphenol with **74k-Tether** (*vide supra*) using Method A.

Isolated yield = 68%, 823 mg.

^{1}H NMR (500 MHz, $CDCl_3$): δ ppm 7.53 (dd, *J*=7.60, 1.46 1H), 7.45 (d, *J*=7.02 Hz, 2H), 7.20-7.30 (m, 3H), 7.08-7.16 (m, 2H), 6.97 (t, *J*=7.45 Hz, 1H), 6.84 (d, *J*=8.18 Hz, 1H), 5.69 (dd, *J*=17.83, 1.17 Hz, 1H), 5.23-5.26 (m, 1H), 4.62 (s, 1H), 1.55-1.62 (m, 1H), 1.39-1.45 (m, 1H), 1.15-1.21 (m, 6H) 0.99-1.07 (m, 6H). ^{13}C NMR (126 MHz, $CDCl_3$): δ ppm 13.1, 13.2, 17.4, 17.5, 17.6, 17.7, 17.8, 18.0, 38.2,113.9, 119.4, 121.7, 126.6, 127.4, 128.5, 128.6, 128.7, 129.3, 131.9, 139.6, 152.1. HRMS (ESI) calcd. for $C_{21}H_{28}BrOSi$ [M+H]: 403.1093, found: 403.1088.

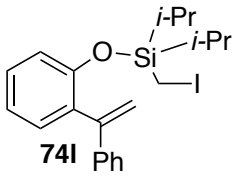

74l

Coupling of 2-(1-phenylvinyl)phenol[43] with **69** using Method A.

Isolated yield = 87%, 1.17 g.

^{1}H NMR (500 MHz, $CDCl_3$): δ ppm 7.22-7.33 (m, 7H), 6.99-7.03 (m, 1H), 6.87 (d, *J*=8.1 Hz, 1H), 5.75 (s, 1H), 5.32 (s, 1H), 2.03 (s, 2H), 1.19-1.25 (m, 2H), 0.91-0.97 (m, 12H). ^{13}C NMR (126 MHz, $CDCl_3$): δ ppm 12.5, 17.1, 17.5, 115.7, 119.0, 121.4, 126.6, 127.4, 128.1, 128.8, 131.7, 133.0, 140.5, 147.4, 152.5. HRMS (ESI) calcd. for $C_{21}H_{27}IOSi$ [M+H]: 451.0954, found: 451.0947.

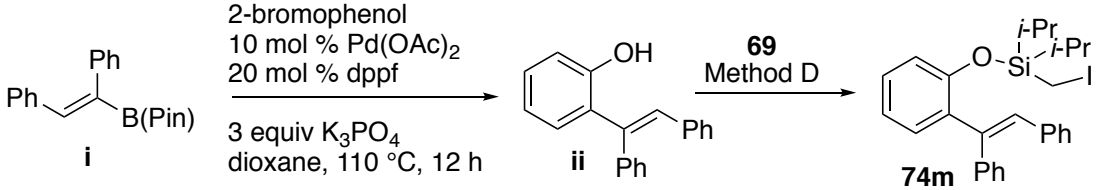

In a V-vial charged with 2-bromophenol (34 μL, 1 equiv, 0.3 mmol), vinyl-B(Pin) (**i**)[44](0.184 g, 2 equiv, 0.6 mmol), $Pd(OAc)_2$ (6.8 mg, 0.1 equiv, 0.03mmol), dppf (33 mg, 0.2 equiv, 0.06 mmol), K_3PO_4 (0.191 g, 3 equiv, 0.9 mmol) under N_2 atmosphere (glove box). Dry dioxane was added via syringe and the reaction vessel was capped with pressure screw cap. The reaction mixture was heated at 110 °C for 12 h. The resulting mixture was cooled down to room temperature and filtered through a short layer of silica gel over Celite plug with the aid of DCM. The filtrate was concentrated under reduced pressure and purified by column chromatography 2:1 Hex:EtOAc. Isolated yield of **ii** = 88%, 72 mg. ^{1}H NMR (500 MHz, $CDCl_3$): δ ppm 7.30-7.39 (m, 7H), 7.21 (s, 1H), 7.17-7.19 (m, 3H) 7.08-7.12 (m, 3H) 6.94-6.98 (t, 2H), 5.06 (s, 1H). ^{13}C NMR (126 MHz, $CDCl_3$): δ ppm 115.9, 121.1, 125.9, 127.1, 127.8, 128.2, 128.4,128.6, 128.9, 129.7, 130.5, 131.0, 136.2, 136.4, 141.7, 153.8. HRMS (EI) calcd. for $C_{20}H_{16}O$ [M]: 272.1201, found: 272.1201.

Synthesis of **74m** was obtained via coupling of **ii** with **69** using Method D.

Isolated yield = 76%, 1.2 g.

^{1}H NMR (500 MHz, $CDCl_3$): δ ppm 7.41-7.43 (m, 2H), 7.28-7.35 (m, 4H), 7.13-7.19 (m, 7H), 6.92-7.01 (m, 2H), 2.05 (s, 2H), 1.15-1.27 (m, 2H), 0.91-0.97 (m, 12H). ^{13}C NMR (126MHz, $CDCl_3$): δ ppm 12.7, 17.3, 17.5, 118.7, 121.7, 127.3, 128.0, 128.2, 128.8, 128.9, 129.3, 131.0, 132.4, 137.6, 139.4, 142.5. 153.0. HRMS (ESI) calcd. for $C_{27}H_{31}IOSi$ [M+H]: 527.1267, found: 527.1262.

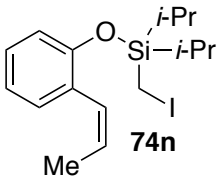

74n

Coupling of (*Z*)-2-(prop-1-enyl)phenol[45]with **69** using Method A.

Isolated yield = 58%, 675 mg.

^{1}H NMR (500 MHz, $CDCl_3$): δ ppm 7.23-7.31 (m, 1 H) 7.09-7.17 (m, 1 H) 6.93 - 7.02 (m, 1 H) 6.88 (d, *J*=8.07 Hz, 1 H) 6.56 (d, *J*=11.74 Hz, 1 H) 5.82 (dq, *J*=11.55, 7.03 Hz, 1 H) 2.24 (m, 2 H) 1.84 (dd, *J*=6.97, 1.83 Hz, 3 H) 1.41 (m, 2 H) 1.06 - 1.19 (m, 12 H). ^{13}C NMR (126 MHz, $CDCl_3$): δ ppm 12.7, 14.6, 17.3, 17.7, 119.4, 121.2, 126.2, 126.8, 127.8, 128.7, 130.5, 152.8. HRMS (EI) calcd. for $C_{16}H_{25}IOSi$ [M]: 388.0709, found 388.0708

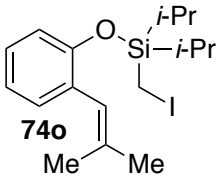

74o

Coupling of 2-(2-methylprop-1-enyl)phenol[40] with **69** using Method A.

Isolated yield = 72%, 869 mg.

^{1}H NMR (500 MHz, $CDCl_3$): δ ppm 7.18 (d, *J*=7.34 Hz, 1 H) 7.07 - 7.13 (m, 1 H) 6.93 - 6.98 (m, 1 H) 6.86 (d, *J*=8.07 Hz, 1 H) 6.33 (br. s., 1 H), 2.20 (s, 2H) 1.92 (s, 3H), 1.79 (s, 3H) 1.37-1.42 (m, 2H), 1.10-1.15 (m, 12H). ^{13}C NMR (126 MHz, $CDCl_3$): δ ppm 12.6, 17.3, 17.6, 19.4, 26.4, 119.4, 121.3, 121.7, 127.2, 130.13, 130.6, 135.14, 152.7. HRMS (EI) calcd. for $C_{17}H_{27}IOSi$ [M]: 403.0954, found: 403.0954.

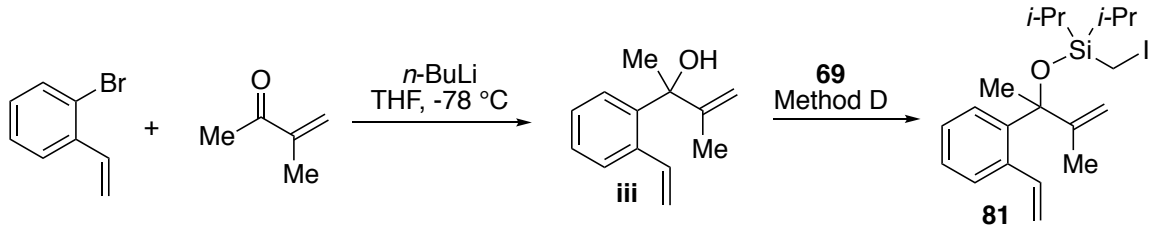

A 25 mL Schlenk flask under argon was charged with 2-bromostyrene (0.62 mL, 1 equiv, 5 mmol) and THF (10 mL). The solution was cooled to -78 °C. *n*-BuLi (2.12 mL, 1.1 equiv, 2.6 M, 5.5 mmol) was added dropwise. After stirring at -78 °C for 1 h, 3-methyl-buten-2-one (0.54 mL, 1.1 equiv, 5.5 mmol) in 5 mL THF was added to the reaction pot. The reaction was allowed to stir for 1 h at -78 °C. A saturated ammonium chloride solution was added and the aqueous phase was extracted with DCM (3 x 50 mL). The organic phase was dried over Na_2SO_4, filtered and concentrated. The compound was purified by column chromatography (10:1 Hex:EtOAc) to give **iii** a clear oil (72%, 683 mg).

^{1}H NMR (500 MHz, $CDCl_3$): δ ppm 7.54-7.56 (m, 1H), 7.44-7.46 (m, 1H), 7.25-7.31 (m, 3H), 5.51-5.55 (d, 1H), 5.21-5.23 (d, 1H), 5.12 (s, 1H), 4.97 (s, 1H), 2.07 (s, 1H), 1.74 (s, 3H), 1.65 (s, 3H). ^{13}C NMR (126 MHz, $CDCl_3$): δ ppm 19.6, 28.9, 20.6, 111.3, 115.5, 125,9, 127.4, 127.4, 127.8, 142.4, 150.3.

Synthesis of **81** was obtained via coupling of **iii** with **69** using Method D.

Isolated yield = 48%, 637 mg.

^{1}H NMR (500 MHz, $CDCl_3$): δ ppm 7.55-7.49 (m, 2H), 7.32-7.38 (dd, *J*=17.24, 11.00 Hz, 1H), 7.23-7.26 (m, 2H), 5.50 (dd, J=17.24, 1.47 Hz, 1 H) 5.20 (s, 1 H) 5.11 (dd, *J*=10.82, 1.28 Hz, 1 H) 4.91-4.94 (m, 1 H), 1.94-2.01 (m, 2H) 1.83 (s, 3H) 1.56 (s, 3H) 1.21-1.28 (m, 1H) 1.11-1.16 (m, 1H) 1.07-1.08 (dd, *J*=7.34, 1.47 Hz, 6H) 0.94-0.99 (t, *J*=8.07 Hz, 6H). ^{13}C NMR (500 MHz, $CDCl_3$): δ ppm 13.5, 13.6, 17.7, 17.8, 17.9, 18.1,

19.8, 29.3, 79.9, 113.8, 126.1, 127.1, 127.2, 127.6, 137.0, 137.2, 142.4, 150.9.HRMS (EI) calcd. for $C_{20}H_{31}IOSi$ [M]: 442.1189, found: 442.1192.

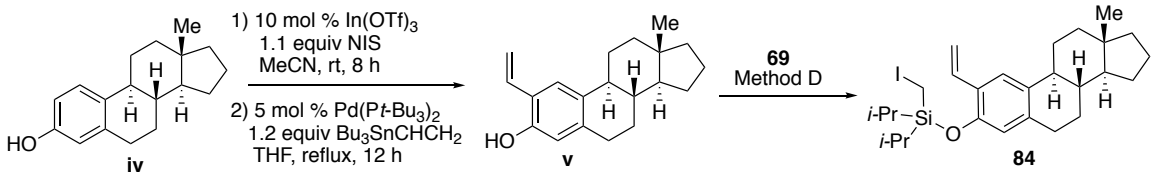

To a 100 mL flask equipped with a stirring bar, argon inlet, and septum, deoxoestrone substrate **iv**[46] (1.35 g, 1 equiv, 5.27 mmol), $In(OTf)_3$ (296 mg, 0.1 equiv, 0.527 mmol), NIS (1.3 g, 1.1 equiv, 5.8 mmol) and MeCN (10 mL) was added. The reaction was then stirred at room temperature for 8 h. Upon completion as judged by GC/MS, the reaction was filtered through Celite and concentrated. The residue was purified by column chromatography 9:1 Hex: EtOAc. The iodination intermediate was obtained as white crystals (59%, 118 g). In a V-vial charged with iodinated steroid (0.77 g, 1 equiv, 2.01 mmol), vinyltributlytin (1.17 mL, 2 equiv, 4.02 mmol), $Pd(P\textit{t}\text{-}Bu_3)_2$ (52 mg, 0.05 equiv, 0.1mmol), under N_2 atmosphere (glove box). Dry THF (10 mL) was added via syringes and the reaction vessel was capped with pressure screw cap. The reaction mixture was heated at 110 °C for 12 h. The resulting mixture was cooled down to room temperature and filtered through a short layer of silica gel over Celite plug with the aid of DCM. The filtrate was concentrated under reduced pressure and purified by column chromatography 9:1 Hex:EtOAc to yield **v** as white crystals (86%, 490 mg). Overall yield = 48% over two steps.

^{1}H NMR (500 MHz, $CDCl_3$): δ ppm 7.33 (s, 1H), 6.89-6.95 (dd, 1H), 6.53 (s, 1H), 5.69-5.73 (dd, 1H), 5.30-5.32 (dd, 1H), 4.99 (s, 1H), 2.80-2.84 (m, 2H), 2.31-2.35 (m, 1H),

2.18-2.21 (m, 1H), 1.89-1.92 (m, 2H), 1.69-1.80 (4H), 1.52-1.54 (m, 2H), 1.13-1.40, (m, 10H), 0.94-0.97, (t, 1H), 0.77 (s, 3H). ^{13}C NMR (126 MHz, $CDCl_3$): δ ppm 13.6, 17.6, 20.6, 25.3, 26.8, 28.1, 29.5, 38.8, 39.2, 41.1, 43.9, 53.6, 114.7, 115.8, 124.3, 131.9, 133.4, 138.1, 150.6.

Synthesis of **84** was obtained via coupling of **v** with **69** using Method D.

Isolated yield = 66%, 1.06 g.

^{1}H NMR (500 MHz, $CDCl_3$): δ ppm 7.41 (s, 1H), 7.03 (dd, J=17.79, 11.19 Hz, 1 H), 6.52 (s, 1H), 5.63 (d, *J*=17.61 Hz, 1 H), 5.17 (d, *J*=11.37 Hz, 1 H), 2.74-2.81, (m, 2H), 2.31-2.34 (m, 1H) 2.23 (s, 2H) 2.18-2.19 (m, 1H), 1.87-1.92 (m, 2H) 1.64-1.69 (m, 3H) 1.49-1.58 (m, 2H), 1.22-1.45 (m, 9H), 1.07-1.16 (m, 16H), 0.75 (s, 3H). ^{13}C NMR (126 MHz, $CDCl_3$): δ ppm 12.3, 12.7, 17.4, 17.6, 17.6, 17.7, 18.7, 20.6, 25.2, 26.7, 28.1, 29.6, 31.6, 39.1, 40.5, 41.1, 44.1, 53.6, 59.5, 112.7, 119.1, 122.9, 125.9, 132.2, 134.0, 137.7, 149.9. HRMS (ESI) calcd. for $C_{27}H_{41}IOSi$ [M+H]: 537.2050, found: 537.2054.

Silyl-tethered aliphatic alkenols, 76a-j:

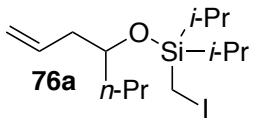

Coupling of 1-heptene-4-ol with **69** using Method B.

Isolated yield = 79%, 873 mg.

^{1}H NMR (500 MHz, $CDCl_3$): δ ppm 5.79-5.87 (m, 1H), 5.04-5.08 (m, 2H), 3.90-3.95 (m, 1H), 2.22-2.32 (m, 2H), 2.08 (s, 2H), 1.43-1.50 (m, 2H), 1.31-1.40 (m, 2H), 1.18-1.25 (m, 2H), 1.07-1.10 (t, *J*=7.34 Hz, 12H), 0.91 (t, *J*=7.34 Hz, 3H). ^{13}C NMR (126 MHz, $CDCl_3$): δ ppm 12.6, 14.3, 17.5, 17.8, 18.3, 38.9, 41.6, 72.5, 116.9, 134.9, HRMS (CI) calcd. for $C_{14}H_{29}IOSi$ [M+H]: 369.1111, found: 369.1108

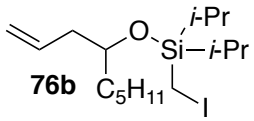

76b

Coupling of 1-nonene-4-ol with **69** Method B.

Isolated yield = 77%, 915 mg.

^{1}H NMR (500 MHz, $CDCl_3$): δ ppm 5.87-5.79 (m, 1 H), 5.08-5.03 (m, 2 H), 3.94-3.89 (m, 1 H), 2.32-2.22 (m, 2 H), 2.08 (s, 2 H), 1.51-1.44 (m, 2H), 1.36-1.12 (m, 8 H), 1.09 (t, *J* = 7.7 Hz, 12 H), 0.89 (t, *J* = 6.6 Hz, 3 H). ^{13}C NMR (126 MHz, $CDCl_3$): δ ppm 12.6, 14.0, 17.5, 17.8, 22.6, 24.7, 32.0, 36.6, 41.5, 72.7, 116.9, 135.0. HRMS (CI) calcd. for $C_{16}H_{34}OISi$ [M+H]: 397.14240, found: 397.14168.

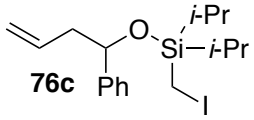

76c

Coupling 4-phenyl-1-butene-4-ol with **69** using Method B.

Isolated yield = 79%, 953 mg.

^{1}H NMR (500 MHz, $CDCl_3$): δ ppm 7.30-7.32 (m, 3H), 7.23-7.28 (m, 1H), 5.71-5.80 (m, 1H), 5.02-5.04 (m, 2H), 5.00 (s, 1H), 4.85-4.88, (t, 3H), 2.52-2.58 (m, 1H), 2.42-2.47 (m, 1H), 1.94 (d, 2H), 1.20-1.27 (m, 1H), 1.14-1.18 (m, 1H), 1.07-1.11 (dd, *J*=15.22, 7.52 Hz, 6H) 0.94-1.00 (m, 6H). ^{13}C NMR (126MHz, $CDCl_3$): δ ppm 12.4, 12.5, 17.3, 17.5, 17.6, 17.9, 45.5, 75.5, 117.3, 126.0, 127.3, 128.1, 134.6, 144.5. HRMS (CI) calcd. for $C_{17}H_{27}IOSi$ [M+H]: 403.09545, found: 403.09531.

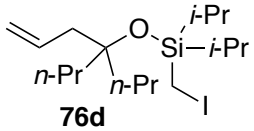

76d

Coupling 4-n-propyl-1-heptene-4-ol with **69** using Method D.

Isolated yield = 58%, 739 mg.

^{1}H NMR (500 MHz, $CDCl_3$): δ ppm 5.79-5.88 (m, 1H), 5.02-5.06 (m, 2H), 2.27-2.28 (d, 2H), 2.10 (s, 2H), 1.44-1.55 (m, 4H), 1.32-1.36 (m, 4H), 1.14-1.26 (m, 2H), 1.07-1.10, (m, 14H), 0.88-0.91 (t, *J*=7.34 Hz, 6H). ^{13}C NMR (126 MHz, $CDCl_3$): δ ppm 13.7, 14.7, 17.1, 17.5, 17.9, 18.2, 42.7, 44.8, 78.6, 117.0, 134.9. HRMS (CI) calcd. for $C_{17}H_{35}IOSi$ [M+H]: 411.15805, found: 411.15814.

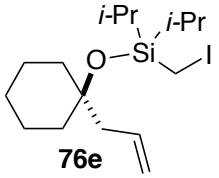

76e

Coupling of 1-allyl-cyclohexanol with **69** using Method D.

Isolated yield = 44%, 520 mg.

^{1}H NMR (500 MHz, $CDCl_3$): δ ppm 5.82-5.91 (m, 1H), 5.02-5.07 (m, 2H), 2.33-2.34 (d, *J*=7.3 Hz, 2H), 2.12 (s, 2H), 1.59-1.65 (m, 4H), 1.47-1.50 (m, 2H), 1.15-1.25 (m, 2H), 1.08-1.10, (m, 12H). ^{13}C NMR (126 MHz, $CDCl_3$): δ ppm 13.7, 17.1, 17.5, 17.9, 18.2, 22.8, 25.5, 38.1, 75.9, 117.0, 134.7. HRMS (EI) calcd. for $C_{16}H_{31}IOSi$ [M+H]: 394.1189 found: 394.1189.

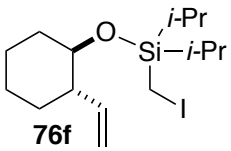

76f

Coupling of (1*R*,2*S*)-2-vinylcyclohexanol[47] with **69** using Method B.

Isolated yield = 65%, 741 mg.

^{1}H NMR (500 MHz, $CDCl_3$): δ ppm 5.81-5.90 (m, 1H), 4.98-5.05 (m, 2H), 3.50-3.56 (m, 1H), 2.07 (s, 2H), 1.73-2.00 (m, 2H), 1.54-1.75 (m, 3H), 1.30-1.43 (m, 1H) 1.14-1.30 (m,

5H), 1.05-1.09, (m, 12H). ^{13}C NMR (126 MHz, $CDCl_3$): δ ppm 13.0, 13.1, 17.9, 18.0, 18.2, 18.4, 24.9, 25.1, 30.8, 36.1, 50.2, 75.7, 114.6, 142.1. HRMS (CI) calcd. for $C_{15}H_{29}IOSi$ [M+H]: 381.11110, found: 381.11144.

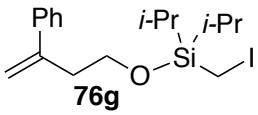

76g

Coupling of 3-phenylbut-3-en-1-ol[48] with **69** using Method B.

Isolated yield = 72%, 869 mg.

^{1}H NMR (500 MHz, $CDCl_3$): δ ppm 7.41-7.44 (m, 2H), 7.32-7.35 (t, 2H), 7.26-7.29 (m, 1H), 5.36 (s, 1H), 5.13 (s, 1H), 3.85 (t, *J*=7.15 Hz, 2H), 2.79-2.82 (t, *J*=7.15 Hz, 2H), 2.03 (s, 2H), 1.17-1.21 (m, 2H), 1.04-1.06, (m, 12H). ^{13}C NMR (126 MHz, $CDCl_3$): δ ppm 12.2, 17.4, 17.7,38.7, 62.9, 114.1, 126.1, 127.4, 128.3, 140.9, 145.1. HRMS (EI) calcd. for $C_{17}H_{27}IOSi$ [M+H]: 402.0876, found: 402.0880.

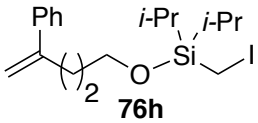

76h

Coupling of 4-phenylpent-4-en-1-ol[49]with **69** using Method B.

Isolated yield = 74%, 924 mg.

^{1}H NMR (500 MHz, $CDCl_3$): δ ppm 7.42-7.44 (m, 2H), 7.31-7.35 (m, 2H), 7.26-7.28 (m, 1H), 5.31 (s, 1H), 5.09 (s, 1H), 3.77 (t, *J*=6.24 Hz, 2H), 2.61 (t, J=7.70 Hz, 2H), 2.07 (s, 2H), 1.70-1.74 (m, 2H), 1.19-1.25 (m, 2H), 1.05-1.09, (m, 12H). ^{13}C NMR (126 MHz, $CDCl_3$): δ ppm 12.3, 17.5, 17.7, 31.4, 31.5, 63.2, 112.4, 126.1, 127.4, 128.3, 141.1, 148.1. HRMS (EI) calcd. for $C_{18}H_{29}IOSi$ [M+H]: 416.1032, found: 416.1040.

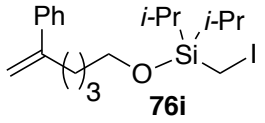

76i

Coupling of 5-phenylhex-5-en-1-ol[50]with **69** using Method B.

Isolated yield= 69%, 891 mg.

^{1}H NMR (500 MHz, $CDCl_3$): δ ppm 7.40-7.42 (d, 2H), 7.31-7.34 (t, 2H), 7.26-7.28 (d, 1H), 5.27-5.28 (dd, 1H), 5.07-5.07 (dd, 1H), 3.74 (t, *J*=6.42 Hz, 2H), 2.54 (t, *J*=7.34 Hz, 2H), 2.06 (s, 2H), 1.52-1.62 (m, 4H), 1.17-1.25 (m, 2H), 1.03-1.09, (m, 12H). ^{13}C NMR (126 MHz, $CDCl_3$): δ ppm 12.3, 17.4, 17.7, 24.4, 32.4, 35.0, 63.6, 112.3, 126.1, 127.3, 128.3, 141.3, 148.5. HRMS (ESI) calcd. for $C_{19}H_{31}IOSi$ [M+H]: 431.1267, found: 431.1268.

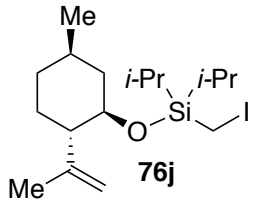

76j

Coupling of isopulegol with **69** using Method C.

Isolated yield= 68%, 833 mg.

^{1}H NMR (500 MHz, $CDCl_3$): δ ppm 4.75-4.77 (m, 2H), 3.70-3.76 (m, 1H), 3.72-3.75 (t, 2H), 2.05-2.06 (m, 2H), 1.88-1.97 (m, 2H), 1.72 (s, 3H), 1.59-1.64, (m, 2H), 1.41-1.48 (m, 1H), 1.26-1.35 (m, 1H), 1.11-1.23 (m, 2H), 1.04-1.09 (m, 12H), 0.87-0.94 (m, 4H).^{13}C NMR (126 MHz, $CDCl_3$): δ ppm 12.7, 12.9, 17.5, 17.6, 17.8, 17.9, 20.9, 22.3, 30.6, 31.6, 34.3, 45.4, 53.6, 73.8, 111.2, 126.1, 147.8. HRMS (ESI) calcd. for $C_{17}H_{33}IOSi$ [M]+H: 409.1424, found: 409.1421

3.2.2. Endo-Selective Silyl Methyl Heck Reaction

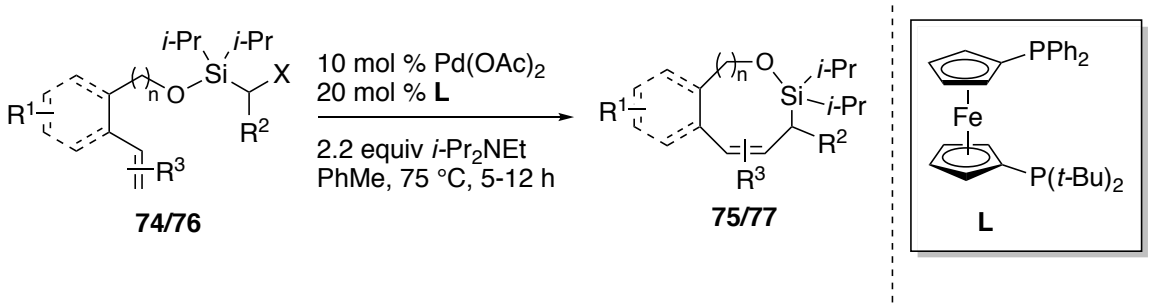

An oven dried 2.5 mL Wheaton V-vial, containing a stirring bar, was charged with phenol/alcohol-derived iodomethylsilanes (0.2 mmol), $Pd(OAc)_2$ (4.5 mg, 0.01 mmol), Ligand **L** (20.6 mg, 0.02 mmol), (and AgOTf (51.2 mg, 0.2 mmol) for **74m**, **76a-c** and **76f-i**) under N_2 atmosphere (glove box). 2 mL of dry toluene (5 mL toluene for **74j-k**, **76i)** and *i*-Pr_2NEt (76 μL, 0.44 mmol) (DABCO instead of *i*-Pr_2NEt, 50 mg, 0.44 mmol for **76d-c**) were added via syringes and the reaction vessel was capped with pressure screw cap. The reaction mixture was heated at 75 °C for 5-20 h (extended time (36 h) and higher temperature (110-130 °C) are required for **74i**, **74j-k**, **74m**, **76i**). The resulting mixture was cooled down to room temperature and filtered through a short layer of silica gel over Celite plug with the aid of DCM. The filtrate was concentrated under reduced pressure and purified by column chromatography (Hexanes - **75i-2j**, **77a-f**. Hexanes: EtOAc = 50:1 – **75i**, **75l**, **75p**, **75r**, **77f**, **77j**. Hexanes: EtOAc = 50:1 → 35:1 – **75j-k**, **75m**, **76g-i**.)

<u>Endo Silyl Methyl Heck products of Benzene Tethered Systems, 75a-o:</u>

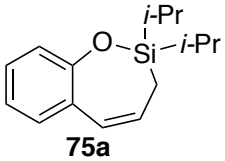

75a

0.2 mmol scale: Isolated yield = 79%, 38.9 mg. Endo:Exo = 33:1 (GC Ratio)

3.8 mmol scale: Isolated yield = 72%, 674 mg. Endo:Exo = 33:1 (GC Ratio)

^{1}H NMR (500 MHz, $CDCl_3$): δ ppm 7.13-7.18 (m, 1H), 7.07-7.10 (m, 1H), 6.93-7.00 (m, 2H), 6.29 (d, *J* = 10.8 Hz, 1H), 6.06-6.13 (m, 1H), 1.63 (d, *J* = 7.6 Hz, 2H), 1.08-1.23 (m, 14H). ^{13}C NMR (126 MHz, $CDCl_3$): δ ppm 12.4, 13.6, 17.5, 17.7, 120.9, 121.6, 126.1, 127.8, 128.1, 130.9, 154.2. HRMS (ESI) calcd. for $C_{15}H_{22}OSi$ [M+H]: 247.1518, found: 247.1520.

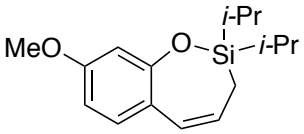

75b

Isolated yield = 87%, 48.1 mg. Endo:Exo = 99: 1 (GC Ratio)

^{1}H NMR (500 MHz, $CDCl_3$): δ ppm 6.96-6.99 (m, 1H), 6.53-6.55 (m, 2H), 6.21 (d, *J* = 11 Hz, 1H), 5.96-5.99 (m, 1H), 3.79 (s, 3H), 1.61 (d, *J* = 7.3 Hz, 2H), 1.06-1.19 (m, 14H). ^{13}C NMR (126 MHz, $CDCl_3$): δ ppm 12.1, 13.6, 17.4, 17.7, 55.3, 106.6, 107.5, 121.0, 125.8, 126.3, 131.6, 155.1, 159.5. HRMS (ESI) calcd. for $C_{16}H_{24}O_2Si$ [M+H]: 277.1624, found: 277.1622.

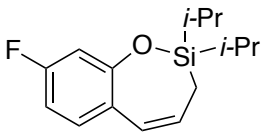

75c

Isolated yield = 74%, 39.1 mg. Endo:Exo = 99:1 (GC Ratio)

^{1}H NMR (500 MHz, $CDCl_3$): δ ppm 6.99-7.00 (m, 1H), 6.65-6.70 (m, 2H), 6.21 (d, *J*= 10.6, 1H), 6.01-6.07 (m, 1H), 1.61 (d, *J* = 7.7 Hz, 2H), 1.06-1.20 (m, 14H). ^{13}C NMR (126 MHz, $CDCl_3$): δ ppm 12.4, 13.6, 17.4, 17.6, 108.2, 108.3, 108.5, 108.6,124.4, 125.3,

127.7, 131.6, 131.7, 155.0. HRMS (ESI) calcd. for $C_{15}H_{21}FOSi$ [M+H]: 265.1413, found: 265.1419.

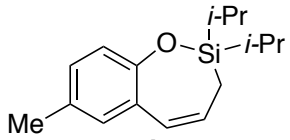

75d

Isolated yield = 76%, 39.5 mg. Endo:Exo = 25:1 (GC Ratio)

^{1}H NMR (500 MHz, $CDCl_3$): δ ppm 6.95-6.97 (m, 1H), 6.88-6.90 (m, 2H), 6.25 (d, *J* = 11 Hz, 1H), 6.06-6.12 (m, 1H), 2.30 (s, 3H), 1.61 (d, *J* = 7.4 Hz, 2H), 1.08-1.20 (m, 14H). ^{13}C NMR (126 MHz, $CDCl_3$): δ ppm 12.3, 13.6, 17.5, 17.7, 20.5, 121.4, 127.9, 128.0, 128.5, 130.1, 131.2, 151.9. HRMS (ESI) calcd. for $C_{16}H_{24}OSi$ [M+H]: 261.1675, found: 261.1668.

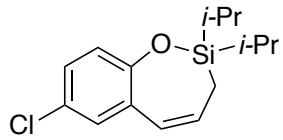

75e

Isolated yield= 72%, 40.4 mg. Endo:Exo = 25:1 (GC Ratio)

^{1}H NMR (500 MHz, $CDCl_3$): δ ppm 7.07-7.09 (m, 1H), 7.04 (s, 1H), 6.88-6.90 (m, 1H), 6.18 (d, *J* = 11 Hz, 1H), 6.09-6.14 (m, 1H), 1.62 (d, *J* = 7.3 Hz, 2H), 1.05-1.18 (m, 14H). ^{13}C NMR (126 MHz, $CDCl_3$): δ ppm 12.4, 13.6, 17.4, 17.7, 122.9, 124.9, 125.7, 127.6, 129.5, 130.2, 152.7. HRMS (ESI) calcd. for $C_{15}H_{21}ClOSi$ [M+H]: 281.1128, found: 281.1132.

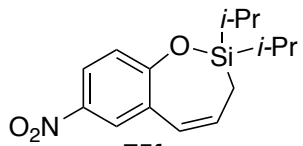

75f

Isolated yield= 33%, 19.2 mg. Endo:Exo = 32:1 (GC Ratio)

^{1}H NMR (500 MHz, $CDCl_3$): δ ppm 8.01-8.03 (m, 2H), 7.01-7.03 (m, 1H), 6.27 (d, *J*= 11, 1H), 6.18-6.23 (m, 1H), 1.66 (d, *J* = 7.3 Hz, 2H), 1.16-1.23 (m, 2H), 1.06-1.10 (m, 12H). ^{13}C NMR (126 MHz, $CDCl_3$): δ ppm 12.6, 13.6, 17.3, 17.5, 122.2, 123.4, 124.5, 127.1, 128.8, 130.5, 141.7, 159.6. HRMS (ESI) calcd. for $C_{15}H_{21}NO_3Si$ [M+H]: 292.1369, found: 292.1372.

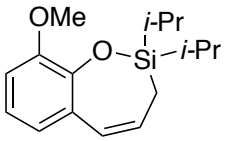

75g

Isolated yield= 90%, 49.7 mg. Endo:Exo = 99:1 (GC Ratio)

^{1}H NMR (500 MHz, $CDCl_3$): δ ppm 6.87-6.90 (m, 1H), 6.76-6.78 (m, 2H), 6.68-6.69 (m, 2H), 6.26 (d, *J* = 11 Hz, 1H), 6.09-6.13 (m, 1H), 3.85 (s, 3H), 1.61 (d, *J* = 7.3 Hz, 2H), 1.07-1.20 (m, 14H). ^{13}C NMR (126 MHz, $CDCl_3$): δ ppm 12.1, 13.6, 17.4, 17.7, 55.8, 110.2, 120.7, 122.5, 125.7, 128.7, 129.4, 143.6, 151.5. HRMS (ESI) calcd. for $C_{16}H_{24}O_2Si$ [M+H]: 277.1624, found: 277.1629.

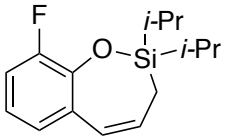

75h

Isolated yield= 74%, 39.1 mg. Endo:Exo = 99:1 (GC Ratio)

^{1}H NMR (500 MHz, $CDCl_3$): δ ppm 6.93-6.97 (m, 1H), 6.82-6.87 (m, 2H), 6.26 (d, *J*= 10.6, 1H), 6.10-6.15 (m, 1H), 1.64 (d, *J* = 7.34 Hz, 2H), 1.07-1.23 (m, 14H). ^{13}C NMR (126 MHz, $CDCl_3$): δ ppm 12.4, 13.6, 17.2, 17.4, 114.0, 114.2, 120.5, 120.6, 125.1,

125.2, 125.63, 125.66, 129.2, 130.8, 142.2, 142.3, 153.8, 155.8. HRMS (ESI) calcd. for $C_{15}H_{21}FOSi$ [M]: 265.1424, found: 265.1424.

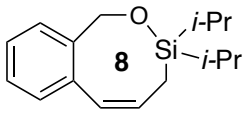

75i

Isolated yield= 60%, 31.2 mg. Endo:Exo:Hydrodehalogenation = 92:0:8 (GC Ratio)

^{1}H NMR (500 MHz, $CDCl_3$): δ ppm 7.47-7.49 (m, 1H), 7.28-7.32 (m, 2H), 7.15-7.16 (m, 1H), 6.50 (d, *J* = 11.0 Hz, 1H), 6.06-6.11 (m, 1H), 4.71 (s, 2H), 1.40 (d, *J* = 8.4 Hz, 2H), 0.99-1.10 (m, 14H). ^{13}C NMR (126 MHz, $CDCl_3$): δ ppm 12.2, 14.5, 17.3, 17.4, 65.2, 126.3, 127.2, 127.9, 128.0, 130.1, 131.1, 137.8. HRMS (ESI) calcd. for $C_{16}H_{24}OSi$ [M+H]: 261.1675, found: 261.1677.

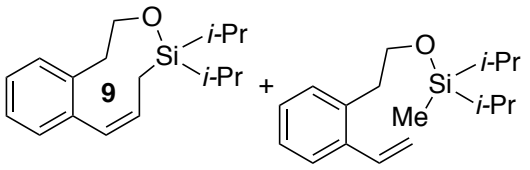

75j : **75j'**

Isolated yield= 33% of compound A, 18 mg. Total yield = 53%, 29 mg.

Endo: Exo: Dehal = 1.6 : 0 : 1 (NMR Ratio)

^{1}H NMR (500 MHz, $CDCl_3$): δ ppm 7.00-7.35 (m, 4H), 6.44 (d, *J* = 10.8 Hz, 1H), 6.06-6.11 (m, 1H), 4.10-4.13 (t, *J*=7.15 Hz, 2H), 2.83-2.87 (t, *J*=7.15 Hz, 2H) 1.38 (d, *J* = 8.4 Hz, 2H), 0.93-1.1 (m, 14H).^{13}C NMR (126MHz, $CDCl_3$): δ ppm 12.9, 15.7, 17.5, 17.7, 65.1, 126.1, 126.9, 127.2, 128.6, 129.4, 130.0, 131.5, 139.3. HRMS (EI) calcd. for $C_{17}H_{26}OSi$ [M+H]: 275.1831, found: 275.1829.

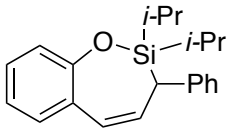

75k

Isolated yield= 67%, 43.2 mg. Endo:Exo = >99 : 1 (GC Ratio).

^{1}H NMR (500 MHz, $CDCl_3$): δ ppm7.29-7.32 (m, 2H), 7.13-7.25 (m, 4H), 6.98-7.06 (m, 3H), 6.33-6.36 (m, 1H), 6.25-6.30 (m, 1H), 3.41-3.43 (m, 1H), 1.07-1.37 (m, 14H).^{13}C NMR (126 MHz, $CDCl_3$): δ ppm 12.4, 14.3, 17.3, 17.5, 18.0, 18.8, 36.9, 121.1, 121.6, 123.9, 125.3, 127.7, 127.8, 128.2, 128.3, 128.7, 130.9, 134.3, 140.7, 154.1. HRMS (EI) calcd. for $C_{21}H_{26}OSi$ [M+H]: 322.1753, found: 322.1756.

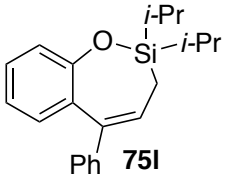

75l

Isolated yield = 96%, 62 mg. Endo:Exo = 100: 0 (GC Ratio)

^{1}H NMR (500 MHz, $CDCl_3$): δ ppm 7.20-7.30 (m, 6H), 7.06-7.07 (m, 1H), 6.91-6.96 (m, 2H), 6.34 (t, *J*= 8.1, 1H), 1.74 (d, *J* = 8.1 Hz, 2H), 1.16-1.24 (m, 2H), 1.09-1.11 (d, 12H). ^{13}C NMR (126 MHz, $CDCl_3$): δ ppm 13.4, 13.5, 17.5, 17.8, 121.3, 121.6, 126.0, 126.5, 128.0, 128.3, 130.7, 131.9, 137.1, 143.9 154.9. HRMS (ESI) calcd. for $C_{21}H_{26}OSi$ [M+H]: 323.1831, found: 323.1830.

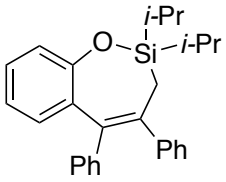

75m

Isolated yield = 64%, 51 mg. Endo:Exo = 100:0 (GC Ratio)

^{1}H NMR (500 MHz, $CDCl_3$): δ ppm 6.84-7.34 (m, 14H), 0.88-1.33 (m, 16H). ^{13}C NMR (126 MHz, $CDCl_3$): δ ppm 17.5, 17.8, 21.3, 121.9, 122.1, 125.8, 126.2,127.5, 127.7, 128.1, 128.4, 129.7, 130.1, 131.7, 132.6, 133.6, 133.9, 137.3, 143.9, 144.1. HRMS (ESI) calcd. for $C_{27}H_{30}OSi$ [M+H]: 398.2066, found: 398.2071.

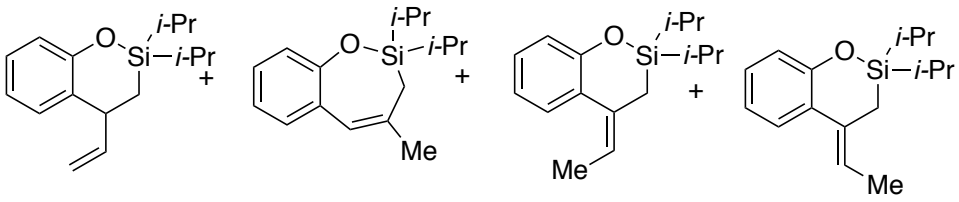

75n : 75n' : 75n'' : 75n'''

Isolated = 78%, 40.6 mg. Ratio = 4.8 : 3.8 : 1.4 : 1

^{1}H NMR (500 MHz, $CDCl_3$): δ ppm only olefinic proton were analyzed: **75n'** = 6.10 (s, 3.8H), **75n'''**= 5.66-5.71 (m, 1H), **75n''**=5.50 – 5.55 (m, 1.4H), **75n**= 5.08-5.17 (m, 4.8H). ^{13}C NMR (500 MHz, $CDCl_3$): δ ppm – See below. HRMS (ESI) calcd. for $C_{16}H_{24}OSi$ [M]+H: 261.165, found: 261.1672

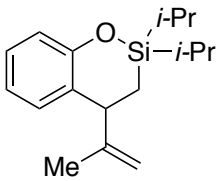

75o

Isolated yield = 76%, 41.7 mg. Endo:Exo = 0:100 (GC Ratio)

^{1}H NMR (500 MHz, $CDCl_3$): δ ppm 7.11-7.14 (m, 1H), 6.99-7.01 (m, 1H), 6.90-6.92 (m, 1H), 6.84-6.88 (m, 1H), 5.01(s, 1H), 4.87 (s, 1H), 3.64 (dd, *J*=11.9, 4.2 Hz, 1H), 1.85 (s, 3H), 0.99-1.24 (m, 16H). ^{13}C NMR (126 MHz, $CDCl_3$): δ ppm 11.1, 12.8, 13.2, 16.9, 17.1, 17.3, 19.8, 43.5,112.9, 119.6, 120.5, 127.6, 127.9, 130.9, 147.9, 155.4. HRMS (ESI) calcd. for $C_{17}H_{26}OSi$ [M+H]: 275.1831, found: 275.1828

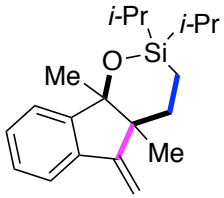

82

Isolated yield = 87%, 54.7 mg.

^{1}H NMR (500 MHz, $CDCl_3$): δ ppm 7.44-7.46 (m, 2H), 7.23-7.32 (m, 2H), 5.47 (s, 1H), 4.89 (s, 1H), 1.78-1.86 (m, 1H), 1.68-1.75 (m, 1H), 1.31 (s, 3H), 1.25 (s, 3H), 1.09 -1.11 (d, 3H), 1.02-1.03 (d, 3H), 0.76-0.80 (m, 7H), 0.64-0.73 (m, 2H), 0.54-0.61 (m, 1H). ^{13}C NMR (126 MHz, $CDCl_3$): δ ppm 1.4, 13.2, 13.4, 16.9, 17.1, 17.3, 17.5, 20.7, 28.0, 33.3, 51.2, 84.32, 102.2, 120.5, 123.4, 127.6, 128.6, 137.5, 150.6. HRMS (EI) calcd. for $C_{20}H_{30}O_2Si$ [M+H]: 315.2144, found: 315.2145.

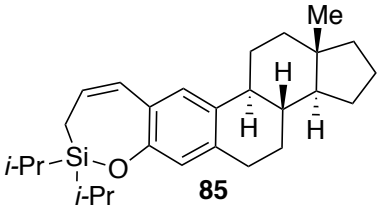

85

Isolated yield = 82%, 67 mg. Endo:Exo = 99:1 (GC Ratio)

^{1}H NMR (500 MHz, $CDCl_3$): δ ppm 6.99 (s, 1H), 6.70 (s, 1H), 6.24 (d, J=11 Hz, 1H), 5.98-6.03 (m, 1H), 2.82 (t, 2H), 2.19-2.29, (m, 2H), 1.86-1.93 (m, 2H), 1.65-1.78 (m, 3H) 1.61 (d, *J*= 7.7 Hz, 2H), 1.49-1.56 (m, 3H), 1.31-1.40 (m, 3H), 1.21-1.30 (m, 3H), 1.06-1.18 (m, 14H) 0.75 (s, 3H). ^{13}C NMR (126MHz, $CDCl_3$): δ ppm 12.4, 13.6, 13.7, 17.5, 17.6, 17.7, 20.6, 25.2, 26.7, 28.2, 29.4, 38.9, 39.1, 40.5, 41.1, 44.0, 53.6, 121.2, 125.3, 126.5, 127.1, 127.8, 133.3, 136.8, 151.8. HRMS (EI) calcd. for $C_{27}H_{40}OSi$ [M+H]: 408.2848, found: 408.2854.

Endo Silyl Methyl Heck Reaction Products of Aliphatic Systems, 77a-j:

2,2-diisopropyl-7-propyl-2,3,4,7-tetrahydro-1,2-oxasilepine, **4a**:

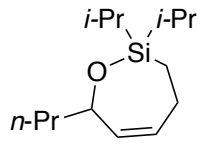

77a

Isolated yield = 65%, 31.2 mg. Endo: Exo = >50 : 1 (GC Ratio).

^{1}H NMR (500 MHz, $CDCl_3$): δ ppm 5.81-5.85 (m, 1H), 5.47-5.52 (m, 1H), 3.91-3.94 (m, 1H), 2.17-2.32 (m, 2H), 1.57-1.64 (m, 2H), 1.42-1.53 (m, 2H), 1.30-1.39 (m, 2H), 0.98-1.09 (m, 12H), 0.88-0.92 (m, 3H). ^{13}C NMR (126 MHz, $CDCl_3$): δ ppm 11.6, 12.9, 13.1, 14.1, 17.5, 17.6, 17.7, 19.1, 36.9, 40.9, 72.3, 126.0, 127.5. HRMS (ESI) calcd. for $C_{14}H_{28}OSi$ [M+H]: 241.1988, found 241.1991.

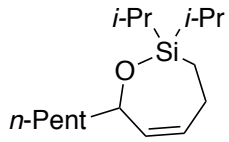

77b

Isolated yield = 76% 40.8 mg. Endo:Exo = 36:1 (GC Ratio)

^{1}H NMR (500 MHz, $CDCl_3$): δ ppm 5.81-5.85 (m, 1H), 5.47-5.51 (m, 1H), 3.89-3.93 (m, 1H), 2.19-2.31 (m, 2H), 1.58-1.63 (m, 2H), 1.41-1.52 (m, 2H), 1.26-1.38 (m, 10H), 0.98-1.09 (m, 14H), 0.87-0.92 (m, 5H). ^{13}C NMR (126MHz, $CDCl_3$): δ ppm 11.6, 12.9, 13.2, 14.1, 17.5, 17.6, 17.7, 22.7, 25.6, 29.7, 31.8, 36.9, 38.7, 72.6, 126.0, 127.6. HRMS (ESI) calcd.for $C_{16}H_{32}OSi$ [M+H]: 269.2301, found: 269.2302.

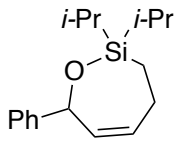

77c

Isolated yield = 83%, 45.5 mg, isomers are separable.

^{1}H NMR (500 MHz, $CDCl_3$): δ ppm 7.40 (d, *J* =7.34 Hz, 2H), 7.34 (t, *J* =7.34 Hz, 2H), 7.23-7.26 (m, 1H), 5.92-5.97 (m, 1H), 5.53-5.58 (m, 1H), 5.11 (d, *J* =9.2 Hz 1H), 2.56-2.62 (m, 1H), 2.45-2.50 (m, 1H), 1.75-1.80 (m, 1H), 1.66-1.71 (m, 1H), 0.99-1.21 (m, 14H). ^{13}C NMR (500 MHz, $CDCl_3$): δ ppm 11.6, 12.9, 13.1, 17.6, 17.7, 17.8, 40.1, 74.3, 125.3, 125.8, 126.7, 128.0, 128.2, 145.8. HRMS (ESI) calcd. for $C_{17}H_{26}OSi$ [M+H]: 275.1831, found: 275.1825.

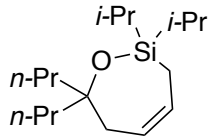

77d

Isolated yield= 80%, 45.2 mg. Endo:Exo = 25:1 (GC Ratio)

^{1}H NMR (500 MHz, $CDCl_3$): δ ppm 5.90-5.95 (m, 1H), 5.44-5.50 (m, 1H), 2.27 (d, *J*= 7.7 Hz, 2H), 1.59 (d, *J*=6.97 Hz, 2H), 1.43-1.47 (m, 1H), 1.20-1.47 (m, 6H), 1.07-1.11 (t, 4H), 0.99-0.98 (m, 12H), 0.89 (t, *J*=7.34 Hz, 6H). ^{13}C NMR (126 MHz, $CDCl_3$): δ ppm: 12.0, 13.1, 13.9, 14.8, 17.3, 17.4, 17.70, 17.73, 74.3, 38.0, 42.0, 77.2, 124.5, 129.3. HRMS (ESI) calcd. for $C_{17}H_{34}OSi$ [M]+H: 283.2457, found: 283.2461.

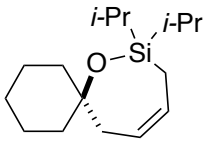

77e

Isolated yield= 75%, 39 mg. Endo:Exo = 16:1 (NMR Ratio)

^{1}H NMR (500 MHz, $CDCl_3$): δ ppm 5.90-5.95 (m, 1H), 5.47-5.52 (m, 1H), 2.27 (d, *J*= 7.7 Hz, 2H), 1.58-1.68 (m, 6H), 1.16-1.42(m, 6H), 0.99-1.01 (dd, 12H), 0.86-0.91 (m,

2H), 1.04-1.21 (m, 14H). ^{13}C NMR (126MHz, $CDCl_3$): δ ppm 11.8, 13.9, 13.1, 17.4, 17.5, 17.7, 17.8, 22.3, 26.2, 38.8, 40.1, 73.6, 124.2, 129.1. HRMS (ESI) calcd. for $C_{16}H_{30}OSi$ [M]+H: 267.2144, found: 267.2146.

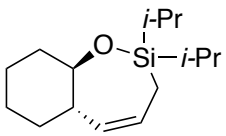

77f

Isolated yield= 71%, 35.8 mg. Endo:Exo = 50:1 (GC Ratio)

^{1}H NMR (500 MHz, $CDCl_3$): δ ppm 5.72-5.77 (m, 1H), 5.11-5.14 (m, 1H), 3.58-3.62 (m, 1H), 2.23 (d, *J*= 7.7 Hz, 1H), 1.98-2.01 (m, 1H), 1.50-1.74 (m, 5H), 1.09-1.35 (m, 4H) 0.88-1.02 (m, 14H). ^{13}C NMR (126 MHz, $CDCl_3$): δ ppm 11.3, 12.2, 13.23, 13.8, 17.5, 17.7, 17.8, 25.1, 25.5, 32.6, 36.4, 46.4, 75.2, 125.2, 132.5. HRMS (ESI) calcd. for $C_{15}H_{28}OSi$ [M+H]: 253.1988, found: 253.1990.

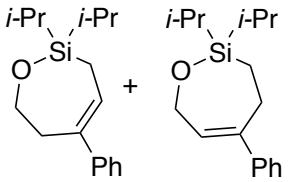

77g : **77g'**

Isolated yield= 80%, 44 mg. **77g** : **77g'** = 7: 1 (NMR Ratio)

^{1}H NMR (500 MHz, $CDCl_3$): δ ppm 7.29-7.36 (m, 5H), 6.23 (t, *J*=7.45 Hz, 1H), 4.07 (t, *J* = 5.3 Hz, 2H), 2.87 (t, *J* = 5.3 Hz 2H), 1.83 (d, *J*=7.6 Hz, 2H), 0.98-1.07 (m, 14H). ^{13}C NMR (126 MHz, $CDCl_3$): δ ppm 13.1, 17.6, 17.7, 34.9, 63.6, 125.5, 126.1, 126.3, 128.3, 137.4, 143.5. HRMS (ESI) calcd. for $C_{17}H_{26}OSi$ [M+H]: 275.1831, found: 274.1833

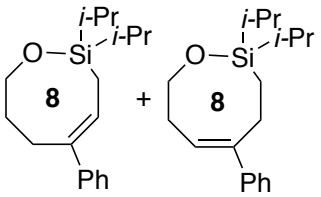

77h : **77h'**

Isolated yield= 85%, 49 mg. **77h** : **77h'** = 17 : 1 (NMR Ratio)

^{1}H NMR (500 MHz, $CDCl_3$): δ ppm 7.38-7.40 (m, 2H), 7.29-7.34 (m, 2H), 7.20-7.23 (m, 1H), 6.20 (t, *J*=8.18 Hz, 1H), 3.72 (t, *J*=5.3 Hz, 2H), 2.72 (t, *J*=5.3 Hz, 2H), 1.81 (d, *J*=8.5 Hz, 2H), 1.72-1.78 (m, 2H), 1.08-1.15 (m, 12H), 0.94-1.04 (m, 2H). ^{13}C NMR (126 MHz, $CDCl_3$): δ ppm 12.6, 14.85, 17.6, 17.8, 24.5, 30.2, 60.6, 124.9, 125.6, 126.3, 128.4, 135.9, 142.1. HRMS (EI) calcd. for $C_{18}H_{28}OSi$ [M]: 289.1988, found: 289.1992.

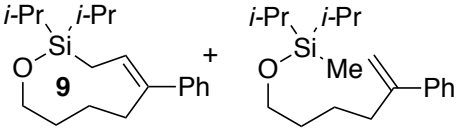

77i : **77i'**

Total yield = 88%, 53.2 mg. **77i** : **77i'** = 1 : 1 (NMR Ratio), Yield of **77i** = 44%, 26.6 mg. ^{1}H NMR (500 MHz, $CDCl_3$): δ ppm -only olefinic proton were analyzed: **77i** = 5.61 (t, *J*=8.8 Hz, 1H), **77i'**= 5.28 (s, 1H), **77i'**=5.07 (s, 1H), ^{13}C NMR (126 MHz, $CDCl_3$): δ ppm – See below. HRMS (ESI) calcd. for $C_{19}H_{30}OSi$ [M]: 303.2144, found: 303.2142.

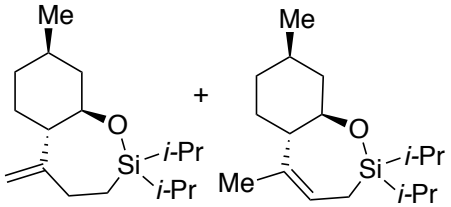

77j : **77j'**

Total yield = 90%, 50 mg. **77j** : **77j'** = 3.5 : 1 (NMR Ratio).

Isomers are separable. Yield of **77j** = 45%, 25.2 mg.

^{1}H NMR (500 MHz, $CDCl_3$): δ ppm of **4j** = 4.84 (s, 2H), 4.80 (s, 1H), 3.51-3.56 (m, 1H), 2.33-2.39 (m, 1H), 2.21-2.26 (m, 1H), 1.93-2.05 (m, 2H) 1.55-1.64 (m, 2H), 1.42-1.46 (m, 1H), 1.26-1.36 (m, 1H), 0.91-1.11 (m, 19H), 0.76-0.83 (m, 2H). ^{13}C NMR (126 MHz, $CDCl_3$): δ ppm 11.8, 12.8, 13.7, 17.3, 17.5, 17.9, 22.1, 29.5, 31.7, 31.8, 34.5, 44.7, 53.3, 74.9, 111.7, 155.4. HRMS (ESI) calcd. for $C_{17}H_{32}OSi$ [M]+H: 281.2301, found: 281.2302.

3.3. Further Transformations of Obtained Siloxycyclic Products

Ring opening:

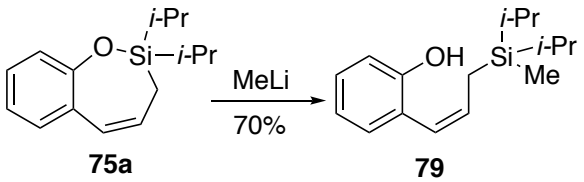

75a **79**

A 50 mL Schlenk flask equipped with a magnetic stir bar under Ar atmosphere was charged with compound **2a** (0.611 g, 2.48 mmol, 1 eq) and 14 mL of dry THF. The mixture was cooled to -78 °C and 4.65 mL (7.44 mmol, 3 eq) MeLi in diethylether (1.6 M in Et_2O) was added drop-wise via syringe. Then, the reaction mixture was stirred at r.t. for 2 h. Upon completion (monitored by GC), the reaction was quenched with NH_4Cl solution (20 mL) at 0 °C and 35 mL of CH_2Cl_2 was added. The aqueous layer was extracted 3x with 30 mL of CH_2Cl_2. The combined extracts were washed with brine and then dried with Na_2SO_4. The organic layer was concentrated *in vacuo* and the crude product was purified by silica gel column chromatography (EA: Hexanes – 1:50) to produce compound **79** as a clear and colorless oil.

Isolated yield = 70%, 456 mg.

^{1}H NMR (500 MHz, $CDCl_3$): δ ppm 7.16 (t, J = 7.3 Hz, 1 H), 7.09 (d, J = 7.3 Hz, 1 H), 6.92 - 6.87 (m, 2 H), 6.21 (d, J = 11.2 Hz, 1 H), 6.05 - 6.00 (m, 1 H), 5.16 (s, 1 H), 1.61 (dd, J = 8.4, 1.1 Hz, 2 H), 0.91-0.88 (m, 12 H), 0.12 (s, 3H). ^{13}C NMR (126 MHz, $CDCl_3$): δ ppm 9.2, 11.8, 14.3, 17.9, 114.9, 120.7, 128.4, 129.7, 134.3. HRMS (EI) calcd. for $C_{16}H_{27}OSi$ [M+H]: 263.1831, found: 263.1833.

Intramolecular Hosomi-Sakurai Reaction:

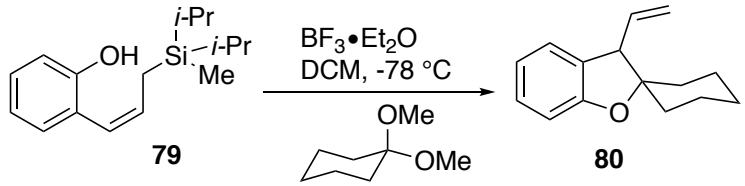

A 2 mL vial equipped with a magnetic stir bar under Ar atmosphere was charged with compound **11** (100 mg, 0.38 mmol) and 1,1-dimethoxycyclohexane (66 mg, 0.46 mmol) with 1 mL of CH_2Cl_2. The reaction mixture was cooled to -78 °C, followed by addition of boron trifluoride diethyl etherate (108 mg, 0.76 mmol). The reaction mixture was stirred at r.t. for 60-90 min. Upon the completion (monitored by GC), the reaction was quenched with 5% $NaHCO_3$ solution (2 mL). The aqueous layer was extracted 3x3 mL of CH_2Cl_2. The combined organic layers was then washed with brine and dried with Na_2SO_4. The organic layer was concentrated *in vacuo* and the crude product was purified bysilica gel column chromatography (EA:Hexanes = 1:100) to produce **80** as a clear and colorless oil (91%, 74 mg).

^{1}H NMR (500 MHz, $CDCl_3$): δ ppm 7.13 (t, *J* = 7.7 Hz, 1 H), 7.05 (d, *J* = 7.4 Hz, 1 H), 6.83 (dt, J = 7.3, 0.7 Hz, 1 H), 6.78 (d, *J* = 7.7 Hz, 1 H), 5.88-5.81 (m, 1 H), 5.21 - 5.17

(m, 2 H), 3.62 (d, J = 9.5 Hz, 1 H), 1.89-1.26 (m, 10 H). ^{13}C NMR (126 MHz, $CDCl_3$):δ ppm 22.2, 22.7, 25.4, 32.1, 37.1, 56.8, 90.6, 109.8, 117.4, 120.0, 125.4, 128.4, 130.0, 136.0, 158.3. HRMS (EI) calcd. for $C_{15}H_{19}O$ [M+H]: 215.1436, found: 215.1434.

Tamao oxidation of 75a and 85:

A 10 mL flask, containing a stirring bar, was charged with **75a** (24.6 mg, 0.1 mmol) or **85** (40.8 mg, 0.1 mmol), $KHCO_3$ (100 mg, 1 mmol), and DMF (1 mL) and 50%. H_2O_2 (80 μL) was added via syringes under Ar atmosphere. The reaction mixture was heated at 70 °C for 6 h. The reaction was then cooled to room temperature, followed by addition of KF on Al_2O_3 (36.5 mg, 0.3 mmol). The reaction mixture was stirred for another 4h at room temperature. The product was purified by silica gel column chromatography (eluent: hexanes/AcOEt 4:1-1:1) to give **78** or **86** as white solids.

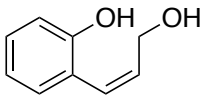

78

Yield= 87%, 13 mg.

^{1}H NMR (500 MHz, DMSO-d_6) δ ppm 9.46 (s, 1 H), 7.07 (t, J = 7.7 Hz, 1 H), 7.01 (d, J = 7.4 Hz, 1 H), 6.81 (d, J = 8.0 Hz, 1 H), 6.75 (t, J = 7.3 Hz, 1 H), 6.51 (d, J = 12.2 Hz, 1 H), 5.74 - 5.69 (m, 1 H), 4.76 (t, J = 5.2 Hz, 1 H), 4.15-4.12 (m, 2 H). ^{13}C NMR (126 MHz, DMSO-d_6) δ ppm 58.7, 115.6, 118.9, 123.9, 124.9, 128.9, 130.4, 132.5, 155.4. HRMS (EI) calcd. for $C_9H_{10}O_2$ [M]: 150.0681, found: 150.0679.

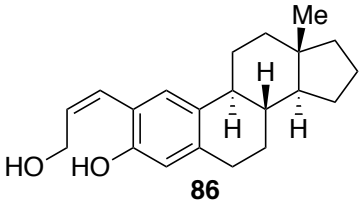

86

Yield after extraction = 80%, 25 mg.

A small portion was recrystallized in DCM for NMR spectra.

^{1}H NMR (500 MHz, DMSO-d_6): δ ppm 9.12 (s, 1H), 6.90 (s, 1H), 6.48 (s, 1H), 6.46 (s, 1H), 5.62-5.67 (m, 1H), 4.73 (t, *J*=5.14 Hz, 1H),) 4.14 (t, *J*=5.32 Hz, 3H), 2.65-2.71 (m, 2H), 2.49 (s, 2H), 2.20-2.23 (d, 1H), 2.09-2.12 (t, 1H), 1.80 (d, *J*=10.6 Hz, 2H), 1.59-1.71 (m, 3H), 1.43-1.47 (m, 1H), 1.26-1.37 (m, 3H), 1.16-1.26 (m, 4H), 1.06-1.12 (m, 1H), 0.7 (s, 3H). ^{13}C NMR (126 MHz, DMSO-d_6): δ ppm 17.9, 20.6, 25.2, 26.9, 28.1, 29.4, 30.9, 38.8, 39.3, 41.1, 43.8, 53.4, 58.8, 115.3, 121.4, 125.2, 125.4, 127.2, 130.5, 131.5, 131.9, 136.9, 153.0. HRMS (ESI) calcd. For $C_{21}H_{28}O_2$ [M+Na]: 325.1987, found: 325.1986.

Woerpel oxidation of 82 leading to 83:

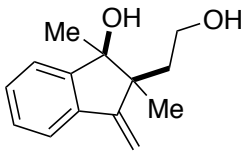

83

To an ice-cooled (0 °C) stirred solution of KH (57.8 mg, 1.44 mmol, dry powder, 95%.) in 1.5 mL of NMP was added *tert*-butyl hydroperoxide (0.22 mL, 5.0 ~ 6.0 M in decane) dropwise. The mixture was allowed to warm up to room temperature and kept for 10 min, then was added a solution of **82** (38 mg, 0.12 mmol) in 1.2 mL of NMP. The mixture was stirred overnight and then 1.5 mL TBAF (0.6mmol, 1.0 M solution in THF) was added. The mixture was stirred for another 3h and cooled to 0°C. 1.0 g of $Na_2S_2O_3$•$5H_2O$ and 5.0 mL of water were added. The mixture was stirred at 0°C for 30 min and neutralized of addition of NH_4Cl. The mixture was extracted with diethyl ether (3 × 50 mL). The combined organic layers were washed with H_2O (4 × 10 mL) and brine (10 mL), dried (Na_2SO_4), and concentrated. Flash silica gel column chromatography (1:2 - 1:1

EtOAc/hexanes) purification of the residue gave **83** as a white solid.

Isolated yield = 82%, 22 mg.

^{1}H NMR (500 MHz, $CDCl_3$): δ ppm 7.44 (dd, J=13.57, 7.70 Hz, 2 H), 7.24-7.32 (m, 2 H), 5.55 (s, 1 H), 4.94 (s, 1 H), 3.53-3.59 (m, 1 H), 3.31 - 3.37 (m, 1 H), 2.00-2.07 (m, 1 H), 1.61 (ddd, J=14.7, 5.7, 2.9 Hz, 1 H), 1.31 (s, 3 H), 1.26 (br. s, 1H), 1.24 (s, 3 H) ^{13}C NMR (126 MHz, $CDCl_3$): δ ppm 21.9, 26.9, 41.7, 59.3, 81.8, 103.4, 120.2, 122.9, 128.1, 129.1, 150.6, 154.9. HRMS (APCG) calcd. for $C_{14}H_{28}O_2$ [M-H_2O]: 200.1201, found 200.1207.

3.4. Mechanistic Experiments

Radical Clock Experiments:

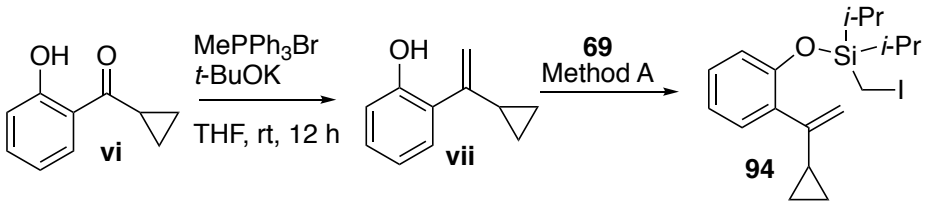

To a suspension of $MePPh_3Br$ (8.8 equiv) in THF (50 mL), *t*-BuOK was added in one portion (8.8 equiv) and the resulting mixture was stirred at room temperature 2 h. The reaction mixture was cooled to -78 °C and **vi**[51] (1.0 equiv) was added over 10 min. The mixture was stirred overnight at room temperature. A saturated ammonium chloride solution was added and the aqueous phase was extracted with ether (3 x 50 mL). The organic phase was dried over Na_2SO_4, filtered and concentrated. The compound was purified by flash (20:1 Hex:EtOAc) to give **vii** a clear/yellow oil.

Isolated yield = 28%, 180 mg.

^{1}H NMR (500 MHz, $CDCl_3$) δ ppm 7.19 (dt, J = 7.3, 1.5 Hz, 1 H), 7.14 (dd, J = 7.6, 1.8 Hz, 1 H), 6.93 (dd, J = 8.2, 0.6 Hz, 1 H), 7.14 (dt, J = 7.3, 1.2 Hz, 1 H), 5.63 (s, 1 H),

5.30 (s, 1 H), 5.05 (d, J = 1.2 Hz, 1 H), 1.68 - 1.59 (m, 1 H), 0.82 - 0.77 (m, 2 H), 0.56 - 0.52 (m, 2 H).[13]C NMR (126 MHz, $CDCl_3$) δ ppm 152.4, 147.3, 128.9, 128.8, 119.9, 115.3, 112.8, 17.1, 6.81.HRMS (EI) calcd. for $C_{17}H_{29}OSi$ [M]+: 277.1988, found: 277.1984.

Synthesis of **94** was obtained via coupling of **vii** with **69** using Method A.

Isolated Yield: 70%, 870 mg.

[1]H NMR (500 MHz, $CDCl_3$) δ ppm 7.18-7.15 (m, 2 H), 6.95 (t, J = 7.3 Hz, 1 H), 6.87 (d, J = 8.5 Hz, 1 H), 5.08 (s, 1 H), 4.96 (s, 1 H), 2.26 (s, 2H), 1.78 - 1.75 (m, 1 H), 1.46 - 1.40 (m, 2 H), 1.17 (d, J = 7.3 Hz, 6 H), 1.13 (d, J = 7.3 Hz, 6 H), 0.73 - 0.70 (m, 2 H), 0.52 – 0.48 (m, 2 H). [13]C NMR (126 MHz, $CDCl_3$) δ ppm 7.0, 12.6, 16.9, 17.4, 17.7, 111.3, 119.3, 121.4, 128.1, 130.5, 133.7, 149.6, 152.0. HRMS (ESI) calcd. for $C_{18}H_{27}OISi$ [M]+H: 414.0954, found: 414.0952

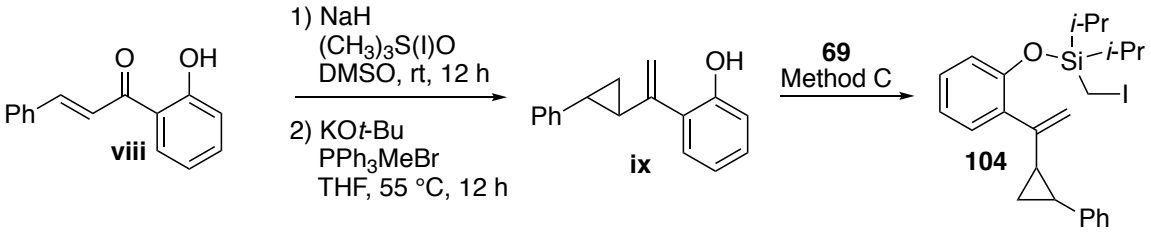

To a 100 mL flask equipped with a magnetic stir bar, argon inlet, and septum, NaH (1.06 g, 44 mmol) and trimethylsulfoxonium iodide (9.68 g, 44 mmol) was added. Followed by slow addition of DMSO (30 mL) and stirred at r.t. for 30 min. After H_2 evolution, 2'-Hydroxychalcone **viii** in 10 mL DMSO was added slowly. The reaction was stirred overnight at r.t. Then, the reaction was quenched by addition of 50 mL H_2O and extracted 3x with 30 mL Et_2O. The organic phase was dried over Na_2SO_4, filtered and concentrated. The compound was purified by column chromatography (20:1 Hex:EtOAc) to give cyclopropane derivative as a clear/yellow oil (44%, 2.72 g). Next, *t*-BuOK was

added to a suspension of $MePPh_3Br$ (2.2 equiv, 7.2 g, 20.1 mmol) in THF (30 mL) in one portion (2.2 equiv, 2.26 g, 20.1) and the resulting mixture was stirred at room temperature 2 h. The reaction mixture was cooled to 0 °C and cyclopropane derivative (1.0 equiv, 2.72 g, 8.76 mmol) in 10 mL THF was added over 10 min. The mixture was stirred overnight at 55 °C. A saturated ammonium chloride solution was added and the aqueous phase was extracted with ether (3 x 50 mL). The organic phase was dried over Na_2SO_4, filtered and concentrated. The compound was purified by flash (20:1 Hex:EtOAc) to give **ix** clear/yellow oil (41%, 857 mg). ^{1}H NMR (500 MHz, $CDCl_3$) δ ppm 7.27-7.30 (m, 2H), 7.10-7.22 (m, 6H), 6.94-6.96 (m, 1 H), 6.88-6.91 (m,1H), 5.54 (s, 1 H), 5.40 (s, 1 H), 5.14 (s, 1 H), 2.00-2.03 (m, 1 H), 1.93-1.97 (m, 1H) , 1.96-2.05 (m, 1 H), 1.24-1.29 (m, 2 H). ^{13}C NMR (126 MHz, $CDCl_3$) δ ppm 152.41, 146.1, 141.8, 129.0, 128.9, 128.5, 125.9, 125.8, 120.1, 115.5, 113.5, 29.3, 25.6, 15.9. HRMS (ESI) calcd. for $C_{17}H_{16}OSi$ [M]+H: 237.1279, found: 237.1278.

Synthesis of **104** was obtained via coupling of **ix** with **69** using Method C.

Isolated yield = 47%, 691 mg.

^{1}H NMR (500 MHz, $CDCl_3$) δ ppm 7.23-7.26 (t, *J*=8.8 Hz, 2H), 7.12-7.16 (m, 3H), 7.07 (d, *J*=8.8 Hz, 2H), 6.92-6.95 (td, *J*=7.7, 1.1 Hz, 1H), 6.83-6.85 (d, *J*=8.5, 1H), 5.15 (s, 1H), 5.02 (s, 1H), 2.19 (s, 2 H), 2.02-2.06 (m, 1H), 1.93-1.97 (m, 1H), 1.35-1.41 (m, 2H), 1.15-1.22 (m, 2H), 1.06-1.12 (m, 14H).^{13}C NMR (126 MHz, $CDCl_3$) δ ppm 12.6, 17.3, 17.7, 25.7, 29.1, 111.9, 119.3, 121.4, 125.5, 125.8, 128.2, 128.3, 130.5, 133.3, 142.8, 148.2, 152.1. HRMS (ESI) calcd. for $C_{24}H_{31}OISi$ [M+H]: 491.1268, found: 491.1267.

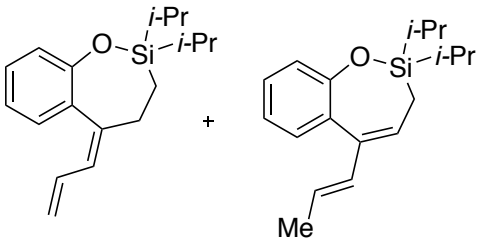

96 : 97

Isolated yield= 58%, 33.2 mg. Endo:Exo = >99 : 1 (GC Ratio), **96**: **97** = 1:1, Isomers are separable.

Running the reaction at 110 °C for 36 h: Isolated yield = 68%, 38.9 mg, **96**:**97** = 0:100

96

^{1}H NMR (500 MHz, $CDCl_3$): δ ppm 7.13-7.19 (m, 2H), 6.88-7.00 (m, 2H), 6.70-6.78 (m, 1H), 6.14-6.20 (m, 1H), 4.91-5.32 (m, 2H), 2.67-2.74 (m, 2H), 0.97-1.22 (m, 16H). HRMS (EI) calcd. for $C_{17}H_{26}OSi$ [M]+H: 286.1753, found: 286.1750.

97

^{1}H NMR (500 MHz, $CDCl_3$): δ ppm 7.24 (d, *J*=7.70 Hz, 1H), 7.18 (t, *J*=7.70 Hz, 1H), 6.96-7.01 (m, 2H), 6.17 (d, *J*=15.4 Hz, 1H), 5.97 (t, *J*=8.1 Hz, 1H), 5.46 (dd, *J*=15.22, 6.79 Hz, 1H), 1.73 (d, J=6.6 Hz, 3H), 1.57 (d, J=8.07 Hz, 2H) 1.06-1.17 (m, 14H).^{13}C NMR (126 MHz, $CDCl_3$): δ ppm 12.6, 13.3, 17.5, 17.7, 18.2, 120.9, 121.8, 124.3, 125.7, 128.1, 128.7, 131.3, 133.9, 135.1, 154.1. HRMS (EI) calcd. for $C_{18}H_{26}OSi$ [M]+H: 286.1753, found: 286.1753.

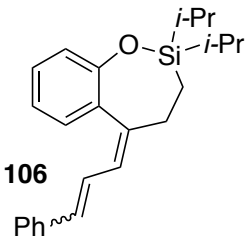

Isolated yield = 91%, 66 mg. *E*:*Z* = 7 : 1

^{1}H NMR (500 MHz, $CDCl_3$): δ ppm 7.52 (d, *J*=7.7 Hz, 2H), 7.39 (t, *J*=7.7 Hz, 2H), 7.19-7.30 (m, 5H), 6.95-6.98 (m, 2H), 6.69 (d, *J*=15.8 Hz, 1H), 6.38 (d, *J*=11.0 Hz, 1H), 2.87-2.90 (m, 2H), 1.15-1.18 (m, 2H), 1.04-1.14 (m, 14H). ^{13}C NMR (126 MHz, $CDCl_3$): δ ppm 10.4, 13.2, 17.1, 17.2., 26.1, 120.9, 121.2, 124.7, 126.4, 126.5, 127.5, 128.6, 128.7, 129.1, 129.9, 133.3, 153.6. HRMS (ESI) calcd. for $C_{24}H_{30}OSi$ [M]+H: 363.2144, found: 363.2139.

Deuterium Labeled Study:

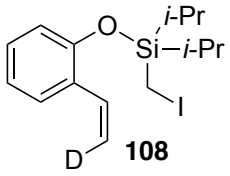

108

Coupling of (*Z*)-2-(vinyl-2-*d*)phenol[52] with **69** using Method A.

Isolated yield= 51%, 574 mg. 88% D-incorporation.

^{1}H NMR (500 MHz, $CDCl_3$): δ ppm 7.50 (m, 1 H), 7.12-7.15 (m, 1 H), 7.07-7.09 (m, 1H), 6.96 (t, J = 7.3 Hz, 1 H), 6.84 (d, J = 8.1 Hz, 1 H), 5.68 (d, J = 17.7 Hz, 0.1 H), 5.25 (d, J = 11.0 Hz, 0.9 H), 2.24 (s, 2 H), 1.40-1.46 (m, 2 H), 1.16 (s, 3 H), 1.15 (s, 3 H), 1.14 (s, 3H), 1.12 (s, 3H). ^{13}C NMR (126 MHz, $CDCl_3$): δ ppm -21.3, 12.7, 17.4, 17.7, 113.6, 114.0, 119.4, 121.8, 126.3, 128.7, 129.0, 131.8, 152.3. ^{2}H NMR (500 MHz, CCl_4): δ ppm 5.99-6.02. HRMS (EI) calcd. for $C_{15}H_{22}DOSiI$ [M]: 376.0704, found: 376.0704

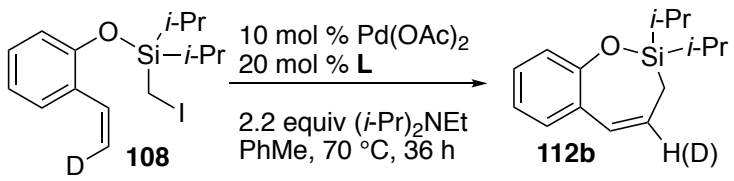

108 **112b**

88% D incorporation

74% Isolated yield
47% D incorporation

Isolated yield = 74%, 36.5 mg. Endo:Exo = 28:1 (GC ratio).

^{1}H NMR (500 MHz, $CDCl_3$): δ ppm 7.13-7.16 (m, 1H), 7.07-7.09 (m, 2H), 6.93-6.99 (m, 2H), 6.27-6.29 (m, 1H), 6.06-6.11 (m, 0.53H), 1.62-1.63 (m, 2H), 1.15-1.23 (m, 2H), 1.07-1.14 (m, 14H). ^{13}C NMR (126 MHz, $CDCl_3$): δ ppm 12.2, 12.3, 13.6, 17.4, 17.7, 120.9, 121.6, 125.9, 128.1, 128.4, 130.9, 154.1. ^{2}H NMR (500 MHz, CCl_4): δ ppm 6.36. HRMS calcd. for $C_{15}H_{21}DOSi$[M]: 247.1503, found: 247.1500.

Comparison Study:

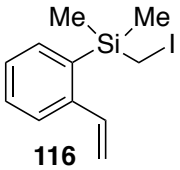

116

Isolated yield= 50% (over two steps)

^{1}H NMR (500 MHz, $CDCl_3$): δ ppm 7.56-7.50 (m, 2H), 7.39 (t, *J* = 7.7, 1H), 7.28-7.26 (m, 1H), 6.99 (ddd, *J*=16.87, 11.00, 2.93 Hz, 1 H) 5.65 (dd, *J*=17.24, 2.93 Hz, 1 H) 5.32 (dd, *J*=10.82, 2.75 Hz, 1 H), 2.30 (s, 3H), 0.51 (s, 6H). ^{13}C NMR (500 MHz, $CDCl_3$): δ ppm -12.6, -1.3, 116.0, 125.6, 127.0, 130.1, 134.8, 136.5, 137.7, 144.0.

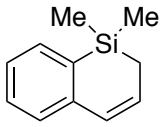

117a, *endo*

Isolated yield = 80%

^{1}H NMR (500 MHz, $CDCl_3$): δ ppm 7.59 (d, *J*=7.3 Hz, 1H), 7.42-7.46 (m, 1H), 7.30-7.34 (m, 1H), 7.18-7.20 (d, *J*=7.6 Hz, 1H), 6.51 (dd, *J*=10.5, 2.1 Hz, 1H), 6.14-6.19 (m, 1H), 1.69-1.71 (dd, *J*=5.6, 2.1 Hz, 2H), 0.41 (s, 6H). ^{13}C NMR (500 MHz, CDCl3): δ ppm 2.2, 13.2, 126.6, 127.1, 128.1, 129.8, 130.7, 132.9, 133.4, 141.9. HRMS (EI) calcd. for $C_{11}H_{14}Si$ [M]: 174.0865, found : 174.0866.

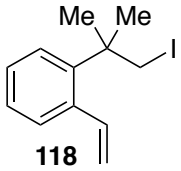

118

Isolated Yield = 7%.

^{1}H NMR (500 MHz, DMSO-*d6*) δ = 7.37 - 7.25 (m, 4H), 5.53 - 5.49 (m, 1H), 5.35 - 5.32 (m, 1H), 3.70-3.69 (m, 2H), 1.60 (s, 3H), 1.59 (s, 3H). ^{13}C NMR (126 MHz, DMSO-*d6*) δ = 142.6, 138.3, 130.1, 127.7, 126.6, 116.9, 39.7, 29.3, 23.3.

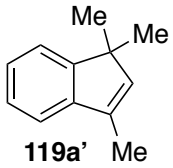

119a'

Isolated yield = 58%

^{1}H NMR (500 MHz, $CDCl_3$) δ = 7.32-7.20 (m, 4 H), 6.04 (s, 1 H), 2.11 (s, 3 H), 1.31 (s, 6H), 1.60 (s, 3 H), 1.59 (s, 3 H). ^{13}C NMR (126 MHz, $CDCl_3$) δ = 154.0, 144.1, 142.2, 135.6, 126.3, 124.9, 120.9, 119.1, 48.1, 24.7, 12.8.

PART TWO: VISIBLE LIGHT-INDUCED PALLADIUM-CATALYZED DESATURATION OF ALIPHATIC ALCOHOLS

4.1. Introduction

The alkene moiety is one of the most privileged functional groups in organic synthesis due to its intrinsic reactivity and functionalization capabilities.[53] Over the past century, a plethora of fundamental transformations have been developed in order to access these privileged synthons (Scheme 36). However, all of these approaches suffer from one common limitation: pre-functionalized substrates are required for the synthesis of alkenes. To date, methods for a direct desaturation of an aliphatic chain into an alkene moiety are underdeveloped owning to the inherent difficulty of activating kinetically stable C(sp^3)–H bonds. Nature, however, can accomplish this feat easily with desaturase enzymes. One well-studied example is the site-selective desaturation of fatty acids (Scheme 37).[54] It is believed that the desaturase enzyme enables a hydrogen atom abstraction event (**127→128**) to occur at the C-9 position of the fatty acid, which forms alkyl radical intermediate **128**. Ensuing oxidation of **128** results in carbocation intermediate **129**, followed by a proton loss step that results in desaturation product **130**. Inspired by this phenomenon, many research groups have focused their efforts on desaturation of aliphatic systems into privileged olefins. Modern approaches can be divided into two categories, transition metal-catalyzed desaturation via concerted metalation-deprotonation (CMD)[55] and oxidative radical desaturation,[56] Scheme 38. Although these approaches have enabled challenging remote desaturation of aliphatic systems, considerable limitations exist. For instance, the transition metal-catalyzed approach suffers from limited substrate scope, low selectivity and efficiency, and harsh

reaction conditions are typically employed. Moreover, the site of functionalization is often restricted to the inherent preference for a 5/6-membered TM-cyclic intermediate and is limited to activation of 1° and 2° γ-/δ-C–H bonds.[55] Whereas, the oxidative radical approach typically enables activation of 3° γ-/δ-C–H bonds under milder reaction conditions, however, it provides low variability of C–H activation sites.[56] In addition, due to the nature of the mechanism, this approach is plagued with regioselectivity issues due to a non-selective proton elimination step from the cationic intermediates. Both of these protocols have found limited applications in chemical synthesis due to these aforementioned limitations.

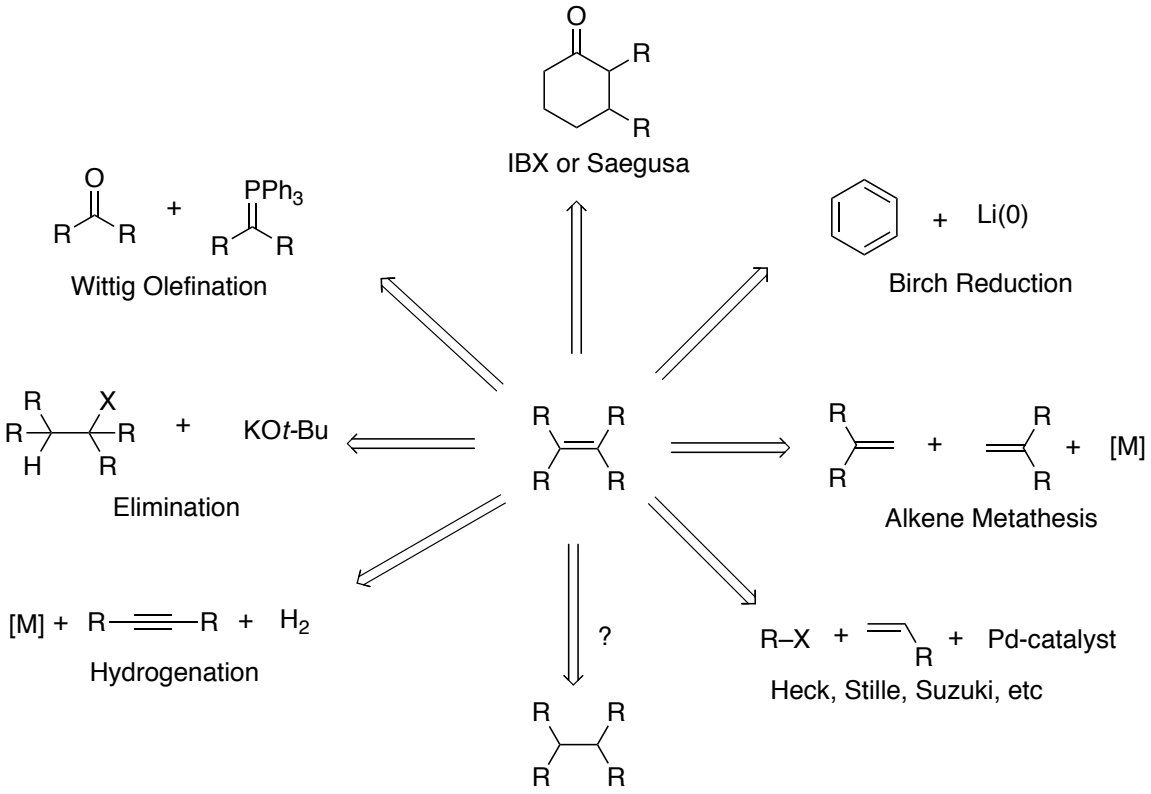

Scheme 36: Methods for synthesis of olefins.

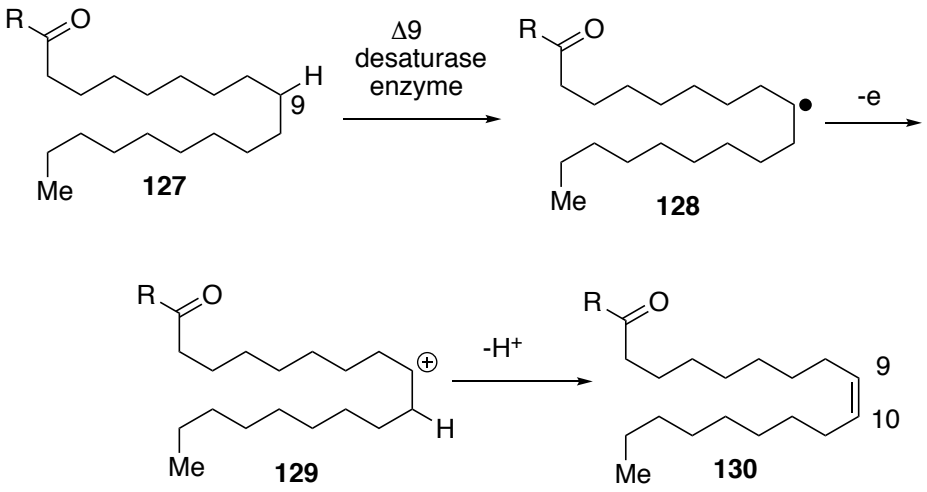

Scheme 37: Biosynthetic desaturation of fatty acids with desaturase enzymes.

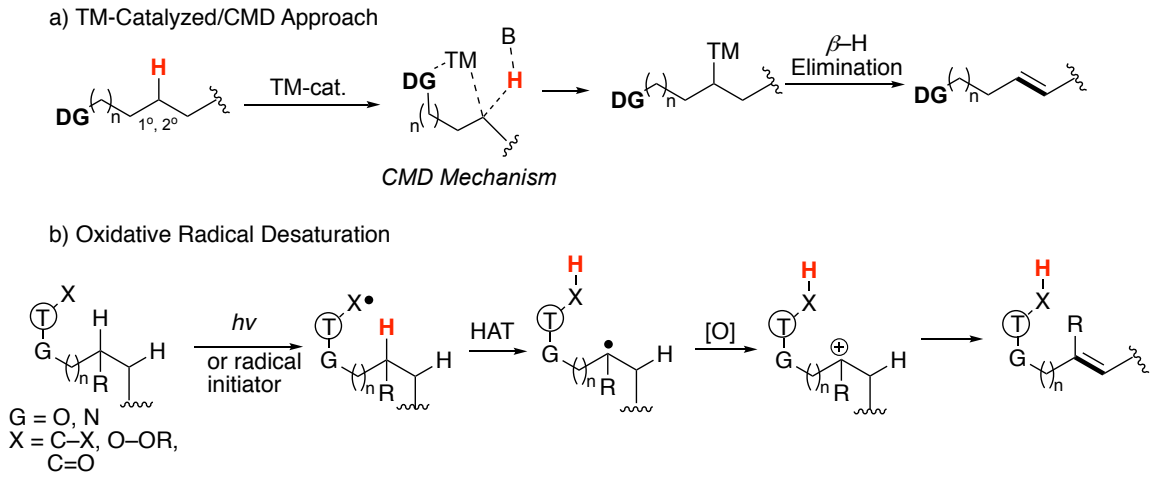

Scheme 38: Approaches for desaturation of aliphatic systems. a) CMD mechanism. b) Oxidative radical desaturation.

4.1.1. Pd-Catalyzed Desaturation of Aliphatic Systems.

In his pioneering report, Baudoin and co-workers reported the Pd-catalyzed *β*-/*γ*-desaturation of propyl benzene derivatives (Scheme 39) via a CMD mechanism.[57] In most cases, the primary *γ*-C-H site was activated, leading to modest yields of the *β*-/*γ*-desaturation products via a Pd-involved *β*-H elimination step (**132a-d**). However, the scope of the transformation was found to be limited to substrates possessing quaternary

benzylic carbon atom (**132e**).[58] Notably, activation of challenging secondary C–H sites was achieved, resulting in internal olefin **132f** in good yield and selectivity. However, in cases with competitive C–H activation sites (**131g**), not surprisingly, activation of the primary C–H was preferred, leading to terminal olefin **132g**. Interestingly, subjecting substrate **131h**, possessing a methyl substituent at the benzylic position, formation of cyclobutane product **132h'** was formed predominately over the *β*-/*γ*- desaturation product **132h**. This result highlights the inherent preference for formation of the favorable 5-membered palladacycle (*vide infra*), which resulted in **132h'** via a subsequent reductive elimination.[55] The applicability of the authors' transformation was demonstrated in the total synthesis of verapamil (**131i→132i**).[59] Finally, a general CMD mechanism of transformation for the mechanism was proposed (Scheme 40).[55]

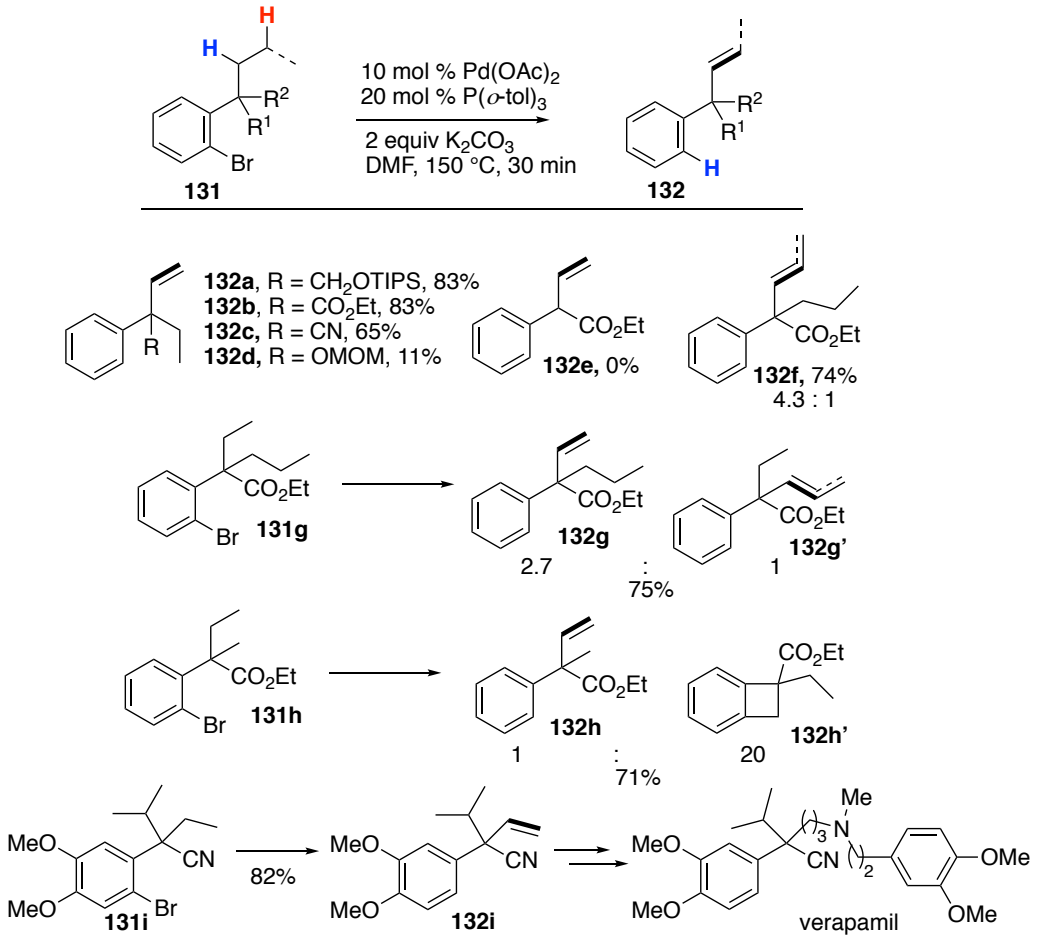

Scheme 39: Baudoin's Pd-catalyzed *β*-/*γ*-desaturation of propyl benzene derivatives

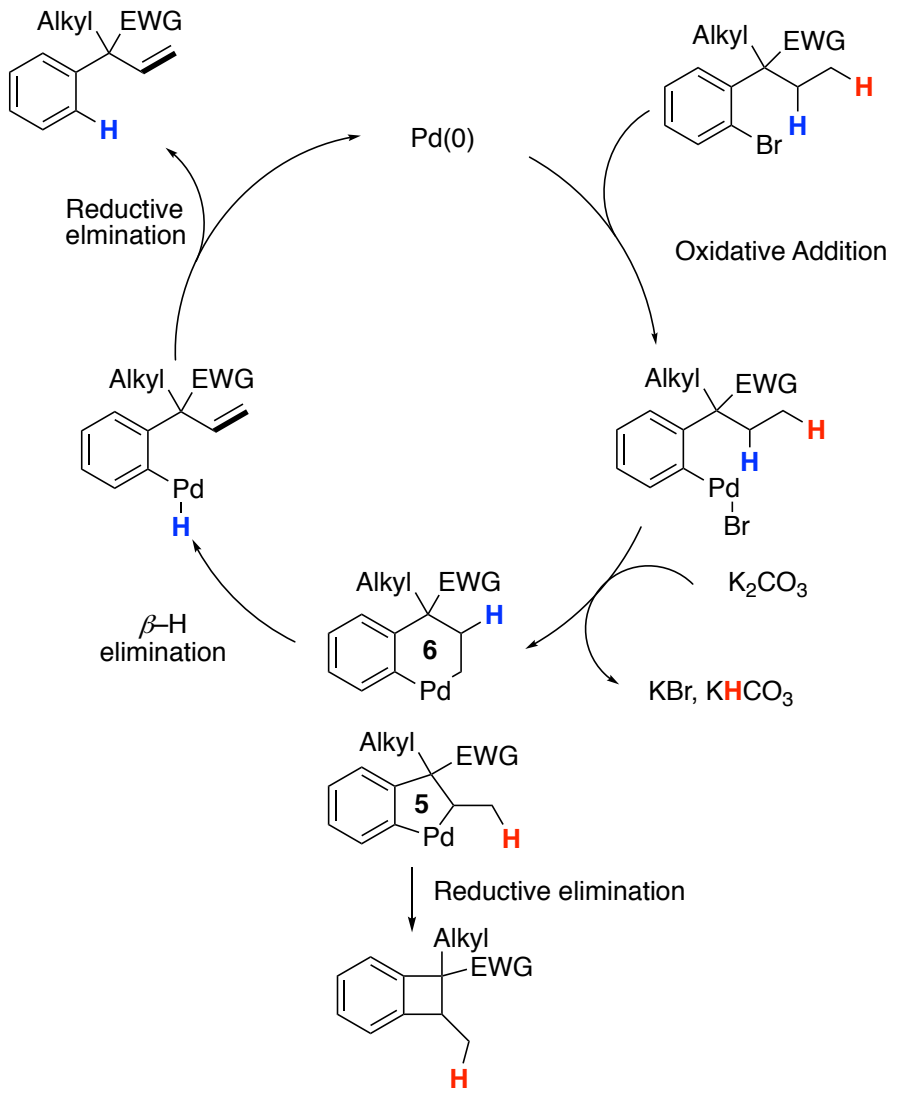

Scheme 40: Baudoin's Pd-catalyzed *β*-/*γ*-desaturation of propyl benzene derivatives.

Catellani and co-workers reported a similar strategy for the *α*-/*β*-desaturation of alkyl- and alkoxy-substituted arenes leading to styrene and aryl enol ethers, respectively (Scheme 41).[60] Two reaction modes were disclosed: (A) a Catellani-type[61]/desaturation reaction involving norborandiene and (B) a CMD-type desaturation reaction.[55,57] The former mode empowered desaturation of linear alkylated systems (**134a-c**), whereas the latter allowed for desaturation of branched alkyl arenes (**136a-c**). Notably, when a methyl

group (**133d**) was present, desaturation via mode A did not occur, but instead the product of C–H activation leading to **134d'** was obtained selectively. This result indicates the preference of this method for activation of less sterically hindered primary C–H sites. Overall, for both modes, milder reaction conditions were employed compared to that of the Baudoin's approach,[57] however, the substrate scope and reaction yields were modest.

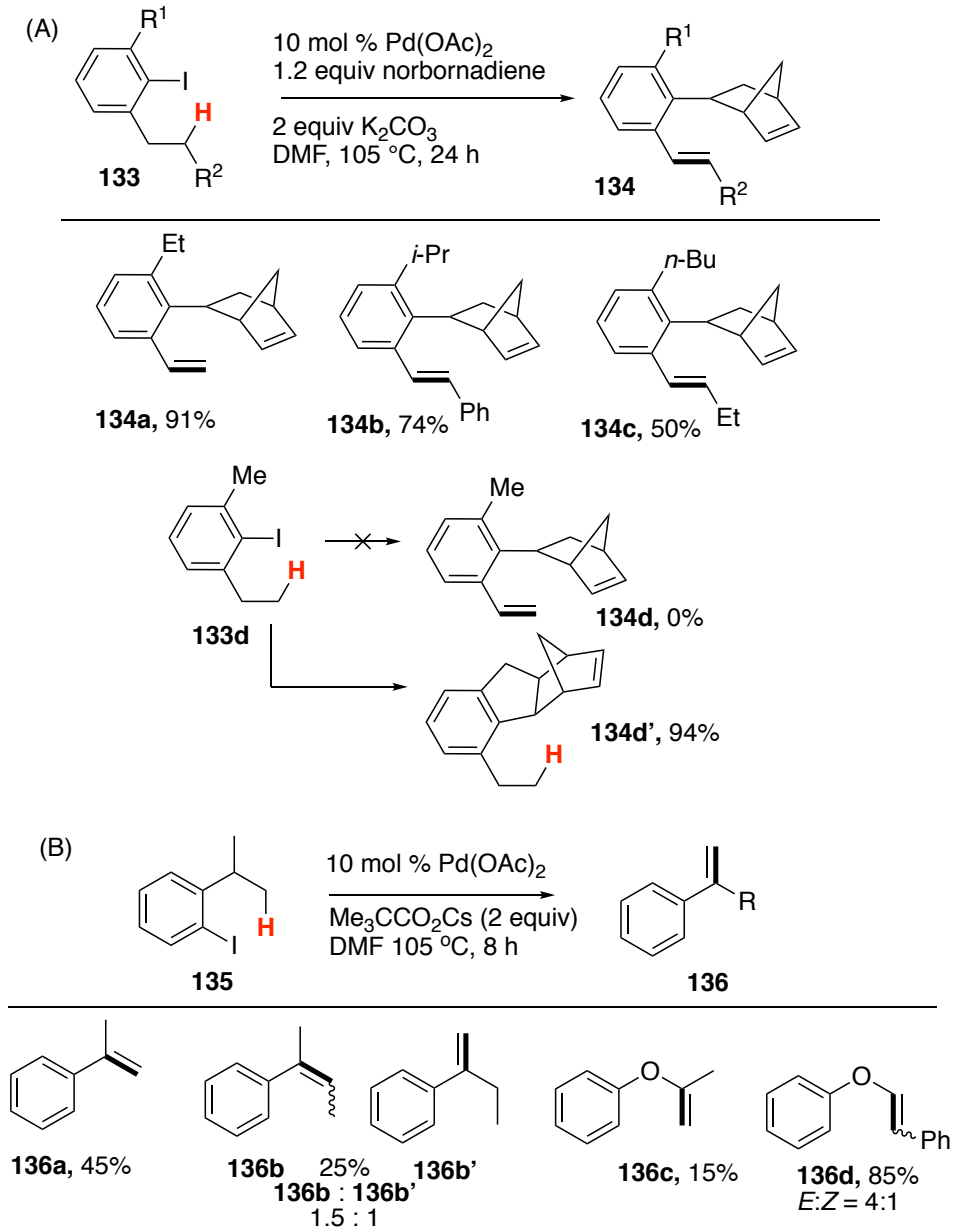

Scheme 41: Catellani's Pd-catalyzed α-/β-desaturation of propyl benzene derivatives.

In 2011, Stahl and co-workers reported an oxidative Pd-catalyzed α-/β-desaturation of cyclic ketones under mild reaction conditions.[62] Importantly, no over-oxidation of the reaction products (into phenol derivatives) was observed. Cyclohexylketone derivatives underwent smooth α-/β-desaturation in good yields (**138a-d**). Moreover, heterocycles such as methylpiperidinone and chromanone reacted well, resulting in desaturation products **138e** and **138g** in 74% and 80% yields, respectively. For unsymmetrical substrates possessing a phenyl substituent at the α-position, desaturation resulted in the conjugated product **138h**, selectively. However, when the phenyl substituent was moved to the β-position, desaturation of **137i** resulted in the non-conjugated product **138i** due to steric effects. Next, Stahl and co-workers successfully applied their desaturation methodology in a complex setting, where desaturation of complex steroid derivatives occurred efficiently (**138j-k**). The authors showcased the power of their method in the synthesis of **138l**, an important core *en route* to natural product (-)-terpestain. It was found that employment of these conditions, resulted in core **138l** in 90% yield, whereas classical approaches relying on IBX oxidation[63] or use of stoichiometric amounts of Pd-metal[64] resulted in no reaction or lower efficiency of the product **138l**, respectively. Stahl and co-workers proposed the following mechanism (Scheme 43). Ligand exchange with the Pd(II)X_2 catalyst and cyclic ketone substrate **137** results in C–Pd enolate intermediate **140**.[65] Next a subsequent β-hydride elimination process occurs to form the α-/β-desaturation product **138** and Pd(II)HX species. The latter species undergoes a reductive elimination event to form the Pd(0) complex, which is successively oxidized into the active Pd(II) species **139** with molecular oxygen.

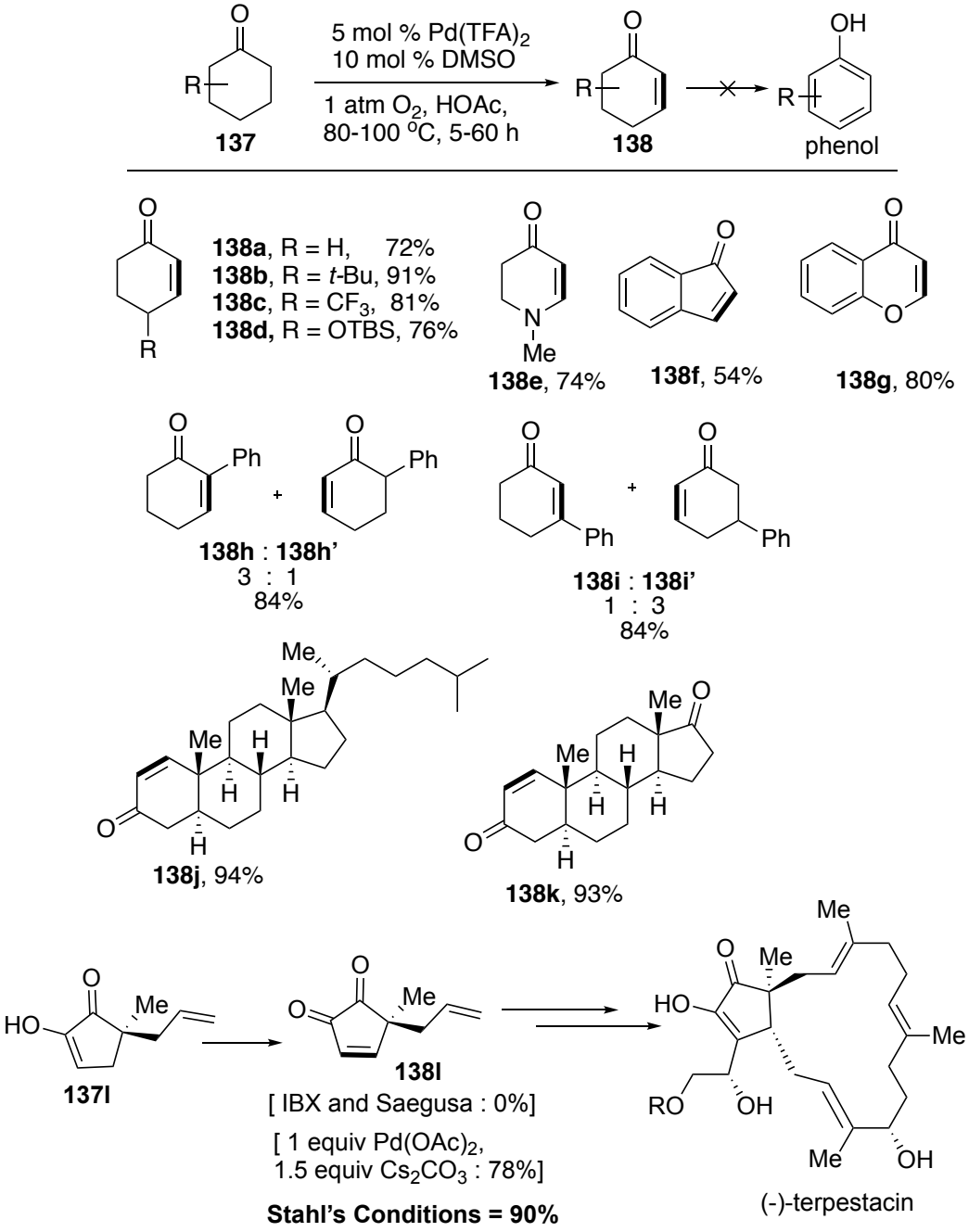

Scheme 42: Stahl's α-/β-desaturation of cyclic ketones.

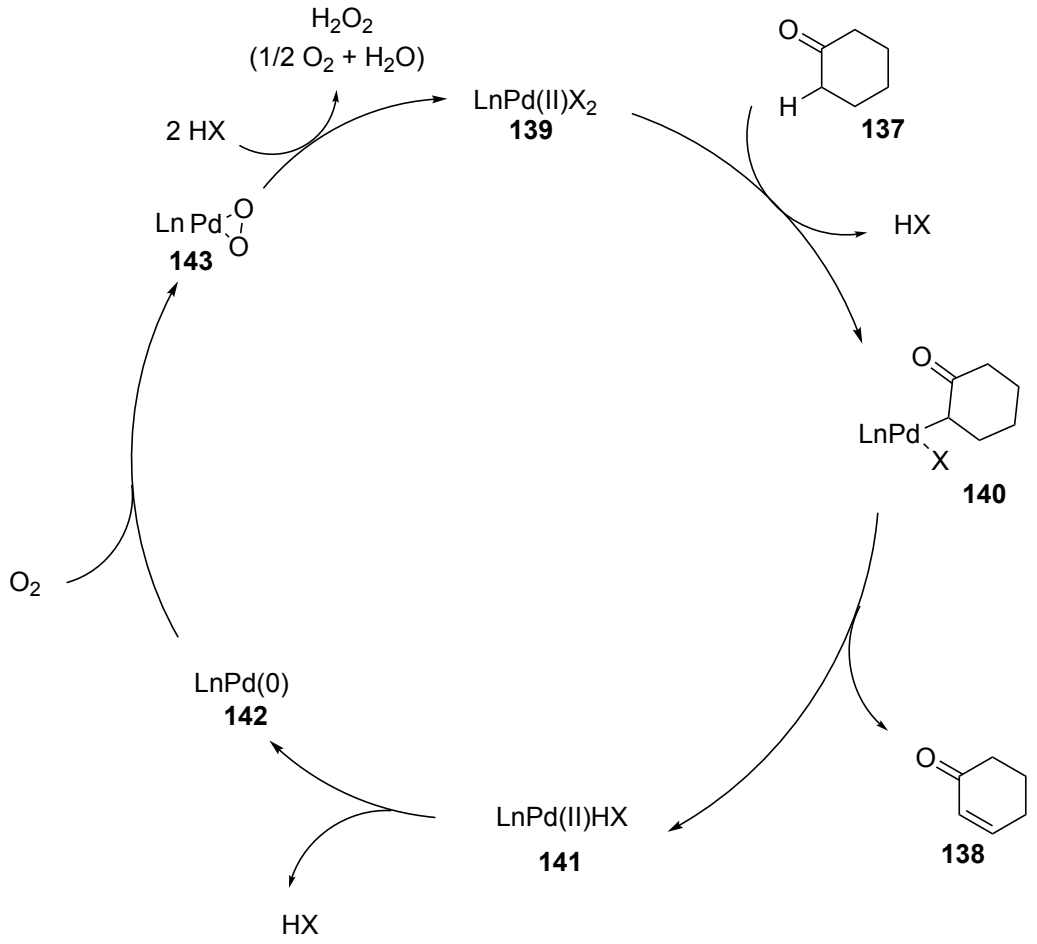

Scheme 43: Mechanism of Stahl's α-/β-desaturation of cyclic ketones.

Later, Newhouse and co-workers reported a novel Pd-catalyzed α-/β-desaturation of esters, nitriles, and amides (Scheme 44).[66] Notably, their transformation enabled efficient desaturation of both cyclic and linear systems (**144→145**). The mechanism of Newhouse's transformation (Scheme 45), however, does not involve a typical CMD step but a transmetalation step of the formed "hard" enolate with an electrophilic allylPd(II) intermediate (**146→147**) and a subsequent β–H elimination (Scheme 45). Following Newhouse's work, Dong and co-workers reported the Pd-catalyzed α-/β-desaturation of amides/lactams.[67] Compared to Newhouse's method, Dong's approach involves the

formation of a "soft" enolate species **150** (Scheme 46) and precludes the use of strong base, which consequently broadens the overall scope of the transformation.

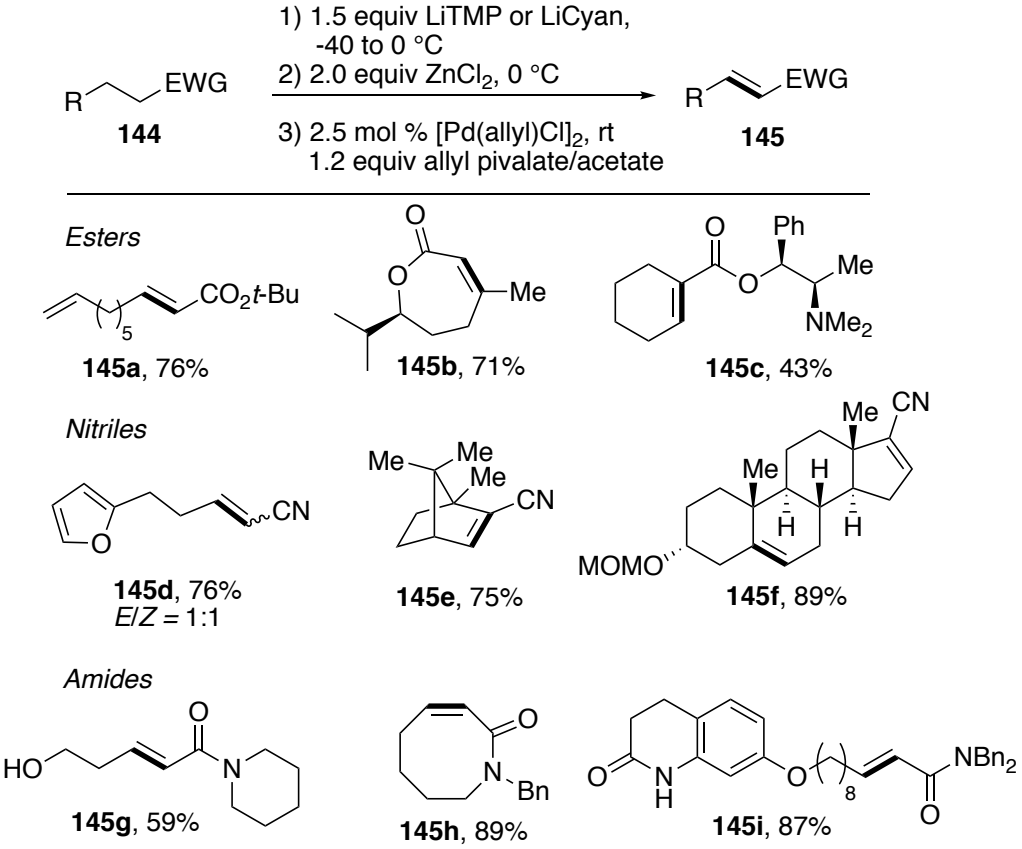

Scheme 44: Newhouse's Pd-catalyzed desaturation of activated systems.

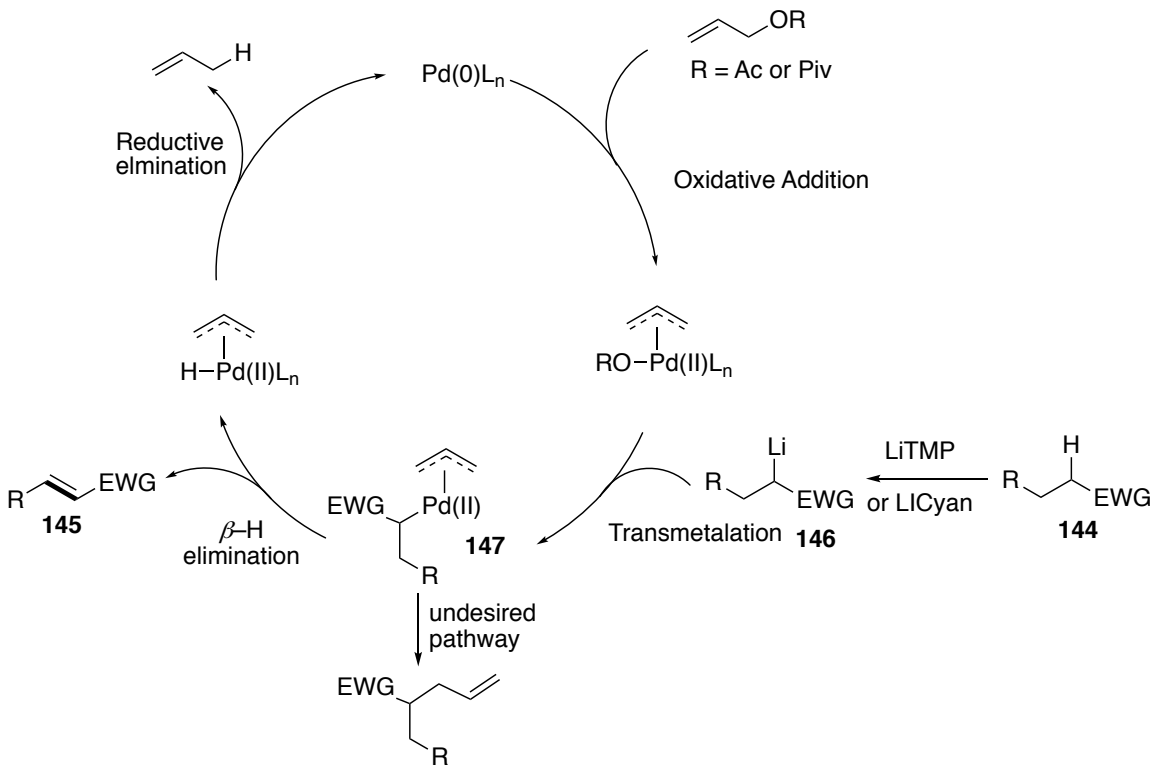

Scheme 45: Mechanism of Newhouse's Pd-catalyzed desaturation of activated systems.

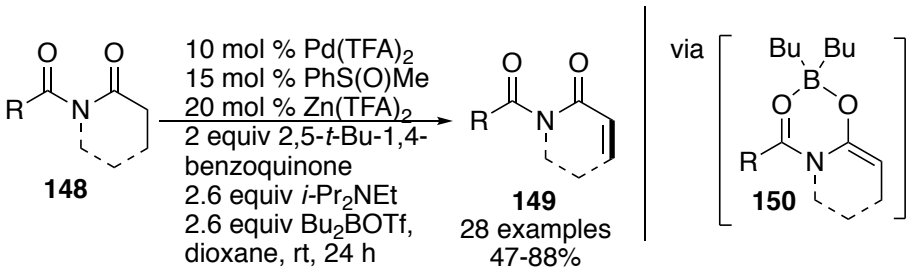

Scheme 46: Dong's Pd-catalyzed desaturation of lactams.

To this point, the presented above Pd-catalyzed desaturation methods all require employment of pre-functionalized substrates. In 2008, Yu and co-workers showed that a Pd-catalyzed desaturation of challenging inert alkyl groups is possible.[68] Their stoichiometric studies involved the use of a tandem amide and oxazoline bidentate

directing group (Scheme 47, **151**), which facilitated a CMD event of the primary γ–C–H site (**152**), followed by β–H elimination to produce terminal olefin **153** in 66% yield. In order to render this approach catalytic, the aid of on an external oxidant benzoquinone was required. Unfortunately, catalytic desaturation was found to be quite challenging, as desaturation of linear and cyclic systems were inefficient (Scheme 48). Only desaturation of substrate **151c**, possessing an α-C–H site, worked well (**154c**). Although a substantial reaction development is needed, this seminal work constitutes a significant advance in the area of remote desaturation of aliphatic systems.

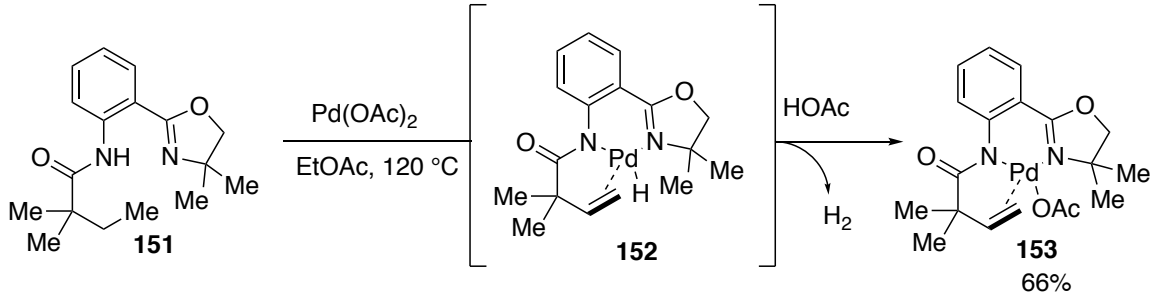

Scheme 47: Yu's stoichiometric studies on desaturation of aliphatic systems.

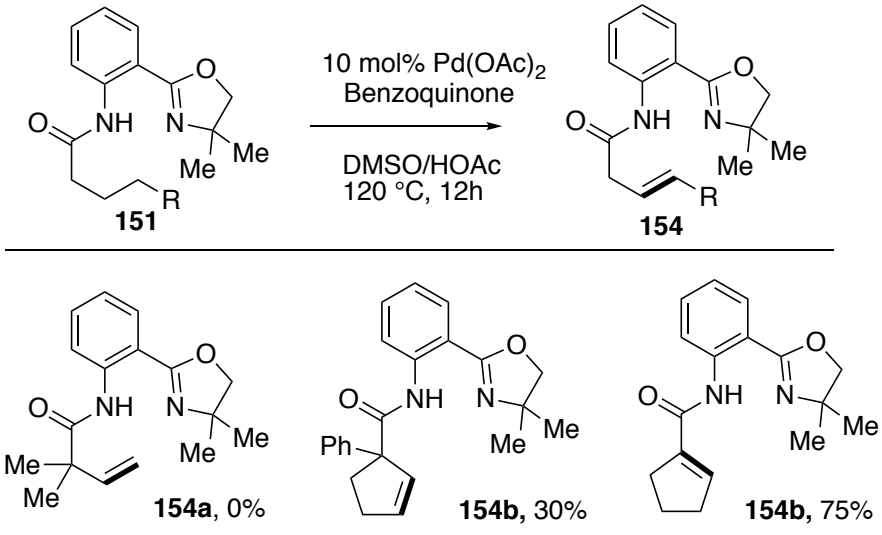

Scheme 48: Yu's Pd(II)-catalyzed desaturation of unactivated aliphatic systems.

Another common method for desaturation of unactivated aliphatic systems is the transfer hydrogenation approach pioneered by Crabtree (Scheme 49A) using his well-studied Ir-catalyst.[69] However, the obtained TON (turnover number) was significantly low and the required high reaction temperatures employed led to catalyst decomposition. Later, Goldman[70] and Brookhart[71] developed a thermodynamically stable Ir-pincer complex **157** that allowed the reaction to run at higher temperatures, which accordingly led to higher TONs for desaturation of unactivated systems (Scheme 49B). Although many advances have been made in this area,[72] the substrate scope of the transformation is not general. Only cycloalkanes possessing high degrees of transannular strain reacted well (**144→145**), whereas linear alkanes[73] generated a mixture of alkene isomers under these reaction conditions (Scheme 50). The mechanism of this transformation is depicted in Scheme 51.

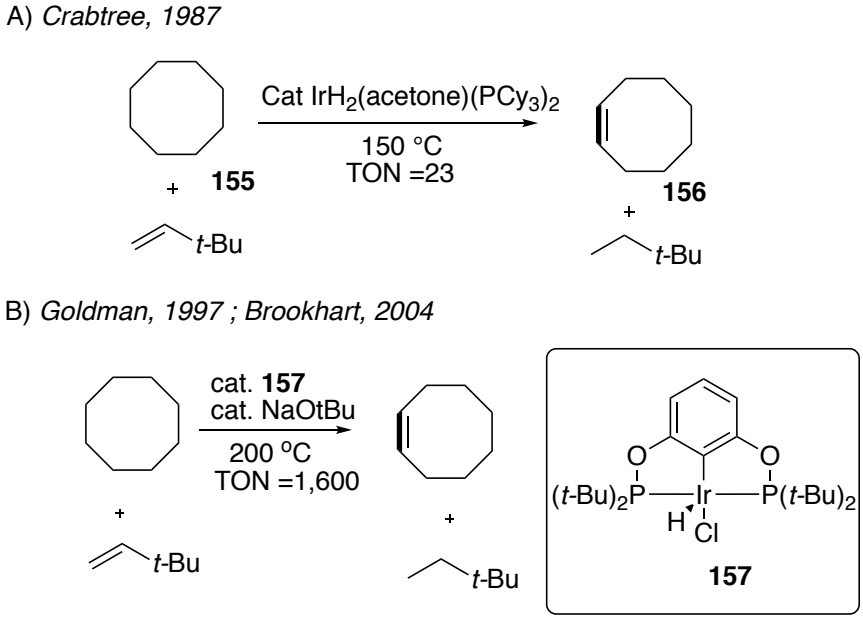

Scheme 49: Ir-catalyzed transfer hydrogenation reactions. (A) Crabtree's seminal work. (B) Goldman and Brookhart's modification using Ir-pincer catalyst **157**.

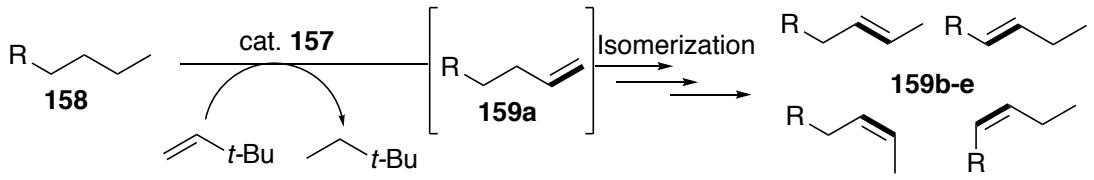

Scheme 50: Ir-catalyzed transfer hydrogenation of linear alkanes into alkenes.

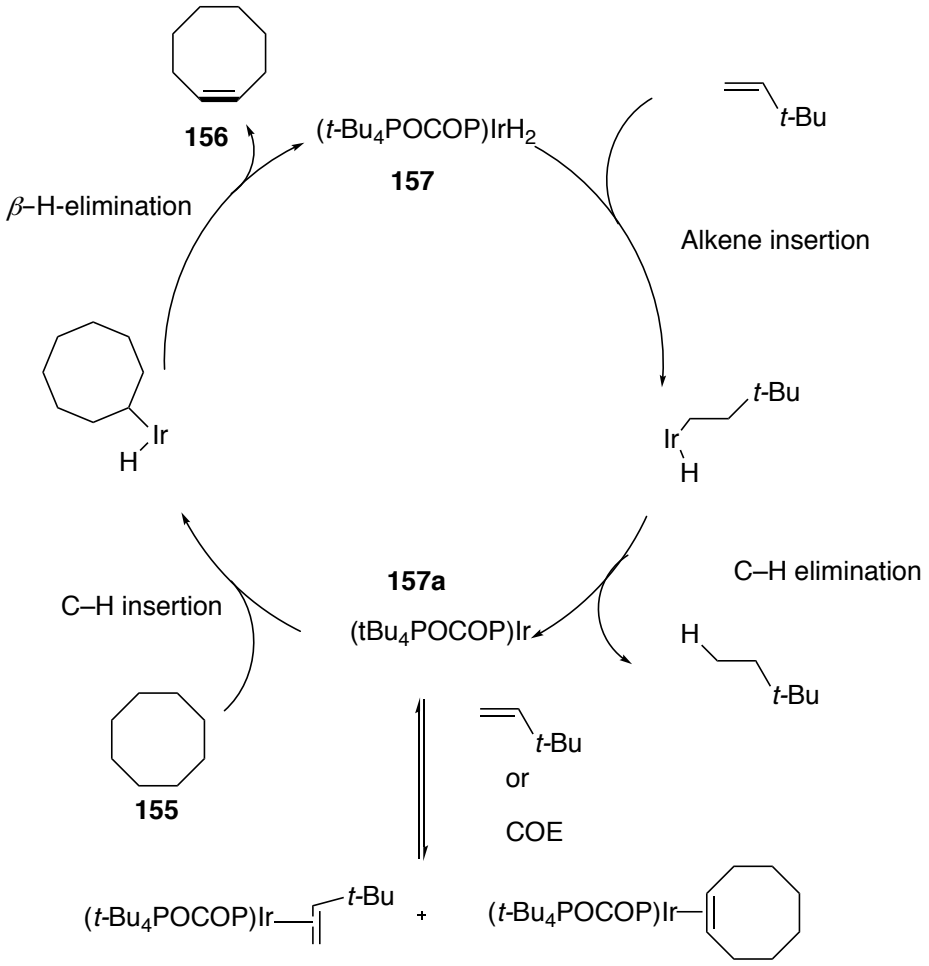

Scheme 51: Mechanism of Ir-pincer-catalyzed transfer hydrogenation of linear alkanes into alkenes.

The aforementioned methods represent a significant advance in the promising area of TM-catalyzed desaturation of aliphatic systems. However, due to limited substrate scope, employment of harsh reaction conditions, and low site-control of desaturation,

these approaches are not practical and will likely not translate to the industrial and pharmaceutical sectors. In addition, TM-catalyzed site-selective desaturation of aliphatic systems via activation of 3° C–H sites have not been reported.

4.1.2. Desaturation of Aliphatic Systems via Oxidative Radical Approaches.

Classical radical approaches have provided solutions for functionalization of unactivated 3° C–H sites. Thus, in 1979, Breslow reported a novel remote desaturation at the A-ring of steroid frameworks (Scheme 52, **160→161**).[74] In this pioneering work, Breslow employed a benzophenone-tether (**160**), which adopted a favorable quasi-linear confirmation for C_{14}–H-specific functionalization. The mechanism for desaturation involved the photolytic formation of high-energy diradical intermediate **162**. Based on the design of the template, the oxygen radical from **162** undergoes site-selective hydrogen atom abstraction of C-14 to generate alkyl radical **163**. Then, this intermediate undergoes a subsequent HAT event at the adjacent C–H site (C-15) and a successive radical collapse to generate desaturation product **161**. Although incredibly innovative, this design is limited to specific steroids systems, lacks generality and practically due to the employment of harmful UV-light, and low variability for C–H abstraction.

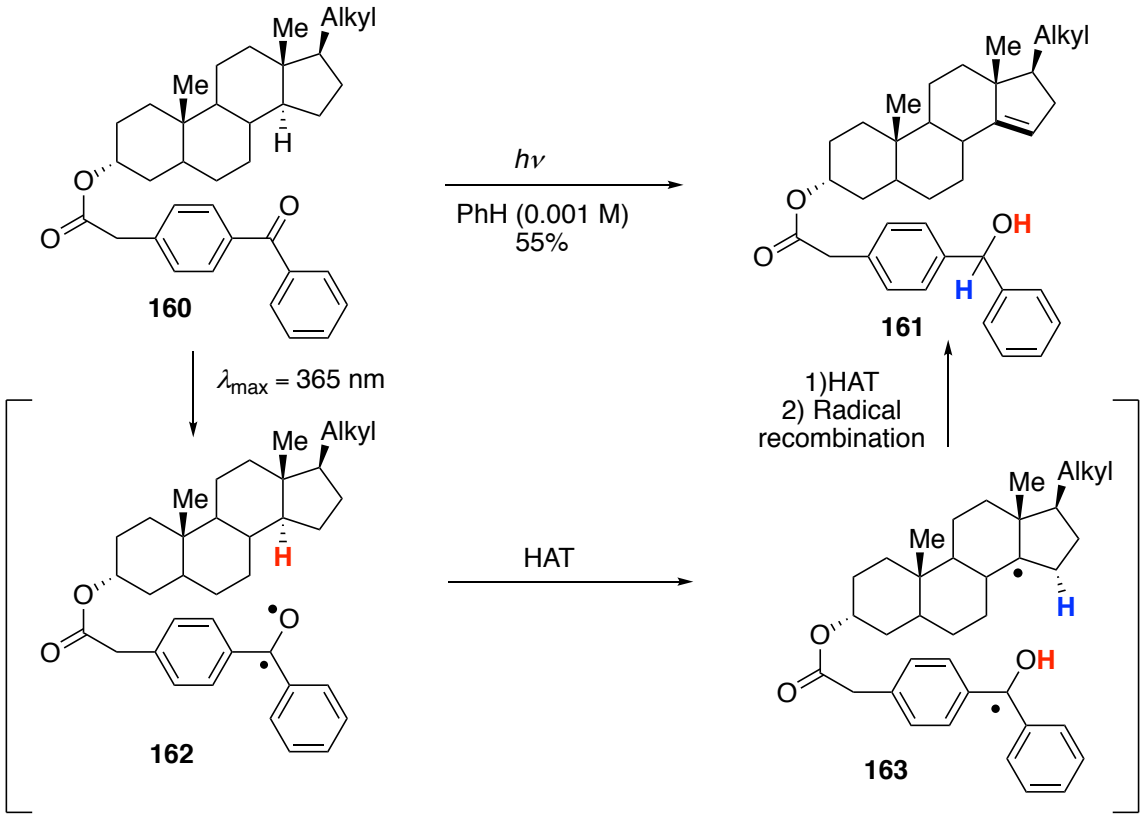

Scheme 52: Breslow's remote desaturation of steroids.

Though limited, the above method outlines an important feature of overcoming the kinetic stability of C–H bonds via hydrogen atom abstraction of heteroatom radical species. A few years later, Čekovic reported desaturation of alkyl hydroperoxides in the presence of stoichiometric amounts of Fe and Cu metals via formation of oxygen radicals (Scheme 53).[75] The scope of this transformation is very limited and not efficient, but contains some notable entries. Amazingly, it was found that *δ*-/*ε*-desaturation of **164a** and **164c**, possessing only 2°C–H sites, worked well. Also, desaturation of **164e** generated product **166e** with no detectable amounts of Wagner-Meerwein (cationic) rearrangement products,[76] which argues against the formation of cationic intermediates for this transformation. Furthermore, submitting **164d** to the reaction conditions resulted in cyclic

tetrahydrofuran derivative **166d** in good yield, via activation of the 1°δ-C–H bond, which is a rather difficult task in field of radical chemistry. Again, no rearrangement products were observed and based on the cyclization product obtained, it was speculated that the transformation proceeds via formation of an alkyl-Cu intermediate. Based on the reaction scope and mechanistic studies, the authors proposed the following mechanism (Scheme 54). First, the alkyl hydroperoxide **164** decomposes into oxygen radical intermediate **165** mediated by Fe(II). Next, 1,5-HAT of **165** results in the formation of transposed alkyl radical intermediate **167**, which subsequently reacts with Cu(II)OAc to form **169**. A concerted elimination of the latter forms the desaturated alcohols **166**/**166'**. Overall, Čekovic's work highlights the power and reactivity of heteroatom radicals, namely oxygen radicals, for HAT from which many works are derived from.[77] However, the presented method suffers from lack of practically due employment of inconvenient starting materials, use of stoichiometric amounts of transition metals, and low regiocontrol of the elimination step.

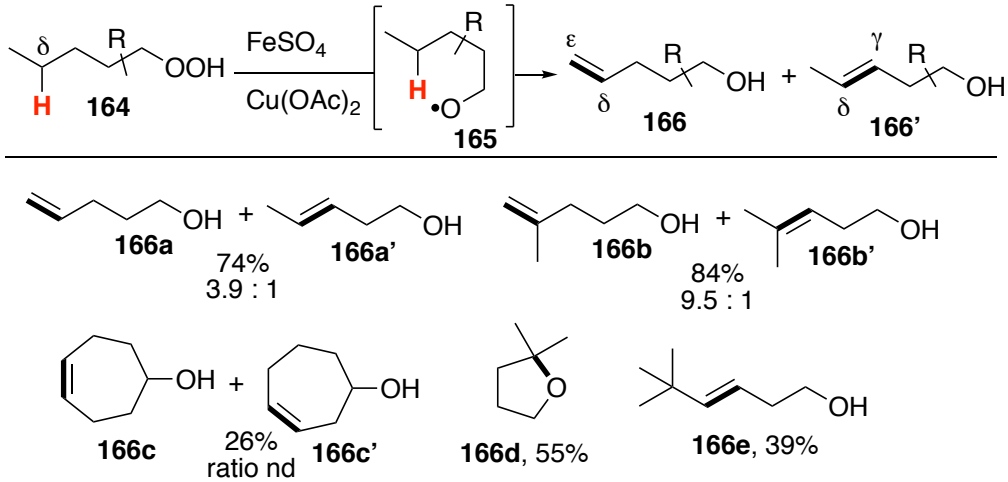

Scheme 53: Čekovic's desaturation of alkyl peroxides into alkenols.

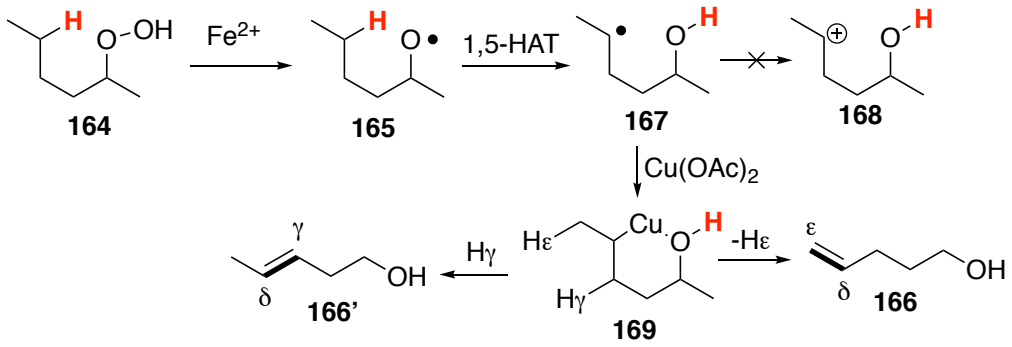

Scheme 54: Mechanism of Čekovic's desaturation of alkyl peroxides into alkenols.

Although the development of radical chemistry grew over the next few decades, methods for remote desaturation methodology remained scarce. The importance of developing a general remote desaturation method became apparent during Baran's total synthesis of epieudesmantetraol **176** (Scheme 55).[78] Synthesis of vital intermediate **175** was achieved by a taxing 3-step procedure involving oxidation of amide **170** into **171**; formation of nitrogen radical by photolysis and a subsequent 1,6-HAT/atom-transfer event (**172→173**), which resulted in formation of **174**; and finally base-induced elimination of the latter species to generate the desired desaturation product **175**. In order to obviate the need for a multi-step desaturation procedure, Baran and co-workers reported a novel strategy for a one-step, guided and site-selective, *γ*-/*δ*-desaturation of alcohols and amines involving a sulfone hydrogen-atom-abstracting tether (Scheme 56).[79] The sulfone tether possesses a triazene group (**177**) that decomposes into diazo species **178**. Next, SET from TEMPO to **178**, results in formation of cationic TEMPO and the aryl radical species **179**. Interestingly, the latter undergoes an unconventional 1,7-HAT event to furnish the transposed radical species **180**. Next, oxidation of intermediate **180** occurs with cationic TEMPO to furnish cationic species **181**, which upon a proton-loss event results in desaturated product **182**. The concept of this work was derived from

Breslow's pioneering work (tether approach, Scheme 52) and the biosynthesis of fatty acids via desaturases (mechanism, Scheme 37). The scope of transformation was found to be quite broad, as a number of aliphatic alcohols and amine possessing important functional groups worked well (Scheme 57). Secondary alcohols possessing competitive sites for functionalization resulted in selective γ-/δ-desaturation at tertiary C–H sites (**184a-d**), albeit with low efficiency. Also, employment of amino acid derivatives was found to competent substrates, as the corresponding γ-/δ-desaturation products were formed efficiently. However, not surprisingly, due to the formation of cationic intermediate **181** (Scheme 56), a handful of substrates resulted in low yields and regioselectivity of the reaction products (**184e,f,k**), and, in some cases, the employed substrates resulted in formation of undesired rearrangements products (**183q→184q'**). Nevertheless, prior to our work, Baran's invention represented the state-of-the-art method for desaturation of aliphatic systems.

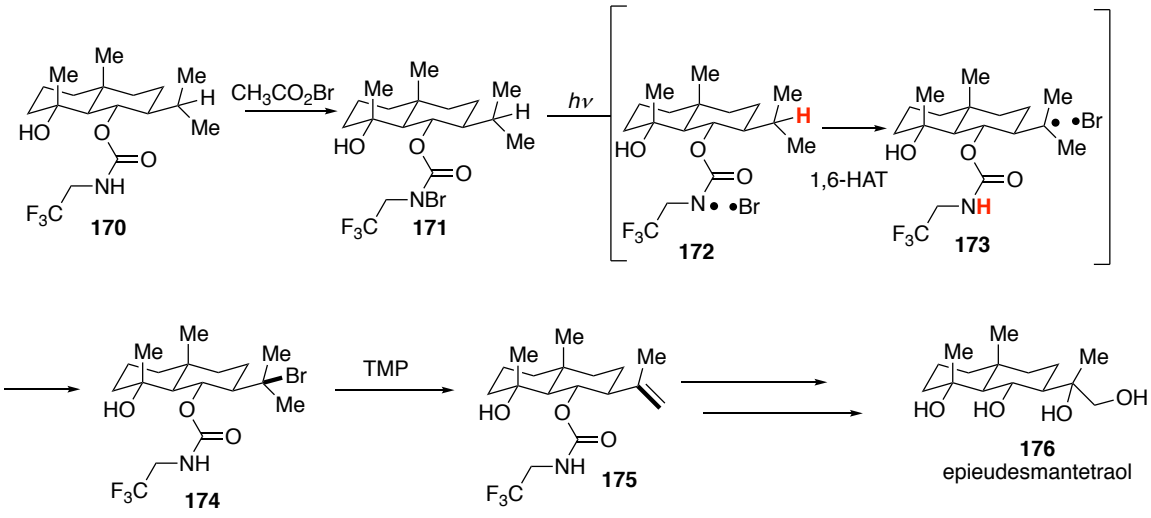

Scheme 55: Baran's synthesis of intermediate **175** *en route* to epieudesmantetrol.

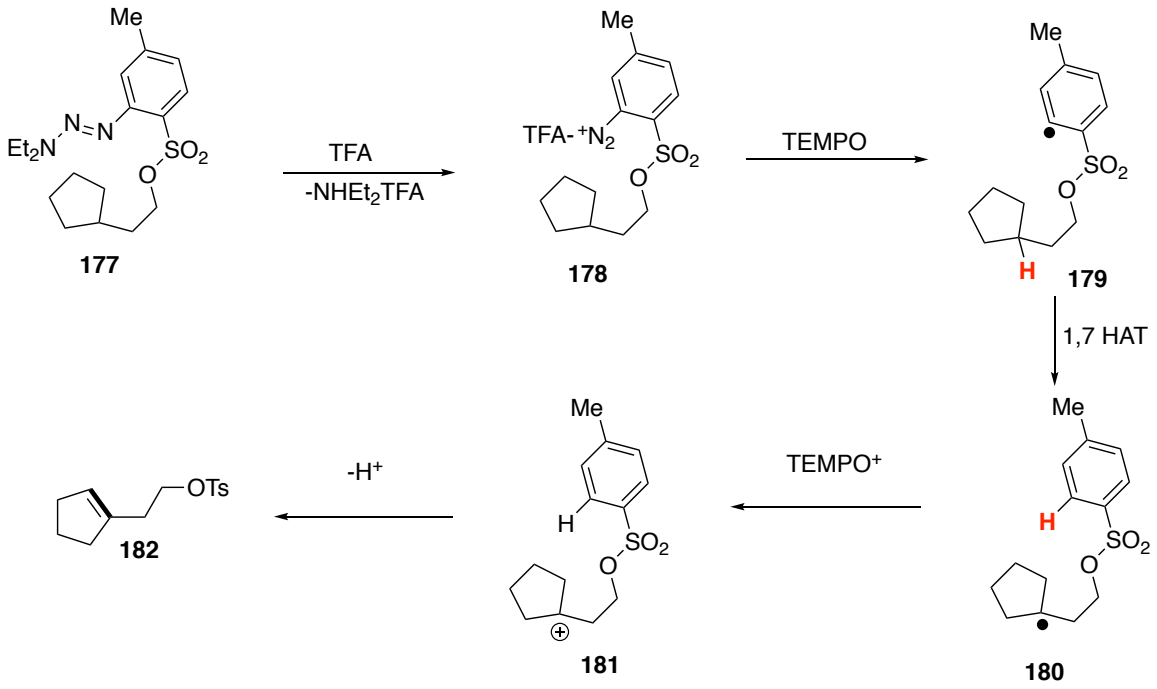

Scheme 56: Baran's concept of remote desaturation using a tether approach.

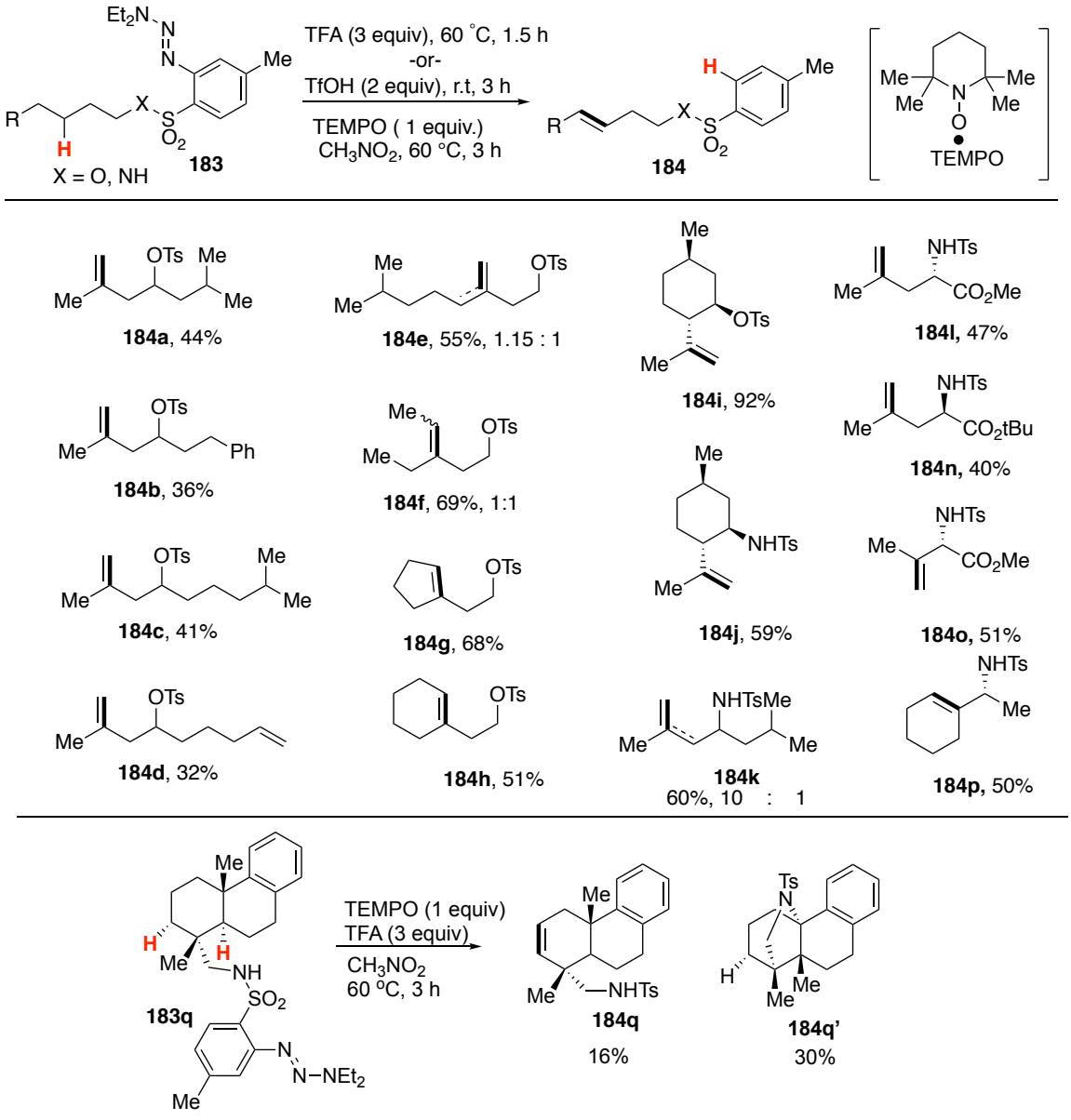

Scheme 57: Scope of Baran's desaturation method.

4.1.2. Conclusion

To date, methods for desaturation of aliphatic systems are still underdeveloped. Strategies over the past decades in transition-metal catalyzed desaturation via CMD and oxidative radical chemistry have provided significant advances for this important transformation. However, numerous limitations exist in each direction. For the TM-catalyzed approach, site-controlled functionalization is often limited to activation of 1° and 2° γ-/δ-C–H bonds and good regiocontrol of elimination. In contrast, for oxidative radical methods, activation is limited to 3° γ-/δ-C–H sites and the regiocontrol of elimination is very poor. Both approaches employ hash or unpractical reaction conditions and suffer from low efficiency and variability of the functionalization site. Hence, development for a general, site-controlled, and efficient desaturation of aliphatic systems is highly justified.

5. Photoinduced Formation of Hybrid Aryl Pd-Radicals Species Capable of 1,5-HAT: Catalytic Oxidation of Silyl Ethers into Silyl Enol Ethers (Previously Published as Parasram, M.; Chuentragool, P.; Sarkar, D.; Gevorgyan, V. "Photoinduced Formation of Hybrid Aryl Pd-Radical Species Capable of 1,5-HAT: Selective Catalytic Oxidation of Silyl Ethers into Silyl Enol Ethers." *J. Am. Chem. Soc.* 2016, *138*, 6340.)

5.1. Reaction Development

Aryl halides are widely used starting materials for many transition metal-catalyzed reactions. In the presence of Pd(0), these substrates undergo a concerted three-centered two-electron oxidative addition process (**185→186**) to generate Pd(II) complex **187** (Scheme 58).[22] This complex is a key intermediate featured in many cross-coupling reactions that has led the development of important C–C bond forming events.[80] Although well defined and established, changing the nature of this intermediate into a hybrid Pd-radical species has not been investigated.[81] Thus, we envisioned, if direct formation of a novel hybrid aryl Pd-radical species, possessing both Pd and radical character, could be realized (**185→188**), it may empower the development of new transformations.

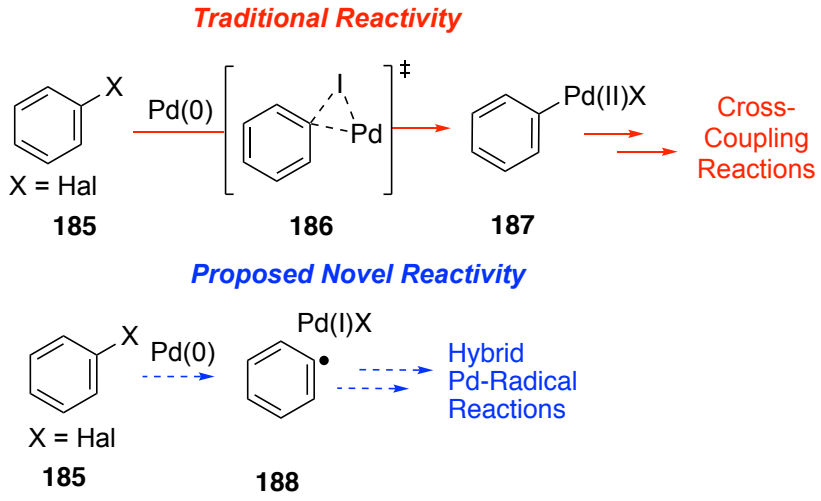

Scheme 58: Mechanism of OA with ArX and proposed formation of **188**.

Although the transition metal-catalyzed formation of aryl radicals (from aryl halides) are scarce,[17,82] they are easily formed and widely used intermediates in radical chemistry. In 1988, Curran reported an impressive remote C–H functionalization strategy via radical 1,5-hydrogen translocation of the formed C(sp^2) radicals from aryl/vinyl halides to a remote C(sp^3)–H sites.[83] One striking example was his remote C–H functionalization of alcohols utilizing a halo-aryl silane tether **189** (Scheme 59). Exposure of **189** to standard reductive radical initiation resulted in formation of aryl radical **190**, which underwent 1,5-HAT to generate alkyl radical species **191**. This transposed radical species can undergo further free radical-type reactions, such as reductive cyclization and coupling with alkenes. Inspired by Curran's transposition of radical species, we thought adopting this approach for translocation of putative hybrid Pd-radical species as a new approach for remote C–H functionalization.

Curran, 1988

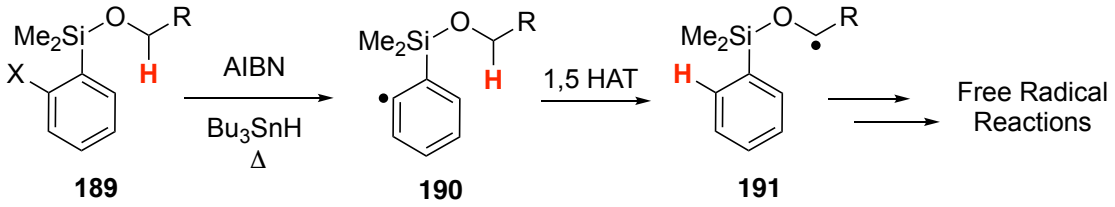

Scheme 59: Curran's translocation chemistry.

We hypothesized that if an aryl hybrid Pd-radical species (**193**) could be generated (Scheme 60); it, due to its inherent radical characteristics, may enable a translocation event to occur via HAT (**193→194**). Then, the transposed radical could recombine with the putative Pd species to form the alkyl-Pd intermediate **195**, which would allow for Pd-type transformation to occur at a remote C(sp^3)–H site. One transformation, in particular, is *β*–H elimination (**195→196**),[9,14,84] which would generate alkene **196**. Overall, our proposed transformation is formally an oxidative version of Curran's chemistry that allows for the direct desaturation of silyl ethers into synthetically valuable silyl enol ethers (**192→196**), to which only a few inefficient methods exist.[85] Also, the proposed transformation represents a new mechanistic mode for Pd-catalyzed C–H functionalization of aliphatic systems.

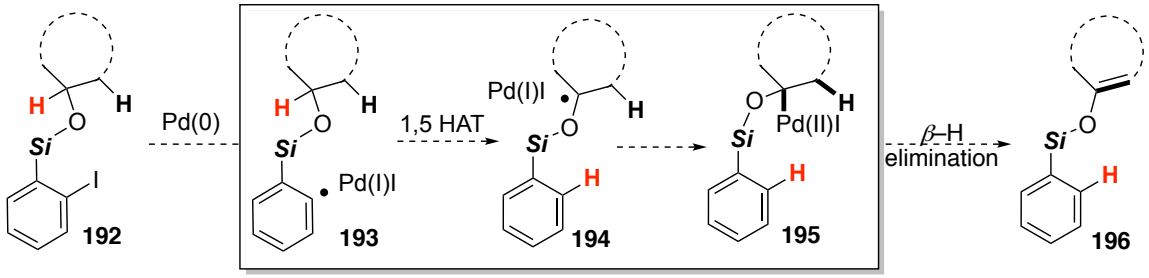

Scheme 60: Proposed direct desaturation of silyl ether in silyl enol ethers via formation of novel aryl hybrid Pd-radical intermediates.

5.2. Optimization of Reaction Conditions, Scope, and Limitations

This project was a collaborative effort in which my colleagues Padon Chuentragool and Dr. Dhruba Sarkar optimized the reaction parameters and developed the substrate scope of the transformation. Scheme 61 contains a brief summary of their results. In summary, it was found that transformation was promoted by visible-light,[86] without exogenous photosensitizers,[87] and the employed of ligand (**L**) provided optimal yields of the desaturated products. Also, the scope was found to be quite board, as desaturation of cyclic-, acyclic-, and unsymmetrical linear-silyl ethers worked well. My work for this project focused on the development of the concept and deducing the operative mechanism of the transformation by conducting various mechanistic studies. Hence, the rest of this chapter will focus on my specific contributions to this project.

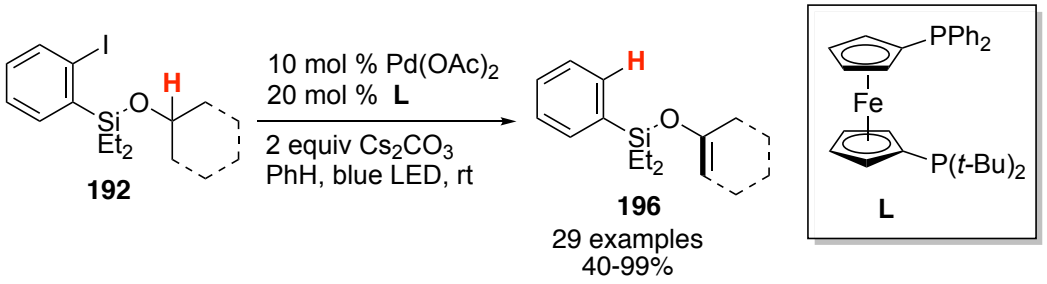

Scheme 61: Visible-light induced Pd-catalyzed desaturation reaction of silyl enols into silyl enol ethers.

5.3. Mechanistic Considerations

Based on our proposed hypothesis (Scheme 60) and the literature precedents for Pd-catalyzed remote C–H functionalization reactions, two distinct mechanistic scenarios were considered (Scheme 62).

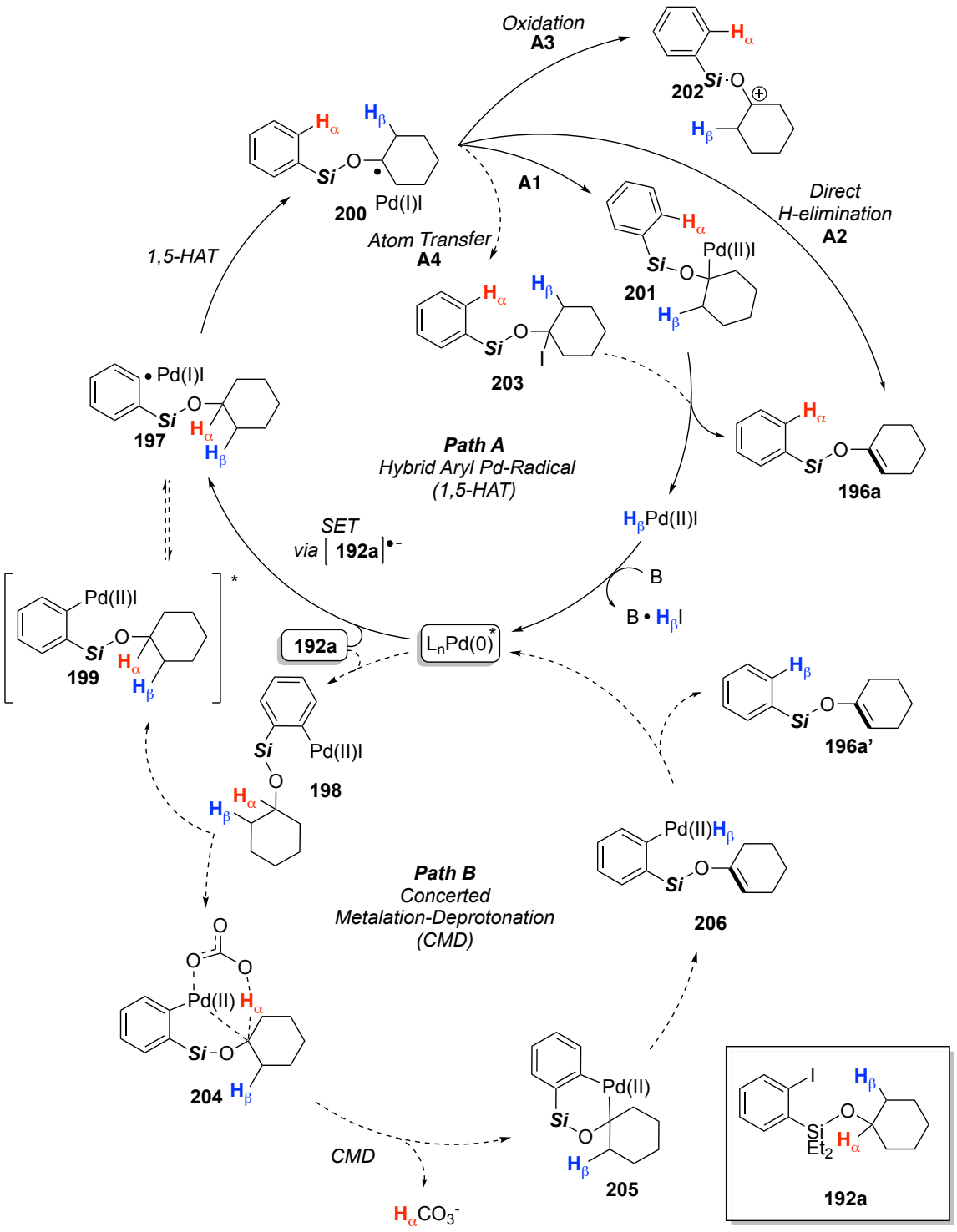

Scheme 62: Potential mechanisms for the transformation.

The first scenario is the aryl hybrid-Pd radical mechanism (Path A). First, the Pd(0) species undergoes photoexcitation with visible light to form excited Pd(0),[88] which

consequently undergoes a SET event with aryl iodide **192a** to produce aryl hybrid Pd-radical intermediate **197** via decomposition of the formed radical anion of **192a**. Intermediate **197**, however, can be formed through an alternative pathway involving oxidative addition of Pd(0) with **192a** to generate **198**, followed by its excitation with visible light into higher energy complex **199** and successive photoinduced homolysis.[89] Nevertheless, once formed, complex **197** undergoes a 1,5-HAT of Hα to furnish alkyl hybrid Pd-radical intermediate **200**. Next, radical-Pd recombination affords alkyl Pd complex **201**,[14] which undergoes facile *β*-hydride (Hβ) elimination to generate silyl enol ether **196** and the active Pd(0) catalyst. Alternatively, **196** can be formed via different endgame pathways from **200**, one of which is the Pd-involved direct Hβ-atom elimination (A2).[90] Other pathways involve oxidation of the radical **200** with Pd(I)I to form cationic intermediate **202**, followed by proton-loss step (A3). [91] Lastly, an atom-transfer/elimination (**200→203→196**) protocol could be operative (A4).[92] The second scenario involves a typical CMD mechanism (Path B).[55] The oxidative addition adduct **198** undergoes a CMD process of Hα (**198→204**) with the carbonate base to form palladacyle intermediate **205**. The subsequent *β*-H_β elimination results in **206**, followed by reductive elimination to form silyl enol ether **196a'** and the active Pd(0) catalyst.

Apparently, depending on the operative mechanism, a different H-atom is incorporated in the aryl of the silane tether, Hα for Path A and H_β for Path B. Thus, isotope labeling at a particular H-atom site and tracking the site of incorporation in the final product would distinguish the working mechanism (Scheme 63). α-Deuterium-labeled substrate **192-*d*** was synthesized with >98% *d*-incorporation and subjected to the reaction conditions. It was found that desaturation of **192-*d*** resulted in **196-*d*** as the sole

product with full deuterium-incorporation at the aryl silane tether. Therefore, a hybrid Pd-radical pathway (Path A) appears to be an operative mechanism. Kinetic isotope effect (KIE) studies were also conducted (Scheme 64), which resulted in a value of 3.3 and 3.0 for parallel and intermolecular KIE, respectively. These values indicate that HAT step is a rate-limiting event.[93]

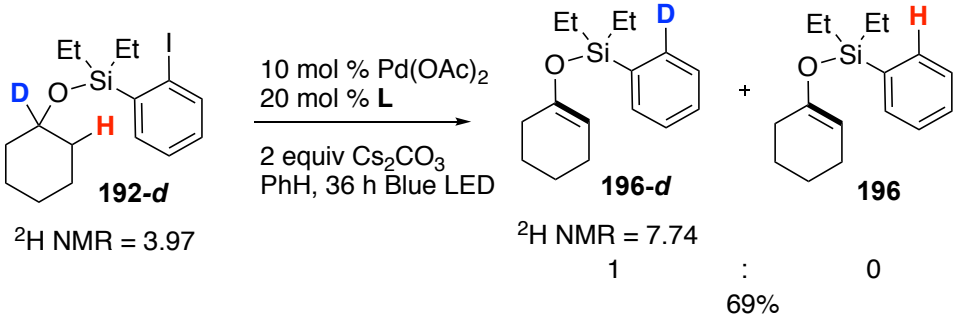

Scheme 63: Isotope labeling studies.

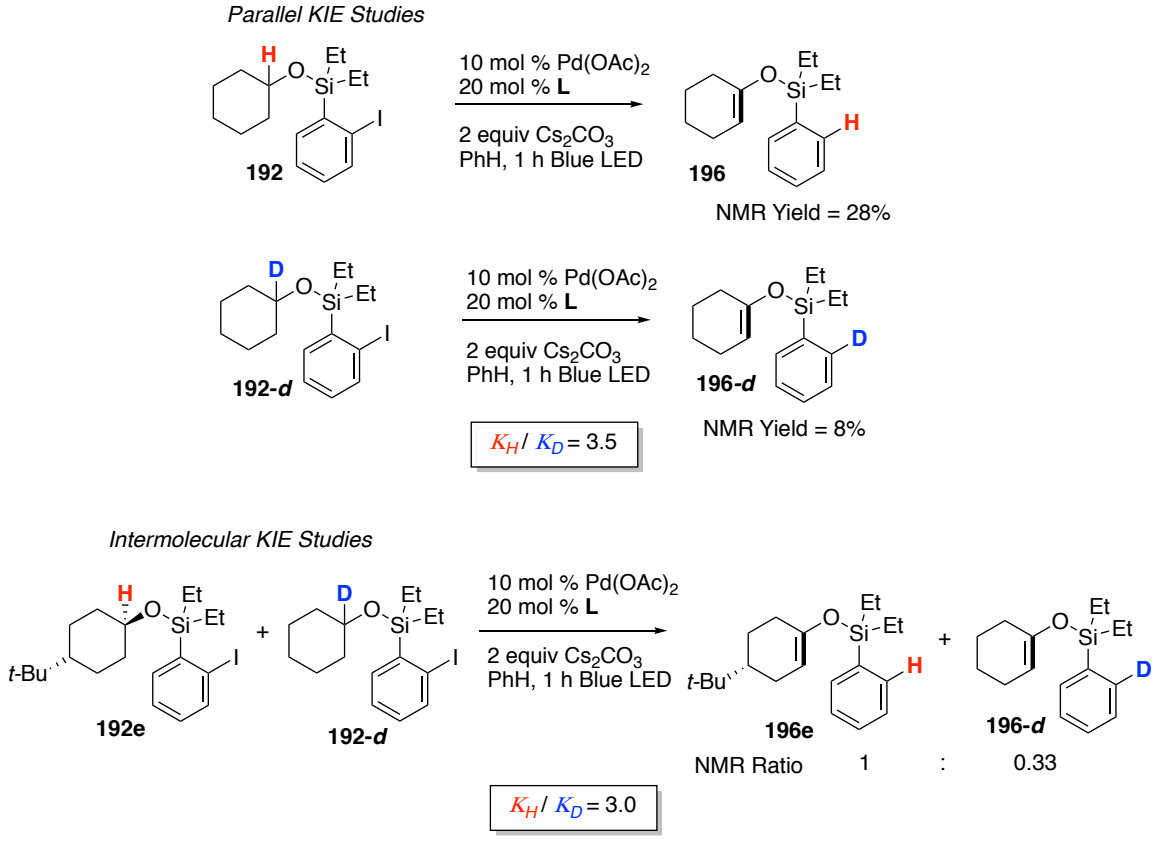

Scheme 64: Kinetic isotope effect (KIE) studies.

In order to provide further support for the Path A mechanism, radical trap and radical clock studies were performed. In the presence of various radical scavengers, the reaction either resulted in diminished yields of the desaturation product or completely shut down the reaction (Scheme 65). A radical clock test was conducted with **207**, which resulted in smooth regioselective radical-ring opening adduct **210** as the sole product (Scheme 66).[35] No products of intact cyclopropane unit **208** and/or Pd-β–Carbon elimination **209** were detected.[37] Thus, the nature of the translocated species is radical in character. The outcomes of theses studies support the intermediacy of radicals in this transformation.

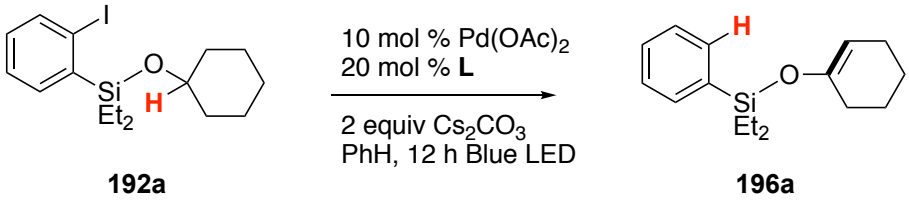

192a **196a**

Radical Traps	NMR Yield, %
None	79
BHT	65
Galvinyloxy	NR
TEMPO	NR

Scheme 65: Radical Trap Studies.

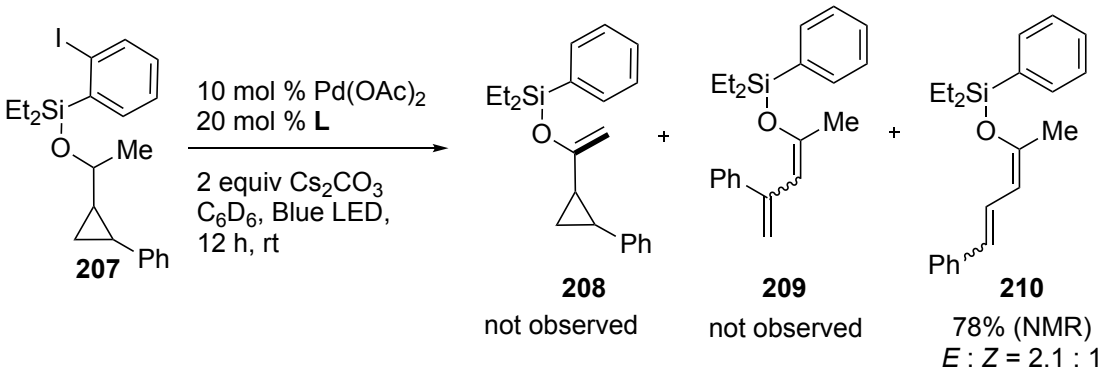

207 **208** not observed **209** not observed **210** 78% (NMR) *E* : *Z* = 2.1 : 1

Scheme 66: Radical Clock Studies.

Although the above experiments support the hybrid-Pd-radical pathway, the mechanism for formation of radical intermediate **197** was still unclear (Scheme 67). As mentioned above, this intermediate can be formed either by SET pathway (Route 1)[14] or via photoinduced homolysis of the oxidative addition intermediate **199** (Route 2).[89] In order to probe the latter pathway, we aimed to prepare the oxidative intermediate **199** independently and test its outcome under photoirradiation (Scheme 68). However, under various reactions conditions and employment of different Pd(0) sources, the desired oxidation adduct was not obtained (**198**), only the starting material (**192a**) remained (Table 7). Presumably, oxidative addition was impeded due to unfavorable steric interactions with the bulky silane tether and the Pd(0) precursors.[22,94] Interestingly, irradiating the stoichiometric reaction mixture with visible light resulted in full conversion of the starting material (**192**) into the desaturation product (**196**) by GC/MS analysis (Table 8). Importantly, no detectable amounts of the oxidative addition product **198** were observed by NMR analysis of this reaction. Based on these results, it is very likely that formation of radical intermediate **197** occurs via a photoinduced SET process (Route 1) and not via oxidative addition/homolysis pathway (Route 2).

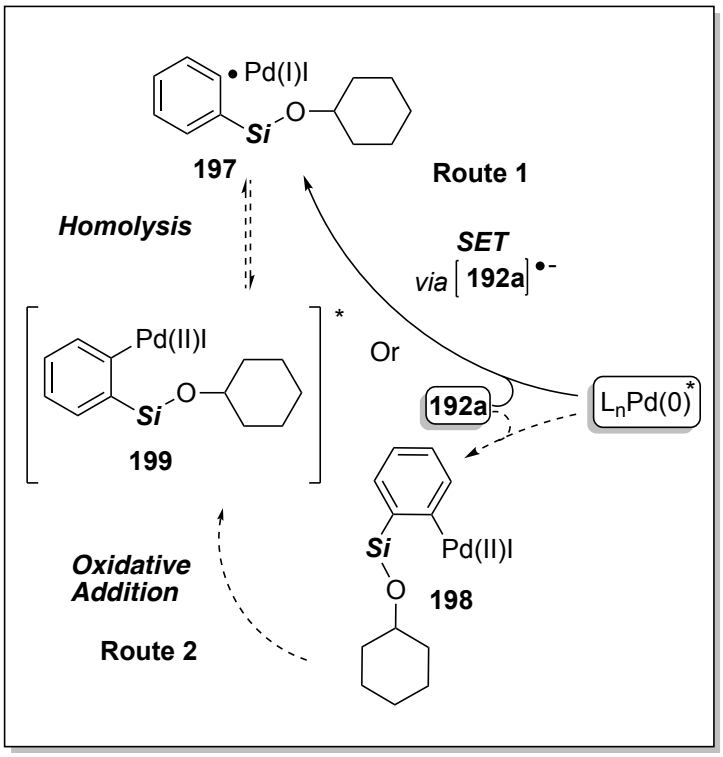

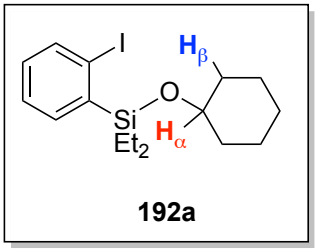

Scheme 67: Possible pathways for the formation of radical intermediate **197**.

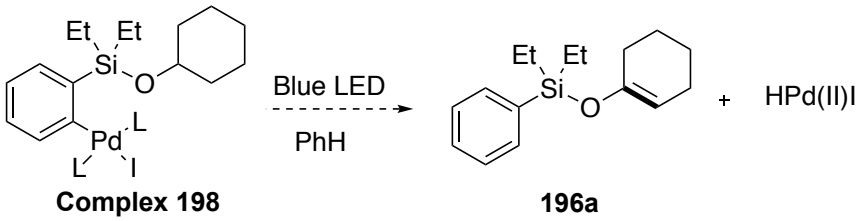

Scheme 68: Rationale for stoichiometric studies.

Table 7: Attempts to obtained complex **198** by stoichiometric studies.

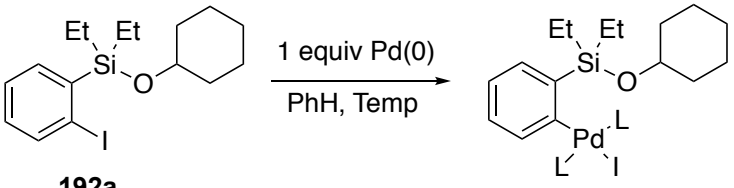

192a **Complex 198**

Entry	Pd(0)	Temp, ^{o}C	GC
1	$Pd(PPh_3)_4$	rt	NR, **192a** stays
2	$Pd(PPh_3)_4$	85	NR, **192a** stays
3	$Pd(PPh_3)_4$	150	NR, **192a** stays
4	$Pd(dba)_2$/**L**	rt	NR, **192a** stays
5	$Pd(dba)_2$/**L**	85	NR, **192a** stays
6	$Pd(dba)_2$/dppf	rt	NR, **192a** stays
7	$Pd(dba)_2$/dppf	85	NR, **192a** stays
8	$Pd(OAc)_2$/**L**	rt	NR, **192a** stays
9	$Pd(OAc)_2$/**L**	85	NR, **192a** stays
10	$Pd(OAc)_2$/**L**	120	NR, decomposition, complex **192a** was not observed by NMR

Table 8: Photoinduced desaturation of **192a** with stoichiometric amounts of Pd(0)

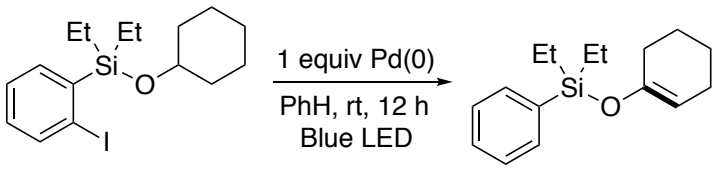

192a **196a**

Entry	Pd(0)	GC
1	$Pd(PPh_3)_4$	100% conversion of **192a** into **196a**
2	$Pd(OAc)_2$/**L**	100% conversion of **192a** into **196a**

As depicted in Scheme 69, formation of the silyl enol ether from intermediate **200** can proceed via four different endgame possibilities: (A1) β-H-elimination; (A2) direct H-atom elimination; (A3) oxidation; and (A4) atom-transfer/elimination. However, at this stage, only route A4 can be ruled out based on the stoichiometric studies without employment of base, where no atom transfer intermediate **211** could be detected/observed by NMR/GCMS analysis of the crude reaction mixture (Table 9). For the other cases, more mechanistic studies are needed to elucidate the operative mechanism.

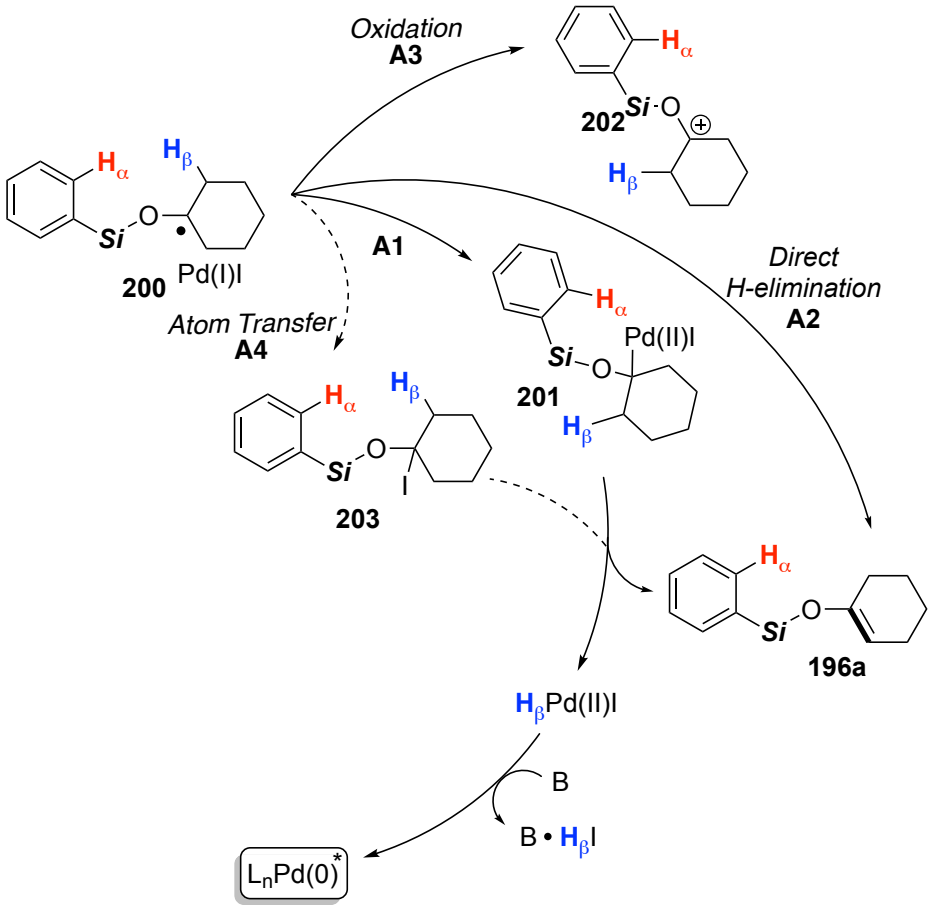

Scheme 69: Possible endgame pathways from **200** *en route* to **196a**.

Table 9: Route A4 studies.

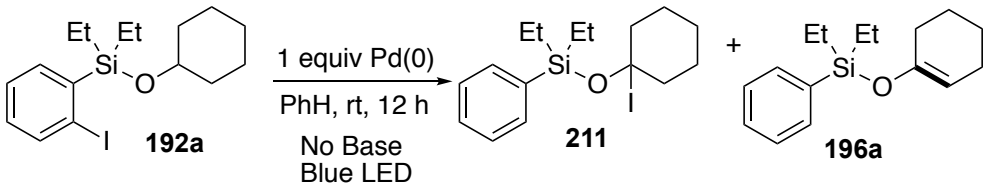

Entry	Pd(0)	**211** (GCMS/NMR)	**196** (GC yield,%)
1	$Pd(PPh_3)_4$	not observed	68
2	$Pd(OAc)_2$/**L**	not observed	70
3	$Pd(OAc)_2$ (10%) / **L** (20%)	not observed	NR

5.4 Summary

In summary, we have shown the first photoinduced generation of an aryl Pd-radical hybrid species, and its ability to enable a remote C–H functionalization event via a 1,5-HAT process. Overall, our photoinduced strategy enabled a mild, general, and direct synthesis of valuable silyl enol ethers from silyl ethers at room temperature without the use of exogenous photosensitizers or oxidants. Mechanistic studies supported the radical nature of this unprecedented transformation and provided evidence that the formation of the aryl radical intermediate occurs via a photoinduced SET process and not the expected oxidation addition/homolysis path.

6. General Remote Desaturation of Aliphatic Alcohols at Unactivated C(sp^3)–H Sites Enabled by Auxiliary Controlled Visible Light-induced Hybrid Pd-Radical Catalysis

6.1. Reaction Development

Alkenols, such as allylic-, homoallylic-, and bis-homoallylic alcohols, are an important class of functional groups, widely present in an array of important natural products (Scheme 70), and extensively used as building blocks in organic synthesis.[95] However, accessing these important moieties requires pre-functionalized systems and multi-step procedures.[96] An attractive approach would be a direct desaturation of an aliphatic alcohol into the alkenol moiety, as it would enable late-stage desaturation of complex molecules and significantly reduce the number of steps toward accessing these fragments.

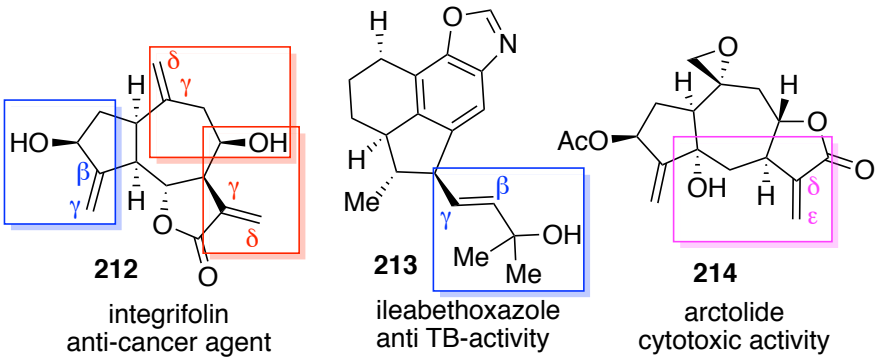

Scheme 70: Important natural products possessing alkenol fragments.

Among the state-of-the-art approaches (*vide supra*), Baran's guided desaturation of alcohols is the most notable achievement (Scheme 71). Although very innovative, considerable limitations exist that precludes it for general use. For instance, Baran's

approach is limited to the formation of homoallylic alcohols (**218**), via *γ*-/*δ*-desaturation of the parent aliphatic precursor (**215**), and due to the low variability of C–H activation of the employed tether **219**. Also, the reaction products are formed with modest yields and low regioselectivity (Scheme 57). This is due to the nature of the mechanism, which involves formation of carbocation intermediate **217** and an "uncontrollable" proton loss step (**217→218**).

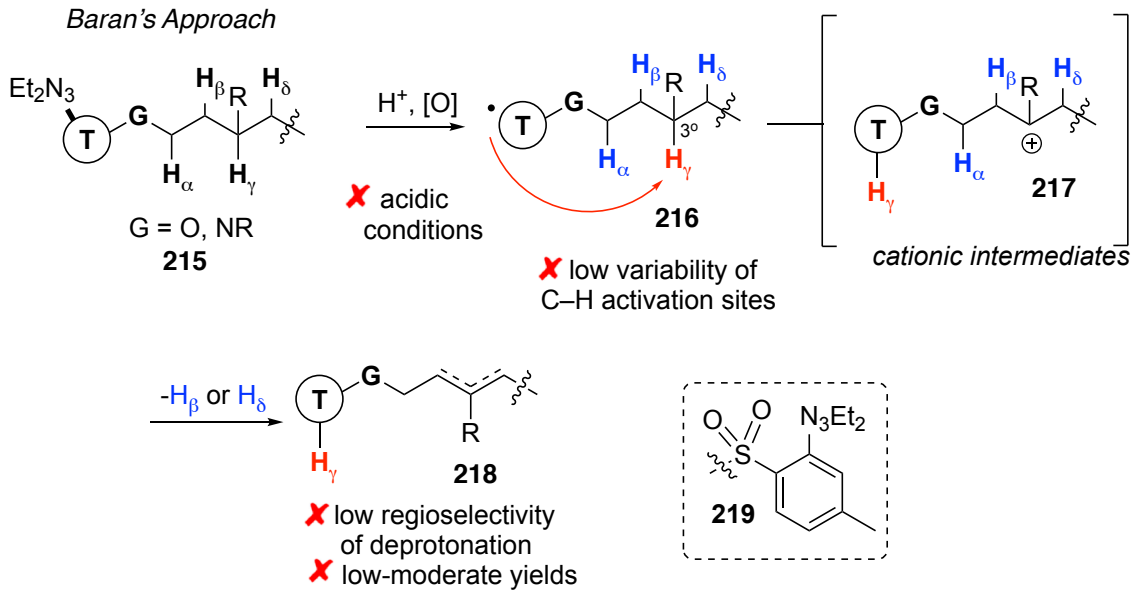

Scheme 71: Baran's state-of-the-art desaturation of alcohols.

Based on our previous work on the *α*-/*β*- desaturation of silyl ethers into silyl enol ethers, we envisioned that applying our translocative hybrid-Pd radical strategy (Scheme 72) for remote C–H desaturation could solve the inherent limitations of Baran's strategy, such as regioselectivity and efficiency issues. Specifically, our proposed mechanism involves an endgame Pd-involved *β*-H elimination step (**223→224**),[14] which will provide a "controlled" elimination that will furnish alkenols with high degrees of regioselectivity. Moreover, we envisioned by leveraging the flexibility of easily installable/removable

reactive Si-tethers,[97] it will allow for an auxiliary-controlled activation of *β*-, *γ*-, or *δ*-C(sp^3)–H bonds (**221**), resulting in site-selective desaturation of aliphatic alcohols to afford allylic-, homoallylic, and bis-homoallylic alkenols (**223→224**). Not only will the presented concept provide a general strategy for a mild and efficient desaturation, but it will also feature a new mechanistic approach for Pd-catalyzed remote C(sp^3)–H functionalization.

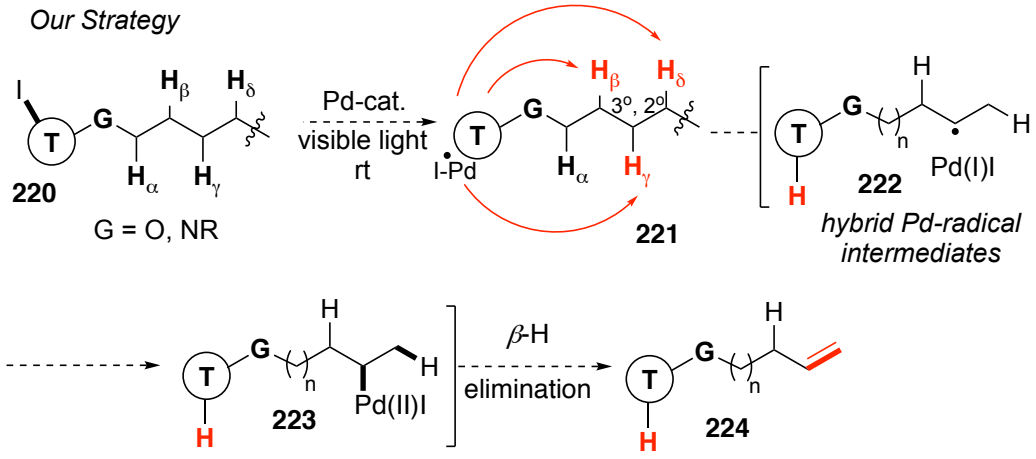

Scheme 72: Our strategy for targeted remote desaturation of aliphatic alcohols involving hybrid-Pd radical intermediates.

6.2. Optimization of the Reaction Conditions

In the context of our prior work, employment of an aryl silyl-tether **225** (Scheme 73) enabled a site-selective *α*-C–H abstraction event due to geometrical constraints, and a favored 1,5-HAT process, which allowed for efficient *α*-/*β*-desaturation of silyl ethers into silyl enol ethers. In order to achieve site-selective functionalization of unactivated remote C–H sites, employment of an auxiliary that is capable of HAT beyond *α*-C–H site is required. We reasoned that positioning the formed radical species closer to the silane

tether may trigger a 1,*n*-HAT (n≥5) process of unactivated C(sp^3)–H sites and, thus, empower a remote desaturation process (e.g. **226**). Hence, we turned our attention toward employment of iodomethylsilane tethers (**227-228**) for the following reasons: (1) Based on our previous work, silyl methyl hybrid-Pd radicals can be easily formed in the presence of Pd(0) (Chapter 2); (2) there have been scattered reports on the propensity of silyl methyl radical species to undergo 1,*n*-HAT (*n*=5-8) with activated C(sp^3)–H sites under reductive radical conditions;[83e,98] and (3) based on the stability of Me_3SiCH_2–H (~100 kcal/mol) bonds, HAT of silyl methyl radical species with unactivated tertiary (95 kcal/mol) and secondary (98 kcal/mol) C–H sites may be feasible.[99] The above hypothesis was tested on Baran's challenging alcohol (**229**) using iodomethylsilane tether ($\mathbf{T_1}$). Gratifyingly, under our previously optimized visible light-induced conditions, **229** resulted in *γ*-/*δ*-desaturation homoallylic alcohol **230a** in *77% yield as the sole regioisomer*. Compared to Baran's approach (using $\mathbf{T_B}$, 55% yield, r.r. = 1.15:1), the reaction efficiency and regioselectivity outcome of our method was superior. This result supports our hypothesis, where the favorable nature of this novel mechanism provides a "controlled" Pd-involved *β*-H elimination[9,14,22,84] event rather than an "uncontrolled" proton loss as in Baran's protocol (*vide supra*).[79] Test experiments indicated that light is required to promote the transformation; and attempts on performing this transformation under thermal means were ineffective (Scheme 74).

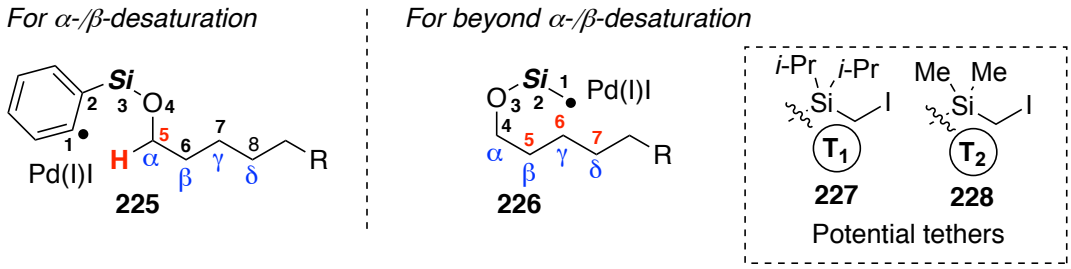

Scheme 73: Preference for C–H abstraction using different tethers based on distance of the formed radical.

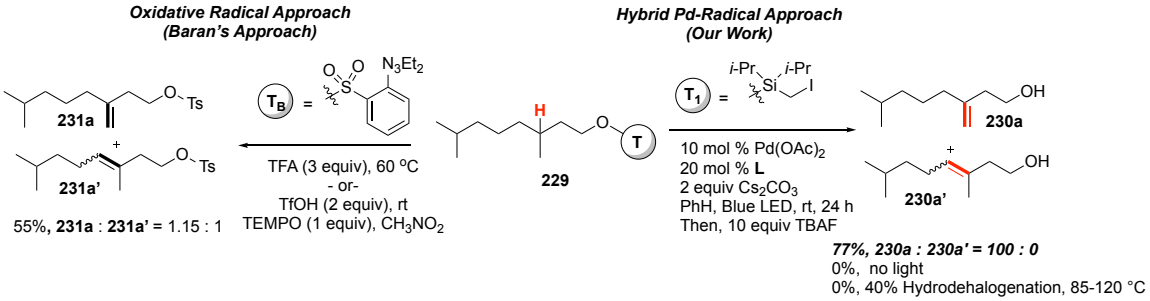

Scheme 74: Initial results and comparison to prior art.

Based on our previous work on the *endo* selective silyl methyl Heck reaction using $\mathbf{T_1}$ (**69**, *vide supra*), installation of bulky $\mathbf{T_1}$ onto secondary and tertiary alcohols required harsh reaction conditions and was inefficient. Hence, in order to obviate the need of forcing reaction conditions and use of high molecular weight silicon tethers for installation onto bulkier alcohols, we opted to employ sterically less hindered dimethyl(iodomethyl)silane tether ($\mathbf{T_2}$). The synthesis of $\mathbf{T_2}$**-Cl** (**232**) is depicted in Scheme 75. Next, optimization of the reaction parameters was conducted on $\mathbf{T_2}$-tethered-(-)-menthol (**229f**). It was found, however, that our previous reaction conditions were the most efficient (Table 10, entry 11). Interestingly, ligands that are typically employed for photoredox catalysis, such as bipyridine and phenantroline, were inefficient (entry 1-2).[87]

In addition, a control study indicated that the Pd-catalyst is required for this transformation (entry 14).

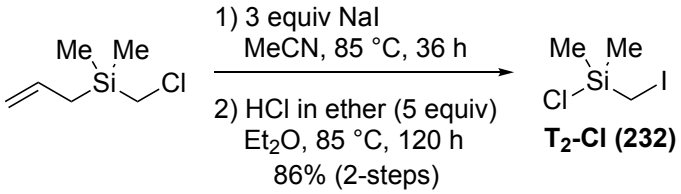

Scheme 75: Synthesis of **T_2-Cl** (**232**).

Table 10: Optimization of the reaction conditions using benchmark substrate **229f**.

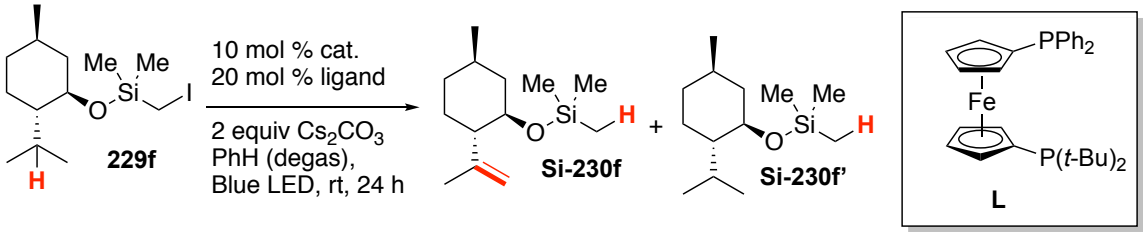

#	catalyst	ligand	**Si-230f : Si-230f'**	GC yield,[a]%
1	$Pd(OAc)_2$	bipy	-	NR
2	$Pd(OAc)_2$	1,10-phen	-	NR
3	$Pd(PPh_3)_4$	-	4 : 1	57
4	$Pd(OAc)_2$	SiPr	-	NR
5	$Pd(OAc)_2$	dppe	-	Traces
6	$Pd(OAc)_2$	Triphos	1 : 1	28
7	$Pd(OAc)_2$	DPEphos	-	NR
8	$Pd(OAc)_2$	Binap	1 : 0	47
9	$Pd(OAc)_2$	dppf	1 : 1	12
10	$Pd(OAc)_2$	xantphos	-	72
11	**$Pd(OAc)_2$**	**L**	**20 : 1**	**94**
12[b]	$Pd(OAc)_2$	**L**	20 : 1	60
13	$Pd(OAc)_2$	-	-	<2
14	-	**L**	-	<2

[a]GC yields were calibrated using pentadecane as an internal standard. [b]5 mol % Pd /10 mol % **L**

6.3. Scope and Limitations

After identifying the optimized reaction conditions, the scope of the *γ*-/*δ*-desaturation of aliphatic alcohols toward homoallylic alcohols was examined (Scheme 76). It should be mentioned that upon completion of the desaturation reaction, the silyl-based tethers were removed by a standard desilylation protocol with TBAF (one-pot). For cases where desilylation would generate volatile alkenols, the silyl-protected alkenols were isolated instead. Various primary alcohols, possessing important functionalities such as alcohols (**229b-c**) and amides (**229e**), underwent smooth *γ*-/*δ*-desaturation into the corresponding homoallylic alcohols (**230b-c,e**) in good yield. Next, desaturation of secondary alcohols was tested (**1f-1h**). Important terpene building block (-)-isopulegol (**230f**) was obtained in 79% yield via *γ*-/*δ*-desaturation of a precursor (-)-menthol (**229f**). Desaturation of substrate **229g**, possessing a remote olefin, resulted in diene **230g** in good yield. Importantly, employment of substrates **229h** and **229i** possessing competitive sites of abstraction, H*β*/H*γ* and H*γ*/H*δ,* respectively, resulted in selective activation of *γ*-C–H bonds, thus resulting in formation of **230h** and **230i** in good yields with high levels of regioselectivity. Based on these studies, the regiochemical preference for HAT using tethers $\mathbf{T_1}$ and $\mathbf{T_2}$ for substrates containing C–H sites with similar BDE[99] is as follows: 1,6 HAT of H*γ* >1,5 HAT of H*β* > 1,7 HAT of H*δ.* Tertiary alcohols were found to be also compatible with our desaturation protocol, as desaturation of **229j→230j** proceeded efficiently. Excitingly, desaturation of challenging tertiary alcohol **229k,** possessing inert 2° C–H bonds, was also accomplished, producing **230k** in good yield. Finally, we tested our *γ*-/*δ*-desaturation protocol on complex natural products and derivatives. It was found that desaturation of abietol worked quite well, generating **230l** in respectable yield. Also,

γ-/δ-desaturation of steroid systems, such as secondary cis-androsterone (**229m**) and tertiary cholestanol derivative (**229n**), were efficient, furnishing **230m** and **230n** in good yields.

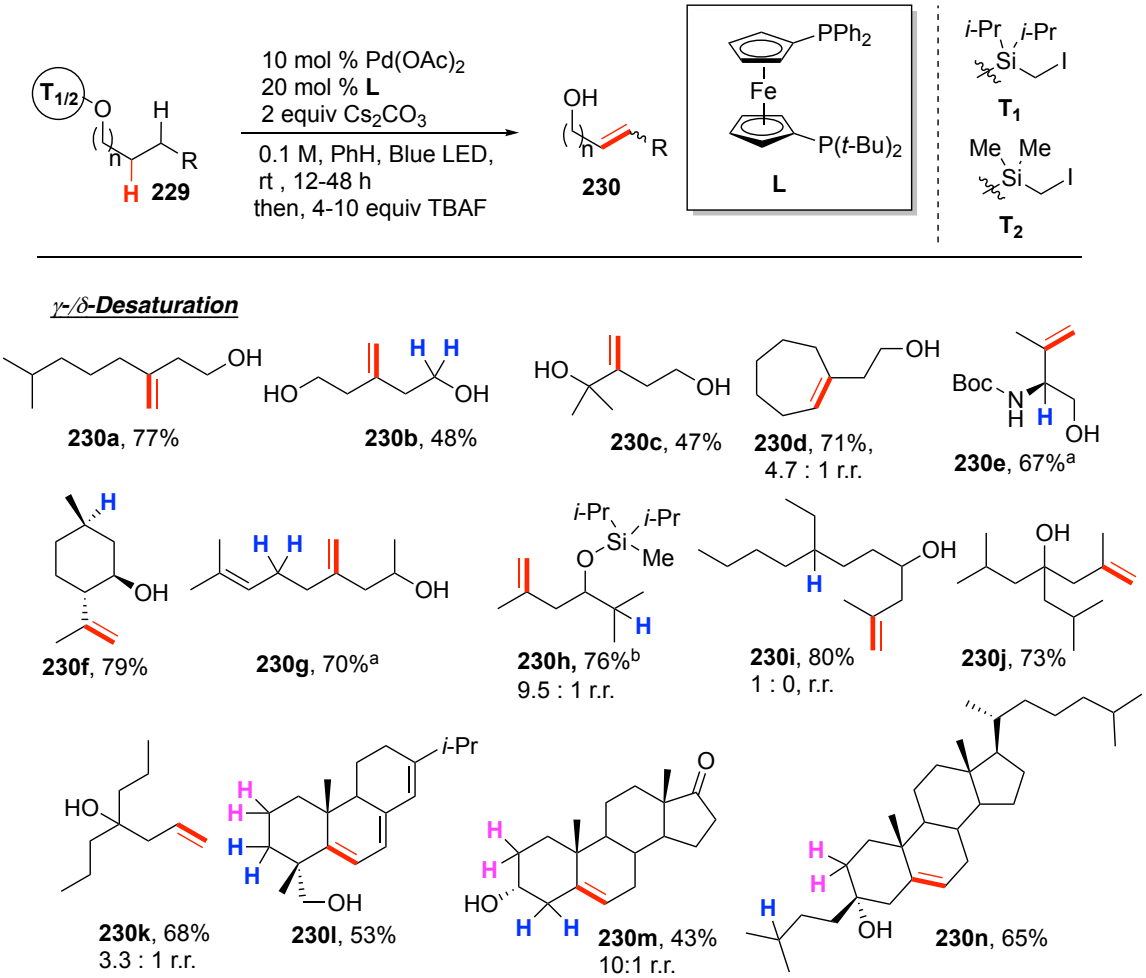

Scheme 76: γ-/δ-desaturation of aliphatic alcohols toward homoallylic alcohols. [a]Contains minor amount of hydrodehalogenation by-product. [b]The desilylation step (TBAF) was omitted. r.r. = regioisomeric ratio.

Interestingly, when secondary alcohol **229o-T$_2$**, possessing a 3° β-C–H site and a competitive 2° γ-C–H site, was exposed to the reaction conditions, desaturation product

2o–T$_2$ was produced as a 1:1.5 mixture of *β*-/*γ*- and *γ*-/*δ*-desaturation products, respectively (Scheme 76). This result indicates that the innate preference for 1,6-HAT occurs regardless of the BDE[99] of *γ*–C–H bond. Conversely, when **T$_1$** was employed on the same alcohol (**229o-1**), the *β*-/*γ*-desaturation product **230–1** was formed predominantly. In this case, it is likely that the steric interactions between the bulky isopropyl groups on Si-tether of **T$_1$** and the isopropyl group of the substrate disfavors the usually preferred confirmation for 1,6-HAT (**230-T$_1$**), which consequently promoted for activation of the *β*-C–H site via 1,5-HAT.

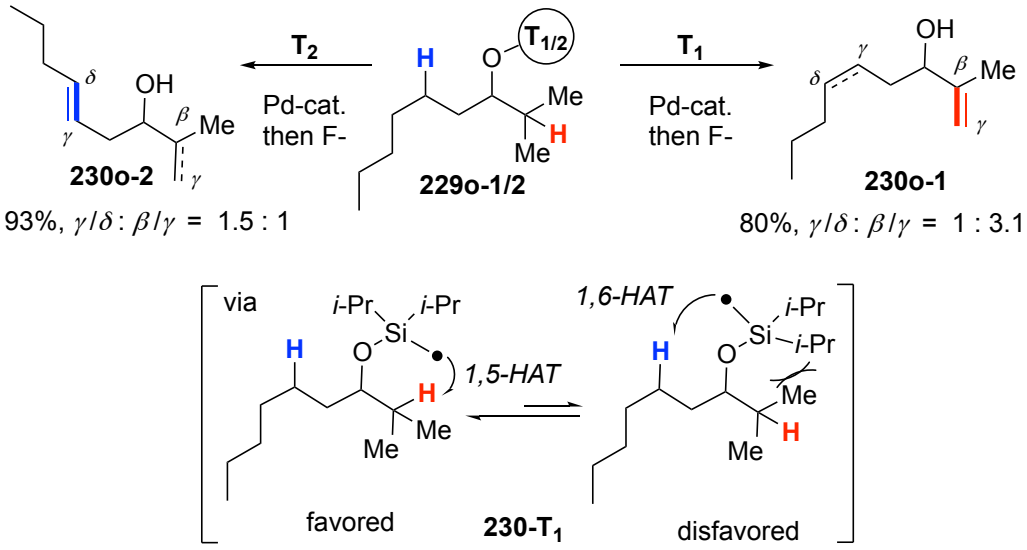

Scheme 77: Regiodivergent desaturation of ambident substrates employing different tethers.

Based on the aforementioned observations, we sought to expand our method toward *β*-*γ*-desaturation alcohols into synthetic valuable allylic alcohols using **T$_2$** (Scheme 78).[96e] In certain cases, however, **T$_2$** was required for sterically encumbered alcohols. Desaturation of secondary alcohols bearing an isopropyl group resulted in efficient formation of allylic alcohols (**230p-r**). Moreover, tertiary cyclic- and bicyclic

alcohols were found to be competent substrates as well, generating the corresponding products **230s-t** in good yields. Next, desaturation of *β*-methyl cycloalkanes was tested. Exposure of the 5-membered cycloalkane **229u** to the reaction conditions resulted in the thermodynamic alkene product **230u**. Contrariwise, 6-membered cycloalkanes underwent desaturation into the kinetic *exo*-methylene products **230v**–**w**. Also, complex limonene derivative **1x** underwent smooth *β*-/*γ*-desaturation, furnishing *exo*-alkene **230x** in 70% yield. Then, reaction of ambident substrate **229y**, possessing competing *β*-/*γ*- and *δ*-/ε-desaturation sites, was examined. Expectedly, it was found that desaturation occurred selectively at the former site, leading to allylic alcohol **230y** in 73% yield (*vide supra*).

Finally, we pushed the limits of developed methodology toward unprecedented *δ*-/ε- desaturation of alcohols. It was found that employment of primary (**229z**), secondary (**229aa**), and tertiary alcohols (**229aa**) all underwent smooth *δ*-/ε- desaturation in moderate to excellent yield (**230z,aa-ab**). Interestingly, desaturation of complex derivative, dehydroabietol **229ac**, resulted in selective formation of *δ*-/ε- desaturation product **230ac**, probably via a rare 2° *ε*- C–H activation event through 1,8-HAT.[83e]

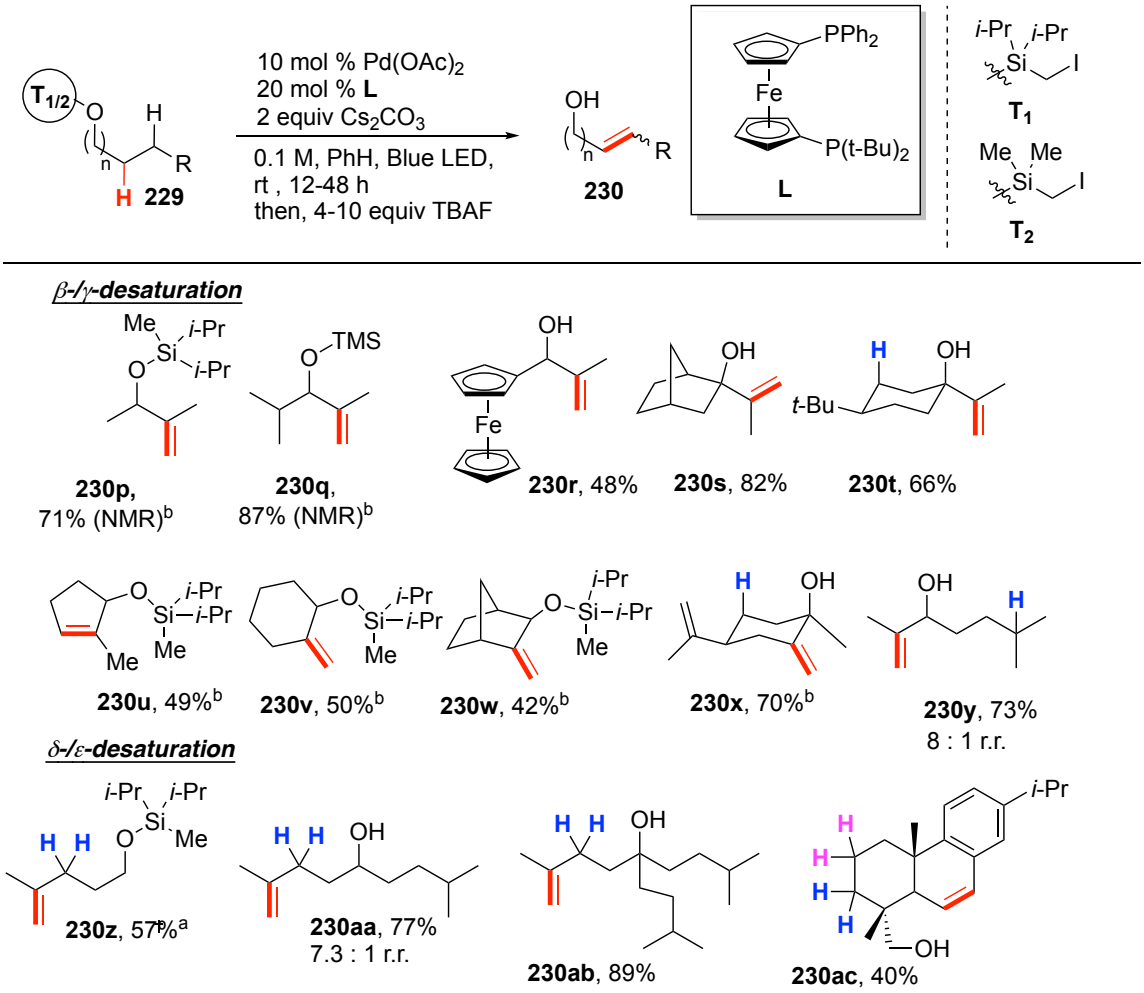

Scheme 78: Beyond γ-/δ-desaturation. β-/γ- and δ-/ε-desaturation of aliphatic alcohols toward homoallylic and bis-homoallylic alcohols, respectively. [a]Contains minor amount of hydrodehalogenation by-product. [b]The desilylation step (TBAF) was omitted. r.r. = regioisomeric ratio.

6.4. Mechanistic Considerations

As discussed above, our desaturation approach resulted in superior regioselectivity of the desaturation products compared to that of Baran's method. Hence, it is very likely that our transformation does not operate via cationic intermediates, as in

Baran's case, but via a hybrid-Pd-radical mechanism.[14] In order to verify the intermediacy radicals in this transformation, typical radical test experiments were conducted (Scheme 79). In the presence of TEMPO, **229f** resulted in TEMPO trapped adduct **233** in 49% NMR yield, which indicates that the radical is initially formed at the silyl methyl position. In addition, a radical clock study was performed. Cyclopropane radical clock substrate **234** was subjected to the reaction conditions and resulted in selective radical ring-opening product **237**.[35] This result supports the formation of a translocated radical species via the 1,6-HAT process. Based on these studies, a hybrid-Pd-radical mechanism was proposed for this transformation (Scheme 80). The active photoinduced Pd(0) complex undergoes SET with Si-tethered alcohol **229** to generate the Pd(I)I complex and the silyl methyl radical species **238**. The latter undergoes a 1,*n*-HAT (*n*=5-8) event to furnish alkyl hybrid-Pd radical intermediate **239**. Next, a subsequent radical recombination of **239** with Pd(I)I produces alkyl Pd-intermediate **240**. Finally, the latter undergoes a "controlled" Pd-involved *β*-hydride elimination step (**240→230**),[9,14,22,84] which forms the desired alkenol fragment **230** and the Pd(II) complex. The latter undergoes base-induced reductive elimination to form the active Pd(0) complex and closes the catalytic cycle.

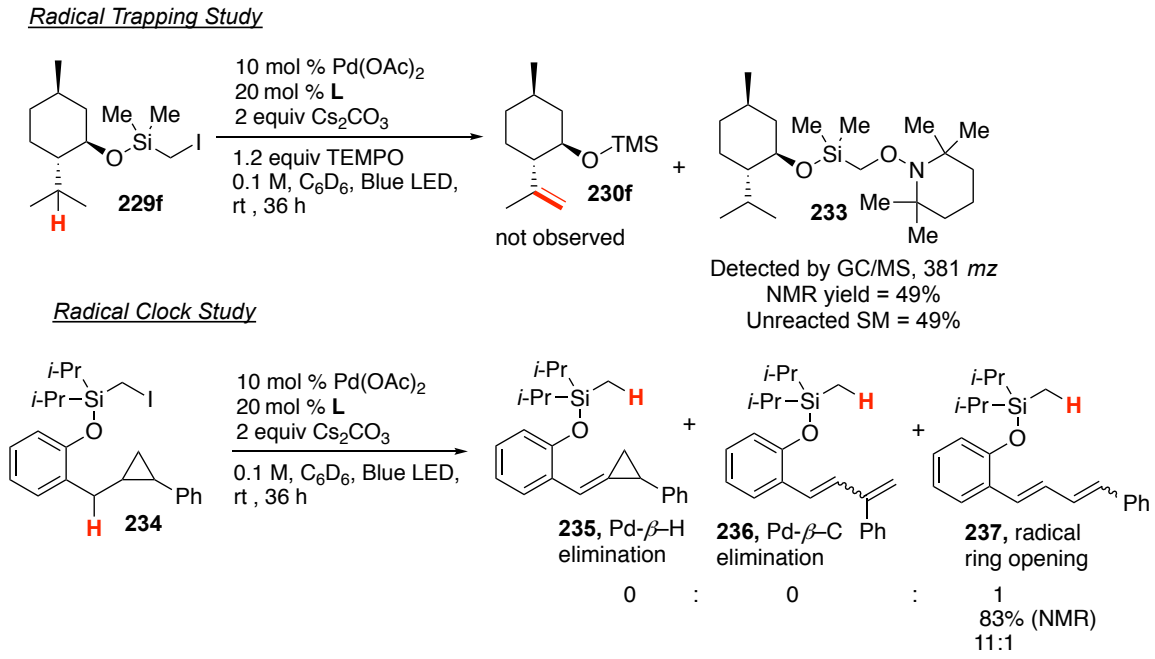

Scheme 79: Mechanistic studies.

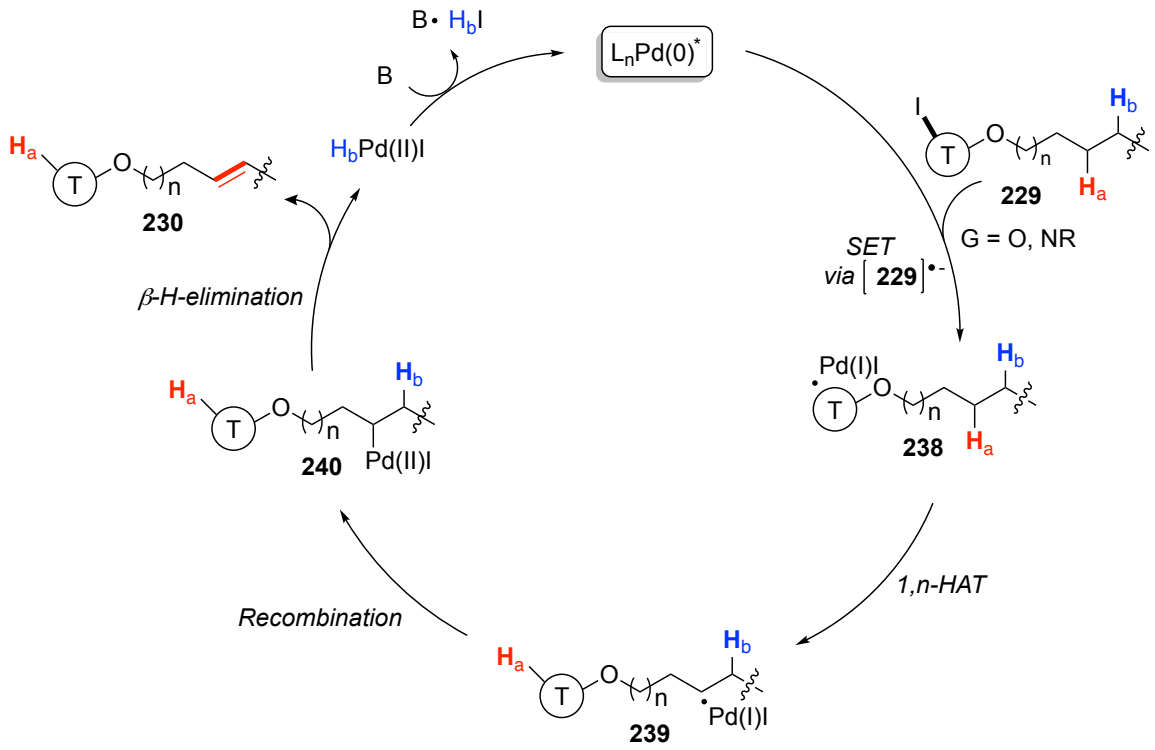

Scheme 80: Mechanism of the Pd-catalyzed desaturation of aliphatic alcohols.

6.5. Summary

In summary, we have developed a mild, general, and selective Pd-catalyzed method for desaturation of aliphatic alcohols. The mechanism of this method operates via a hybrid-Pd radical approach, which synergistically combines the best features of the radical and Pd chemistry and thus, empowers this novel desaturation protocol to occur. It was shown for the first time that the formed hybrid Pd-radical intermediates are capable of a facile 1,*n*-HAT process at remote unactivated C(sp^3)–H sites. Formation of these key hybrid Pd-radical intermediates are efficiently induced by visible light, without exogenous photosensitizers, from alkyl-iodides and Pd(0) complexes, thus, allowing desaturation of aliphatic alcohols to occur under neutral conditions at room temperature. Moreover, based on the nature of the mechanism, the endgame desaturation step occurs via "controlled," Pd-involved *β*–H elimination step, which generates the alkenol products with unmatched for radical chemistry degrees of regioselectivity. In addition, our concept involves the utilization of easily installable/removable tethers capable of targeted activation of 2°/3°- *β*-, *γ*-, and *δ*-positions of aliphatic systems, resulting in valuable unsaturated alcohols. Overall, due to the nature of this novel mechanism, our approach solves the inherent limitations of previously developed desaturation protocols and provides a new direction for site-controlled Pd-catalyzed C–H functionalization of aliphatic molecules.

7. Experimental Section

7.1. General Information

NMR spectra were recorded on Bruker Avance DRX-500 (500 MHz) or DPX-400 (400 MHz) instrument. 1H signals are referenced to residual $CHCl_3$ at 7.26 ppm. ^{13}C signals are referenced to $CDCl_3$ at 77.0 ppm. GC/MS analysis was performed on a Hewlett Packard Model 6890 GC interfaced to a Hewlett Packard Model 5973 mass selective detector (15 m x 0.25 mm capillary column, HP-5MS). Column chromatography was carried out employing Silicycle Silica-P flash silica gel (40-63 μm). Precoated silica gel plates F-254 were used for thin-layer analytical chromatography. LRMS and HRMS analyses were performed on Micromass 70 VSE mass spectrometer. Anhydrous solvents purchased from Aldrich were additionally purified on PureSolv PS-400-4 by Innovative Technology, Inc. purification system and/or stored over calcium hydride. All starting materials were purchased from Strem Chemicals, Aldrich, Gelest Inc., TCI America, or Alfa Aesar, or synthesized via known literature procedures. The 34 W Blue LED lamp (Kessil KSH150B LED Grow Light), 23W Philips Household CFL, and Vornado 133 Small Air Circulator fan were purchased from amazon.com. All manipulations with transition metal catalysts were conducted in oven-dried glassware under inert atmosphere using a combination of glovebox and standard Schlenk techniques.

7.2. Photoinduced Formation of Hybrid Aryl Pd-Radicals Species Capable of 1,5-HAT: Catalytic Oxidation of Silyl Ethers into Silyl Enol Ethers (Previously Published as Parasram, M.; Chuentragool, P.; Sarkar, D.; Gevorgyan, V. "Photoinduced Formation of Hybrid Aryl Pd-Radical Species Capable of 1,5-HAT: Selective Catalytic Oxidation of Silyl Ethers into Silyl Enol Ethers." *J. Am. Chem. Soc.* 2016, *138*, 6340.)

7.2.1 Analytics of the Substrates Employed for Mechanistic Studies

Starting Materials:

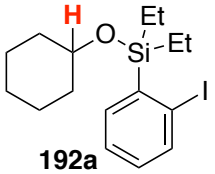

192a

Isolated yield = 32% yield. Colorless oil. R_f (hexanes): 0.31.

^{1}H NMR (500 MHz, $CDCl_3$): δ ppm 7.83-7.85 (m, 1H), 7.64-7.62 (m, 1H), 7.36-7.33 (m, 1H), 7.05-7.01 (m, 1H), 3.80-3.74 (m, 1H), 1.87-1.85 (m, 2H), 1.76-1.75 (m, 2H), 1.52-1.42 (m, 3H), 1.28-1.23 (m, 3H), 1.14-1.0.98 (m, 4H), 0.96-0.93 (m, 6H). ^{13}C NMR (126 MHz, $CDCl_3$) δ ppm 5.5, 7.0, 24.2, 25.6, 35.9, 71.4, 102.7, 126.8, 130.9, 138.1, 139.6, 142.8. HRMS (EI+) calcd. for C16H25IOSi [M]: 388.0720, found: 388.0722.

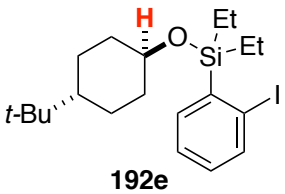

192e

Isolated yield = 41%. Colorless oil. Rf (hexanes): 0.35.

^{1}H NMR (500 MHz, $CDCl_3$): δ ppm 7.85-7.84 (m, 1H), 7.61-7.59 (m, 1H), 7.35-7.32 (m, 1H), 7.05-7.01 (m, 1H), 3.68-3.61 (m, 1H), 2.02-2.00 (m, 2H), 1.77-1.75 (m, 2H), 1.43-1.37 (m, 2H), 1.13-1.03 (m, 2H), 1.03-1.01 (m, 1H), 1.01-0.98 (m, 2H), 0.98-0.94 (m, 8H), 0.85-0.83 (m, 9H). ^{13}C NMR (126 MHz, $CDCl_3$) δ ppm 5.4, 7.0, 25.8, 27.6, 32.3, 36.4, 47.2, 72.6, 102.7, 126.8, 130.9, 138.1, 139.7, 142.8. HRMS (ESI) calcd. for $C_{20}H_{33}IOSi$ [M+1]: 444.1345, found: 444.1347.

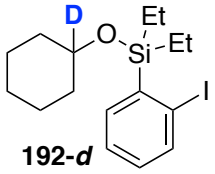

192-*d*

Isolated yield = 55%. >98% D incorporation. Colorless oil. R_f (hexanes): 0.20. ^{1}H NMR (500 MHz, $CDCl_3$): δ ppm 7.85 (d, *J* = 8.07 Hz, 1H), 7.64 (dd, *J* = 7.34 Hz, *J* = 1.47 Hz, 1H), 7.34 (m, 1H), 7.03 (td, *J* = 8.07 Hz, *J* = 1.83 Hz, 1H), 1.87-1.85 (m, 2H), 1.76-1.73 (m, 2H), 1.52-1.43 (m, 3H), 1.31-1.22 (m, 3H), 1.14-0.98 (m, 4H), 0.96-0.94 (m, 6H). ^{13}C NMR (126 MHz, $CDCl_3$) δ ppm 5.4, 7.0, 24.2, 25.7, 35.8, 102.7, 126.8, 130.9, 138.1, 139.7, 142.8. ^{2}H NMR (77 MHz, CCl_4) δ ppm 3.97. HRMS (EI+) calcd. for $C_{16}H_{24}DIOSi$ [M]: 389.0782, found: 375.0794.

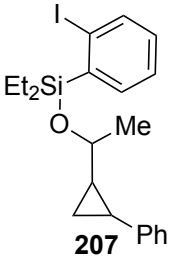

207

Isolated yield = 40% yield. Diastereomeric Ratio = 1.5:1 (GC). Clear and Colorless oil. Rf (50:1 Hexanes : Ethyl Acetate): 0.3. ^{1}H NMR (500 MHz, $CDCl_3$): δ ppm 7.88-7.82 (m, 1H), 7.65- 7.59 (m, 1H), 7.37-7.24 (m, 3H), 7.17-7.14 (m, 1H), 7.07-7.00 (m, 3H), 3.71-3.67 (m, 1H), 1.91-1.79 (m, 1H), 1.39-1.36 (m, 3H), 1.18-0.88 (m, 13H). ^{13}C NMR

(126 MHz, $CDCl_3$) δ ppm 5.3, 5.4, 5.5, 5.6, 6.9, 7.0, 13.4, 14.5, 20.6, 21.7, 23.7, 23.9, 30.8, 31.0, 71.9, 72.0, 102.7, 102.8, 125.3, 125.4, 125.8, 125.9, 126.9, 128.2, 128.3, 130.9, 131.0, 138.0, 138.2, 139.7, 139.8, 142.5, 142.6, 143.0, 143.2. HRMS (EI) calcd. for $C_{21}H_{27}IOSi$ [M]: : 450.0876, found: 450.0880.

Reaction Products:

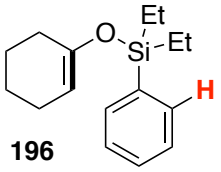

196

Isolated yield = 79%. Yellow oil. R_f (hexanes): 0.34.

^{1}H NMR (500 MHz, $CDCl^3$): δ ppm 7.60-7.58 (m, 2H), 7.39-7.36 (m, 3H), 4.88-4.86 (m, 1H), 2.04-2.01 (m, 2H), 1.98-1.95 (m, 2H), 1.66-1.61 (m, 2H), 1.51-1.46 (m, 2H), 1.14-1.07 (m, 2H), 1.03-0.90 (m, 8H). ^{13}C NMR (126 MHz, $CDCl_3$) δ ppm 6.6, 6.7, 22.3, 23.2, 23.8, 29.8, 104.3, 127.7, 129.4, 133.9, 136.4, 150.4. HRMS (ESI) calcd. for $C_{16}H_{24}OSi$ [M]+1: 261.1677, found: 261.1675.

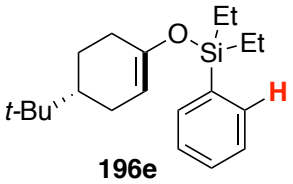

196e

Isolated yield = 65%. Yellow oil. R_f (hexanes): 0.35.

^{1}H NMR (500 MHz, $CDCl_3$): δ ppm 7.60-7.58 (m, 2H), 7.40-7.7.36 (m, 3H), 4.85-4.85 (m, 1H), 2.14-2.03 (m, 2H), 1.80-1.77 (m, 3H), 1.27-1.22 (m, 2H), 1.12-0.97 (m, 10H), 0.86-0.83 (s, 9H). ^{13}C NMR (126 MHz, $CDCl_3$) δ ppm 5.5, 7.0, 24.4, 25.1, 27.3, 27.6, 30.8, 43.9, 103.9, 127.7, 129.4, 133.6, 133.9, 150.3. HRMS (ESI) calcd. for $C_{20}H_{32}OSi$ [M]+1: 317.2301, found: 317.2311.

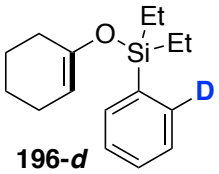

196-*d*

Isolated yield = 69% yield. Clear and colorless oil. R_f (hexanes): 0.34. ^{1}H NMR (500 MHz, $CDCl_3$): δ ppm 7.53-7.51 (m, 1H), 7.33-7.31 (m, 3H), 4.77-4.76 (m, 1H), 2.03-2.01 (m, 2H), 1.99-1.96 (m, 4H), 1.67-1.63 (m, 2H), 1.53-1.49 (m, 2H), 1.03-0.99 (m, 6H), 0.88-0.92 (m, 4H). ^{2}H NMR (77 MHz, CCl_4) δ ppm 7.75. HRMS (AP+) calcd. for $C_{16}H_{24}DOSi$ [M]+1: 262.1737, found: 262.1746.

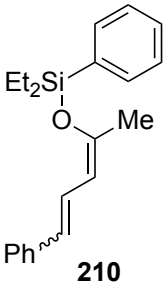

210

53% NMR yield of **Trans** and 25% NMR yield of **Cis**; Total Yield = 78%. Crude ^{1}H NMR (500 MHz, C_6D_6) **Trans** (only olefinic and the methyl group protons are reported): δ ppm 7.57 (dd, *J* = 10.6 Hz, *J* = 15.7 Hz, 1H), 6.50 (d, *J* = 16.4 Hz, 1H), 5.48 (d, *J* = 10.6 Hz, 1H), 1.79 (s, 3H). Crude ^{1}H NMR (500 MHz, C6D6) **Cis** (only Olefinic and the methyl group protons are reported): δ ppm 6.93 (dd, *J* = 11.0 Hz, *J* = 15.4 Hz, 1H), 5.94 (d, *J* = 11.0 Hz, 1H), 1.95 (s, 3H). HRMS (EI) calcd. for $C_{21}H_{26}OSi$ [M]: 322.1753, found: 322.1749.

7.3. General Remote Desaturation of Aliphatic Alcohols at Unactivated C(sp^3)–H Sites Enabled by Auxiliary Controlled Visible Light-induced Hybrid Pd-Radical Catalysis

7.3.1. Preparation of Starting Materials

Synthesis of chloro(iodomethyl)dimethylsilane tether (T_2-Cl):

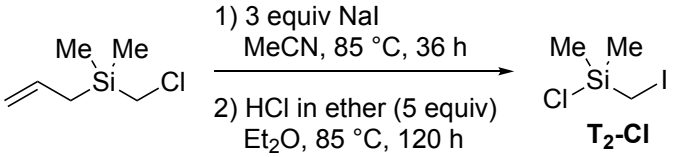

Allyl(chloromethyl)dimethylsilane (5.6 mL, 34 mmol, 1 equiv) in MeCN (10 mL) was added to the solution of sodium iodide (15.4 g, 102 mmol, 3 equiv) in MeCN (20 mL) under Ar atmosphere. The mixture was refluxed for 36 hours. The reaction was cooled to rt, diluted with EtOAc (60 mL), then washed with $Na_2S_2O_{3(sat)}$ solution (30 mL) and water (30 mL), dried over $Na_2SO_{4(anh)}$, concentrated and purified by flash chromatography (hexanes) to afford 4.8 g (67%) of the Finkelstein reaction product. The product was transferred to a 250 mL Schlenk flask equipped with a reflux condenser and then purged with Ar. The substrate was diluted with dry Et_2O (20 mL). Then, dry HCl (48 mL, 97 mmol, 2 M Et_2O) was added at rt under Ar. The mixture was then refluxed at 85 °C for 120 h. After completion, the mixture was cooled down to rt and then filtered with Celite under Ar atmosphere. The mixture was then concentrated *in vacuo* to furnish 3.9 g (86%, 95% pure) **T_2-Cl** as a greenish-yellow oil. The substrate was used for the next step without further purification. *Warning: **T_2-Cl** is highly moisture sensitive!* ^{1}H NMR (500 MHz, $CDCl_3$): δ ppm 2.24 (s, 2H), 0.6 (s, 6H). ^{13}C NMR (126 MHz, $CDCl_3$): δ ppm -0.14, 0.99.

General Method for Synthesis of T_1 and T_2 tethered alcohols

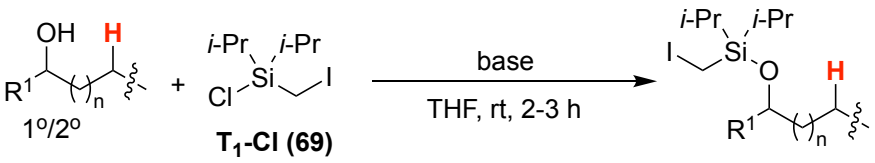

Method A: To a stirred mixture of imidazole (410 mg, 4 mmol, 2 equiv) and THF (5 mL), chlorosilane **T_1-Cl** (640 mg, 2.2 mmol, 1.1 equiv) was added at rt under Ar atmosphere. To this mixture, primary alcohol (2 mmol, 1 equiv) in 5 mL of THF was added. The mixture was stirred until completion of the reaction as judged by GC/MS analysis. To this mixture, hexanes (10 mL) was added and then filtered. The filtrate was then concentrated under reduced pressure. The residue was purified by column chromatography in hexanes.

Method B: To a stirred mixture of primary/secondary alcohol (2 mmol, 1 equiv) and THF (5 mL), MeLi (1.34 mL, 1.5 M, 2 mmol, 1 equiv) was added dropwise at 0 °C under Ar atmosphere. To this mixture, HMPA (0.35 mL, 2 mmol, 1 equiv) was added, followed by, **T_1-Cl** (640 mg, 2.2 mmol, 1.1 equiv) in 5 mL of THF at 0 °C. The mixture was stirred until completion of the reaction as judged by GC/MS analysis. Then, the mixture was quenched with $NH_4Cl_{(sat)}$ solution (30 mL) and extracted with Et_2O (3 x 20 mL). The combined organic layer was washed with brine. The organic layer was dried and filtered. The filtrate was then concentrated under reduced pressure. The residue was purified by column chromatography in hexanes.

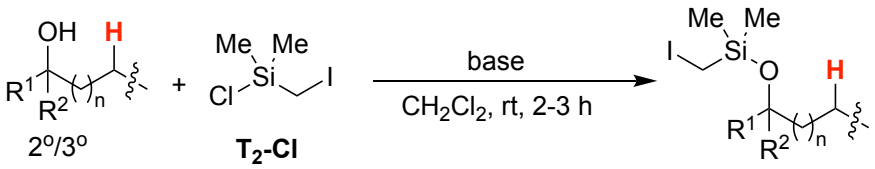

Method C: To a stirred mixture of imidazole (410 mg, 4 mmol, 2 equiv) and THF (5 mL), chlorosilane **T_2-Cl** (520 mg, 2.2 mmol, 1.1equiv) was added at rt under Ar atmosphere. To this mixture, secondary/tertiary alcohol (2 mmol, 1 equiv) in 5 mL of THF was added. The mixture was stirred until completion of the reaction as judged by GC/MS analysis. To this mixture, hexanes (10 mL) was added and then filtered. The filtrate was then concentrated under reduced pressure. The residue was purified by column chromatography in hexanes.

Method D: To a stirred mixture of imidazole (410 mg, 4 mmol, 2 equiv) and MeCN (3 mL), dimethyl(bromomethyl-)chlorosilane (0.3 mL, 2.2 mmol, 1.1 equiv) was added at rt under Ar atmosphere. To this mixture, secondary/tertiary alcohol (2 mmol, 1 equiv) in 2 mL of MeCN was added. The mixture was stirred until completion of the reaction as judged by GC/MS analysis. Then, NaI (900 mg, 3 equiv) was added directly to the reaction mixture. The mixture was heated to 85 ^{o}C for 2-12 h. After completion, the mixture was cooled to rt, diluted with EtOAc (60 mL), then washed with $Na_2S_2O_{3(sat)}$ solution (30 mL) and water (30 mL), dried over $Na_2SO_{4(anh)}$, concentrated and purified by flash chromatography in hexanes.

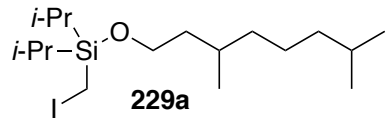

229a

229a was prepared according to the general Method **A** in 71% yield. Clear and colorless liquid. R_f (hexanes): 0.60. ^{1}H NMR (500 MHz, $CDCl_3$): δ ppm 3.79-3.72 (m, 1H), 2.08 (s, 2H), 1.59-1.50 (m, 3H), 1.38-1.12 (m, 6H), 1.16-1.03 (m, 16H), 0.87 (t, *J* = 6.6 Hz, 9H). ^{13}C NMR (126 MHz, $CDCl_3$): δ ppm 12.3, 17.4, 17.6, 19.9, 22.6, 22.7, 24.7, 27.9, 29.4, 39.2, 39.9, 62.2.

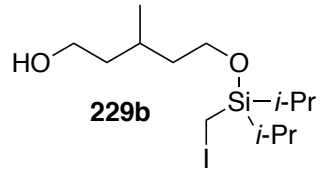

229b

229b was prepared according to the general Method **A** in 40% yield. Clear and colorless liquid. R_f (hexanes:EtOAc = 9:1): 0.20. ^{1}H NMR (500 MHz, $CDCl_3$): δ ppm 3.81-3.68 (m, 4H), 2.80-2.07 (s, 2H), 1.77-1.75 (m, 1H), 1.64-1.60 (m, 2H), 1.46-1.40 (m, 2H), 1.32 (bs, 1H), 1.25-1.19 (m, 2H), 1.09-1.06 (m, 13H), 0.94-0.92 (m, 3H). ^{13}C NMR (126 MHz, $CDCl_3$): δ ppm 12.3, 17.4, 17.7, 19.9, 26.3, 39.7, 39.9, 61.1, 61.9.

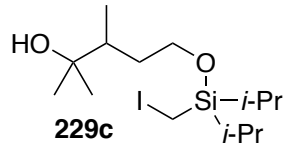

229c

229c was prepared according to the general Method **A** in 62% yield. Clear and colorless liquid. R_f (hexanes:EtOAc = 9:1): 0.38. ^{1}H NMR (500 MHz, $CDCl_3$): δ ppm 3.89-3.87 (m, 1H), 3.78-3.76 (m, 1H), 2,09 (s, 2H), 1.98 (bs, 1H), 1.90-1.85 (m, 1H), 1.65-1.62 (m, 1H), 1.38-1.32 (m, 1H), 1.27-1.21, (m, 2H), 1.19 (s, 3H), 1.17-1.15 (m, 3H), 1.10-1.07

(m, 12H), 0.95-0.93 (d, J = 6.9 Hz, 3H). ^{13}C NMR (126 MHz, $CDCl_3$): δ ppm 12.3, 17.4, 17.7, 25.8, 27.7, 35.0, 41.3, 62.7, 72.8.

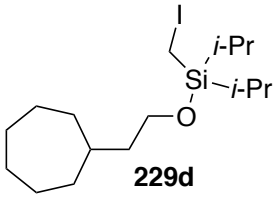

229d

229d was prepared according to the general Method **A** in 58% yield. Clear and colorless liquid. R_f (hexanes): 0.58. ^{1}H NMR (500 MHz, $CDCl_3$): δ ppm 3.76 (t, J = 6.7 Hz, 1H), 2.08 (s, 2H), 1.72-1.40 (m, 14H), 1.26-1.15 (m, 4H), 1.09-1.03 (m, 12H). ^{13}C NMR (126 MHz, $CDCl_3$): δ ppm 12.3, 17.4, 17.7, 26.4, 28.5, 34.6, 35.6, 40.9, 62.3.

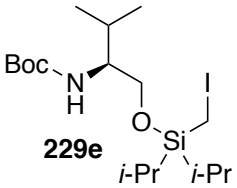

229e

229e was prepared according to the general Method **A** in 58% yield. Clear and colorless oil. R_f (hexanes): 0.48. ^{1}H NMR (500 MHz, $CDCl_3$): δ ppm 4.72-4.74 (m, 1H), 3.79 (dd, J = 10.2, 3.8 Hz, 1H), 3.39 (m, 1H), 2.09 (s, 2H), 1.93-1.84 (m, 1H), 1.44 (m, 9H), 1.29-1.18 (m, 2H), 1.09-1.06 (m, 12H), 0.96-0.93 (m, 6H). ^{13}CNMR (126 MHz, $CDCl_3$): δ ppm 12.3, 17.3, 17.4, 17.5, 17.6, 17.7, 18.8, 19.7, 28.4, 29.0, 57.1, 63.9, 79.9, 155.9.

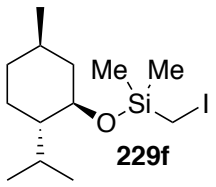

229f

229f was prepared according to the general Method **D** in 58% yield. Clear and colorless liquid. R_f (hexanes): 0.20. ^{1}H NMR (500 MHz, $CDCl_3$): δ ppm 3.48-3.43 (m, 1H), 2.16-2.13 (m, 1H), 2.04 (s, 2H), 1.85-1.84 (m, 1H), 1.65-1.58 (m, 2H), 1.39-1.36 (m, 1H), 1.16-1.12 (m, 1H), 1.06-0.99 (m, 1H), 0.90-0.89 (m, 7H), 0.87-0.81 (m, 1H), 0.73 (d, *J* = 6.9 Hz, 3H), 0.30 (s, 6H). ^{13}C NMR (126 MHz, $CDCl_3$): δ ppm -1.8, 15.9, 21.2, 22.3, 22.9, 25.3, 31.7, 34.4, 45.4, 49.9, 73.2.

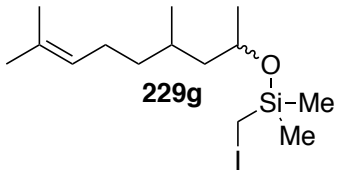

229g

1g was prepared according to the general Method **D** in 53% yield. dr = 1:1. Clear and colorless liquid. R_f (hexanes): 0.71. ^{1}H NMR (500 MHz, $CDCl_3$): δ ppm 5.09-5.08 (m, 1H), 3.96-3.91 (m, 1H), 2.02-1.93 (m, 5H), 1.68 (s, 3H), 1.60 (s, 3H), 1.53-1.47 (m, 1H), 1.36-1.26 (m, 3H), 1.17-1.09, (m, 6H), 0.89-0.86 (m, 4H), 0.29 (m, 6H). ^{13}C NMR (126 MHz, $CDCl_3$): δ ppm -2.0, 17.6, 19.5, 20.0, 23.9, 24.6, 25.4, 25.7, 28.8, 29.3, 37.1, 37.6, 47.1, 67.3, 67.6, 124.8, 131.1.

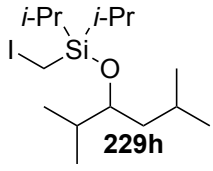

229h

229h was prepared according to the general Method **A** in 78% yield. Colorless liquid. R_f (hexanes): 0.62. ^{1}H NMR (500 MHz, $CDCl_3$): δ ppm 3.83-3.80 (m, 1H), 2.08 (s, 2H), 1.79-1.76 (m, 1H), 1.67-1.65 (m, 1H), 1.31-1.18 (m, 4H), 1.10-1.07 (m, 12H), 0.92-0.88

(m, 9H), 0.83-0.81 (d, J = 6.6 Hz, 3H). ^{13}C NMR (126 MHz, $CDCl_3$): δ ppm 12.8, 16.7, 17.6, 17.8, 17.9, 22.8, 23.2, 24.5, 32.8, 42.2, 75.5.

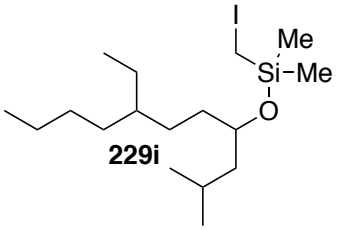

229i

229i was prepared according to the general Method **D** in 94% yield. 92% Purity. Clear and colorless liquid. R_f (hexanes): 0.43. ^{1}H NMR (500 MHz, $CDCl_3$): δ ppm 3.75-3.70 (m, 1H), 2.04 (m, 2H), 1.71-1.63 (m, 1H), 1.43-1.23 (m, 15H), 0.91-0.82 (m, 12H), 0.29 (s, 6H). ^{13}C NMR (126 MHz, $CDCl_3$): δ ppm -1.9, 10.9, 14.2, 22.5, 23.1, 23.3, 24.5, 25.8, 28.6, 28.9, 32.7, 34.7, 38.9, 46.5, 72.1.

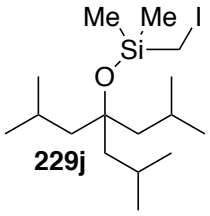

229j

229j was prepared according to the general Method **C** in 50% yield. Clear and colorless liquid. R_f (hexanes): 0.79. ^{1}H NMR (500 MHz, $CDCl_3$): δ ppm 2.06 (s, 2H), 1.75-1.68 (m, 3H), 1.43 (d, J = 5.5 Hz, 6H), 0.94 (d, J = 6.7 Hz, 18H), 0.3 (s, 6H). ^{13}C NMR (126 MHz, $CDCl_3$): δ ppm -14.0 (not shown), 0.4, 24.2, 25.1, 49.1, 81.4.

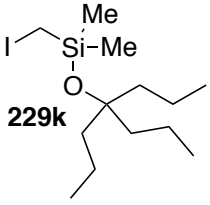

229k

229k was prepared according to the general Method **C** in 65% yield. Clear and colorless liquid. R_f (hexanes): 0.61. ^{1}H NMR (500 MHz, $CDCl_3$): δ ppm 2.02 (s, 2H), 1.41-1.38 (m, 6H), 1.30-1.25 (m, 6H), 0.90-0.87 (m, 9H), 0.28 (s, 6H). ^{13}C NMR (126 MHz, $CDCl_3$): δ ppm -14.0 (not shown), 0.2, 14.7, 17.1, 42.2, 79.4.

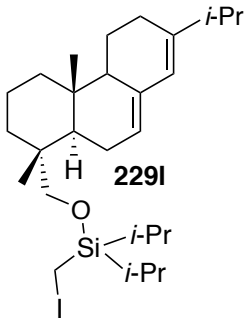

2291

229l was prepared according to the general Method **B** in 36% yield. Clear and colorless thick liquid. R_f (hexanes): 0.77. ^{1}H NMR (500 MHz, $CDCl_3$): δ ppm 5.78 (s, 1H), 5.40-5.39 (m, 1H), 3.44 (d, J = 9.4 Hz, 1H), 3.25 (d, J = 9.4 Hz, 1H), 2.22 (d, 1H), 2.10-2.08 (m, 3H), 2.05 (s, 2H), 1.98-1.95 (m, 1H), 1.90-1.79 (m, 3H), 1.63-1.16 (m, 8H), 1.09-1.00 (m, 20H), 0.86 (s, 3H), 0.81 (s, 3H). ^{13}C NMR (126 MHz, $CDCl_3$): δ ppm 12.2, 12.3, 14.2, 17.5, 17.6, 17.7, 18.3, 20.8, 21.4, 22.7, 24.0, 27.4, 34.6, 34.8, 36.1, 37.9, 38.9, 43.6, 50.7, 72.6, 121.2, 122.6, 135.3, 144.9.

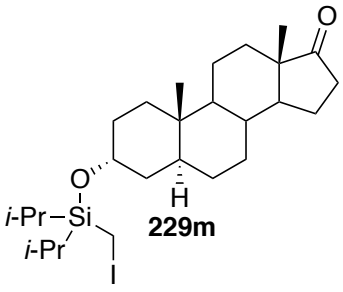

229m

229m was prepared according to the general Method **A** in 40% yield. Clear and colorless thick liquid. R_f (hexanes:EtOAc = 9:1): 0.47. ^{1}H NMR (500 MHz, $CDCl_3$): δ ppm 4.16-

4.15 (m, 1H), 2.43 (dd, J = 19.1 Hz, 8.4 Hz, 1H), 2.06 (s, 2H), 1.95-1.90 (m, 1H), 1.80-1.79 (m, 2H), 1.69-1.16 (m, 18H), 1.09-1.00 (m, 14H), 0.85 (s, 3H), 0.78 (s, 3H). ^{13}C NMR (126 MHz, $CDCl_3$): δ ppm 11.4, 12.6, 13.8, 17.6, 17.7, 17.8, 20.1, 21.8, 28.3, 29.8, 30.9, 31.6, 32.4, 35.1, 35.9, 36.2, 36.8, 39.1, 47.8, 51.5, 54.5, 67.7, 221.6.

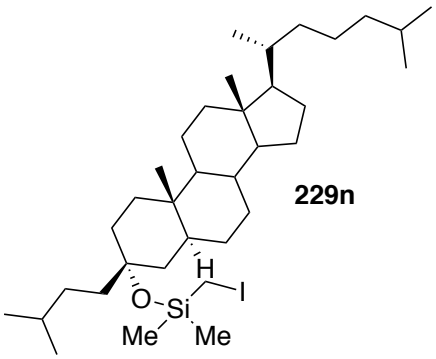

229n

229n was prepared according to the general Method **C** in 46% yield. White-pale solid. R_f (hexanes): 0.78. ^{1}H NMR (500 MHz, $CDCl_3$): δ ppm 2.04 (s, 2H), 2.02 (s, 1H), 1.98-1.95 (m, 1H), 1.83-0.96 (m, 36H), 0.91-0.85 (m, 16H), 0.72 (s, 3H), 0.65 (s, 3H), 0.3 (s, 6H). ^{13}C NMR (126 MHz, $CDCl_3$): δ ppm -14.0 (not shown), 0.36, 0.23, 11.6, 12.1, 18.7, 21.0, 22.5, 22.7, 22.8, 23.8, 24.2, 28.0, 28.3, 28.5, 28.7, 32.2, 32.7, 33.4, 34.1, 35.6, 35.7, 35.8, 36.2, 39.5, 40.1, 40.4, 40.7, 42.4, 42.6, 54.4, 56.3, 56.3. 76.9.

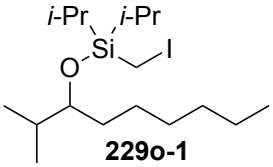

229o-1

229o-1 was prepared according to the general Method **A** in 67% yield. Colorless liquid. R_f (hexanes): 0.61. ^{1}H NMR (500 MHz, $CDCl_3$): δ ppm 3.70-3.67 (m, 1H), 2.08 (s, 2H), 1.78-1.74 (m, 1H), 1.41-1.41 (m, 2H), 1.32-1.19 (m, 10H), 1.09 (t, J = 7.34 Hz, 12H),

0.90-0.84 (m, 9H). ^{13}C NMR (126 MHz, $CDCl_3$): δ ppm 12.8, 14.1, 17.3, 17.5, 18.1, 22.7, 25.6, 29.6, 31.9, 32.7, 33.2, 77.8.

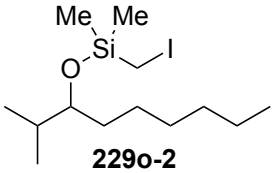

229o-2

229o-2 was prepared according to the general Method **D** in 45% yield. Colorless liquid. R_f (hexanes): 0.54. ^{1}H NMR (500 MHz, $CDCl_3$): δ ppm 3.48-3.47 (m, 1H), 2.04 (s, 2H), 1.69-1.68 (m, 1H), 1.40-1.27 (m, 10H), 0.90-0.84 (m, 9H), 0.29 (m, 6H). ^{13}C NMR (126 MHz, $CDCl_3$): δ ppm -1.9, 14.1, 17.7, 18.4, 22.7, 25.7, 29.5, 31.9, 33.1, 33.5, 78.3.

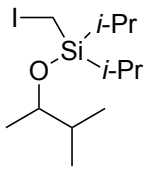

229p

229p was prepared according to the general Method **A** in 42% yield. Clear and colorless liquid. R_f (hexanes): 0.58. ^{1}H NMR (500 MHz, $CDCl_3$): δ ppm 3.85-3.81 (m, 1H), 2.08 (s, 2H), 1.71-1.65 (m, 1H), 1.23-1.18 (m, 2H), 1.12-1.05 (m, 15H), 0.87 (d, J = 7.0 Hz, 6H). ^{13}C NMR (126 MHz, $CDCl_3$): δ ppm 12.6, 12.7, 17.4, 17.5, 17.6, 17.8, 17.9, 18.0, 19.6, 35.3, 73.6.

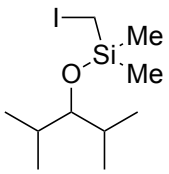

229q

229q was prepared according to the general Method **D** in 48% yield. Colorless liquid. R_f (hexanes): 0.55. ^{1}H NMR (500 MHz, $CDCl_3$): δ ppm 3.17-3.14 (m, 1H), 2.07 (s, 2H), 1.78-1.72 (m, 2H), 0.86 (dd, *J* = 6.8 Hz, *J* = 3.3 Hz, 12H), 0.32 (s, 6H). ^{13}C NMR (126 MHz, $CDCl_3$): δ ppm -1.8, 17.7, 20.4, 30.9, 84.3.

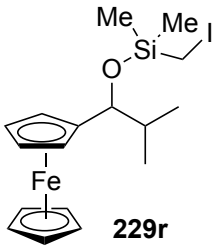

229r

229r was prepared according to the general Method **C** in 20% yield. Yellow liquid. R_f (hexanes:EtOAc = 20:1): 0.40. ^{1}H NMR (500 MHz, $CDCl_3$): δ ppm 4.55 (d, *J* = 4.0 Hz, 1H), 4.23 (s, 1H), 4.11 (s, 5H), 4.08 (s, 2H), 4.05 (s, 1H), 2.09 (s, 2H), 1.93-1.86 (m, 1H), 0.83 (d, *J* = 8.5 Hz, 3H), 0.77 (d, *J* = 8.5 Hz, 3H), 0.39 (s, 3H), 0.38 (s, 3H). ^{13}C NMR (126 MHz, $CDCl_3$): δ ppm -1.8, -1.6, 17.4, 18.1, 35.5, 66.4, 66.7, 67.2, 67.8, 68.6.

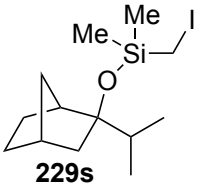

229s

229s was prepared according to the general Method **C** in 31% yield. Clear and colorless liquid. R_f (hexanes): 0.70. ^{1}H NMR (500 MHz, $CDCl_3$): δ ppm 2.29 (s, 1H), 2.17 (s, 1H), 2.09 (s, 2H), 1.80-1.75 (m, 1H), 1.68-1.62 (m, 2H), 1.56-1.51 (m, 1H), 1.40-1.23 (m, 3H), 1.20-1.09 (m, 2H), 0.92-0.84 (m, 6H), 0.34 (s, 6H). ^{13}C NMR (126 MHz, $CDCl_3$): δ ppm 0.0, 17.2, 17.7, 17.8, 23.3, 28.5, 36.9, 37.0, 37.5, 43.7, 45.1, 86.9.

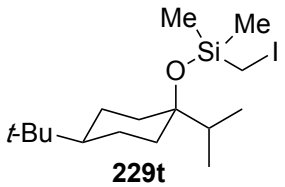

229t

229t was prepared according to the general Method **C** in 45% yield. Clear and colorless liquid. R_f (hexanes): 0.56. ^{1}H NMR (500 MHz, $CDCl_3$): δ ppm 2.08-2.03 (m, 2H), 1.64-1.52 (m, 5H), 1.32-1.25 (m, 4H), 0.92-0.83 (m, 16H), 0.34-0.23 (m, 6H). ^{13}C NMR (126 MHz, $CDCl_3$): δ ppm 0.1, 0.4, 16.2, 17.7, 22.5, 22.6, 24.1, 27.6, 32.4, 34.0, 37.6, 39.0, 47.9, 79.1.

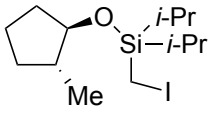

229u

229u was prepared according to the general Method **A** in 67% yield. Colorless liquid. R_f (hexanes): 0.58. ^{1}H NMR (500 MHz, $CDCl_3$): δ ppm 3.84 (m, 1H), 2.08 (s, 2H), 1.89-1.81 (m, 2H), 1.71-1.66 (m, 1H), 1.58-1.52 (m, 2H), 1.24-1.18 (m, 2H), 1.09-1.06 (m, 12H), 0.96-0.94 (d, J = 6.9 Hz, 1H). ^{13}C NMR (126 MHz, $CDCl_3$): δ ppm 12.4, 17.4, 17.7, 17.8, 18.4, 21.4, 31.1, 34.6, 42.7, 81.3.

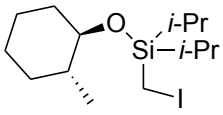

229v

229v was prepared according to the general Method **A** in 75% yield. Clear and colorless liquid. R_f (hexanes): 0.60. ^{1}H NMR (500 MHz, $CDCl_3$): δ ppm 3.37-3.32 (m, 1H), 2.09

(s, 2H), 1.91-1.86 (m, 1H), 1.72-1.67 (m, 2H), 1.59-1.53 (m, 1H), 1.41-1.08 (m, 6H), 1.11-1.06 (m, 12H), 0.99-0.96 (m, 4H). ^{13}C NMR (126 MHz, $CDCl_3$): δ ppm 12.7, 12.8, 17.5, 17.6, 17.8, 18.0, 19.2, 25.0, 25.3, 33.3, 35.9, 40.3, 77.7.

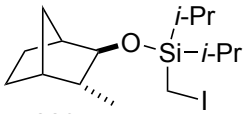

229w

229w was prepared according to the general Method **A** in 75% yield. Colorless liquid. R_f (hexanes/EtOAc = 50:1): 0.66. ^{1}H NMR (500 MHz, $CDCl_3$): δ ppm 3.19 (s, 1H), 2.08-2.04 (m, 3H), 2.03-2.00 (m, 1H), 1.74-1.70 (m, 2H), 1.48-1.44 (m, 1H), 1.38-1.33 (m, 1H), 1.22-1.15 (m, 4H), 1.10-1.03 (m, 14H), 0.95 (d, *J* = 7.0 Hz, 3H). ^{13}C NMR (126 MHz, $CDCl_3$): δ ppm 12.4, 15.3, 17.4, 17.5, 17.7, 17.8, 21.3, 24.7, 36.5, 40.7, 46.0, 46.8, 83.5.

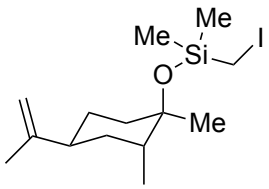

229x

229x was prepared according to the general Method **C** in 35% yield. Colorless liquid. ^{1}H NMR (500 MHz, $CDCl_3$): δ ppm 4.72-4.68 (m, 2H), 2.06-2.01 (m, 3H), 1.96-1.92 (m, 1H), 1.80-1.77 (m, 1H), 1.71 (s, 3H), 1.66-1.61 (m, 1H), 1.57-1.48 (m, 3H), 1.49-1.44 (m, 1H), 1.31-1.25 (m, 1H), 1.20 (s, 3H), 0.95-0.92 (m, 3H), 0.89-0.87 (m, 1H), 0.30 (s, 6H). ^{13}C NMR (126 MHz, $CDCl_3$): δ ppm 0.2, 16.3, 20.9, 26.9, 28.0, 34.0, 34.7, 37.9, 38.0, 40.0, 108.4, 150.6.

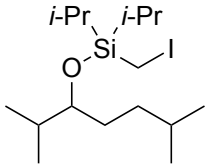

229y

229y was prepared according to the general Method **A** in 82% yield. Colorless liquid. R_f (hexanes): 0.46. ^{1}H NMR (500 MHz, $CDCl_3$): δ ppm 3.71-3.65 (m, 1H), 2.09 (s, 2H), 1.80-1.74 (m, 1H), 1.54-1.49 (m, 1H), 1.45-1.43 (m, 2H), 1.26-1.18 (m, 4 H), 1.12-1.09 (m, 12H), 0.92-086 (m, 12H). ^{13}C NMR (126 MHz, $CDCl_3$): δ ppm 12.8, 17.2, 17.6, 17.9, 18.2, 22.6, 22.7, 28.3, 31.2, 32.6, 34.7, 78.0.

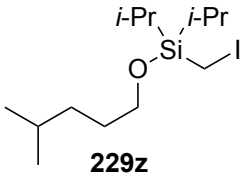

229z

229z was prepared according to the general Method **A** in 70% yield. Clear and colorless liquid. R_f (hexanes): 0.30. ^{1}H NMR (500 MHz, $CDCl_3$): δ ppm 3.71 (t, J = 6.7 Hz, 2H), 2.08 (s, 2H), 1.59-1.53 (m, 3H), 1.24-1.18 (m, 4H), 1.08 (m, 12H), 0.88 (d, J = 6.7 Hz, 6H). ^{13}C NMR (126 MHz, $CDCl_3$): δ ppm 12.3, 17.4, 17.7, 22.6, 27.8, 30.7, 34.9, 84.2.

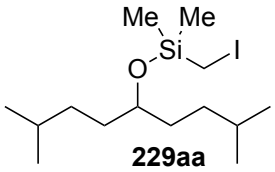

229aa

229aa was prepared according to the general Method **C** in 40% yield. Clear and colorless liquid. R_f (hexanes): 0.39. ^{1}H NMR (500 MHz, $CDCl_3$): δ ppm 3.67-3.61 (m, 1H), 2.03

(s, 2H), 1.56-1.41 (m, 6H), 1.28-1.10 (m, 4H), 0.90-0.86 (m, 12H), 0.29 (s, 6H). ^{13}C NMR (126 MHz, $CDCl_3$): δ ppm -2.0, 22.5, 22.6, 28.1, 34.6, 34.7, 35.0, 35.2, 74.0.

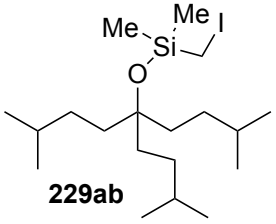

229ab

229ab was prepared according to the general Method **C** in 29% yield. Clear and colorless liquid. R_f (hexanes): 0.65. ^{1}H NMR (500 MHz, $CDCl_3$): δ ppm 2.02 (s, 2H), 1.50-1.38 (m, 9H), 1.17-1.10 (m, 6H), 0.89 (d, J = 8.2 Hz, 18H), 0.29 (s, 6H). ^{13}C NMR (126 MHz, $CDCl_3$): δ ppm 0.4, 22.8, 28.7, 32.8, 37.4, 79.6.

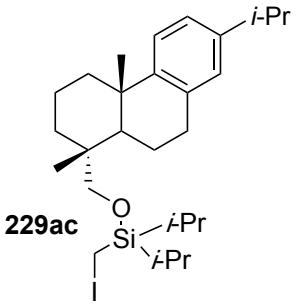

229ac

229ac was prepared according to the general Method **B** in 36% yield. Clear and colorless oil. R_f (hexanes): 0.50. ^{1}H NMR (500 MHz, $CDCl_3$): δ ppm 7.18 (d, J = 8.0 Hz, 1H), 7.00 (d, J = 8.0 Hz, 1H), 6.9 (s, 1H), 3.60 (d, J = 9.5 Hz, 1H), 3.26 (d, J = 9.5 Hz, 1H), 2.86-2.82 (m, 3H), 2.25 (d, J = 12.5 Hz, 1H), 2.07 (s, 2H), 1.80-1.73 (m, 3H), 1.66-1.50 (m, 5H), 1.39-1.30 (m, 2H), 1.25-1.20 (m, 9H), 1.08-1.02 (m, 12H), 0.85 (s, 3H). ^{13}C NMR (126 MHz, $CDCl_3$): δ ppm 12.3, 17.4, 17.5, 17.8, 18.8, 19.0, 24.0, 25.6, 30.5, 33.4, 35.3, 38.3, 38.4, 43.6, 72.4, 123.7, 124.4, 126.8, 135.0, 147.5.

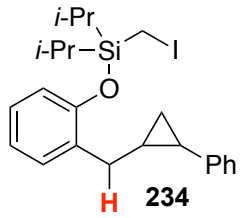

234

40% isolated yield. Clear and colorless oil. R_f (hex): 0.38. ^{1}H NMR (500 MHz, C_6D_6): δ ppm 7.33 (d, *J*= 7.6 Hz, 1H), 7.20 (t, *J*= 7.3 Hz, 2H), 7.12-7.09 (m, 2H), 7.08 (d, *J*= 7.0 Hz, 2H), 6.96 (t, *J*= 7.6 Hz, 1H), 6.83 (d, *J*= 7.6 Hz, 1H), 2.88 (dd, *J*= 7.0, 2.3 Hz, 2H), 2.00 (s, 2H), 1.51-1.47 (m, 2H), 1.22-1.03 (m, 14H), 0.99-0.89 (m, 2H). LRMS (EI) calcd. for $C_{23}H_{31}IOSi$ [M]: 478.49, found: 478.01.

7.3.2. Visible Light-Induced Pd-catalyzed Desaturation of Aliphatic Alcohols

General Procedure A for Desaturation of Alcohols using T_1.

An oven dried 5 mL Wheaton V-vial containing a stirring bar was charged with silyl tethered alcohols **229** (0.2 mmol), $Pd(OAc)_2$ (4.49 mg, 0.02 mmol), ligand **L** (20.6 mg, 0.04 mmol) and Cs_2CO_3 (130 mg, 0.4 mmol) under N_2 atmosphere (glovebox). Dry degassed benzene (2 mL) was added and the reaction vessel was capped with a pressure screw cap. The vial was irradiated with 34 W Blue LED lamp (Kessil KSH150B LED Grow Light) for 12-48 h (monitored by GC/MS), with cooling from a fan (vial temperature reached 37 °C). The vial distance from the lamp was about 2-3 cm. After completion, judged by GC/MS analysis, 10 equiv of TBAF (2 mL, 1 M THF) was added directly to the reaction mixture. The reaction was stirred for an additional 2-12 h (monitored by GC/MS).The resulting mixture was diluted with DCM (10 mL), filtered (Celite), and concentrated under a reduced pressure. The residue was purified by filtration through silica gel (hexanes:EtOAc = 9:1 to 4:1) affording the corresponding desaturated alcohols.

General Procedure B for Desaturation of Alcohols using T_2.

An oven dried 3 mL Wheaton V-vial containing a stirring bar was charged with silyl tethered alcohols **229** (0.2 mmol), $Pd(OAc)_2$ (4.49 mg, 0.02 mmol), ligand **L** (20.6 mg, 0.04 mmol) and Cs_2CO_3 (130 mg, 0.4 mmol) under N_2 atmosphere (glovebox). Dry degassed benzene (2 mL) was added and the reaction vessel was capped with a pressure screw cap. The vial was irradiated with 34 W Blue LED lamp (Kessil KSH150B LED Grow Light) for 12-48 h (monitored by GC/MS), with cooling from a fan (vial temperature reached 37 °C). The vial distance from the lamp was about 2-3

cm. After completion, judged by GC/MS analysis, 5 equiv of TBAF (1 mL, 1 M THF) was added directly to the reaction mixture. The reaction was stirred for an additional 2-12 h (monitored by GC/MS). The resulting mixture was diluted with DCM (10 mL), filtered (Celite), and concentrated under a reduced pressure. The residue was purified by filtration through silica gel (hexanes:EtOAc = 9:1 to 4:1) affording the corresponding desaturated alcohols.

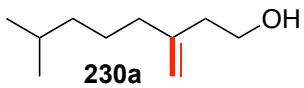

230a

230a was prepared according to the general procedure **A** in 77% yield. Slightly yellow oil. R_f (hexanes/EtOAc = 4:1): 0.44. ^{1}H NMR (500 MHz, $CDCl_3$): δ ppm 4.86 (s, 1H), 4.81 (s, 1H), 3.71 (t, *J* = 6.3 Hz, 2H), 2.29 (t, *J* = 6.6 Hz, 2H), 2.01 (t, *J* = 7.7 Hz, 2H), 1.57-1.51 (m, 3H), 1.46-1.40 (m, 2H), 1.20-1.13 (s, 2H), 0.90-0.86 (m, 7H). ^{13}C NMR (126 MHz, $CDCl_3$): δ ppm 12.7, 17.1, 22.6, 25.5, 27.9, 36.7, 39.1, 62.9, 110.4, 146.9. HRMS (EI+) calcd. for $C_{10}H_{20}O$ [M]: 156.1514, found: 155.1512.

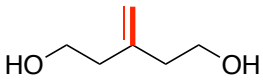

230b

230b was prepared according to the general procedure **A** (two-step procedure) in 48% yield. Clear and colorless oil. R_f (hexanes/EtOAc = 1:4): 0.25. ^{1}H NMR (500 MHz, $CDCl_3$): δ ppm 5.01 (s, 2H), 3.79 (t, *J* = 6.2 Hz, 4H), 2.36 (t, *J* = 6.2 Hz, 4H), 1.75 (bs, 2H). ^{13}C NMR (126 MHz, $CDCl_3$): δ ppm 38.8, 60.6, 114.3, 143.0. LRMS (EI+) calcd. for $C_6H_{12}O_2$ [M-H_2O]: 98.16, found 98.10.

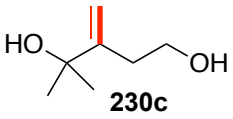

230c

230c was prepared according to the general procedure **A** (two-step procedure) in 47% yield. Clear and colorless oil. R_f (hexanes/EtOAc = 1:4): 0.61. ^{1}H NMR (500 MHz, $CDCl_3$): δ ppm 5.18 (s, 1H), 4.90 (s, 1H), 3.83 (t, *J* = 5.8 Hz, 2H), 2.46 (t, *J* = 5.1 Hz, 2H), 1.42 (s, 6H), 1.28 (bs, 2H). ^{13}C NMR (126 MHz, $CDCl_3$): δ ppm 29.7, 34.7, 63.1, 72.7, 110.1, 153.3. HRMS (EI+) calcd. for $C_7H_{14}O_2$ [M]: 129.09156, found: 129.09097.

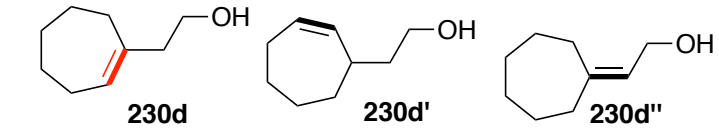

230d **230d'** **230d''**

71%, 14 : 2 : 1

230d was prepared according to the general procedure **A** in calcd. 58% yield. Yellow oil. R_f (hexanes/EtOAc = 4:1): 0.40. ^{1}H NMR (500 MHz, $CDCl_3$): δ ppm 5.67 (t, *J* = 6.6 Hz, 1H), 3.63 (t, *J* = 6.2 Hz, 2H), 2.24 (t, *J* = 5.8 Hz, 2H), 2.13-2.09 (m, 4H), 1.77-1.72 (m, 2H), 1.51-1.45 (m, 5H). ^{13}C NMR (126 MHz, $CDCl_3$): δ ppm 26.4, 26.9, 27.3, 28.4, 32.5, 43.3, 59.3, 129.8, 140.7. LRMS (EI+) calcd. for $C_9H_{16}O$ [M]: 140.23, found: 140.00.

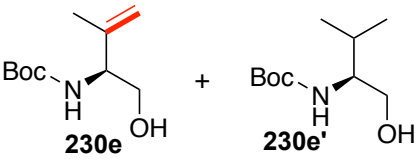

230e **230e'**

5 : 1

67%

230e was prepared according to the general procedure **A** in calcd. 56% yield of **2e**. White solid. R_f (hexanes/EtOAc = 1:1): 0.48. ^{1}H NMR (500 MHz, $CDCl_3$): δ 4.97 (s, 1H), 4.94 (s, 1H), 4.11 (br, 1H), 3.68 (s, 2H), 1.79 (s, 3H), 1.45 (s, 9H), 1.25 (bs, 1H). ^{13}C NMR

(126 MHz, $CDCl_3$): δ 20.4, 28.4, 57.4, 63.8, 79.8, 112.3, 142.6, 155.9. HRMS (ESI) calcd. for $C_{10}H_{19}O_3$ [M+Na]: 224.1263, found: 224.1260.

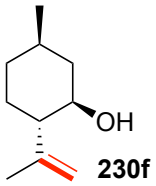

230f

230f was prepared according to the general procedure **B** in 79% yield. Clear and colorless oil. R_f (hexanes/EtOAc = 4:1): 0.39. ^{1}H NMR (500 MHz, $CDCl_3$): δ ppm 4.90 (s, 1H), 4.85 (s, 1H), 3.46 (t, *J* = 5.4 Hz, 1H), 2.05-2.03 (s, *J* = 12.5 Hz, 1H), 1.90-1.85 (m, 2H), 1.71 (s, 3H), 1.69-1.66 (m, 1H), 1.50 (bs, 1H), 1.36-1.25 (m, 2H), 0.98-0.92 (m, 6H). ^{13}C NMR (126 MHz, $CDCl_3$): δ ppm 19.2, 22.2, 29.6, 31.4, 34.3, 42.6, 55.1, 70.3, 112.9, 146.6. HRMS (EI+) calcd. for $C_{10}H_{18}O$ [M]: 154.1358, found: 154.1360.

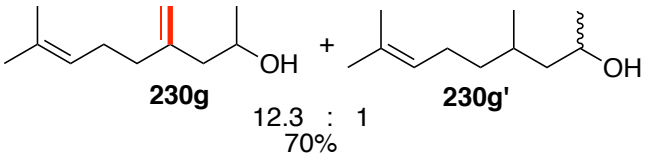

230g 12.3 : 1 **230g'**

70%

230g was prepared according to the general procedure **B** in calcd. 65% yield of **2g**. Clear and colorless oil. R_f (hexanes/EtOAc = 4:1): 0.40. ^{1}H NMR (500 MHz, $CDCl_3$): δ ppm 5.09 (t, *J* = 6.4 Hz, 1H), 4.89 (s, 1H), 4.85 (s, 1H), 3.93-3.87 (m, 1H), 2.24-2.02 (m, 6H), 1.75 (bs, 1H), 1.68 (s, 3H), 1.61 (s, 3H), 1.21 (d, *J* = 6.1 Hz, 2H). ^{13}C NMR (126 MHz, $CDCl_3$): δ ppm 17.7, 22.9, 25.6, 26.3, 35.8, 46.5, 65.1, 70.3, 112.3, 123.7, 131.9, 146.6. HRMS (ES+) calcd. for $C_{11}H_{20}O$ [M+1]: 169.1592, found: 169.1597.

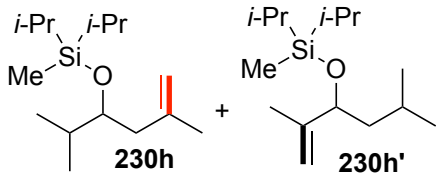

9.5 : 1
76%

230h was prepared according to the general procedure **A** (two-steps) in calcd. 69% yield. Clear and colorless oil. R_f (hexanes): 0.62. ^{1}H NMR (500 MHz, $CDCl_3$): δ ppm 4.75 (s, 1H), 4.72 (s, 1H), 3.74-3.71 (m, 1H), 2.20-2.10 (m, 2H), 1.72 (s, 3H), 1.00 (d, 14H), 0.91-0.88 (m, 8H), 0.84 (d, J = 7.0 Hz, 3H). ^{13}C NMR (126 MHz, $CDCl_3$): δ ppm -7.3, 13.6, 16.1, 17.5, 17.6, 18.8, 22.8, 32.2, 42.6, 74.9, 112.6, 143.2. LRMS (ES+) calcd. for $C_{15}H_{32}OSi$ [M]: 256.49, found: 255.20.

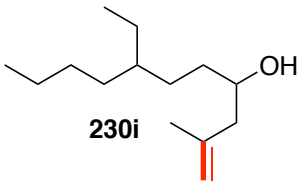

230i was prepared according to the general procedure **B** in 80% yield. Clear and colorless oil. R_f (hexanes/EtOAc = 4:1): 0.55. ^{1}H NMR (500 MHz, $CDCl_3$): δ ppm 4.88 (s, 1H), 4.80 (s, 1H), 3.68 (m, 1H), 2.23 (dd, J = 13.6, 2.9 Hz, 1H), 2.08 (dd, J = 13.6, 9.5 Hz, 1H), 1.76 (s, 3H), 1.47-1.34 (m, 4H), 1.28-1.24 (m, 10H), 0.93-0.83 (m, 6H). ^{13}C NMR (126 MHz, $CDCl_3$): δ ppm 10.8, 14.1, 22.4, 24.6, 25.7, 28.9, 29.1, 32.7, 34.3, 38.9, 46.2, 69.1, 113.4, 142.9. HRMS (EI+) calcd. For $C_{14}H_{28}O$ [M]: 212.2140, found 212.2140.

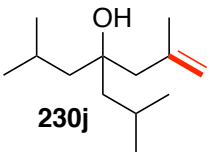

230j was prepared according to the general procedure **B** in 73% yield. Clear and colorless oil. R_f (hexanes/EtOAc = 4:1): 0.61. ^{1}H NMR (500 MHz, $CDCl_3$): δ ppm 4.93 (s, 1H), 4.75 (s, 1H), 2.2 (s, 1H), 1.84-1.78 (m, 5H), 1.44-1.36 (m, 5H), 0.97-0.95 (m, 14H). ^{13}C NMR (126 MHz, $CDCl_3$): δ ppm 24.0, 24.7, 24.9, 24.6, 48.3, 48.6, 75.3, 114.9, 143.0. LRMS (ES+) calcd. for $C_{13}H_{26}O$ [M]: 198.35, found: 198.20.

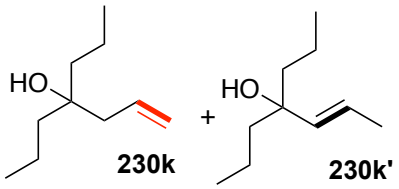

230k was prepared according to the general procedure **B** in calcd. 52% yield. Clear and colorless oil. R_f (hexanes/EtOAc = 4:1): 0.62. ^{1}H NMR (500 MHz, $CDCl_3$): δ ppm 5.88-5.80 (m, 1H), 5.14-5.08 (m, 2H), 2.20 (d, *J* = 6.6 Hz, 2H), 1.49-1.25 (m, 8H), 0.93-0.88 (m, 6H). ^{13}C NMR (126 MHz, $CDCl_3$): δ ppm 14.6, 16.7, 41.5, 43.4, 43.9, 74.9, 118.4, 134.0. HRMS (EI+) calcd. for $C_{10}H_{19}O$ [M-1]: 155.1436, found 155.1431.

2k' ^{1}H NMR (500 MHz, $CDCl_3$): δ ppm 5.61-5.57 (m, 1H), 5.44 (dd, *J* = 15.4, 1.5 Hz, 1H), 1.70 (dd, *J* = 7.7, 1.5 Hz, 2H), 1.49-1.25 (m, 8H), 0.93-0.88 (m, 6H). ^{13}C NMR (126 MHz, $CDCl_3$): δ ppm 14.7, 16.8, 17.7, 41.7, 74.9, 122.7, 137.2. HRMS (EI+) calcd. for $C_{10}H_{19}O$ [M]: 155.1436, found 155.1431.

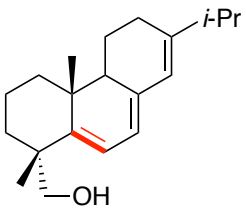

230l

230l was prepared according to the general procedure **A** (two-steps) in 53% yield. White solid. R_f (hexanes/EtOAc = 4:1): 0.39. ^{1}H NMR (500 MHz, $CDCl_3$): δ ppm 5.95 (s, 1H), 5.91 (d, J = 5.5 Hz, 1H), 5.69 (s,1H), 3.78 (d, J = 11.3 Hz, 1H), 3.16 (d, J = 11.0 Hz, 1H), 2.30-2.22 (m, 2H), 2.13-2.01 (m, 2H), 1.88-1.17 (m, 6H), 1.07-0.98 (m, 12H), 0.89 (s, 3H). ^{13}C NMR (126 MHz, $CDCl_3$): δ ppm 17.1, 17.4, 17.8, 20.1, 21.3, 22.3, 27.9, 28.2, 33.8, 35.3, 38.2, 40.9, 47.7, 70.5, 117.3, 119.5, 121.7, 136.2, 148.3, 148.6. HRMS (ES+) calcd. For $C_{20}H_{30}O$ [M+1]: 287.2375, found: 287.2367.

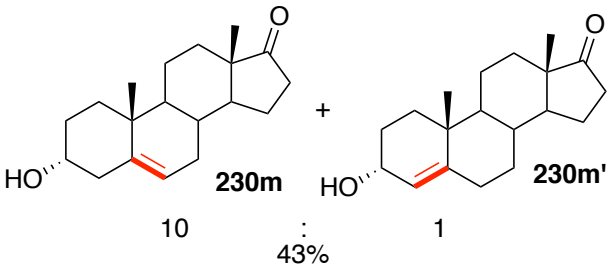

2m was prepared according to the general procedure **A** in calcd. 40% yield of **2m**. White solid. R_f (hexanes/EtOAc = 1:1): 0.59. ^{1}H NMR (500 MHz, $CDCl_3$): δ ppm 5.44 (m, 1H), 4.03 (m, 1H), 2.78 (d, J = 15.5 Hz, 1H), 2.46 (dd, J = 19.1, 8.8 Hz, 1H), 2.13-1.15 (m, 18H), 1.04 (s, 3H), 0.89 (s, 3H). ^{13}C NMR (126 MHz, $CDCl_3$): δ ppm 13.5, 18.7, 20.1, 21.9, 28.9, 30.9, 31.4, 33.1, 35.8, 37.8, 39.8, 47.5, 50.4, 51.8, 66.9, 132.0, 138.9, 221.2. HRMS (ES+) calcd. for $C_{19}H_{28}O_2$ [M+1]: 289.2168, found: 289.2161.

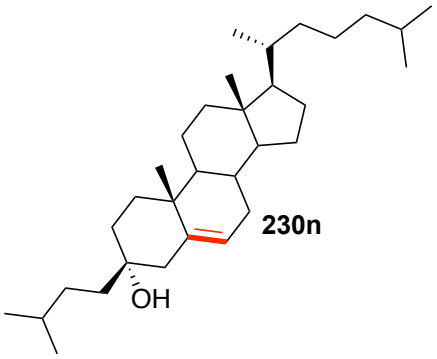

230n was prepared according to the general procedure **B** in 65% yield. White solid. R_f (hexanes/EtOAc = 9:1): 0.62. ^{1}H NMR (500 MHz, $CDCl_3$): δ ppm 5.40-5.39 (d, *J* = 5.4 Hz, 1H), 2.38 (dd, *J* = 14.3, 2.2 Hz, 1H), 2.03-0.85 (m, 51H), 0.68 (s, 3H). ^{13}C NMR (126 MHz, $CDCl_3$): δ ppm 11.8, 18.6, 18.7, 20.9, 22.5, 22.6, 22.7, 22.8, 23.8, 24.9, 28.0, 28.2, 28.6, 31.9, 32.0, 32.2, 33.0, 35.1, 35.8, 36.2, 37.0, 39.5, 39.8, 40.6, 42.3, 44.1, 50.4, 56.1, 56.7, 71.9, 123.9, 139.9. HRMS (ES+) calcd. For $C_{32}H_{56}O$ [M]: 456.4331, found 456.4331.

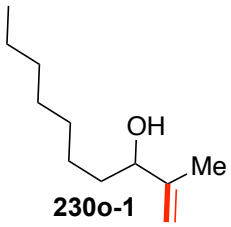

230o-1 was prepared according to the general procedure **A** in calcd. 56% yield (80% yield, r.r. = 3.1:1). Clear and colorless oil. R_f (hexanes/EtOAc = 4:1): 0.47. ^{1}H NMR (500 MHz, $CDCl_3$): δ ppm 4.93 (s, 1H), 4.83 (s, 1H), 4.05 (s, 1H), 1.72 (s, 3H), 1.55-1.51 (m, 2H), 1.44 (bs, 1H), 1.34-1.26 (m, 8H), 0.88 (t, *J* = 5.4 Hz, 3H). ^{13}C NMR (500 MHz, $CDCl_3$): δ ppm 14.1, 17.5, 22.6, 25.5, 29.2, 31.8, 34.9, 76.0, 110.9, 147.7. HRMS (EI+) calcd. for $C_{10}H_{20}O$ [M]: 140.1201, found: 140.1197.

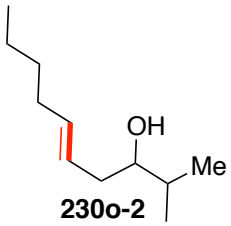

230o-2

230o-2 was prepared according to the general procedure **B** in calcd. 38% yield (93%, r.r. = 1:1.5). Slightly yellow oil. R_f (hexanes/EtOAc = 4:1): 0.53. ^{1}H NMR (500 MHz, $CDCl_3$): δ ppm 5.56-5.52 (m, 1H), 5.43-5.39 (m, 1H), 3.33 (m, 1H), 2.27 (m, 1H), 2.07-1.98 (m, 2H), 1.71-1.64 (m, 1H), 1.59 (d, J = 11.4 Hz, 1H), 1.42-1.35 (m, 2H), 1.29-1.25 (m, 1H), 0.94-0.87 (m, 9H). ^{13}C NMR (500 MHz, $CDCl_3$): δ ppm 13.6, 17.6, 18.7, 22.6, 32.9, 34.8, 37.6, 75.5, 126.5, 134.4. HRMS (EI+) calcd. for $C_{10}H_{20}O$ [M]: 140.1201, found: 140.1197.

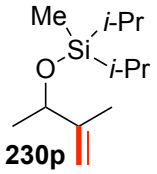

230p

230p was prepared according to the general procedure **B** in 76% yield (NMR).^{1}H NMR (500 MHz, C_6D_6): δ ppm 5.09 (s, 1H), 4.83 (s, 1H), 4.31-4.26 (m, 1H), 1.77 (s, 3H), 1.31 (d, J = 6.4 Hz, 1H), 1.19-1.11 (m, 14H), 0.12 (s, 3H). LRMS (EI+) calcd. for $C_{12}H_{26}OSi$ [M+1]: 214.42, found: 214.10.

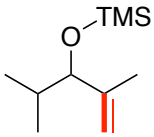

230q

230q was prepared according to the general procedure **B** in 87% yield (NMR). ^{1}H NMR (500 MHz, C_6D_6): δ ppm 4.97 (s, 1H), 4.89 (s, 1H), 3.70 (d, *J* = 7.3 Hz, 1H), 1.83-1.79 (m, 3H), 1.73 (s, 3H), 1.10 (d, *J* = 6.6 Hz, 3H), 0.89 (d, *J* = 6.6 Hz, 3H), 0.24 (s, 9H). HRMS (ES+) calcd. for $C_{10}H_{22}OSi$ [M+1]: 186.37, found: 186.10.

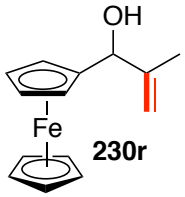

230r

230r was prepared according to the general procedure **B** in 48% yield. R_f (hexanes/EtOAc = 9:1): 0.38. ^{1}H NMR (500 MHz, $CDCl_3$): δ ppm 5.02 (s, 1H), 4.80 (s, 2H), 4.27-4.17 (m, 9H), 2.20 (bs, 1H), 1.69 (s, 3H). ^{13}C NMR (126 MHz, $CDCl_3$): δ ppm 18.2, 65.2, 67.8, 67.9, 68.4, 73.6, 92.9, 110.9, 146.6. HRMS (ES+) calcd. for $C_{14}H_{16}OFe$ [M+1]: 257.029, found: 257.0638.

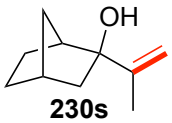

230s

230s was prepared according to the general procedure **B** in 82% yield. R_f (hexanes/EtOAc = 4:1): 0.60. ^{1}H NMR (500 MHz, $CDCl_3$): δ ppm 4.91 (s, 1H), 4.78 (s, 2H), 2.40 (bs, 1H), 2.20 (bs, 1H), 2.04-1.94 (m, 2H), 1.82 (s, 3H), 1.59-0.89 (m, 7H). ^{13}C NMR (126 MHz, $CDCl_3$): δ ppm 18.7, 22.1, 28.8, 37.0, 38.9, 44.1, 44.8, 81.2, 109.4, 149.8. HRMS (EI+) calcd. for $C_{10}H_{16}O$ [M]: 152.12012, found: 152.11963.

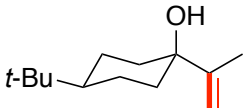

230t

230t was prepared according to the general procedure **B** 66% yield. R_f (hexanes/EtOAc = 4:1): 0.60. ^{1}H NMR (500 MHz, $CDCl_3$): δ ppm 5.01 (s, 1H), 4.79 (s, 1H), 1.80 (s, 3H), 1.68-1.57 (m, 6H), 1.45-1.40 (m, 2H), 0.97-0.90 (m, 1H), 0.87 (s, 9H). ^{13}C NMR (126 MHz, $CDCl_3$): δ ppm 16.8, 9.0, 22.5, 27.5, 29.1, 32.3, 36.2, 46.6, 73.2, 108.7, 152.5. HRMS (ES+) calcd. for $C_{13}H_{24}O$ [M]: 196.18272, found: 196.18239.

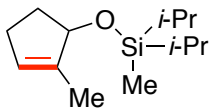

230u

230u was prepared according to the general procedure **A** (without TBAF) 49% yield. R_f (hexanes): 0.24. ^{1}H NMR (500 MHz, $CDCl_3$): δ ppm 5.46 (s, 1H), 4.86 (s, 1H), 2.36-2.15 (m, 4H), 1.73 (s, 3H), 1.04-0.92 (m, 14H), 0.60 (s, 1H). ^{13}C NMR (126 MHz, $CDCl_3$): δ ppm -7.7, 13.2, 17.4, 29.6, 34.5, 39.3, 80.1, 126.8, 142.2. HRMS (EI+) calcd. for $C_{13}H_{26}OSi$ [M]: 226.17530, found: 226.17480.

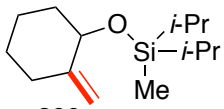

230v

230v was prepared according to the general procedure **A** (without TBAF) 50% yield. R_f (hexanes): 0.42. ^{1}H NMR (500 MHz, $CDCl_3$): δ ppm 4.91 (s, 1H), 4.69 (s, 1H), 4.06 (s, 1H), 2.40-2.38 (m, 1H), 1.99-1.94 (m, 1H), 1.84-1.79 (m, 2H), 1.60-1.56 (m, 1H), 1.46-1.38 (m, 3H), 1.02-0.90 (m, 14H), 0.02 (s, 3H). ^{13}C NMR (126 MHz, $CDCl_3$): δ ppm -

8.1, 13.2, 17.5, 23.8, 27.9, 33.6, 37.6, 73.2, 105.4, 151.5. HRMS (EI+) calcd. for $C_{14}H_{28}OSi$ [M]: 240.19095, found: 240.19050.

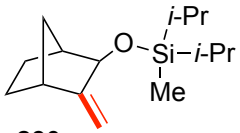

230w

230w was prepared according to the general procedure **A** (without the TBAF step) in 42% yield. Slightly yellow oil. R_f (hexanes/EtOAc = 50:1): 0.61. ^{1}H NMR (500 MHz, $CDCl_3$): δ ppm 5.01 (s, 1H), 4.92 (s, 1H), 3.89 (s, 1H), 2.69 (s, 1H), 2.17 (s, 1H), 1.82-1.79 (m, 1H), 1.55 (s, 2H), 1.27-1.26 (m, 1H), 1.21-1.16 (m, 2H), 1.02-0.95 (m, 12H), 0.95-0.91 (m, 2H), 0.07 (s, 3H). ^{13}C NMR (126 MHz, $CDCl_3$): δ ppm -7.9, 13.2, 13.4, 17.4, 17.5, 23.9, 29.2, 35.4, 43.9, 44.9, 106.2, 159.2. LRMS (ES+) calcd. for $C_{15}H_{28}OSi$ [M]: 252.1, found: 252.1.

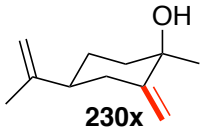

230x

230x was prepared according to the general procedure **B** 70% yield. R_f (hexanes/EtOAc = 9:1): 0.42. ^{1}H NMR (500 MHz, $CDCl_3$): δ ppm 4.88 (s, 1H), 4.78 (s, 1H), 4.74 (s, 1H), 4.71 (m, 1H), 2.46 (t, J = 12.1 Hz, 1H), 2.20 (d, J = 12.4 Hz, 2H), 1.98 (t, J = 11.4 Hz, 1H), 1.89-1.84 (m, 1H), 1.74 (m, 3H), 1.62-1.60 (m, 1H), 1.47-1.43 (m, 1H), 1.40 (s, 3H), 1.36 (bs, 1H). ^{13}C NMR (126 MHz, $CDCl_3$): δ ppm 20.8, 26.9, 27.5, 37.5, 40.2, 46.7, 70.8, 107.5, 108.3, 149.5, 152.4. LRMS (EI+) calcd. for $C_{11}H_{18}O$ [M]: 166.26, found: 166.10.

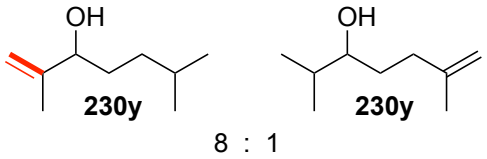

230y was prepared according to the general Method **D** in 73% yield. 85% purity (GC). Colorless liquid. R_f (hexanes/EtOAc 9:1): 0.40. For major isomer **2y**, ^{1}H NMR (500 MHz, $CDCl_3$): δ ppm 4.94 (s, 1H), 4.84 (s, 1H) 4.06-4.03 (m, 1H), 1.74 (s, 3H), 1.57-1.53 (m, 2H), 1.27-1.25 (m, 1H), 1.04-0.99 (m, 2H), 0.93-0.89 (m, 6 H). ^{13}C NMR (126 MHz, $CDCl_3$): δ ppm 17.2, 17.4, 22.6, 32.7, 34.6, 76.3, 111.1, 147.6. LRMS (EI+) calcd. for $C_9H_{18}O$ [M]: 142.1, found: 142.1.

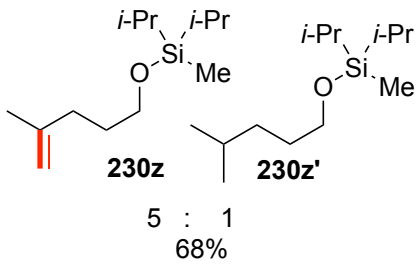

230z was prepared according to the general procedure **A** (without the TBAF step) in calcd. 57% yield. Yellow oil. R_f (hexanes/EtOAc = 20:1): 0.41. ^{1}H NMR (500 MHz, $CDCl_3$): δ ppm 4.69 (d, J = 11.6 Hz, 2H), 3.64-3.56 (m, 2H), 2.07-1.99 (m, 2H), 1.72 (s, 3H), 1.69-1.64 (s, 2H), 1.03-0.99 (m, 14H), 0.01 (s, 3H). ^{13}C NMR (126 MHz, $CDCl_3$): δ ppm -8.7, 12.9, 17.4, 22.4, 30.9, 33.9, 63.0, 109.7, 127.2. LRMS (EI+) calcd. for $C_{13}H_{28}OSi$ [M]: 228.45, found: 229.10.

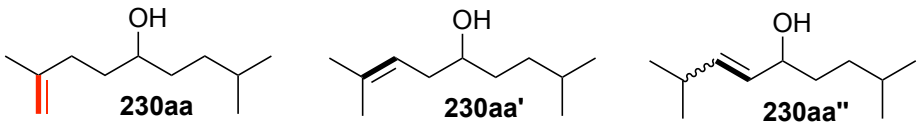

16.7 : 1.3 : 1

88%

230aa was prepared according to the general procedure **B** in calcd. 77% yield. Clear and colorless oil. R_f (hexanes/EtOAc = 4:1): 0.54. ^{1}H NMR (500 MHz, $CDCl_3$): δ ppm 4.72 (s, 2H), 3.60-3.54 (m, 1H), 2.17-2.08 (m, 2H), 1.74 (s, 3H), 1.65-1.16 (m, 8H), 0.99-0.88 (m, 6H). ^{13}C NMR (126 MHz, $CDCl_3$): δ ppm 22.4, 22.5, 22.7, 28.1, 34.1, 35.2, 35.3, 72.1, 110.0, 145.9. HRMS (EI+) calcd. for $C_{11}H_{22}O$ [M]: 170.16707, found: 170.16688.

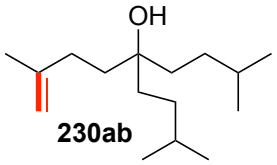

230ab was prepared according to the general procedure **B** in 89 % yield .Clear and colorless oil. R_f (hexanes/EtOAc = 4:1): 0.63. ^{1}H NMR (500 MHz, $CDCl_3$): δ ppm 4.70 (s, 2H), 2.03-2.00 (m, 2H), 1.54 (s, 3H), 1.49-1.38 (m, 9H), 1.19-1.14 (m, 4H), 0.90-0.89 (m, 12H). ^{13}C NMR (126 MHz, $CDCl_3$): δ ppm 22.7, 28.6, 31.7, 32.4, 36.8, 37.2, 74.3, 109.7, 146.4. HRMS (ESI+) calcd. for $C_{16}H_{32}O$ [M]+Na: 263.2351, found: 263.2359.

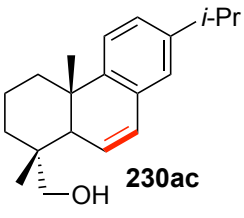

230ac was prepared according to the general procedure **A** (two-steps) in 40% yield. Clear and colorless oil. R_f (hexanes/EtOAc = 4:1): 0.28. ^{1}H NMR (500 MHz, $CDCl_3$): δ ppm

7.10 (d, *J* = 7.7 Hz, 2H), 7.06 (d, *J* = 8.1 Hz, 1H), 6.90 (s, 1H), 6.55 (dd, *J* = 9.5, 2.9 Hz, 1H), 5.97 (d, *J* = 9.2, 2.2 Hz, 1H), 3.49 (d, *J* = 11.0 Hz, 1H), 3.27 (d, *J* = 11.0 Hz, 1H), 2.89-2.82 (m, 1H), 2.40 (bs, 1H), 2.18 (d, 12.8 Hz, 1H), 1.83-1.74 (m, 2H), 1.64-1.41 (m, 4H), 1.28-1.23 (m, 6H), 1.08 (s, 3H), 1.02 (s, 3H). ^{13}C NMR (126 MHz, $CDCl_3$): δ ppm 18.2, 18.3, 20.8, 24.0, 33.5, 29.7, 33.7, 34.4, 35.7, 37.2, 45.1, 71.6, 121.8, 124.6, 125.7, 128.5, 128.7, 132.6, 145.6, 146.2. HRMS (ES+) calcd. for $C_{20}H_{28}O$ [M+1]: 285.2218, found: 285.2224.

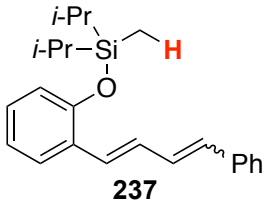

237

237 was prepared according to the general procedure in 83% NMR yield. ^{1}H NMR (500 MHz, C_6D_6): δ ppm 7.62 (dd, *J*= 7.7, 1.5 Hz, 1H), 7.36 (d, *J*= 10.3 Hz, 2H), 7.21 (t, *J*= 7.7 Hz, 2H), 7.14-7.06 (m, 5H), 6.98 (t, *J*= 7.3 Hz, 1H), 6.94 (d, *J*= 8, 1H), 6.66 (d, *J*=15.04, 1H), 1.22-1.11 (m, 14H), 0.25 (s, 3H). ^{13}C-dept displayed no CH_2 signals in the olefin region. LRMS (EI) calcd. for $C_{23}H_{30}OSi$ [M]: 350.58, found: 350.20.

APPENDICES

^{1}H Spectrum of **69**

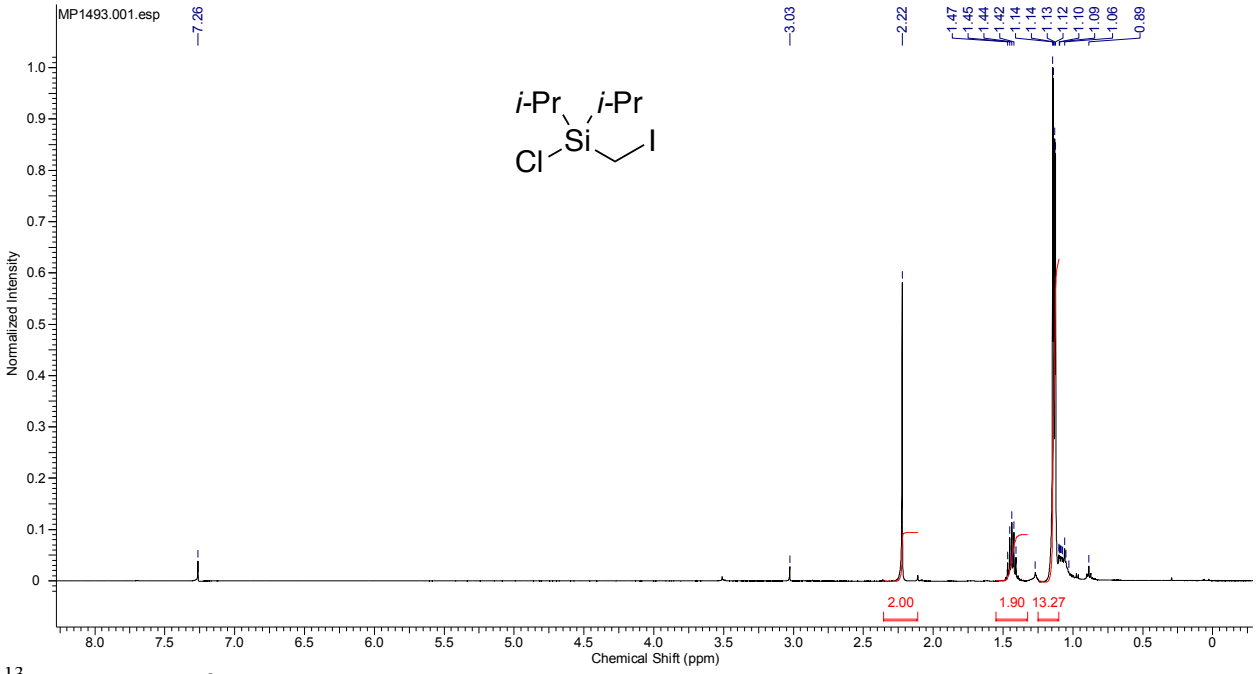

^{13}C Spectrum of **69**

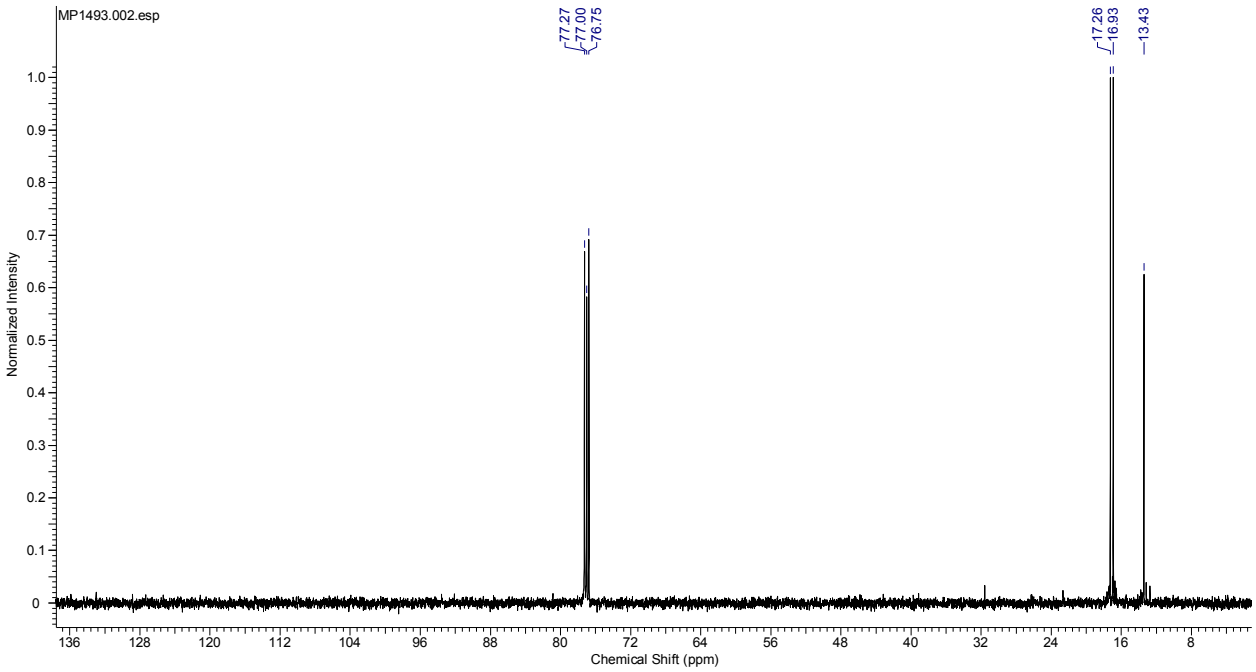

^{1}H Spectrum of **75a**

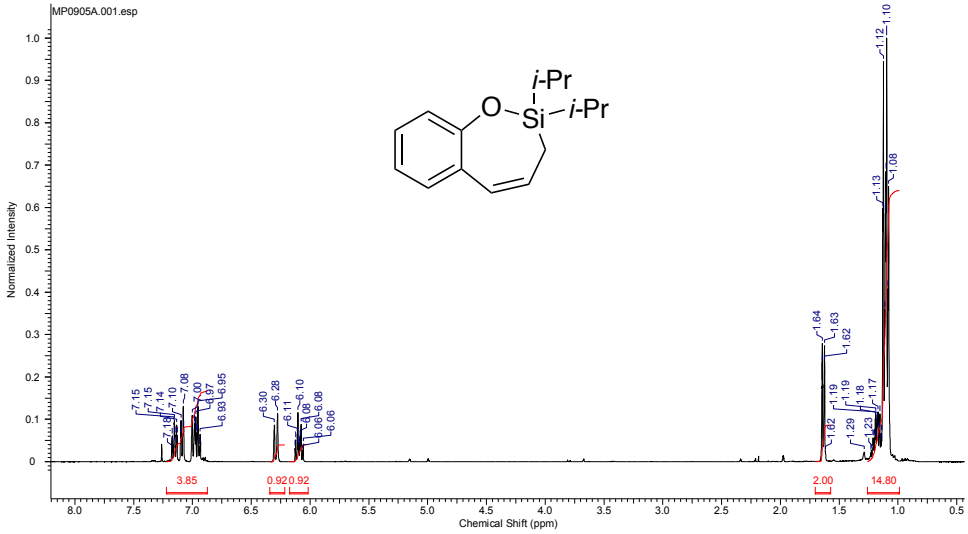

^{13}C Spectrum of **74a**

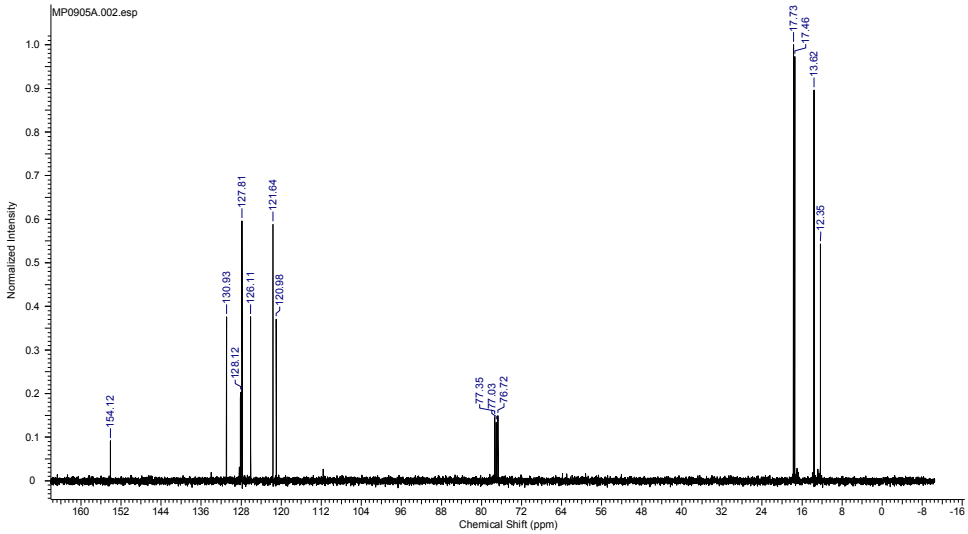

^{13}C DEPT Spectrum of **74a**

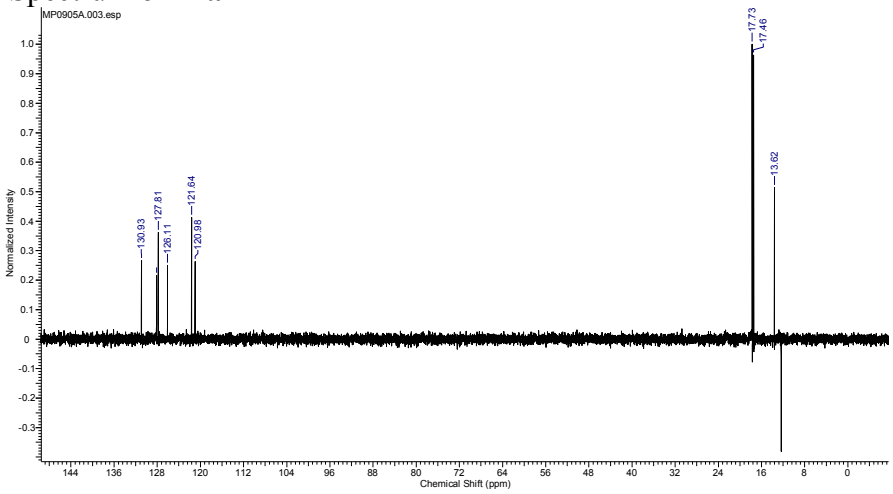

^{1}H Spectrum of **75b**

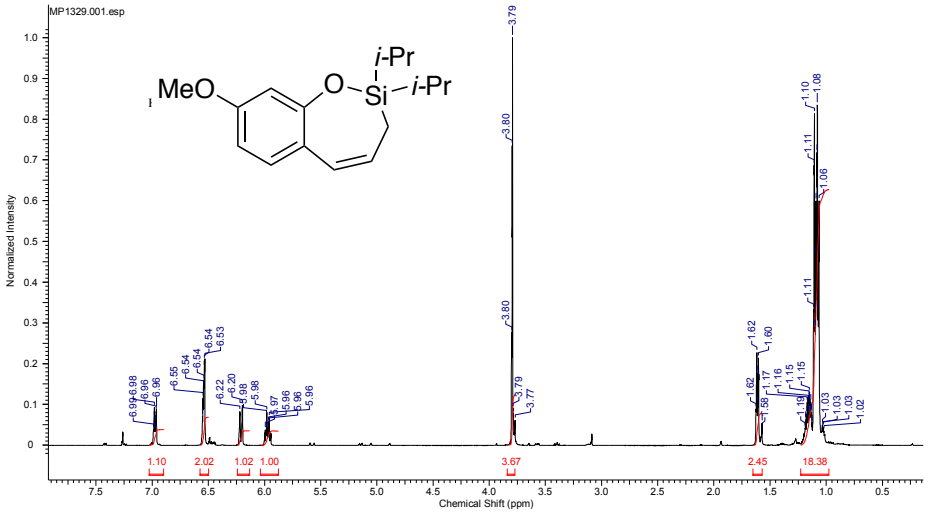

^{13}C Spectrum of **75b**

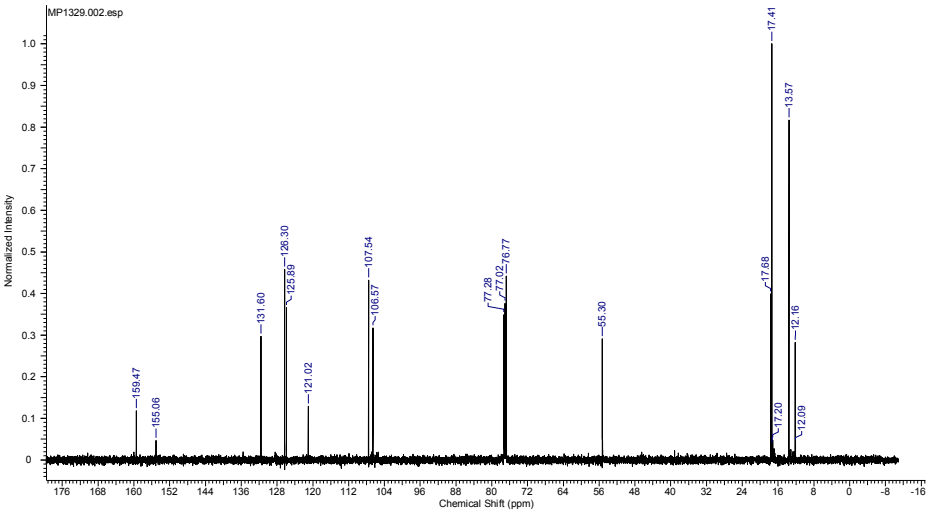

^{13}C DEPT Spectrum of **75b**

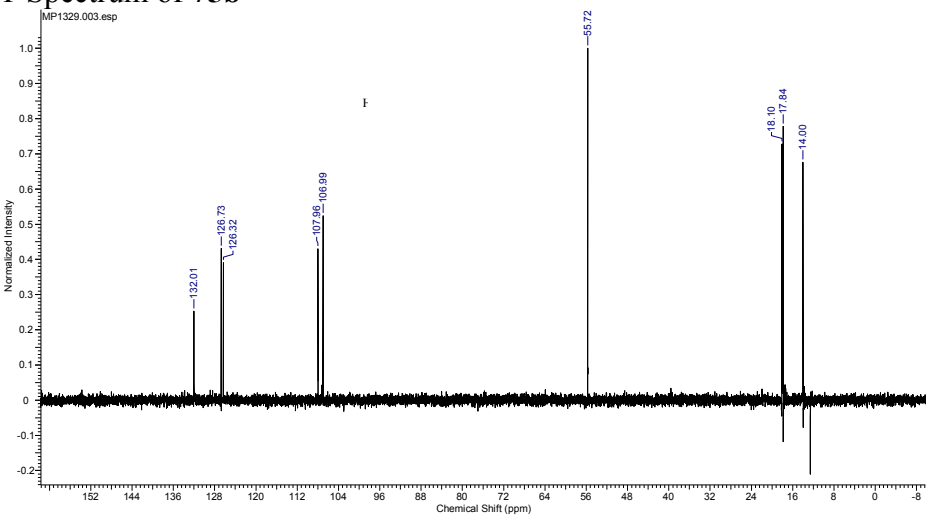

^{1}H Spectrum of **75c**

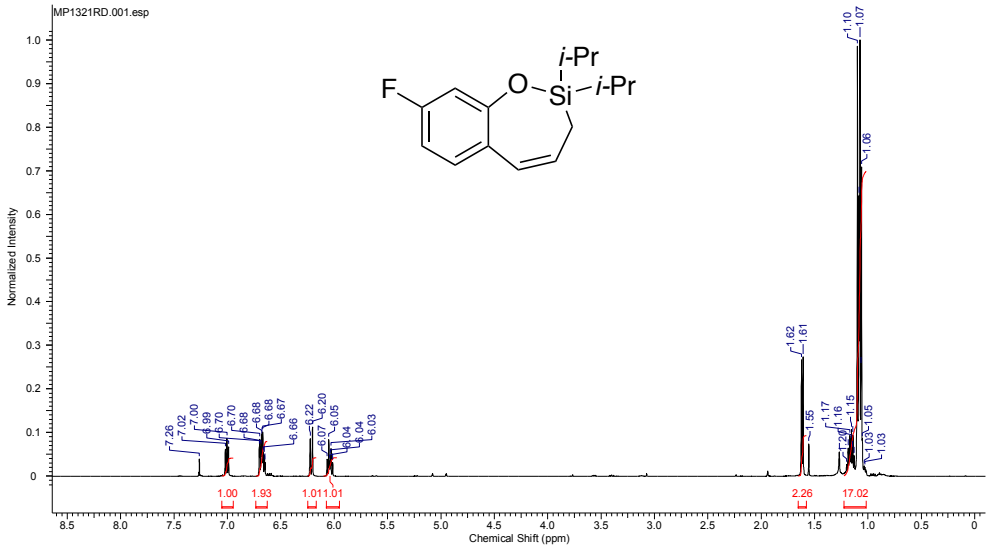

^{13}C Spectrum of **2c**

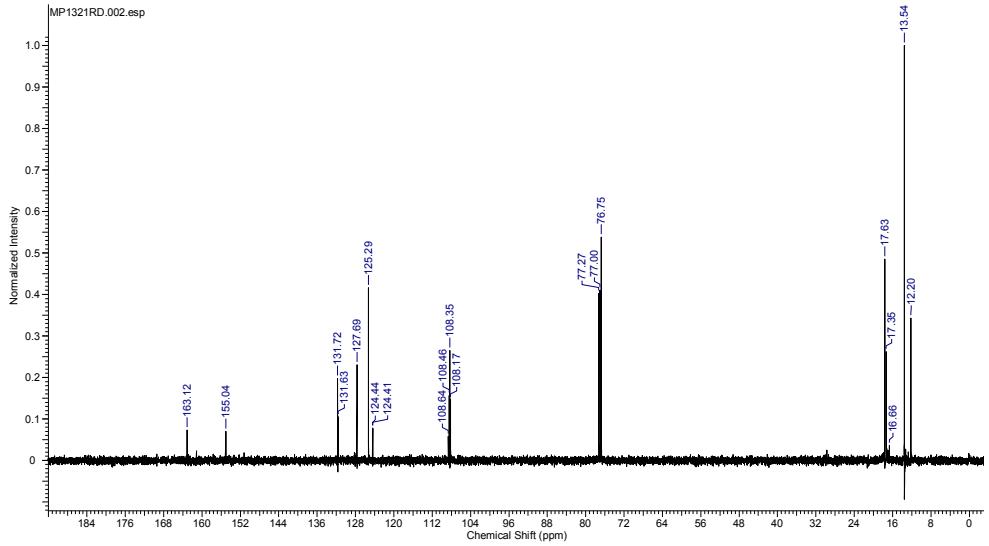

^{13}C DEPT Spectrum of **2c**

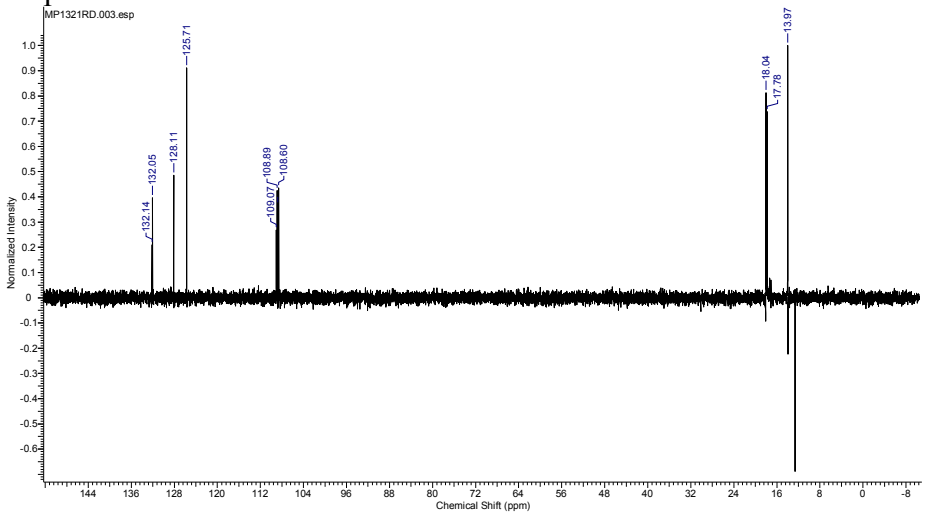

^{1}H Spectrum of **75d**

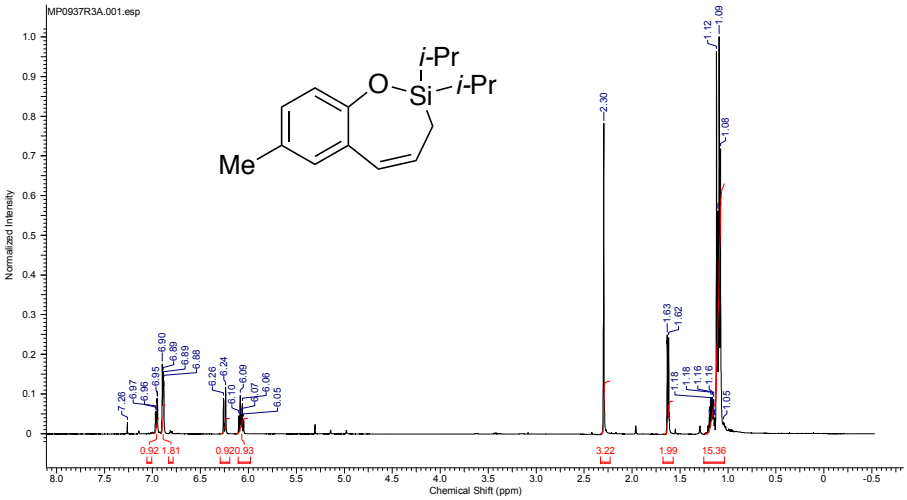

^{13}C Spectrum of **75d**

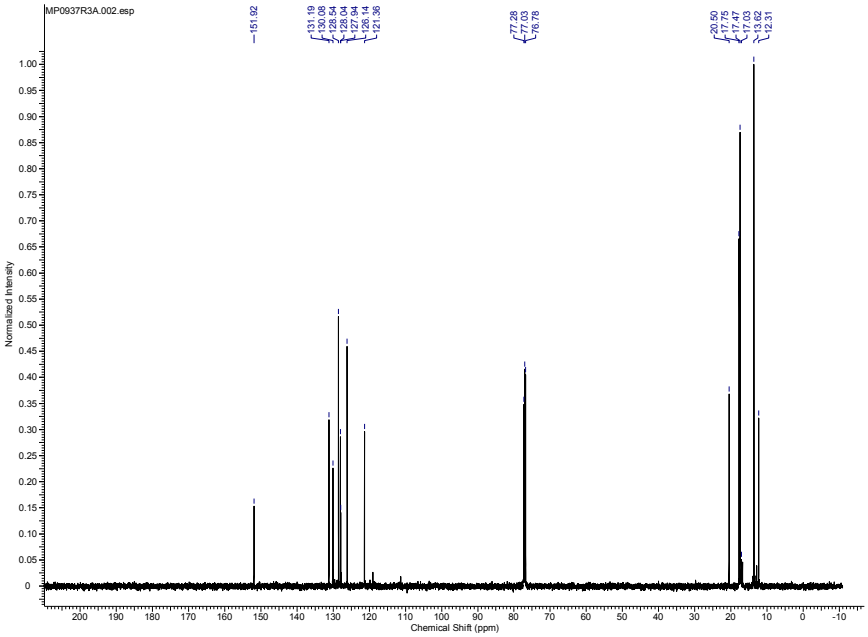

^{13}C DEPT Spectrum of **75d**

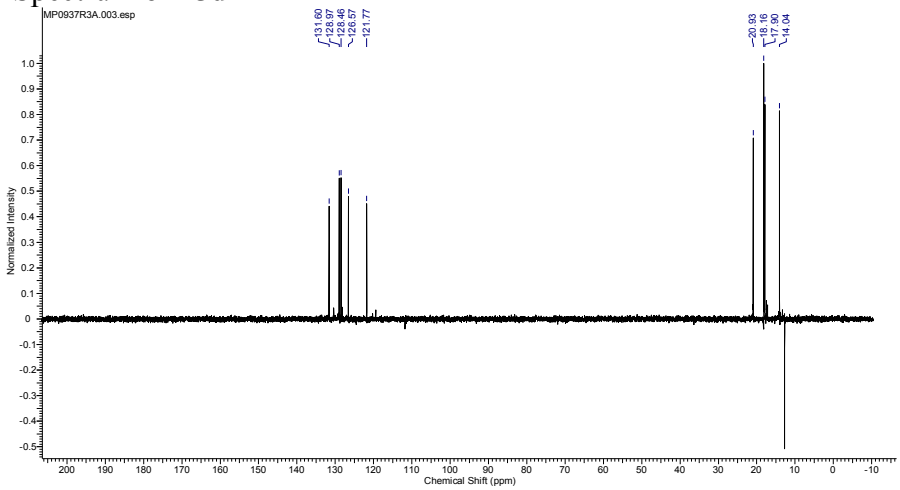

^{1}H Spectrum of **75e**

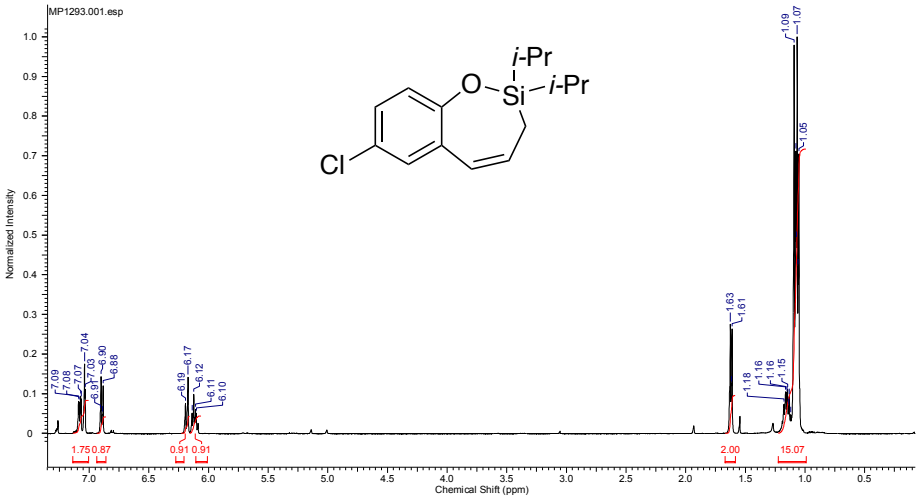

^{13}C Spectrum of **75e**

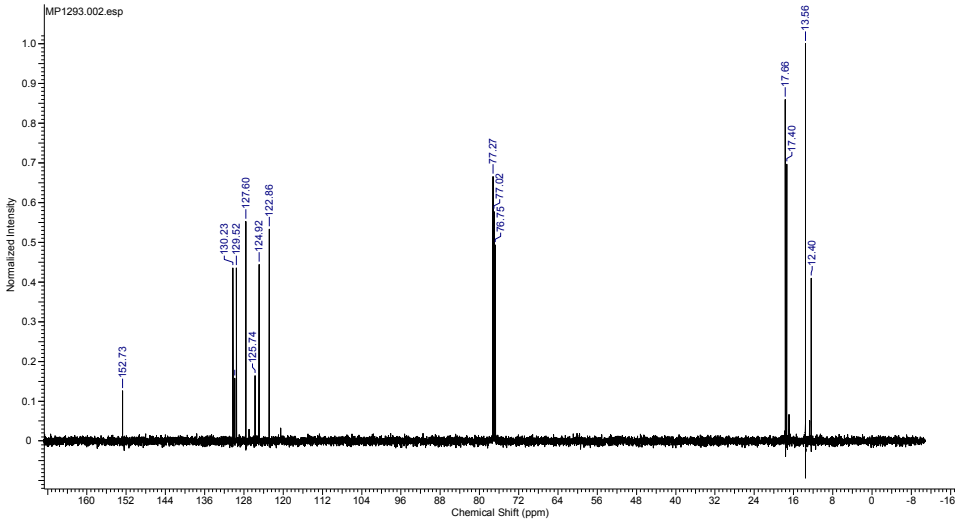

^{13}C DEPT Spectrum of **75e**

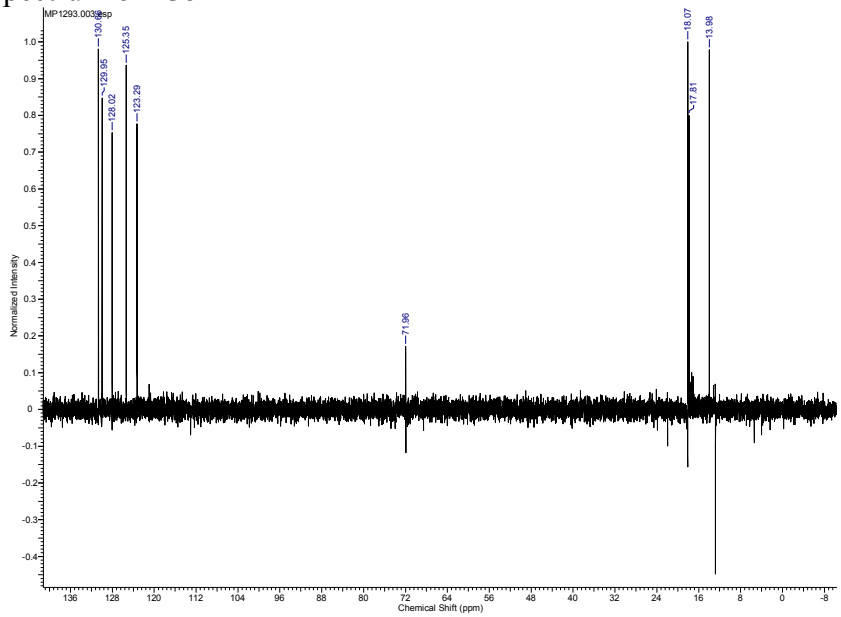

^{1}H Spectrum of **75f**

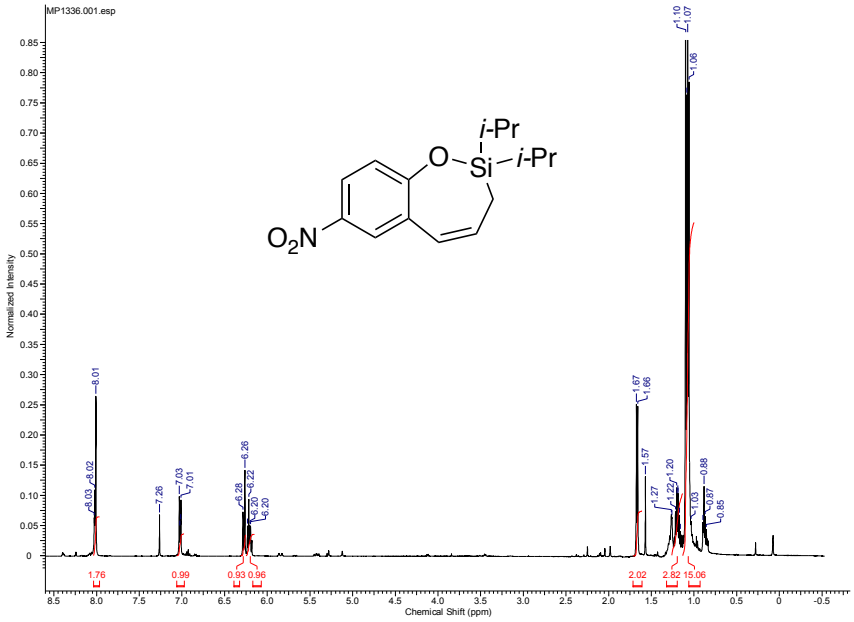

^{13}C Spectrum of **75f**

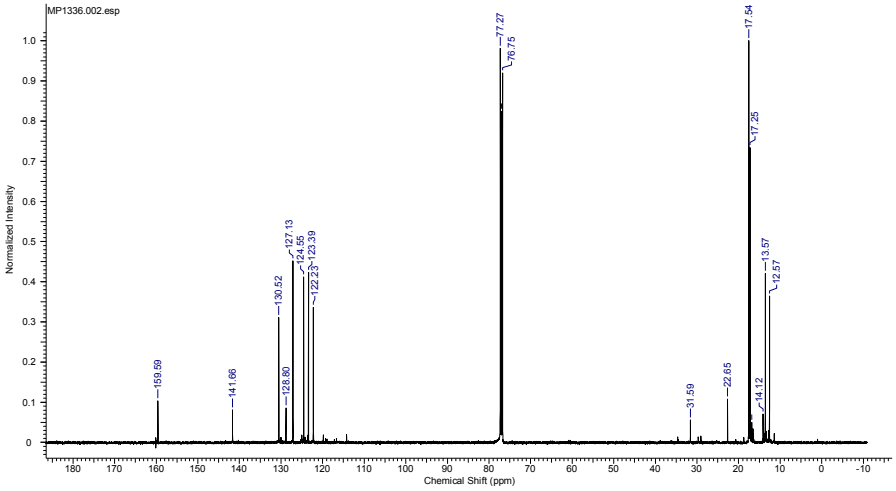

^{13}C DEPT Spectrum of **75f**

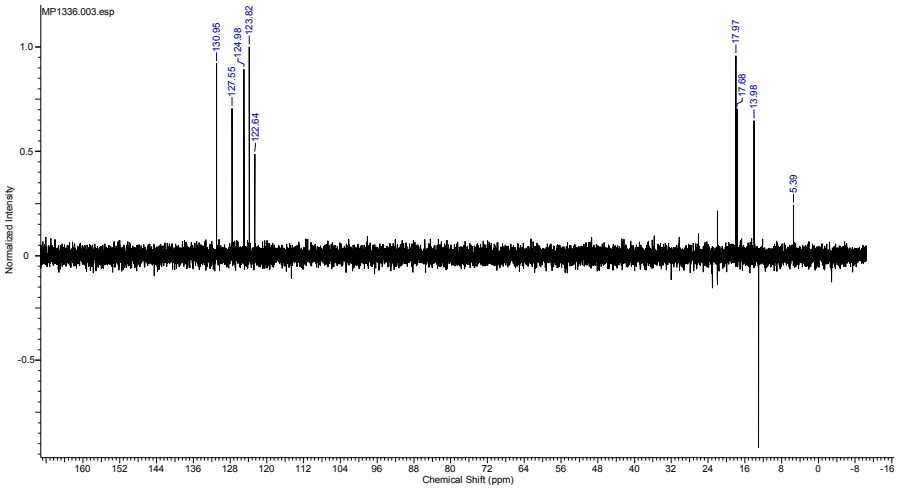

^{1}H Spectrum of **75g**

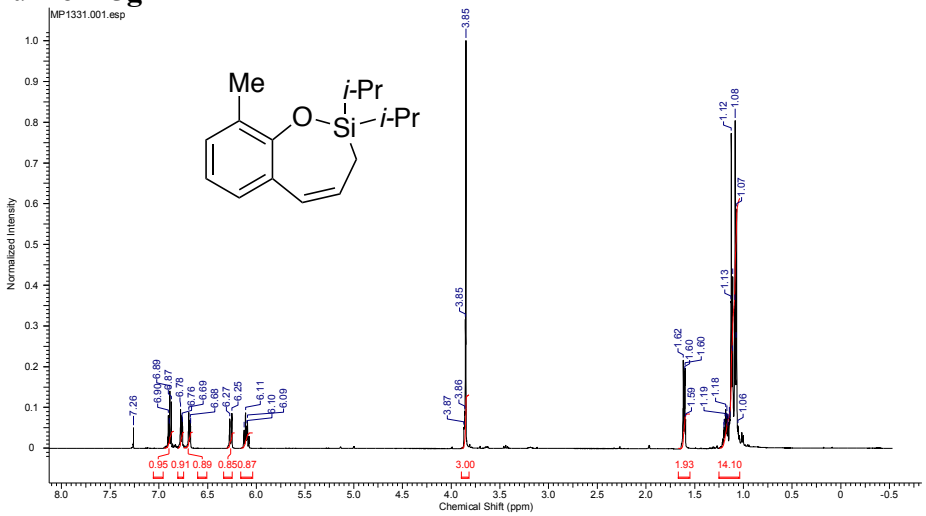

^{13}C Spectrum of **75g**

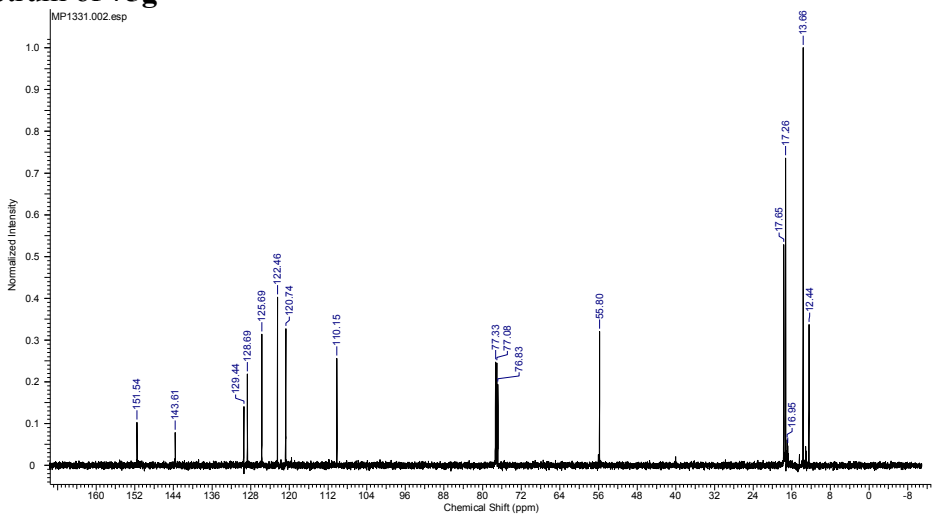

^{13}C DEPT Spectrum of **75g**

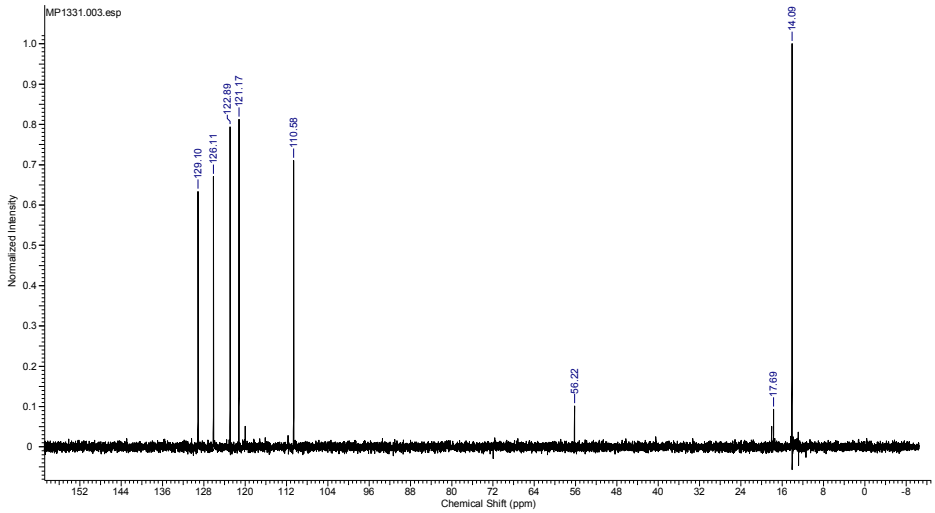

^{1}H Spectrum of **2h**

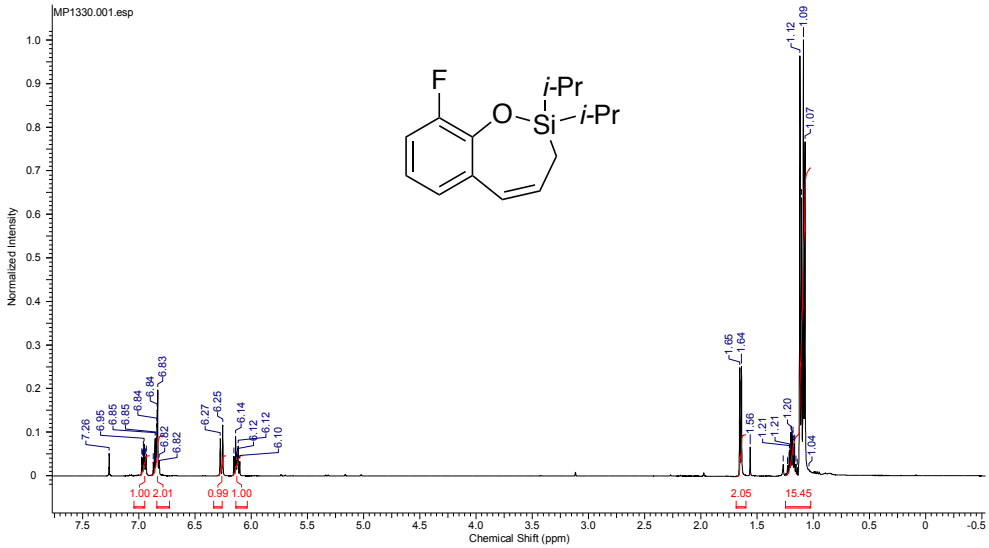

^{13}C Spectrum of **2h**

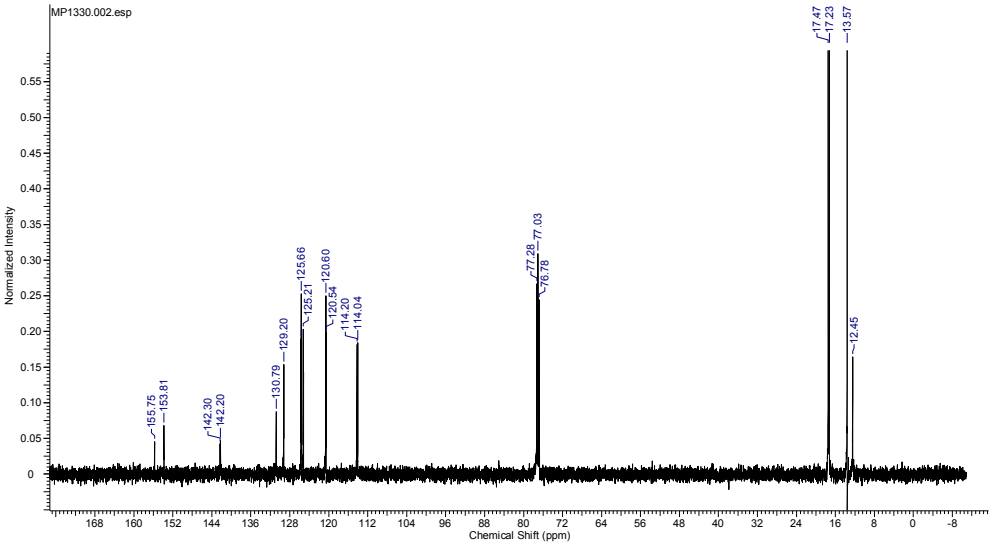

^{13}C DEPT Spectrum of **2h**

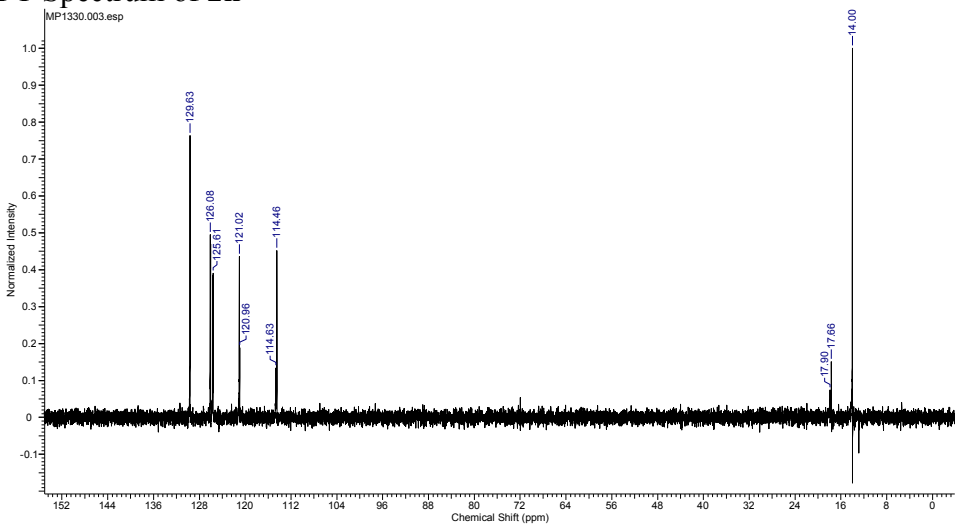

^{1}H Spectrum of **75i**

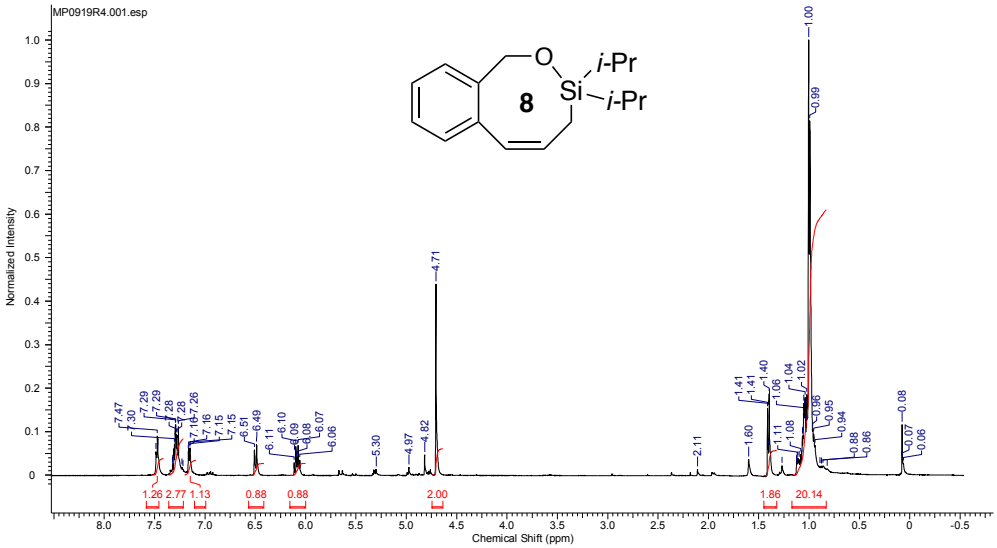

^{13}C Spectrum of **75i**

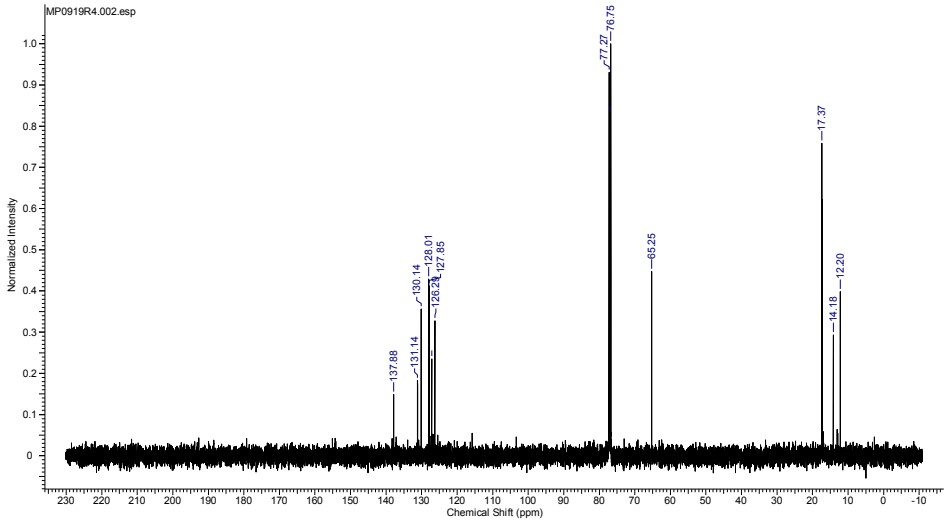

^{13}C DEPT Spectrum of **75i**

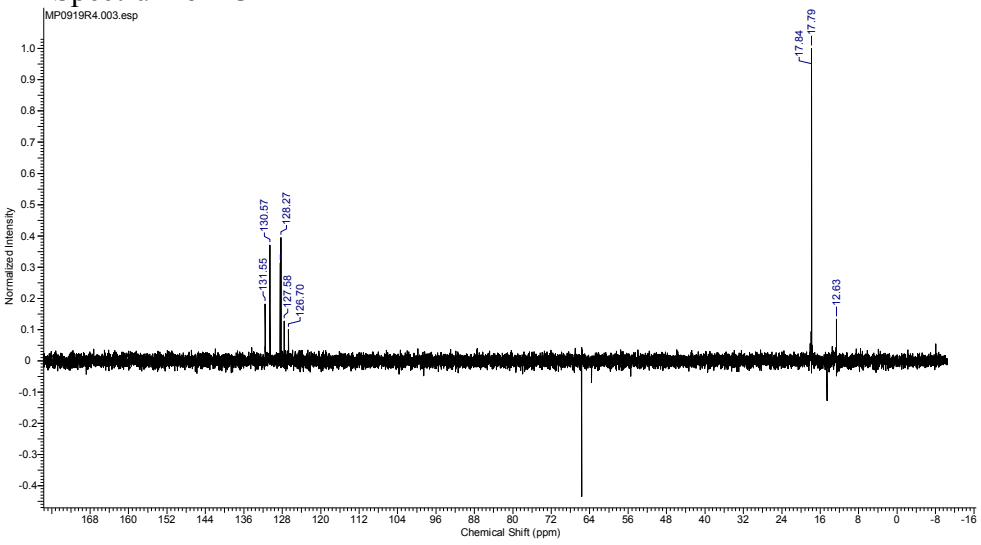

^{1}H Spectrum of **75j** and **75j'**

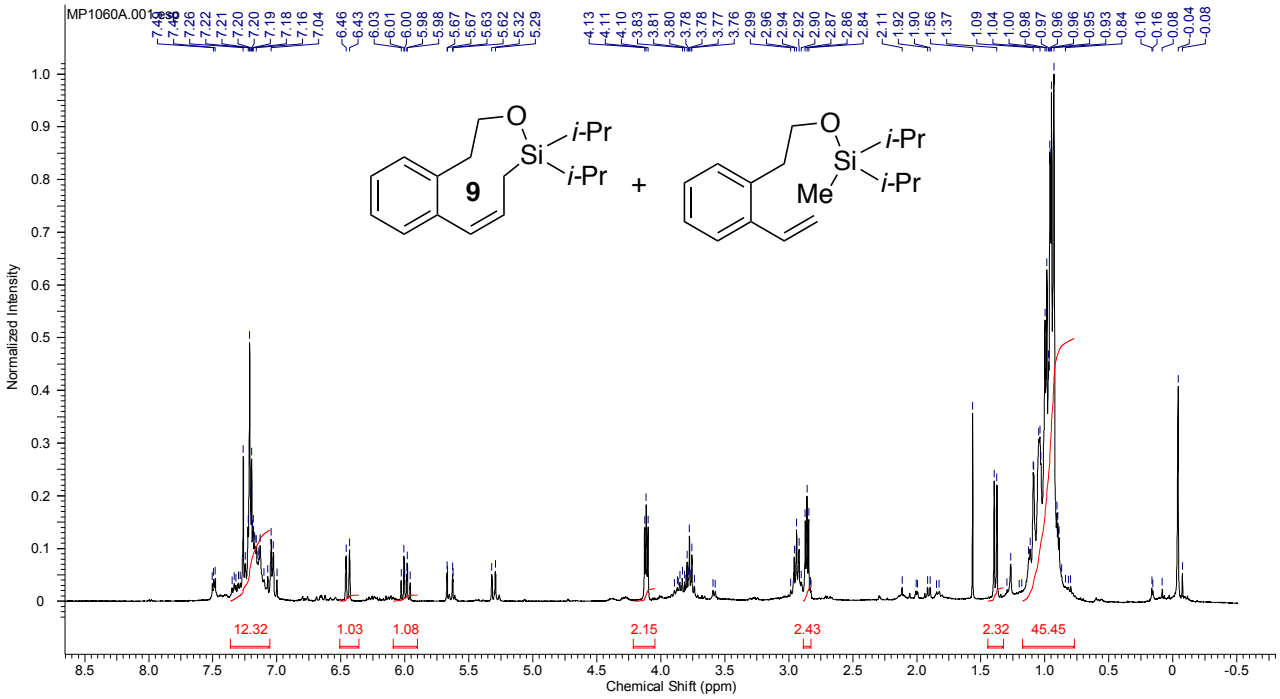

^{13}C Spectrum of **75j** and **2j'**

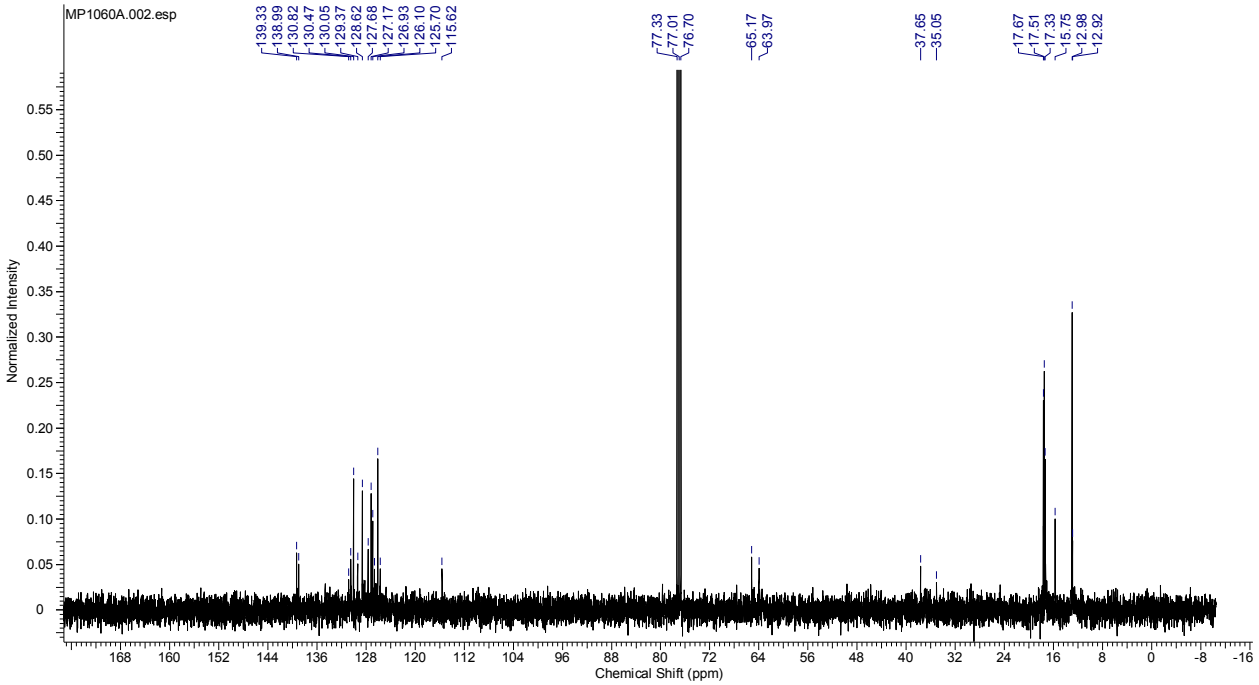

^{1}H Spectrum of **75k**

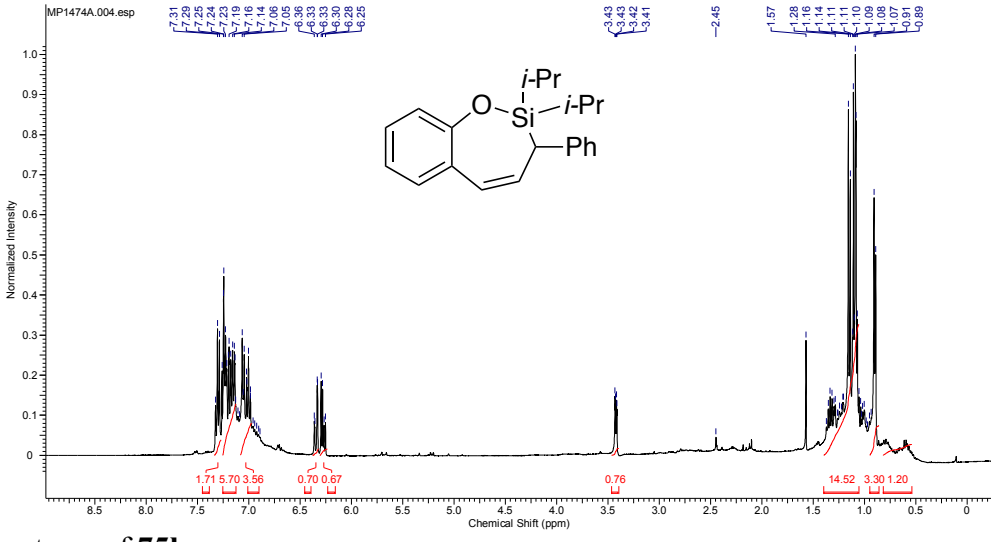

^{13}C Spectrum of **75k**

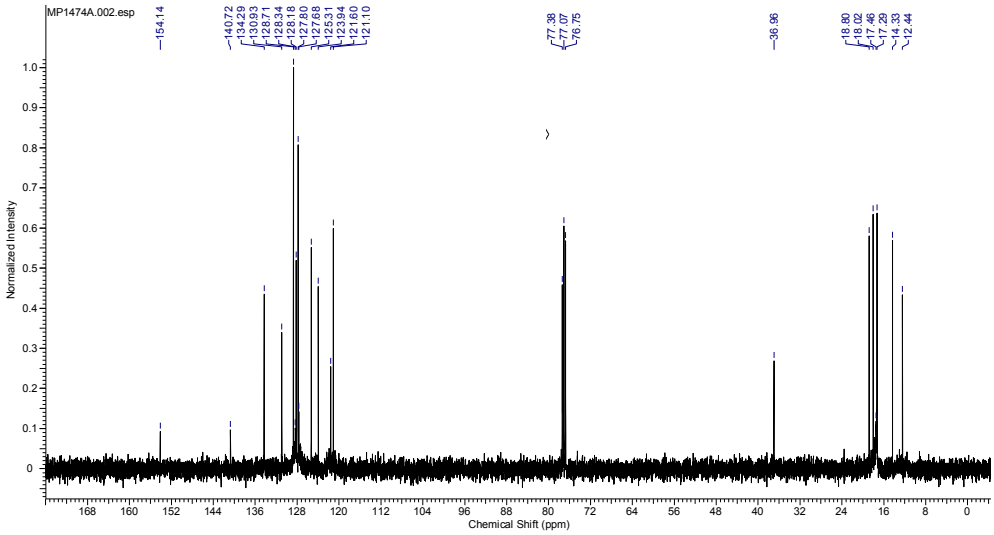

^{13}C DEPT Spectrum of **75k**

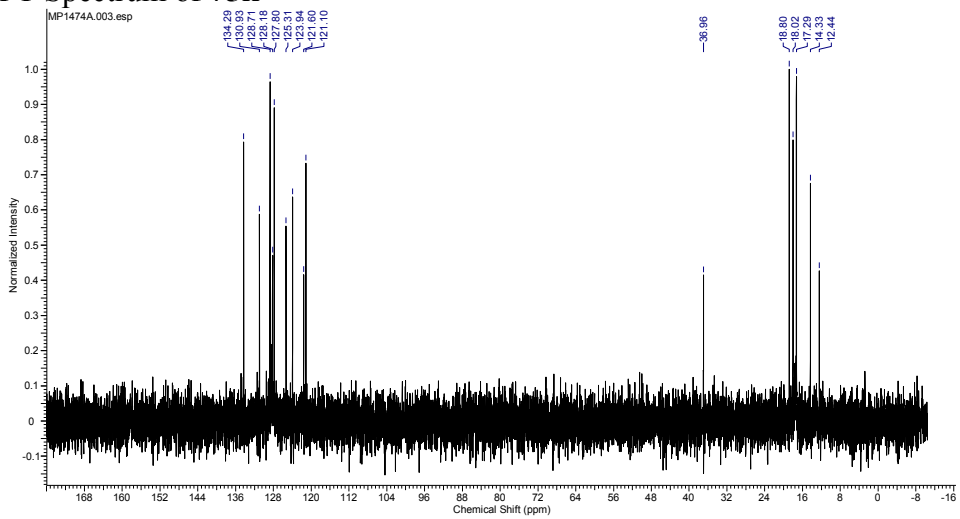

^{1}H Spectrum of **75l**

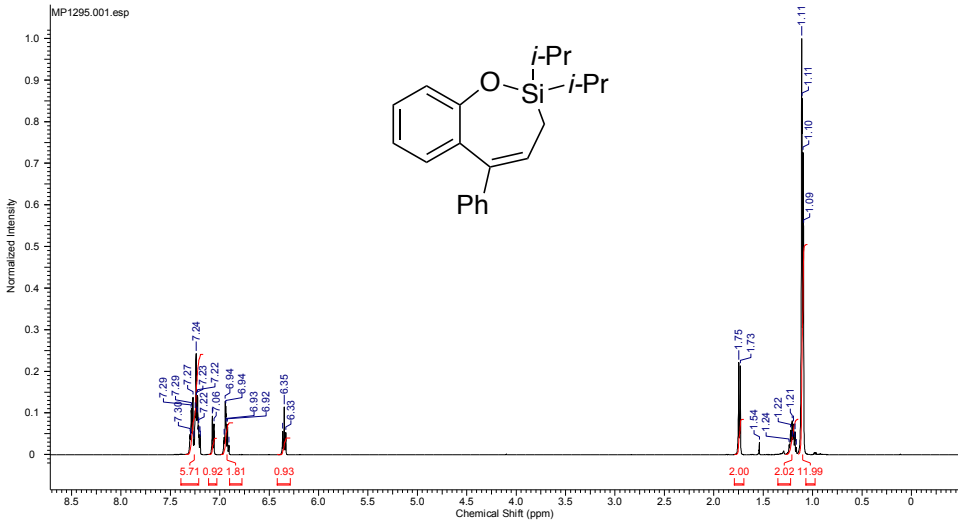

^{13}C Spectrum of **75l**

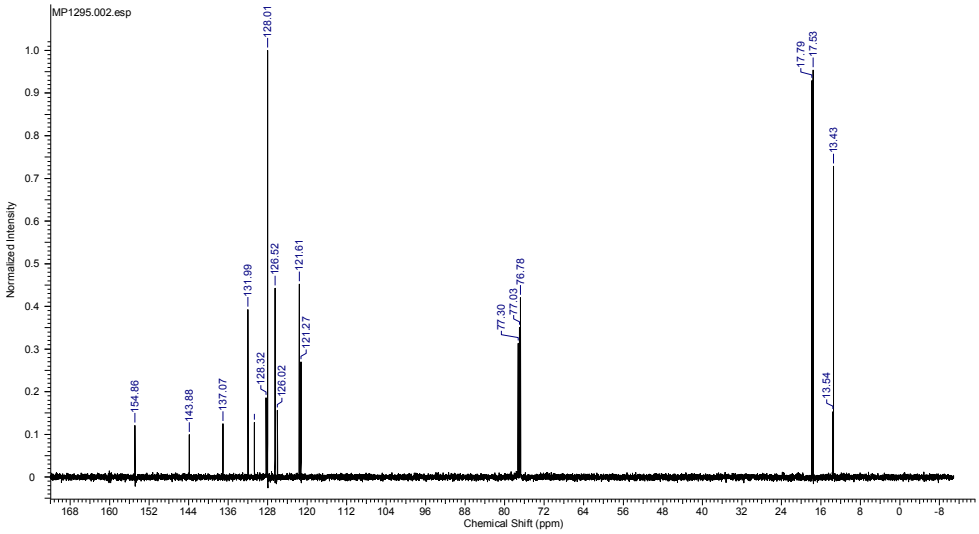

^{13}C DEPT Spectrum of **75l**

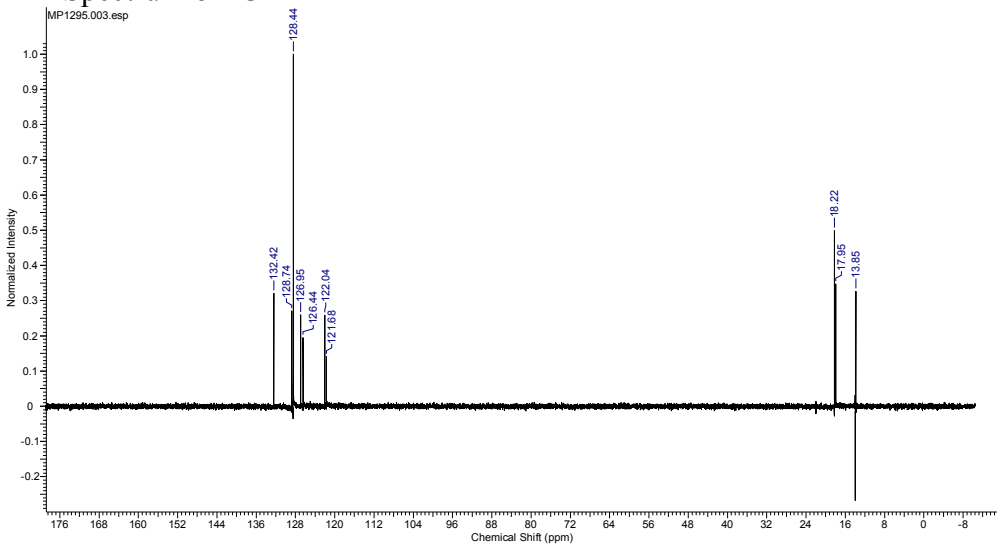

^{1}H Spectrum of **75m**

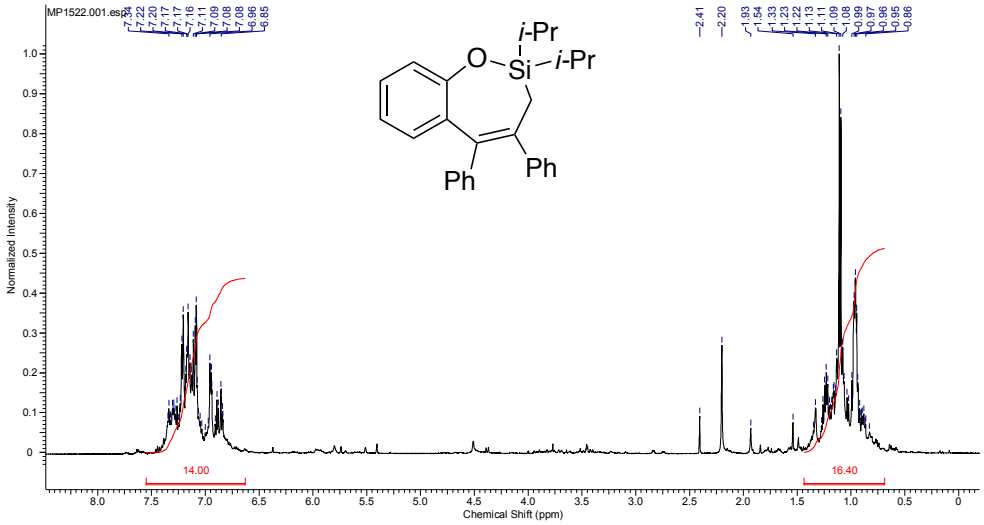

^{13}C Spectrum of **75m**

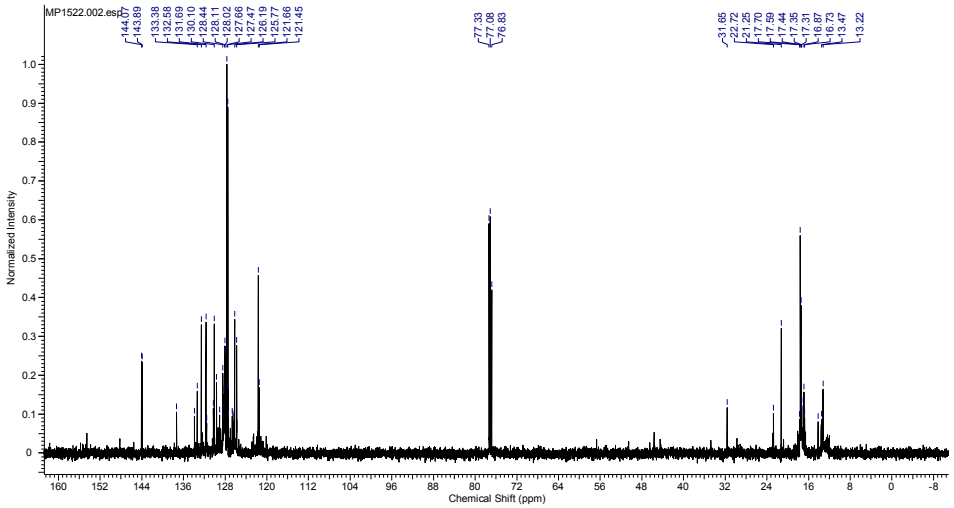

^{13}C DEPT Spectrum of **75m**

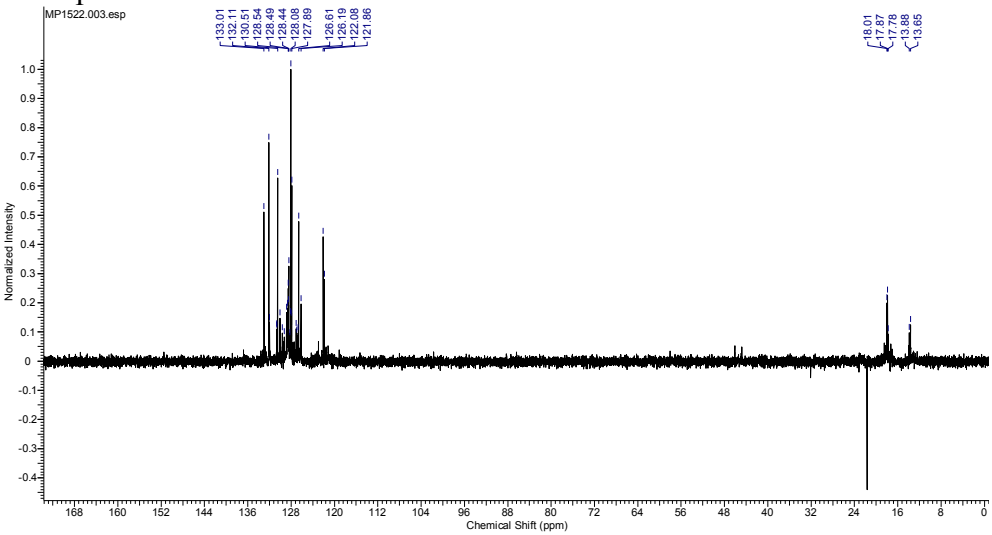

^{1}H Spectrum of **75n, 75n', 75n'', 75n'''**

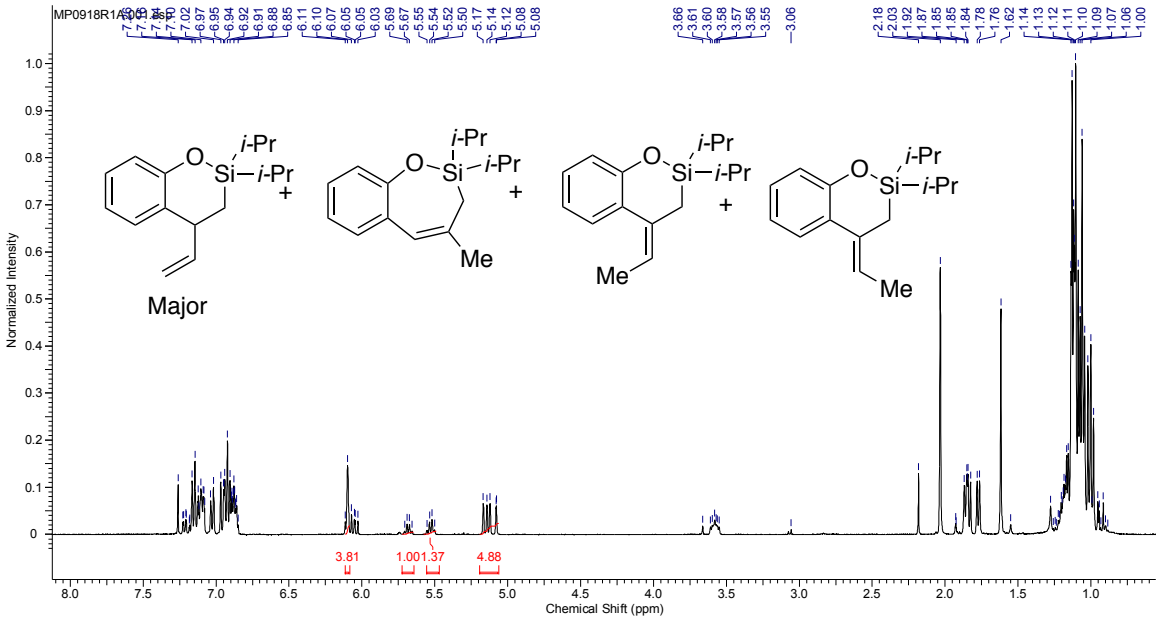

^{13}C Spectrum of **75n, 75n', 75n'', 75n'''**

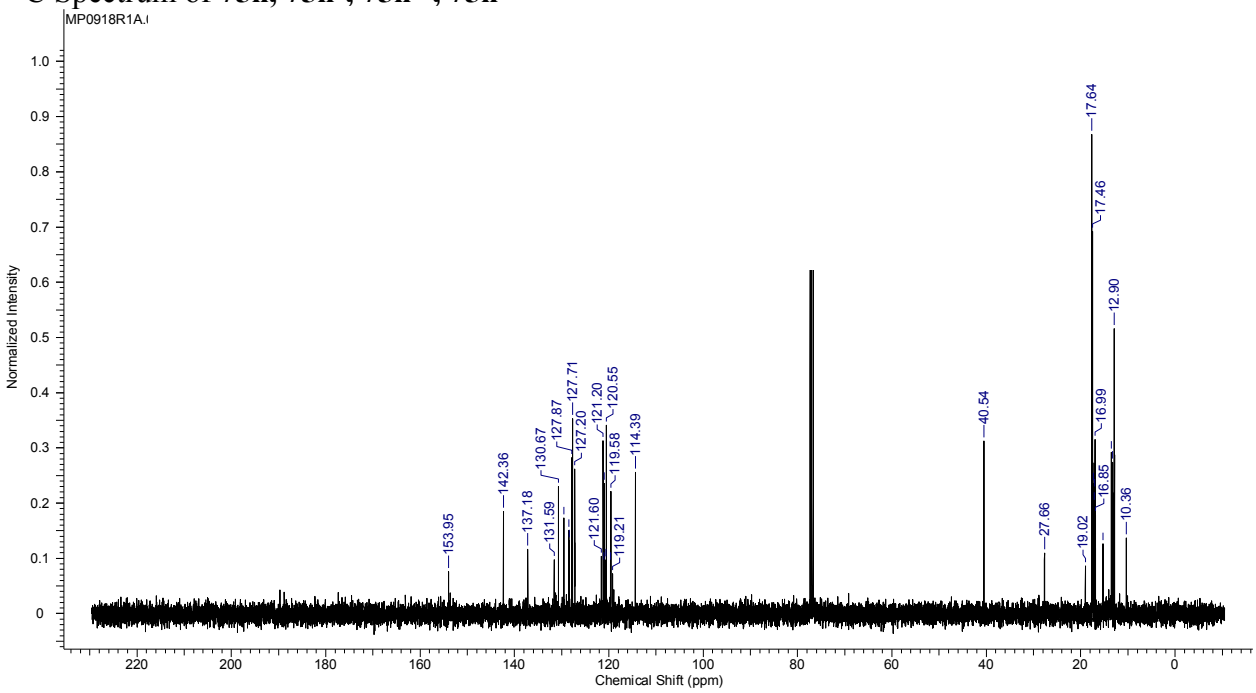

^{1}H Spectrum of **75o**

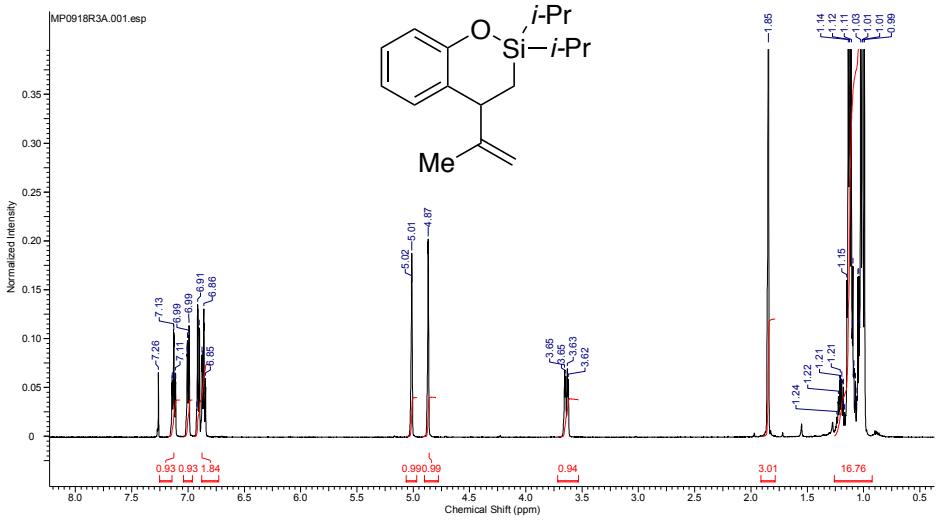

^{13}C Spectrum of **75o**

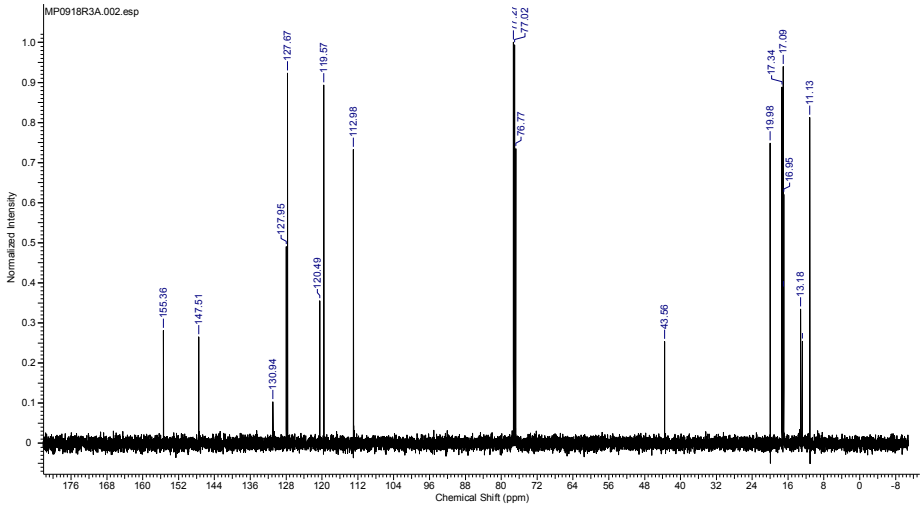

^{13}C DEPT Spectrum of **75o**

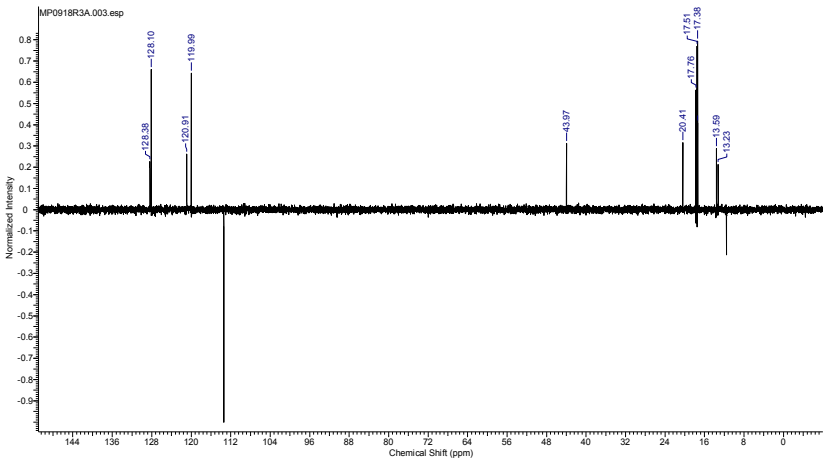

^{1}H Spectrum of **75p**

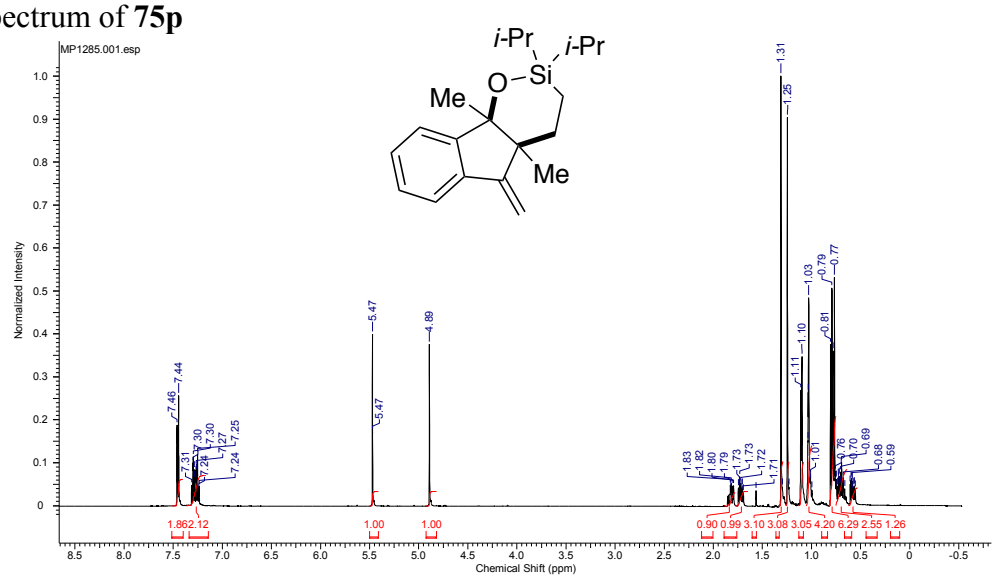

^{13}C Spectrum of **75p**

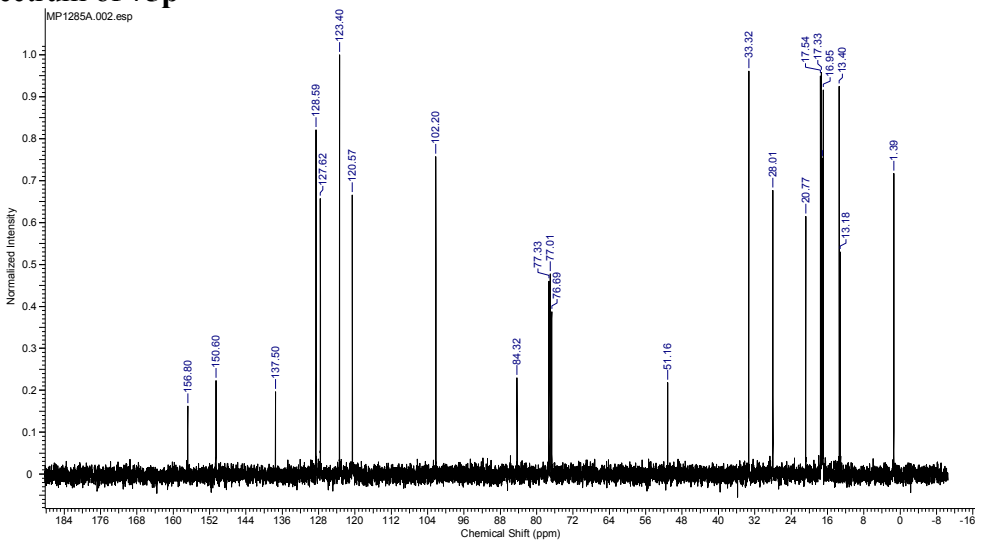

^{13}C DEPT Spectrum of **75p**

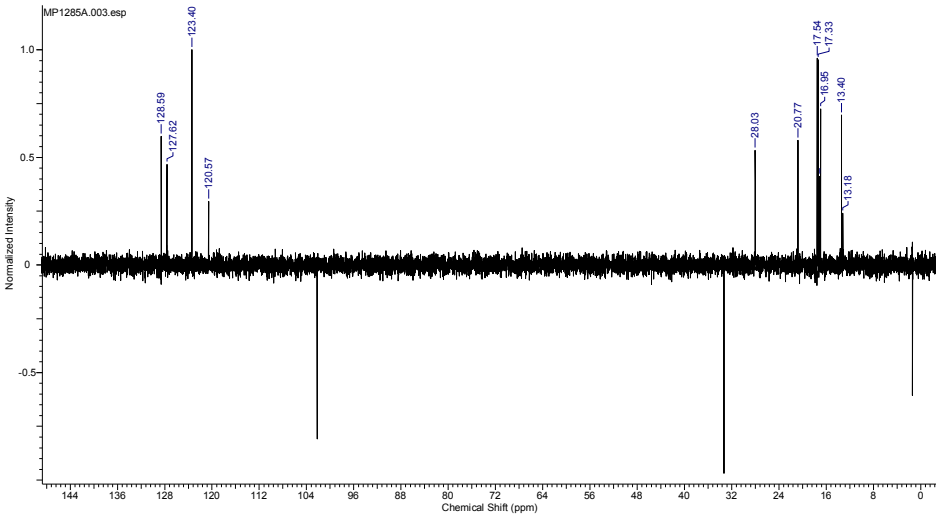

^{1}H Spectrum of **75q**

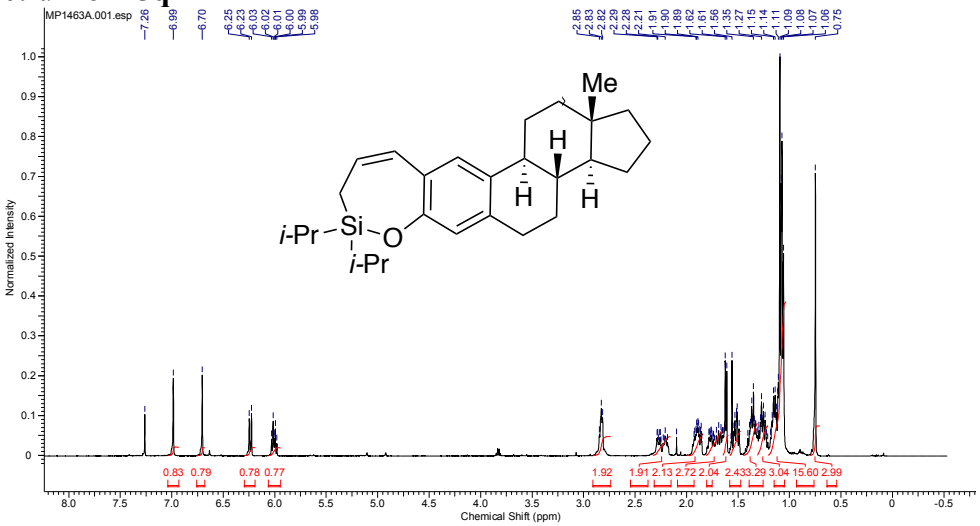

^{13}C Spectrum of **75q**

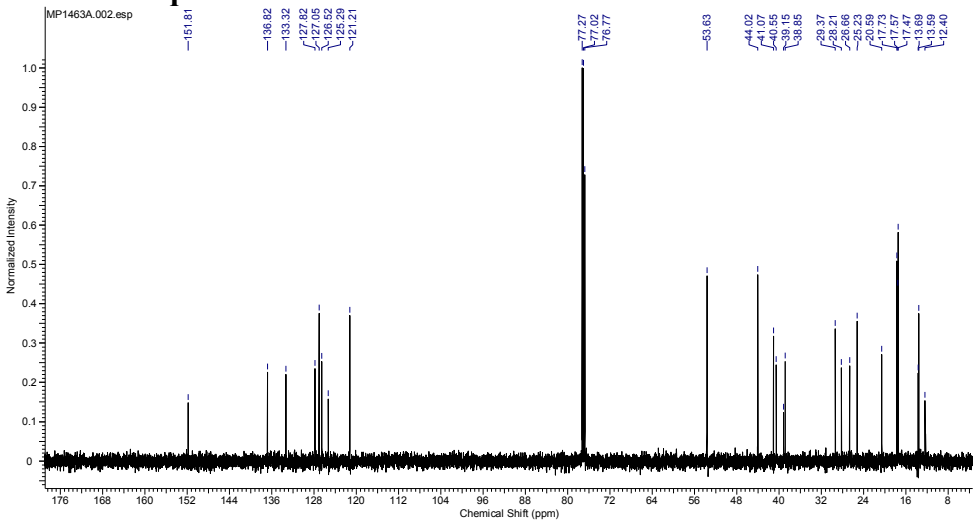

^{13}C DEPT Spectrum of **75q**

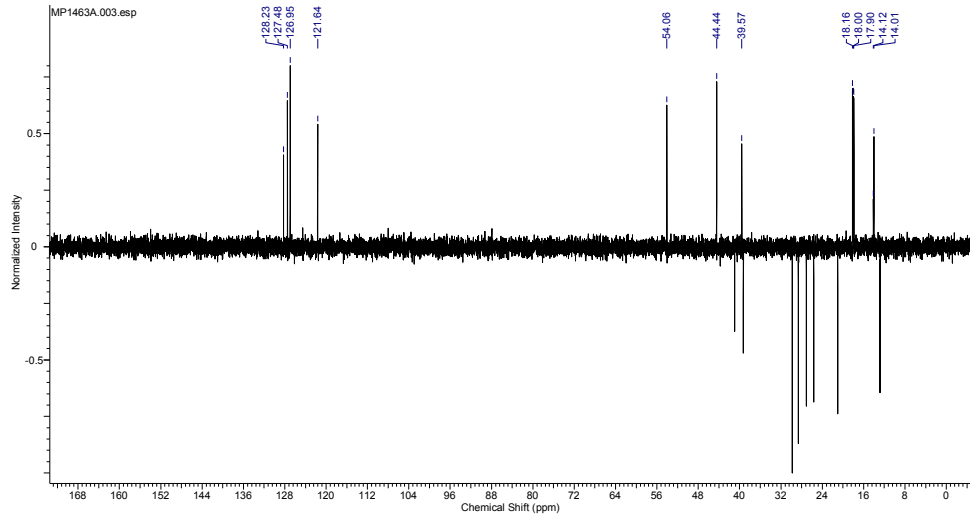

^{1}H Spectrum of **77a**

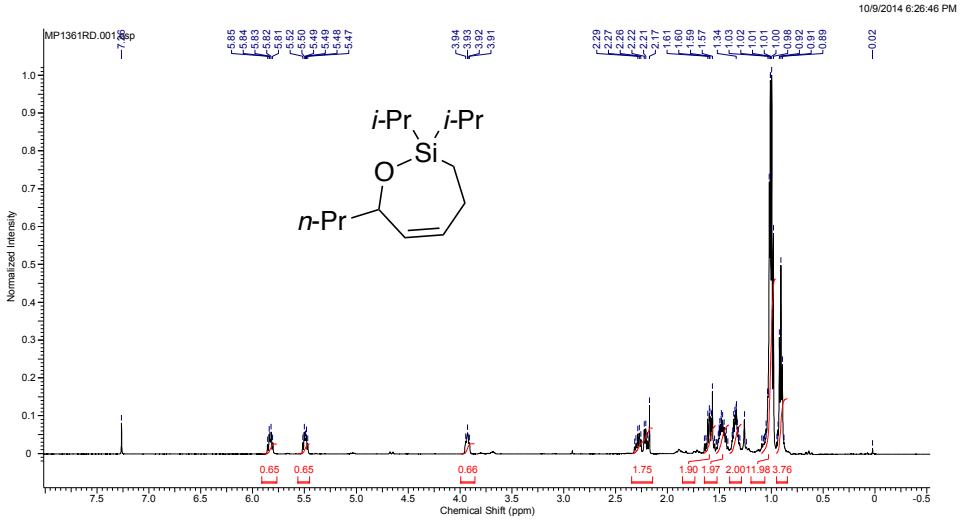

^{13}C Spectrum of **77a**

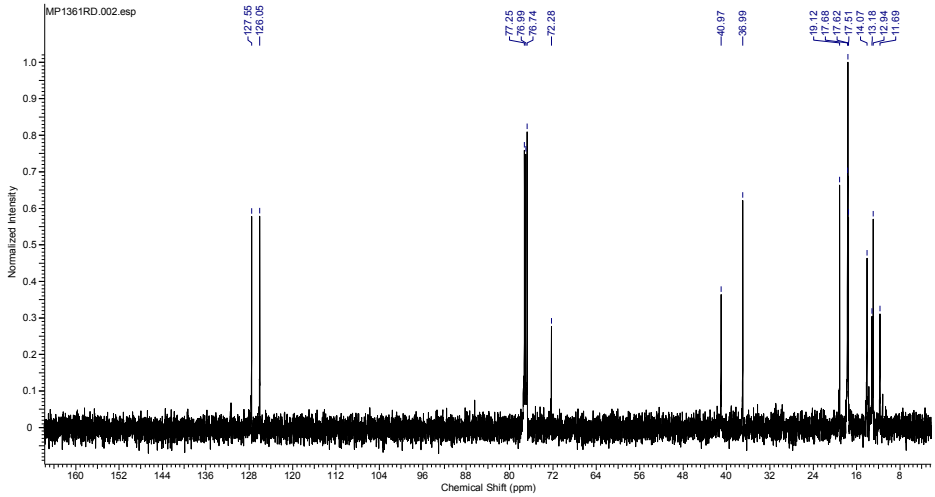

^{13}C DEPT Spectrum of **77a**

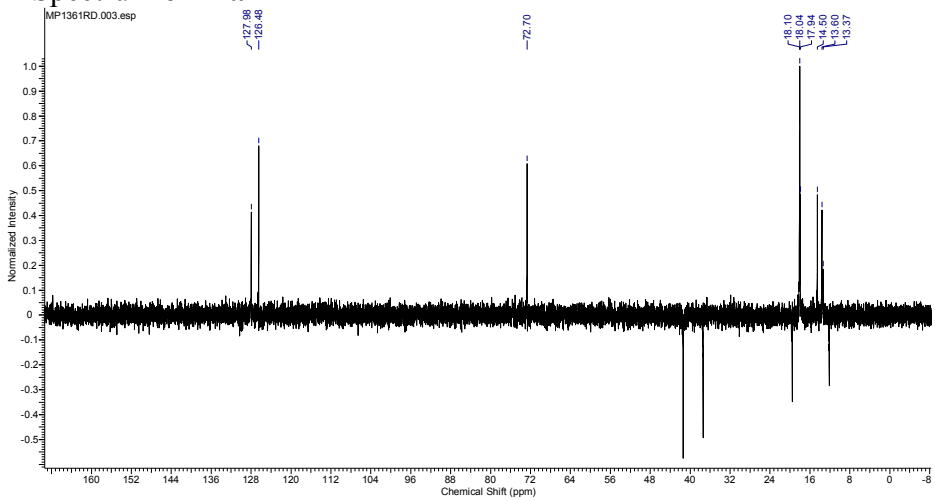

^{1}H Spectrum of **77b**

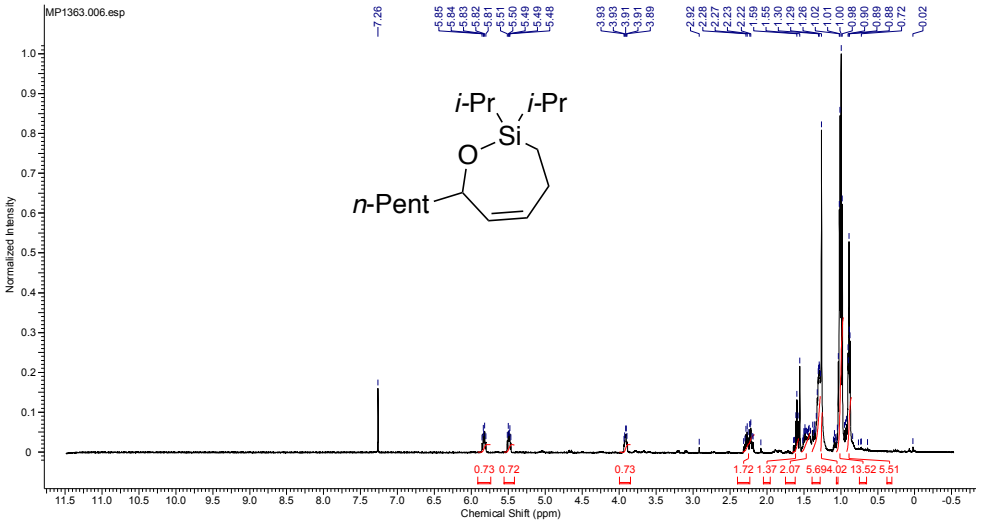

^{13}C Spectrum of **77b**

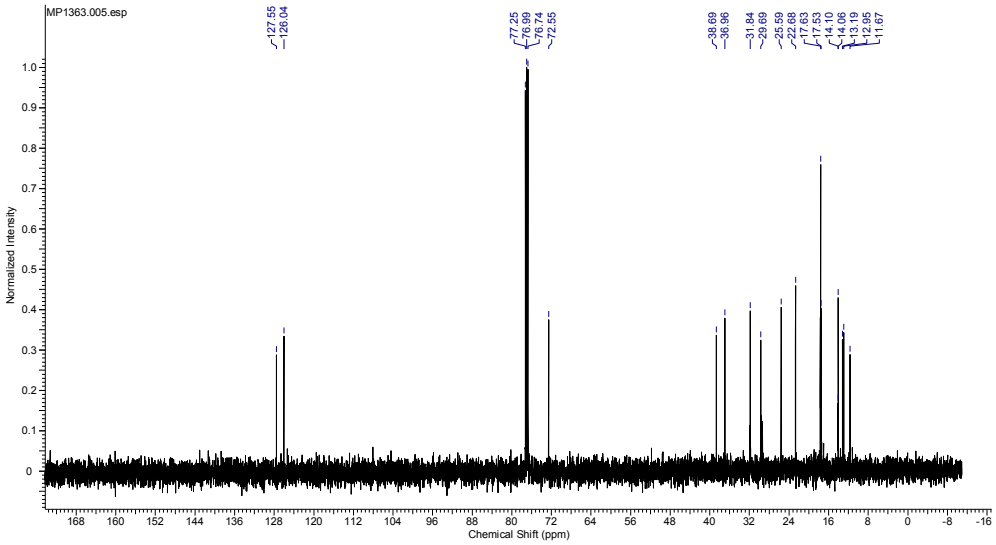

^{13}C Spectrum of **77b**

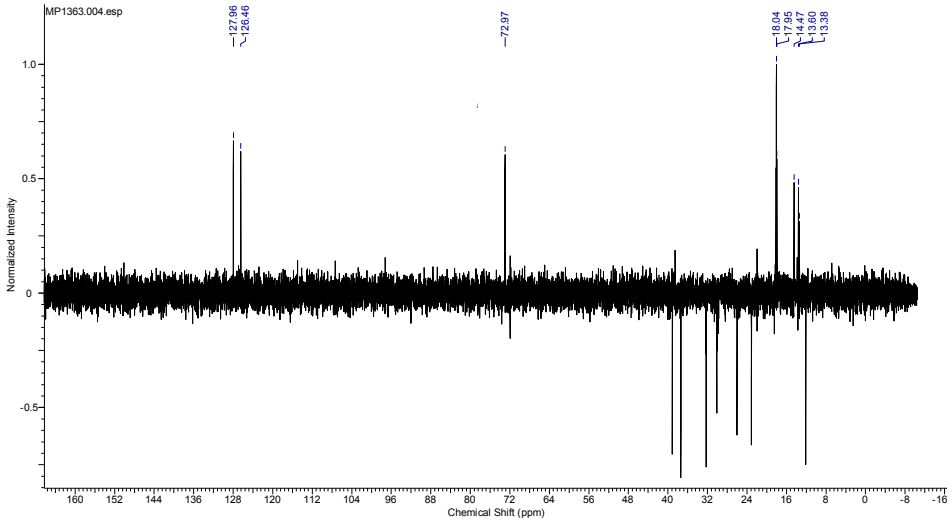

^{1}H Spectrum of **77c**

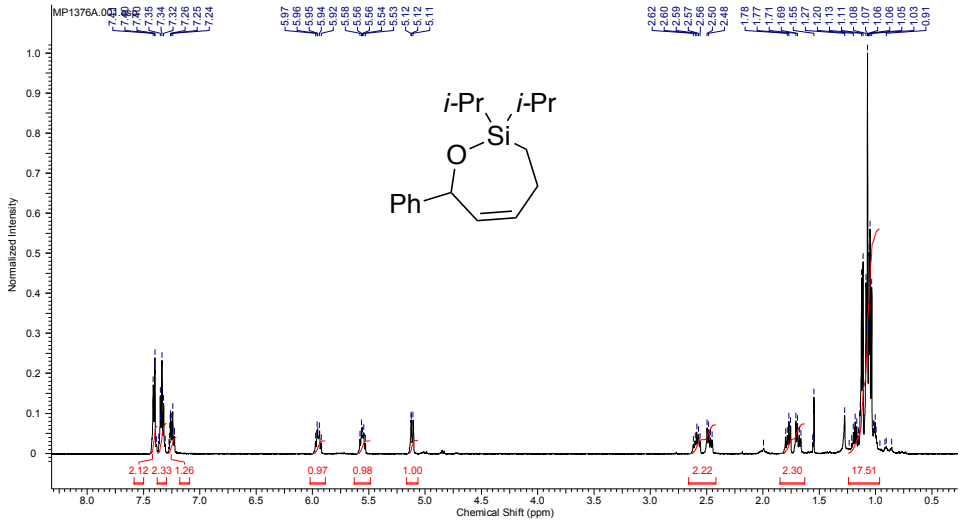

^{13}C Spectrum of **77c**

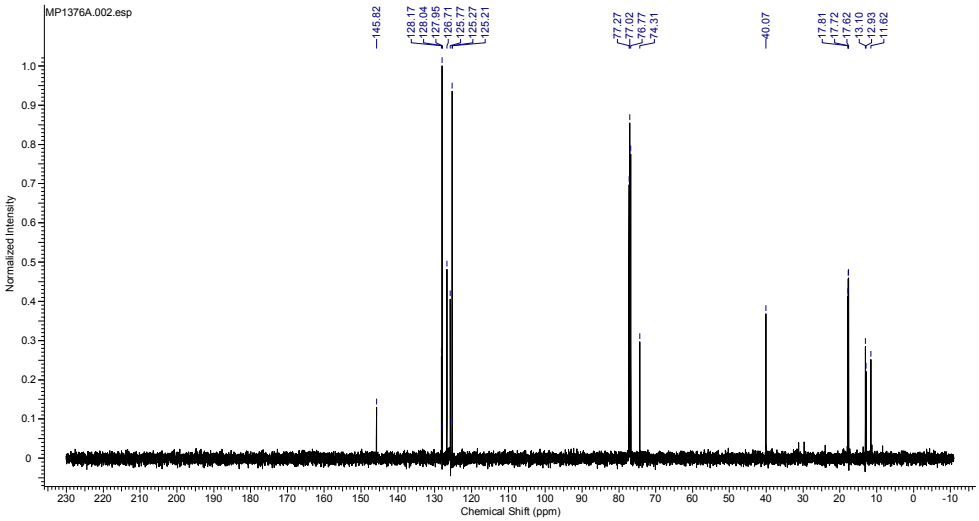

^{13}C DEPT Spectrum of **77c**

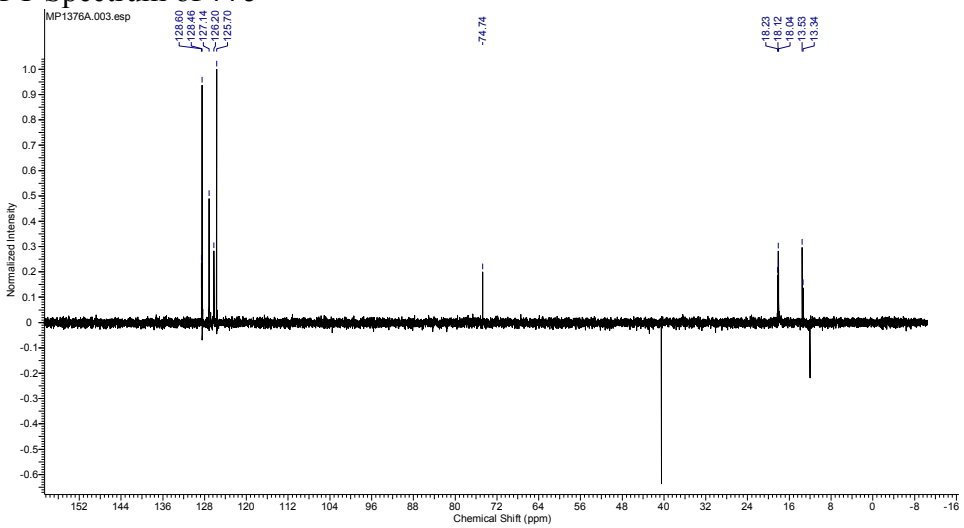

^{1}H Spectrum of **77d**

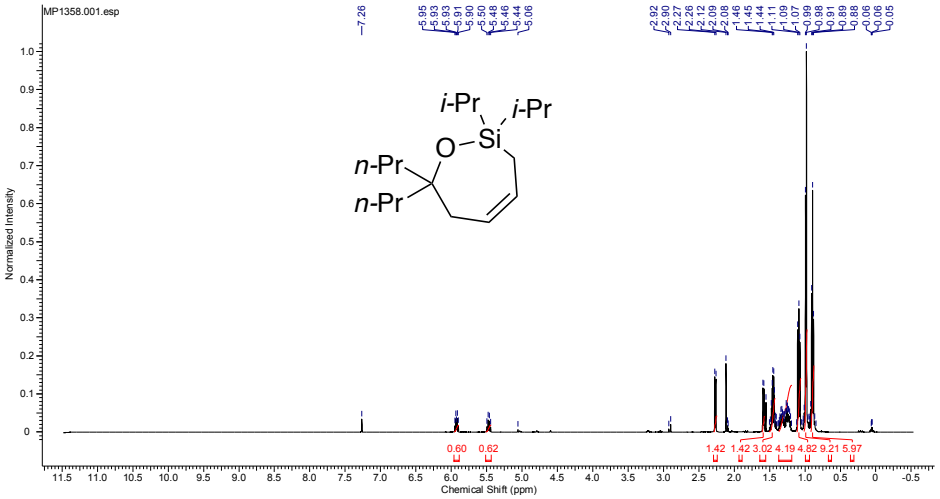

^{13}C Spectrum of **77d**

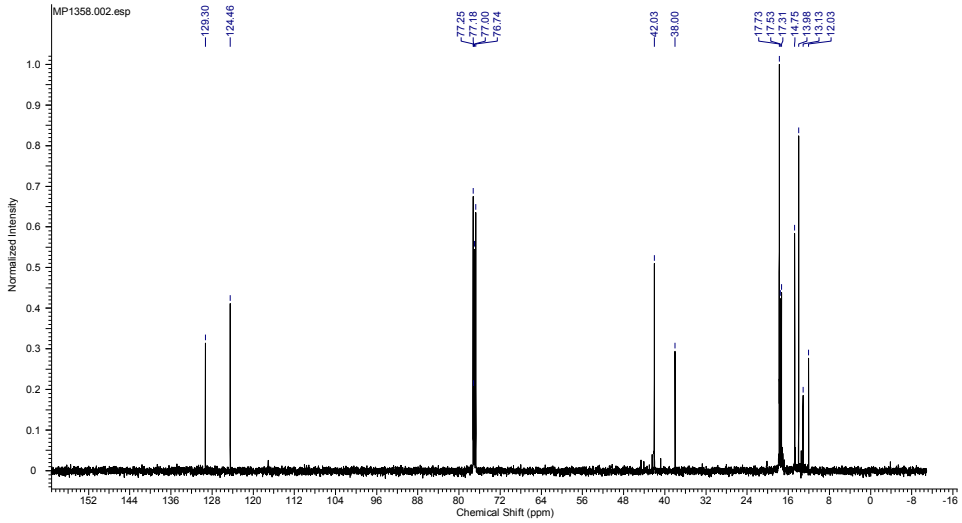

^{13}C DEPT Spectrum of **77d**

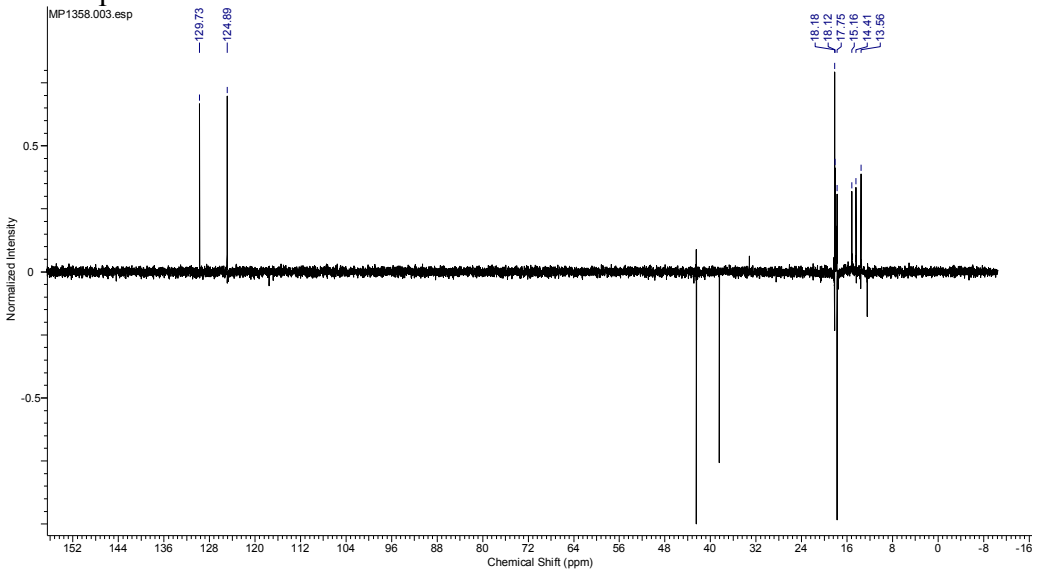

^{1}H Spectrum of **77e**

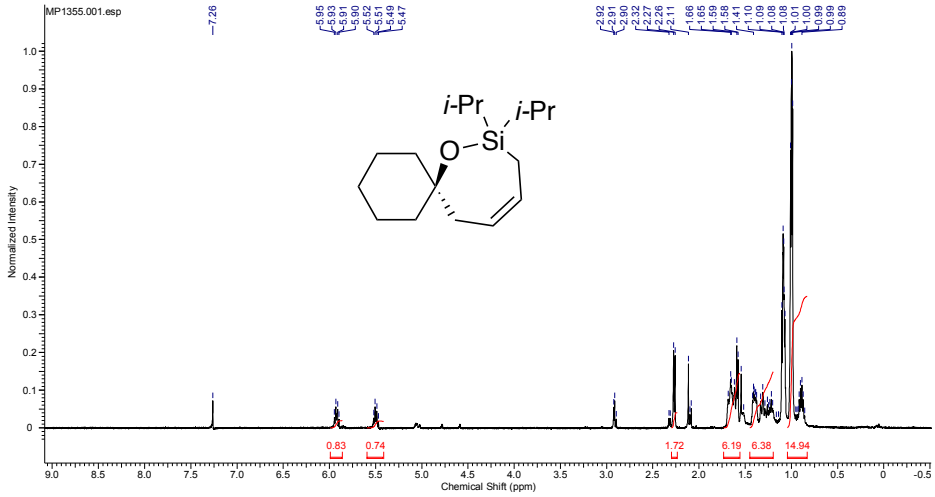

^{13}C Spectrum of **77e**

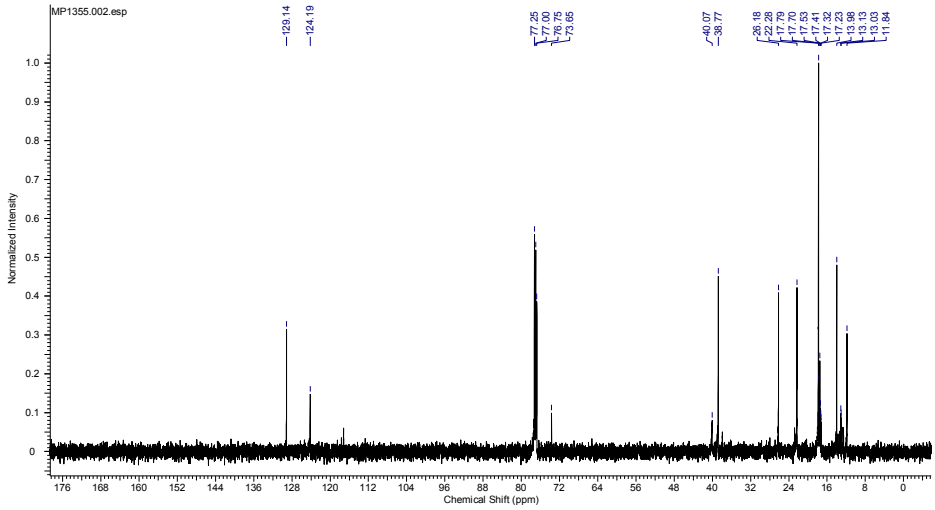

^{13}C DEPT Spectrum of **77e**

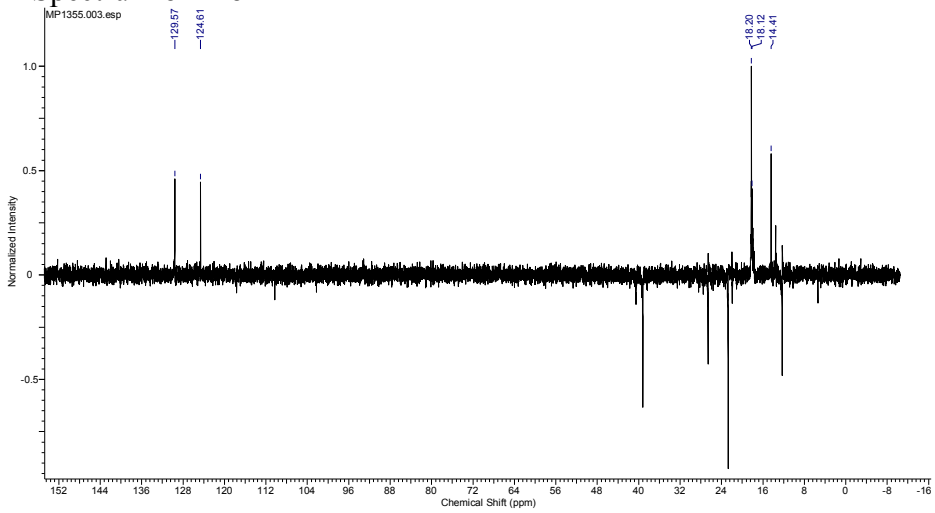

^{1}H Spectrum of **77f**

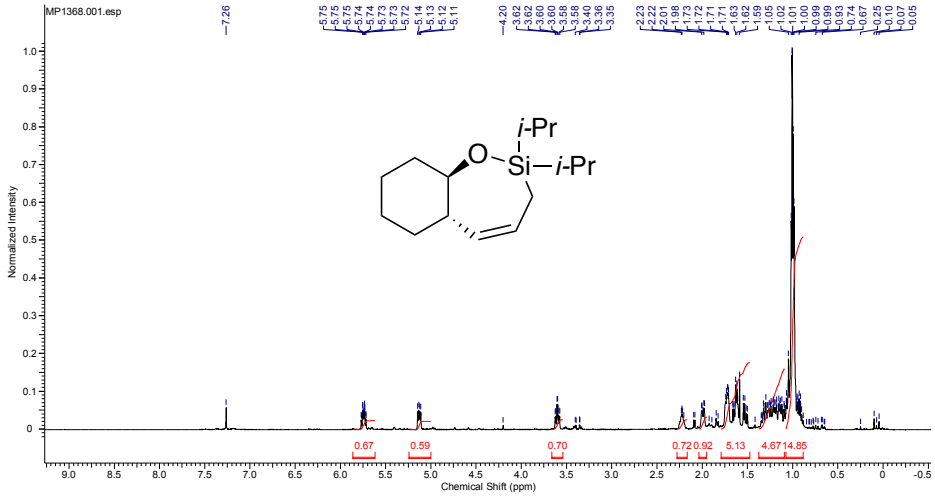

^{13}C Spectrum of **77f**

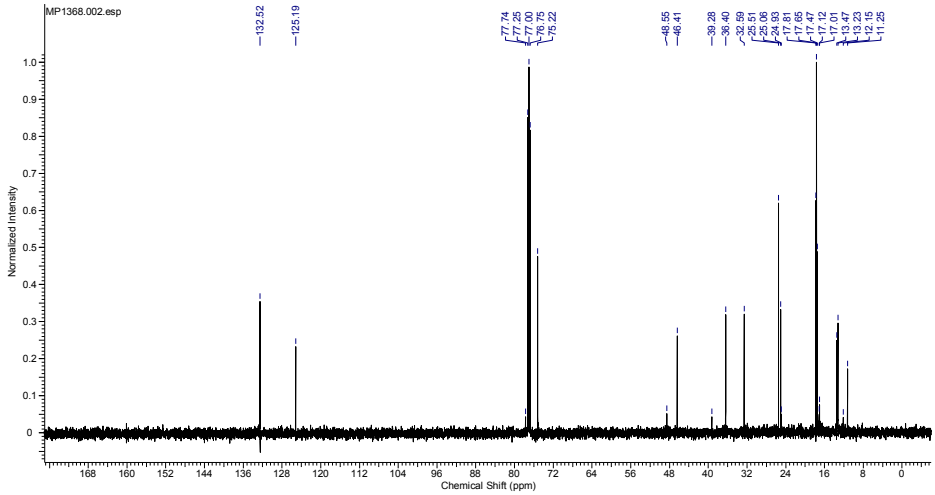

^{13}C DEPT Spectrum of **77f**

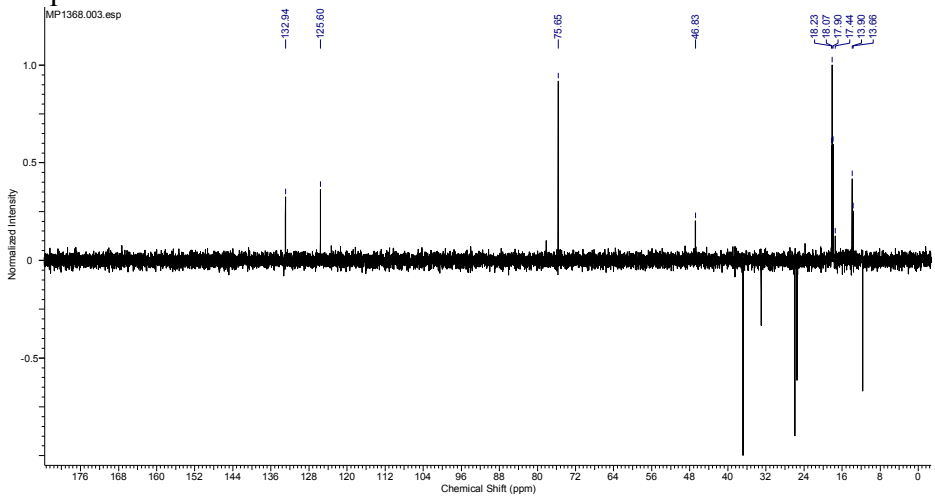

^{1}H Spectrum of **77g**

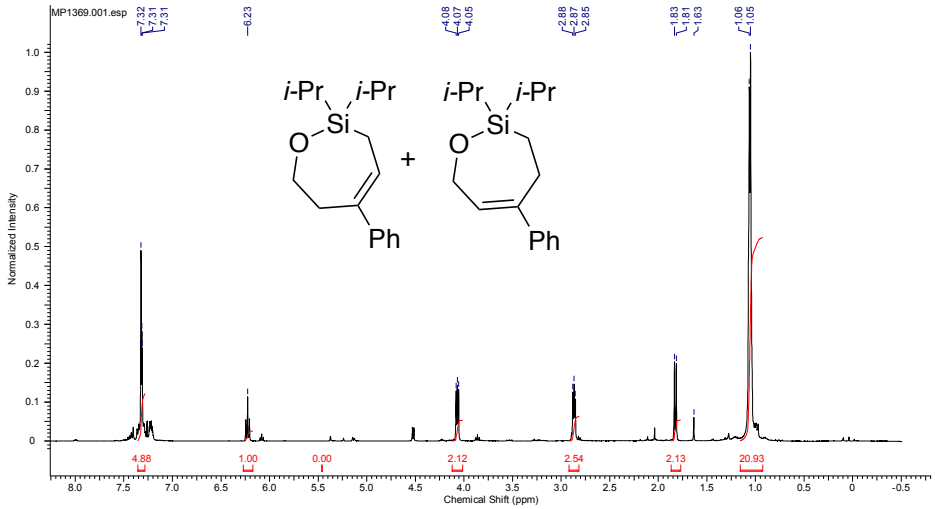

^{13}C Spectrum of **77g**

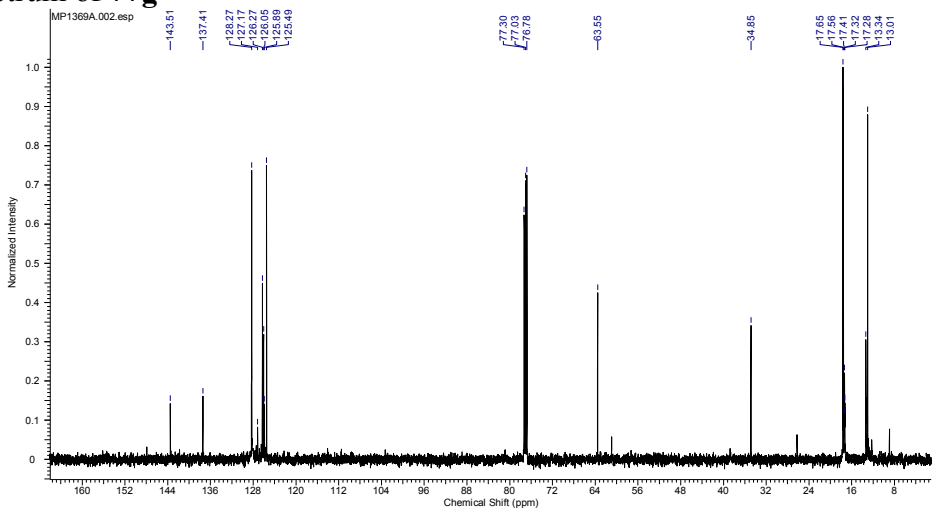

^{13}C DEPT Spectrum of **77g**

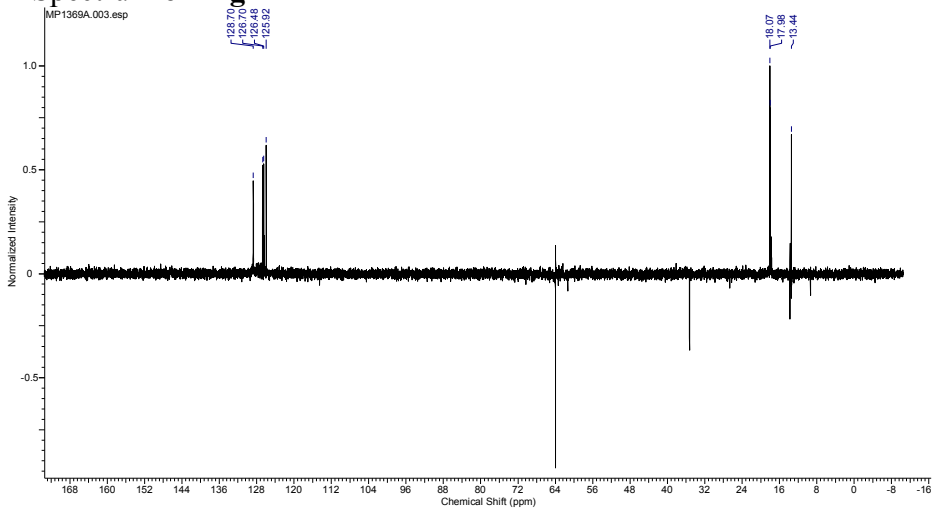

^{1}H Spectrum of **77h** and **77h'**

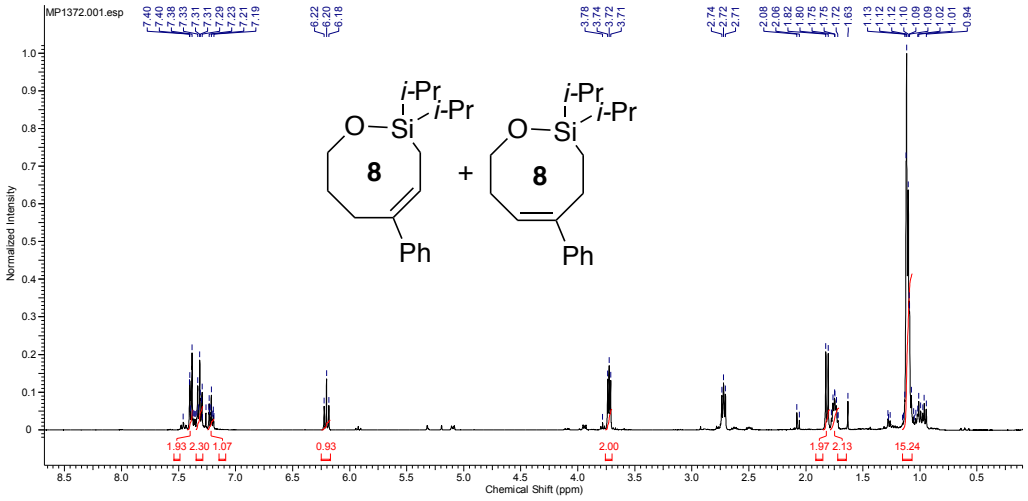

^{13}C Spectrum of **77h** and **77h'**

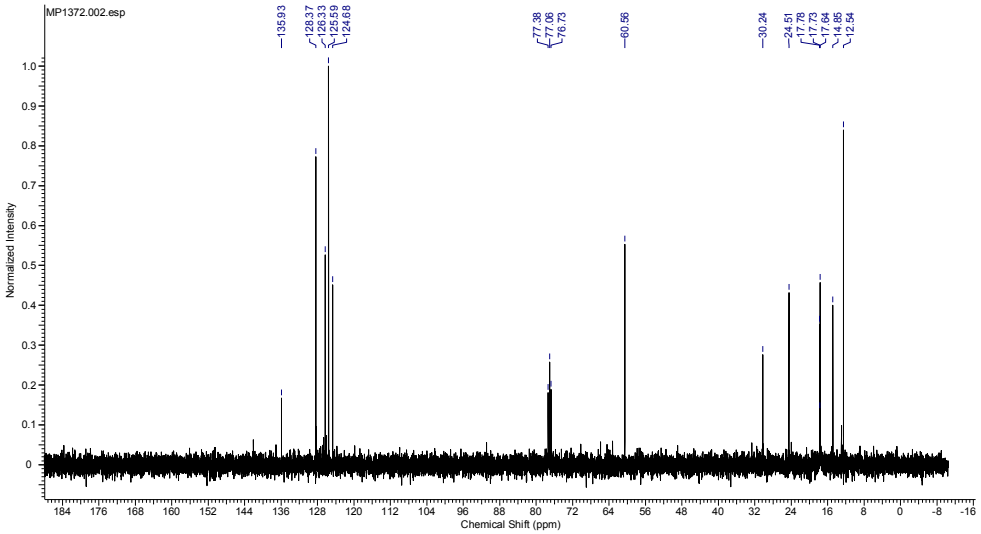

^{13}C DEPT Spectrum of **77h** and **77h'**

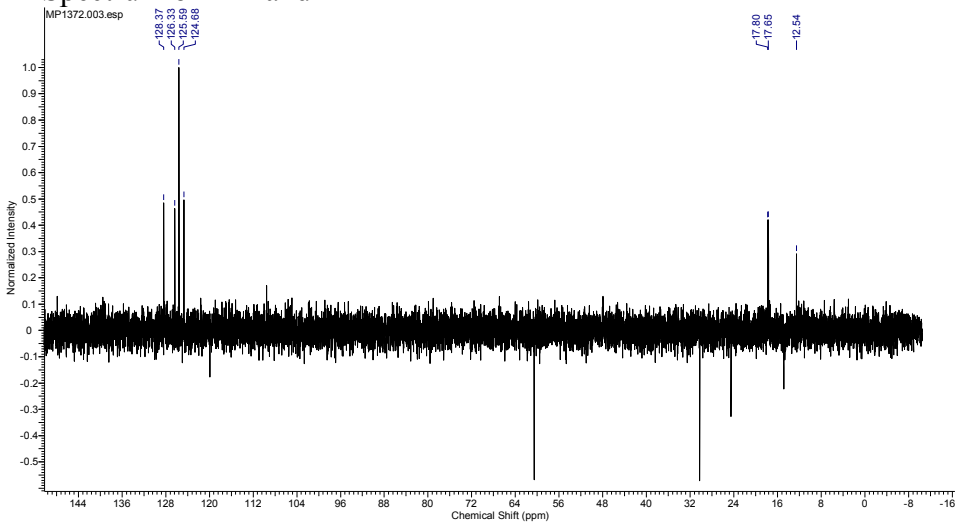

^{1}H Spectrum of **77i** and **77i'**

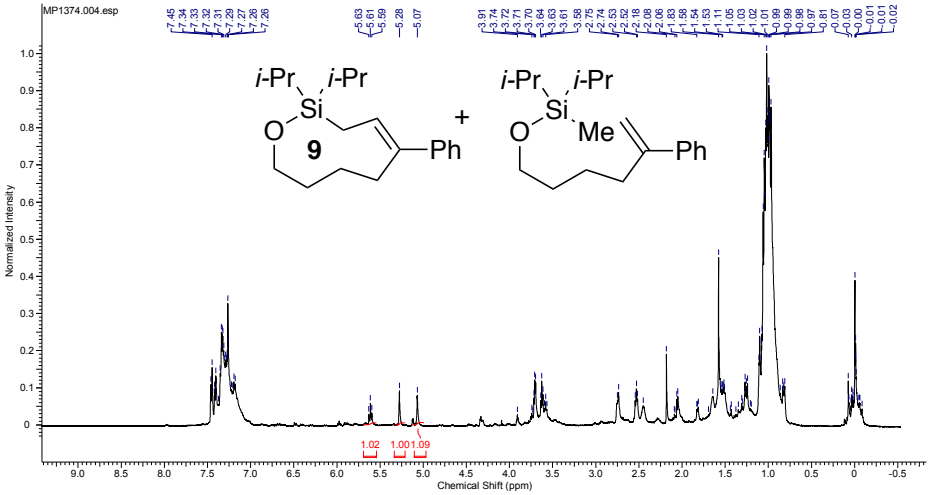

^{13}C Spectrum of **77i** and **77i'**

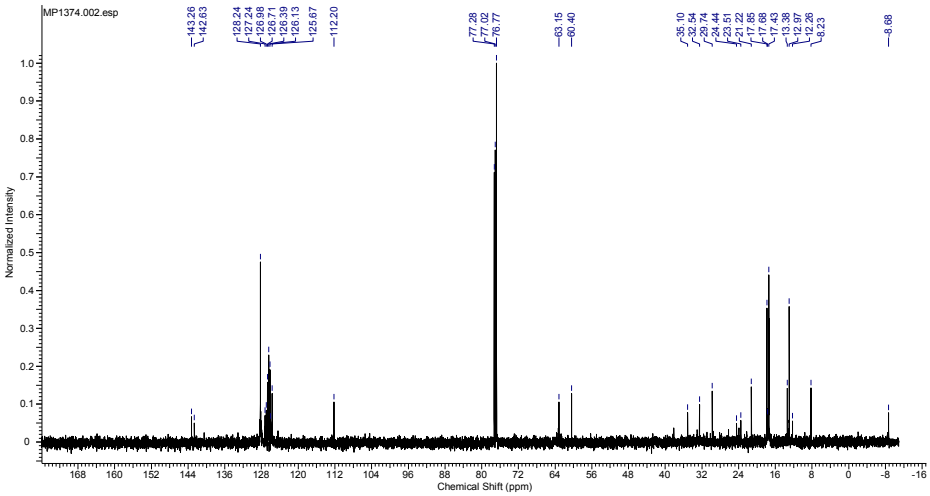

^{13}C Spectrum of **77i** and **77i'**

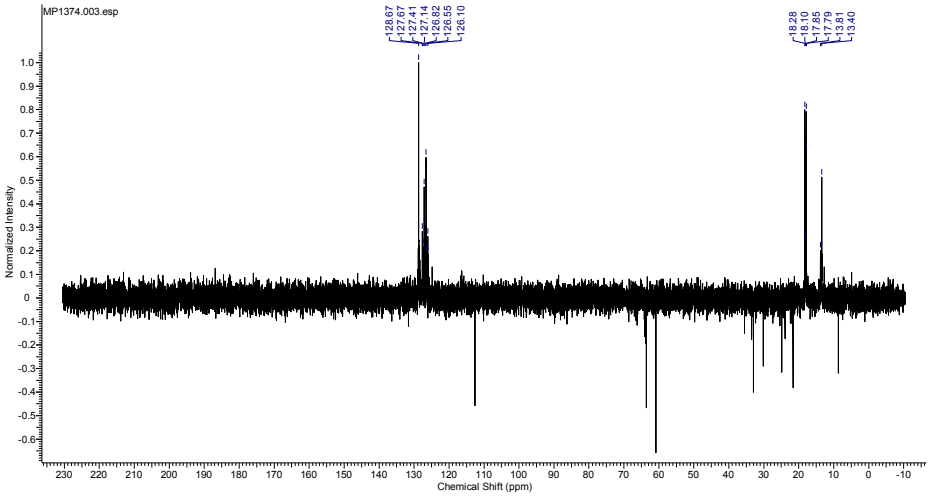

^{1}H Spectrum of **77j**

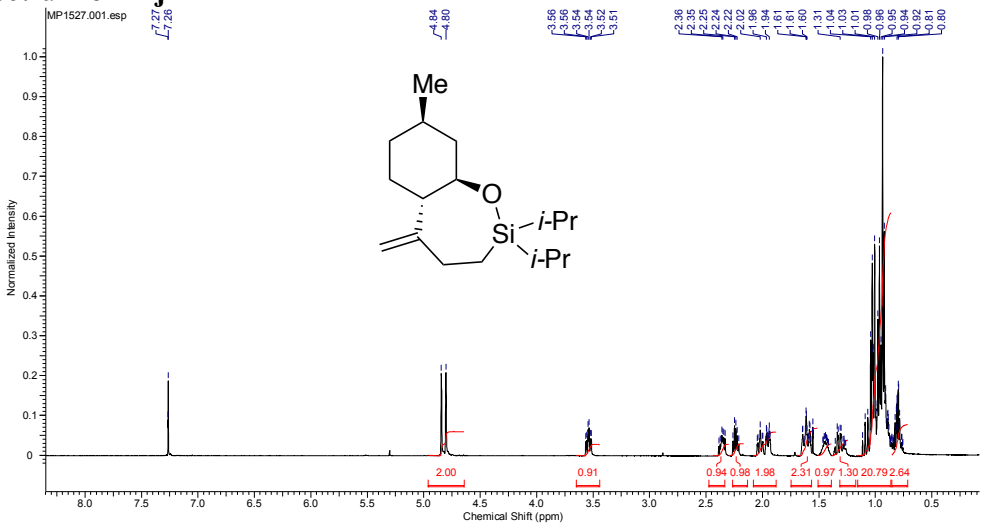

^{13}C Spectrum of **77j**

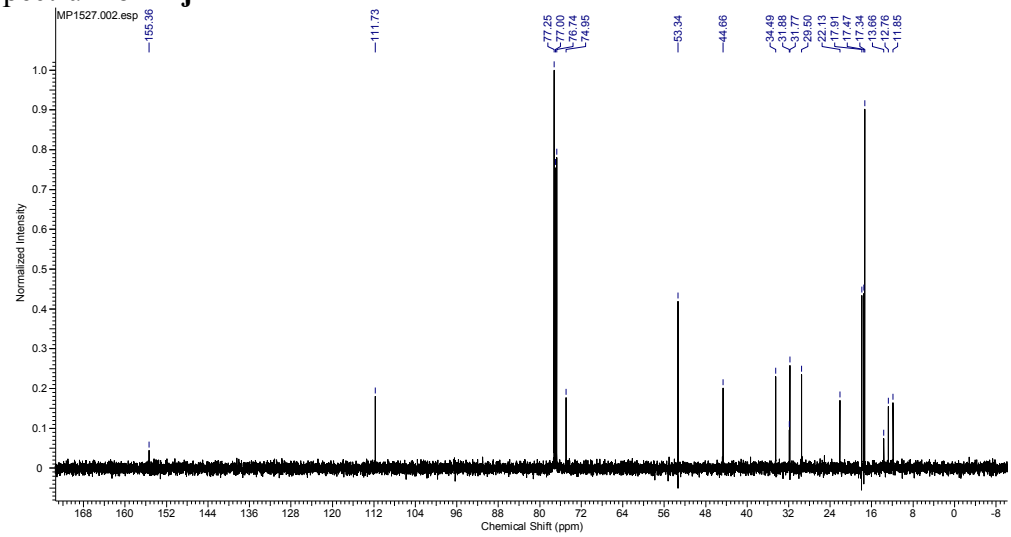

^{13}C DEPT Spectrum of **77j**

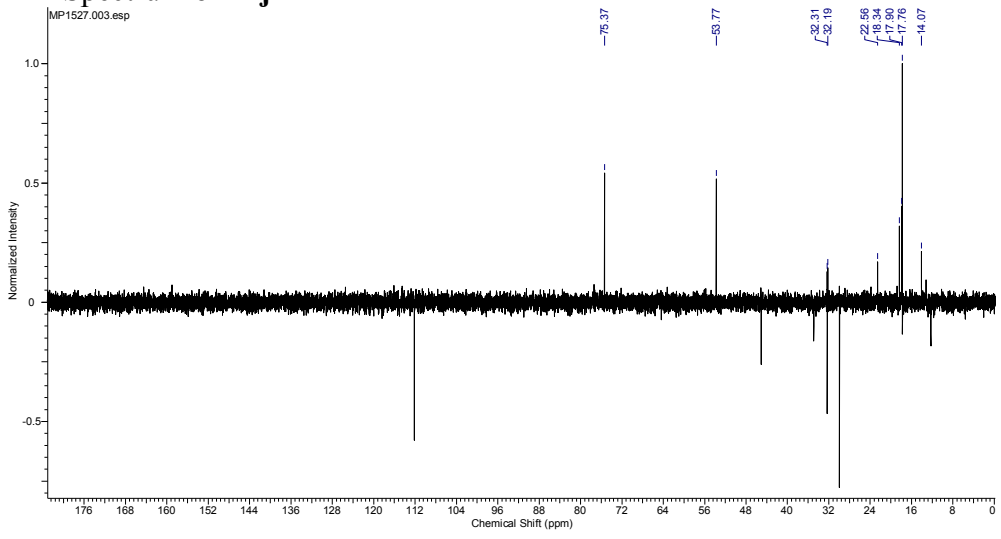

^{1}H Spectrum of **96**

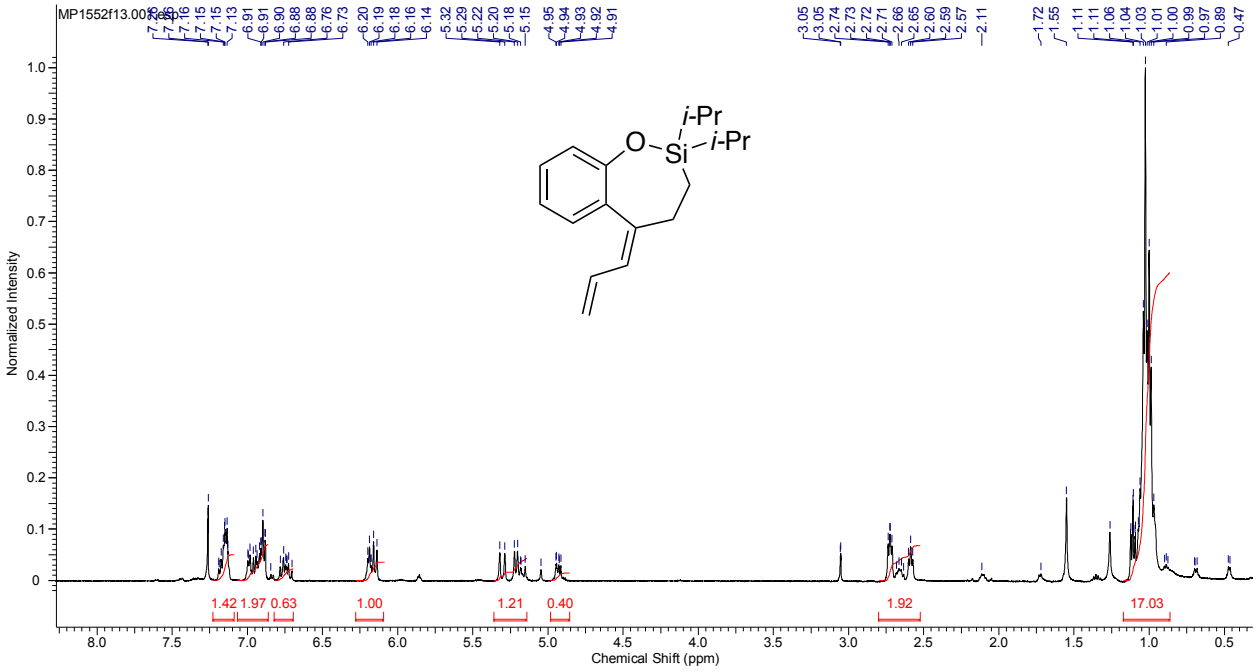

^{1}H Spectrum of **97**

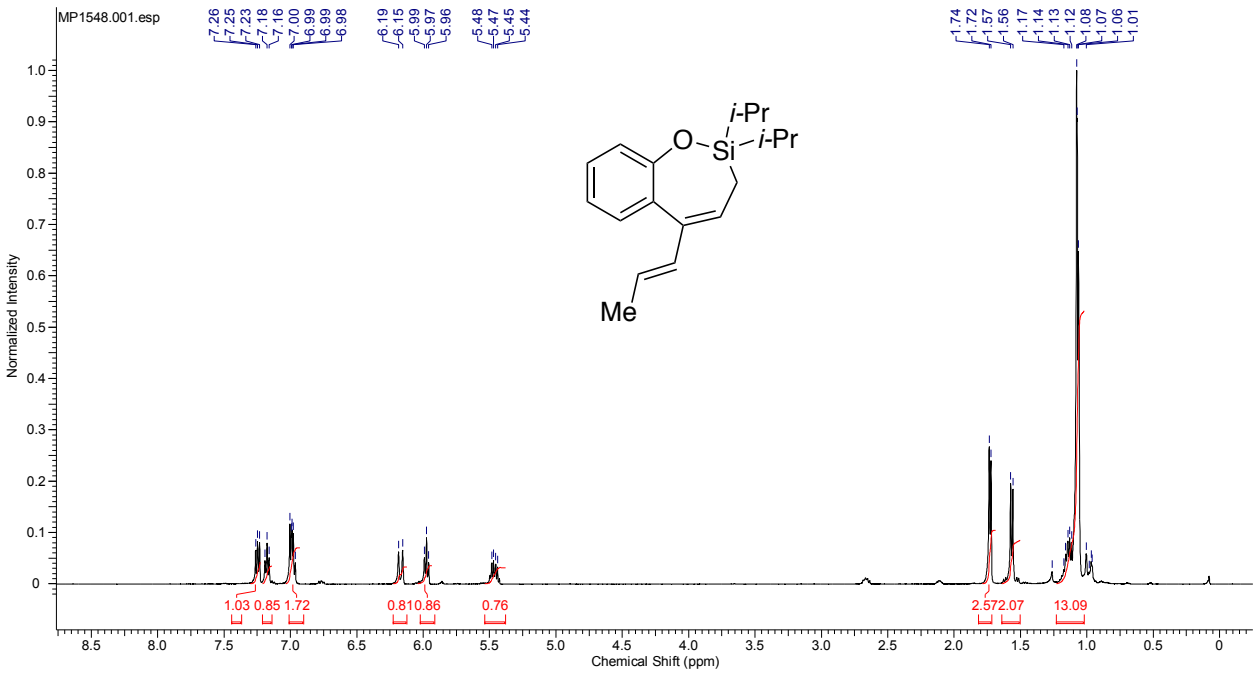

^{13}C Spectrum of **97**

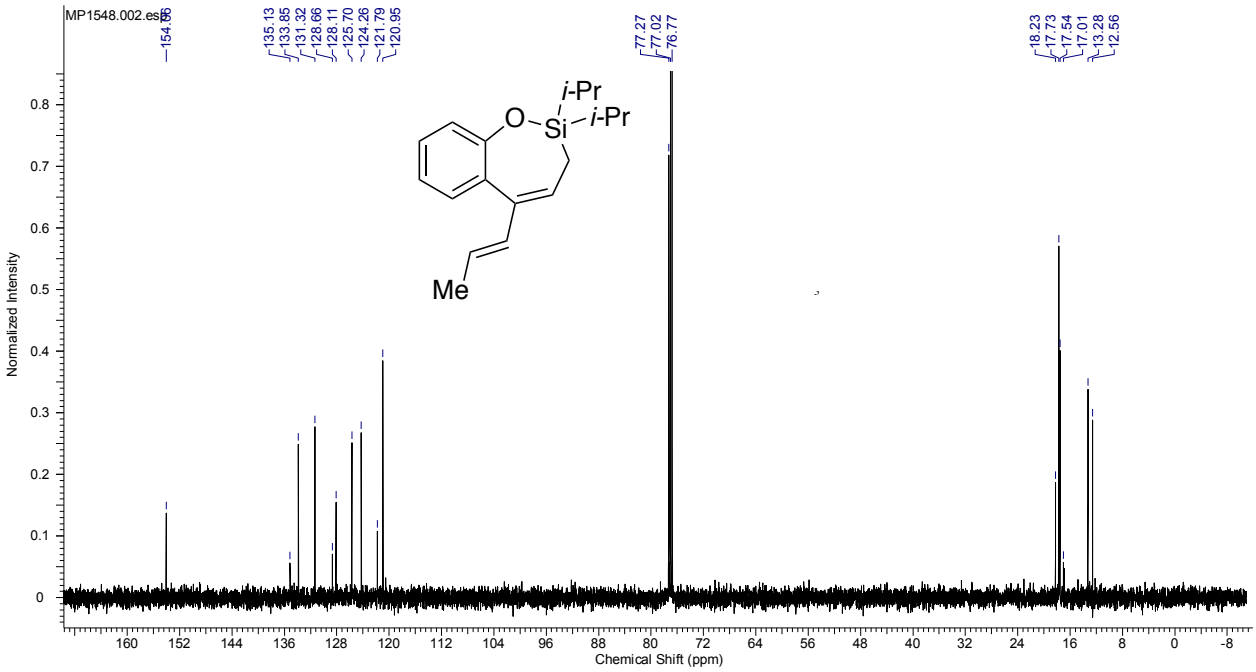

^{13}C DEPT Spectrum of **97**

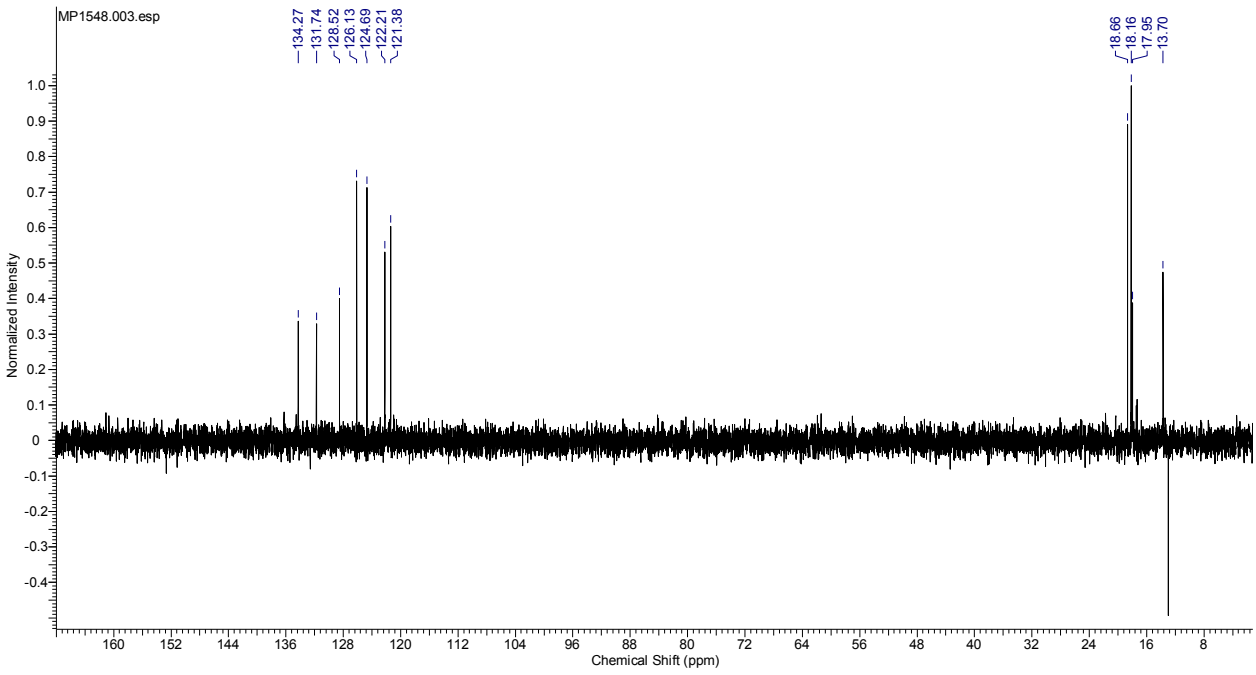

^{1}H Spectrum of **106**

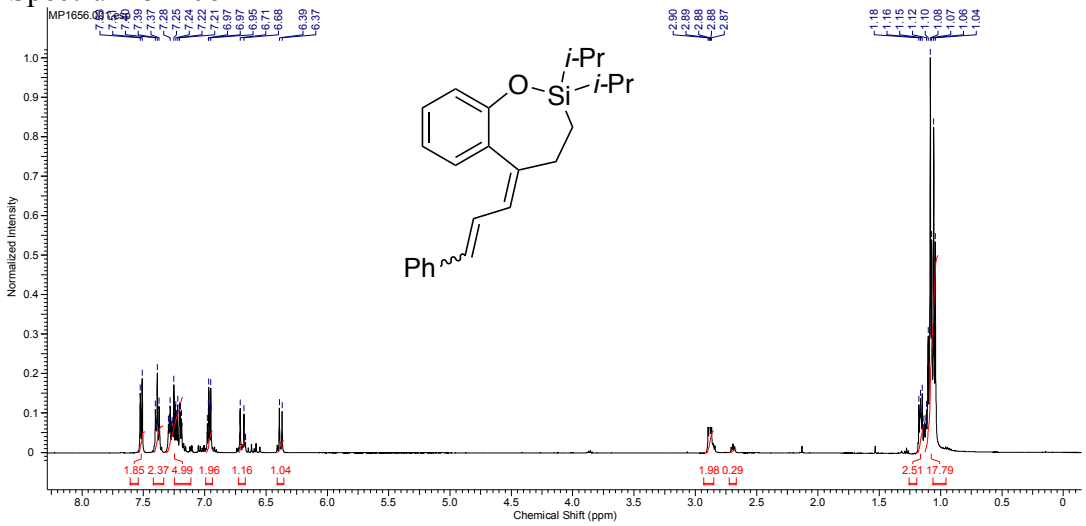

^{13}C Spectrum of **106**

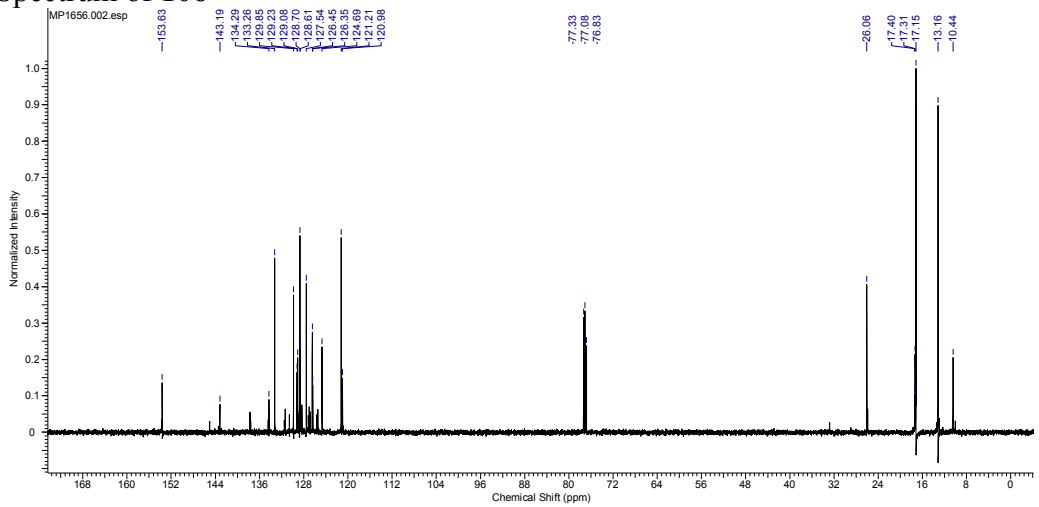

^{13}C DEPT Spectrum of **106**

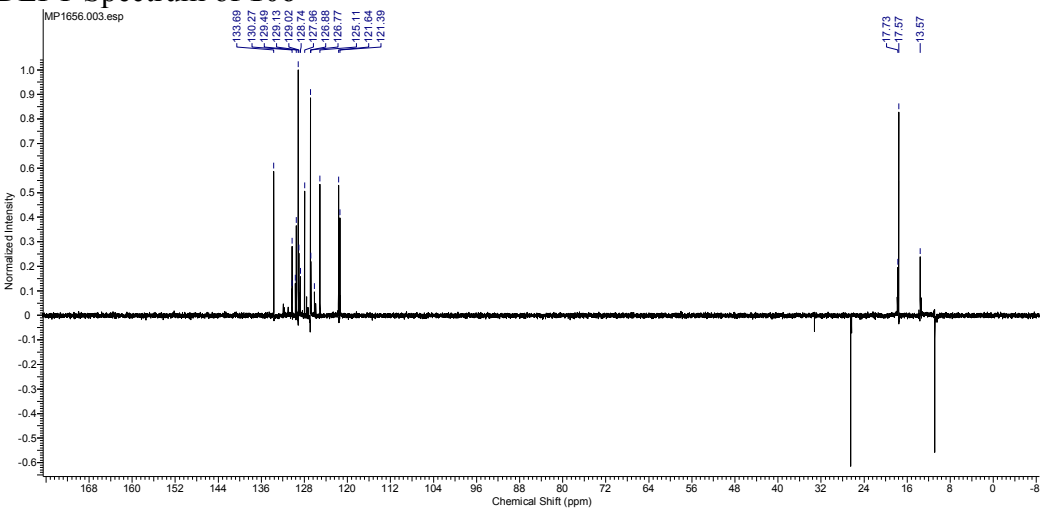

^{1}H Spectrum of **78**

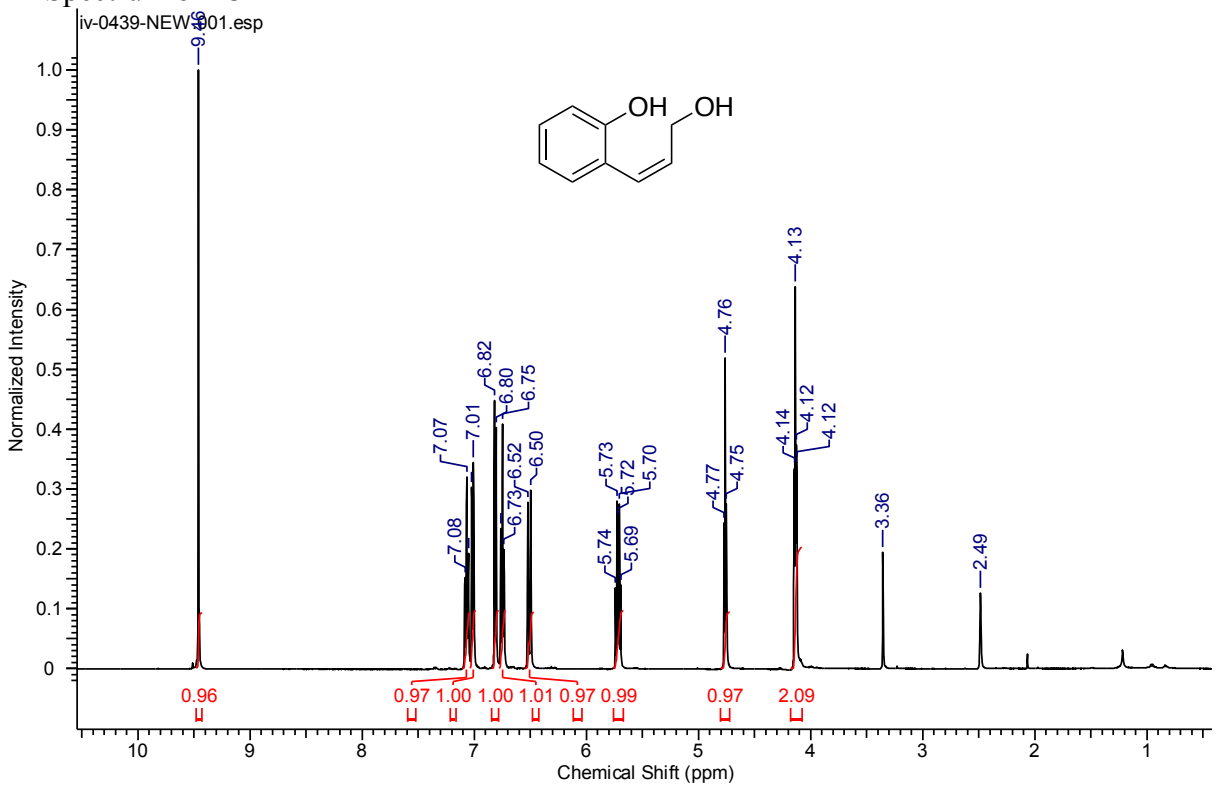

^{13}C Spectrum of **78**

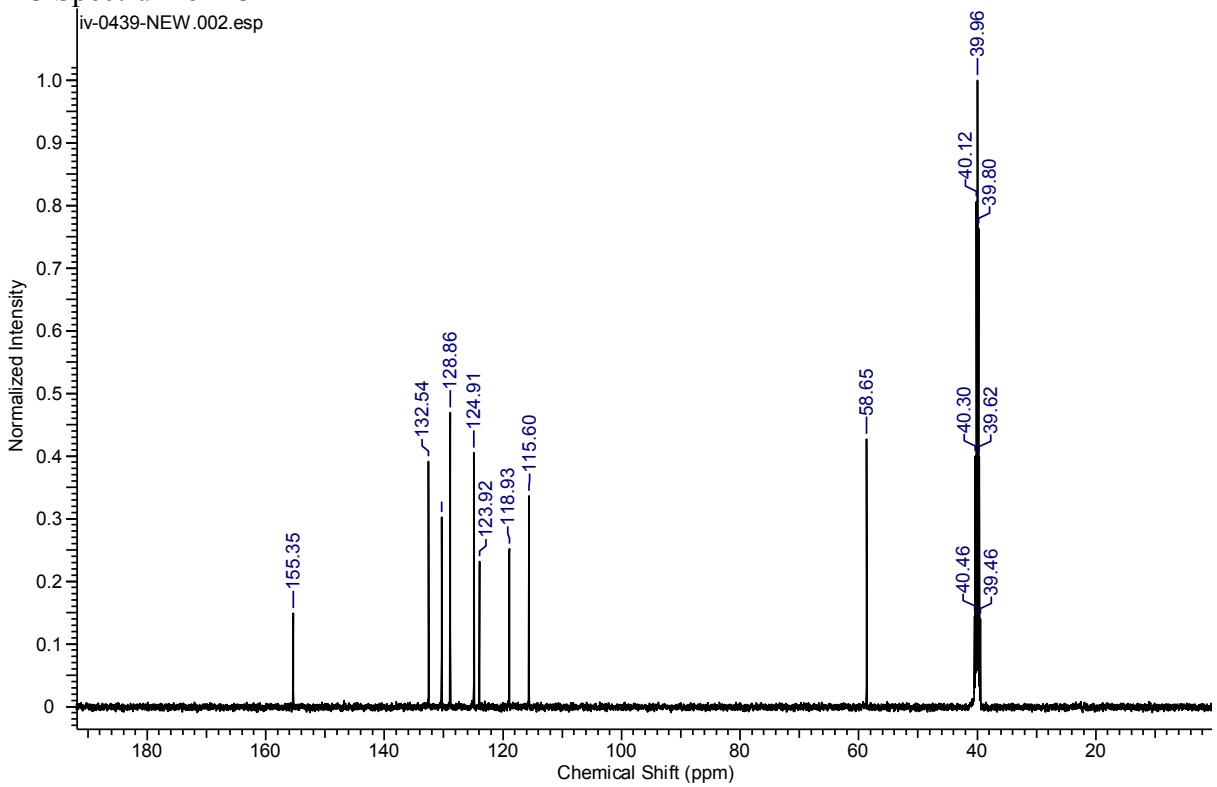

^{1}H Spectrum of **79**

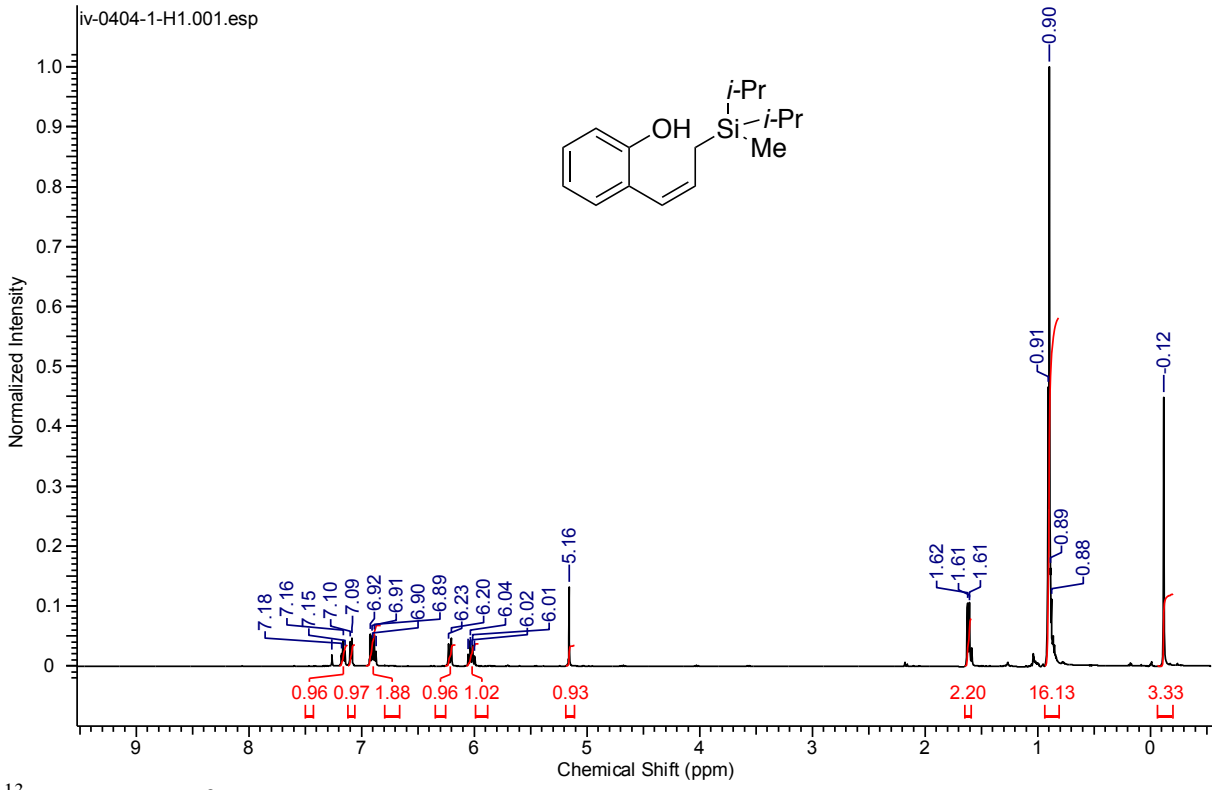

^{13}C Spectrum of **79**

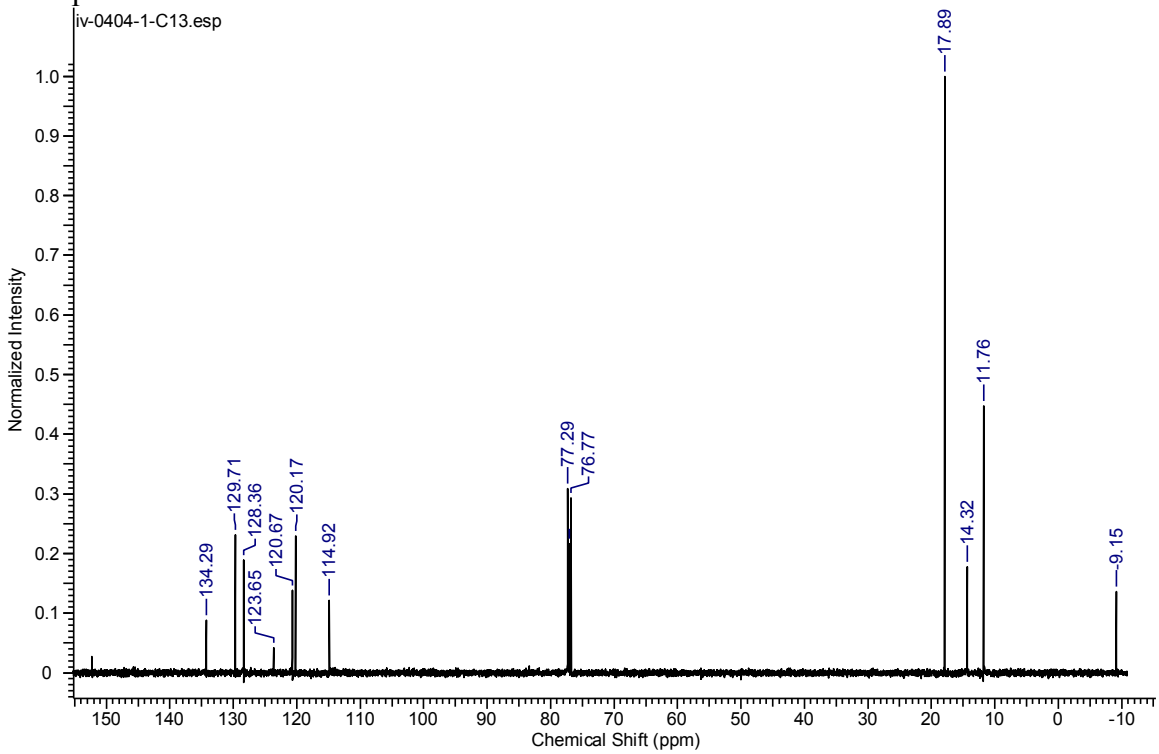

^{1}H Spectrum of **80**

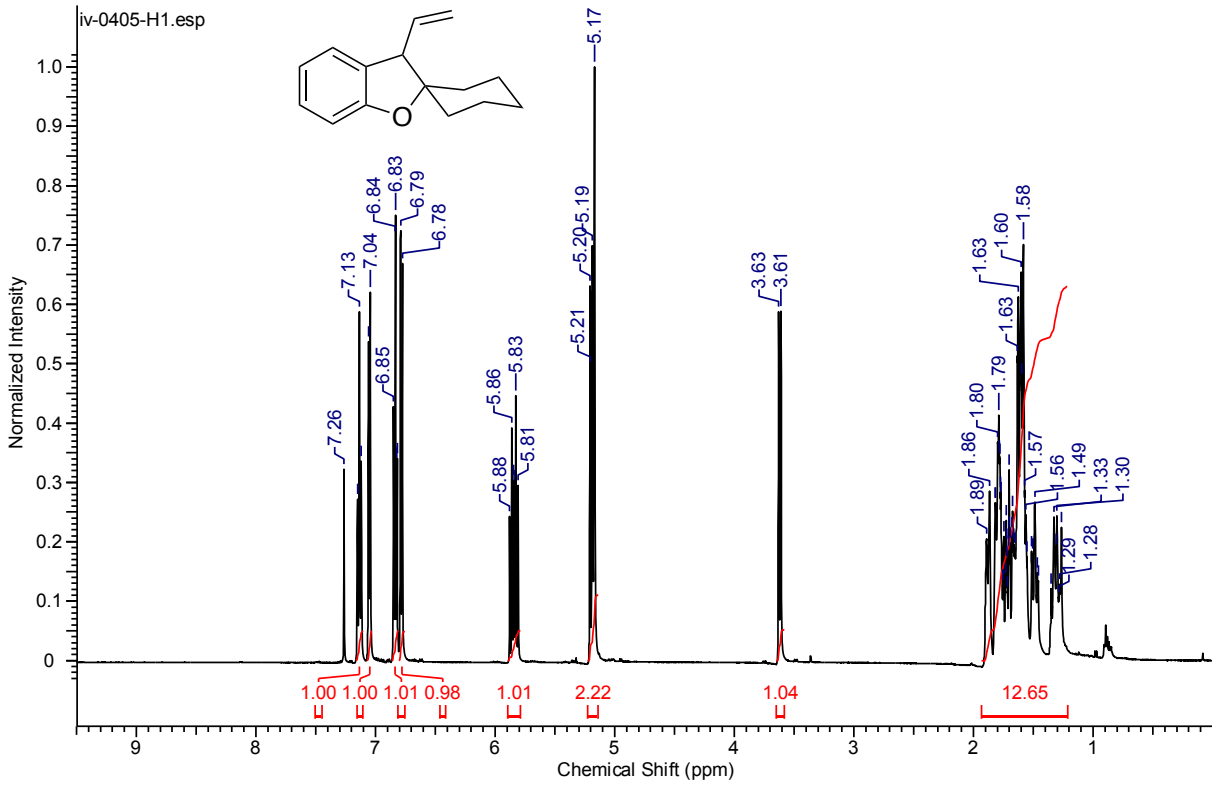

^{13}C Spectrum of **80**

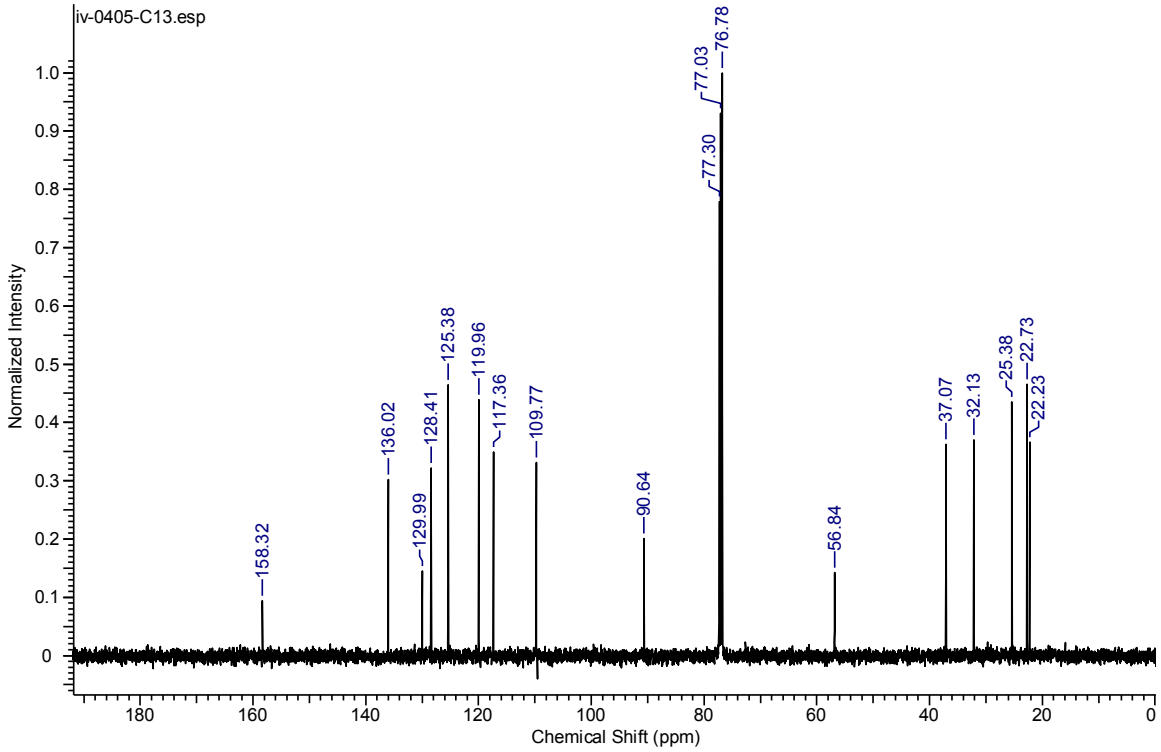

^{1}H Spectrum of **83**

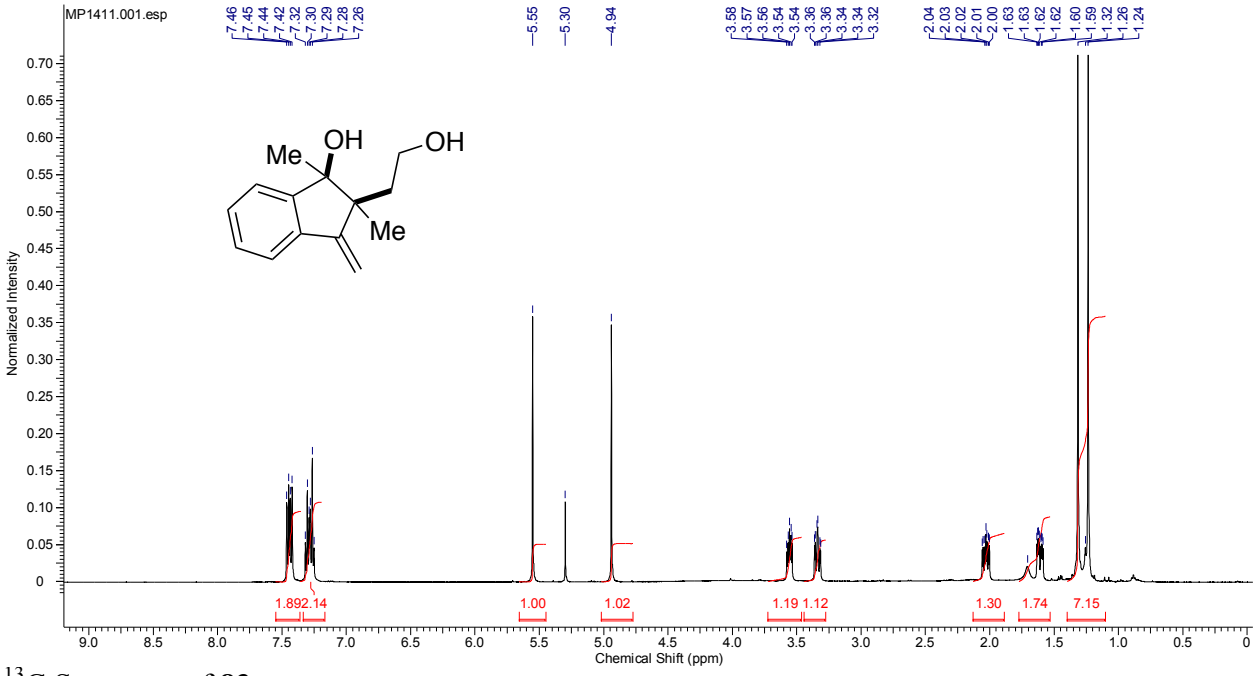

^{13}C Spectrum of **83**

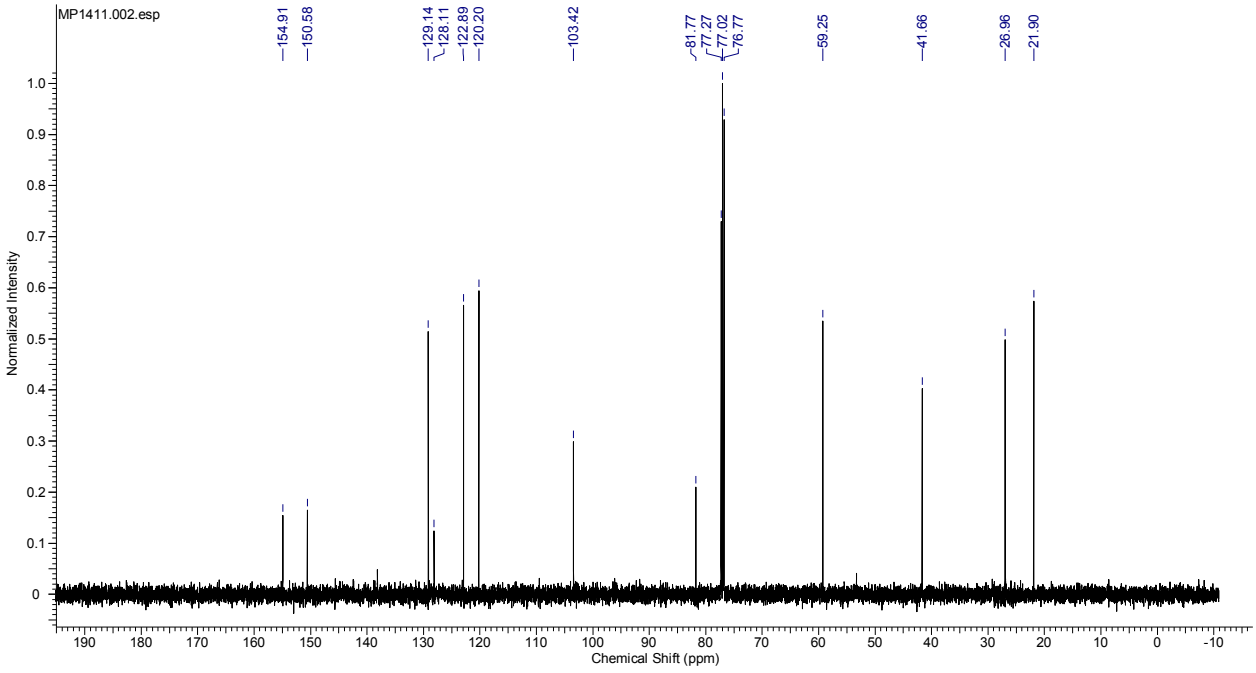

^{1}H Spectrum of **86**

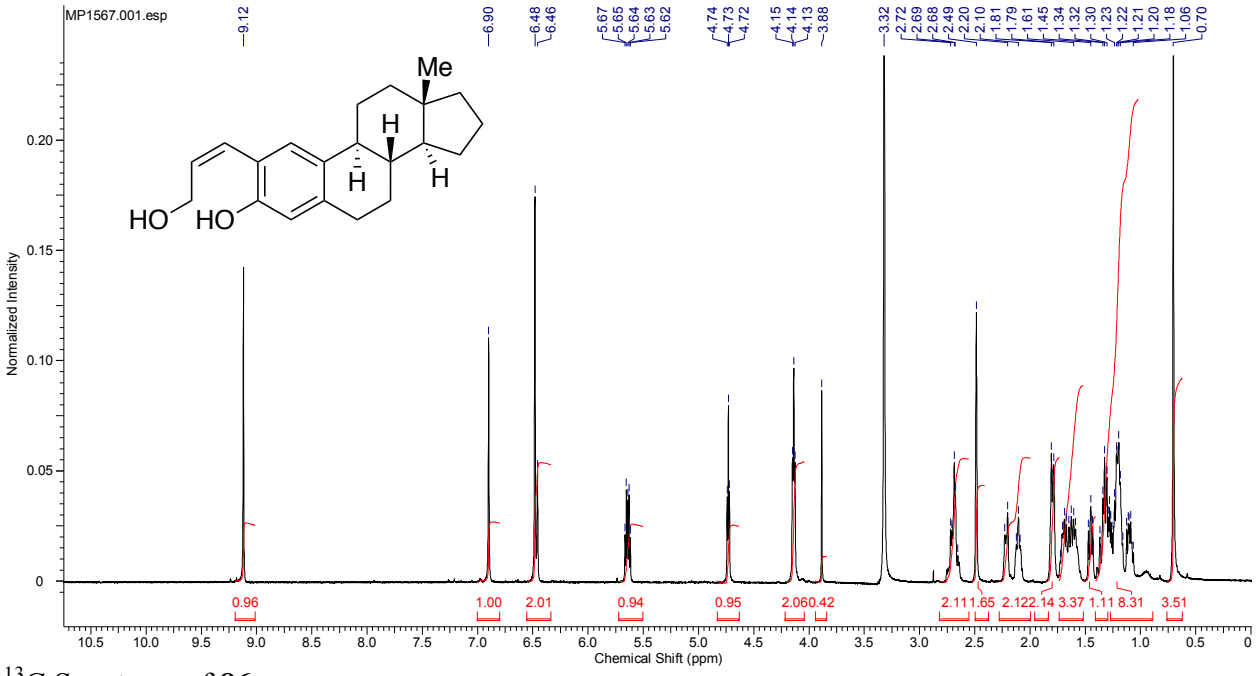

^{13}C Spectrum of **86**

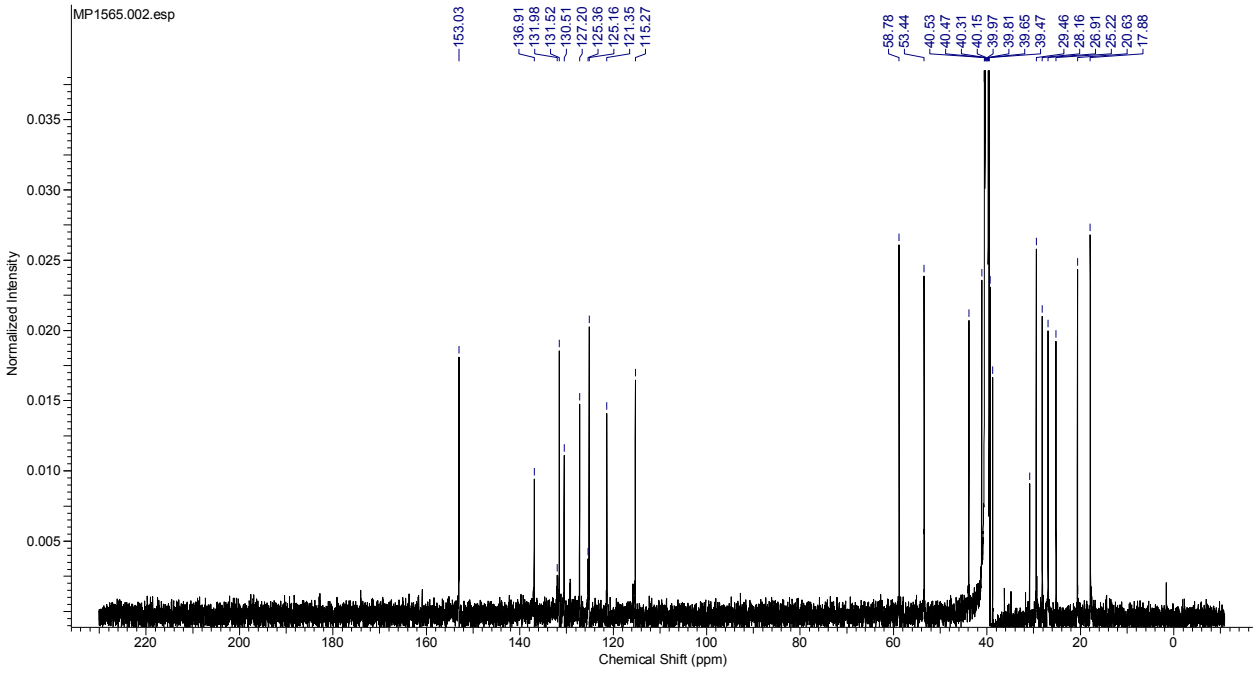

^{1}H Spectrum of **112b**

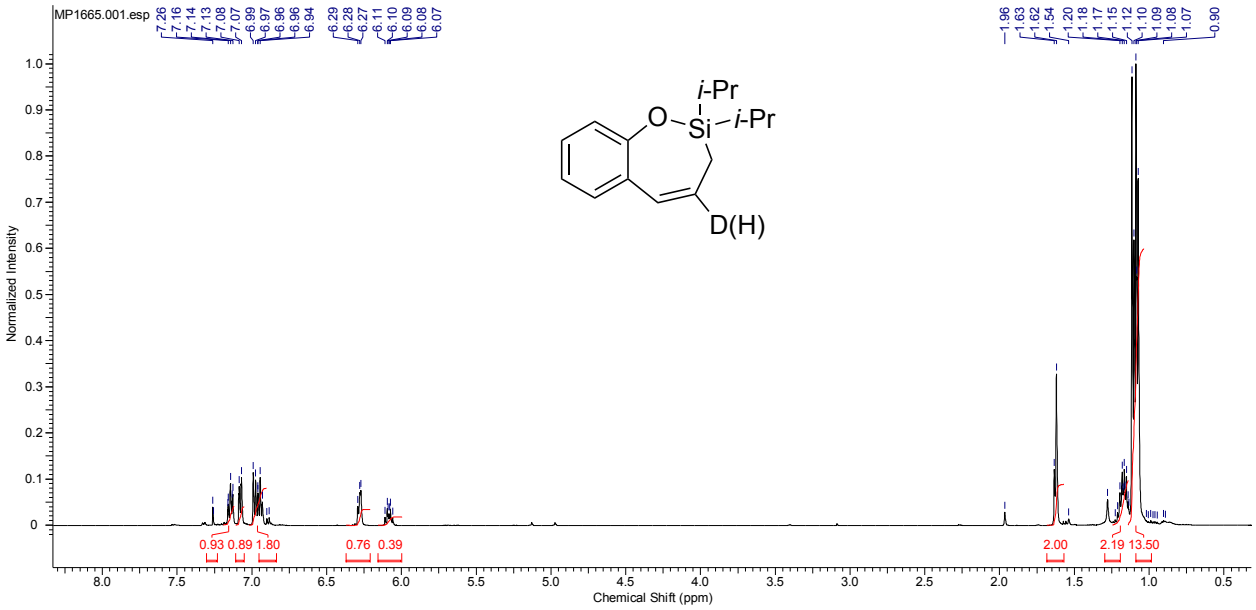

^{13}C Spectrum of **112b**

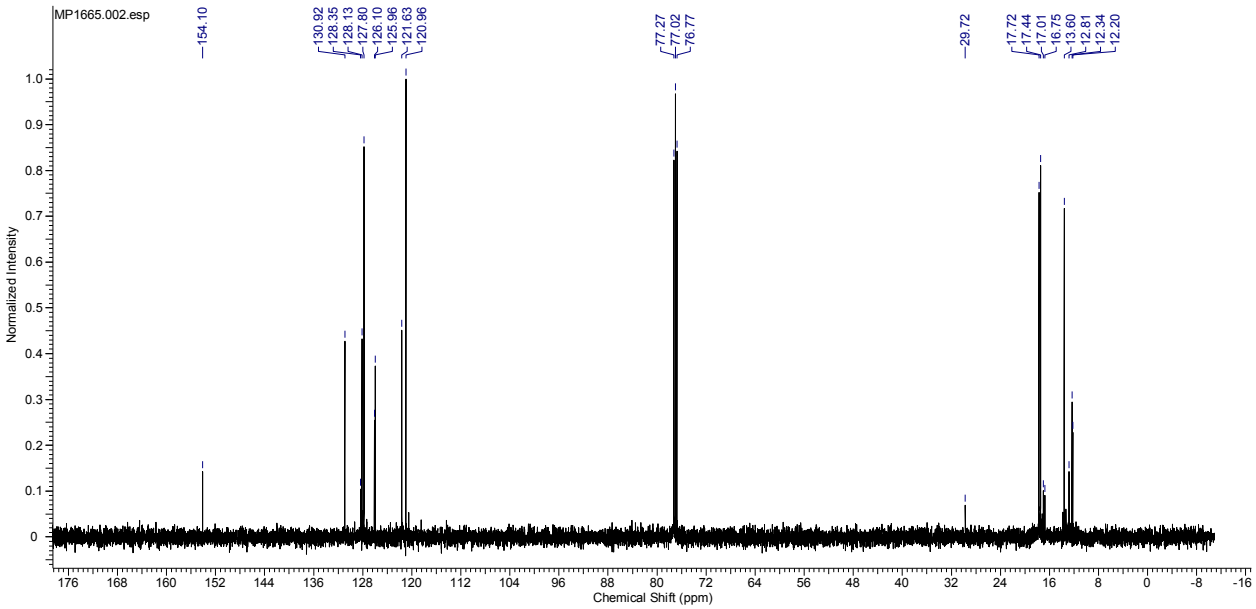

^{13}C DEPT Spectrum of **112b**

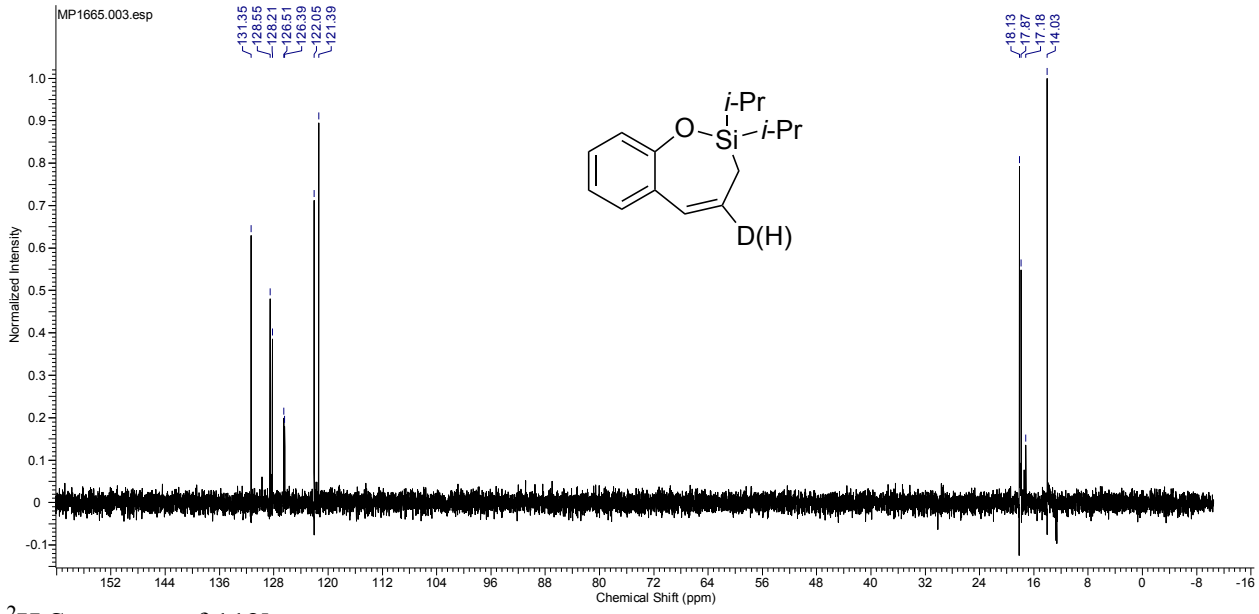

^{2}H Spectrum of **112b**

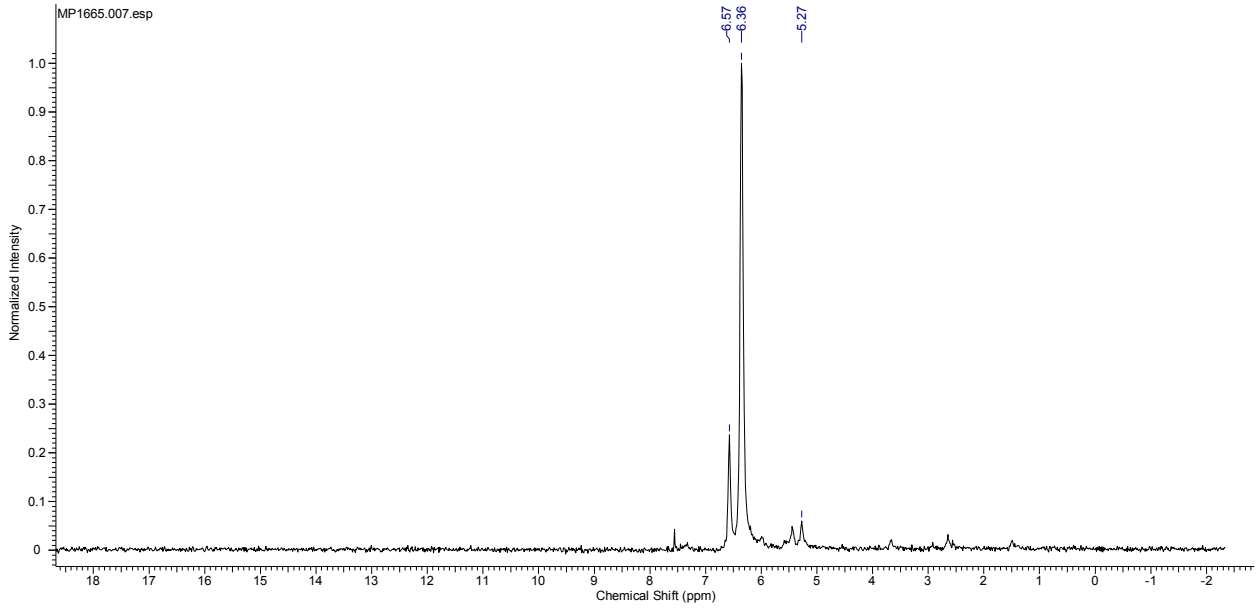

^{1}H Spectrum of **117a**

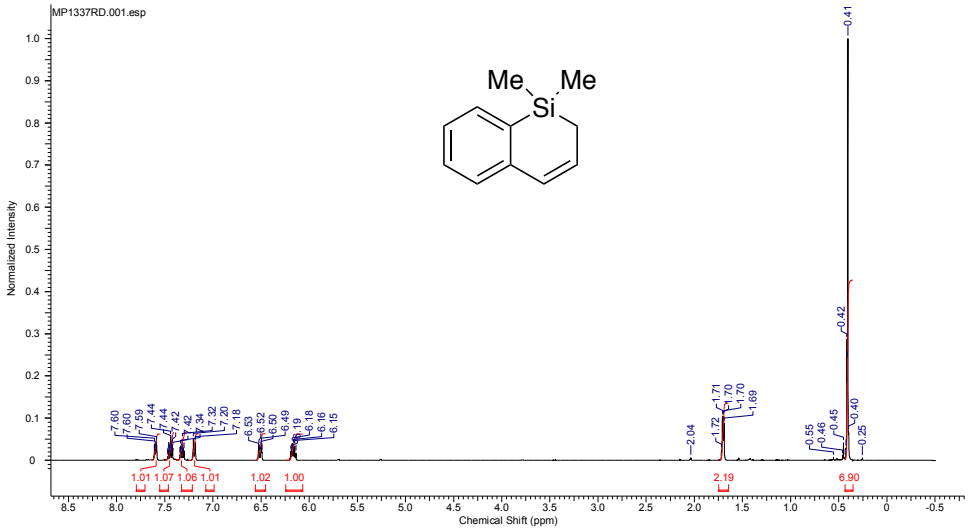

^{13}C Spectrum of **117a**

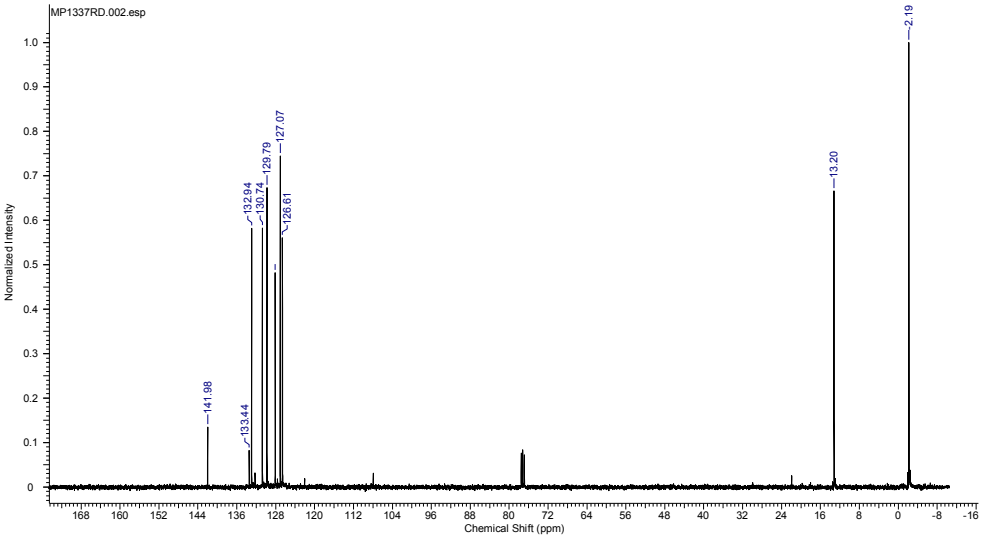

^{13}C Dept Spectrum of **117a**

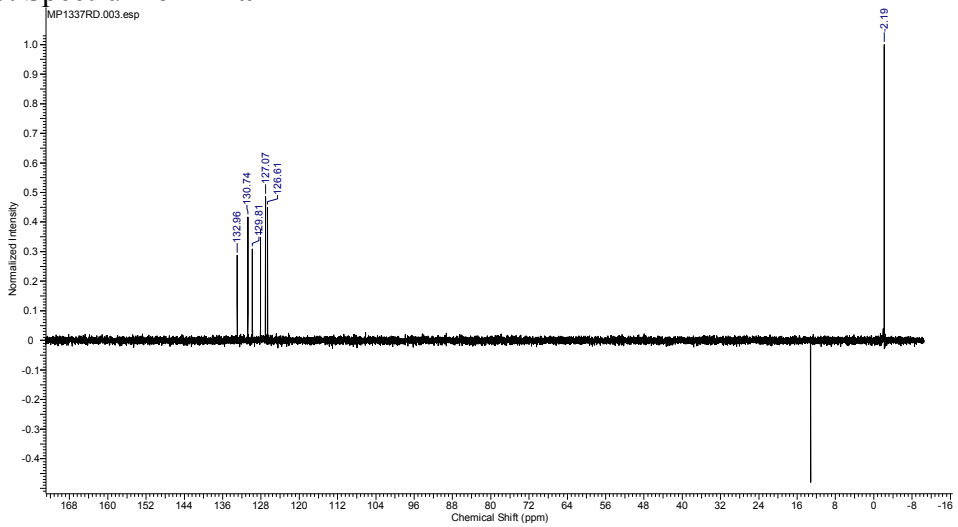

^{1}H Spectrum of **119a'**

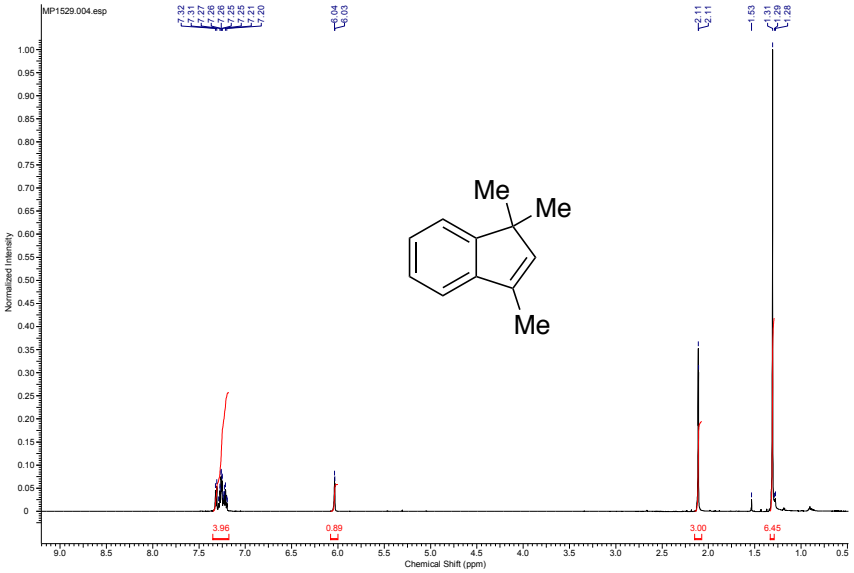

^{13}C Spectrum of **119a'**

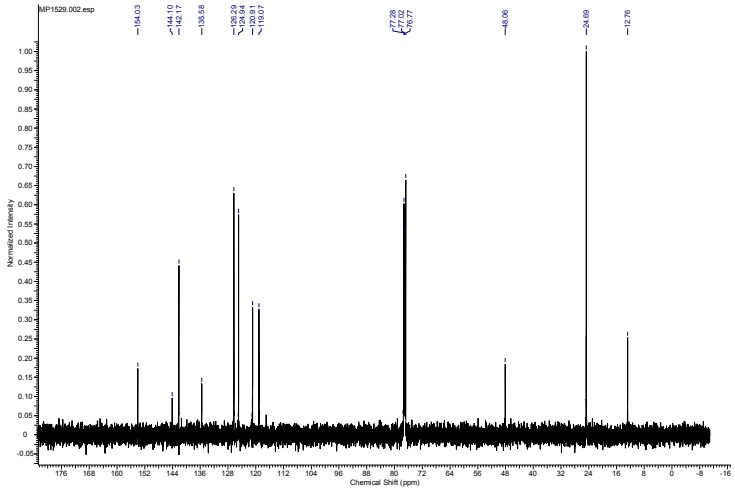

^{13}C Dept Spectrum of **119a'**

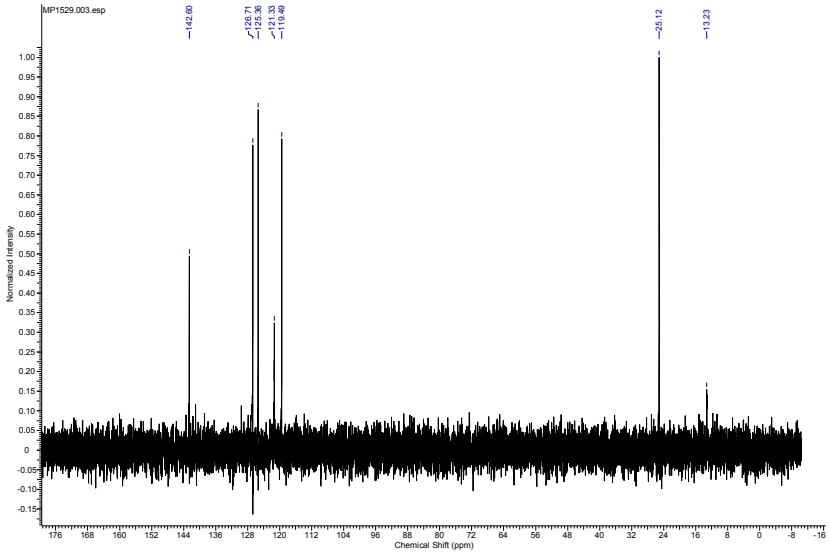

^{1}H Spectrum of **196a**

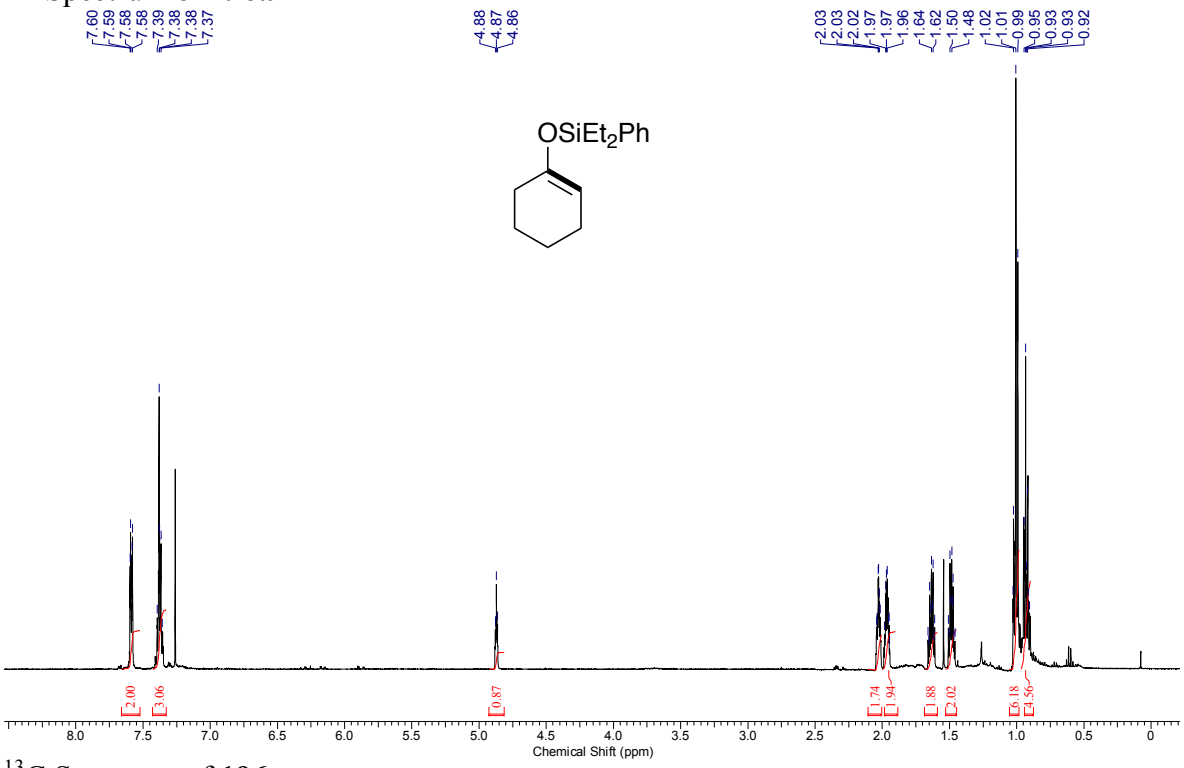

^{13}C Spectrum of **196a**

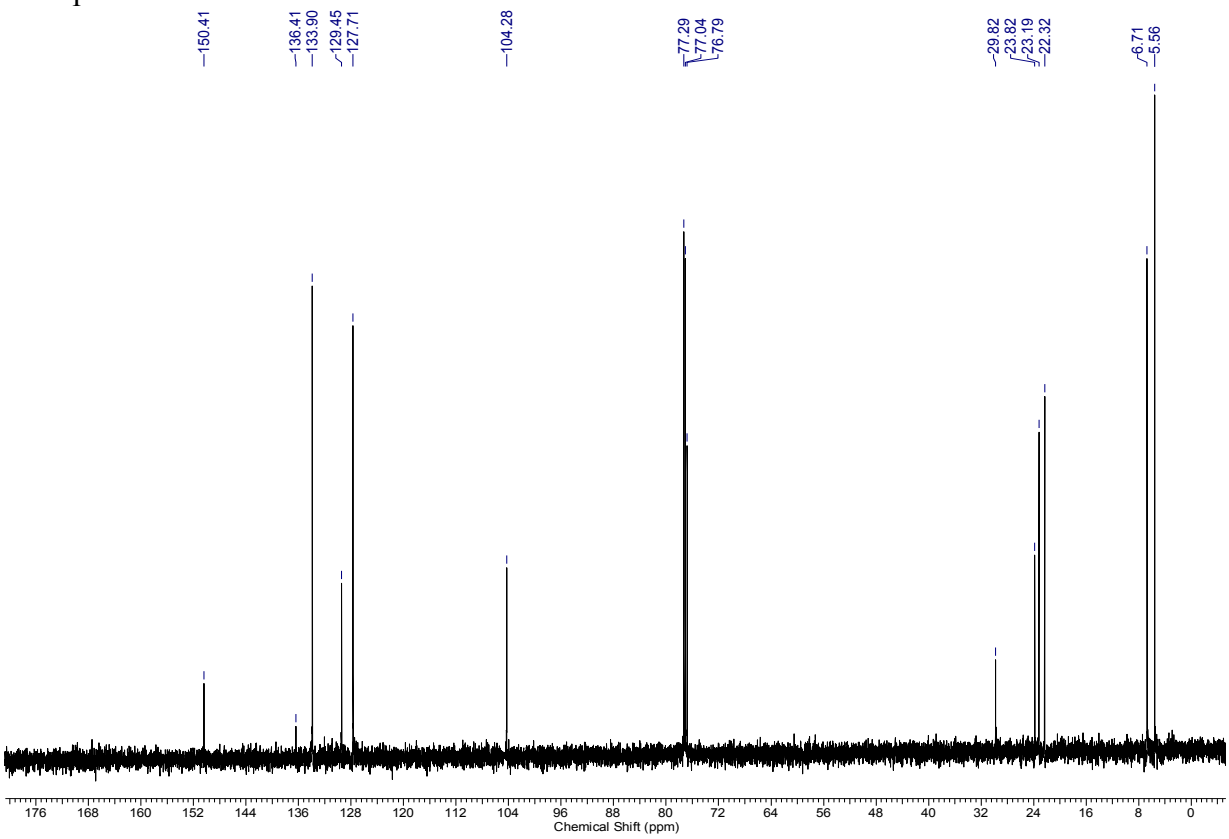

^{1}H Spectrum of **196e**

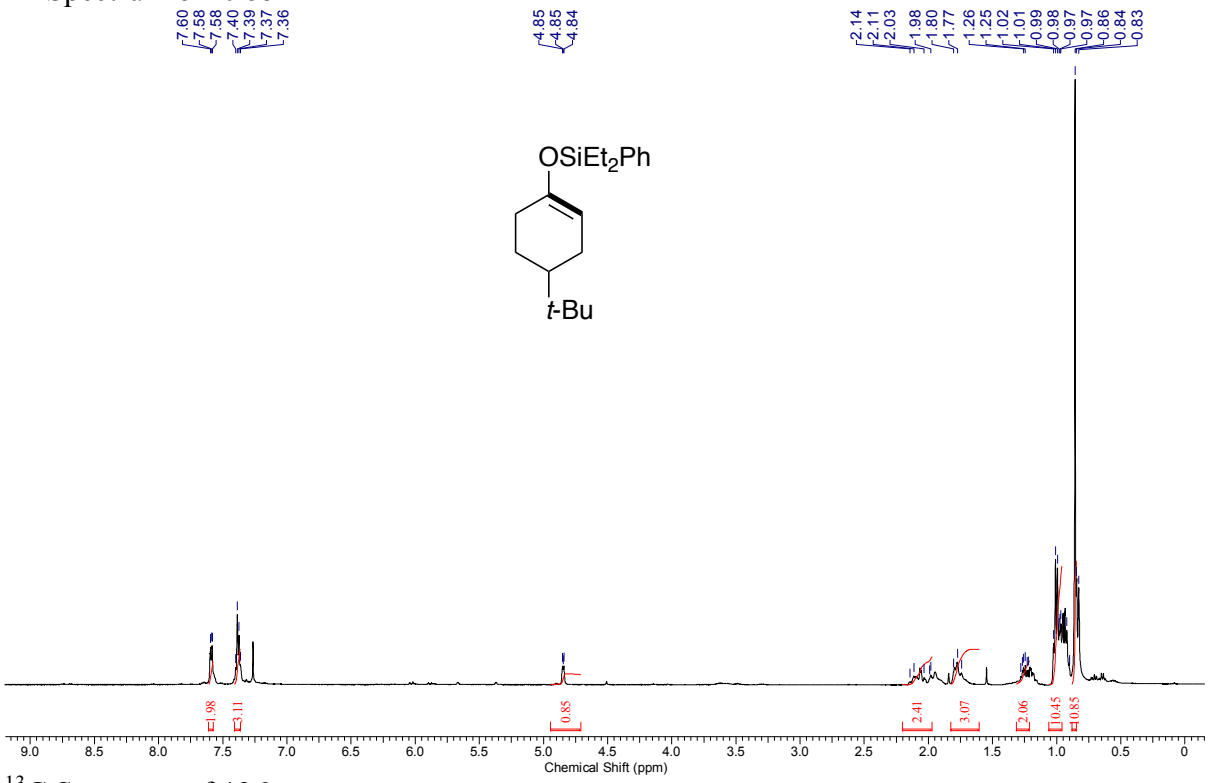

^{13}C Spectrum of **196e**

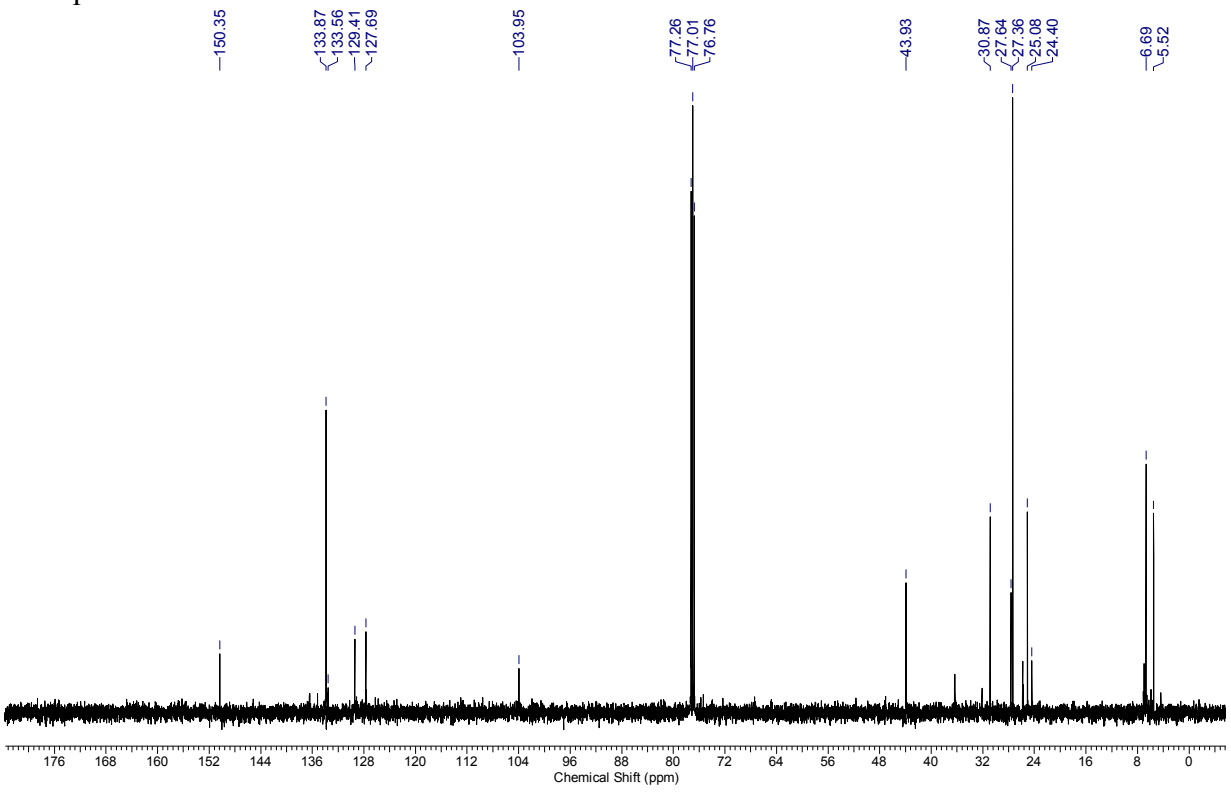

^{1}H Spectrum of **196a-*d***

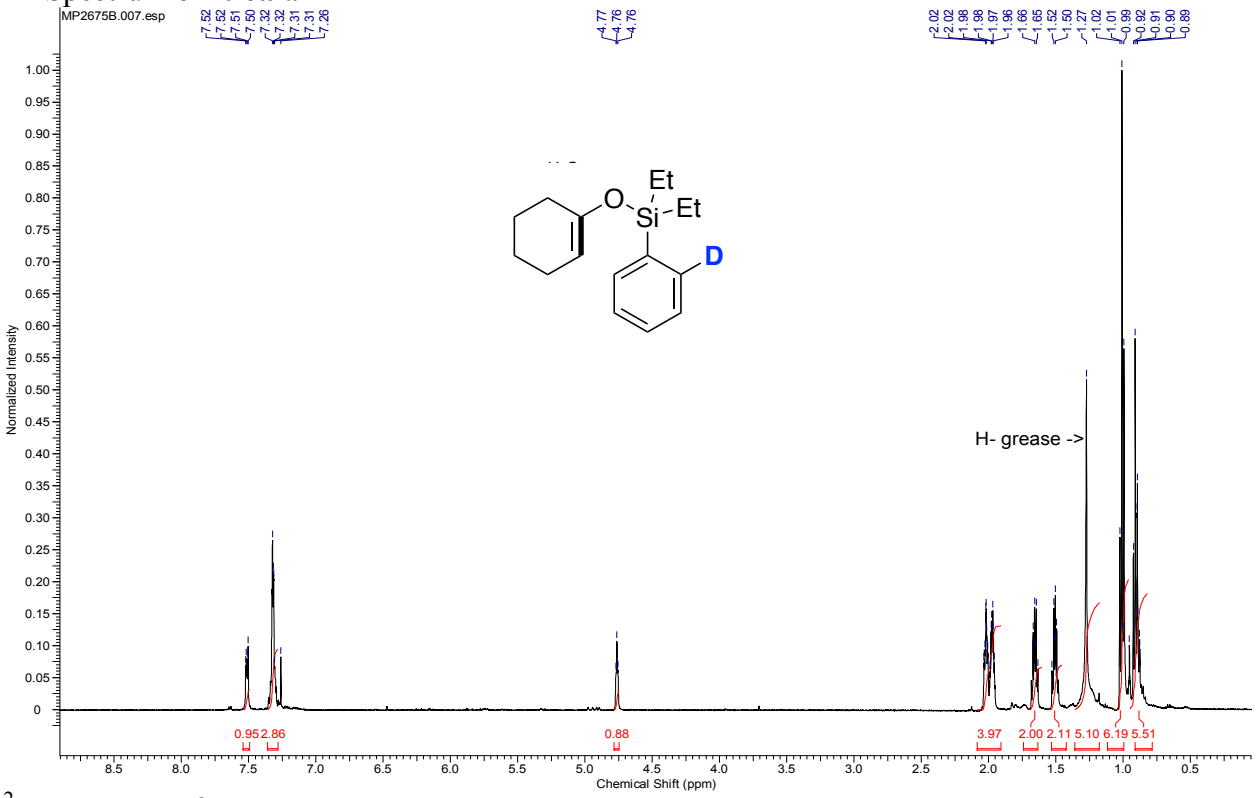

^{2}H Spectrum of **196-*d***

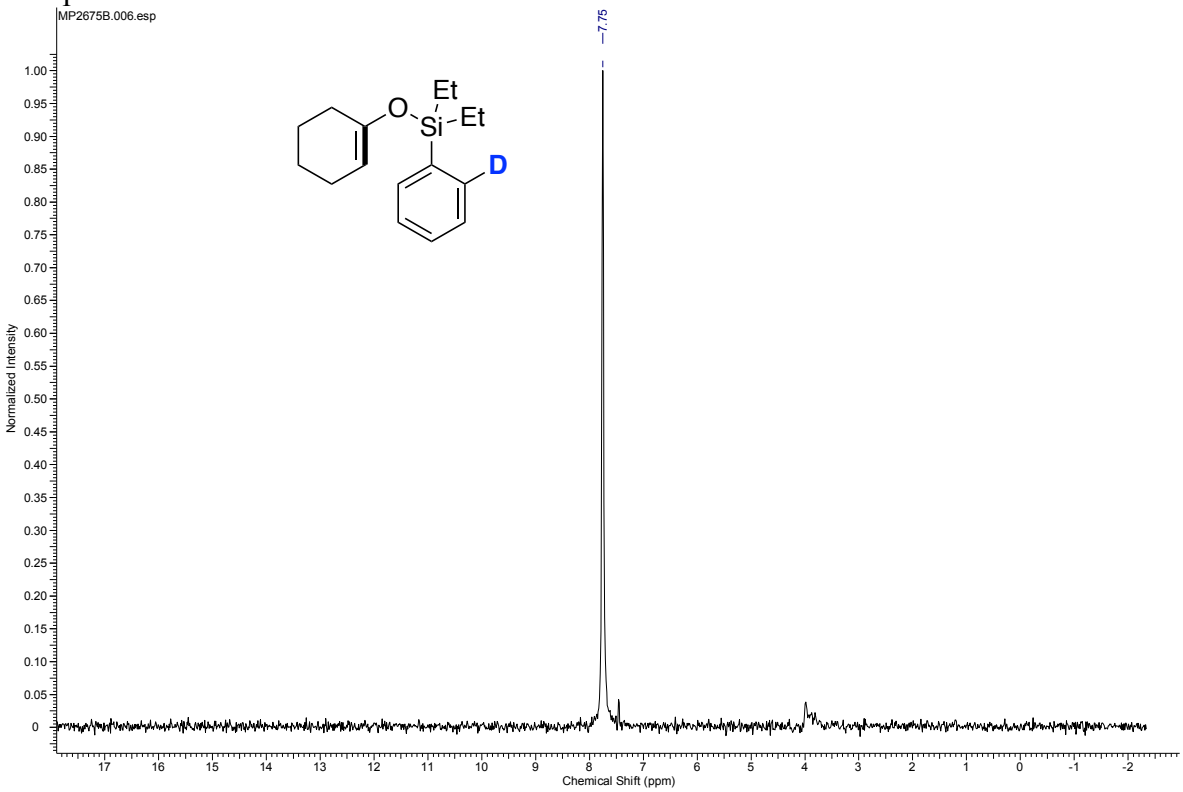

Crude ^{1}H Spectrum of **210**

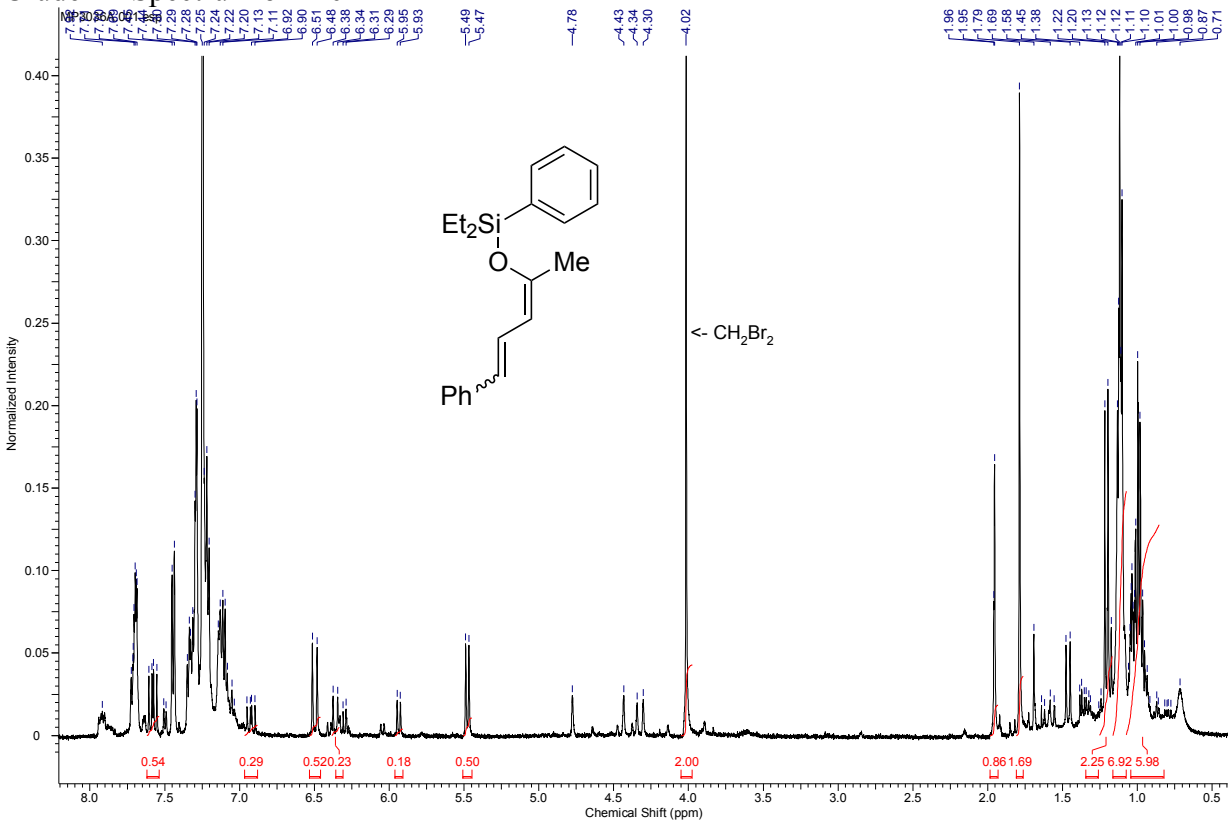

^{1}H Spectrum of **T_2-Cl (232)**

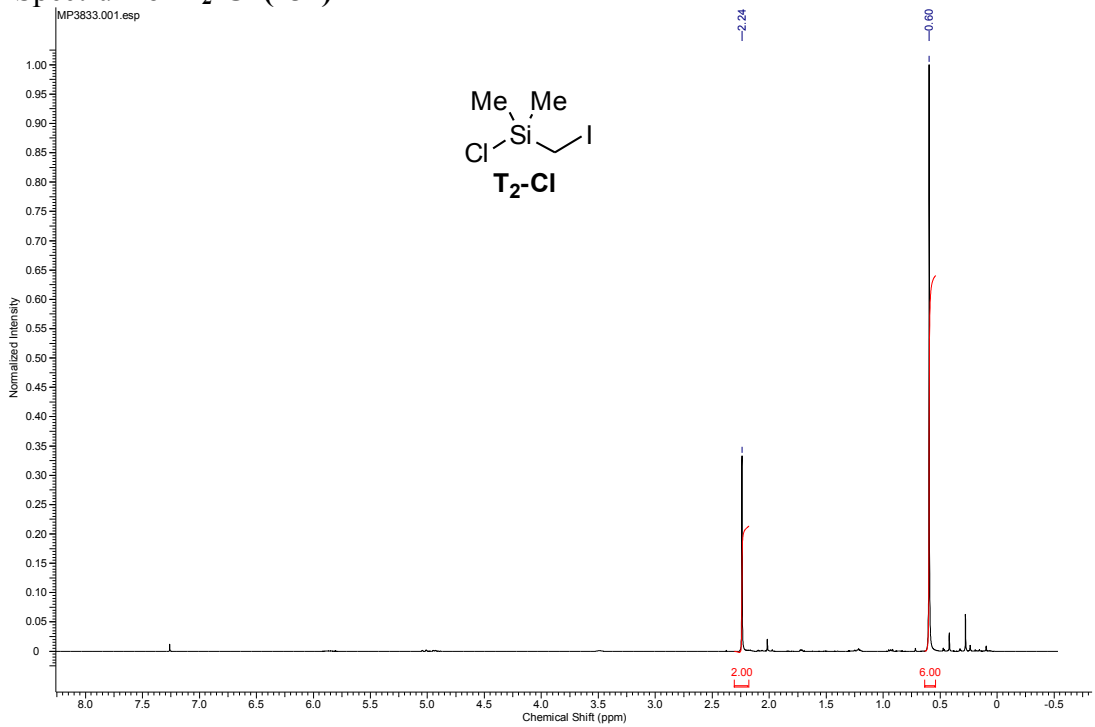

^{13}C Spectrum of **T_2-Cl (232)**

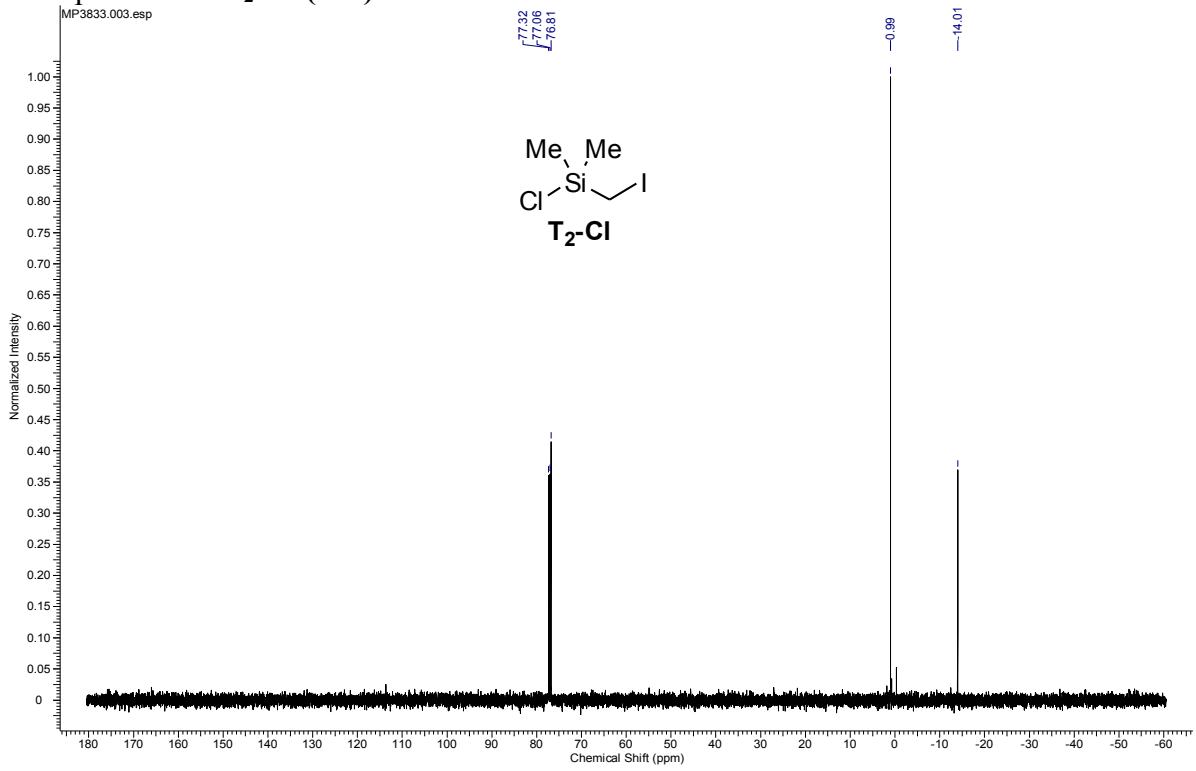

^{1}H Spectrum of **230a**

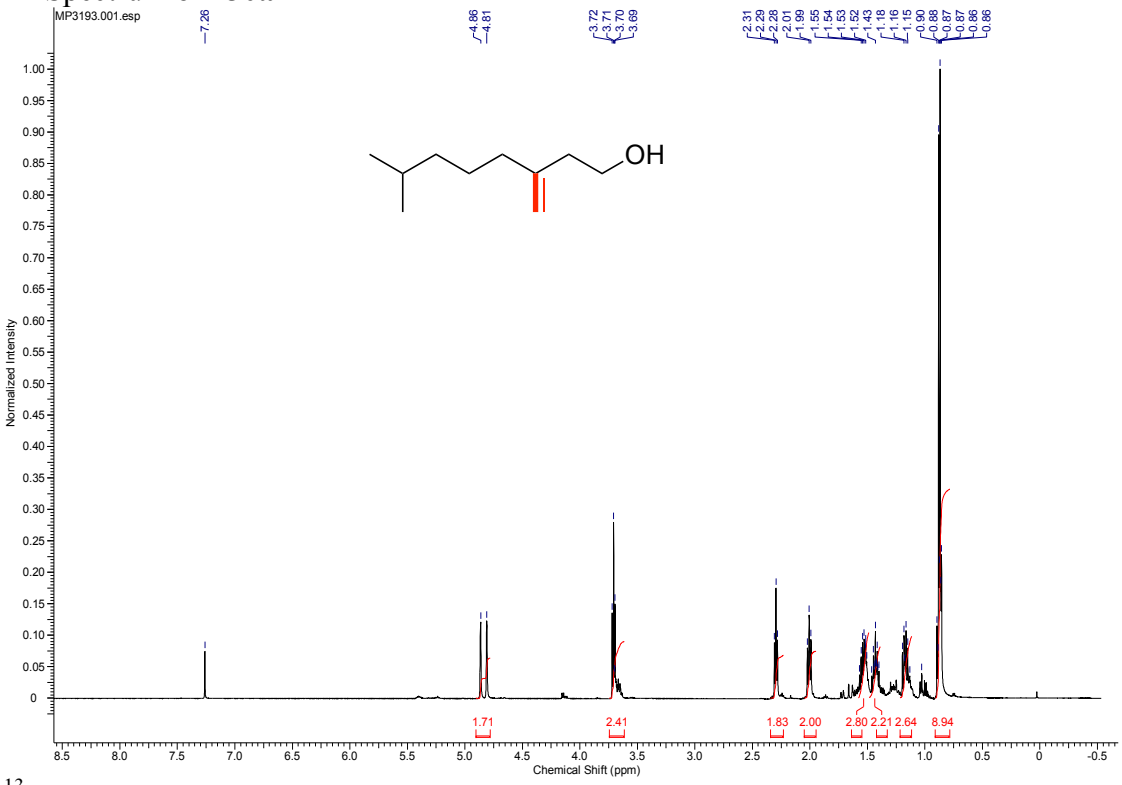

^{13}C Spectrum of **230a**

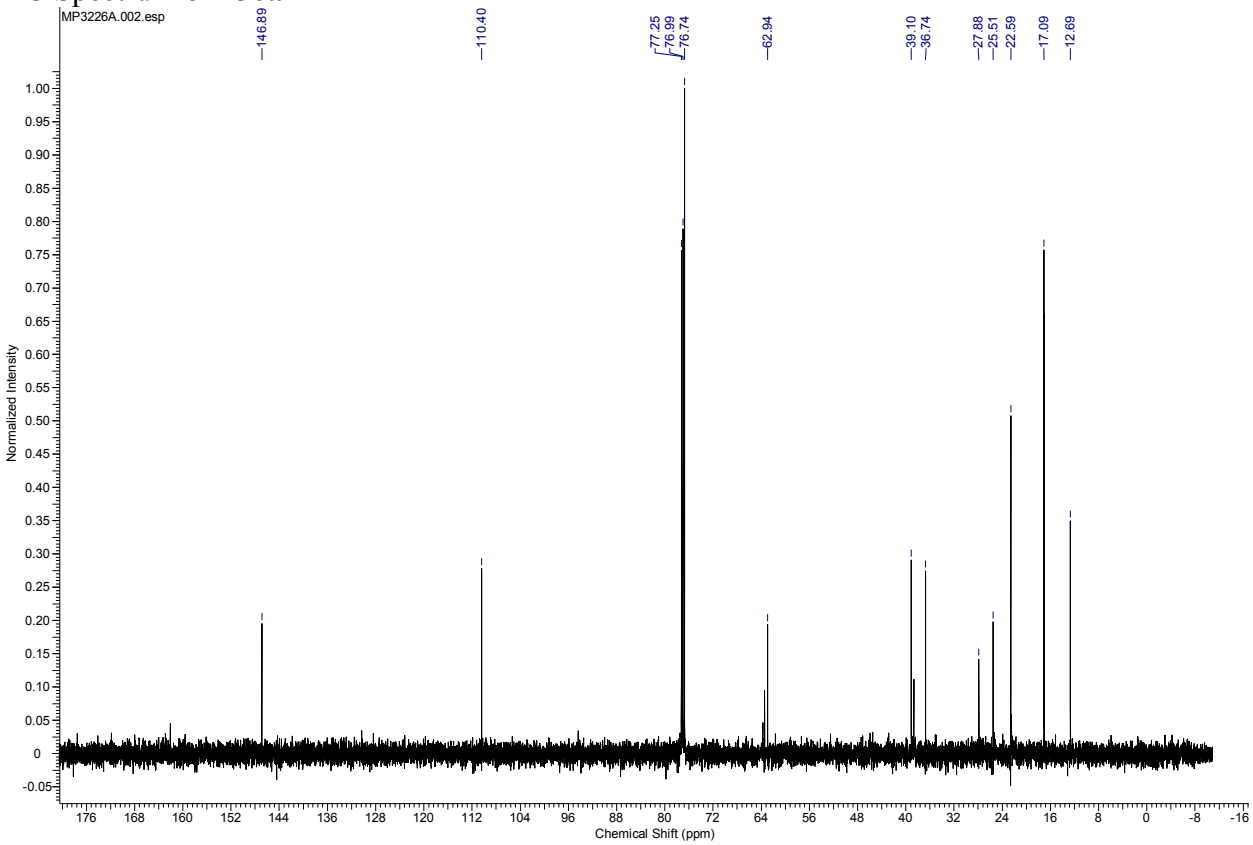

^{1}H Spectrum of **230b**

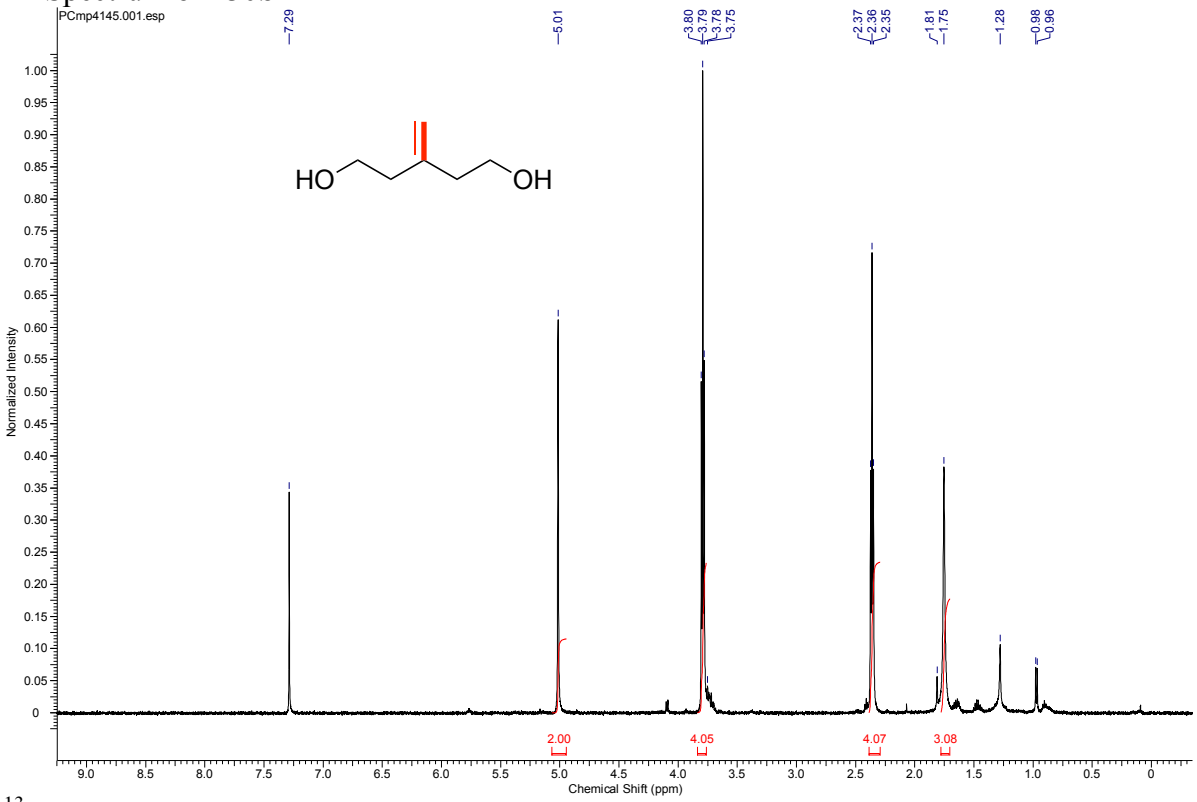

^{13}C Spectrum of **230b**

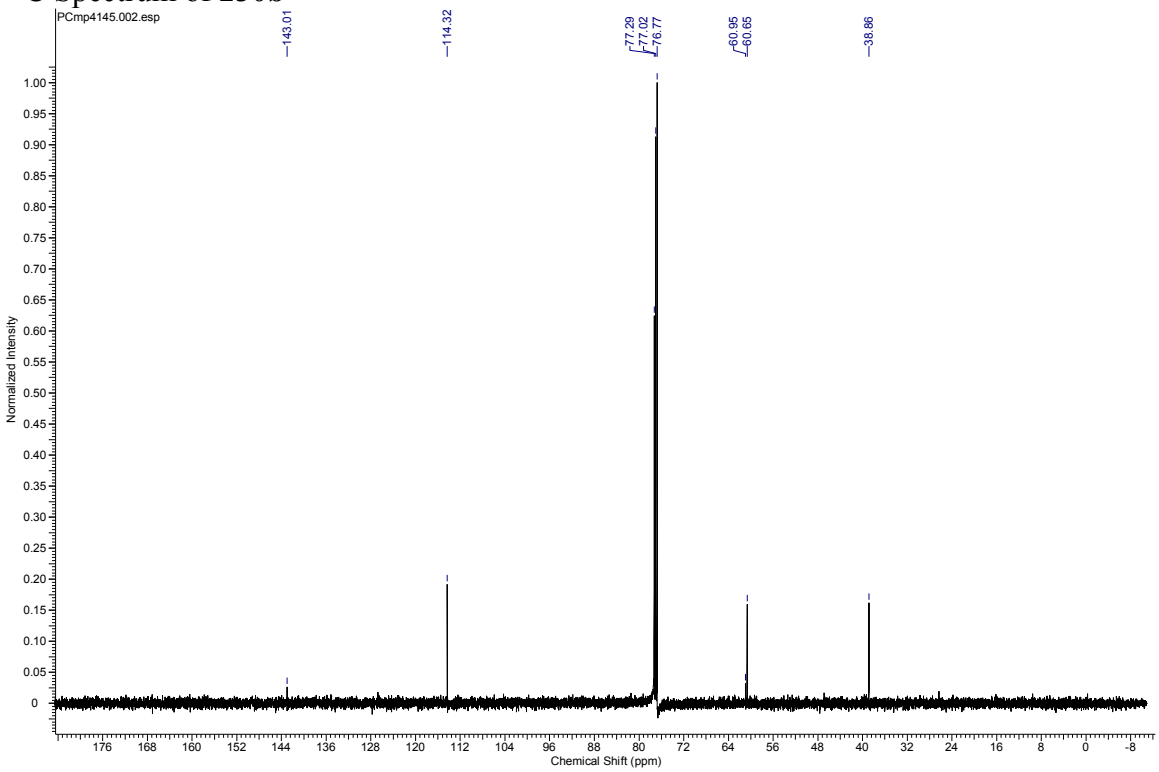

^{1}H Spectrum of **230c**

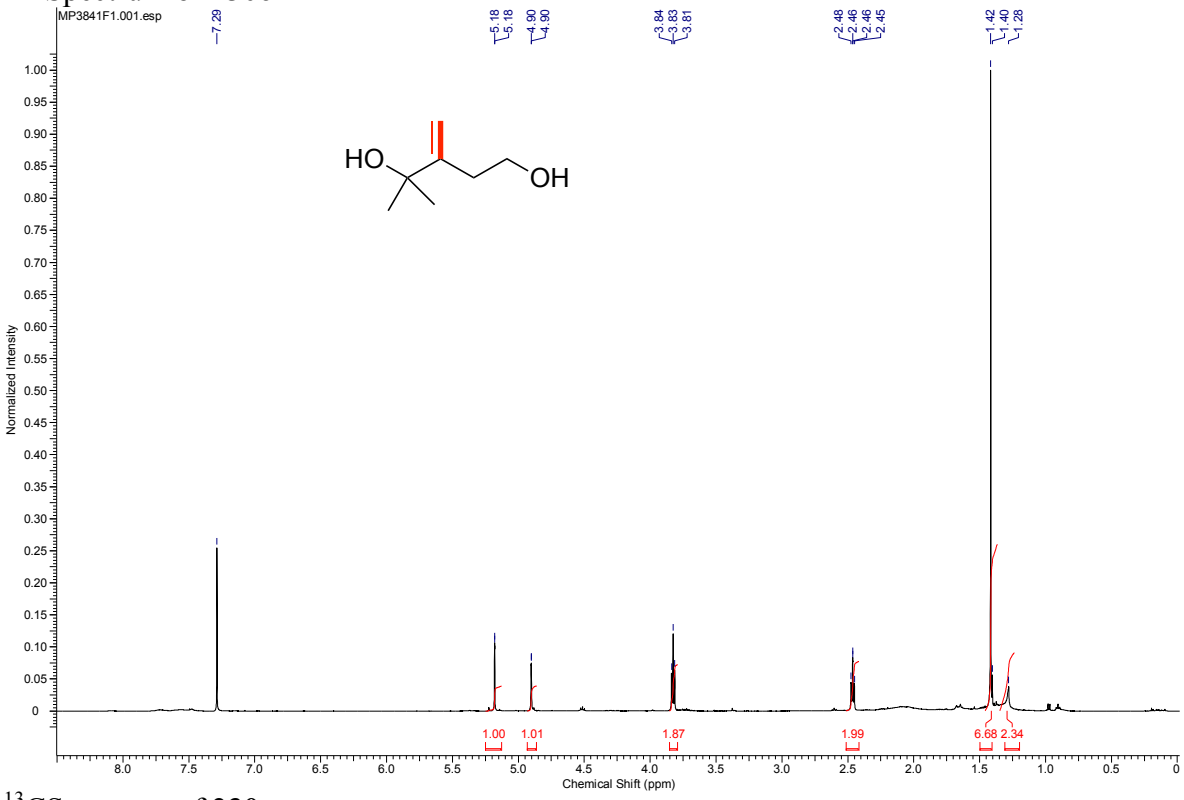

^{13}CSpectrum of **230c**

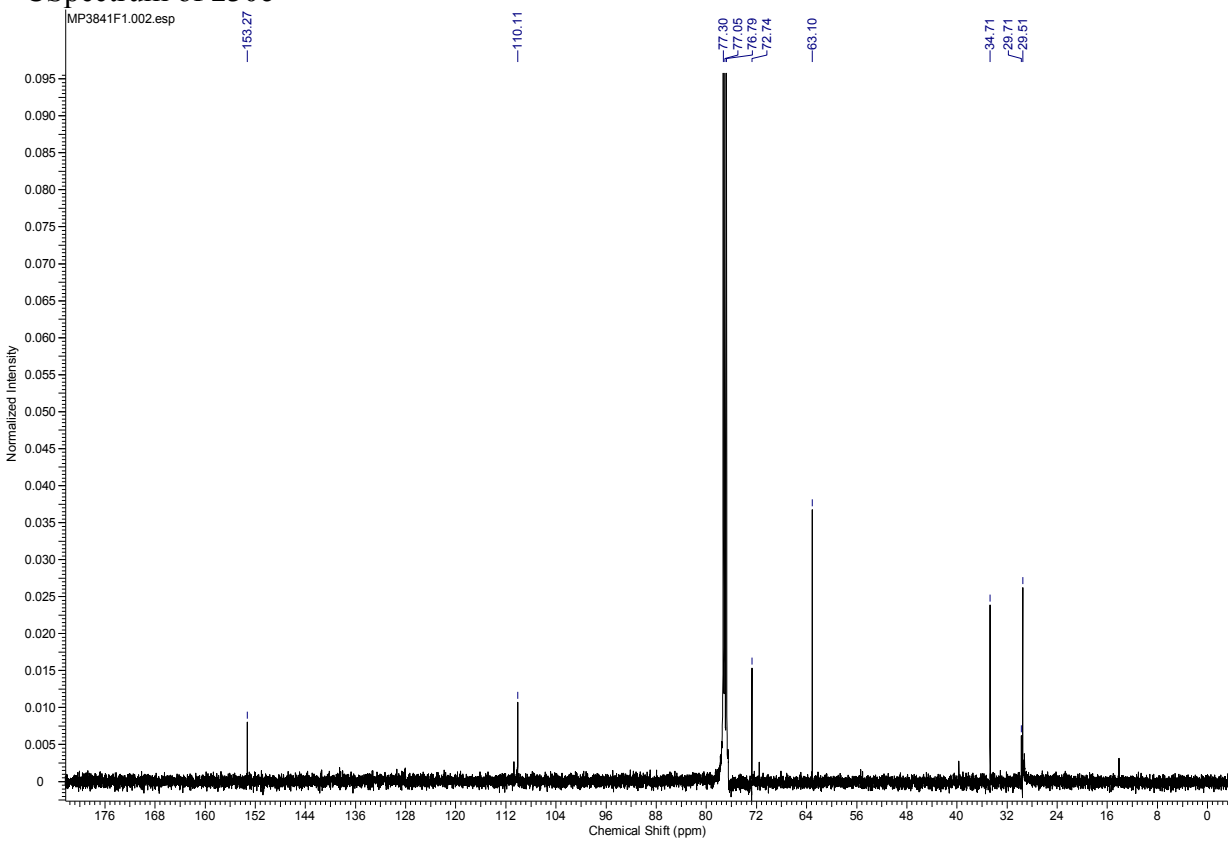

^{1}H Spectrum of **220d, 230d'**, and **230d''**

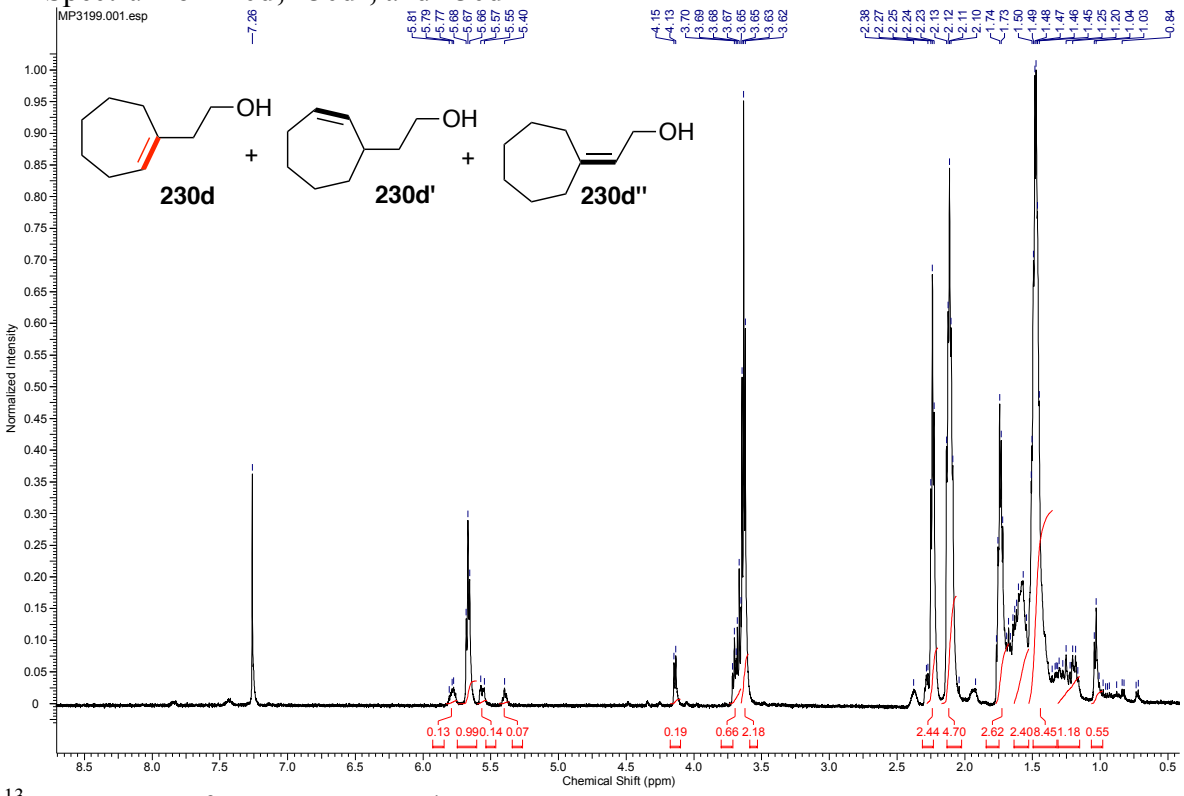

^{13}C Spectrum of **230d, 230d'**, and **230d''**

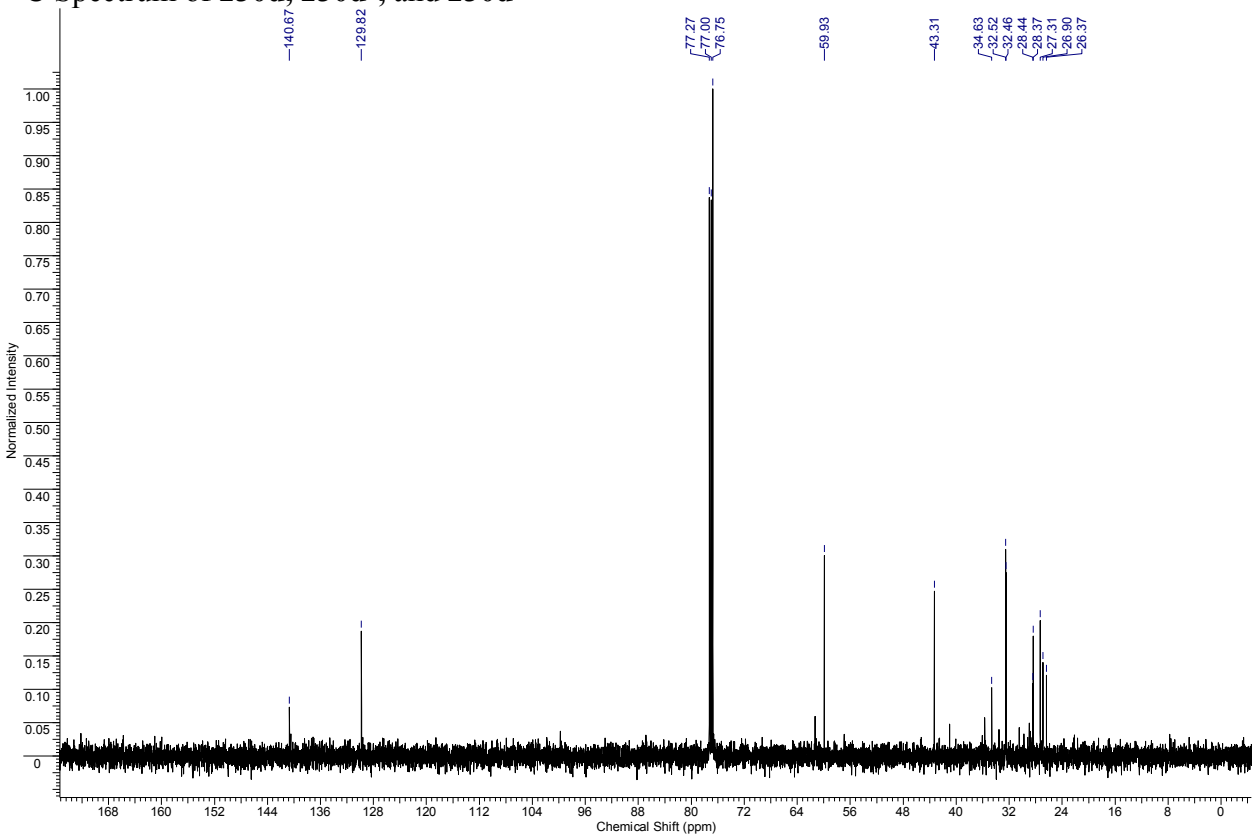

^{1}H Spectrum of **230e** and **230e'**

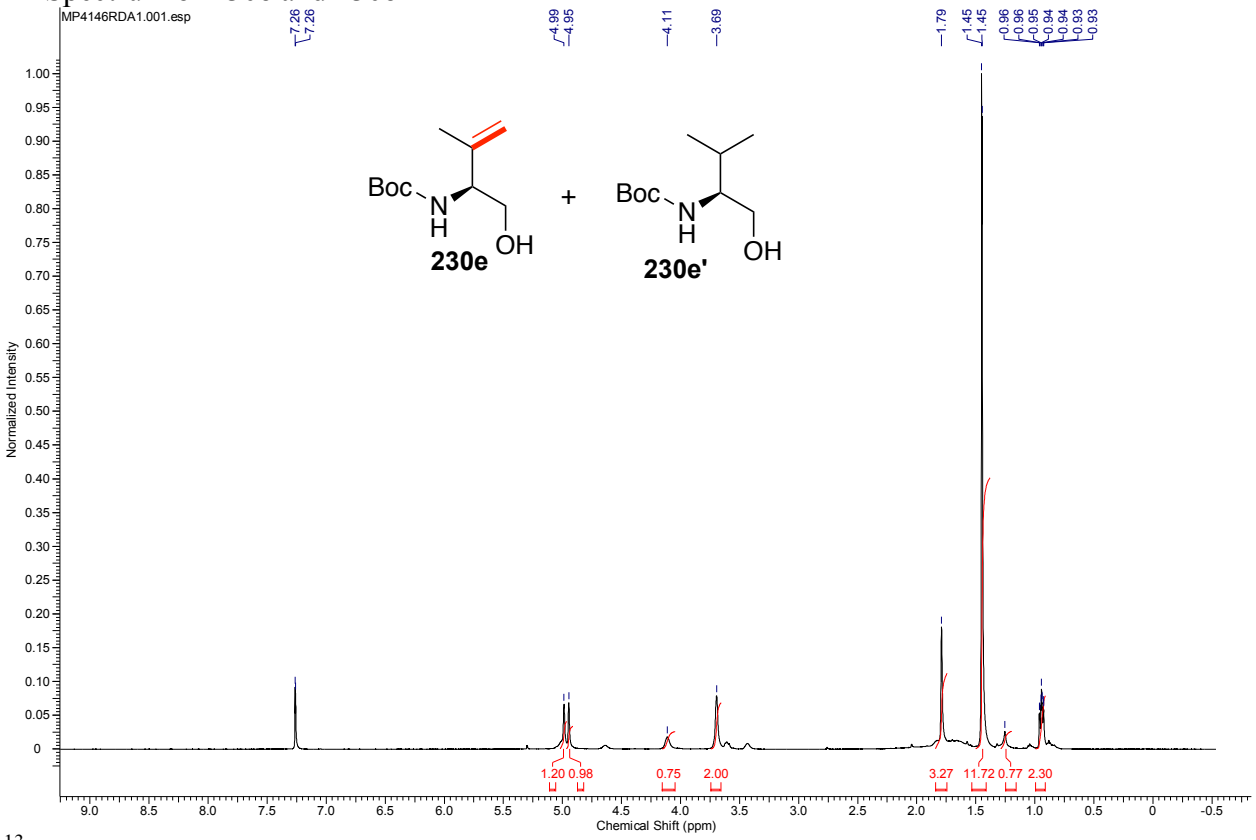

^{13}C Spectrum of **230e**

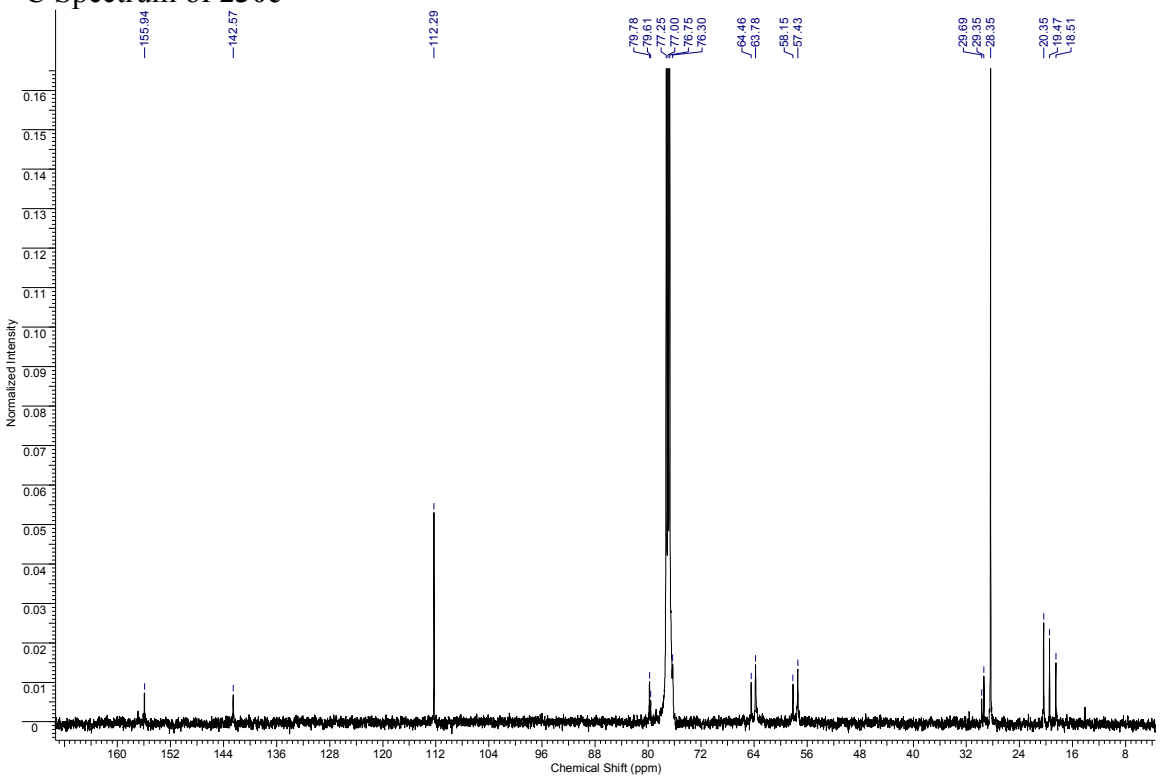

^{1}H Spectrum of **230f**

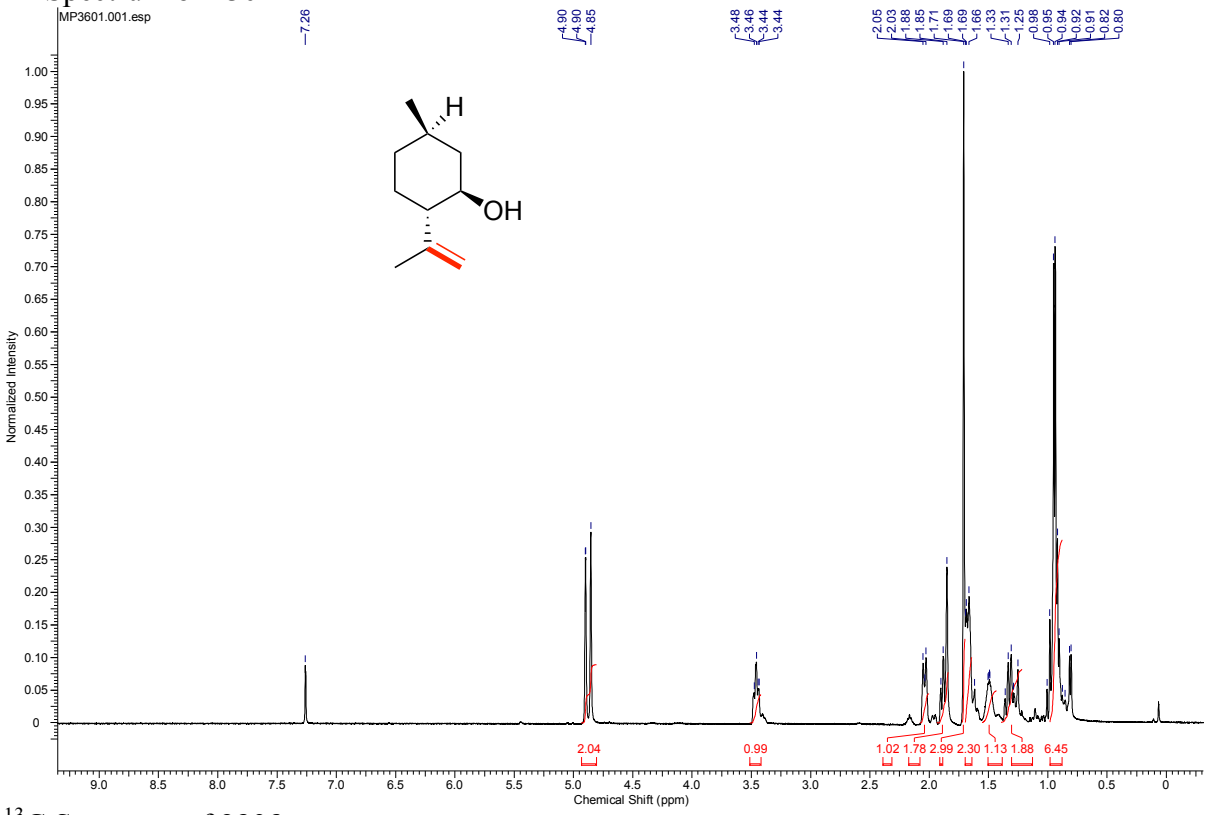

^{13}C Spectrum of **230f**

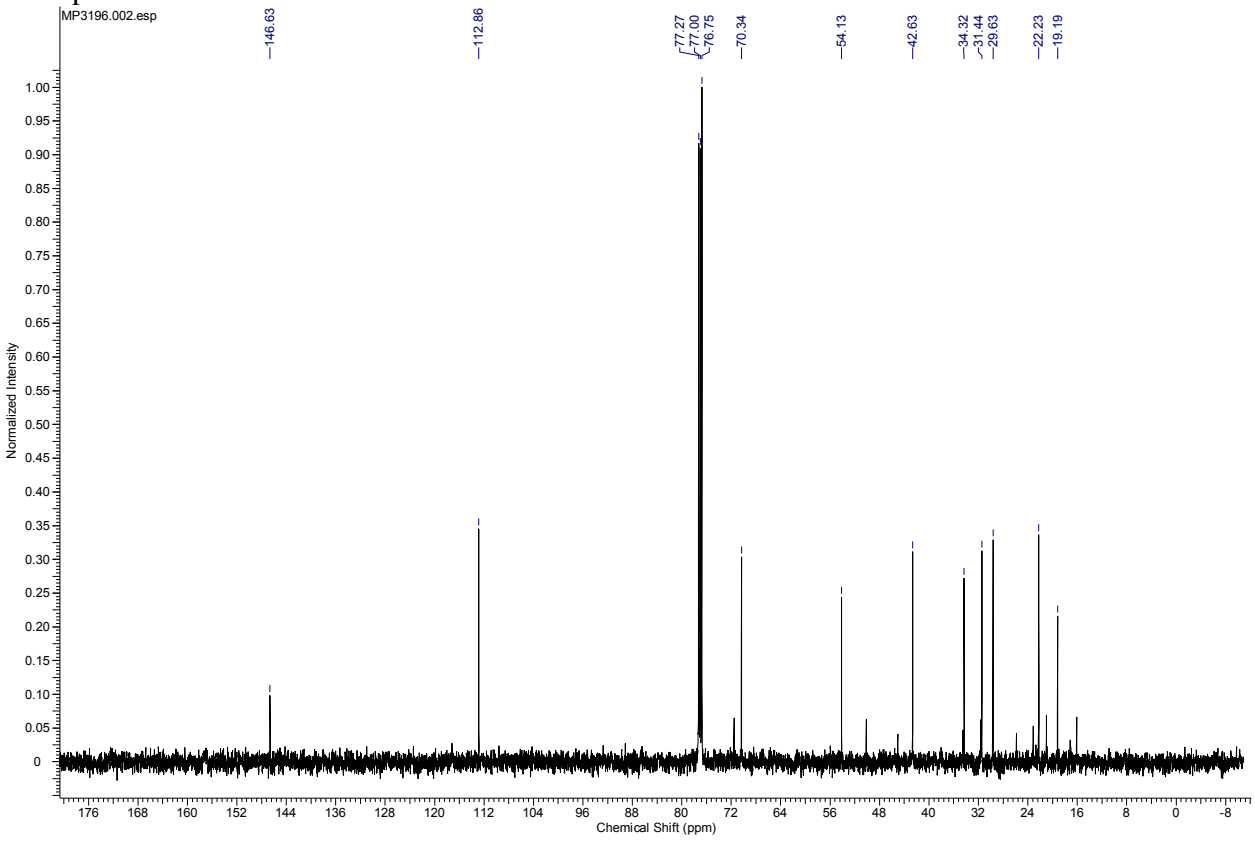

^{1}H Spectrum of **230g**

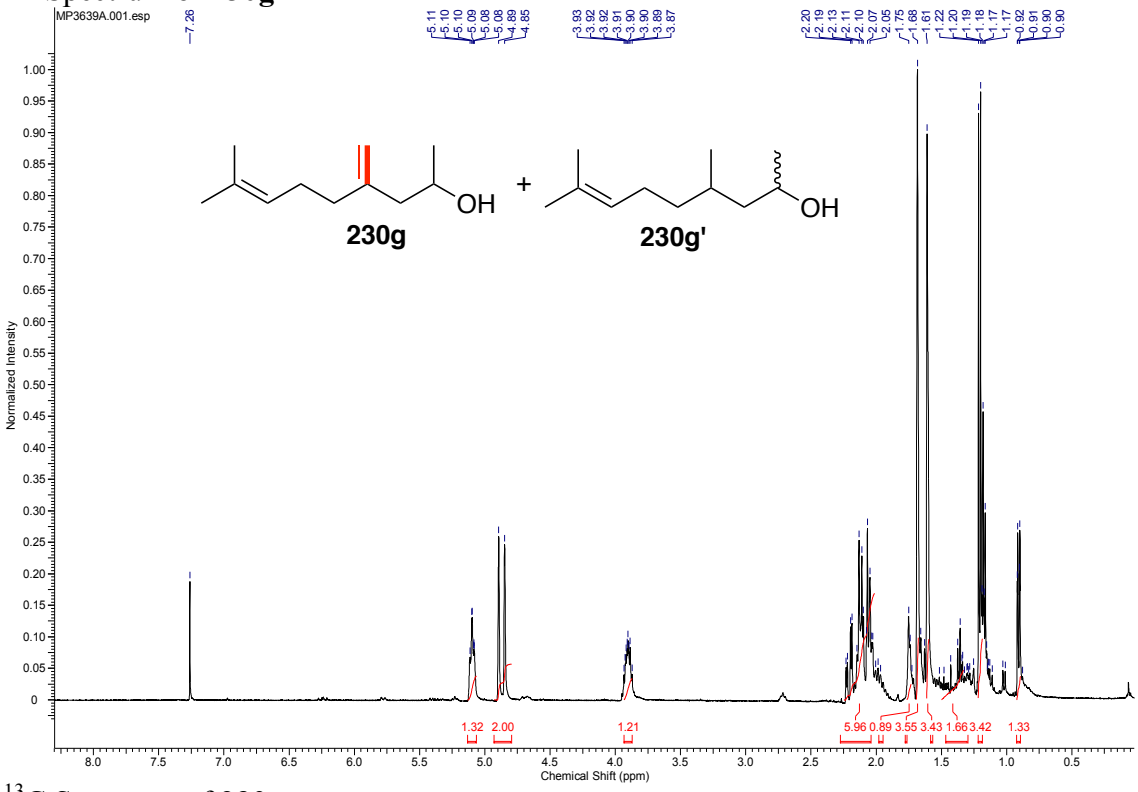

^{13}C Spectrum of **230g**

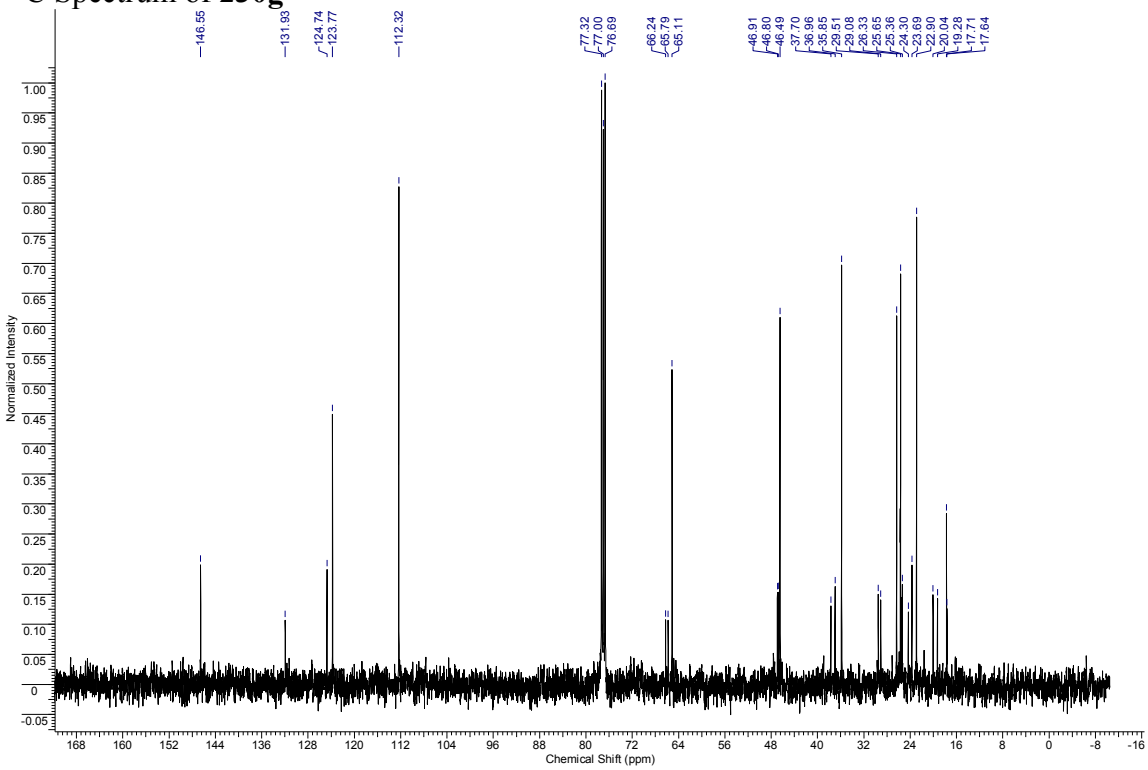

^{1}H Spectrum of **230h**

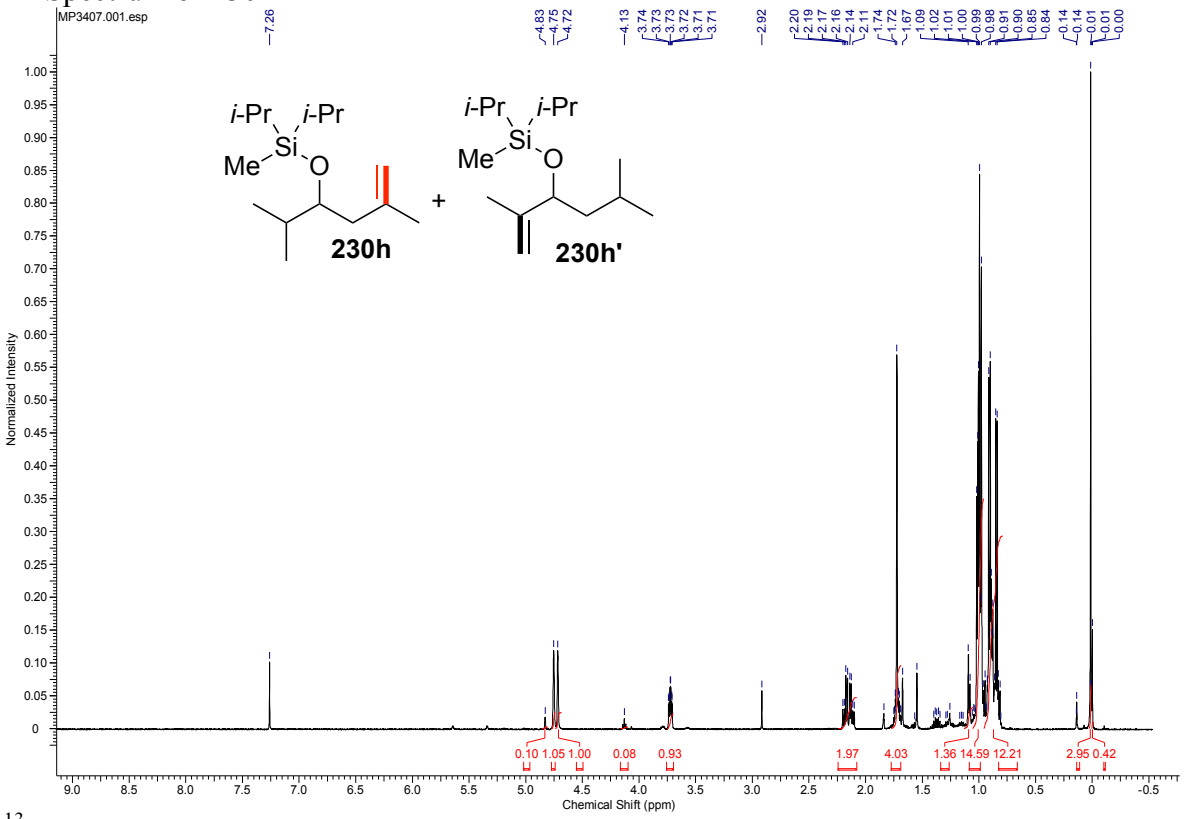

^{13}C Spectrum of **230h**

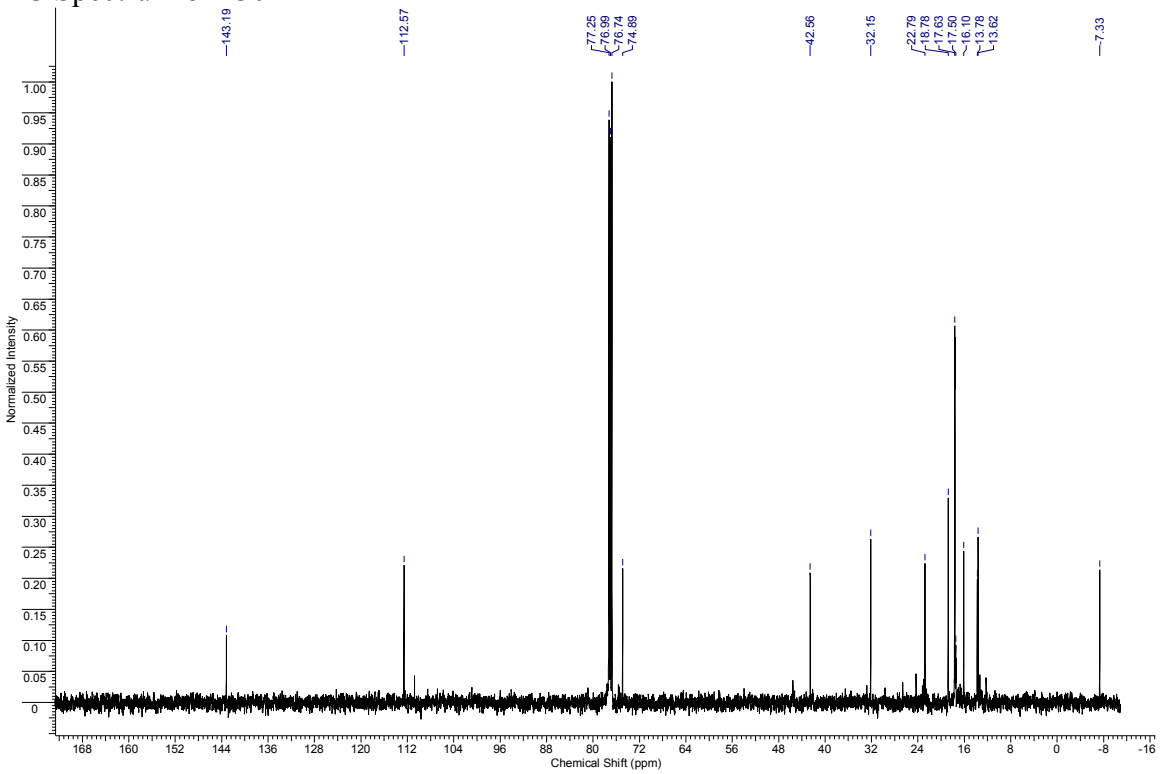

^{1}H Spectrum of **230i**

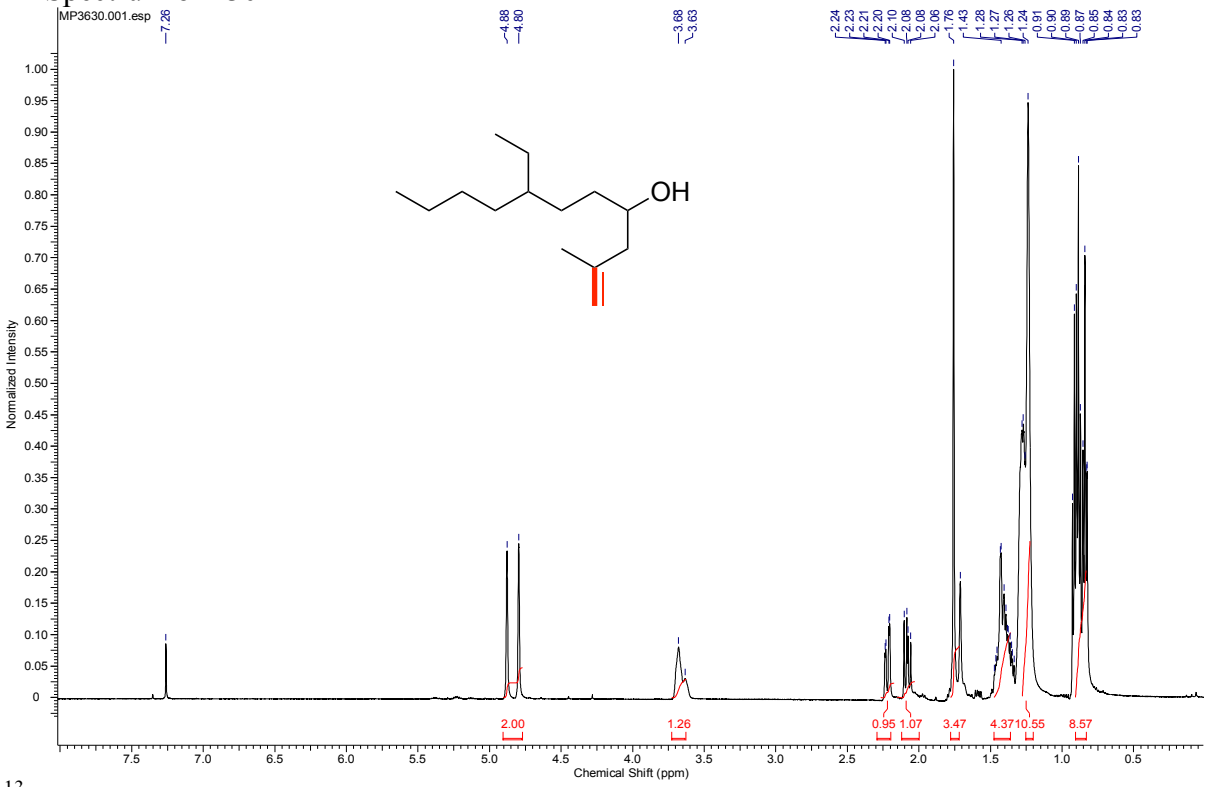

^{13}C Spectrum of **230i**

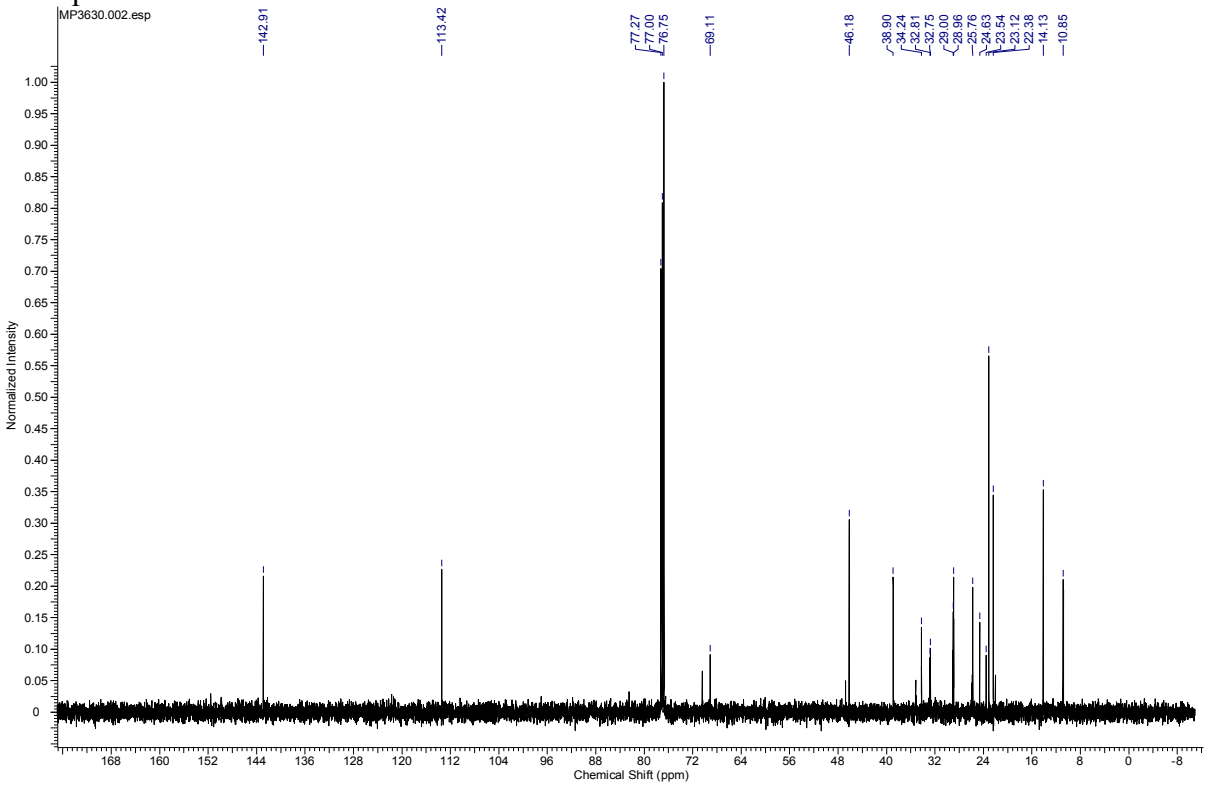

^{1}H Spectrum of **230j**

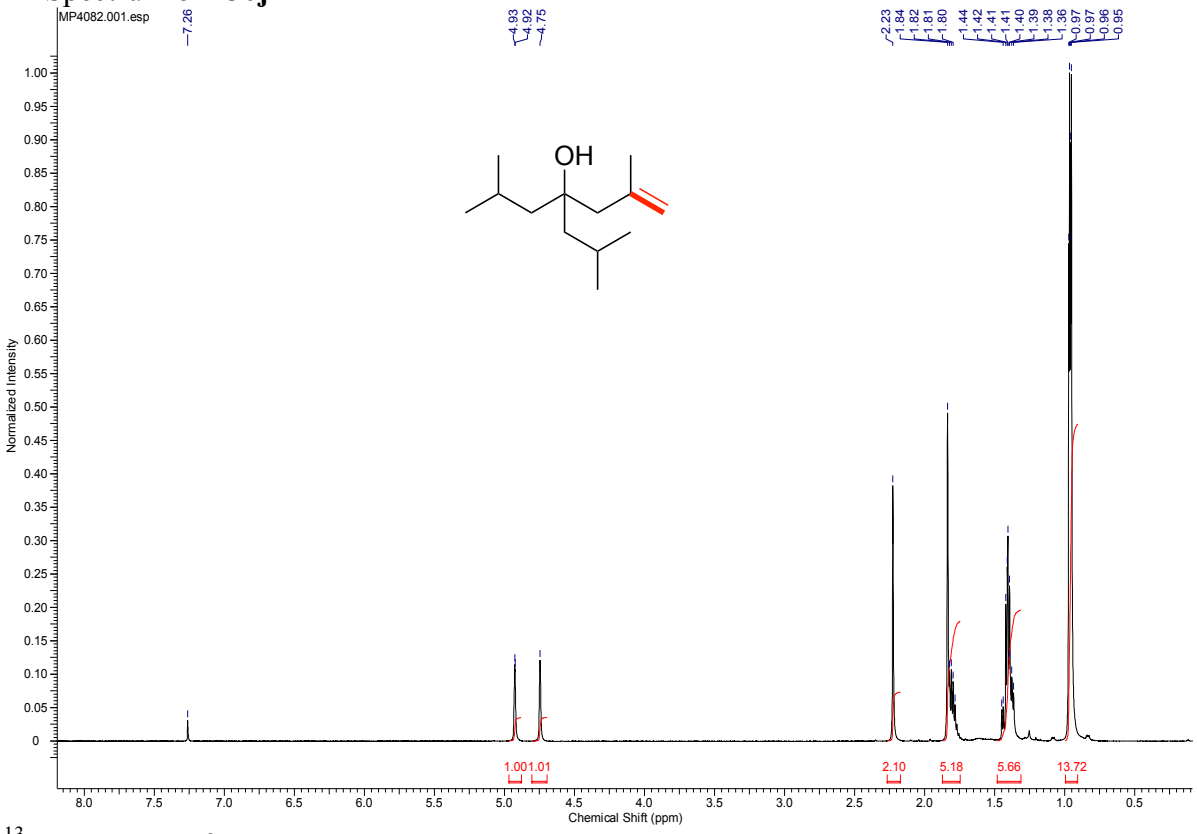

^{13}C Spectrum of **230j**

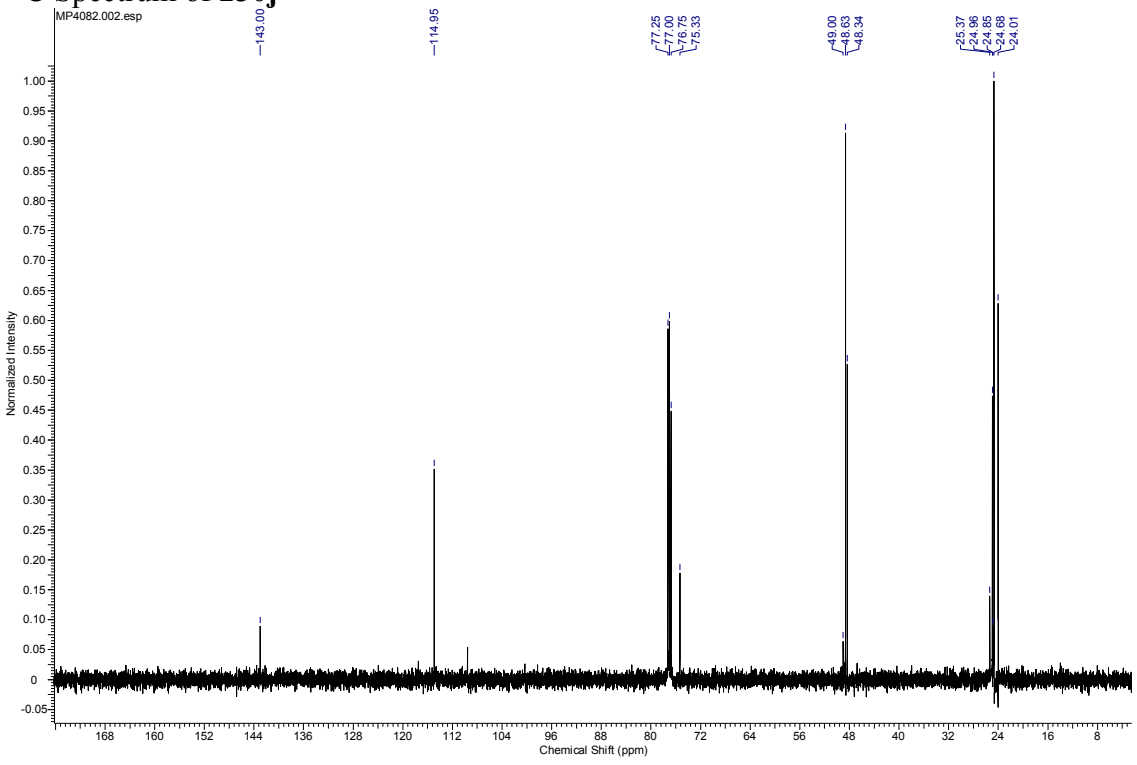

^{1}H Spectrum of **230k**

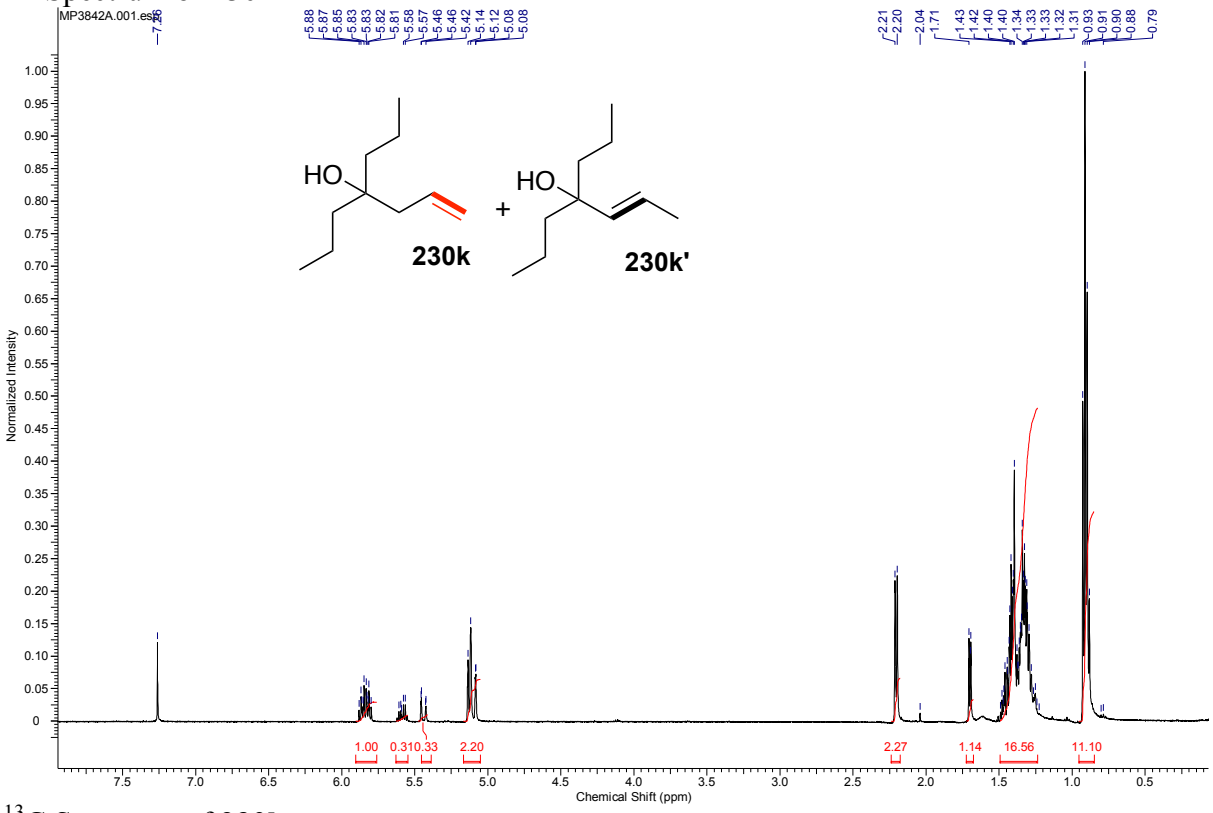

^{13}C Spectrum of **230k**

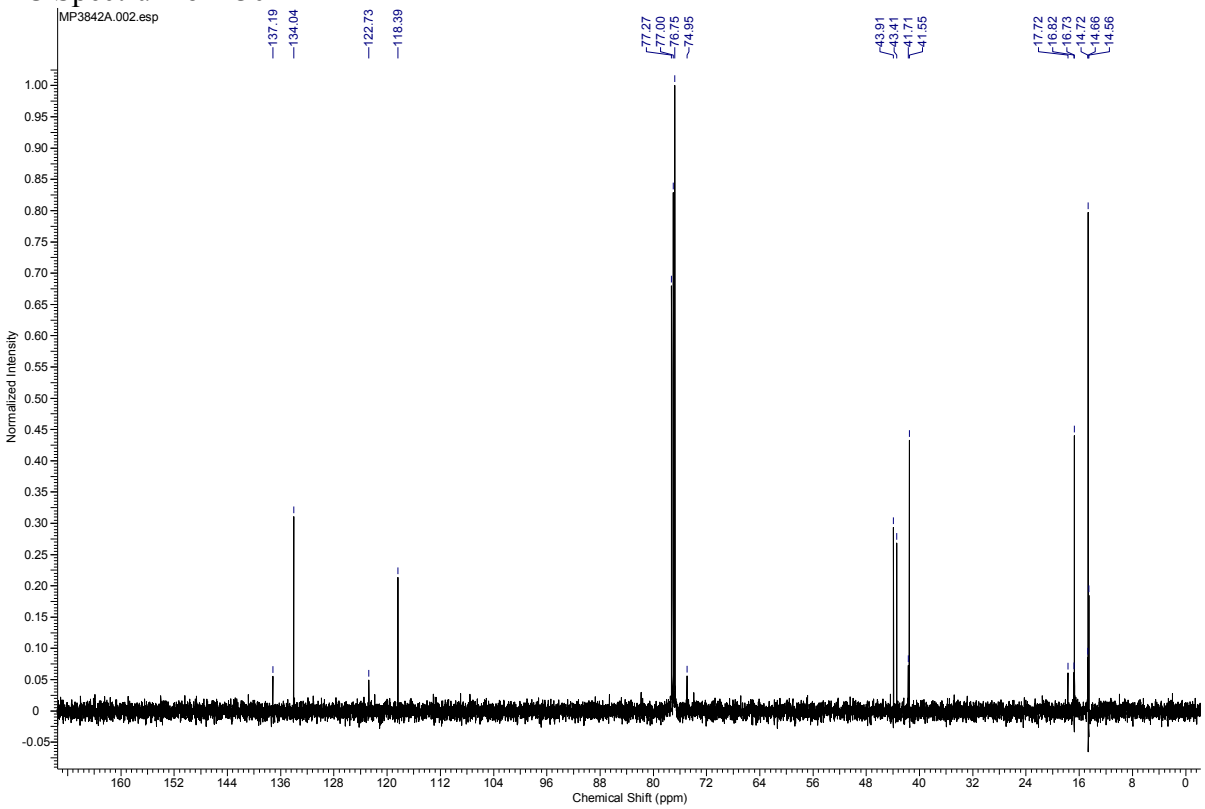

^{1}H Spectrum of **230l**

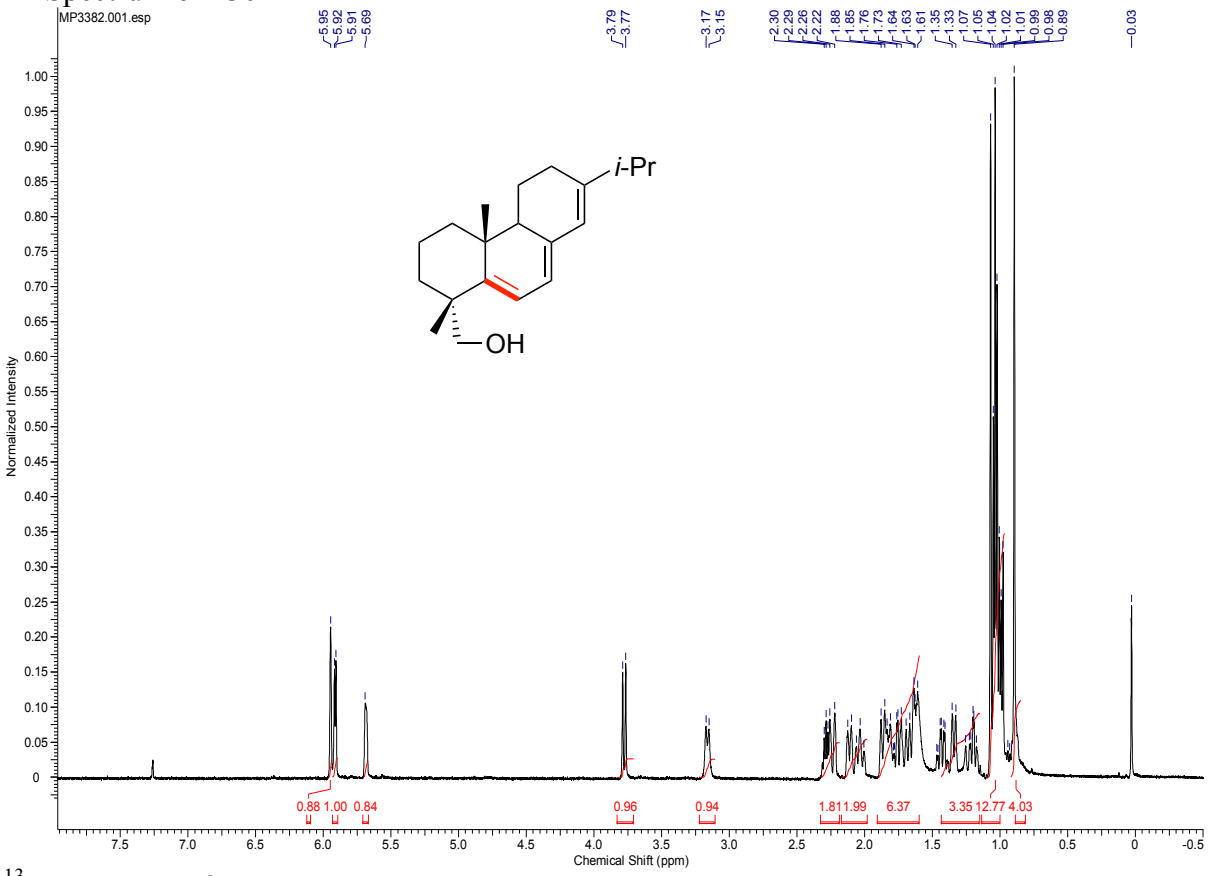

^{13}C Spectrum of **230l**

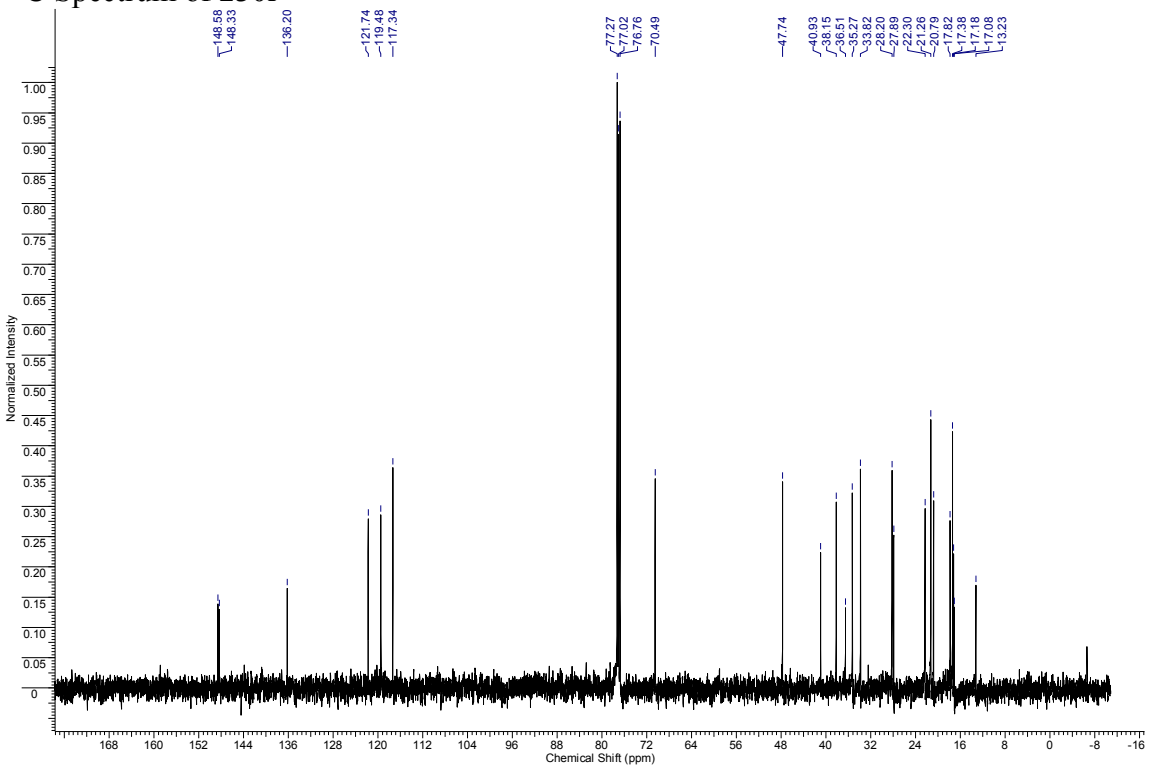

^{1}H Spectrum of **230m**

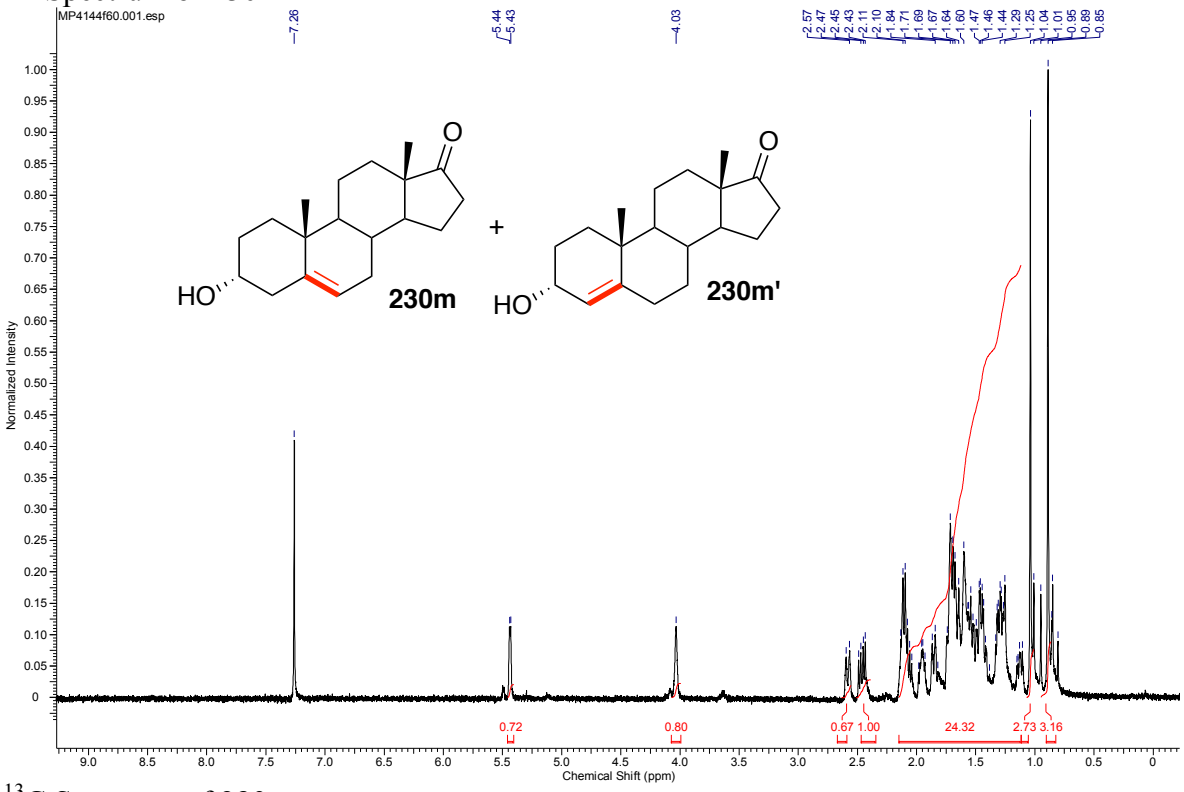

^{13}C Spectrum of **230m**

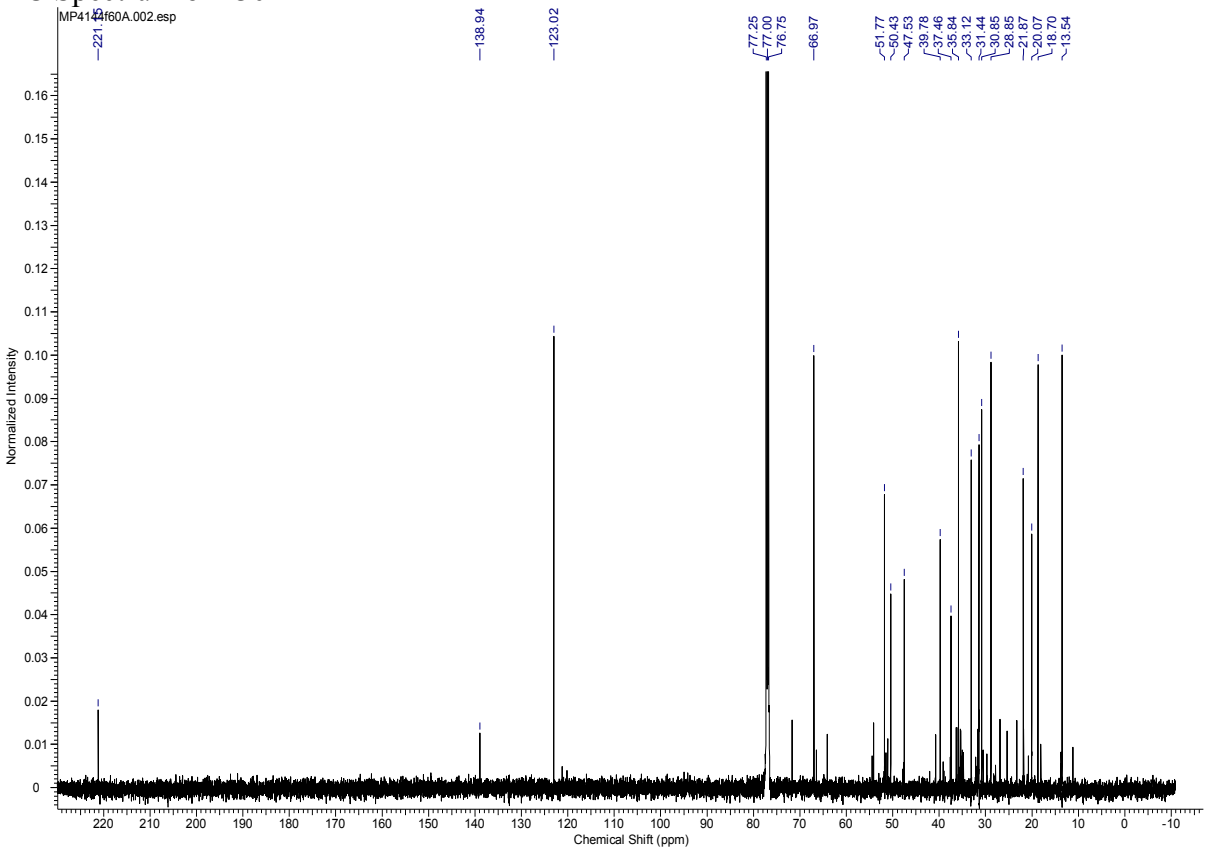

^{1}H Spectrum of **230n**

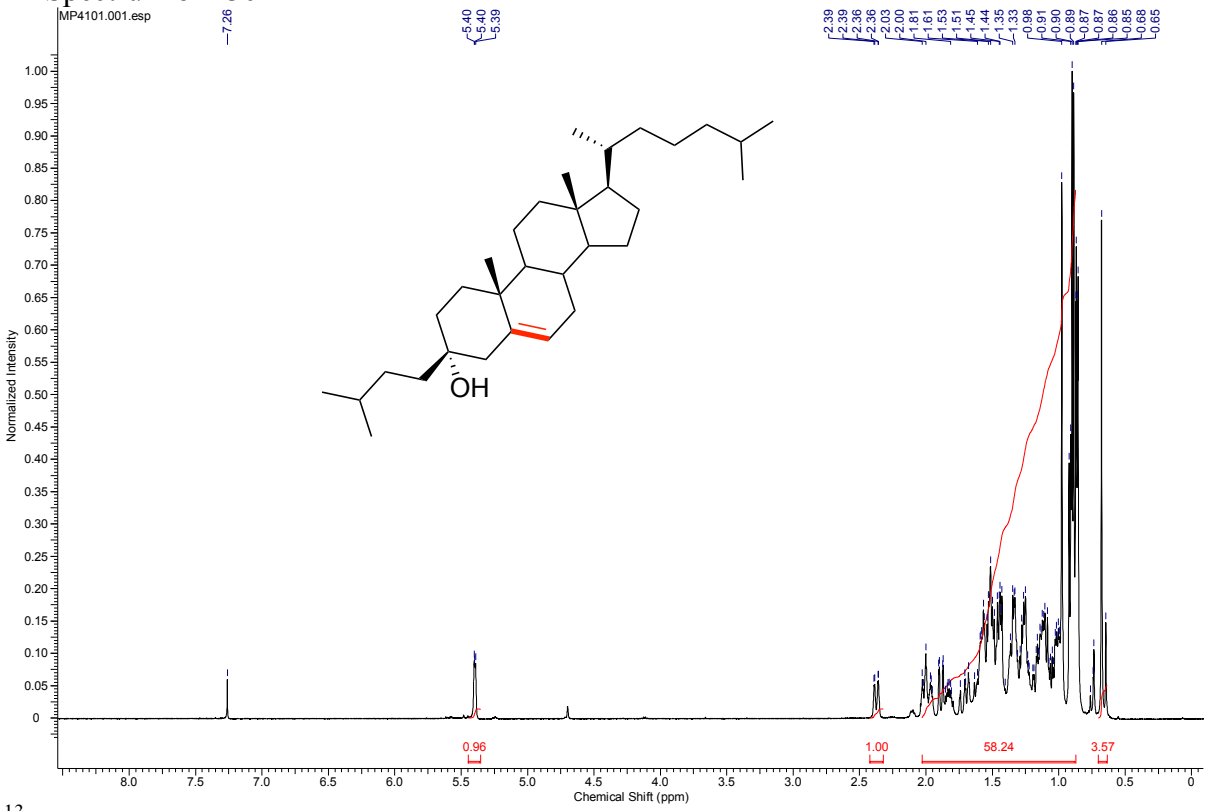

^{13}C Spectrum of **230n**

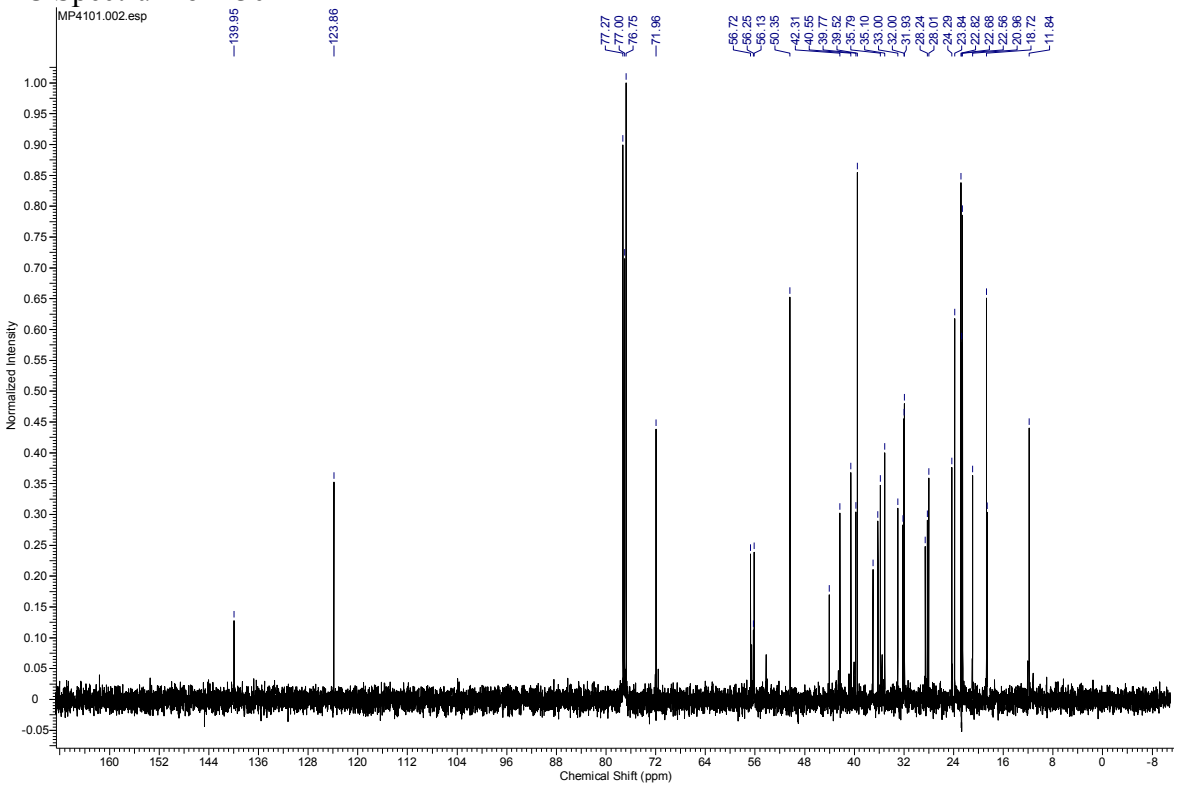

^{1}H Spectrum of **230o-1**

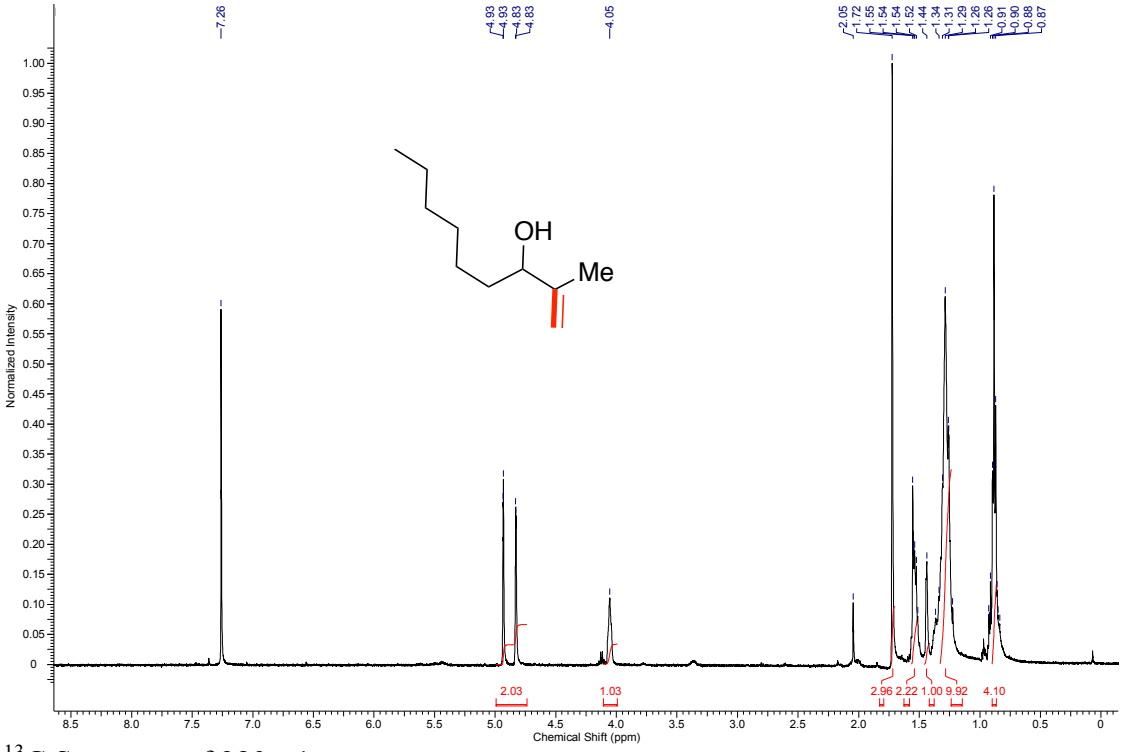

^{13}C Spectrum of **230o-1**

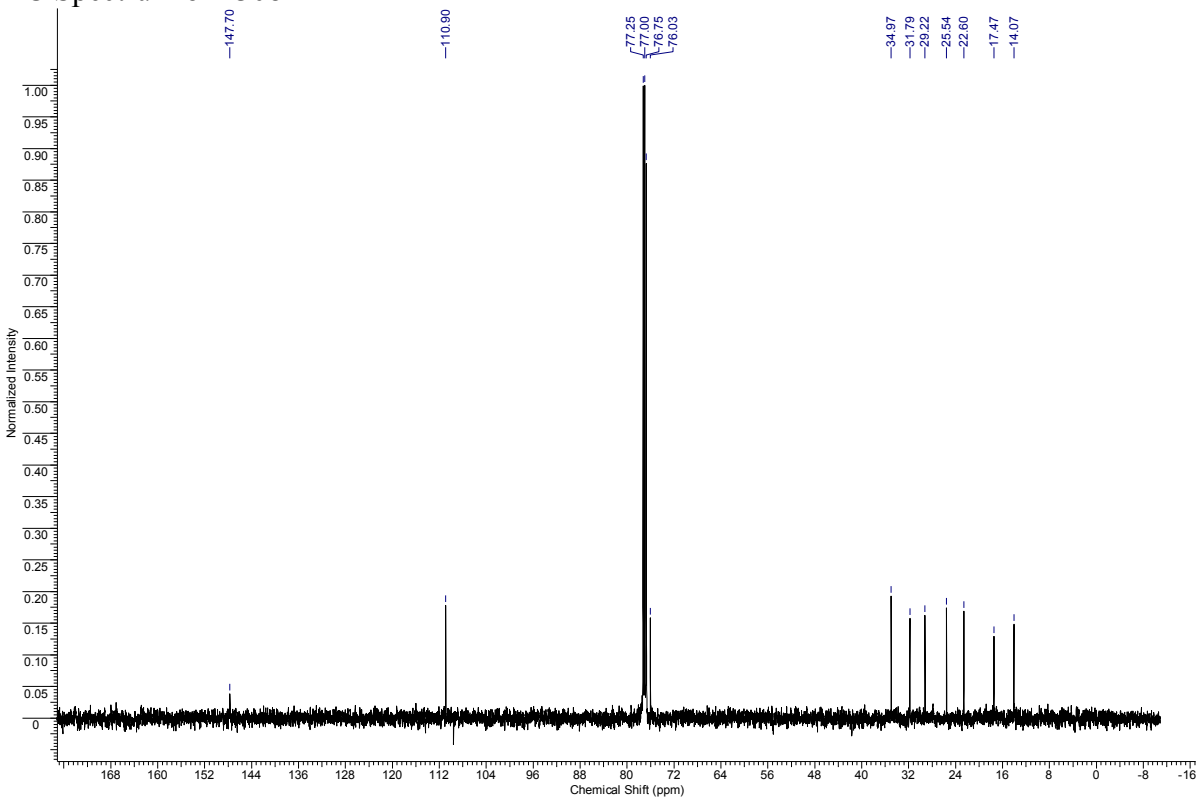

^{1}H Spectrum of **230o-2**

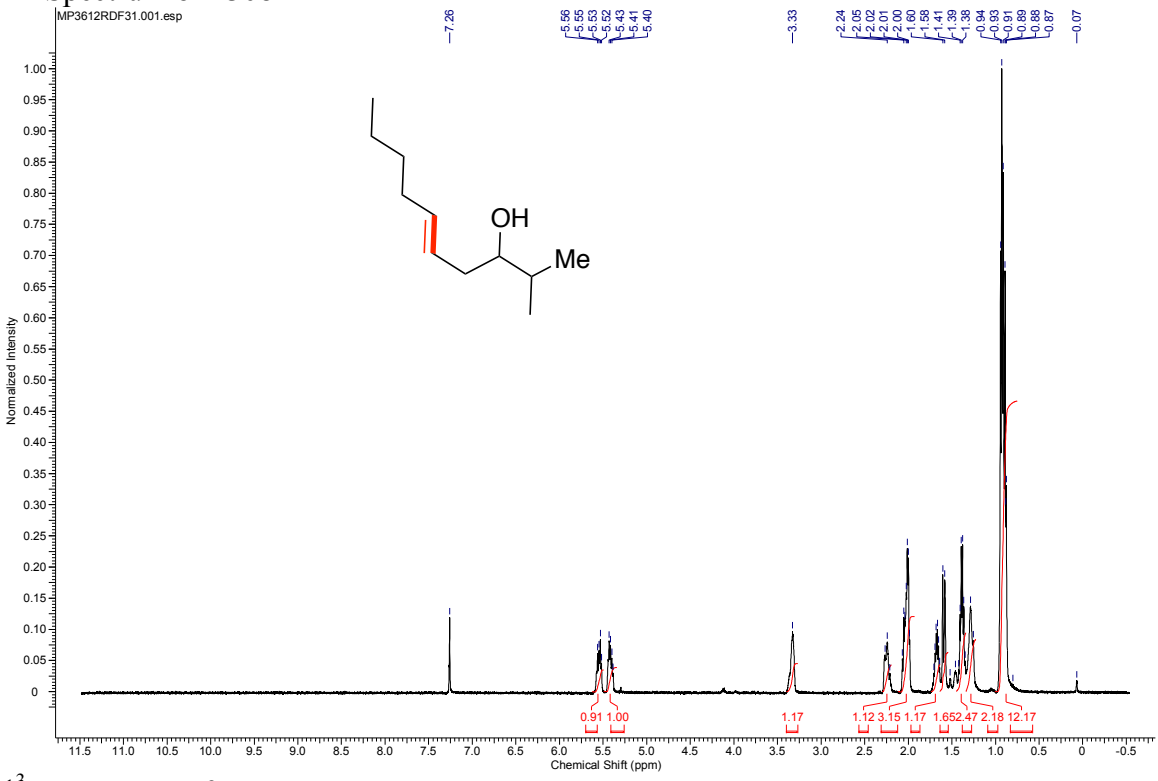

^{13}C Spectrum of **230o-2**

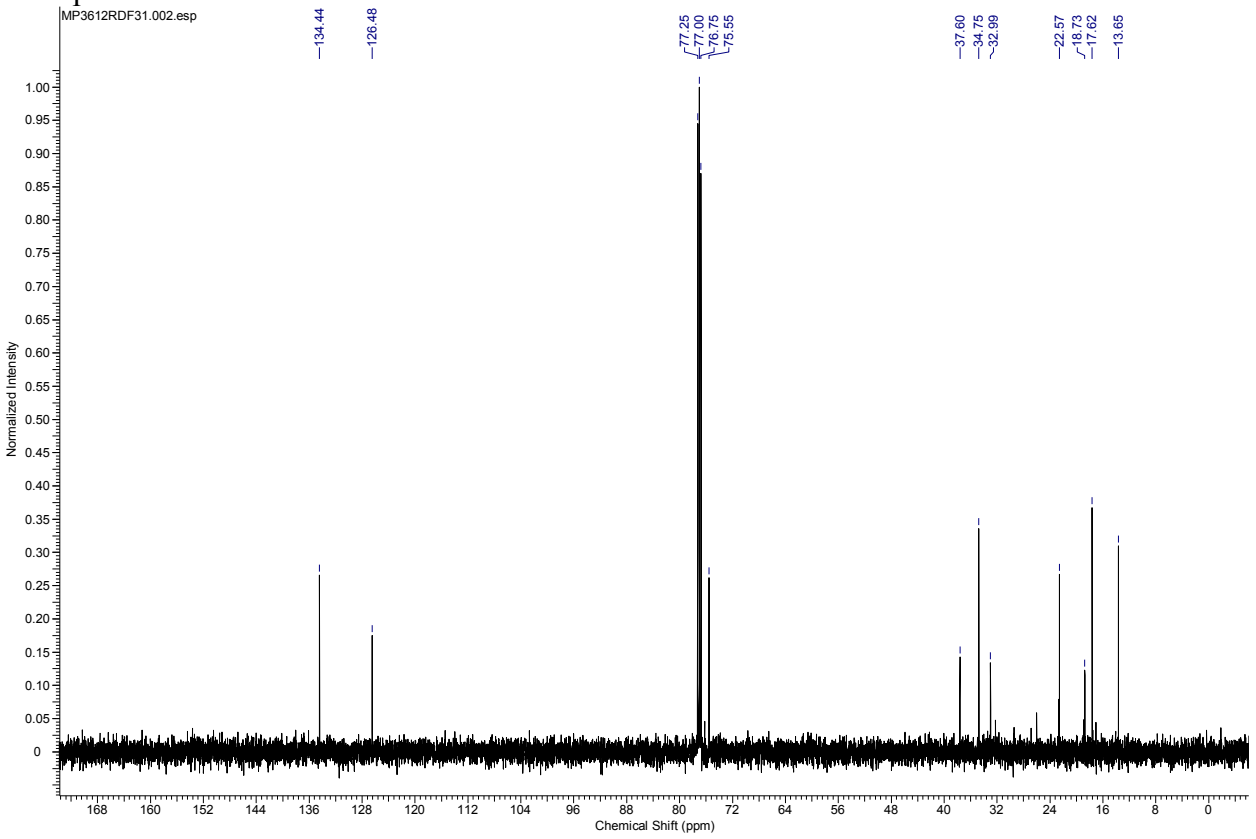

^{1}H Spectrum of **230p**

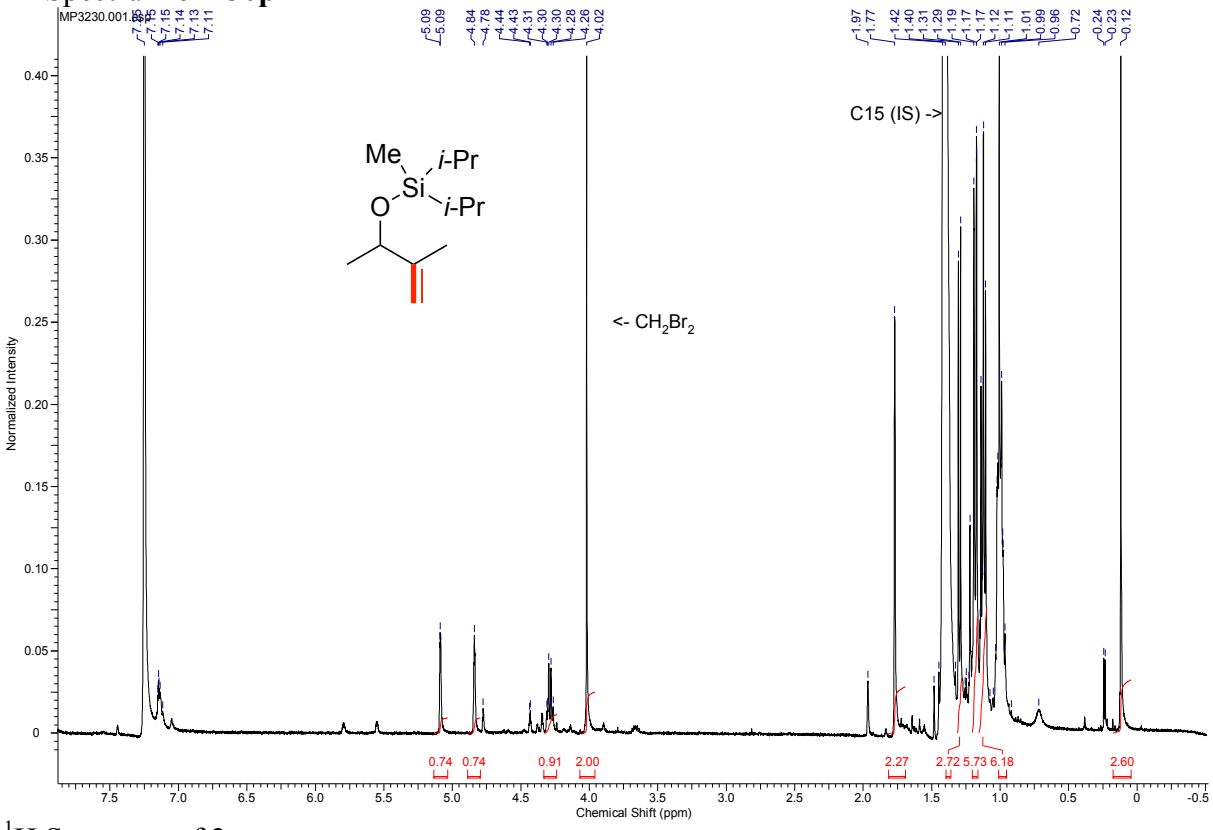

^{1}H Spectrum of **2q**

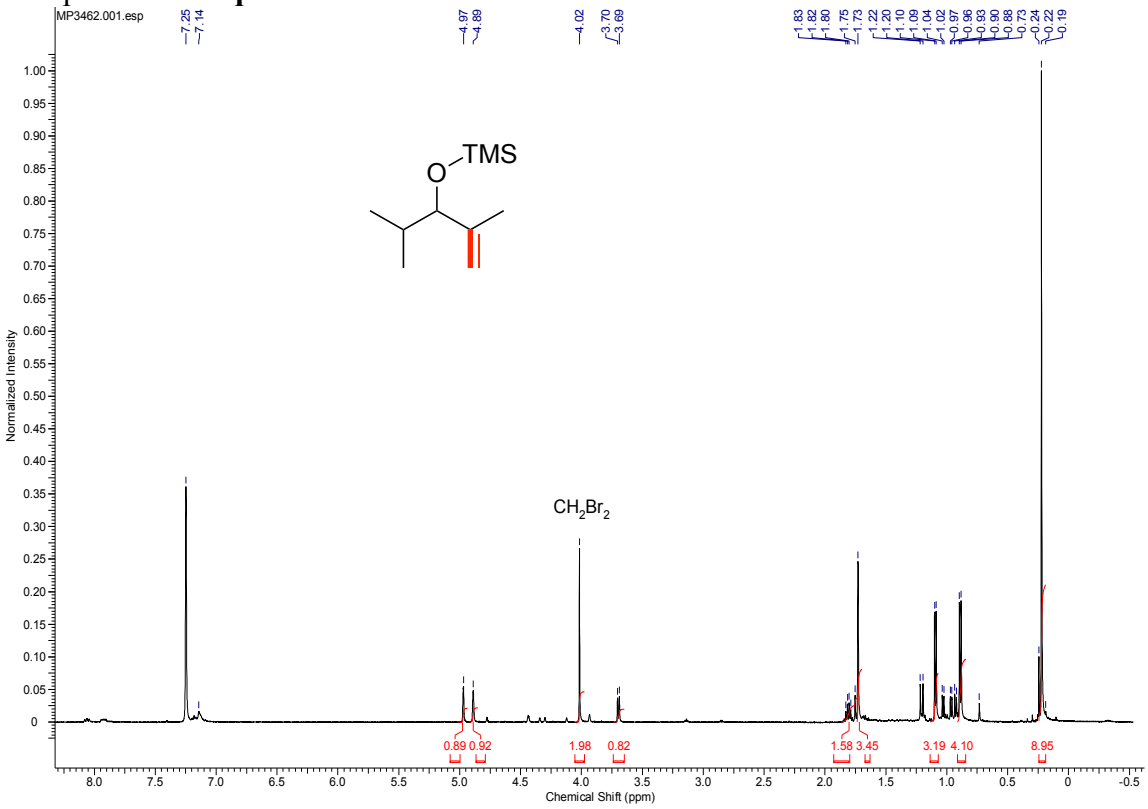

^{1}H Spectrum of **2r**

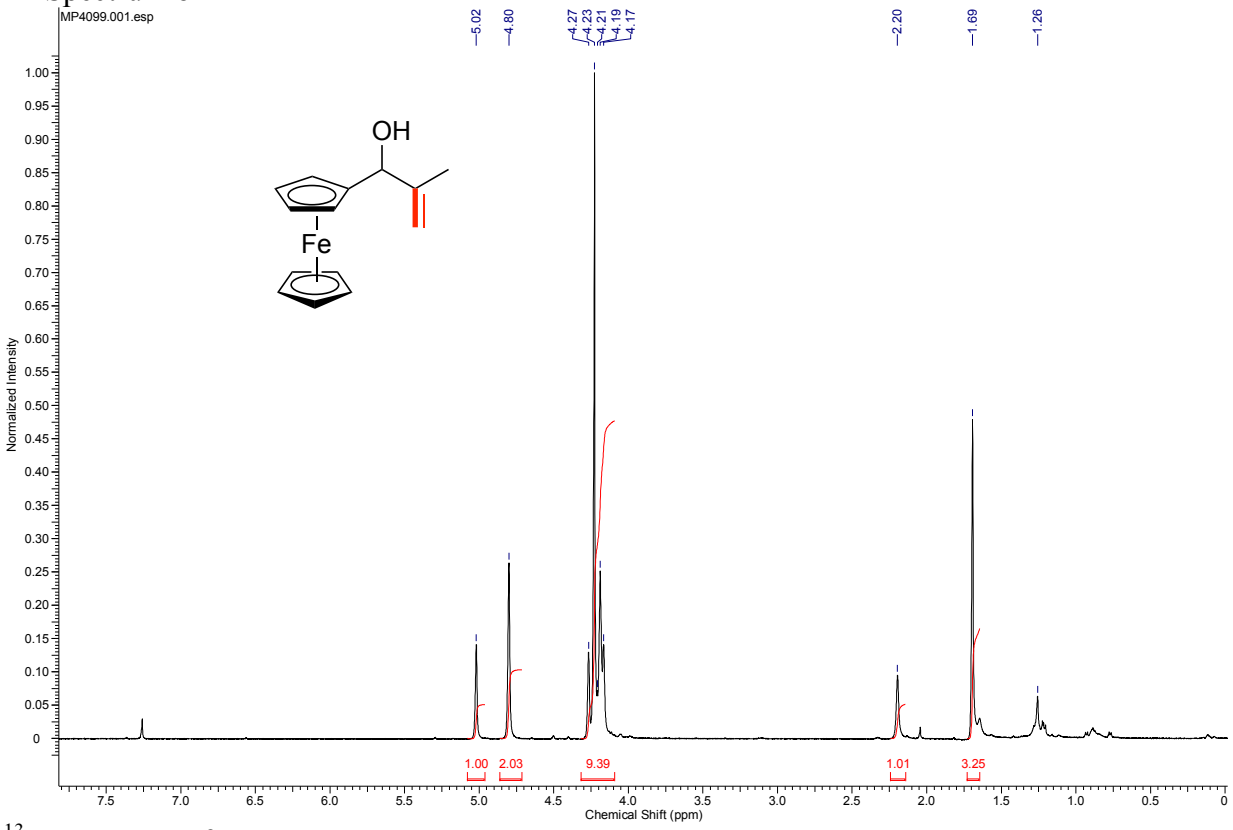

^{13}C Spectrum of **2r**

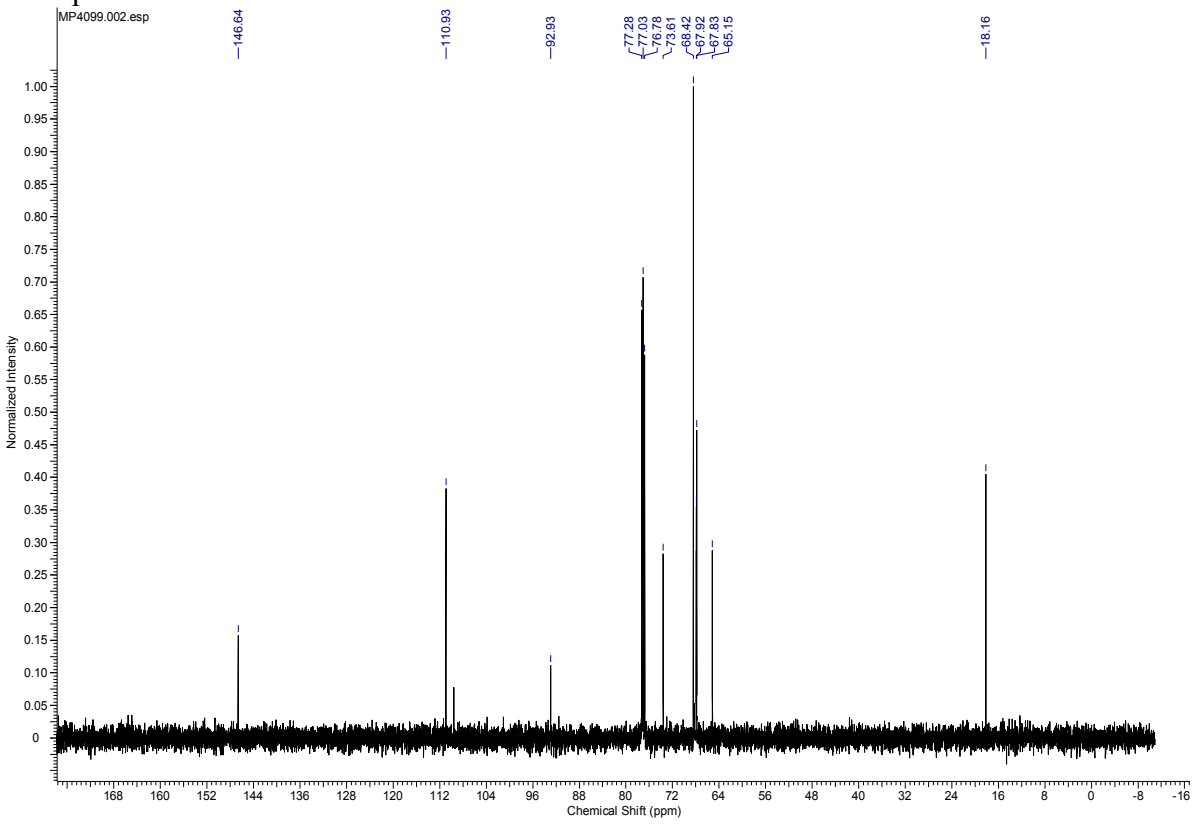

^{1}H Spectrum of **230s**

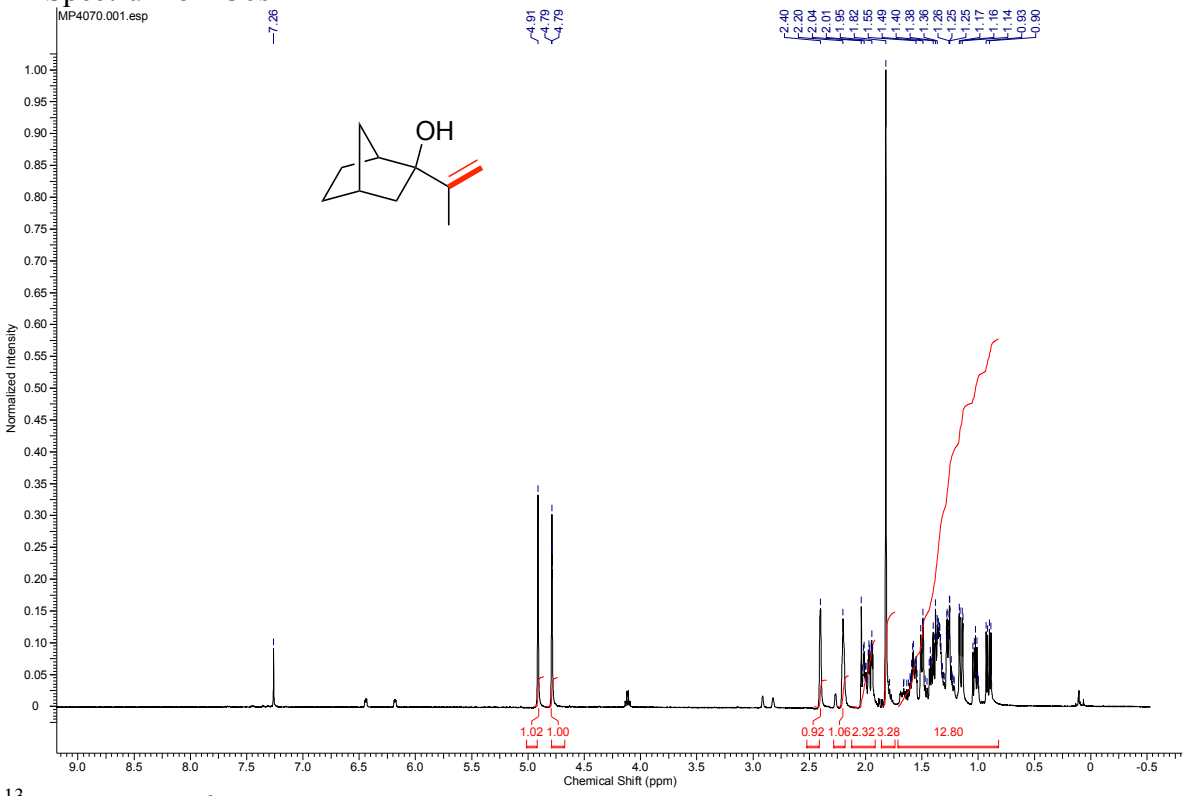

^{13}C Spectrum of **230s**

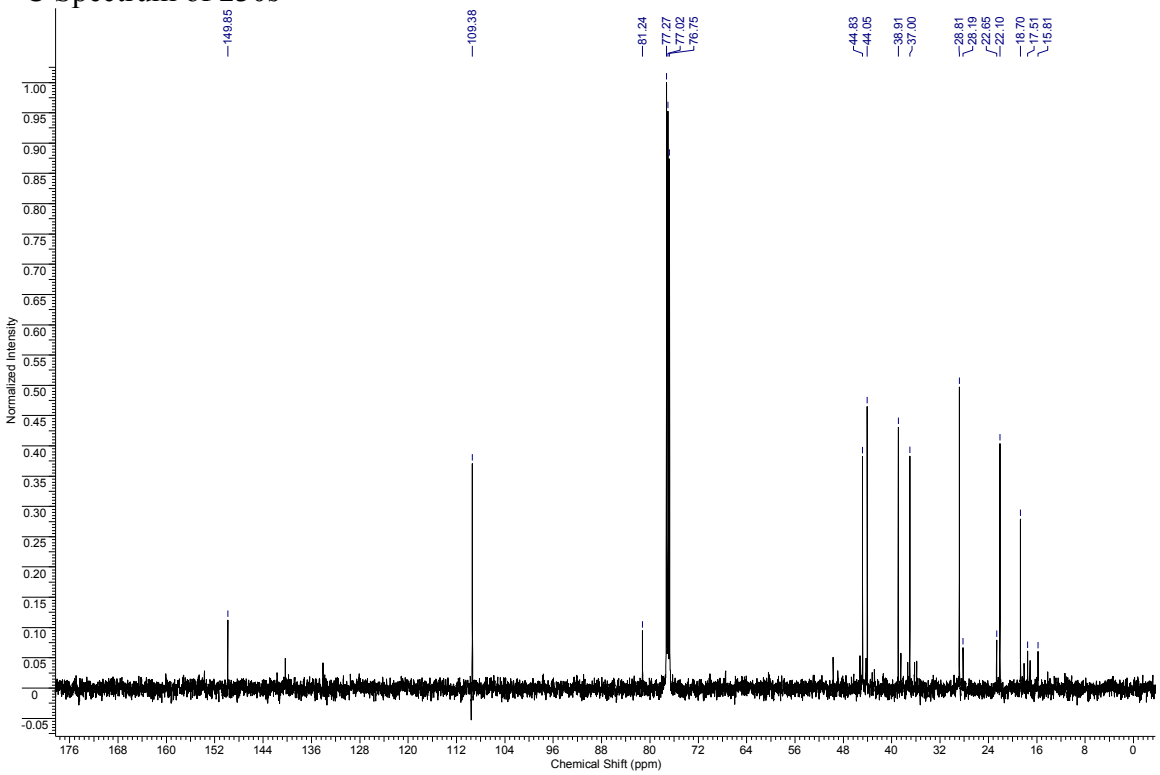

^{1}H Spectrum of **230t**

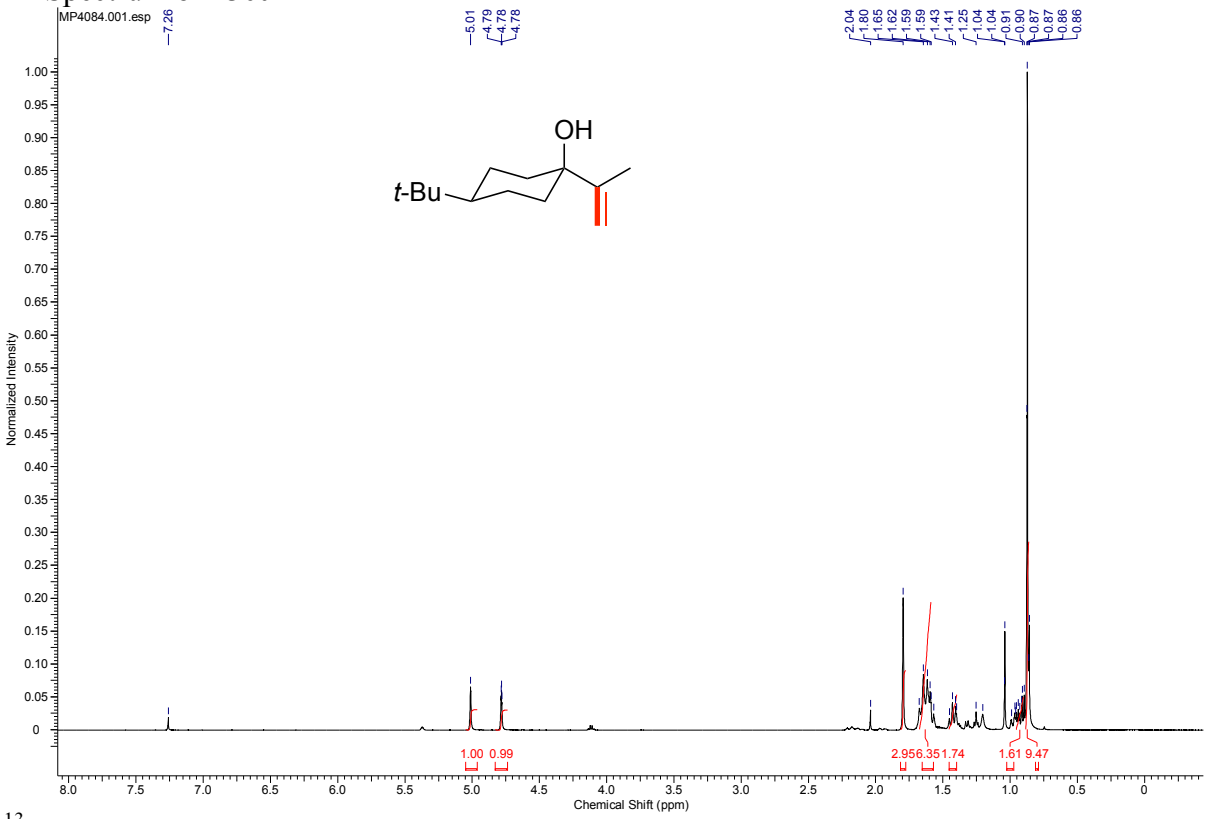

^{13}C Spectrum of **230t**

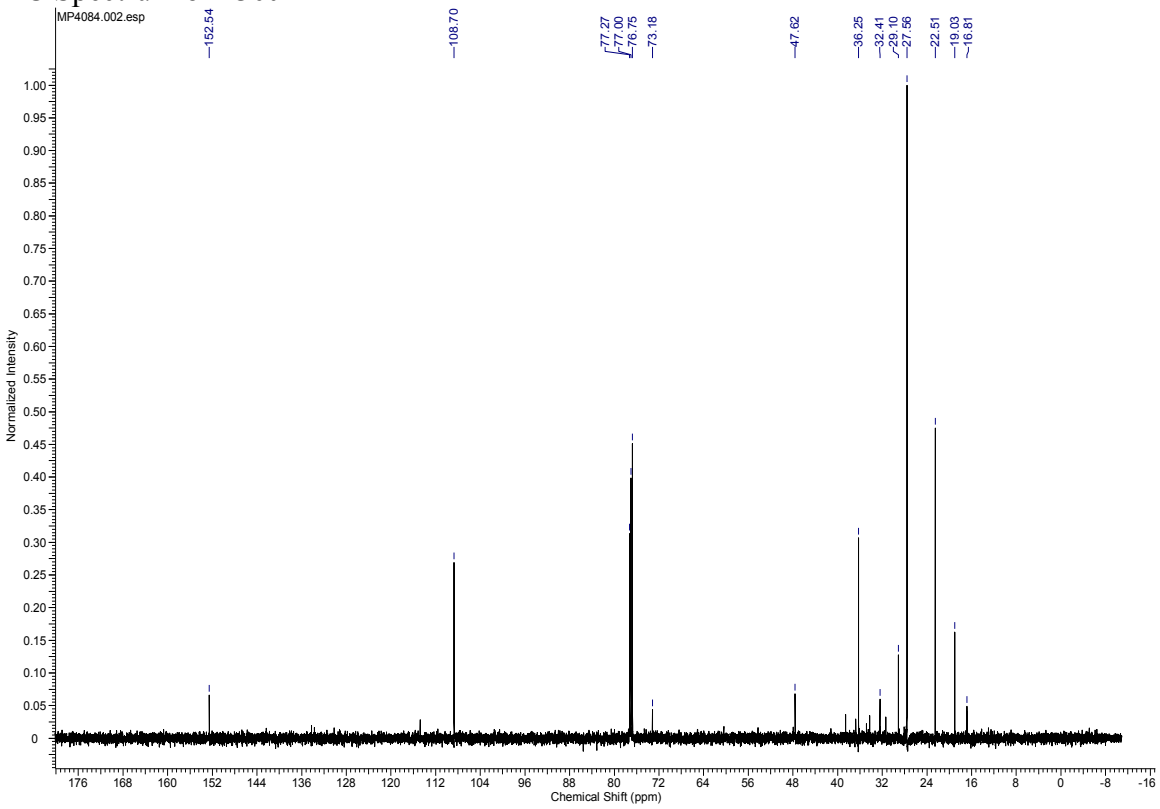

^{1}H Spectrum of **230u**

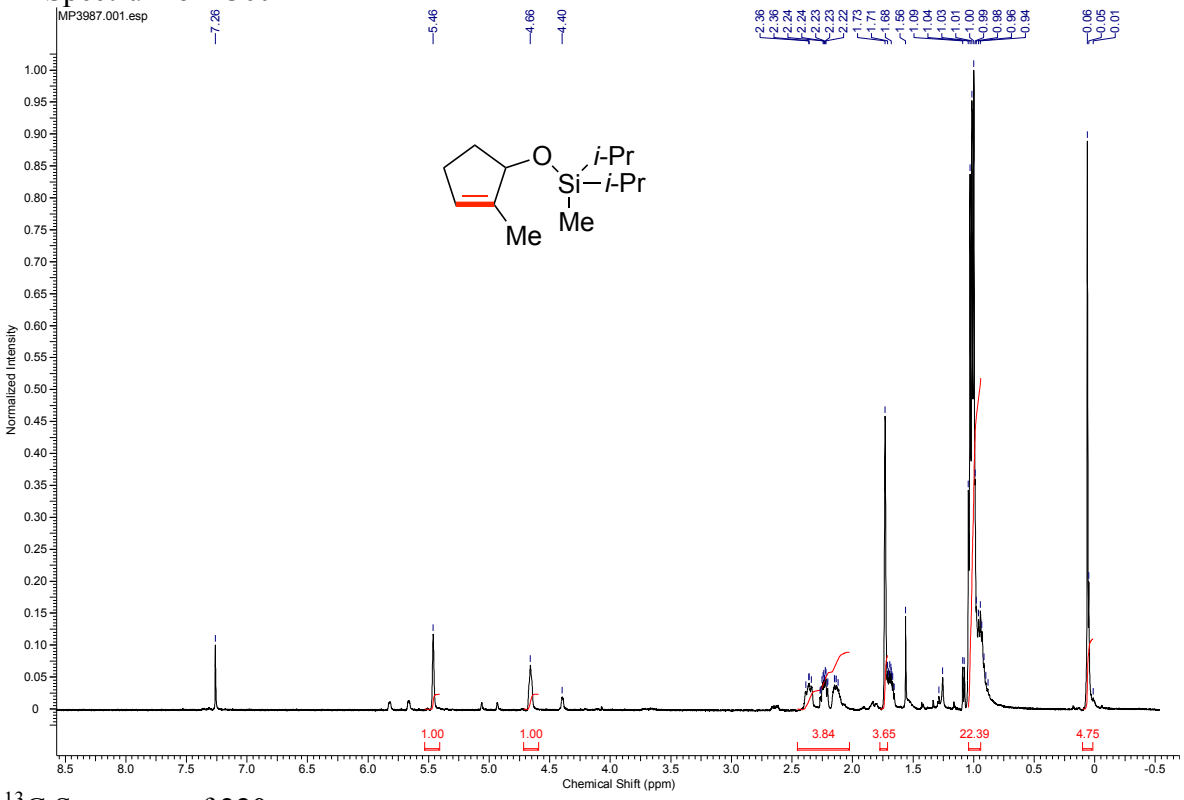

^{13}C Spectrum of **230u**

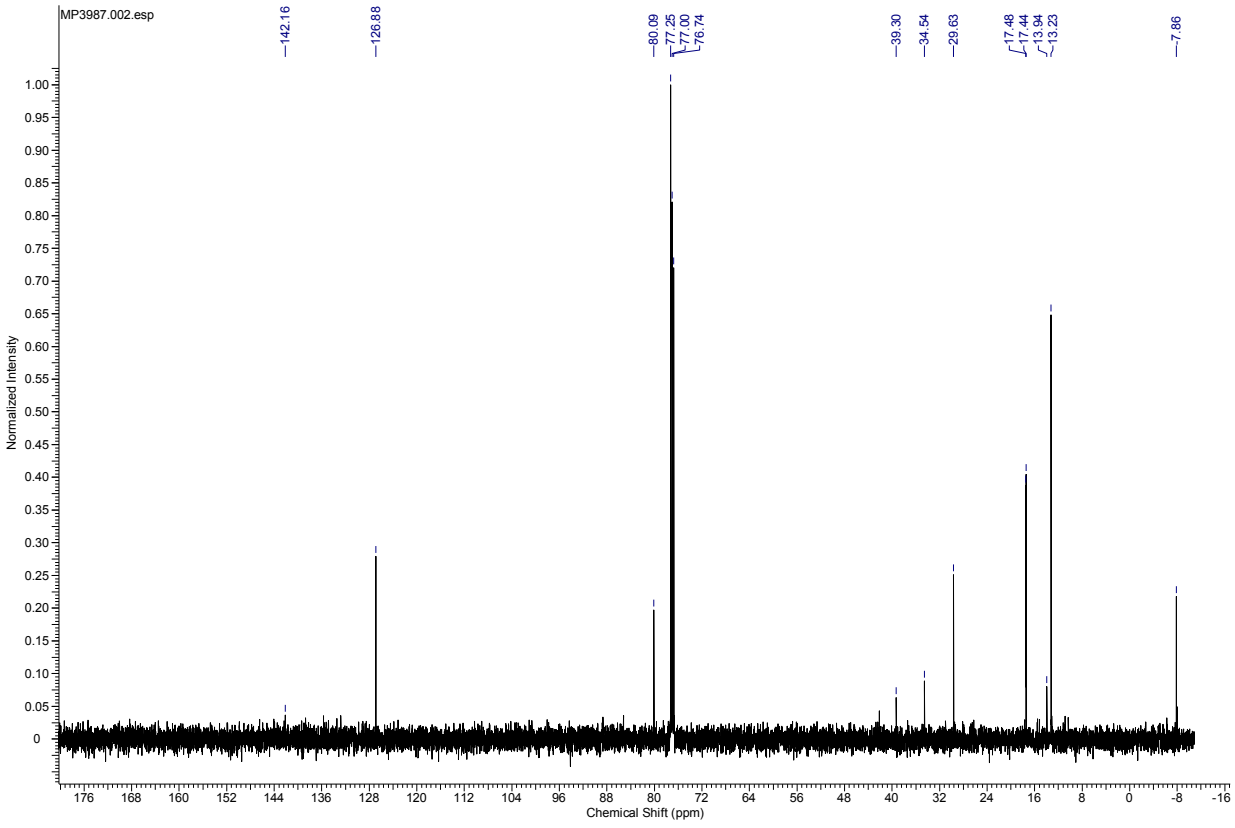

^{1}H Spectrum of **230v**

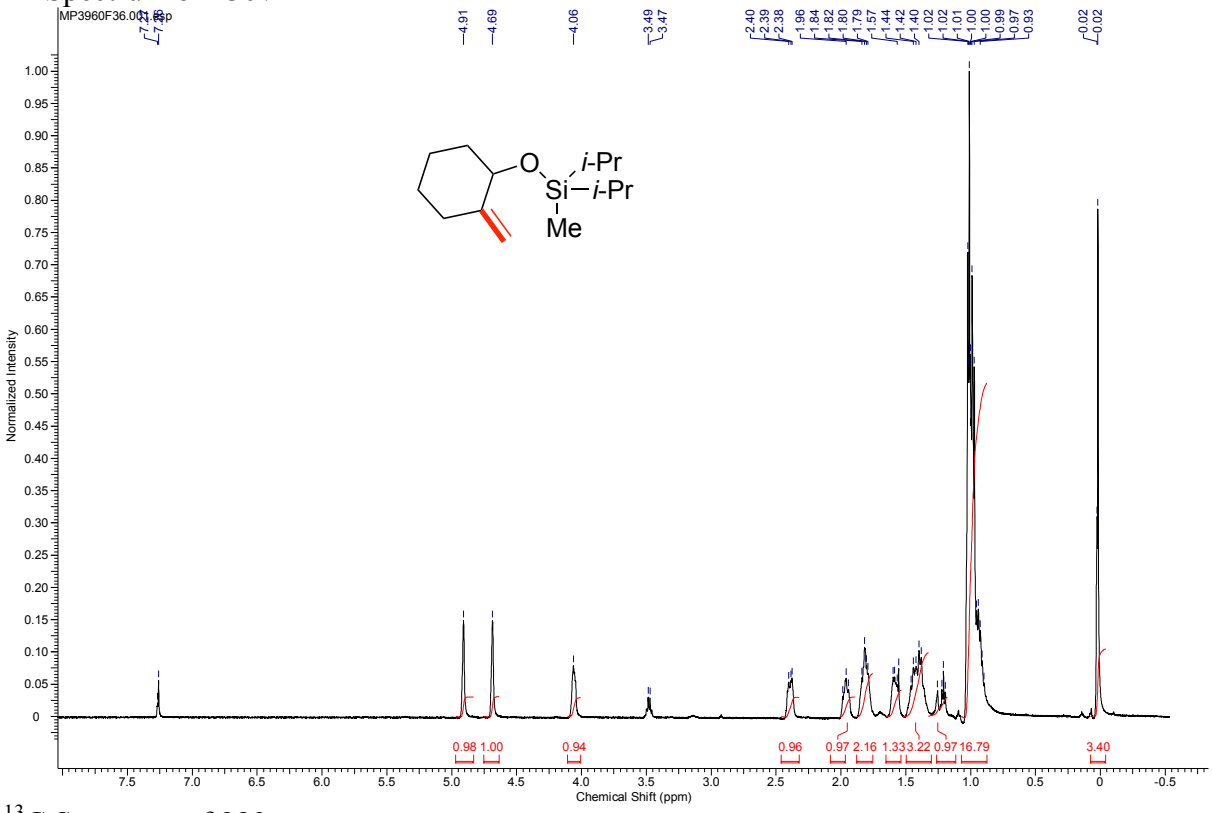

^{13}C Spectrum of **230v**

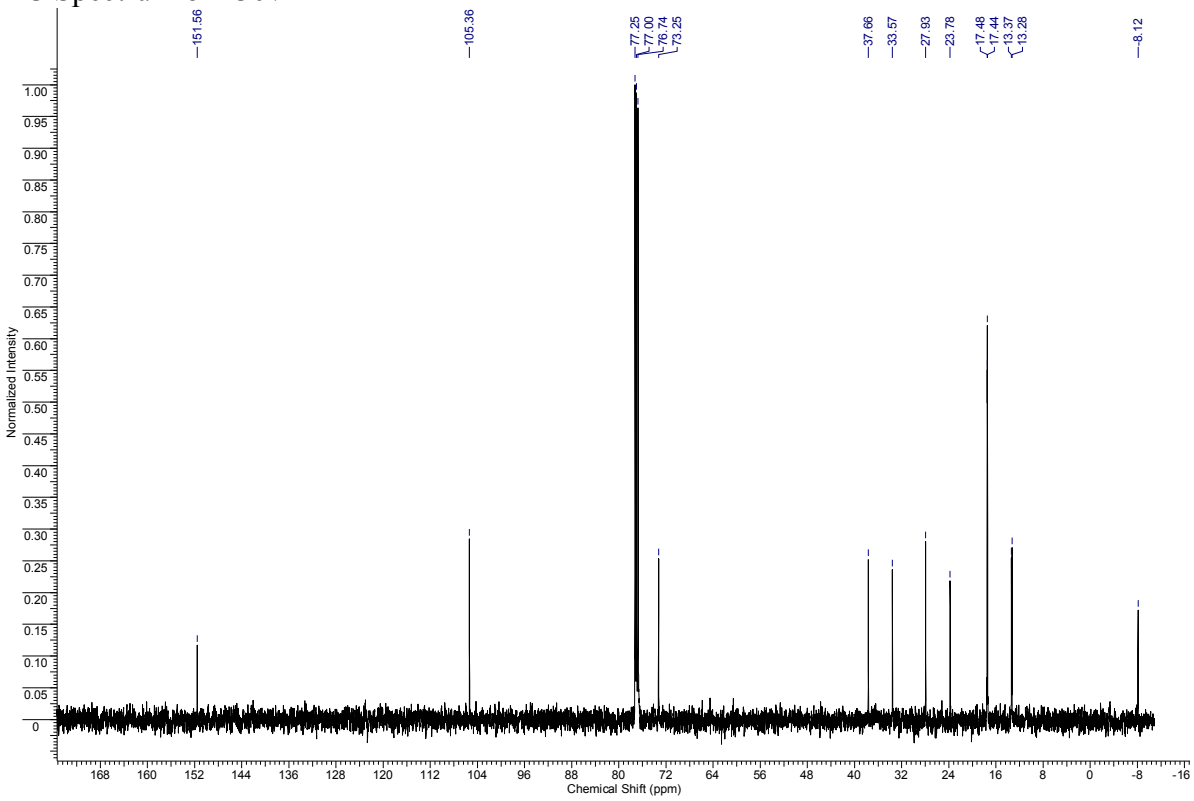

^{1}H Spectrum of **230w**

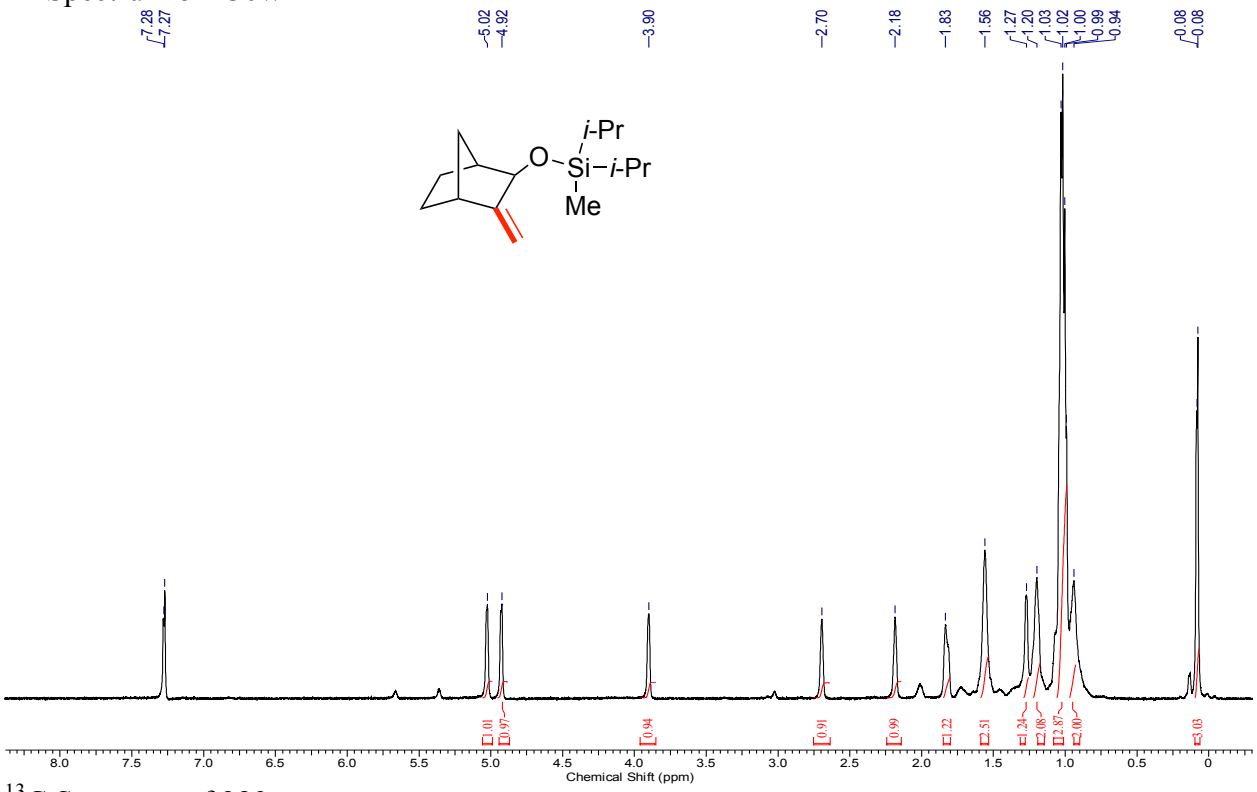

^{13}C Spectrum of **230w**

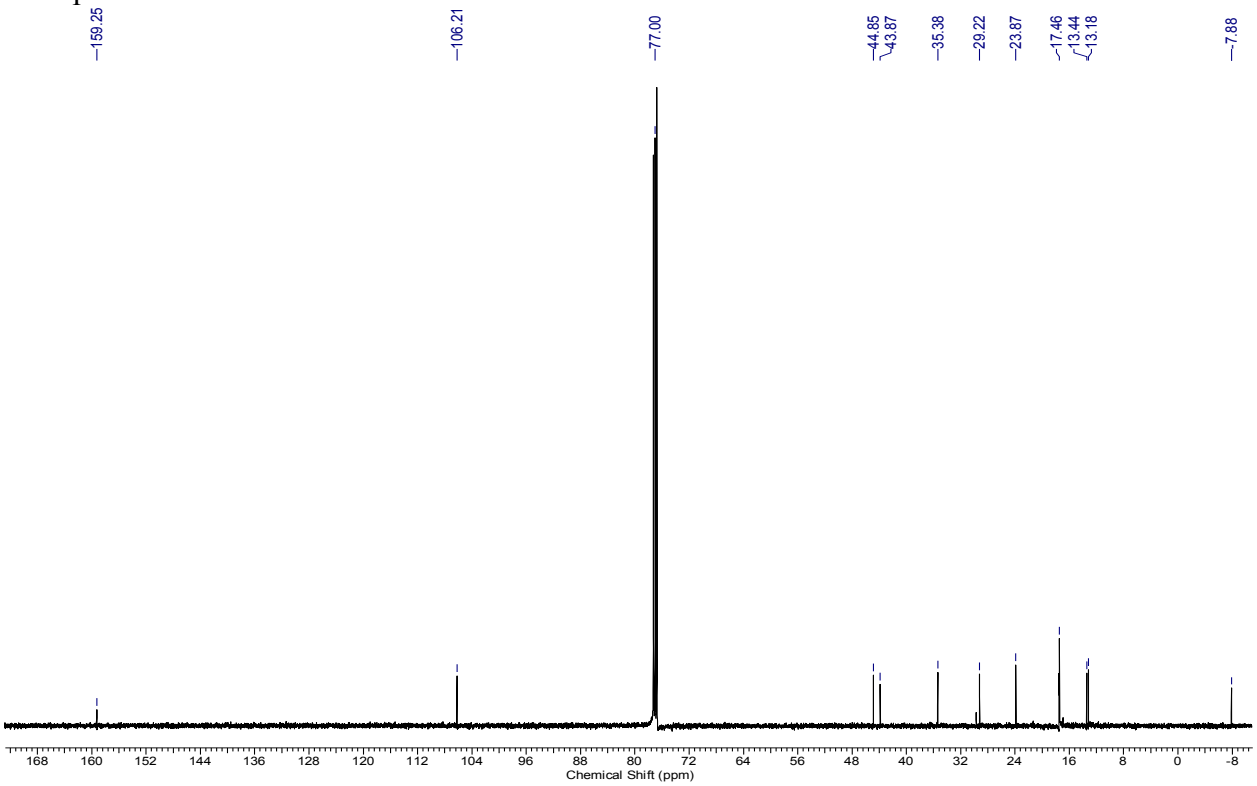

^{1}H Spectrum of **230x**

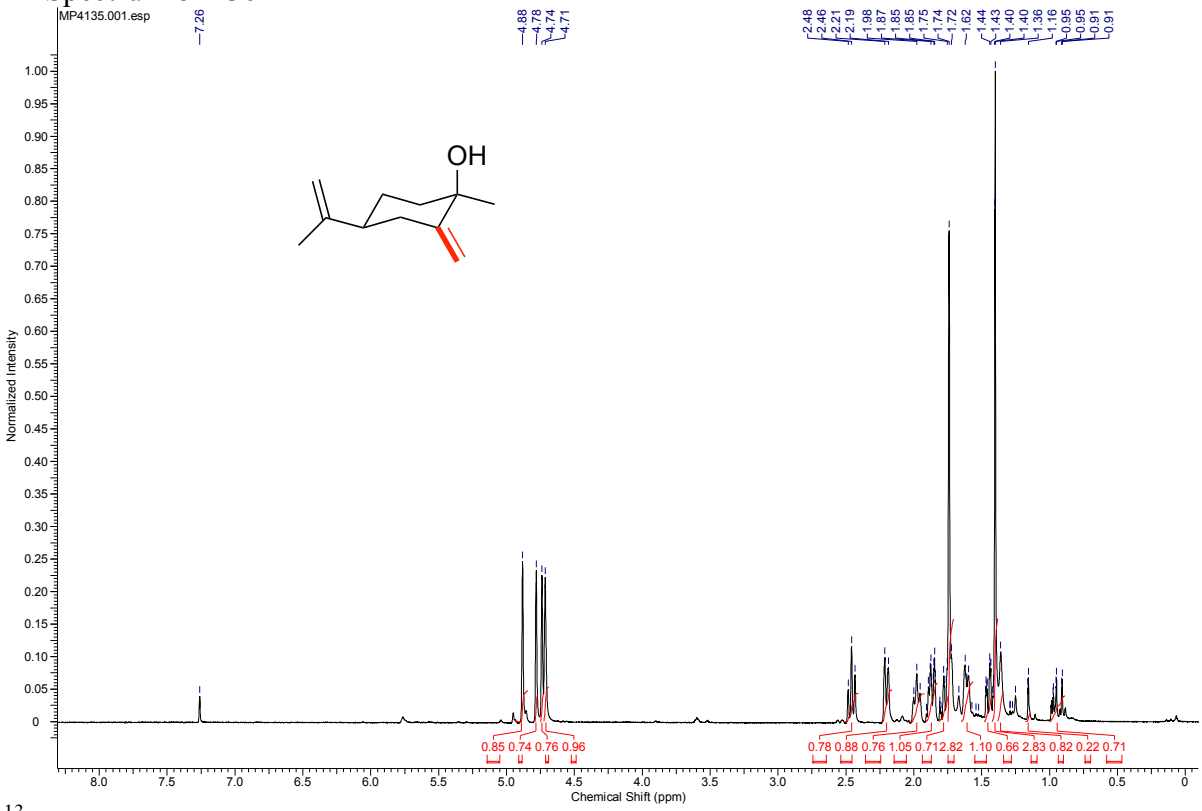

^{13}C Spectrum of **230x**

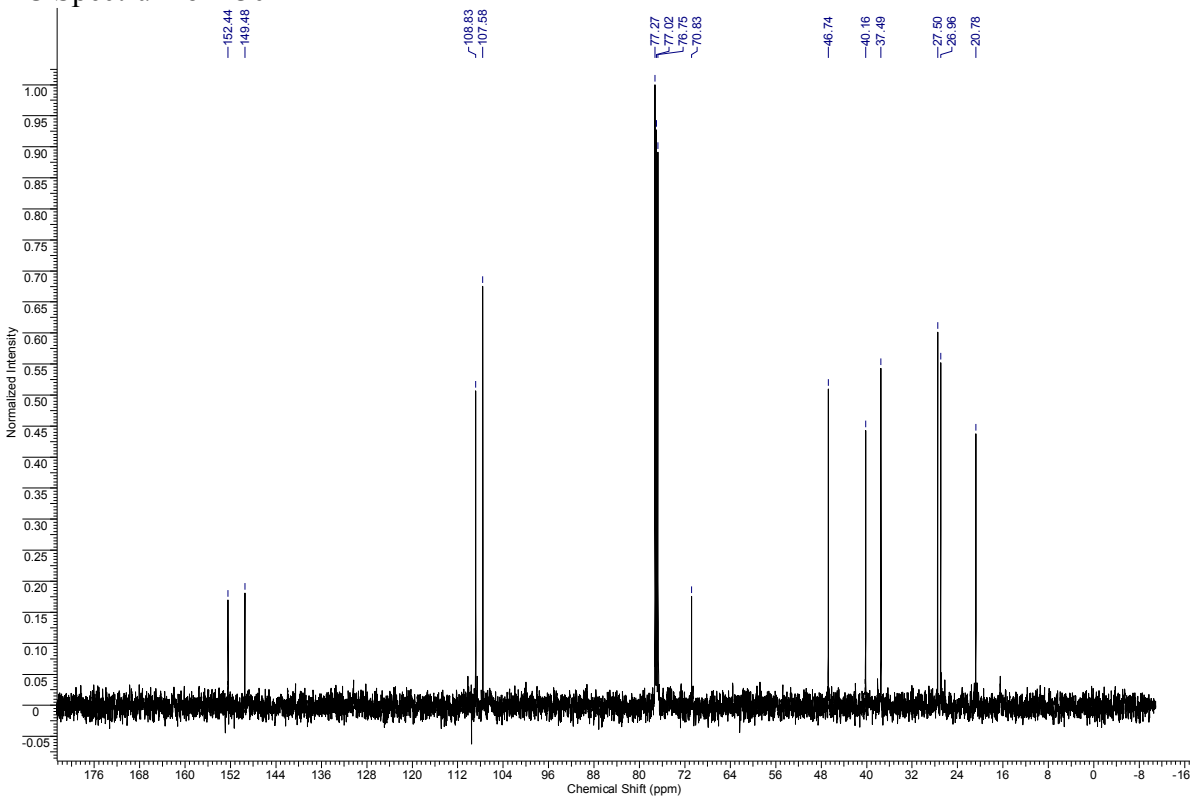

^{1}H Spectrum of **2y** and **2y'**

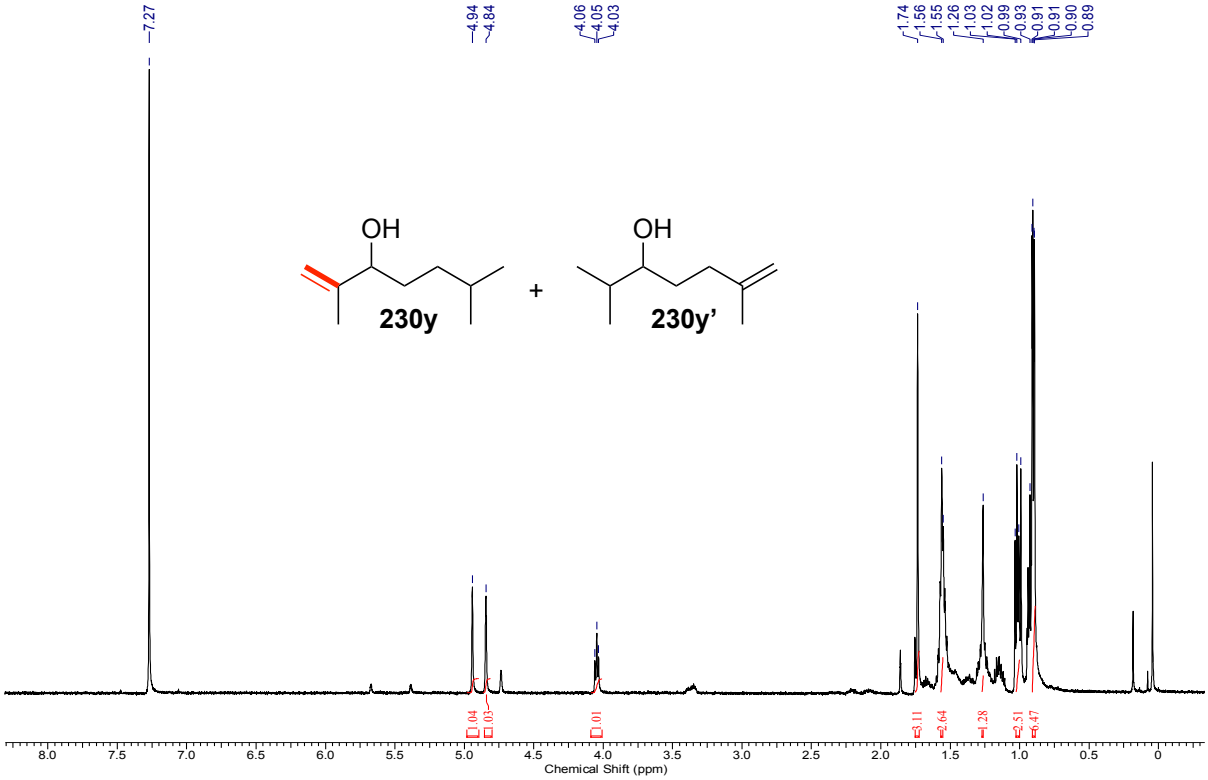

^{13}C Spectrum of **230y** and **230y'**

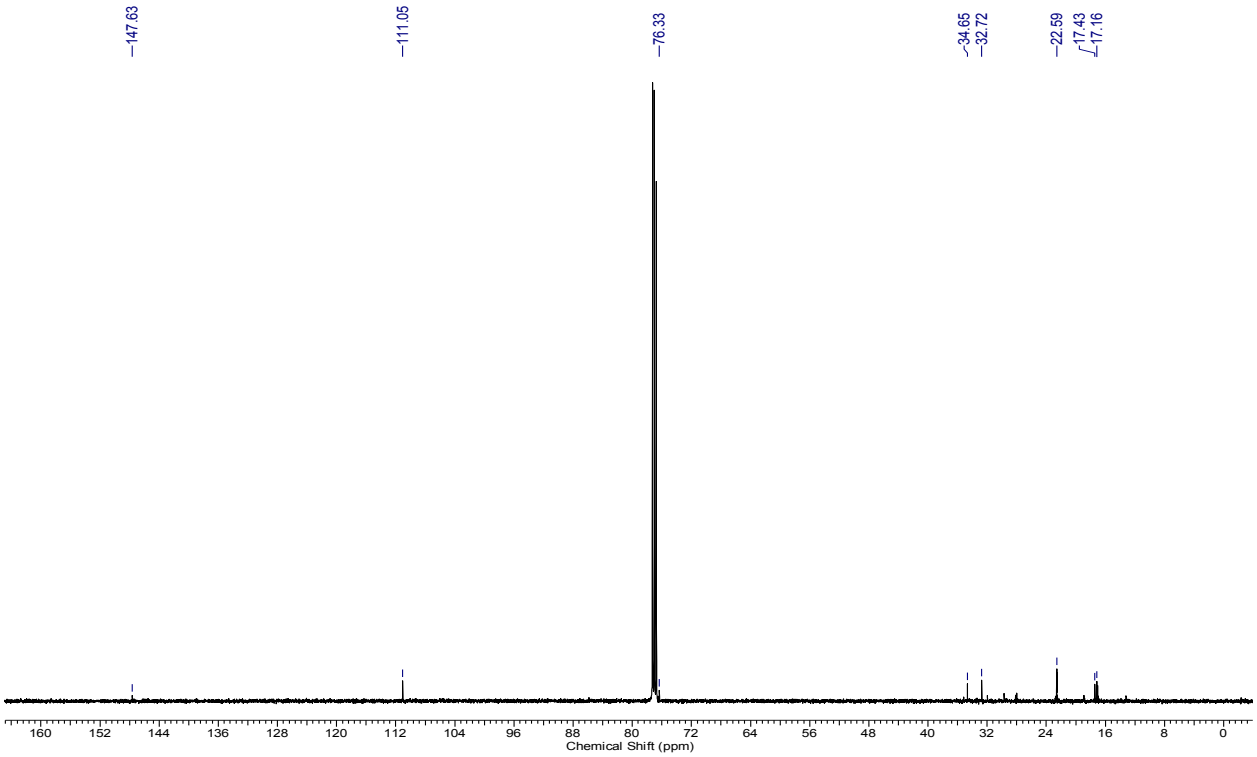

^{1}H Spectrum of **230z**

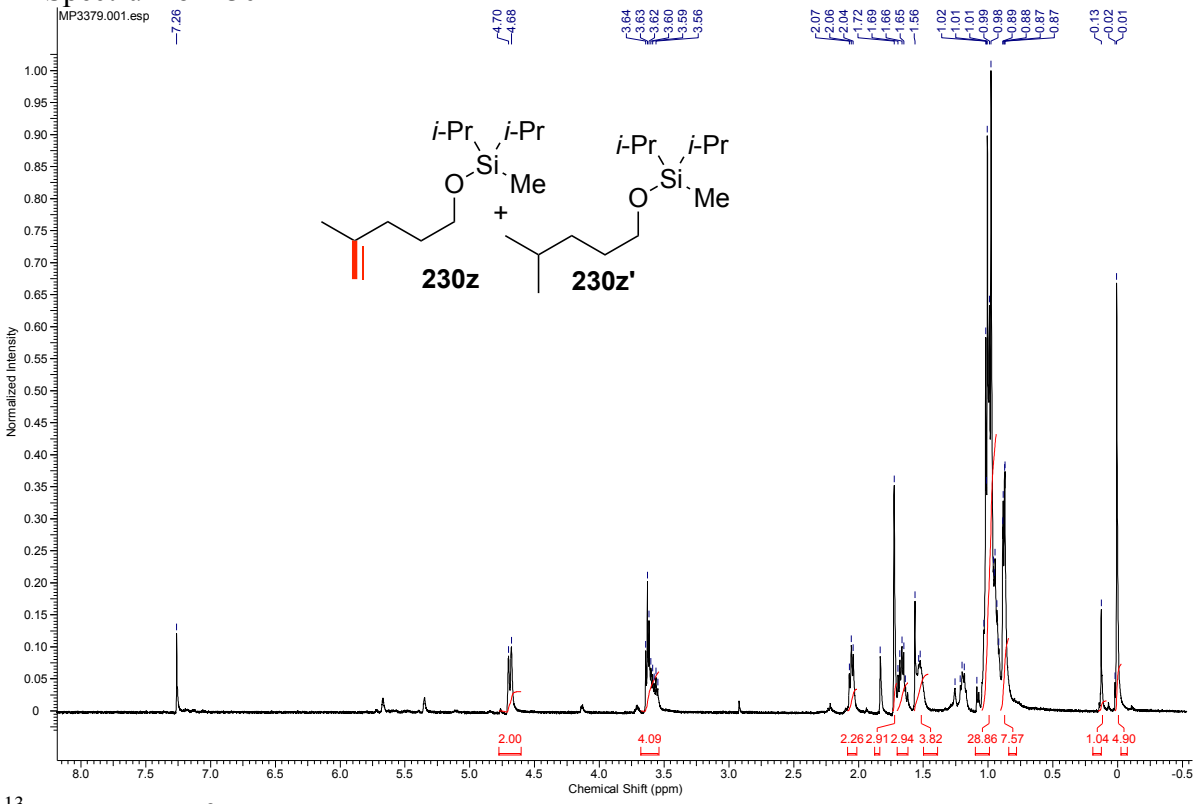

^{13}C Spectrum of **230z**

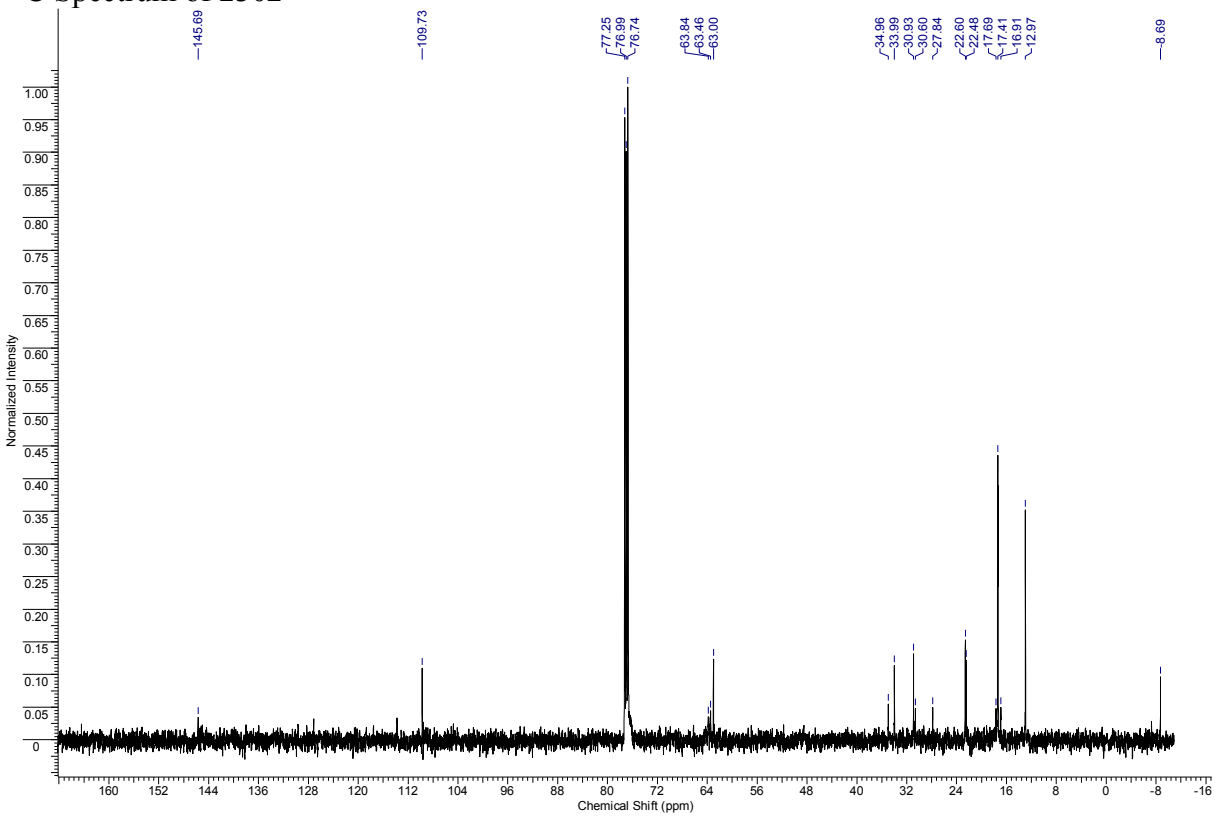

^{1}H Spectrum of **230aa, 230aa', and 230aa''**

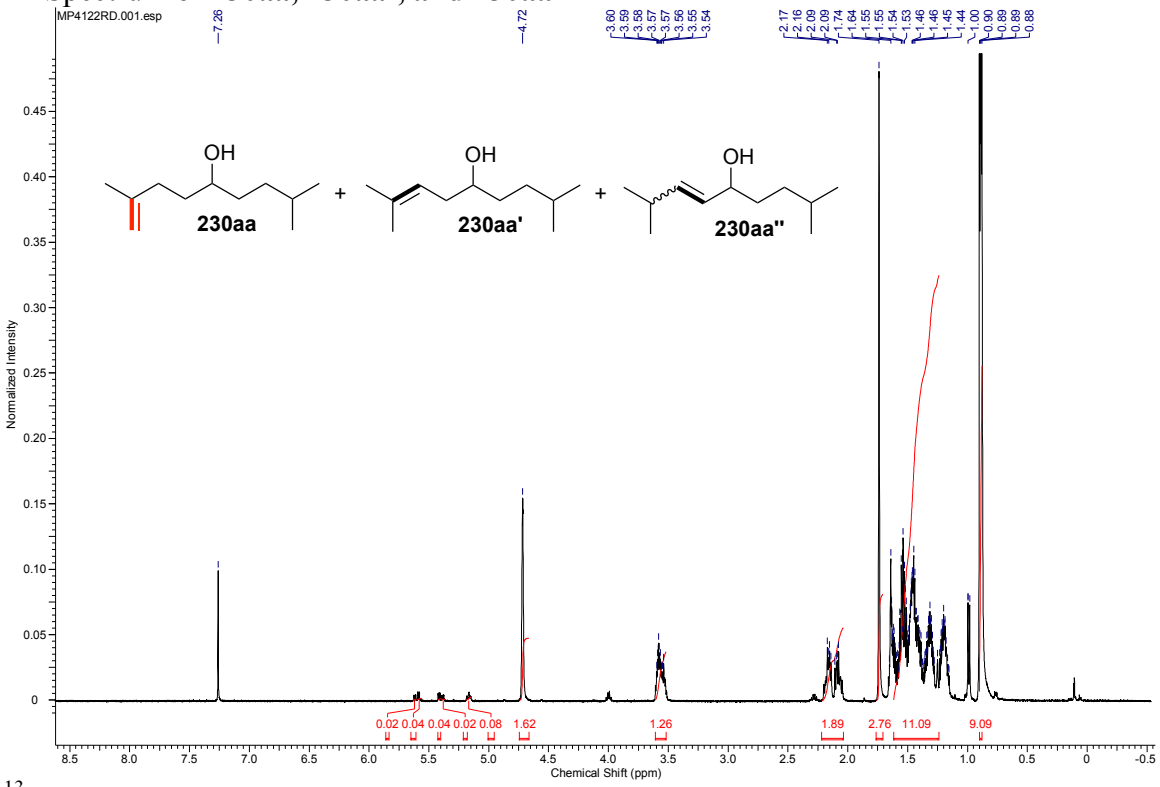

^{13}C Spectrum of **230aa**

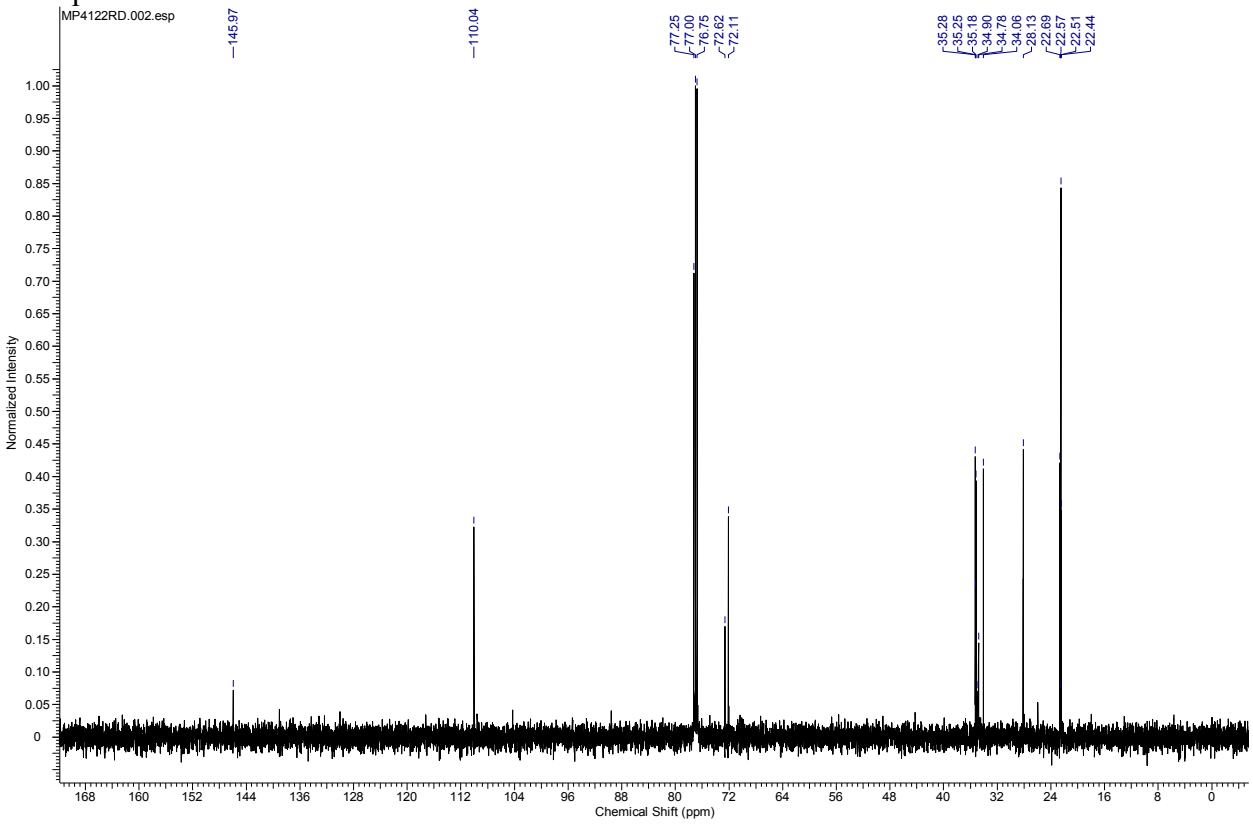

^{1}H Spectrum of **230ab**

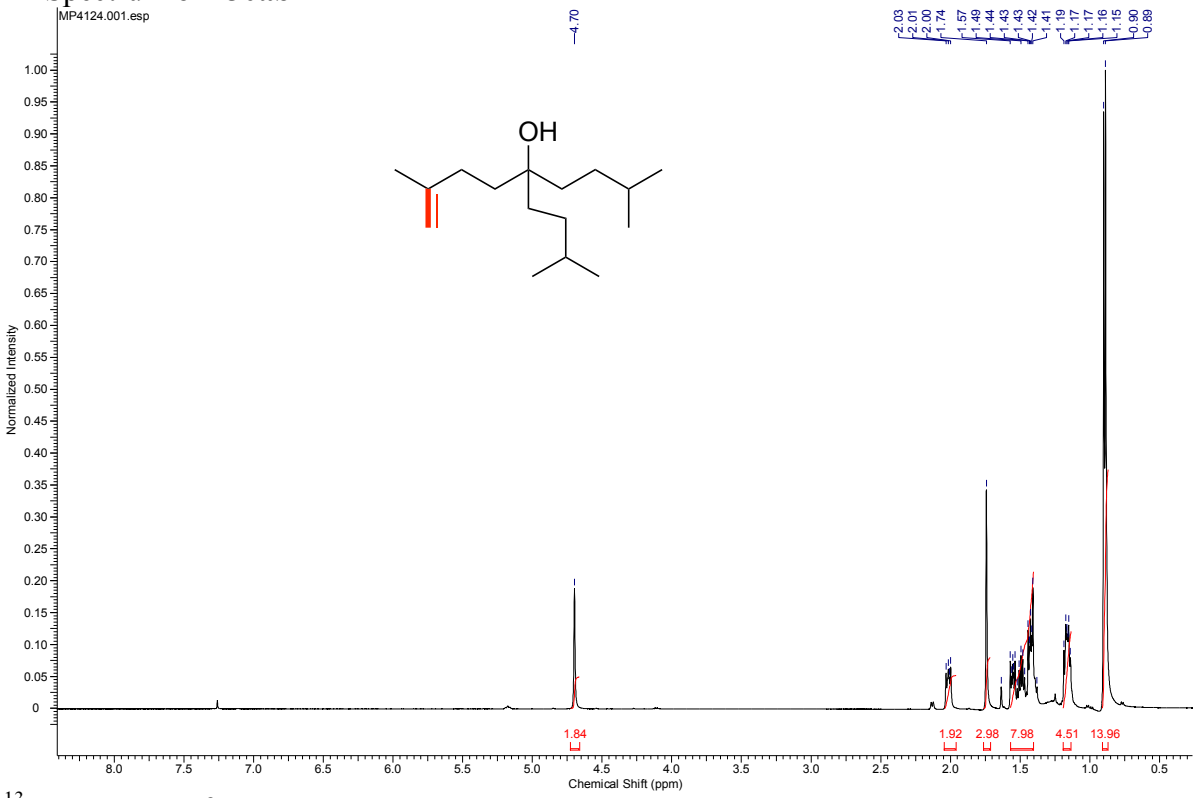

^{13}C Spectrum of **230ab**

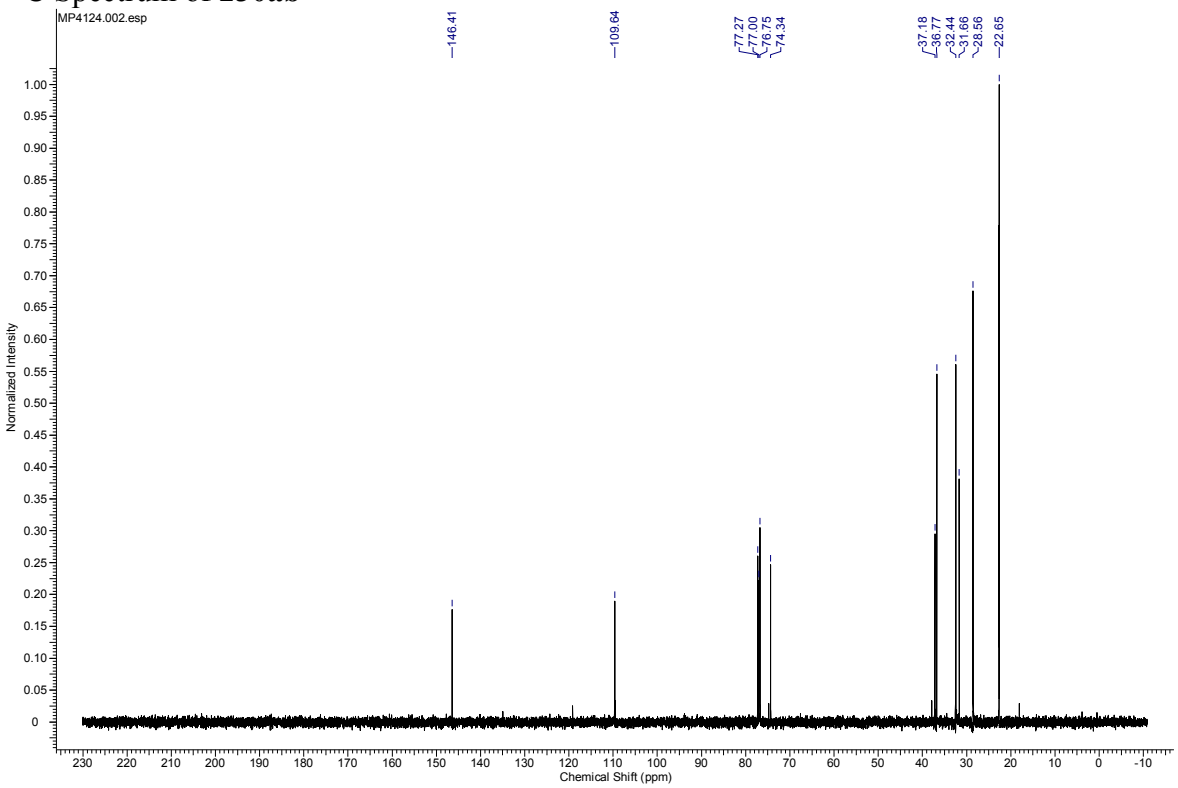

^{1}H Spectrum of **230ac**

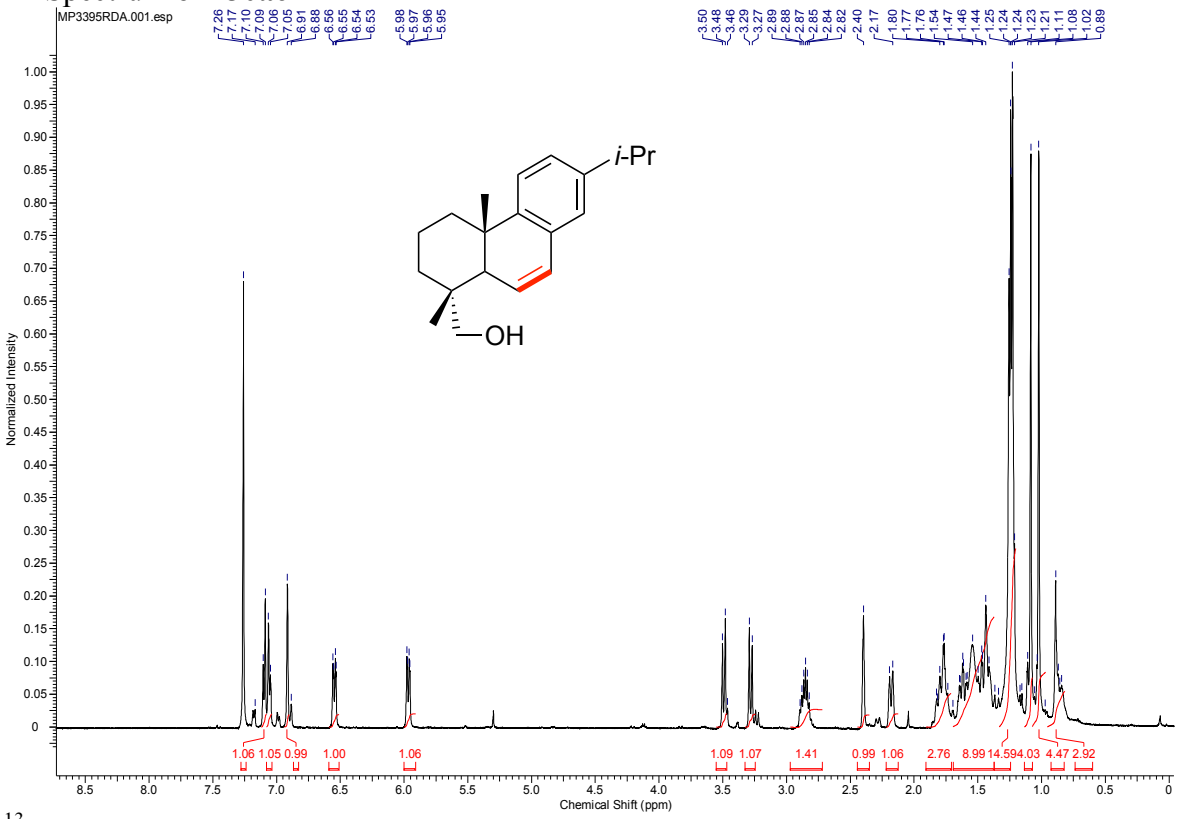

^{13}C Spectrum of **230ac**

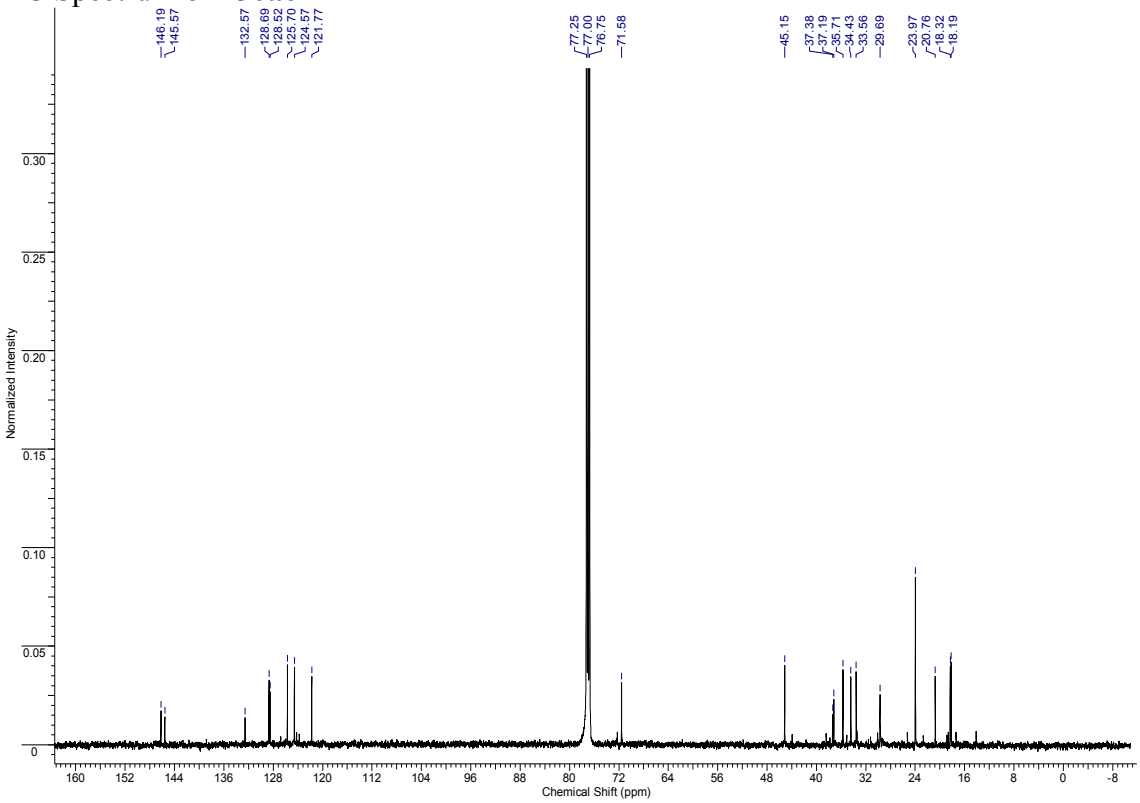

^{1}H Spectrum of **237**

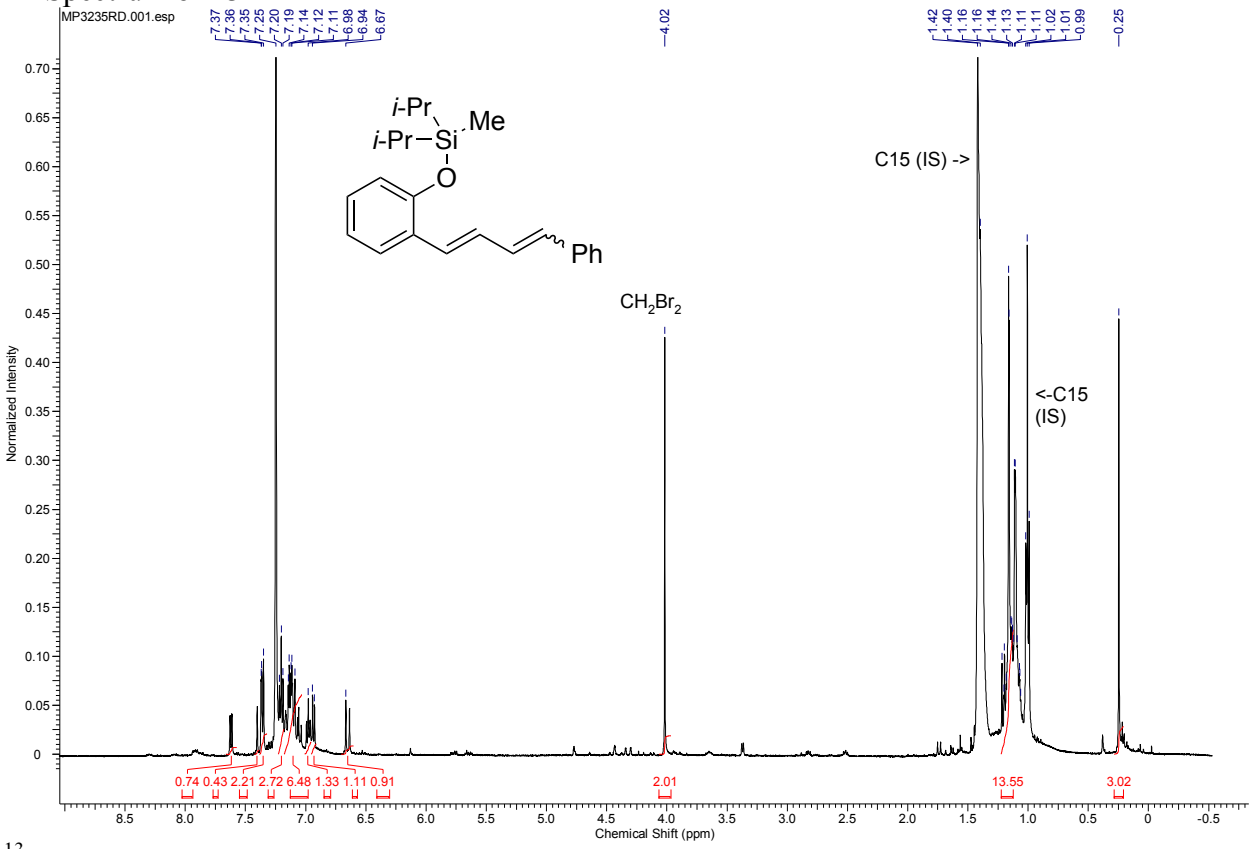

^{13}C-Dept Spectrum of **237**

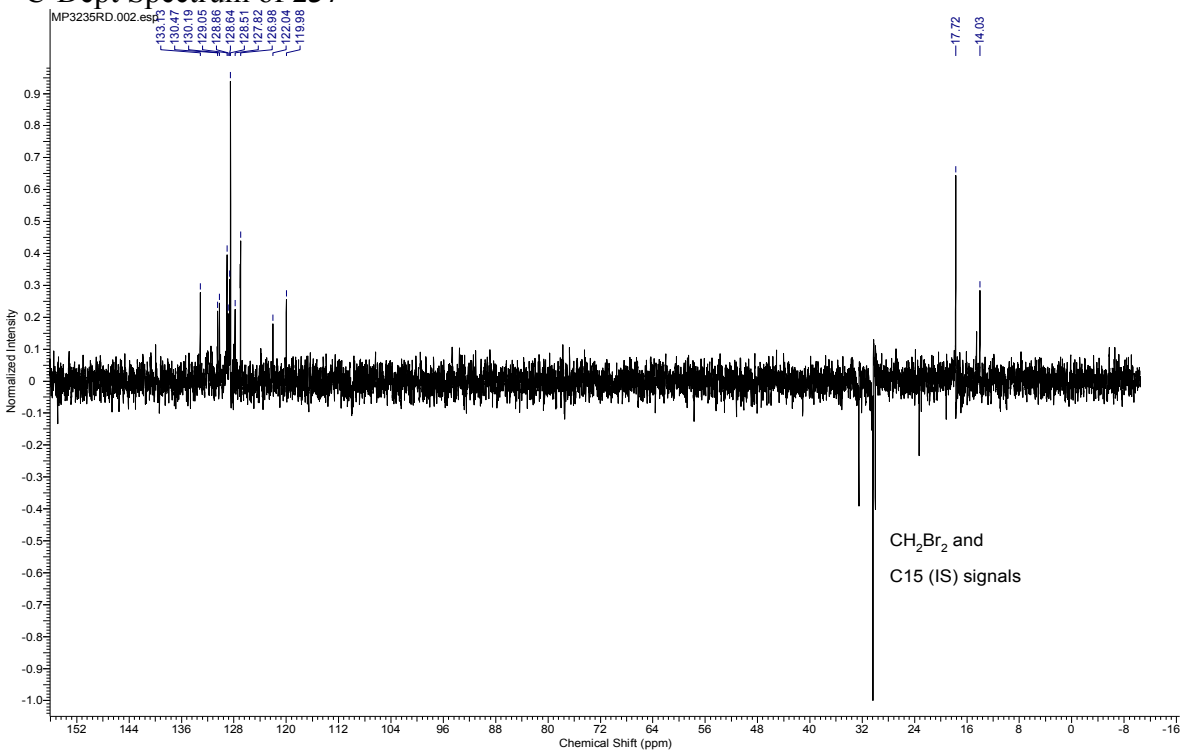

^{1}H Spectrum of **233** (NMR Yield)

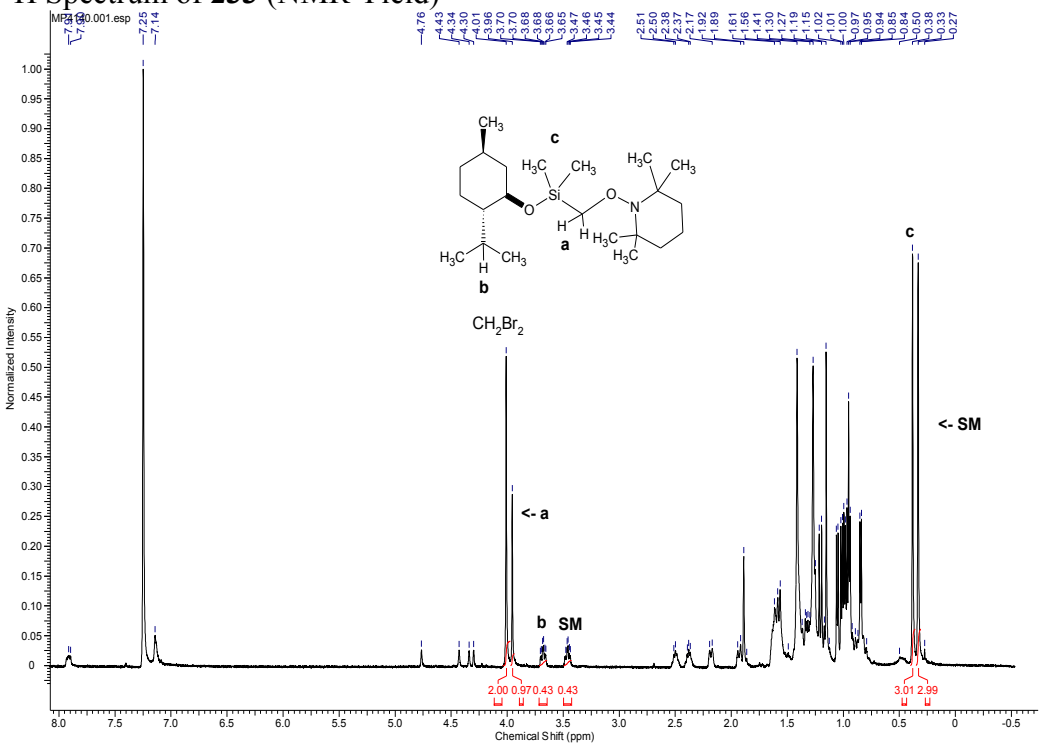

Copyright Permissions

Chapter 2 reproduced in part with permission from:

"Endo-Selective Pd-Catalyzed Silyl Methyl Heck Reaction " Parasram, M.; Iaroshenko, V. O.; Gevorgyan, V. *J. Am. Chem. Soc.* **2014**, *136*, 17926. *ACS AuthorChoice*. Copyright 2014 American Chemical Society.

Chapter 5 reproduced in part with permission from:

"Photoinduced Formation of Hybrid Aryl Pd-Radical Species Capable of 1,5-HAT: Selective Catalytic Oxidation of Silyl Ethers into Silyl Enol Ethers" Parasram, M.; Chuentragool, P.; Sarkar, D.; Gevorgyan, V. *J. Am. Chem. Soc.* **2016**, *138*, 6340. Copyright 2016 American Chemical Society.

American Chemical Society's Policy on Theses and Dissertations

If your university requires you to obtain permission, you must use the RightsLink permission system.
See RightsLink instructions at http://pubs.acs.org/page/copyright/permissions.html.

This is regarding request for permission to include **your** paper(s) or portions of text from **your** paper(s) in your thesis. Permission is now automatically granted; please pay special attention to the **implications** paragraph below. The Copyright Subcommittee of the Joint Board/Council Committees on Publications approved the following:

Copyright permission for published and submitted material from theses and dissertations
ACS extends blanket permission to students to include in their theses and dissertations their own articles, or portions thereof, that have been published in ACS journals or submitted to ACS journals for publication, provided that the ACS copyright credit line is noted on the appropriate page(s).

Publishing **implications** of electronic publication of theses and dissertation material
Students and their mentors should be aware that posting of theses and dissertation material on the Web prior to submission of material from that thesis or dissertation to an ACS journal may affect publication in that journal. Whether Web posting is considered prior publication may be evaluated on a case-by-case basis by the journal's editor. If an ACS journal editor considers Web posting to be "prior publication", the paper will not be accepted for publication in that journal. If you intend to submit your unpublished paper to ACS for publication, check with the appropriate editor prior to posting your manuscript electronically.

Reuse/Republication of the Entire Work in Theses or Collections: Authors may reuse all or part of the Submitted, Accepted or Published Work in a thesis or dissertation that the author writes and is required to submit to satisfy the criteria of degree-granting institutions. Such reuse is permitted subject to the ACS' "Ethical Guidelines to Publication of Chemical Research" (http://pubs.acs.org/page/policy/ethics/index.html); the author should secure written confirmation (via letter or email) from the respective ACS journal editor(s) to avoid potential conflicts with journal prior publication*/embargo policies. Appropriate citation of the Published Work must be made. If the thesis or dissertation to be published is in electronic format, a direct link to the Published Work must also be included using the ACS Articles on Request author-directed link – see http://pubs.acs.org/page/policy/articlesonrequest/index.html

* Prior publication policies of ACS journals are posted on the ACS website at
http://pubs.acs.org/page/policy/prior/index.html

If your paper has **not** yet been published by ACS, please print the following credit line on the first page of your article: "Reproduced (or 'Reproduced in part') with permission from [JOURNAL NAME], in press (or 'submitted for publication'). Unpublished work copyright [CURRENT YEAR] American Chemical Society." Include appropriate information.

If your paper has already been published by ACS and you want to include the text or portions of the text in your thesis/dissertation, please print the ACS copyright credit line on the first page of your article: "Reproduced (or 'Reproduced in part') with permission from [FULL REFERENCE CITATION.] Copyright [YEAR] American Chemical Society." Include appropriate information.

Submission to a Dissertation Distributor: If you plan to submit your thesis to UMI or to another dissertation distributor, you should not include the unpublished ACS paper in your thesis if the thesis will be disseminated electronically, until ACS has published your paper. After publication of the paper by ACS, you may release the entire thesis (**not the individual ACS article by itself**) for electronic dissemination through the distributor; ACS's copyright credit line should be printed on the first page of the ACS paper.

10/10/03, 01/15/04, 06/07/06, 04/07/10, 08/24/10, 02/28/11

iii. The inclusion or incorporation of article content in other works or services (other than normal quotations with an appropriate citation) that is then available for sale or licensing, for a fee;

iv. Use of articles or article content (other than normal quotations with appropriate citation) by a for-profit organizations for promotional purposes, whether for a fee or otherwise;

v. Sale of translated versions of the article that have not been authorized by license or other permission from the ACS

4. TERMINATION

ACS reserves the right to limit, suspend, or terminate your access to and use of the ACS Publications Division website and/or all ACS articles immediately upon detecting a breach of this License.

5. COPYRIGHTS; OTHER INTELLECTUAL PROPERTY RIGHTS

Except as otherwise specifically noted, ACS is the owner of all right, title and interest in the content of this ACS article, including, without limitations, graphs, charts, tables illustrations, and copyrightable supporting information. This ACS article is protected under the Copyright Laws of the United States Codified in Title 17 c the U.S. Code and subject to the Universal Copyright Convention and the Berne Copyright Convention. You agree not to remove or obscure copyright notices. You acknowledge that You have no claim to ownership of any part of this ACS article or other proprietary information accessed under this Agreement.

The names “American Chemical Society,” “ACS” and the titles of the journals and other ACS products are trademarks of ACS.

6. DISCLAIMER OF WARRANTIES; LIMITATION OF LIABILITY

ACS warrants that it is entitled to grant this Agreement.

EXCEPT AS SET FORTH IN THE PRECEDING SENTENCE, ACS MAKES NO WARRANTY OR REPRESENTATION OF ANY KIND, EXPRESS OR IMPLIED, WITH RESPECT TO THIS ACS ARTICLE INCLUDING, BUT NOT LIMITED TO WARRANTIES AS TO THE ACCURACY OR COMPLETENESS OF THE ACS ARTICLE, ITS QUALITY, ORIGINALITY, SUITABILITY, SEARCHABILITY, OPERATION, PERFORMANCE, COMPLIANCE WITH ANY COMPUTATIONAL PROCESS, MERCHANTABILITY OR FITNESS FOR A PARTICULAR PURPOSE.

ACS SHALL NOT BE LIABLE FOR: EXEMPLARY, SPECIAL, INDIRECT, INCIDENTAL, CONSEQUENTIAL OR OTHER DAMAGES ARISING OUT OF OR IN CONNECTION WITH THE AGREEMENT GRANTED HEREUNDER, THE USE OR INABILITY TO USE ANY ACS PRODUCT, ACS’S PERFORMANCE UNDER THIS AGREEMENT, TERMINATION OF THIS AGREEMENT BY ACS OR THE LOSS OF DATA, BUSINESS OR GOODWILL EVEN IF ACS IS ADVISED OR AWARE OF THE POSSIBILITY OF SUCH DAMAGES. IN NO EVENT SHALL THE TOTAL AGGREGATE LIABILITY OF ACS OUT OF ANY BREACH OR TERMINATION OF THIS AGREEMENT EXCEED THE TOTAL AMOUNT PAID BY YOU TO ACS FOR ACCESS TO THIS ACS ARTICLE FOR THE CURRENT YEAR IN WHICH SUCH CLAIM, LOSS OR DAMAGE OCCURRED, WHETHER IN CONTRACT, TORT OR OTHERWISE, INCLUDING, WITHOUT LIMITATION, DUE TO NEGLIGENCE.

The foregoing limitations and exclusions of certain damages shall apply regardless of the success or effectiveness of other remedies. No claim may be made against ACS unless suit is filed within one (1) year after the event giving rise to the claim.

7. GENERAL

This Agreement sets forth the entire understanding of the Parties. The validity, construction and performance of this Agreement shall be governed by and construed in accordance with the laws of the District of Columbia USA without reference to its conflicts of laws principles. You acknowledge that the delivery of the ACS article will occur in the District of Columbia, USA. You shall pay any taxes lawfully due from it, other than taxes on ACS's net income, arising out of your use of this ACS article and/or other rights granted under this Agreement. You may not assign or transfer its rights under this Agreement without the express written consent of ACS.

8. ACCEPTANCE

You warrant that You have read, understand, and accept the terms and conditions of this Agreement. ACS reserves the right to modify this Agreement at any time by posting the modified terms and conditions on the ACS Publications Web site. Any use of this ACS article after such posting shall constitute acceptance of the terms and conditions as modified.

Title: Photoinduced Formation of Hybrid Aryl Pd-Radical Species Capable of 1,5-HAT: Selective Catalytic Oxidation of Silyl Ethers into Silyl Enol Ethers

Author: Marvin Parasram, Padon Chuentragool, Dhruba Sarkar, et al

Publication: Journal of the American Chemical Society

Publisher: American Chemical Society

Date: May 1, 2016

PERMISSION/LICENSE IS GRANTED FOR YOUR ORDER AT NO CHARGE

This type of permission/license, instead of the standard Terms & Conditions, is sent to you because no fee is being charged for your order. Please note the following:

- Permission is granted for your request in both print and electronic formats, and translations.
- If figures and/or tables were requested, they may be adapted or used in part.
- Please print this page for your records and send a copy of it to your publisher/graduate school.
- Appropriate credit for the requested material should be given as follows: "Reprinted (adapted) with permission from (COMPLETE REFERENCE CITATION). Copyright (YEAR) American Chemical Society." Insert appropriate information in place of the capitalized words.
- One-time permission is granted only for the use specified in your request. No additional uses are granted (such as derivative works or other editions). For any other uses, please submit a new request.

BACK CLOSE WINDOW

CITED LITERATURE

[1] *The Mizoroki-Heck Reaction*; Oestreich, M. Ed.; John Wiley & Sons: West Sussex, U.K.; 2009.

[2] (a) Mizoroki, T.; Mori, K.; Ozaki, A. *Bull. Chem. Soc. Jpn.* **1971**, *44*, 581. (b) Heck, R. F.; Nolley, J. P. *J. Org. Chem.* **1972**, *37*, 2320.

[3] (a) Dounay, A. B.; Overman, L. E. *Chem. Rev.* **2003**, *103*, 2945. (b) Torborg, C.; Beller, M. *Adv. Synth. Catal.* **2009**, *351*, 3027.

[4] (a) Baldwin, J. E. *J. Chem. Soc., Chem. Commun.* **1976**, 734. (b) Gilmore, K.; Alabugin, I. V. *Chem. Rev.* **2011**, *111*, 6513.

[5] (a) Iimura, S.; Overman, L. E.; Paulini, R.; Zakarian, A. *J. Am. Chem. Soc.* **2006**, *128*, 13095. (b) Vital, P.; Norrby, P.-O.; Tanner, D. *Synlett* **2006**, *2006*, 3140. (c) Klein, J. E. M. N.; Műller-Bunz, H.; Ortin, Y.; Evans, P. *Tetrahedron Letters* **2008**, *49*, 7187.

[6] (a) Rigby, J. H.; Hughes, R. C.; Heeg, M. J. *J. Am. Chem. Soc.* **1995**, *117*, 7834. (b) Lemaire-Audoire, S.; Savignac, M.; Dupuis, C.; Genêt, J.-P. *Tetrahedron Lett.***1996**, *37*, 2003.

[7] (a) O'Connor, B.; Zhang, Y.; Negishi, E.-i.; Luo, F.-T.; Cheng, J.-W. *Tetrahedron Lett.***1988**, *29*, 3903. (b) Hegedus, L. S.; Sestrick, M. R.; Michaelson, E. T.; Harrington, P. J. *J. Org. Chem.* **1989**, *54*, 4141. (c)

[8] Owczarczyk, Z.; Lamaty, F.; Vawter, E. J.; Negishi, E. *J. Am. Chem. Soc.* **1992**, *114*, 10091.

[9] Sigman, M. S.; Werner, E. W. *Acc. Chem. Res.* **2012**, *45*, 874.

[10] Jun, T.; Hiroyasu, W.; Masako, M.; Nobuaki, K. *Bull. Chem. Soc. Jpn.* **2003**, *76*, 2209.

[11] Affo, W.; Ohmiya, H.; Fujioka, T.; Ikeda, Y.; Nakamura, T.; Yorimitsu, H.; Oshima, K.; Imamura, Y.; Mizuta, T.; Miyoshi, K. *J. Am. Chem. Soc.* **2006**, *128*, 8068.

[12] Firmansjah, L.; Fu, G. C. *J. Am. Chem. Soc.* **2007**, *129*, 11340.

[13] (a) Bloome, K. S.; McMahen, R. L.; Alexanian, E. J. *J. Am. Chem. Soc.* **2011**, *133*, 20146. (b) Venning, A. R. O.; Kwiatkowski, M. R.; Roque Peña, J. E.; Lainhart, B. C.; Guruparan, A. A.; Alexanian, E. J. *J. Am, Chem. Soc.* **2017**, DOI: 10.1021/jacs.7b06794. For intermolecular alkyl Heck reactions, see: (c) McMahon, C. M.; Alexanian, E. J. *Angew. Chem. Int. Ed.* **2014**, *53*, 5974. (d) Zou, Y.; Zhou, J. *Chem. Commun.* **2014**, *50*, 3725.

[14] Liu, Q.; Dong, X.; Li, J.; Xiao, J.; Dong, Y.; Liu, H. *ACS Catal.* **2015**, *5*, 6111.

[15] (a) Wilt, J. W. *J. Am. Chem. Soc.* **1981**, *103*, 5251. (b) Wilt, J. W. *Tetrahedron* **1985**, *41*, 3979. (c) Wilt, J. W.; Lusztyk, J.; Peeran, M.; Ingold, K. U. *J. Am. Chem. Soc.* **1988**, *110*, 281

[16] Koreeda, M.; Hamann, L. G. *J. Am. Chem. Soc.* **1990**, *112*, 8175.

[17] Jahn, U. In *Radicals in Synthesis III*; Heinrich, M., Gansäuer, A., Eds.; Springer Berlin Heidelberg: Berlin, Heidelberg, 2012, p 121-451.

[18] Weiss, M. E.; Carreira, E. M. *Angew. Chem. Int., Ed.* **2011**, *50*, 11501.

[19] Weiss, M. E.; Kreis, L. M.; Lauber, A.; Carreira, E. M. *Angew. Chem. Int., Ed.* **2011**, *50*, 11125.

[20] Millán, A.; Álvarez de Cienfuegos, L.; Miguel, D.; Campaña, A. G.; Cuerva, J. M. *Org. Lett.* **2012**, *14*, 5984.

[21] Fairlamb, I. J. S.; Kapdi, A. R.; Lee, A. F.; McGlacken, G. P.; Weissburger, F.; de Vries, A. H. M.; Schmieder-van de Vondervoort, L. *Chem. Eur. J.* **2006**, *12*, 8750.

[22] Hartwig, J. F. In *Organotransition Metal Chemistry: From Bonding to Catalysis*; University Science Books, 2009, p 379-417.

[23] Dong, X.; Han, Y.; Yan, F.; Liu, Q.; Wang, P.; Chen, K.; Li, Y.; Zhao, Z.; Dong, Y.; Liu, H. *Org. Lett.* **2016**, *18*, 3774.

[24] (a) Bols, M.; Skrydstrup, T. *Chem. Rev.***1995**, *95*, 1253. (b) Fensterbank, L.; Malacria, M.; Sieburth, S. M. N. *Synthesis* **1997**, *1997*, 813. (c) Bracegirdle, S.; Anderson, E. A. *Chem. Soc. Rev.***2010**, *39*, 4114. (d) Arnason, I.; Oberhammer, H. *J. Mol. Struct.* **2001**, *598*, 245.

[25] Nishiyama, H.; Kitajima, T.; Matsumoto, M.; Itoh, K. *J. Org. Chem.* **1984**, *49*, 2298.

[26] Koreeda, M.; George, I. A. *J. Am. Chem. Soc.* **1986**, *108*, 8098.

[27] Esposito, O.; Roberts, D. E.; Cloke, F. G. N.; Caddick, S.; Green, J. C.; Hazari, N.; Hitchcock, P. B. *Eur. J. Inorg. Chem.* **2009**, *2009*, 1844.

[28] (a) Chernyak, N.; Dudnik, A. S.; Huang, C.; Gevorgyan, V. *J. Am. Chem. Soc.* **2010**, *132*, 8270. (b) Huang, C.; Gevorgyan, V. *Org. Lett.* **2010**, *12*, 2442.

[29] (a) McAtee, J. R.; Yap, G. P. A.; Watson, D. A. *J. Am. Chem. Soc.* **2014**, *136*, 10166. (b) McAtee, J. R.; Martin, S. E. S.; Ahneman, D. T.; Johnson, K. A.; Watson, D. A. *Angew. Chem. Int., Ed.* **2012**, *51*, 3663.

[30] (a) Hosomi, A.; Sakurai, H. *Tetrahedron Lett.* **1976**, *17*, 1295. (b) Akira, H.; Masahiko, E.; Hideki, S. *Chem. Lett.* **1976**, *5*, 941. (c) Denmark, S. E.; Fu, J. *Chem. Rev.* **2003**, *103*, 2763. (d) Jiménez-González, L.; García-Muñoz, S.; Álvarez-Corral, M.; Muñoz-Dorado, M.; Rodríguez-García, I. *Chem. Eur. J.* **2007**, *13*, 557.

[31] Muzart, J. *Tetrahedron* **2013**, *69*, 6735.

[32] Smitrovich, J. H.; Woerpel, K. A. *J. Org. Chem.* **1996**, *61*, 6044.

[33] Tamao, K.; Kumada, M.; Maeda, K. *Tetrahedron Lett.* **1984**, *25*, 321.

[34] Albéniz, A. C.; Espinet, P.; López-Fernández, R.; Sen, A. *J. Am. Chem. Soc.* **2002**, *124*, 11278.

[35] Newcomb, M.; Toy, P. H. *Acc. Chem. Res.* **2000**, *33*, 449.

[36] Phapale, V. B.; Buñuel, E.; García-Iglesias, M.; Cárdenas, D. J. *Angew. Chem. Int., Ed.* **2007**, *46*, 8790.

[37] Satoh, T.; Miura, M. *Top. Organomet. Chem.* **2005**, *14*, 1.

[38] Marsault, E.; Hoveyda, H. R.; Peterson, M. L.; Saint-Louis, C.; Landry, A.; Vézina, M.; Ouellet, L.;Wang, Z.; Ramaseshan, M.; Beaubien, S.; Benakli, K.; Beauchemin, S.; Déziel, R.; Peeters, T.; Fraser, G. L. *J. Med. Chem.***2006**, *49*, 7190.

[39]Hu, J.; Hirao, H.; Li, Y.; Zhou, J. *Angew. Chem., Int. Ed* .**2013**, *52*, 8676.

[40]Konishi, H.; Ueda, T.; Muto, T.; Manabe, K. *Org. Lett.* **2012**, *14*, 4722.

[41]Bharath, Y.; Thirupathi, B.; Ranjit, G.; Mohapatra, D. K. *Asian. J. Org. Chem.* **2013**, *2*, 848.

[42]Yoshida, M.; Ohno, S.; Namba, K. *Angew. Chem., Int. Ed.* **2013**, *52*, 13597.

[43]Moure, M. J.; SanMartin, R.; Dominguez, E. *Angew. Chem. Int. Ed.* **2012**, *51*, 3220.

[44] Kim, H. R.; Yun, J. *Chem. Commun*. **2011**, *47*, 2943.

[45]Sato, T.; Komine, N.; Hirano, M.; Komiya, S. *Chem. Lett.* **1999**, *28*, 441.

[46]Shah, J. H.; Agoston, G. E.; Suwandi, L.; Hunsucker, K.; Pribluda, V.; Zhan, X. H.; Swartz, G. M.; LaVallee, T. M.; Treston, A. M. *Bioorg. Med. Chem.* **2009**, *17*, 7344.

[47]Tobia, D.; Rickborn, B. *J. of Org. Chem.* **1989**, *54*, 777.

[48]Reetz, M. T.; Guo, H.; Ma, J.-A.; Goddard, R.; Mynott, R. J. *J. Am. Chem. Soc.* **2009**, *131*, 4136.

[49]Takemiya, A.; Hartwig, J. F. *J. Am. Chem. Soc.* **2006**, *128*, 6042.

[50]Karila, D.; Leman, L.; Dodd, R. H. *Org. Lett.* **2011**, *13*, 5830.

[51]Choy, P. Y.; Kwong, F. Y. *Org. Lett*. **2013**,*15*, 270.

[52]Yus, M.; Foubelo, F.; Ferrández, José V. *Eur. J Org. Chem.* **2001**, 2809.

[53] *Comprehensive Organic Transformation*; Larock, R. C.; Wiley: **1999**.

[54] (a) Buist, P. H. *Nat. Prod. Rep.* **2004**, *21*, 249. (b) Cavellini, L.; Meurisse, J.; Findinier, J.; Erpapazoglou, Z.; Belgareh-Touzé, N.; Weissman, A. M.; Cohen, M. M. *Nat. Commun.* **2017**, *8*, 15832. (c) Li, J.; Condello, S.; Thomes-Pepin, J.; Ma, X.; Xia, Y.; Hurley, T. D.; Matei, D.; Cheng, J.-X. *Cell Stem Cell* **2017**, *20*, 303. (d) Niu, D.; Willoughby, P. H.; Woods, B. P.; Baire, B.; Hoye, T. R. *Nature* **2013**, *501*, 531.

[55] (a) Baudoin, O. *Acc. Chem. Res.* **2017**, *50*, 1114. (b) Gorelsky, S. I. *Coord. Chem. Rev.* **2013**, *257*, 153. (c) Livendahl, M.; Echavarren , A. M. *Isr. J. Chem.* **2010**, *50*, 630. (d) Fagnou, K. In *C-H Activation*; Yu, J.-Q., Shi, Z., Eds.; Springer Berlin Heidelberg: Berlin, Heidelberg, 2010, p 35.

[56] (a) Guo, S.-r.; Kumar, P. S.; Yang, M. *Adv. Synth. Catal.* **2017**, *359*, 2. (b) Liu, C.; Liu, D.; Lei, A. *Acc. Chem. Res.* **2014**, *47*, 3459. (c) Zhang, S.-Y.; Zhang, F.-M.; Tu, Y.-Q. *Chem. Soc. Rev.* **2011**, *40*, 1937.

[57] Baudoin, O.; Herrbach, A.; Guéritte, F. *Angew. Chem., Int. Ed.* **2003**, *42*, 5736.

[58] Beesley, R. M.; Ingold, C. K.; Thorpe, J. F. *J. Chem. Soc., Trans.* **1915**, *107*, 1080.

[59] Hitce, J.; Retailleau, P.; Baudoin, O. *Chem. Eur. J.* **2007**, *13*, 792.

[60] Motti, E.; Catellani, M. *Adv. Synth. Catal.* **2008**, *350*, 565.

[61] Della Ca', N.; Fontana, M.; Motti, E.; Catellani, M. *Acc. Chem. Res.* **2016**, *49*, 1389.

[62] (a) Diao, T.; Stahl, S. S. *J. Am. Chem. Soc.* **2011**, *133*, 14566. (b) Diao, T.; Pun, D.; Stahl, S. S. *J. Am. Chem. Soc.* **2013**, *135*, 8205. (c) Pun, D.; Diao, T.; Stahl, S. S. *J. Am. Chem. Soc.* **2013**, *135*, 8213.

[63] Nakajima, R.; Ogino, T.; Yokoshima, S.; Fukuyama, T. *J. Am. Chem. Soc.* **2010**, *132*, 1236.

[64] Trost, B. M.; Dong, G.; Vance, J. A. *Chem. Eur. J.* **2010**, *16*, 6265.

[65] Ito, Y.; Hirao, T.; Saegusa, T. *J. Org. Chem.* **1978**, *43*, 1011.

[66] (a) Chen, Y.; Romaire, J. P.; Newhouse, T. R. *J. Am. Chem. Soc.* **2015**, *137*, 5875. (b) Chen, Y.; Turlik, A.; Newhouse, T. R. *J. Am. Chem. Soc.* **2016**, *138*, 1166.

[67] Chen, M.; Dong, G. *J. Am. Chem. Soc.* **2017**, *139*, 7757.

[68] Giri, R.; Maugel, N.; Foxman, B. M.; Yu, J.-Q. *Organometallics* **2008**, *27*, 1667.

[69] (a) Crabtree, R. H.; Burk, M. J. *J. Am. Chem. Soc.* **1987**, *109*, 8025. (b) Dobereiner, G. E.; Crabtree, R. H. *Chem. Rev.* **2010**, *110*, 681.

[70] Xu, W.-w.; P. Rosini, G.; Krogh-Jespersen, K.; S. Goldman, A.; Gupta, M.; M. Jensen, C.; C. Kaska, W. *Chem. Commun.* **1997**, 2273.

[71] Göttker-Schnetmann, I.; White, P.; Brookhart, M. *J. Am. Chem. Soc.* **2004**, *126*, 1804.

[72] Choi, J.; MacArthur, A. H. R.; Brookhart, M.; Goldman, A. S. *Chem. Rev.* **2011**, *111*, 1761.

[73] Liu, F.; Pak, E. B.; Singh, B.; Jensen, C. M.; Goldman, A. S. *J. Am. Chem. Soc.* **1999**, *121*, 4086.

[74] Breslow, R.; Baldwin, S.; Flechtner, T.; Kalicky, P.; Liu, S.; Washburn, W. *J. Am. Chem. Soc.* **1973**, *95*, 3251.

[75] Čeković, Ž.; Dimttruević, L.; Djokić, G.; Srnić, T. *Tetrahedron* **1979**, *35*, 2021.

[76] (a) Hogeveen, H.; van Kruchten, E. M. G. A. *In Memory of H. L. Meerwein*; Springer Berlin Heidelberg: Berlin, Heidelberg, 1979, p 89. (b) Hanson, J. R. In *Comprehensive Organic Synthesis*; Fleming, I., Ed.; Pergamon: Oxford, 1991, p 705. (c) Olah, G. A. *Acc. Chem. Res.* **1976**, *9*, 41.

[77] (a) Čeković, Ž.; Dimttruević, L.; Djokić, G.; Srnić, T. *Tetrahedron* **1979**, *35*, 2021. (b) Wolff, M. E. *Chem. Rev.* **1963**, *63*, 55. (c) Gansäuer, A.; Lauterbach, T.; Narayan, S. *Angew. Chem. Int. Ed.* **2003**, *42*, 5556. (d) Stella, L. *Angew. Chem., Int. Ed.* **1983**, *22*, 337. (e) Choi, G. J.; Zhu, Q.; Miller, D. C.; Gu, C. J.; Knowles, R. R. *Nature* **2016**, *539*, 268. (f) Chu, J. C. K.; Rovis, T. *Nature* **2016**, *539*, 272.

[78] Chen, K.; Baran, P. S. *Nature* **2009**, *459*, 824.

[79] Voica, A.-F.; Mendoza, A.; Gutekunst, W. R.; Fraga, J. O.; Baran, P. S. *Nat. Chem.* **2012**, *4*, 629.

[80] Johansson Seechurn, C. C. C.; Kitching, M. O.; Colacot, T. J.; Snieckus, V. *Angew. Chem. Int. Ed.* **2012**, *51*, 5062.

[81] Manolikakes, G.; Knochel, P. *Angew. Chem., Int. Ed*. **2009**, *48*, 205.

[82] Tsou, T. T.; Kochi, J. K. *J. Am. Chem. Soc.* **1979**, *101*, 6319.

[83] (a) Curran, D. P.; Kim, D.; Liu, H. T.; Shen, W. *J. Am Chem Soc*. **1988**, *110*, 5900. For HAT reviews, see: (b) Majetich, G.; Wheless, K. *Tetrahedron* **1995**, *51,* 7095. (c) *Radicals in Organic Synthesis Vol. 2*; Renaud, P.; Sibi, M.P.; Wiley-VCH: Weinheim, **2001**. (d) Robertson, J.; Pillai, J.; Lush, R. K. *Chem. Soc. Rev*. **2001**, *30*, 94. (e) Nechab, M.; Mondal, S.; Bertrand, M. P.; *Chem. Eur. J*. **2014**, *20*, 16034.

[84] Bissember, A. C.; Levina, A.; Fu, G. C. *J. Am. Chem. Soc.* **2012**, *134*, 14232.

[85] (a) Yao, W.; Zhang, Y.; Jia, X.; Huang, Z. *Angew. Chem., Int. Ed*. **2014**, *53*, 1390. (b) Lyons, T.W.; Bezier, D.; Brookhart, M. *Organometallics*. **2015**, *34*, 4058. (c)

[86] For a recent review on visible-light induced TM catalyzed reactions without exogenous photosensitizers, see: Parasram, M.; Gevorgyan, V. *Chem. Soc. Rev.* **2017**. (in press)

[87] (a) Prier, C. K.; Rankic, D. A.; MacMillan, D. W. C. *Chem. Rev*. **2013**, *113*, 5322. (b) Skubi, K. L.; Blum, T. R.; Yoon, T. P. *Chem. Rev*. **2016**, *116*, 10035. (c) Romero, N. A.; Nicewicz, D. A. *Chem. Rev*. **2016**, *116*, 10075. (d) Staveness, D.; Bosque, I.; Stephenson, C. R. J. *Acc. Chem. Res*. **2016**, *49*, 2295. (e) Tellis, J. C.; Kelly, C. B.; Primer, D. N.; Jouffroy, M.; Patel, N. R.; Molander, G. A. *Acc. Chem. Res.* **2016**, *49*, 1429.

[88] Kunkely, H.; Vogler, A. *J. Organomet. Chem.* **1998**, *559*, 215.

[89] (a) Kraatz, H.-B.; van der Boom, M. E.; Ben-David, Y.; Milstein, D. *Isr. J. Chem.* **2001**, *41*, 163. (b) Seligson, A. L.; Trogler, W. C. *J. Am. Chem. Soc.* **1992**, *114*, 7085. (c) Lanci, M. P.; Remy, M. S.; Kaminsky, W.; Mayer, J. M.; Sanford, M. S. *J. Am. Chem. Soc.* **2009**, *131*, 15618. (d) Andersen, T. L.; Kramer, S.; Overgaard, J.; Skrydstrup, T. *Organometallics* **2017**, *36*, 2058.

[90] (a) Kuo, J. L.; Hartung, J.; Han, A.; Norton, J. R. *J. Am. Chem. Soc.* **2015**, *137*, 1036. (b) Hu, Y.; Shaw, A. P.; Estes, D. P.; Norton, J. R. *Chem. Rev.* **2016**, *116*, 8427

[91] Wu, X.; See, J. W. T.; Xu, K.; Hirao, H.; Roger, J.; Hierso, J.-C.; Zhou, J. *Angew. Chem., Int. Ed.* **2014**, *53*, 13573.

[92] Venning, A. R.O.; Kwiatkowski, M. R.; Peña, J. E. R.; Lainhart, B. C.; Guruparan, A. A.; Alexanian, E. J. J. *Am. Chem. Soc.* **2017** DOI: 10.1021/jacs.7b06794.

[93] Simmons, E. M.; Hartwig, J. F. *Angew. Chem. Int. Ed.* **2012**, *51*, 3066.

[94] Stille, J. K.; Lau, K. S. Y. *Acc. Chem. Res.* **1977**, *10*, 434–442

[95] (a) Lumbroso, A.; Cooke, M. L.; Breit, B. *Angew. Chem., Int. Ed.* **2013**, *52*, 1890. (b) Lin, Y. A.; Davis, B. G. *Beilstein J. Org. Chem.* **2010**, *6*, 1219. (c) Cha, M.-R.; Choi, C.-W.; Lee, J.-Y.; Kim, Y.-S.; Yon, G.-H.; Choi, S.-U.; Kim, Y.-H.; Ryu, S.-Y.; *Bull. Korean Chem. Soc*. **2012**, *33*, 337-340. (d) Rodriguez, I. I.; Rodriguez, A. D.; Wang, Y.; Franzblau, S. G. *Tetrahedron Lett.* **2006**, *47*, 3229-3232. (e) Marrero, J.; Rodríguez, A. D.; Baran, P.; Raptis, R. G.; Sánchez, J. A.; Ortega-Barria, E.; Capson, T. L. *Org. Lett*. **2004**, *6*, 1661-1664. (d) Colby, E. A.; O'Brie, K. C.; Jamison, T. F., *J. Am. Chem. Soc.* **2004,** *126*, 998-999. (e) Ghosh, A. K.; Liu, C. *J. Am. Chem. Soc.* **2003,** *125*, 2374-2375. (f) Hu, X.; Xu, S.; Maimone, T. J. *Angew. Chem. Int. Ed.* **2017**, *56*, 1624.

[96] (a) Rycek, L.; Hudlicky, T. *Angew. Chem., Int. Ed.* **2017**, *56*, 6022. (b) Skucas, E.; Ngai, M.-Y.; Komanduri, V.; Krische, M. J. *Acc. Chem. Res.* **2007**, *40*, 1394. (e) Lumbroso, A.; Cooke, M. L.; Breit, B *Angew. Chem., Int. Ed.* **52**, 1890-1932 (2013).

[97] Parasram, M.; Gevorgyan, V. *Acc. Chem. Res.* **2017**, DOI: 10.1021/acs.accounts.7b00306.

[98] (a) Brunckova, J.; Crich, D.; Yao, Q. *Tetrahedron Lett.* **1994**, *35*, 6619. (b) Attouche, A.; Urban, D.; Beau, J.-M. *Angew. Chem. Int. Ed.* **2013**, *52*, 9572.

[99] Blanksby, S. J.; Ellison, G. B. *Acc. Chem. Res.* **2003**, *36*, 255.

VITA

NAME: Marvin Parasram

EDUCATION: B.S., Chemistry, Stony Brook University, Stony Brook, NY, 2010

TEACHING EXPERIENCE: Teaching Assistant, Department of Chemistry, University of Illinois, 2010-2012

HONORS AND AWARDS: *Graduate Student Council Award*, University of Illinois at Chicago, 2015

Gordon Research Conference Carl Storm Underrepresented Minority Fellowship, 2015

Graduate College Student Presenter Award, University of Illinois at Chicago, 2014-2017

AFFILIATIONS: American Chemical Society

PUBLICATIONS: **Parasram, M.;** Chentragool, P.; Wang, Y.; Shi, Y.; Gevorgyan, V. "General Desaturation of Aliphatic Alcohols at Unactivated C(sp^3)–H Sites by Auxiliary-Controlled Photoinduced Hybrid Pd-Radical Catalysis." (*Submitted)*

Kurandina, D.; **Parasram, M.**; Gevorgyan, V. "Visible Light-Induced Room Temperature Intermolecular Reaction of Functionalized Alkyl Iodides with Vinyl Arenes/Heteroarenes." (*Submitted)*

Parasram, M.; Gevorgyan, V. "Visible Light-Induced Transition Metal-Catalyzed Transformations: Beyond Conventional Photosensitizers." *Chem. Soc. Rev.* **2017**. (*Accepted*)

Parasram, M.; Gevorgyan, V. "Silicon-Tethered Strategies for C–H Functionalization Reactions." *Acc. Chem. Res.* **2017**, DOI: 10.1021/acs.accounts.7b00306. (*Review*)

Parasram, M.; Chuentragool, P.; Sarkar, D.; Gevorgyan, V. "Photoinduced Formation of Aryl Hybrid Pd-Radical Species Capable of 1,5-HAT. Selective Oxidation of Silyl Ethers in Silyl Enol Ethers." *J. Am. Chem. Soc.* **2016**, *138*, 6340.

Parasram, M.; Iaroshenko, V. O.; Gevorgyan, V. "Endo-Selective Pd-Catalyzed Silyl Methyl Heck Reaction." *J. Am. Chem. Soc.* **2014**, *136*, 17926.

PRESENTATIONS: **Parasram, M.;** Chuentragool, P.; Sarkar, D.; Gevorgyan, V. "Photoinduced Formation of Aryl Hybrid Pd-Radical Species Capable of 1,5-HAT: Selective Oxidation of Silyl Ethers in Silyl Enol Ethers." Presented at the *ACS Chicago Section – Monthly Meeting*, University of Illinois at Chicago, Chicago, IL, **2017**. (poster)

Parasram, M.; Chuentragool, P.; Sarkar, D.; Gevorgyan, V. "Photoinduced Formation of Aryl Hybrid Pd-Radical Species Capable of 1,5-HAT: Selective Oxidation of Silyl Ethers in Silyl Enol Ethers." Presented at the 7th *Chicago Organic Symposium*, Loyola University, Chicago, IL, **2016** (oral).

Parasram, M.; Iaroshenko, V. O.; Gevorgyan, V. "Endo-Selective Pd-Catalyzed Silyl Methyl Heck Reaction." Presented at the *Key State Laboratory of Fine Chemicals at the Dalian University of Technology*, Dalian, China, **2015**.

Parasram, M.; Iaroshenko, V. O.; Gevorgyan, V. "Endo-Selective Pd-Catalyzed Silyl Methyl Heck Reaction." Presented at the *Gordon Research Conference – Organometallic Chemistry*, Newport, RI, **2015**. (poster)

Parasram, M.; Iaroshenko, V. O.; Gevorgyan, V. "Endo-Selective Pd-Catalyzed Silyl Methyl Heck Reaction." Presented at the *7th Negishi–Brown Lectures,* Purdue, IN, **2014**. (poster).